

TECHNICAL REPORTS SERIES No. **188**

Radiological Safety Aspects of the Operation of Electron Linear Accelerators



INTERNATIONAL ATOMIC ENERGY AGENCY, VIENNA, 1979

**RADIOLOGICAL SAFETY ASPECTS
OF THE OPERATION OF
ELECTRON LINEAR ACCELERATORS**

The following States are Members of the International Atomic Energy Agency:

AFGHANISTAN	HOLY SEE	PHILIPPINES
ALBANIA	HUNGARY	POLAND
ALGERIA	ICELAND	PORTUGAL
ARGENTINA	INDIA	QATAR
AUSTRALIA	INDONESIA	ROMANIA
AUSTRIA	IRAN	SAUDI ARABIA
BANGLADESH	IRAQ	SENEGAL
BELGIUM	IRELAND	SIERRA LEONE
BOLIVIA	ISRAEL	SINGAPORE
BRAZIL	ITALY	SOUTH AFRICA
BULGARIA	IVORY COAST	SPAIN
BURMA	JAMAICA	SRI LANKA
BYELORUSSIAN SOVIET SOCIALIST REPUBLIC	JAPAN	SUDAN
CANADA	JORDAN	SWEDEN
CHILE	KENYA	SWITZERLAND
COLOMBIA	KOREA, REPUBLIC OF	SYRIAN ARAB REPUBLIC
COSTA RICA	KUWAIT	THAILAND
CUBA	LEBANON	TUNISIA
CYPRUS	LIBERIA	TURKEY
CZECHOSLOVAKIA	LIBYAN ARAB JAMAHIRIYA	UGANDA
DEMOCRATIC KAMPUCHEA	LIECHTENSTEIN	UKRAINIAN SOVIET SOCIALIST REPUBLIC
DEMOCRATIC PEOPLE'S REPUBLIC OF KOREA	LUXEMBOURG	UNION OF SOVIET SOCIALIST REPUBLICS
DENMARK	MADAGASCAR	UNITED ARAB EMIRATES
DOMINICAN REPUBLIC	MALAYSIA	UNITED KINGDOM OF GREAT BRITAIN AND NORTHERN IRELAND
ECUADOR	MALI	UNITED REPUBLIC OF CAMEROON
EGYPT	MAURITIUS	UNITED REPUBLIC OF TANZANIA
EL SALVADOR	MEXICO	UNITED STATES OF AMERICA
ETHIOPIA	MONACO	URUGUAY
FINLAND	MONGOLIA	VENEZUELA
FRANCE	MOROCCO	VIET NAM
GABON	NETHERLANDS	YUGOSLAVIA
GERMAN DEMOCRATIC REPUBLIC	NEW ZEALAND	ZAIRE
GERMANY, FEDERAL REPUBLIC OF	NICARAGUA	ZAMBIA
GHANA	NIGER	
GREECE	NIGERIA	
GUATEMALA	NORWAY	
HAITI	PAKISTAN	
	PANAMA	
	PARAGUAY	
	PERU	

The Agency's Statute was approved on 23 October 1956 by the Conference on the Statute of the IAEA held at United Nations Headquarters, New York; it entered into force on 29 July 1957. The Headquarters of the Agency are situated in Vienna. Its principal objective is "to accelerate and enlarge the contribution of atomic energy to peace, health and prosperity throughout the world".

© IAEA, 1979

Permission to reproduce or translate the information contained in this publication may be obtained by writing to the International Atomic Energy Agency, Kärntner Ring 11, P.O. Box 590, A-1011 Vienna, Austria.

Printed by the IAEA in Austria
February 1979

TECHNICAL REPORTS SERIES No.188

RADIOLOGICAL SAFETY ASPECTS
OF THE OPERATION OF
ELECTRON LINEAR ACCELERATORS

A manual written by
William P. SWANSON
Stanford Linear Accelerator Center
Stanford University
United States of America

*Work supported in part by the
United States Department of Energy*

INTERNATIONAL ATOMIC ENERGY AGENCY
VIENNA, 1979

**RADIOLOGICAL SAFETY ASPECTS
OF THE OPERATION OF
ELECTRON LINEAR ACCELERATORS**
IAEA, VIENNA, 1979
STI/DOC/10/188
ISBN 92-0-125179-3

FOREWORD

Electron linear accelerators are being used throughout the world in increasing numbers in a variety of important applications. Foremost among these is their role in the treatment of cancer with both photon and electron radiations in the energy range 4–40 MeV. To a greater extent linear accelerators are replacing ^{60}Co sources and betatrons in medical applications. Commercial uses include non-destructive testing by radiography, food preservation, product sterilization and radiation processing of materials such as plastics and adhesives. Scientific applications include investigations in radiation biology, radiation chemistry, nuclear and elementary-particle physics and radiation research.

This manual is conceived as a source book providing authoritative guidance in radiation protection from an important category of radiation sources. It thus supplements other manuals of the Agency related to the planning and implementation of radiation protection programmes. The author, W.P. Swanson of Stanford Linear Accelerator Center, USA, was engaged as a consultant by the Agency to compile and write the manual, and the Agency wishes to express its gratitude to him.

A draft was sent to a number of experts in various countries. The Agency gratefully acknowledges the helpful comments, which have been taken into account in the final text, from J. Rassow, K. Tesch (Federal Republic of Germany), M. Ladu (Italy), T. Nakamura (Japan), G.R. Higson (United Kingdom), F.H. Attix, R.C. McCall and C.S. Nunan (United States of America). The Agency's officer responsible for this project was F.N. Flakus of the Radiological Safety Section, Division of Nuclear Safety and Environmental Protection.

Comments from readers for possible inclusion in a later edition of the manual would be welcome; they should be addressed to the Director, Division of Nuclear Safety and Environmental Protection, International Atomic Energy Agency, Kärntner Ring 11, P.O. Box 590, A-1011 Vienna, Austria.

CONTENTS

INTRODUCTION	1
Purpose and scope of the Manual	2
Terminology and units	5
Acknowledgements	5
1. USES AND CHARACTERISTICS OF ELECTRON LINEAR ACCELERATORS	7
1.1. Fields of application	7
1.2. Types of electron linear accelerator installations	8
1.3. Parameters of electron linear accelerators	11
2. RADIATIONS AT ELECTRON LINEAR ACCELERATOR INSTALLATIONS	27
2.1. Radiations anticipated and their quality factors	27
2.1.1. Types of radiations and their sources	27
2.1.2. Quality factors	29
2.2. Photon differential track length and estimation of yields	34
2.3. Electron beams	43
2.4. Photons	50
2.4.1. External bremsstrahlung	50
2.4.2. Scattered photons	57
2.5. Neutrons	61
2.5.1. Neutron quality factor and dose equivalent	61
2.5.2. Production mechanisms	65
2.5.3. Neutron yields from electron beams	79
2.5.3.1. The giant-resonance region ($E_0 \gtrsim 35$ MeV) .	82
2.5.3.2. Neutron production for $34 < E_0 < 150$ MeV .	88
2.5.3.3. Neutron production for $E_0 > 150$ MeV	91
2.6. Radioactivity induced in components	97
2.6.1. Installations with $E_0 < 35$ MeV	101
2.6.2. Activity induced by high-energy beams	101
2.7. Activity induced in air and water	126
2.7.1. Airborne radioactivity	126
2.7.1.1. Air activation	126
2.7.1.2. Dust	131
2.7.2. Activity induced in water	136

2.8.	Muons	142
2.9.	Charged-particle secondary beams	147
2.10.	Production of toxic gases	149
	2.10.1. Concentration buildup and removal	151
	2.10.2. Production rates	152
2.11.	X-rays generated by microwave systems	156
	2.11.1. Oscillators and amplifiers	156
	2.11.2. Microwave cavities	158
3.	RADIATION SHIELDING	160
3.1.	Types of areas and shielding criteria	160
	3.1.1. Accelerator scheduling and workload factor W	160
	3.1.2. Primary and secondary barriers and the orientation (use) factor U	162
	3.1.3. Occupancy factor T	164
3.2.	Shielding materials	165
3.3.	Physical considerations	168
3.4.	Shielding against photons	175
	3.4.1. Primary barriers ($E_0 < 100$ MeV)	175
	3.4.2. Secondary barriers ($E_0 < 100$ MeV)	177
	3.4.3. Accelerators operating above 100 MeV	186
3.5.	Shielding against neutrons	189
	3.5.1. Energies below the photopion threshold ($E_0 < 140$ MeV)	190
	3.5.2. High-energy installations ($E_0 > 140$ MeV)	197
3.6.	Labyrinths, doors, voids and penetrations	199
4.	TYPICAL INSTALLATIONS	205
4.1.	Medical installations	205
4.2.	Industrial radiographic installations	207
4.3.	Research and special-purpose installations	214
5.	RADIATION MONITORING AND INTERPRETATION OF MEASUREMENTS	226
5.1.	Characteristics and choice of monitoring equipment	226
5.2.	Duty factor effects on radiation measurements	236
	5.2.1. Dead-time effects in pulse counters	237
	5.2.2. Recombination in ionization chambers	238

5.3.	Neutron monitoring techniques	242
5.3.1.	Fluence measurements	243
5.3.2.	Spectral measurements	252
5.4.	Radiation surveys	255
5.5.	Instrument calibration and maintenance	260
6.	REQUIREMENTS FOR AN EFFECTIVE SAFETY PROGRAMME ..	263
6.1.	Safety organization	263
6.2.	Safety programme	263
6.3.	Radiation safety	265
6.4.	Accelerator safety	268
6.5.	Linear accelerators used in radiation therapy	270
6.5.1.	General radiation safety	271
6.5.2.	Reliability of dosimetry	272
6.5.3.	Control of dose distribution	273
6.5.4.	Safe delivery of the prescribed treatment	274
6.5.5.	Provisions to facilitate accurate patient positioning	276
6.5.6.	Control of unwanted dose to patient	277
6.5.7.	Protection against other risks	279
6.6.	Safety at industrial and research installations	282
7.	GENERAL BIBLIOGRAPHY	286
	APPENDIXES	293
	Appendix A. Physical and numerical constants	294
	Appendix B. Radiation parameters of materials	297
	Appendix C. Rules of thumb	318
	Appendix D. Addresses of organizations	322

INTRODUCTION

More than a decade of experience has been gained since the publication of a manual devoted exclusively to radiological protection at high-energy electron accelerators. Because of the rapidly increasing use of electron linear accelerators, it was felt that it would be useful to prepare such a handbook that would encompass the large body of methods and data which have since been developed. Since the publication of NBS Handbook No.97, significant developments related to radiation protection at electron linear accelerators have occurred along the following lines:

(a) Electron linear accelerators for medical and radiographic purposes operating in the range 4–40 MeV are now widely accepted. The growing number of such machines operating above 10 MeV poses additional problems of undesirable neutron radiations and concomitant component activation.

(b) There has been a trend toward standardization of radiation-protection practices, and development of national and international radiation-protection guidelines for medical accelerators.

(c) The introduction of high-energy, high-power electron machines has brought new types of problems and magnified old ones. The higher energy has necessitated provisions for high-energy neutron dosimetry and shielding, muon dosimetry and shielding, and treatment of the neutron skyshine problem. The higher power has aggravated such problems as radioactive air and water and the possibility of burn-through of shielding by raw electron beams.

(d) Operating flexibility such as *multibeam capability* has placed new demands on personnel protection systems.

(e) Refinement of measurements of photonuclear reactions has made more reliable predictions of neutron production and component activation possible. These developments include improved consistency among cross-section measurements with monochromatic photons in the giant-resonance region, as well as new data on less frequent types of reactions at all energies.

(f) The development of Monte-Carlo techniques to a high degree has made it possible to undertake otherwise practically intractable calculational problems. Very useful calculations are now available on electromagnetic cascade development, on neutron production and transport, and on muon production and transport.

(g) The development of radiation protection practices at other types of accelerators has also provided a source of information useful at electron accelerators. Conferences on accelerator dosimetry and experience held in 1965, 1969 and 1971 presented occasions at which world-wide operating experience at accelerators of all kinds was shared.

(h) The growing sensitivity on the part of the general public to environmental concerns has required a greater degree of attention to radioactive releases.

While these have never been a serious problem at electron accelerators, it still is desirable to be able to make positive statements about the amounts produced and about their disposal.

Since much of this great body of information is scattered widely throughout the literature, it is the goal of this manual to gather it together in an organized usable form.

It is significant that no fatalities to personnel have ever resulted from acute radiation injury at an electron linear accelerator. The few serious accidents at research installations that have occurred were by electrocution and ordinary mechanical injury. A manual devoted to radiological safety is nevertheless useful, because radiation is a 'special' safety hazard connected with these accelerators and its management requires more specialized knowledge and instrumentation than do the programmes of conventional safety.

PURPOSE AND SCOPE OF THE MANUAL

This manual is intended as a guide for the planning and implementation of radiation protection programmes for all types of electron linear accelerators. It is hoped that it will prove useful to accelerator manufacturers, accelerator users, management of institutional and industrial installations, and especially to radiation safety officers and other persons responsible for radiation safety. Material is provided for guidance in the planning and installation stages, as well as for the implementation of radiation protection for continuing operations.

Because of their rapidly growing importance, the problems of installation and radiation safety of standard medical and industrial accelerators are discussed in separate sections. For higher-energy research installations, the basic radiation protection objectives are the same, but more types of potentially harmful radiation must be considered and shielded against. For such facilities, each major type of problem is briefly summarized and references are given to direct the user to more complete information in the literature.

Special discussions are devoted to the radiation protection problems unique to electron accelerators: thick-target bremsstrahlung, the electromagnetic cascade, the estimation of secondary-radiation yields from thick targets, and that annoying operational problem, instrumental corrections for accelerator duty factor. In addition, an extensive review of neutron production is given which includes new calculations of neutron production in various materials. A recalculation of activation in a variety of materials has been done for this manual, and specific gamma-ray constants have been recalculated for a number of nuclides to take into account the contribution of K X-rays. The subjects of air and water activation, as well as toxic gas production in air have been specially reviewed. In the section on radiation shielding, published data on bremsstrahlung attenuation have been

reviewed to estimate a consistent set of attenuation parameters over a broad range of primary energies. Furthermore, the treatment of monochromatic photon reflection of Chilton and Huddleston has been adapted for use with bremsstrahlung spectra. The discussion of neutron shielding utilizes neutron transport calculations from Oak Ridge which properly account for the contribution of neutron-capture gamma rays to the dose equivalent. These data are presented in a form believed most convenient for direct use by the radiation protection specialist.

The present manual does not strive to provide results of great accuracy; this is very difficult unless all aspects of a given situation are taken into account. The intention is rather to present a balanced treatment of the major kinds of radiation and provide means to estimate them with simple algebraic manipulations based on physically well-grounded interpolations. For the sake of completeness and to provide additional perspective for the user, order-of-magnitude estimates are given for some radiations of lesser importance.

Betatrons and electron microtrons operating at the same energy produce essentially the same kind of secondary radiation as electron linacs and the material given in this manual is directly applicable to them. Accelerators which deliver primary beams of other types of particles, particularly protons, deuterons or heavier ions, give rise to secondary radiation of a somewhat different nature, owing to the mass and hadronic interactions of the primary particles; the amount of bremsstrahlung is negligible compared with the intense neutron fluences released by these particles. These accelerators are not discussed in this manual.

During the preparation of this manual, an ongoing dialogue was conducted with accelerator manufacturers and radiation protection specialists at several laboratories (see Acknowledgements). A number of visits were made to clinics and research installations to gather first-hand impressions of safety practices that are actually in use.

The material presented here is of course based on earlier work by many persons and organizations. A reasonable attempt is made to acknowledge, by citation, the work of individuals where appropriate, but as the field of radiation protection extends over many decades, completeness in this regard is impossible. Radiation protection manuals which are heavily drawn upon are listed in the General Bibliography (Section 7). It is recommended that persons responsible for radiation protection have a selection of these references available, for additional perspective on the problems and their solutions.

Recommendations for clinical calibrations of beams used in therapy are not given in this manual, but the reader is referred to reports of international organizations such as the IAEA and ICRU and other authoritative bodies which deal with this important subject (see Section 7).

It should be borne in mind that there may be additional regional and local requirements for radiation protection that must be met. Governmental authorities and qualified experts are best consulted to ensure that each installation is operated in compliance with all legal requirements.

TABLE I. FREQUENTLY USED SYMBOLS AND UNITS

Name	Symbol	Units		
		SI	Special	Conversion factors
Absorbed dose	D	gray (Gy)	rad (rad)	1 rad = 10 mGy = 10 mJ · kg ⁻¹
Absorbed dose rate	\dot{D}	Gy · s ⁻¹	rad · s ⁻¹	1 rad · s ⁻¹ = 10 mGy · s ⁻¹
Exposure	X	coulomb per kilogram (C · kg ⁻¹)	röntgen (R)	1 R = 258 μC · kg ⁻¹
Exposure rate	\dot{X}	C · kg ⁻¹ · s ⁻¹	R · s ⁻¹	1 R · s ⁻¹ = 258 μC · kg ⁻¹ · s ⁻¹
Dose equivalent	H	(dimensions of J · kg ⁻¹)	rem	
Dose equivalent rate	\dot{H}	-	rem · s ⁻¹	
Activity	A	becquerel (Bq)	curie (Ci)	1 Ci = 37 GBq = 3.7 × 10 ¹⁰ s ⁻¹
Quality factor	Q	-	-	
Electron kinetic energy	E	MeV	-	1 MeV = 1.602 × 10 ⁻¹³ J
Incident or initial kinetic energy	E ₀	MeV		
Photon energy	k	MeV		

Useful conversions

1 Bq = 1 radioactive disintegration per second = 1 s⁻¹ = 27.027 pCi

1 Gy = 1 J · kg⁻¹ = 100 rad

1 eV = 1.602 × 10⁻¹⁹ J, approx.

1 MeV ≈ 1.602 × 10⁻¹³ J = 1.602 × 10⁻¹³ kg · Gy = 1.602 × 10⁻⁸ g · rad = 1.602 × 10⁻⁶ erg

1 W = 1 J · s⁻¹ = 1 V · A

Absorbed dose corresponding to an exposure X of 1 C · kg⁻¹: to air: D = 33.7 Gy

to tissue: D = 36.4 Gy (Co-60)

TERMINOLOGY AND UNITS

Where possible, the terminology and units correspond to those defined in ICRU Report 19 (see Bibliography, Section 7). Table I gives frequently used symbols and units. (See Appendix A for additional useful physical and numerical constants.)

Note

The question of an SI-coherent unit with a special name for dose equivalent H is undergoing review. The sievert (Sv), which is the absorbed dose D (in Gy) multiplied by dimensionless modifying factors (in particular the quality factor Q) has been proposed to the Conférence Générale des Poids et Mesures (CGPM) by the International Commission on Radiation Units and Measurements (ICRU) and the International Commission on Radiological Protection (ICRP). The sievert would stand in the same relationship to the gray as the rem does to the rad. Since a final resolution of this matter has not been made at the time of publication, values of dose equivalent H are given in rem in this manual. In all other instances radiation quantities are given in *both* the SI-coherent units and the existing special units. Also note that no special SI-coherent unit has been proposed to the CGPM for exposure X; the SI-derived unit $C \cdot kg^{-1}$ is used for exposure.

ACKNOWLEDGEMENTS

The author gratefully acknowledges the kind hospitality and support of the International Atomic Energy Agency and the Stanford Linear Accelerator Center in the preparation of this manuscript, and particularly thanks F.N. Flakus and R.C. McCall for their personal help and encouragement.

The author is deeply indebted to F.H. Attix, G.R. Higson, M. Ladu, T.G. Martin III, R.C. McCall, T. Nakamura, C.S. Nunan, J. Rassow and K. Tesch for valuable comments on a preliminary draft, and to my colleagues D.D. Busick, T.M. Jenkins, K.R. Kase, W.R. Nelson and G.J. Warren of the Stanford Linear Accelerator Center, and R.H. Thomas of the Lawrence Berkeley Laboratory, for generously sharing their knowledge and experience.

Many other individuals, representing a large number of organizations, were extremely cooperative and helpful in supplying useful information. These include: R. Alvarez, L. Armstrong, A. Asami, M.L. Berger, B. Berman, J. Bly, J. Broberg, A. Burrill, R. Byers, A.B. Chilton, T.R. Chippendale, J.B. Czirr, J. Fenger, H. Fujita, E.G. Fuller, G. Gilbert, T.F. Godlove, T.W. Grunewalt, D. Hankins, P. Hardaker, T.G. Hobbs, J. Jasberg, R. Jean, R. Johnson, J. Kaehler, M.J. Karaffa, C.J. Karzmark, N.N. Kaushal, N.L. Kay, J.G. Kelliher, E.A. Knapp, J.D. Koenig, S. Kurihara, M. Lara, J. Lebacqz, J.E. Leiss, G. Loew, P. Maschka,

T.P. McReynolds, B. Mecklenburg, B. Meyer, V. Moré, R.B. Neal, P. Ogren, S. Penner, F. Peregoy, E. Petersilka, V. Price, D. Reid, J.C. Ritter, R. Rorden, R. Ryan, A. Smith, W. Smith, V. Stieber, I.A. Taub, G. Tochilin, G. Trimble, W. Turchinets, Yu.P. Vakhrushin, R. Van de Vyver, N. Van Hooydonk, D. Walz, K. Whitham, D. Willis, U. Yelin, and many others who provided information about specific accelerator installations or discussed certain portions of the material.

The author acknowledges with deep appreciation the considerable help in the preparation of this manuscript by V. Smoyers and personnel of the SLAC Drafting Department under the leadership of T. Hunter. D. Dupen, W. Field and A. Schwartz provided very helpful advice at critical moments.

1. USES AND CHARACTERISTICS OF ELECTRON LINEAR ACCELERATORS

1.1. Fields of application

Several decades of technological development have culminated in the modern microwave electron linear accelerator, or electron linac, an instrument useful in medicine, industry and science [1, 2, 3]. The technologies combined in this simple and powerful tool are high-power pulsed microwave generation, high-vacuum technology, electronics, and metal forming and assembly. Originally developed as a research instrument to study the basic structure of matter, it has become useful in several other important ways.

(a) Medical applications

In radiation therapy, second- and third-generation electron linacs are widely employed in the treatment of cancer. They offer the advantages of simplicity and reliability, higher output, larger treatment fields, and the choice of both electron and photon irradiations. The higher energies are useful because of the greater penetration of the radiation to treat deep-lying tumours and afford a greater degree of protection to the skin. A small focal spot allows precise beam definition. Space requirements for the accelerators are modest and they are readily adaptable to rotational therapy. Both because of its societal importance and in terms of numbers of accelerators in operation (over 800), cancer therapy is the leading application of the electron linear accelerator [4, 5, 6].

(b) Industrial applications

High-intensity radiography is now an accepted, standard application of the electron linac, such as in the X-ray inspection of large welds, castings, complex assemblies and solid propellants [7]. Radiation processing applications [8] include curing of paint and adhesives, polymerization of plastics, food preservation [9] and sterilization of heat-sensitive medical products [10].

(c) Research applications

A third major category of uses is in scientific research. Research in nuclear physics employs linacs operating in the range 25–500 MeV, generally using the copiously produced photons to study nuclear structures. Facilities for studies using neutron time-of-flight and monoenergetic photons have permitted much greater detail in the experimental results than previously possible [11, 12].

Laboratories doing research in elementary particle physics use linacs producing electron beams with energies as high as 22 GeV and positron beams up to 15 GeV [3] (1 GeV \approx 1000 MeV). The extremely short wavelength corresponding to the electron or positron momentum (10^{-15} cm at 20 GeV) permits the sub-structure of the much larger proton and neutron (radius $\approx 1.2 \times 10^{-13}$ cm) to be explored.

Linacs are used as injectors for electron synchrotrons and electron/positron storage rings for elementary particle research. The discovery in 1974–75 of massive (compared with the nucleon) elementary particles at the $e^+ - e^-$ storage rings is considered one of the most important scientific results of recent times because it reveals the existence of a previously unknown property of matter, with implications concerning nuclear substructure [13].

Pulse radiolysis is a field of chemistry which uses to advantage the short radiation pulses available from electron linacs to study the dynamics of chemical reactions, particularly of free radicals.

A list of experimental uses under study might include such diverse subjects as: the use of intense beams of negative pi mesons (π^-) for cancer therapy, production of short-lived isotopes for prompt use in nuclear medicine, earth tunnelling and free-electron lasing.

1.2. Types of electron linear accelerator installations

The electron linear accelerator itself is fundamentally a conducting tube, usually of copper, accurately shaped to contain an electromagnetic wave of the proper characteristics — a kind of waveguide [14, 15, 16]. The beam energy is proportional to the length and to the electric field strength within the cavity or, equivalently, to the square root of the microwave power inserted. Typical gradients achieved lie in the range 2–4 MeV/ft. Because the electrons achieve relativistic velocities quickly, the spacing of cavities within the tube is uniform almost throughout its length. A high-energy accelerator differs from a low-energy machine mainly in its total length.

Two different configurations are in modern use. In the *travelling wave accelerator* (Figs 1, 2), microwave power is supplied to the input of the accelerator section and travels to the other end, remaining at all times in phase with the moving electron bunches. The accelerator interior is partitioned into accelerating cavities dimensioned in such a way that the phase velocity of the microwave field equals the electron velocity.

Another configuration is the *standing-wave accelerator* [17, 18] in which additional side cavities provide a 180° phase shift between accelerating cavities (Fig.3). This type has the advantage of being less sensitive to temperature or dimensional variations and achieves the same beam energy in a shorter length.



FIG.1. A ten-foot (≈ 3.0 m) travelling-wave accelerator section for SLAC. With a 16-MW klystron (peak RF power), the energy added by such a section is 40 MeV. The uniform partitioning into RF cavities by annular disks is easily seen. (Reproduced with kind permission of the Stanford Linear Accelerator Center and the Energy Research and Development Administration.)

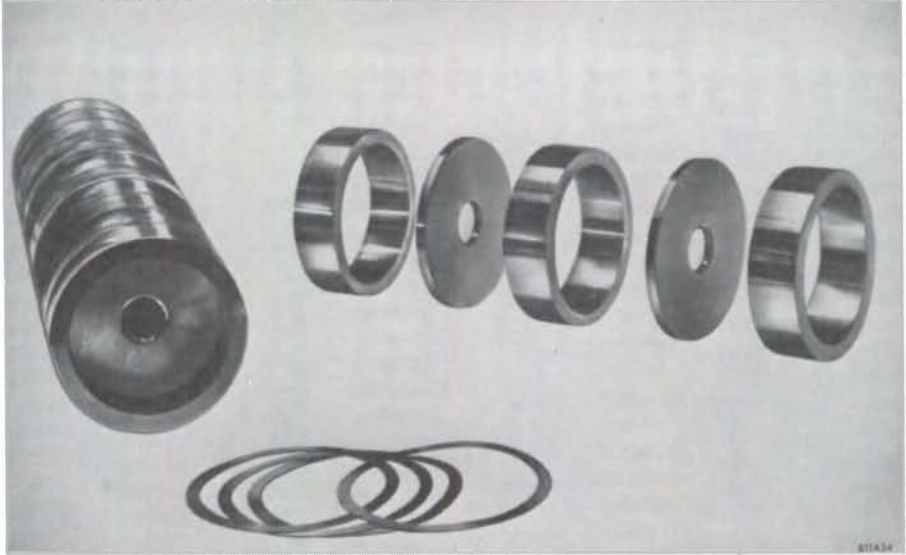


FIG.2. Accelerator disks and cylinders. These components are assembled to form the 10-ft (≈ 3.0 m) sections shown in Fig.1. (Reproduced with kind permission of the Stanford Linear Accelerator Center and the Energy Research and Development Administration.)

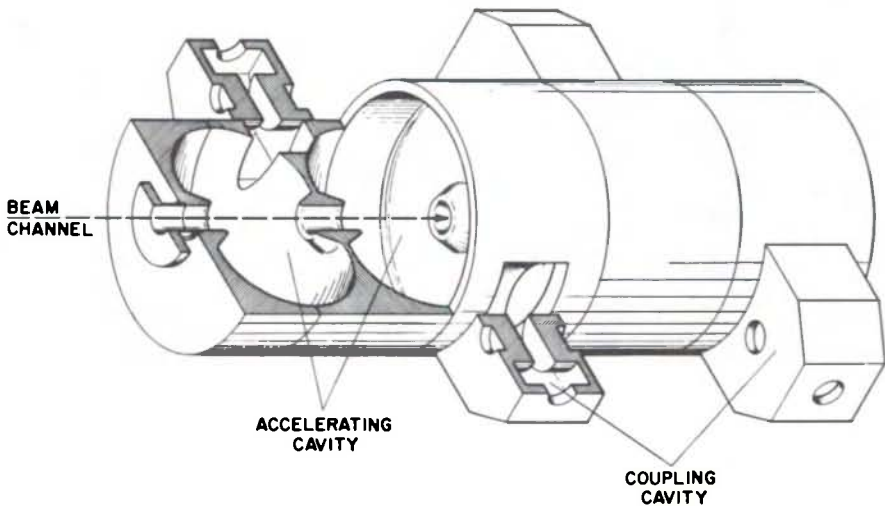


FIG.3. Structure of a standing-wave accelerator. The coupling cavities provide a phase change such that the accelerating cavities maintain a 180° phase shift with respect to each other. (Reproduced with kind permission of E.A. Knapp, the Los Alamos Scientific Laboratory and Review of Scientific Instruments.)

Microwave power for low energies is generally developed by magnetrons, but all higher-energy accelerators use klystrons. The nominal frequency of 3000 Hz (wavelength 10 cm in free space at 2998 MHz) is usually used. Peak RF powers generated per unit are 2–5 MW (magnetrons) and 20–40 MW (klystrons).

The following components are common to all types of installations:

- (a) The injector, containing the gun or electron 'source';
- (b) The accelerator itself, composed of one or more sections, fed by separate microwave generators;
- (c) The microwave generators: one or more magnetrons or klystrons, driven in phase;
- (d) A modulator to energize each microwave generator;
- (e) A target and/or beam dump to provide useful secondary radiations and stop the electrons.

In addition, most installations have at least one beam-transport magnet. Most medical accelerators operating above 6 MeV are equipped with a magnet which is an integral part of the apparatus which deflects the beam by 90° or 270°. Research installations may also have secondary beam lines, transporting a variety of particle types – photons, electrons, positrons and mesons.

Three categories of installations with similar radiation protection problems are easily identifiable: (a) medical, (b) industrial, and (c) research. These categories may differ somewhat in the types of radiations to be protected against, but more so in the physical layout and movements of personnel and members of the general public around them. Special needs of these types of installations are discussed where appropriate, and descriptions of typical installations are given. It is hoped that useful information for meeting the requirements of novel or unique installations will be found in this manual, although every case cannot be foreseen.

1.3. Parameters of electron linear accelerators

A list of physical parameters of the two-mile Stanford Linear Accelerator (Fig.4) is given in Table II. Although the example chosen is at present the highest-energy linac, most of its parameters are quite representative of many other travelling-wave accelerators if the differences related to its great length (multiplicity of sections and therefore of beam energy and power) are taken into account. The particularly unique features of the SLAC facility are the interlaced-multiple-beam capability, the ability to accelerate also positrons and polarized electrons to high energies, and a special facility for extremely short (10 ps) beam pulses.

Tables III, IV and V provide an overview of three classes of linear accelerator installations. It is seen that the development in medical accelerators within the past decade (Table III) has been toward a capability for isocentric therapy using



FIG.4. Aerial view of the Stanford Two-Mile Accelerator (SLAC), a modern high-energy facility for elementary-particle research. The Research Area with multiple-beam capability is in the foreground. The electron-positron storage ring SPEAR is to the lower right. The 360 beam pulses accelerated per second are shared by as many as six different beam paths, each with separately adjustable energy, current and pulse length. (Reproduced with kind permission of the Stanford Linear Accelerator Center and the Energy Research and Development Administration.)

both electrons and photons [4]. The maximum useful energy appears to be approximately 40 MeV. The radiation characteristics at each energy are surprisingly similar among these modern facilities, reflecting a general consensus among manufacturers and users.

Accelerators for industrial radiography are surveyed in Table IV. The very high outputs of these machines may pose a great potential hazard to operating personnel in industrial settings.

Table V contains an abbreviated list of physical parameters of representative operating research and special-purpose installations. There is great variety in the capabilities of these installations, reflecting the purposes to which they are applied. Figure 5 illustrates the general rise in beam power with accelerator energy.

Text continued on p.24

TABLE II. PHYSICAL PARAMETERS OF THE STANFORD TWO-MILE ACCELERATOR (SLAC)

Accelerator length	10 000 ft (3048 m)
Length between feeds	10 ft (3.04 m)
Number of accelerator sections	960
Number of klystrons	245
Peak power per klystron	20 - 40 MW
Beam pulse repetition rate	1 - 360 pulses/s
RF pulse length	2.5 μ s
Filling time	0.83 μ s
Electron energy, unloaded	22.8 GeV (max)
Electron energy, loaded	21.5 GeV
Electron peak beam current	70 mA (max)
Electron average beam current	40 μ A (max)
Electron average beam power	800 kW (max)
Electron beam pulse length	10 ps - 1.6 μ s
Electron beam energy spread (max)	0.5%
Positron energy	15 GeV (max)
Positron average beam current ^a	0.5 μ A
Multiple beam capability	6 interlaced beams with independently adjustable pulse length, energy, and current
Operating frequency	2856 MHz

^a For 140 kW of incident electron beam power at positron source located at one-third point along accelerator length.

TABLE III. RADIATION PARAMETERS OF MEDICAL ELECTRON LINEAR ACCELERATORS INTRODUCED SINCE 1965

Approx. date of introduction	Model	Manufacturer	Beam energies in modality ^a		Type of mount or motion	Rotation	Total structure length and type	Power source	Transport magnet(s)	Maximum photon output ($10^{-2} \text{ Gy} \cdot \text{m}^2 \cdot \text{min}^{-1}$) ($\text{rad} \cdot \text{m}^2 \cdot \text{min}^{-1}$) (flattened)	Maximum field size (photons) (cm^2 at 1 m)	Nominal leakage radiation ^b (photons) (%)
			Photons (MV)	Electrons (MeV)								
1965	SL 75/10	Philips MEL	7-10	4-10	Isocentric 100 cm SAD	370°	2.25 m, TW	2 MW Magnetron	95° (approx.)	600 (300 W electrons at 8 MeV) ^c	30 X 30	0.1
1965	LUE 5	Efremov	5	-	Isocentric 100 cm SAD	$\pm 120^\circ$	TW	1.8 MW Magnetron	90°	300	15 X 17	
1967	LUE 25	Efremov	10, 15	10-25	Stationary ^c	-30° $+45^\circ$	6.5 m, TW (two sections)	20 MW Klystron	90°	1000	18 X 18 (20 X 20) ^d	0.03
1967	Therac 40 Saggitaire	CGR-MeV AECL	10, 25	7-32 (40)	Isocentric 105 cm SAD	$\pm 105^\circ$ (370° with pit)	6.0 m, TW (two sections)	9 MW Klystron	$+37^\circ$ -37° $+37^\circ$ -127°	400 (1000) (2 kW electrons) ^c	38 X 38	0.1 0.3 ^b
1967	LMR 13	Toshiba	10	8-12	Isocentric 100 cm SAD	$\pm 210^\circ$	1.6 m, TW	4.8 MW Magnetron	105° (approx.)	400	30 X 30	0.1
1968	Clinac 4	Varian	4	-	Isocentric 80 cm SAD	360°	0.3 m, SW	2 MW Magnetron	None: straight ahead beam	224	40 X 40	0.1 0.03 ^b
1969	Mevatron VI	Applied Radiation	6	-	Isocentric 100 cm SAD	370°	1.0 m, SW	2 MW Magnetron	261° achromatic	300	40 X 40	0.02
1969	Mevatron XII	Applied Radiation	8, 10	5-11	Isocentric 100 cm SAD	370°	1.3 m, SW	2 MW Magnetron	261° achromatic	300	40 X 40	0.1
1970	ML-15MIIB	Mitsubishi	12	8-15	Isocentric 100 cm SAD	390°	1.7 m, TW	5 MW Klystron	110°	500	30 X 30	0.1
1970	Therapi 4	SHM Nuclear	4	-	Stationary ^c	365°	0.35 m, SW	2 MW Magnetron	None: straight ahead beam	220	40 X 40	0.1
1970	Clinac 35	Varian	8, 25	7-28	Isocentric 100 cm SAD	360°	2.25 m, TW	20 MW Klystron	$+57^\circ$ -90°	1000 (5 kW electrons) ^e	35 X 35	0.1

Approx. date of introduction	Model	Manufacturer	Beam energies in modality ^a		Type of mount or motion	Rotation	Total structure length and type	Power source	Transport magnet(s)	Maximum photon output ($10^{-2} \text{ Gy} \cdot \text{m}^2 \cdot \text{min}^{-1}$) ($\text{rad} \cdot \text{m}^2 \cdot \text{min}^{-1}$) (flattened)	Maximum field size (photons) (cm^2 at 1 m)	Nominal leakage radiation ^b (photons) (%)
			Photons (MV)	Electrons (MeV)								
1970	Dynaray 4	Radiation Dynamics	4	—	Isocentric 100 cm SAD	370°	0.75 m, TW	2 MW Magnetron	266° achromatic	300	30 X 30	0.1
1971	Therac 6 Neptune	CGR-MeV AECL	6	—	Isocentric 100 cm SAD	370°	1.1 m, TW	2 MW Magnetron	262° achromatic	250	40 X 40	0.1
1972	Dynaray 10	Radiation Dynamics	8	3-10	Isocentric 100 cm SAD	370°	2.3 m, TW	2 MW Magnetron	266° achromatic	300	35 X 35	0.1
1972	LMR 4	Toshiba	4	—	Isocentric 80/100 cm SAD	420°	0.3 m, SW	2 MW Magnetron	None: straight ahead beam	225	40 X 40	0.05
1972	LMR 15	Toshiba	10	10-16	Isocentric 100 cm SAD	420°	1.7 m, TW	4.8 MW Magnetron	105° (approx.)	350	30 X 30	0.1
1973	Therac 20 Saturne	CGR-MeV AECL	10, 18	6-20	Isocentric 100 cm SAD	370°	2.3 m, TW	5 MW Klystron	270° achromatic	400	40 X 40	0.1
1973	SL 75/20	Philips MEL	8, 16	5-20	Isocentric 100 cm SAD	360°	2.5 m, TW	5 MW Magnetron	95° (approx.)	400 (900 W electrons at 10-15 MeV) ^c	30 X 30	0.1
1973	ML-4M	Mitsubishi	4	—	Isocentric 80 cm SAD	380°	0.3 m, SW	2 MW Magnetron	None: straight ahead beam	224	30 X 30	0.1
1974	ML-3M	Mitsubishi	2.8	—	Isocentric 80 cm SAD	380°	0.25 m, SW	2 MW Magnetron	None: straight ahead beam	100	30 X 30	0.1
1974	Clinac 18	Varian	10	6-18	Isocentric 100 cm SAD	360°	1.4 m, SW	5 MW Klystron	270° achromatic	500	35 X 35	0.1
1974	Dynaray 18	Radiation Dynamics	6-12	5-18	Isocentric 100 cm SAD	370°	2.3 m, TW	5 MW Klystron	266° achromatic	350	35 X 35	0.1
1975	Clinac 12	Varian	8 (6)	6-12 (4-9)	Isocentric 100 cm SAD	360°	1.2 m, SW	2 MW Magnetron	270° achromatic	350	35 X 35	0.1
1975	Clinac 6X	Varian	6	—	Isocentric 80 cm SAD	360°	0.3 m, SW	2 MW Magnetron	None: straight ahead beam	192	40 X 40	0.1

See footnotes at end of table.

TABLE III. (cont.)

Approx. date of introduction	Model	Manufacturer	Beam energies in modality ^a		Type of mount or motion	Rotation	Total structure length and type	Power source	Transport magnet(s)	Maximum photon output (10^{-2} Gy · m ² · min ⁻¹) (rad · m ² · min ⁻¹) (flattened)	Maximum field size (photons) (cm ² at 1 m)	Nominal leakage radiation ^b (photons) (%)
			Photons (MV)	Electrons (MeV)								
1975	SL 75/5	Philips MEL	4-6	-	Isocentric 100 cm SAD	420°	1.25 m, TW	2 MW Magnetron	95°	350	40 X 40	0.1
1976	Therac 10 Neptune	CGR-MeV AECL	9	6-10	Isocentric 100 cm SAD	370°	1.2 m, SW	2 MW Magnetron	262° achromatic	300	40 X 10	0.1
1976	Dynaray 6	Radiation Dynamics	6	-	Isocentric 100 cm SAD	370°	1.0 m, TW	2 MW Magnetron	266° achromatic	300	35 X 35	0.1
1976	LUE 15M	Efremov	15	10-20	Isocentric 100 cm SAD	± 120°	2.6 m, TW	9 MW Magnetron	270° achromatic	300 (1.5 kW electrons) ^c	30 X 30 20 X 20 ^d	0.1 0.2 ^b
1977	Mevatron XX	Siemens	10, 15	3-18	Isocentric 100 cm SAD	370°	1.3 m, SW	7 MW Klystron	270° achromatic	300	40 X 40	0.1
1977	Clinac 6/100	Varian	6	-	Isocentric 100 cm SAD	360°	0.3 m, SW	2 MW Magnetron	None: straight ahead beam	200	40 X 40	0.1
1977	Clinac 20	Varian	15	6-20	Isocentric 100 cm SAD	360°	1.6 m, SW	5 MW Klystron	270° achromatic	500	35 X 35	0.1
1977	EMI FOUR	EMI Therapy	4	-	Isocentric 100 cm SAD	360°	0.3 m, SW	2 MW Magnetron	None: straight ahead beam	220	40 X 40	0.1
1977	EMI SIX	EMI Therapy	6	-	Isocentric 100 cm SAD	360°	0.3 m, SW	2 MW Magnetron	None: straight ahead beam	220	40 X 40	0.1
1978	LUE 5M	Efremov	4-5	4-5	Isocentric 100 cm SAD	± 120°	0.6 m, TW	3 MW Magnetron	None: straight ahead beam	200	30 X 30 20 X 20 ^d	
1978	SL 75/14	Philips MEL	8, 10	4-14	Isocentric 100 cm SAD	360°	2.25 m, TW	2 MW Magnetron	95°	350	40 X 40	0.1

^a Data in parentheses are non-standard options offered by manufacturer.

^b Averaged over 100 cm² at 1 m. Where two values are given, the first refers to patient plane, the second applies to room shielding.

^c Vertical, rotational adjustment.

^d Where two field sizes are given, the first refers to photon beam therapy, the second to electron therapy.

^e Primary electron beam extracted in research mode.

TABLE IV. RADIATION CHARACTERISTICS OF ELECTRON LINEAR ACCELERATORS FOR INDUSTRIAL RADIOGRAPHY

Manufacturer	Model	Nominal beam energy (MeV)	RF power source (magnetron or klystron)	Maximum X-ray output (unflattened)		Maximum field size (at 1 m) (cm)	Nominal photon leakage radiation (per cent of useful beam at 1 m)
				(Gy·m ² ·s ⁻¹)	(rad·m ² ·min ⁻¹)		
CGR MeV	Neptune 6	6	M	0.13	750	50 (dia.)	0.1
CGR MeV	Neptune 10	10	M	0.33	2 000	50 (dia.)	0.1
Efremov	LUE-15-1.5	15	M	1.7	10 000	30 (dia.)	1.0
Efremov	LUE-10-1D	10	M	0.30	1 800	22 (dia.)	1.0
Efremov	LUE-10-2D	10	M	0.83	5 000	25 (dia.)	1.0
Efremov	LUE-15-15000D	15	M	2.5	15 000	40 (dia.)	1.0
Efremov	LUE-5-500D	5	M	0.08	500	35 (dia.)	0.2
EMI Therapy	Radiograf 4	4	M	0.08	500	26 × 35	0.5
Mitsubishi	ML-1 RII	0.95	M	0.003	20	30 (dia.)	0.1
Mitsubishi	ML-1 RIII	0.45 0.95	M	0.00025 0.0025	1.5 15	30 (dia.)	0.1 0.1
Mitsubishi	ML-3R	1.5	M	0.01	50	30 (dia.)	0.3
Mitsubishi	ML-5R	3	M	0.05	300	30 (dia.)	0.3
Mitsubishi	ML-5RII	4	M	0.06	350	30 (dia.)	0.3
Mitsubishi	ML-10R	8	M	0.33	2 000	30 (dia.)	0.2
Mitsubishi	ML-15RII	12	K	1.2	7 000	30 (dia.)	0.1

TABLE IV (cont.)

Manufacturer	Model	Nominal beam energy (MeV)	RF power source (magnetron or klystron)	Maximum X-ray output (unflattened)		Maximum field size (at 1 m) (cm)	Nominal photon leakage radiation (per cent of useful beam at 1 m)
				(Gy·m ² ·s ⁻¹)	(rad·m ² ·min ⁻¹)		
Radiation Dynamics	Super X 600	4	M	0.1	600	30 (dia.)	0.1
Radiation Dynamics	Super X 2000	8	M	0.33	2 000	30 (dia.)	0.1
Radiation Dynamics	Super XX	12	K	1.0	6 000	30 (dia.)	0.1
Varian	Linatron 200	2	M	0.03	175	77 × 77	0.02
Varian	Linatron 400	4	M	0.07	400	39 × 39	0.1
Varian	Linatron 2000	8	M	0.33	2 000	55 (dia.)	0.1
Varian	Linatron 6000	15	K	1.0	6 000	27 (dia.)	0.1

TABLE V. RADIATION PARAMETERS OF RESEARCH AND SPECIAL-PURPOSE ELECTRON LINEAR ACCELERATORS

Installation location	Nominal peak energy (MeV)	Machine use	Special capabilities	Number and type of sections ^b	RF source ^c	Typical high-power operation (approx.) ⁸						
						Peak current (mA)	Energy (MeV)	T _p (μs)	Pulse rate (Hz)	Duty factor (%)	Electron power (kW)	
1 Amsterdam IKO	500	Nuclear physics Nuclear chemistry	n(0–500 MeV) Large duty factor	25 TW (S)	12 K (1–4)	10	250	50	2500	10.	200	1
2 Argonne	22	Nuclear physics Nuclear chemistry	n(2–20 MeV) 35-ps pulses	2 TW (L)	2 K (20)	2500	14	10	120	0.12	45	2
3 Bariloche	30	Nuclear physics	10–100 ns pulses	1 TW (S)	1 K	300	25	1.2	200	0.024	1.8	3
4 Bedford RADC	12	Radiation research		1 TW (L)	1 K (10)	550	10	4.3	180	0.08	5.0	4
5 Berlin BAM	35	Activation analysis Neutron radiography Radiation protection		2 TW (S)	1 K	180	30	4	300	0.12	6.5	5
6 Berlin HMI	18	Pulse radiolysis	Nanosecond pulses	1 TW (L)	1 K (10)	800	12	5	50	0.025	2.5	6
7 Bethesda AFFRI	55	Radiation research	High current	6 TW (S)	4 K	1000	30	1.0	1000	0.1	30	7
8 Boeing (Seattle)	30	Radiation research		3 TW (S)	1 K	1100	11.5	5	30	0.015	1.9	8
9 Bologna	12	Radiation chemistry Radiation biology Radiation physics	Selectable pulse width High current 11 A in 10-ns pulse	TW (L)	1 K(10)	1400	6	5	300	0.15	12	9
10 Bonn	35	Synchrotron injector		1 TW	1 K (25)	800	20	1	50	0.005	0.8	10
11 Cornell	246	Synchrotron injector		6 TW	3 K	100	150	2.5	60	0.015	2.3	11
12 Daresbury	43	Synchrotron injector		4 TW	2 K (30)	500	43	0.73	53	0.004	0.8	12
13 Darmstadt	70	Nuclear physics	(e ⁺) resolution 30 keV	2 TW (S)	1 K	60	70	5.5	150	0.08	4.0	13
14 DESY I	400	Synchrotron injector	e ⁺ (250–380 MeV) DORIS storage rings PETRA storage rings	14 TW	14 K (25)	200	500	2	50	0.01	10	14
15 DESY II	50	Second injector		5 TW	5 K (6)	70	40	1	50	0.005	0.2	15
16 Frascati	450	Storage ring injector	e ⁺ (60–320 MeV) ADONE storage rings	12 TW (S)	6 K (20)	100	400	3.2	250	0.08	40	16
17 Geel BCMN	150	Nuclear physics	10 A in 3-ns pulse	1 SW (S) 2 TW (S)	3 K	1500	90	0.1	900	0.009	12	17
18 Ghent	90	Nuclear physics	e ⁺ (10–40 MeV)	2 TW (S)	2 K (20)	250	70	2.5	300	0.075	13	18

See footnotes at end of table.

TABLE V. (cont.)

Installation location	Nominal peak energy (MeV)	Machine use	Special capabilities	Number and type of sections ^b	RF source ^c	Typical high-power operation (approx.) ^a						
						Peak current (mA)	Energy (MeV)	T _p (μs)	Pulse rate (Hz)	Duty factor (%)	Electron power (kW)	
19 Giessen	65	Nuclear physics	Mono-E photons (8–35 MeV)	2 TW (S)	1 K	200	65	2	250	0.05	6.8	19
20 Glasgow	130	Nuclear physics	n(0–10 MeV)	12 TW (S)	3 K (20)	300	93	3.5	150	0.05	14	20
21 Hammersmith MRC	8	Radiation physics		1 TW	1 M (2)	25	7	2	300	0.06	0.1	21
22 Harwell I	55	Nuclear physics	n(0–10 MeV)	7 TW (S)	7 K (8)	500	30	2.0	200	0.04	5	22
23 Harwell II	136	Nuclear physics	n(0–30 MeV)	8 TW (L)	4 K (20)	1000	60	5.0	300	0.15	90	23
24 Hebrew University (Jerusalem)	8	Pulse radiolysis	Nanosecond pulses	1 TW	1 M	1400	8	0.01	460	0.0005	1	24
25 Hokaido	45	Neutron diffraction Pulse radiolysis		3 TW (S)		100	45	3	200	0.06	5	25
26 Karlsruhe	22	Food preservation		1 TW	1 K	100	16	4	300	0.1	2	26
27 Kharkov I	500	Nuclear physics										27
28 Kharkov II	2000	Particle physics		49 TW	51 K (20)	20	1600	1.2	50	0.006	2	28
29 Kyoto	48	Neutron production	n(0–14 MeV)	2 TW (L)	2 K (10)	500	25	4	180	0.07	10	29
30 Livermore LLL	180	Nuclear physics	e ⁻ (10–180 MeV) Mono-E photons (5–70 MeV) n(0–30 MeV)	5 TW (S)	15 K (15)	650	75	3	300	0.1	45	30
31 Mainz	320	Nuclear physics	Mono-E photons (10–100 MeV) Nanosecond pulses	8 TW (S)	8 K (25)	150	270	3	150	0.04	15	31
32 Manchester (Paterson Labs)	12	Radiation biology Radiation chemistry	6 Å in 10-ns pulse	1 TW	1 K (20)	500	10	5	50	0.025	1.3	32
33 MIT Bates	400	Nuclear physics	Large duty factor High-res. spectrometer	22 TW (S)	10 K (4)	10	400	15	1250	1.8	60	33
34 Monterey NPGS	100	Nuclear physics		3 TW	2 K	30	105	1	60	0.006	0.2	34
35 Moscow Kurchatov	60	Nuclear physics	Neutron production 50 ms pulse at 900 Hz	6 TW	6 K	1000	60	5.5	150	0.1	55	35

Installation location	Nominal peak energy (MeV)	Machine use	Special capabilities	Number and type of sections ^b	RF source ^c	Typical high-power operation (approx.) ^a						
						Peak current (mA)	Energy (MeV)	T _p (μs)	Pulse rate (Hz)	Duty factor (%)	Electron power (kW)	
36 Natick NARADCOM	15	Food preservation Radiation chemistry	Multiple beam ports	2 TW (S)	2 K (5)	500	10	5	180	0.09	5	36
37 NBS (Washington)	160	Nuclear physics Radiation standards	n(0–20 MeV) e ⁺ (10–40 MeV)	9 TW (L)	12 K	250	100	5	360	0.18	40	37
38 NPL (London)	22	Radiation metrology	5 A in 5-ns pulse	2 TW	1 K (20)	750	15	3.2	240	0.07	8	38
39 NRC (Ottawa)	35	Nuclear physics	Neutron production	4 TW (S)	1 K	250	35	3.2	180	0.06	5	39
40 NRL (Washington)	60	Radiation research	Neutron production	3 TW	3 K	450	50	1	360	0.04	10	40
41 Oak Ridge ORELA	178	Nuclear physics	Nanosecond pulses	4 TW (L)	4 K	15000	140	0.024	1000	0.0024	50	41
42 Ohio State	6	Pulse radiolysis	Nanosecond pulses	1 TW	1 M	325	6	0.01	550	0.0006		42
43 Orsay	2300	Particle physics	e ⁺ (0–1.3 GeV) Storage rings ACO, DCI	39 TW	39 K (20, 25)	60	2000	1.5	50	0.008	9	43
44 Raychenn (Copenhagen)	17	Product irradiation	High current	1 TW	1 K	1100	10	6	200	0.1	10	44
45 Rensselaer	100	Radiation research	n(0–30 MeV) 6 A in short pulse	9 TW (L)	9 K (10)	300	45	4.5	720	0.32	50	45
46 Rio de Janeiro	30	Nuclear physics		3 TW	1 A, 1 K	100	28	3.3	360	0.1	2.8	46
47 RISØ (Roskilde)	14	Radiation research	Nanosecond pulses High current	1 TW	1 K (17)	1100	10	4	200	0.08	8.8	47
48 Saclay I	70	Radiation research	n(0–2 MeV) Mono-E photons (7–40 MeV)	4 TW (S)	4 K	100	70	2	500	0.1	7	48
49 Saclay II	600	Nuclear physics	Mono-E photons (20–120 MeV)	30 TW (S)	15 K (12)	25	400	20	1000	2.0	200	49
50 St. Bartholomews (London)	15	Radiation physics Radiation biology		2 TW (S)	1 K (20)	750	15	5	100	0.05	6	50
51 San Diego IRT	100	Radiation research Product irradiation	Nanosecond pulses e ⁺ (3–75 MeV) Mono-E photons (3–75 MeV)	4 TW (L)	4 K (40)	700	60	4.5	180	0.08	35	51

See footnotes at end of table.

TABLE V (cont.)

Installation location	Nominal peak energy (MeV)	Machine use	Special capabilities	Number and type of sections ^b	RF source ^c	Typical high-power operation (approx.) ^a						
						Peak current (mA)	Energy (MeV)	T _p (μ s)	Pulse rate (Hz)	Duty factor (%)	Electron power (kW)	
52 S. Barbara EG&G	30	Radiation research	50-ps pulses	3 TW (L)	2 K	500	20	4.5	180	0.081	8.1	52
53 São Paulo USP	50	Nuclear physics		2 TW	2 K	10	50	1	120	0.01	0.05	53
54 Saskatchewan	250	Nuclear physics	n(0–150 MeV)	6 TW (S)	2 K (18)	300	200	1.2	400	0.05	30	54
55 Sendai (Tohoku)	280	Nuclear physics	n(0–20 MeV)	5 TW (S)	5 K (20)	100	280	3.3	300	0.1	20	55
56 Stanford HEPL Mk.III	1200	Particle physics	e ⁺ (up to 1 GeV)	31 TW (S)	31 K (20)	30	1200	1.3	120	0.016	6	56
57 Stanford HEPL SC Mark III	2000	Radiation therapy Particle physics	Superconducting linac Duty factor = 100% Pion therapy	8 SW (L)	8 K (0.015)	0.1	2000	CW	CW	100.	200	57
58 SLAC	22800	Particle physics	e ⁺ (0–15 GeV) Interlaced beams SPEAR storage rings Muon and meson beams Picosecond pulses Mono-E, polarized photons Polarized electrons	960 TW (S)	245 K (20–40)	70	21500	1.6	360	0.06	800	58
59 Tokai JAERI	190	Nuclear physics	n(0–20 MeV)	5 TW (S)	5 K (20)	350	100	2	150	0.03	11	59
60 Tokyo ETL	33	Radiation standards Solid-state physics	180° spectrometer	3 TW (S)	2 K (17)	200	30	4	300	0.12	7	60
61 Tokyo INS	15	Synchrotron injector		1 TW (S)	1 K (6)	200	13	1.2	21.5	0.0026	0.07	61
62 Tokyo NERL	35	Neutron physics Pulse radiolysis	20-ps pulses	2 TW (S)	2 K (6.5)	200	35	4	200	0.08	6	62
63 Toronto	50	Nuclear physics	e ⁺ (10–25 MeV) n(0–20 MeV)	4 TW (S)	2 K (20)	400	35	3.5	240	0.084	12	63
64 Warsaw	13	Pulse radiolysis Radiation research	Nanosecond pulses	2 TW	1 K	800	13	3	300	0.09	9	64

Installation location	Nominal peak energy (MeV)	Machine use	Special capabilities	Number and type of sections ^b	RF source ^c	Typical high-power operation (approx.) ^a						
						Peak current (mA)	Energy (MeV)	T _P (μs)	Pulse rate (Hz)	Duty factor (%)	Electron power (kW)	
65 White Sands WSMR	48	Nuclear effects	Nanosecond pulses	2 TW (S)	2 K (20)	600	48	10	120	0.12	35	65
66 Winfrith AEE	15	Radiation research		1 TW (S)	1 K (10)	200	14	4.5	200	0.09	2.5	66
67 Yale	70	Nuclear physics	n(0–20 MeV)	5 TW (L)		700	40	4.5	250	0.11	30	67
68 Yerevan	480	Nuclear physics	Iterative acceleration e* (0–200 MeV)	13 TW (S)	13 K (20)	1500	120	8	100	0.08	140	68

(a) Parameters simultaneously achievable highest electron beam power under continuous operation.

(b) TW = travelling wave, SW = standing wave, S = S-band, L = L-band operating frequency.

(c) Number of klystrons (K), magnetrons (M) or amplitrans (A). Peak power per unit (MW) given in parentheses.

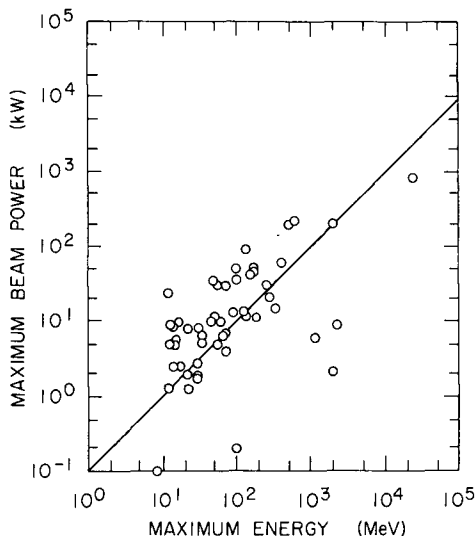


FIG.5. Beam power (kW) of representative electron linacs plotted against beam energy (MeV). The line represents the typical but arbitrary average current of $100 \mu\text{A}$ (corresponding to, e.g., $I_{\text{peak}} = 100 \text{ mA}$, $DF = 0.1\%$).

The parameters which most directly affect radiological safety are:

- (a) Electron beam energy E_0
- (b) Average beam power P
(the product of E_0 and the average beam current I)¹.

The most important derived quantities of radiation protection, such as dose rate or shielding thickness, are generally not simple functions of energy E_0 , and the complete information needed for radiation protection over a broad range of energies requires an extensive set of tables or graphs.

Many quantities are relatively simpler functions of energy when normalized to average beam *power* rather than to average current, and therefore are so presented in this manual. At a given energy E_0 , the dose rate or exposure rate is directly proportional to average beam power P . The required shielding thickness at a given distance, and for a given beam energy E_0 , is approximately proportional to the logarithm of average beam power.

¹ The average power may be obtained from $E_0 I$ because E_0 , when specified in eV, is numerically equal to the potential difference (V) effectively used to accelerate each particle. Potential difference (V) times current (A) is equal to power (W).

The beam is not continually accelerated but comes in short pulses of typically $T_p = 1 - 3 \mu\text{s}$ duration. Where desired, T_p can be made as short as 10 ps. The pulse repetition rates may range between 1 and 1440 Hz, but most are in the range of 60 to 360 Hz. The duty factor DF is the fraction of operating time during which the linac is actually producing radiation, which is generally in the range 10^{-4} to 10^{-3} . It is the product of pulse repetition rate p (in Hz) and pulse length T_p (in seconds):

$$DF = p \cdot T_p \quad (1)$$

This small duty factor is a disadvantage in some research applications but is unimportant in the most common applications such as radiotherapy and industrial radiography. Special large-duty-factor and continuously operating (CW) accelerators have also been developed. Very short pulses (usually 5–10 ns) are used to advantage in pulse radiolysis and neutral-particle spectrometry where precise timing of the reactions studied is crucial.

In radiological protection, the duty factor is important insofar as it may affect radiation measurements; some measurements may be rendered completely useless or even dangerously misleading by duty-factor effects. Any measurement involving the counting of discrete events must be carefully evaluated to ensure that these effects are kept small or properly corrected for. Geiger-Müller and proportional counters are particularly susceptible to saturation, owing to their long dead times. Procedures for correction are explained in Section 5.

REFERENCES TO SECTION 1

- [1] See, for example, papers in: LAPOSTOLLE, P.M., SEPTIER, A.L. (Eds), *Linear Accelerators*, North-Holland Publishing Co., Amsterdam (1970).
- [2] See, for example, papers in: Proc. 1975 Particle Accelerator Conf., Accelerator Engineering and Technology, held in Washington, DC, 12–14 March 1975, IEEE Trans. Nucl. Sci. **NS-22** (1975).
- [3] See, for example, papers in: Proc. IXth Int. Conf. High Energy Accelerators, held at Stanford Linear Accelerator Center, 2–7 May 1974, CONF-740522, UC-28-Accelerators (TID-4500, 60th ed.), National Technical Information Service, Springfield, Virginia (1974).
- [4] KARZMARK, C.J., PERING, N.C., Electron linear accelerators for radiation therapy: history, principles and contemporary developments, *Phys. Med. Biol.* **18** (1973) 321.
- [5] ALMOND, P.R., Some applications of particle accelerators to cancer research and treatment, *Phys. Rep.* **17C** 1 (1975).
- [6] See, for example, papers in: Proc. Conf. Particle Accelerators in Radiation Therapy, held at Los Alamos Scientific Laboratory, 2–5 Oct. 1972, USAEC Rep. LA-5180-C, Technical Information Center, Oak Ridge, TN (1972).
- [7] BLY, J.H., High energy radiography: 1–30 MeV, *Mater. Eval.* (Nov. 1964) 1.
- [8] See, for example, papers in: Large Radiation Sources for Industrial Processing (Proc. Symp. Munich, 1969), IAEA, Vienna (1969).

- [9] See, for example, papers in: Radiation Preservation of Food (Proc. Symp. Bombay, 1972), IAEA, Vienna (1973).
- [10] INTERNATIONAL ATOMIC ENERGY AGENCY, Manual on Radiation Sterilization of Medical and Biological Materials, Technical Reports Series No.149, IAEA, Vienna (1973).
- [11] See, for example, papers in: BERMAN, B.L., Ed., Proc. Int. Conf. Photonuclear Reactions and Applications, Asilomar, California, 26–30 March 1973, Lawrence Livermore Laboratory and USAEC Rep. CONF-730301, Office of Information Services, Oak Ridge, TN (1973).
- [12] FULLER, E.G., “Photonuclear Physics 1973: Where we are and how we got there”, Proc. Int. Conf. Photonuclear Reactions and Applications, Asilomar, California, 26–30 March 1973 (BERMAN, B.L., Ed.), Lawrence Livermore Laboratory and USAEC Rep. CONF-730301, Office of Information Services, Oak Ridge, TN (1973) 1202.
- [13] See, for example, papers in: KIRK, W.T., Ed., Proc. 1975 Int. Symp. Lepton and Photon Interactions at High Energies, held at Stanford University, 21–27 Aug. 1975, Stanford Linear Accelerator Center, Stanford, CA (1975).
- [14] CHODOROW, M., GINZTON, E.L., HANSEN, W.W., KYHL, R.L., NEAL, R.B., PANOFSKY, W.K.H., Stanford high-energy linear accelerator (Mark III), Rev. Sci. Instrum. **27** (1955) 134.
- [15] NEAL, R.B., Gen. Ed., DUPEN, D.W., HOGG, H.A., LOEW, G.A., Eds, The Stanford Two-Mile Accelerator, Benjamin, New York (1968).
- [16] BORCHI, R.P., ELDREDGE, A.L., HELM, R.H., LISIN, A.F., LOEW, G.A., NEAL, R.B., “Design, fabrication, installation, and performance of the accelerator structure”, Ch. 6, Stanford Two-Mile Accelerator (NEAL, R.B., Ed.), Benjamin, New York (1968).
- [17] KNAPP, E.A., KNAPP, B.C., POTTER, J.M., Standing wave high-energy linear accelerator structures, Rev. Sci. Instrum. **39** (1968) 979.
- [18] ONO, K., TAKATA, K., SHIGEMURA, N., A short electron linac of side-coupled structure with low injection voltage, Part. Accel. **5** (1973) 207.

2. RADIATIONS AT ELECTRON LINEAR ACCELERATOR INSTALLATIONS

2.1. Radiations anticipated and their quality factors

2.1.1. Types of radiations and their sources

The useful radiations at electron linear accelerators are generally not the primary electron beams themselves but secondary beams. In most applications the electrons are used to produce bremsstrahlung and the resulting penetrating photon beams are those usefully employed, as in radiography. In high-energy research applications the useful beams may be of other types of secondary particles², such as positrons and mesons.

The important exceptions to this generalization are the widely accepted uses of diffuse electron beams for radiation therapy, and for research in nuclear structure by means of high-energy electron scattering.

The dominant prompt radiation at all energies is composed of photons produced by bremsstrahlung in the materials which absorb the electron beam energy. In fact, other prompt radiations can be neglected completely unless the energy exceeds the threshold for neutron production. Thresholds lie in the range $k_{th} = 6-13$ MeV for most materials.³ Above these energies, giant-resonance neutron production must be considered, both as a form of prompt radiation and as related to induced activity.

At high energies, neutrons are produced in photonuclear reactions via the quasi-deuteron effect or in processes involving pi meson production. Although fewer in number than other types of secondary particles, these neutrons are quite penetrating and in such installations may dominate the shielding requirements.

At yet higher energies, a forward-directed beam of mu mesons (μ^\pm) is produced which requires consideration.

The behaviour of these types of radiation as a function of electron energy E_0 is qualitatively sketched in Fig.6. In this figure, as in several figures and tables in this manual, 'absorbed dose rate' or 'dose-equivalent rate' are represented by quantities which can be represented by $(\text{Gy} \cdot \text{h}^{-1})(\text{kW} \cdot \text{m}^{-2})^{-1}$ ($(\text{rad} \cdot \text{h}^{-1})(\text{kW} \cdot \text{m}^{-2})^{-1}$),

² Since these particles are produced almost entirely by secondary photons, rather than by primary electrons, they could properly be regarded as tertiary. This accounts in part for their lower fluences relative to the electrons and photons. We shall not insist on this distinction but refer to all types of prompt radiation, except the primary beam itself, as 'secondary'.

³ There are some important exceptions. For example, ^2H and ^9Be have anomalously low thresholds of $k_{th} = 2.23$ and 1.67 MeV, respectively. The abundant nuclides ^{12}C (all organic materials) and ^{16}O (air, water) have high thresholds: 18.72 and 15.67 MeV, respectively.

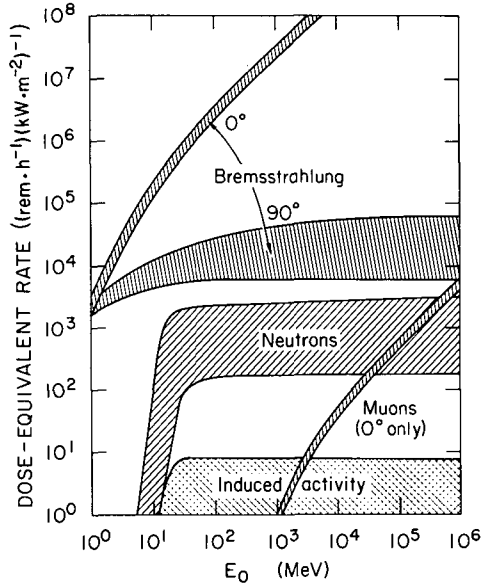


FIG. 6. Dose-equivalent rates per unit primary beam power, produced by various types of 'secondary' radiations from an electron target, as a function of primary beam energy, if no shielding were present (qualitative). The width of the bands suggests the degree of variation found, depending on such factors as target material and thickness.

$(\text{rem} \cdot \text{h}^{-1})(\text{kW} \cdot \text{m}^{-2})^{-1}$, etc. The quantity plotted is then equal to the dose-equivalent rate that would be measured at 1 m from a target onto which a 1-kW electron beam is directed. The unit m^2 is included to suggest an inverse-square dependence on distance from the target for this type of radiation. An inverse-square dependence is strictly true only for unshielded point radiation sources. However, for most purposes in radiological safety, the assumption of inverse-square dependence is accurate enough. Thus, to determine the dose rate ($\text{Gy} \cdot \text{h}^{-1}$ ($\text{rad} \cdot \text{h}^{-1}$)) or dose-equivalent rate ($\text{rem} \cdot \text{h}^{-1}$) at a particular place, one would read the ordinate of the figure, multiply by the true beam power (kW) and divide by the distance squared (m^2) from the target.

In all cases, the primary electron beam can be stopped completely within a short distance, compared with the space needed for the accelerator installation. In the case of medical and radiographic installations the beam is stopped in a target only a few millimetres thick, incorporated in the accelerator unit. In high-energy research installations a specially designed beam dump, which may also serve as a beam monitor (Faraday cup or multi-plate ionization chamber), is usually provided. Even at the highest energies the high-power beam dumps are

of modest dimensions, compared even with the thickness of the required biological shield, and could be a fraction of their actual length (up to about 2 m) if it were not for necessary provision for thermal cooling.

Some fraction of the beam may strike structures such as collimators, beam windows or the accelerator itself. A mis-steered beam may strike a beam pipe or any other piece of equipment. Each object that might be struck by the primary beam must be considered a potential source of secondary radiation. It is good practice to have as few such points as possible in order to simplify the shielding requirements.

In research installations the primary beam is usually directed onto a 'target' before it reaches the beam dump. The target may be of any material and of any thickness, absorbing fractions of beam energy ranging from a small fraction of a per cent to over 99%. The target's efficiency as a source of secondary radiation can be estimated if the target material and thickness, usually expressed in radiation lengths (Appendix B), is known. Because targets can usually be easily changed, it is prudent to assume the worst case, i.e. that the entire beam energy is absorbed at the target location in a material of high Z .

In clinical situations, radiation scattered from the patient must be considered in the room shielding design. In radiographic installations, radiation scattered from the irradiated object must be considered.

Radiation doses due to ingested materials, although possible, are not a significant hazard at electron accelerators. Risk of radiation exposure by inhalation is also quite limited. Table VI summarizes the types of radiations that must be normally considered in the planning of an electron linear accelerator installation.

2.1.2. *Quality factors*

Unless otherwise stated, the quality factors Q given as 'typical' values in Table VII are used in this manual and may be generally assumed in practice.⁴ For more precise dose-equivalent assessment, the quality factors for neutrons

⁴ The quality factor Q is a factor by which the absorbed dose is multiplied to better approximate the relative effect of radiation on human tissue. In the absence of other modifying factors, the product of Q and the absorbed dose D is equal to the dose-equivalent H . The essential difference between Q and the relative biological effectiveness (RBE) is that the RBE is a measurable quantity defined for each quality of radiation for a specific organism or organ and for a well-defined biological endpoint, and usually determined by experiment. Values of Q for radiation protection purposes generally apply to the human body as a whole without referring to any specific biological endpoint. They are *chosen* values which reflect current information on RBE, but averaged for convenient use under a great variety of irradiation conditions. See Refs [3–5] for further discussion.

TABLE VI. RADIATIONS TO BE ANTICIPATED IN PLANNING AN ELECTRON LINEAR ACCELERATOR INSTALLATION

Type of Radiation	Medical Accelerator		Industrial or Research Accelerator	
	Energy (MeV)	Consideration	Energy (MeV)	Consideration
Primary electron beam	Various All	Frequently used for therapy No access for any person, except patient for therapy	All	No access for any person
Photons: (0° bremsstrahlung)	Various All	For therapy Room shielding against useful beam	All	Room shielding
Photons: (wide-angle bremsstrahlung)	All All	Patient protection against unnecessary integral dose Room shielding against "leakage" radiation	All	Room shielding
Photons: (scattered)	All	Room shielding	All	Room shielding
Neutrons: Giant-resonance	> 15 None > 15	Patient protection against unnecessary integral dose Room shielding with concrete walls and ceiling Neutron streaming through labyrinth or other openings	> 15	Room shielding
Induced activity: Components	> 10	Target, jaws, compensating filter	> 10	Targets, collimators, compensating filters, beam dumps
Induced activity: air	None	Negligible	> 15	Present in target room, but usually not limiting
Induced activity: water	None	Negligible	> 20	Above 10 kW, release to air and radiation from cooling-system pipes and vessels
Neutrons: high-energy	None	Negligible	> 150	May determine room shielding
Muons	None	Not produced	> 500	May determine 0° shielding
Charged secondary beams	None	Not produced	> 500	Large research installations only
X-Rays from RF systems	All	Accessible klystrons should be properly shielded	All	Klystrons, RF separators, RF cavities

TABLE VII. QUALITY FACTORS OF ELECTRON LINAC RADIATIONS

Type of Radiation	Quality Factor	
	Typical Value	Comment
Electrons (e^+)	1	LET-dependent ^(a)
Photons (bremsstrahlung and scattered photons)	1	---
Neutrons	10	Energy-dependent ^(b) (Range: $Q \approx 2 - 11$)
Induced Activity:		
Gammas (γ , and β^+ annihilation photons)	1	---
Betas (β^+)	1	---
Muons (μ^+)	1	LET-dependent ^(a)
Mesons (π^+ , K^+)	1	LET-dependent ^(a)
X-rays from RF systems	1	---

(a) LET: Linear energy transfer (see Table VIII).

(b) The effective quality factor depends on incident neutron energy (see Section 2.5).

as a function of energy E_n and for charged particles as a function of LET⁵ or collision stopping power must be considered. The effective quality factor of neutrons is discussed further in Section 2.5. Table VIII and Fig.7 show quality factors for charged particles recommended by the ICRP [1, 2] as functions of LET. Figure 8 shows the quality factors of several types of charged particles as a function of energy, based on their LET. In interpreting these data, one should also consider the change in LET of low-energy particles as they are slowed down or even stopped in tissue. In this case the average quality factor might be significantly higher than the 'entrance' quality factor.

⁵ LET stands for 'linear energy transfer'. It is the component of the stopping power (dE/dX or $dE/d(\rho X)$) due exclusively to collisions with atomic electrons (ionization). It specifically excludes energy loss by radiation (bremsstrahlung) or by interaction with nuclei. In this context, no restriction on the energy of the recoiling electrons is implied. High LET is associated with slowly moving particles and high ionization density. Since the probability of multiple injury to cells is greater, the RBE is generally larger and a higher quality factor Q is assigned. Low LET is associated with fast particles that leave a relatively rarified trail of ions and cause relatively less tissue damage ($Q \approx 1$). See Refs [4-6] for further discussion.

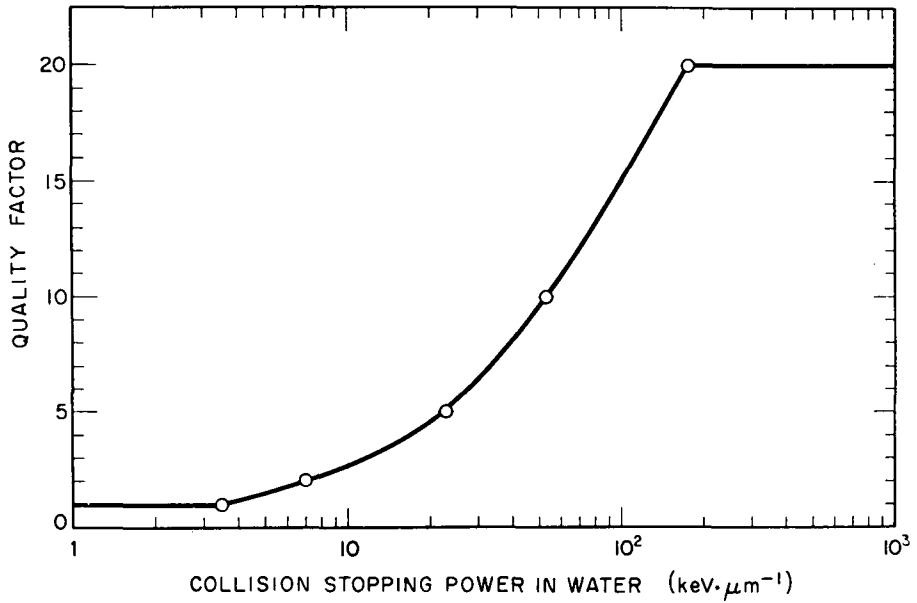


FIG. 7. Quality Factor Q of charged particles as a function of collision stopping power (LET_{∞}) in water, as recommended by ICRP. (Reproduced from ICRP-21 (Ref.[1]), with kind permission of the International Commission on Radiological Protection and Pergamon Press.)

TABLE VIII. QUALITY FACTOR OF CHARGED PARTICLES AS A FUNCTION OF LET (L_{∞})

L_{∞} in water ($keV/\mu m$)	Q
3.5 (and less)	1
7	2
23	5
53	10
175 (and above)	20

(Adapted from ICRP-21 (Ref. [1]), with kind permission of the International Commission on Radiological Protection and Pergamon Press.)

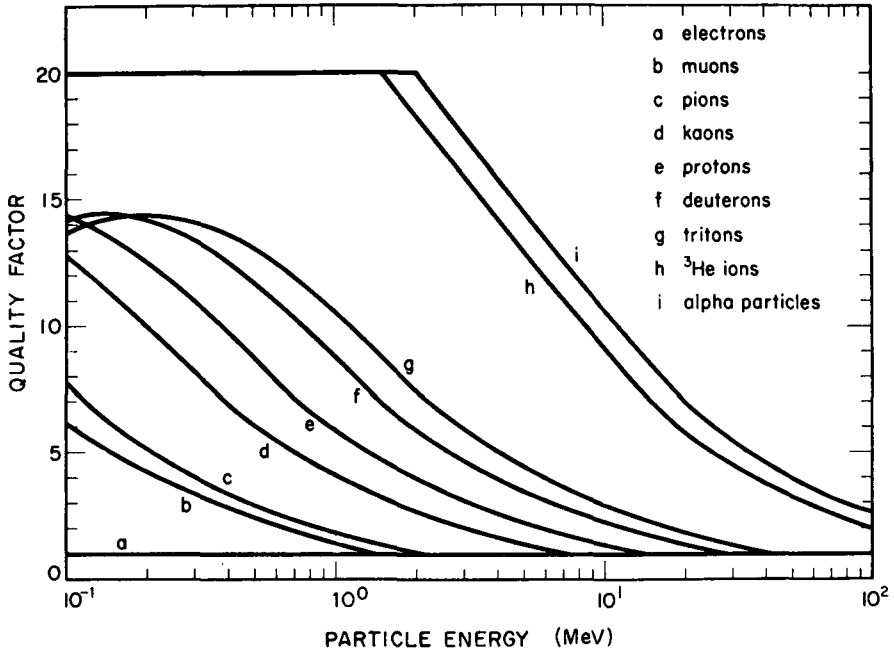


FIG.8. Quality factors of charged particles as a function of energy, as recommended by ICRP. (Reproduced from ICRP-21 (Ref.[1]), with kind permission of the International Commission on Radiological Protection and Pergamon Press.)

REFERENCES TO SECTION 2.1

- [1] INTERNATIONAL COMMISSION ON RADIOLOGICAL PROTECTION, Data for Protection Against Ionizing Radiation from External Sources: Supplement to ICRP Publication 15, Report of ICRP Committee 3, ICRP Publication No.21, Pergamon Press, Oxford (1973).
- [2] INTERNATIONAL COMMISSION ON RADIOLOGICAL PROTECTION, Protection Against Ionizing Radiation from External Sources, Report of ICRP Committee 3, ICRP Publication No.15, Pergamon Press, Oxford (1969).
- [3] INTERNATIONAL COMMISSION ON RADIATION UNITS AND MEASUREMENTS, Radiation Quantities and Units, ICRU Report No.19, Washington, DC (1971).
- [4] INTERNATIONAL COMMISSION ON RADIATION UNITS AND MEASUREMENTS. Dose Equivalent (Supplement to ICRU Report No.19), ICRU Report No.19S, Washington, DC (1973).
- [5] INTERNATIONAL COMMISSION ON RADIATION UNITS AND MEASUREMENTS, Conceptual Basis for the Determination of Dose Equivalent, ICRU Report No.25, Washington, DC (1976).
- [6] INTERNATIONAL COMMISSION ON RADIATION UNITS AND MEASUREMENTS, Linear Energy Transfer, ICRU Report No.16, Washington, DC (1970).

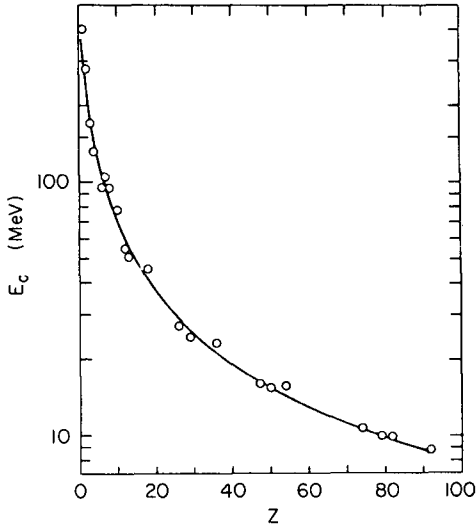


FIG.9. Critical energy E_c as a function of atomic number Z . The curve represents the approximation $E_c(\text{MeV}) = 800/(Z + 1.2)$. (Adapted from Ref.[1], with kind permission of M.J. Berger and S.M. Seltzer, and the National Aeronautics and Space Administration.)

2.2. Photon differential track length and estimation of yields

In the lower energy range in which many electron linacs operate, ionization of atoms of the target material is the dominant mechanism for electron energy deposition in a target. As the energy is increased, the relative importance of energy loss by *radiation* increases and becomes dominant at energies above a value E_c called the 'critical energy'. The value of E_c in MeV is approximately given by

$$E_c = 800/(Z + 1.2) \quad (2)$$

where Z is the atomic number of the target material [1, 2]. For such high- Z materials as tungsten and lead, E_c is about 10 MeV (see Fig.9 and Appendix B, Table B-1).

In the situation where *photons* are incident on matter, the probability of electron-positron *pair production* (threshold energy = $2 \times 0.511 \text{ MeV} \cong 1 \text{ MeV}$) rises with increasing photon energy and becomes important at energies above about 5 MeV in high- Z materials. These two processes together make possible the phenomenon of the electromagnetic shower or cascade [2, 3]. This is a complicated process in which bremsstrahlung (radiation), followed by pair

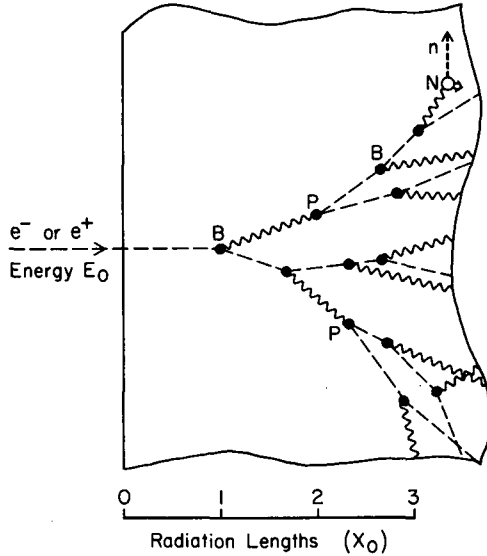


FIG.10. Development of an electromagnetic cascade in a semi-infinite medium at high energy (well above the critical energy). The dashed lines represent electrons or positrons and the wavy lines are photons. An electron or positron of energy E_0 is incident at the left (a cascade can also be initiated by a photon). The spreading in the transverse direction is greatly exaggerated for clarity. Only bremsstrahlung (B) and pair production (P) events are shown, but Compton scattering also plays a role in the dispersal of energy. Energy is deposited in the medium along the dashed lines by ionization. Photonuclear reactions, as illustrated by the (γ, n) reaction at N, may take place along any of the wavy lines if the energy of that photon is high enough. They occur much less frequently than might be inferred from this illustration.

production, followed in turn by more bremsstrahlung, rapidly disperses the incident kinetic energy treelike, among a myriad of photons, electrons and positrons. At very high energies, other mechanisms of energy dispersal, although present, are almost negligible in comparison (see Fig.10).

At very high energies, the distance which an *electron* must travel so that its energy is reduced by an average factor of e^{-1} approaches a constant value called the *radiation length* X_0 (in $\text{g} \cdot \text{cm}^{-2}$), which depends on the atomic number Z and atomic weight A in approximately the following way⁶:

⁶ The factor 716 cm^{-2} is $[4\alpha r_0^2 N_A]^{-1}$, where α is the fine-structure constant ($\sim 1/137$) which determines the strength of the electron-photon interaction, r_0 is the 'classical' electron radius and N_A is Avogadro's number (see Appendix A for values). These same factors appear in the cross-section for pair production. See Ref. [2] for extensive discussion.

$$X_0 \cong 716 A [Z(Z + 1) \ln (183 Z^{1/3})]^{-1} \quad (3)$$

Precise values of radiation lengths for various materials are tabulated in Appendix B.

At very high energies, the distance a *photon* must travel, on the average, before pair production occurs also approaches a constant value which is approximately $9/7 X_0$. This near equality of the two characteristic distances comes about because bremsstrahlung and pair production are merely different manifestations of the same underlying physical process⁶. There is a kind of pleasing symmetry in the electromagnetic cascade phenomenon that also permits some simplifying approximations.

It must be realized that the electrons themselves do not release significant yields of secondary particles directly. The photons have much larger nuclear cross-sections and give rise to the overwhelming majority of secondary particles, especially neutrons, and, at higher energies, mesons as well. To estimate the yields of secondary particles, it is necessary to know not only the photonuclear cross-section $\sigma(k)$ for particle production as a function of photon energy k but also the total length L of material traversed by photons of each energy. (For example, the total photon track length in the portion of the cascade illustrated in Fig. 10 is about $L = 8 X_0$ (all energies combined); for the entire cascade it is much more.) The track-length dependence on photon energy is expressed as the *differential track length* dL/dk , representing the total track length of all photons having energy in the interval $(k, k + dk)$. For electrons of high energy E_0 incident on very *thin* targets, the photon differential track length is approximately

$$dL/dk \cong \frac{1}{2} X^2 X_0^{-1} k^{-1} \quad \begin{cases} X \ll X_0 \\ k < E_0 \\ E_0 > E_c \end{cases} \quad (4)$$

in which L will be in the same units as X_0 and the target thickness X (Appendix B lists X_0 in both $\text{g} \cdot \text{cm}^{-2}$ and cm).

The yield of secondary particles per incident electron $Y(E_0)$ of energy E_0 is obtained by an integration over the photon energy k :

$$Y(E_0) = \frac{N_A \rho}{A} \int_0^{E_0} \sigma(k) \frac{dL(k)}{dk} dk \quad (5)$$

using the production cross-section $\sigma(k)$ (in cm^2) for the secondary particles in question and the differential track length just explained (in $\text{cm} \cdot \text{MeV}^{-1}$). N_A ,

ρ , and A are Avogadro's number, the material density ($\text{g}\cdot\text{cm}^{-3}$), and gram atomic weight, respectively.

A number of approaches to handling the more difficult problem of the photon track-length distribution in *thick* targets are used:

- (a) The simplest method is to use Approximation A of analytical shower theory [2, 3].

This approximation applies to an infinitely thick target, considers only pair production and bremsstrahlung, and assumes constant cross-sections at the high-energy limit for these processes:

$$\frac{dL}{dk} = 0.572 \frac{X_0 E_0}{k^2} \quad (\text{Approximation A}) \quad \begin{cases} X \gg X_0 \\ k < E_0 \\ E_0, E_0 - k > E_c \end{cases} \quad (6)$$

where L is in the same units as X_0 (Appendix B lists X_0 in both $\text{g}\cdot\text{cm}^{-2}$ and cm), and k and E_0 are conveniently expressed in MeV. Approximation A works best at very high energies. Modifications can be made to improve the accuracy of Approximation A, particularly the expression proposed by Clément and Kessler [4, 5]:

$$\frac{dL}{dk} = \frac{0.964 X_0}{E_0} \left[0.686 \left(\frac{k}{E_0} \right)^2 - 0.5 \left(\frac{k}{E_0} \right)^4 - \ln \left(1 - \left(\frac{k}{E_0} \right)^2 \right) \right]^{-1} \quad \begin{cases} X \gg X_0 \\ k < E_0 \end{cases} \quad (7)$$

- (b) The next simplest approach is Approximation B [2, 3], which cannot be written in closed form. This is similar to Approximation A except that electron energy loss by ionization is also considered. Approximation B is more accurate at all energies, but it has the disadvantage that numerical integrations must be made.

(c) A formulation derived by iteration over successive shower generations is discussed by Tsai and Whitis [6]. It is applicable at very high energies and for $k/E_0 \gtrsim 0.5$.

(d) The most satisfactory approach to handling the photon track-length distribution is through Monte-Carlo calculations which can accommodate all of the major physical processes accurately and can be done for any shape or thickness of target, whereas approximations (a) and (b) refer only to infinitely large targets. References to published Monte-Carlo calculations are summarized in Table IX. Those references marked by Note D contain at least some information on the differential photon track-length distribution. Of particular usefulness are

TABLE IX. MONTE-CARLO CALCULATIONS OF THE ELECTROMAGNETIC CASCADE

Authors and year	Ref.	Data ^a	Medium	Initial particle	
				Type ^b	Energy ^a
Varfolomeev and Svetloolobov (1959)	7	D	Emulsion	e	1, 10, 100, 500, 1000, 3000 GeV
Butcher and Messel (1960)	8	D	Air, Al	e, γ	50, 100, 200, 500 MeV; 1, 2, 5, 10, 20, 50 GeV
Messel et al. (1962)	9	D	Pb	e, γ	50, 100, 200, 500, 1000 MeV.
Zerby and Moran (1962)	10	D	Emuls., Pb	e	1 GeV
Zerby and Moran (1962)	11	I	Be, Pb	e	100 MeV
		I	Sn	e	185 MeV
Zerby and Moran (1962)	12	I	Air	e	200 MeV
		I	Al	e, γ	50, 100, 200, 500 MeV
		I	Pb	e	50, 100, 185, 200, 300, 500 MeV; 1 GeV
		I	Pb	γ	50, 100, 200, 300, 500 MeV
		D	Cu	e, γ	50, 100, 200, 400, 700 MeV; 1.4, 3, 5, 10, 20, 45 GeV
Nagel and Schlier (1963)	13	D	Pb	e	200 MeV
Woischnig and Burmeister (1964)	14	I	Pb	e, γ	100, 200, 380 MeV
Crawford and Messel (1965)	15	D	Emulsion, Cu, Pb	e, γ	50, 100, 200, 500 MeV; 1, 2 GeV
Nagel (1965)	16	D	Pb	e	100, 200, 400, 1000 MeV
Tamura (1965)	17	D	Al	e, γ	204 MeV
Völkel (1965)	18	D	Pb	e, γ	6 GeV
Alsmiller and Moran (1966)	19	Y	Cu	e	34 MeV
		DY	Ta	e	30, 100, 150, 200 MeV
		Y	Pb	e	34, 100 MeV
Varfolomeev and Drabkin (1966)	20	D	Pb	e	6 GeV
Alsmiller and Moran (1967)	21	E	H ₂ O	e	100, 200, 500 MeV; 1, 5.2, 10, 20 GeV
		E	H ₂ O	γ	10, 20, 50, 100, 200, 500 MeV; 1, 5.2, 10, 20 GeV
Burfeindt (1967)	22	D	Pb	e	3 GeV

TABLE IX. (cont.)

Authors and year	Ref.	Data ^a	Medium	Initial particle	
				Type ^b	Energy ^a
Völkel (1967)	23	D	Cu	γ	<i>1, 3, 6 GeV</i>
		D	Cu	B	<i>6 GeV</i>
Alsmiller and Moran (1968)	24	D	Pb	γ	<i>15, 25, 35, 45, 60, 75, 100 MeV</i>
Alsmiller and Moran (1969)	25	E	H ₂ O, Al	e	1 GeV
Cioni and Treves (1969)	26	I	Pb-glass	e	50, 150, 300, 500 MeV; 1 GeV
Gabriel and Alsmiller (1969)	27	DY	Cu	e	<i>50, 100, 200, 300, 400 MeV</i>
Alsmiller and Moran (1970)	28	E	H ₂ O, Al	e	1 GeV
Alsmiller and Moran (1970)	29	E	Be, Al	γ	45 GeV
Beck (1970)	30	E	H ₂ O	e, γ	100, 200, 500 MeV; 1, 5.2, 10, 20 GeV
Beck (1970)	31	E	H ₂ O, Al	e	1 GeV
Berger and Seltzer (1970)	32	DY	Ta, W	e	<i>2, 5, 10, 15, 20, 30, 60 MeV</i>
Messel and Crawford (1970)	33	D	Air	e, γ	<i>500 MeV; 1, 10, 50 GeV</i>
		D	Cu	e, γ	<i>50, 100, 200, 500 MeV; 1, 2 GeV</i>
		D	Pb	e, γ	<i>50, 100, 200, 500 MeV; 1, 2, 10 GeV</i>
Beck (1971)	34	E	Pb + H ₂ O ^c	e	1 GeV
		I	Air + Al	e	200, 500 MeV; 1 GeV
		I	Air + Fe	e	200, 500 MeV; 1 GeV
Alsmiller et al. (1974)	35	E	H ₂ O	e	50, 100, 150, 200 MeV
Ford and Nelson (1978)	36	D	Various	e, γ	Various

^a Type of cascade data given:

E: Distribution of energy deposition (absorbed dose) in medium only.

I: Data on electron and/or photon track length, but integrated over energy.

D: Data on electron and/or photon track length, differential in energy or in such a form that some information on differential track length can be derived. Italics indicate those energy values for which such data are given.

Y: Yield of some type of secondary particle is given, in addition to cascade data.

^b Particle type: e: electron (or positron); γ : monoenergetic photon; B: Bremsstrahlung beam of indicated end-point energy.

^c Two-material medium.

the studies of Zerby and Moran [12] and Alsmiller and Moran [19] because extensive tables of photon track-length data are given in a form that can be used directly in Eq.(5). Track-length data for one material can be scaled to another by the ratio of radiation lengths for the two materials. Table XIV (Section 2.5) contains a summary of references to Monte-Carlo calculations of neutron production based on Eq.(5).

In estimating yields of secondary particles for radiation protection work, it is conservative practice to assume the maximum possible yield, i.e. that the production target is infinitely thick but reabsorption of secondary particles is negligible. Where Monte-Carlo yield calculations for infinitely thick targets are available, they are preferred. However, the Approximations A and B are very useful for rapid calculation, and frequent use is made of them. Their range of validity can be stretched to lower energy by correction factors which account for the electron radiative cross-section being less than at the high-energy limit and the photon mean free path being longer than its high-energy limit [37].

Because the track-length dependence on photon energy is approximately as k^{-2} in Eq.(6), the integral in Eq.(5) is approximately proportional to

$$\sigma_{-2}(E_0) \equiv \int_0^{E_0} \sigma(k)k^{-2} dk \quad (8)$$

Because of the role this integral plays in yield calculations, values of Eq.(8) integrated over the region of largest $\sigma(k)$ are useful as indices of activation and secondary yield potential in thick targets (see, for example, Section 2.5.2).

There are a great number of experimental studies of the electromagnetic cascade. This work is essential to a firm theoretical understanding of the phenomenon, but does not generally yield direct information on the photon differential track-length distributions central to this discussion. References [38–42] describe recent experimental results and give extensive references to earlier work.

REFERENCES TO SECTION 2.2

- [1] BERGER, M.J., SELTZER, S.M., Tables of Energy Losses and Ranges of Electrons and Positrons, Paper 10, NAS-NRC Publication 1133, National Academy of Sciences, National Research Council, Washington, DC (1964); and National Aeronautics and Space Administration, Washington, DC, Rep. NASA-SP-3012 (1964).
- [2] ROSSI, B., High-Energy Particles, Ch.5, Prentice-Hall, Englewood Cliffs, NJ (1952).
- [3] ROSSI, B., GREISEN, K., Cosmic-ray theory, Rev. Mod. Phys. **13** (1941) 240.
- [4] CLEMENT, G., KESSLER, P., Electroproduction de muons de très haute énergie, Nuovo Cim. **37** (1965) 876.

- [5] CLEMENT, G., Parcours différentiel des photons produits par un électron de très haute énergie dans une cible épaisse, C.R. Hebd. Acad. Sci. 257 (1963) 2971.
- [6] TSAI, Y.-A., WHITIS, V., Thick-target bremsstrahlung and target considerations for secondary-particle production of electrons, Phys. Rev. 149 (1966) 1248.
- [7] VARFOLOMEEV, A.A., SVETLOLOBOV, I.A., Monte Carlo calculations of electromagnetic cascades with account of the influence of the medium on bremsstrahlung, Zh. Eksp. Teor. Fiz. 36 6 (1959) 1771; Transl.: Sov.Phys.—JETP 36 (1959) 1263.
- [8] BUTCHER, J.C., MESSEL, H., Electron number distribution in electron-photon showers in air and aluminum absorbers, Nucl. Phys. 20 1 (1960) 15.
- [9] CRAWFORD, D.F., MESSEL, H., Energy distribution in low-energy electron-photon showers in lead absorbers, Phys. Rev. 128 5 (1962) 2352.
- [10] MESSEL, H., SMIRNOV, A.D., VARFOLOMEEV, A.A., CRAWFORD, D.F., BUTCHER, J.C., Radial and angular distributions of electrons in electron-photon showers in lead and in emulsion absorbers, Nucl. Phys. 39 1 (1962) 1.
- [11] ZERBY, C.D., MORAN, H.S., A Monte-Carlo Calculation of the Three-Dimensional Development of High-Energy Electron-Photon Cascade Showers, Oak Ridge National Laboratory, Rep. ORNL-TM-422 (1962).
- [12] ZERBY, C.D., MORAN, H.S., Studies of the Longitudinal Development of High-Energy Electron-Photon Cascade Showers in Copper, Oak Ridge National Laboratory, Rep. ORNL-3329 (1962); J. Appl. Phys. 34 8 (1963) 2445. (The ORNL report contains extensive tables not included in the published version.)
- [13] NAGEL, H.H., SCHLIER, Ch., Berechnung von Elektron-Photon-Kaskaden in Blei für eine Primärenergie von 200 MeV, Z. Phys. 174 (1963) 464.
- [14] WOISCHNIG, W., BURMEISTER, H., Berechnung von Elektronen-Photonen-Kaskaden nach der Monte-Carlo-Methode, Z. Phys. 177 (1964) 151.
- [15] CRAWFORD, D.F., MESSEL, H., The electron-photon cascade in lead, emulsion and copper absorbers, Nucl. Phys. 61 (1965) 145.
- [16] NAGEL, H.-H., Elektron-Photon-Kaskaden in Blei, Z. Phys. 186 (1965) 319. (Copies of complete shower tables may be obtained from: Bibliothek des Physikalischen Institutes, 53 Bonn, Nussallee 12, Federal Republic of Germany.)
- [17] TAMURA, M., A study of electron-photon showers by the Monte Carlo method, Prog. Theor. Phys. 34 (1965) 912.
- [18] VÖLKEL, U., Elektron-Photon-Kaskaden in Blei für Primärteilchen der Energie 6 GeV, Deutsches Elektronen-Synchrotron, Hamburg, Rep. DESY-65/6 (1965).
- [19] ALSMILLER, R.G., Jr., MORAN, H.S., Electron-Photon Cascade Calculations and Neutron Yields from Electrons in Thick Targets, Oak Ridge National Laboratory, Rep. ORNL-TM-1502 (1966); Nucl. Instrum. Meth. 48 (1967) 109. (The ORNL report contains extensive tables not included in the published version.)
- [20] VARFOLOMEEV, A.A., DRABKIN, L.B., Calculations of Electromagnetic Showers in Lead with an Initial Energy of 6 GeV, Institute of Atomic Energy, Rep. IAE-1201 (1966); Transl.: Oak Ridge National Laboratory, Rep. ORNL-tr-1923 (1968).
- [21] ALSMILLER, R.G., Jr., MORAN, H.S., Dose Rate from High-Energy Electrons and Photons, Oak Ridge National Laboratory, Rep. ORNL-TM-2026 (1967); Nucl. Instrum. Meth. 58 (1968) 343.
- [22] BURFEINDT, H., Monte-Carlo-Rechnung für 3 GeV-Schauer in Blei, Deutsches Elektronen-Synchrotron, Hamburg, Rep. DESY-67/24 (1967).
- [23] VÖLKEL, U., A Monte Carlo Calculation of Cascade Showers in Copper Due to Primary Photons of 1 GeV, 3 GeV, and 6 GeV, and to a 6-GeV Bremsstrahlung Spectrum, Deutsches Elektronen-Synchrotron, Hamburg, Rep. DESY-67/16 (1967).

- [24] ALSMILLER, R.G., Jr., MORAN, H.S., The Electron-Photon Cascade Induced in Lead by Photons in the Energy Range 15 to 100 MeV, Oak Ridge National Laboratory, Rep. ORNL-4192, UC-34-Physics (1968).
- [25] ALSMILLER, R.G., Jr., MORAN, H.S., Calculation of the Energy Deposited in Thick Targets by High-Energy (1 GeV) Electron-Photon Cascades and Comparison with Experiment, Oak Ridge National Laboratory, Rep. ORNL-TM-2559 (1969); Nucl. Sci. Eng. **38** (1969) 131. (This paper is superseded by Ref.[28].)
- [26] CIONI, G., TREVES, A., A simplified method of simulating electromagnetic showers, Nuovo Cim. **62 B** (1969) 371.
- [27] GABRIEL, T.A., ALSMILLER, R.G., Jr., Photonucleon and Photopion Production from High-Energy (50–400 MeV) Electrons in Thick Copper Targets, Oak Ridge National Laboratory, Rep. ORNL-4443, UC-34-Physics (1969).
- [28] ALSMILLER, R.G., Jr., MORAN, H.S., Calculation of the Energy Deposited in Thick Targets by High-Energy (1 GeV) Electron-Photon Cascades and Comparison with Experiment II, Oak Ridge National Laboratory, Rep. ORNL-TM-2843 (1970); Nucl. Sci. Eng. **40** (1970) 483.
- [29] ALSMILLER, R.G., Jr., MORAN, H.S., Energy Deposition by 45-GeV Photons in Be and Al, Oak Ridge National Laboratory, Rep. ORNL-4631, UC-34-Physics (1970).
- [30] BECK, H.L., A new calculation of dose rates from high energy electrons and photons incident on 30 cm water slabs, Nucl. Instrum. Meth. **78** (1970) 333.
- [31] BECK, H.L., The influence of the density effect on electron-induced cascade showers in water and aluminum, Nucl. Sci. Eng. **39** (1970) 120.
- [32] BERGER, M.J., SELTZER, S.M., Bremsstrahlung and photoneutrons from thick tungsten and tantalum targets, Phys. Rev. **C2 2** (1970) 621.
- [33] MESSEL, H., CRAWFORD, D.F., Electron-Photon Shower Distribution Function, Tables for Lead, Copper and Air Absorbers, Pergamon Press, Oxford (1970).
- [34] BECK, H.L., Monte-Carlo calculations of electromagnetic shower transition effects, Nucl. Instrum. Meth. **91** (1971) 525.
- [35] ALSMILLER, R.G., Jr., BARISH, J., DODGE, S.R., Energy Deposition by High-Energy Electrons (50 to 200 MeV) in Water, Oak Ridge National Laboratory, Rep. ORNL-TM-4419 (1974).
- [36] FORD, R.L., NELSON, W.R., EGS Code System: Computer Programs for the Monte-Carlo Simulation of Electromagnetic Cascade Showers, Stanford Linear Accelerator Center, Rep. SLAC-210 (1978).
- [37] SWANSON, W.P., Calculation of neutron yields released by electrons incident on selected materials, Health Phys. **35** (1978) 353; see also Stanford Linear Accelerator Center, Rep. SLAC-PUB-2211 (1978).
- [38] YUDA, T., MASAIKE, A., KUSUMEGI, A., MURATA, Y., OHTA, I., NISHIMURA, J., Electron-induced cascade showers in lead, copper and aluminum, Nuovo Cim. **65A 1** (1970) 205.
- [39] BATHOW, G., FREYTAG, E., KÖBBERLING, M., TESCH, K., KAJIKAWA, R., Measurements of the longitudinal and lateral development of electromagnetic cascades in lead, copper and aluminum at 6 GeV, Nucl. Phys. **B20** (1970) 592.
- [40] JAKEWAYS, R., CALDER, I.R., An experimental study of the longitudinal development of electron initiated cascades in lead in the energy range 0.5–4.0 GeV, Nucl. Instrum. Meth. **84** (1970) 79.
- [41] BROCKMANN, R., KEIL, P., KNOP, G., WUCHERER, P., Elektron-Photon-Kaskaden in Blei bei Primärenergien von 100, 200 und 400 MeV, Z. Phys. **243** (1971) 464.
- [42] MÜLLER, D., Electron showers of high primary energy in lead, Phys. Rev. **5** (1972) 2677.

2.3. Electron beams

Except for radiation therapy, there is no installation in which access of personnel to a *direct* electron beam from an accelerator can be safely allowed. Inadvertent or deliberate access to a controlled area is prevented by physical barriers, interlocks and warning devices described in Section 6.4. Even when beams are adjusted to negligible levels and limited by electronic devices, sufficient assurance cannot be provided that the mode of operation may not suddenly change, permitting dangerous beam levels in the primary beam line.

The only exception to this is the use of diffuse electron radiation in cancer therapy. Under these conditions, especially designed monitoring and control systems are employed to precisely control the administered dose (Section 6.5).

The fluence of electrons, together with the stopping power of the medium (tissue), determines the absorbed dose. The absorbed dose D in Gy (rad) of a monochromatic beam is approximated by

$$\begin{aligned} D \text{ (Gy)} &= 1.602 \times 10^{-10} \Phi \cdot (S/\rho)_{\text{col}, \infty} \text{ (approx.)} \\ D \text{ (rad)} &= 1.602 \times 10^{-8} \Phi \cdot (S/\rho)_{\text{col}, \infty} \text{ (approx.)} \end{aligned} \tag{9}$$

where Φ is the fluence ($\text{electrons} \cdot \text{cm}^{-2}$) and $(S/\rho)_{\text{col}, \infty}$ is the unrestricted collision stopping power in $\text{MeV} \cdot \text{cm}^2 \cdot \text{g}^{-1}$. The coefficient is merely a conversion from $\text{MeV} \cdot \text{g}^{-1}$ to Gy (rad). Values of $(S/\rho)_{\text{col}}$ from the work of Berger and Seltzer [1, 2] are plotted for water in Fig.11, and tabulated for selected materials in Appendix B. (See also Pages et al., Ref. [3].)

The more precise formulation of absorbed dose is given in ICRU Report No. 21 [4], which includes an integration over the electron energy spectrum and uses the *restricted* stopping power in which a cutoff Δ in energy transfer per collision is imposed.

The actual absorbed dose is difficult to calculate precisely from the stopping power curves, because buildup, scattering and spectral changes all modify dose distributions. However, the extent of the minimum hazard of an accelerated electron beam can be indicated. The minimum stopping power of $1.829 \text{ MeV} \cdot \text{cm}^2 \cdot \text{g}^{-1}$ (at 1.5 MeV) gives an estimate of the minimum dose rate to tissue due to an electron flux density φ in $\text{electrons} \cdot \text{cm}^{-2} \cdot \text{s}^{-1}$:

$$\begin{aligned} \dot{D} \text{ (Gy} \cdot \text{h}^{-1}) &= 1.055 \times 10^{-6} \varphi \text{ (minimum)} \\ \dot{D} \text{ (rad} \cdot \text{h}^{-1}) &= 1.055 \times 10^{-4} \varphi \text{ (minimum)} \end{aligned} \tag{10}$$

The effect of buildup on the dose distribution is shown in Fig.12. These curves should be taken as illustrative only; the shape of the actual dose distribution depends on beam size and other factors that may vary considerably. The maximum

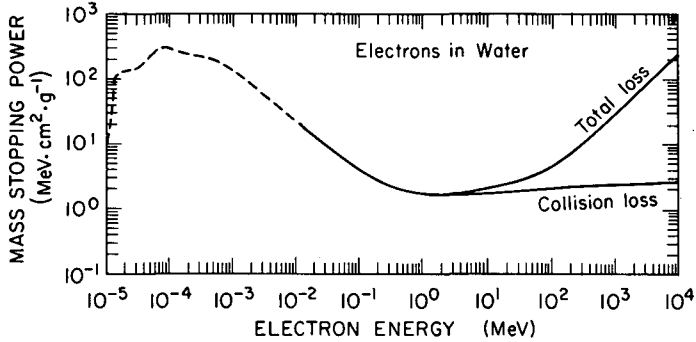


FIG.11. Stopping power of electrons in water as a function of electron energy E (MeV). The continuation labelled 'collision loss' is the energy loss per pathlength due to ionization (collision with atomic electrons) and may be used in the formulae of this section for dose estimation. The 'total loss' includes radiative losses as well. Since soft tissue is so similar to water in the transport of electrons and photons, these data may be used directly for radiation protection purposes.

(Reproduced from Ref.[8], with kind permission of H.W. Patterson and R.H. Thomas, the Lawrence Berkeley Laboratory and Academic Press.)

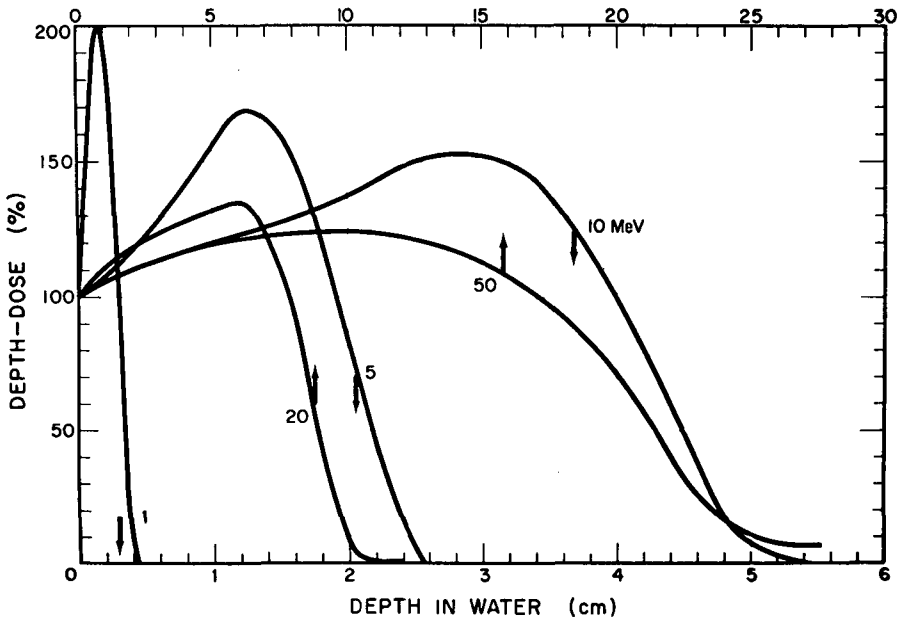


FIG.12. Calculated percentage depth-dose distributions in water for broad beams of normally incident monoenergetic electrons.

(Reproduced from ICRP-21 [5], with kind permission of the International Commission on Radiological Protection and Pergamon Press.)

TABLE X. CONVERSION FACTORS FOR ELECTRONS RECOMMENDED IN ICRP PUBLICATION 21

Electron energy (MeV)	Conversion factor ^a (electrons·cm ⁻² ·s ⁻¹ per mrem·h ⁻¹)
1 × 10 ⁻¹	1.6
2 × 10 ⁻¹	2.6
5 × 10 ⁻¹	3.9
1 × 10 ⁰	4.8
2 × 10 ⁰	5.5
5 × 10 ⁰	6.2
1 × 10 ¹	6.7
2 × 10 ¹	7.2
5 × 10 ¹	7.2
1 × 10 ²	6.7
2 × 10 ²	5.4
5 × 10 ²	3.6
1 × 10 ³	3.0
2 × 10 ³	2.5
5 × 10 ³	2.1
1 × 10 ⁴	1.8
2 × 10 ⁴	1.5

^a Calculated at maximum of depth-dose equivalent curve. (Adapted from ICRP-21 [5], with kind permission of the International Commission on Radiological Protection and Pergamon Press.)

of buildup over the range shown is not very energy dependent, but the initial rise may vary owing to 'pre-buildup' in air, beam windows, collimator edges, etc. Bremsstrahlung contamination will contribute to a slowly decreasing background at greater depths.

Fluence-to-dose-equivalent rate conversion factors recommended by the ICRP [5] are given in Table X and plotted in Fig.13. They refer to irradiation by a unidirectional broad beam of monoenergetic electrons at normal incidence and are evaluated at the maxima of the depth-dose equivalent curves. The quality factor for electrons is assumed to be $Q = 1$.

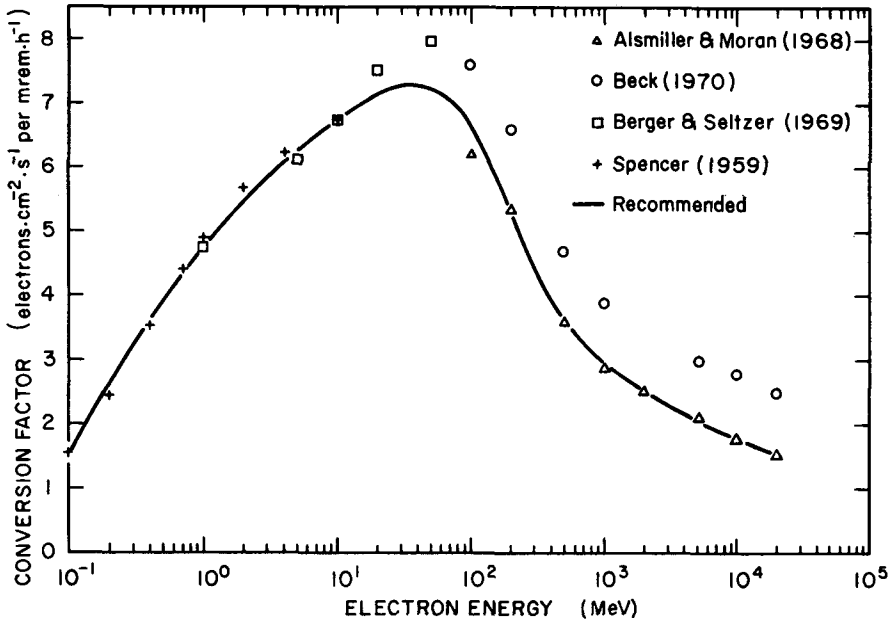


FIG.13. Conversion factor as a function of incident energy E_0 for a unidirectional broad beam of monoenergetic electrons at normal incidence. The curve indicates values recommended by ICRP. (See ICRP-21 [5] for references to original work. Reproduced with kind permission of the International Commission on Radiological Protection and Pergamon Press.)

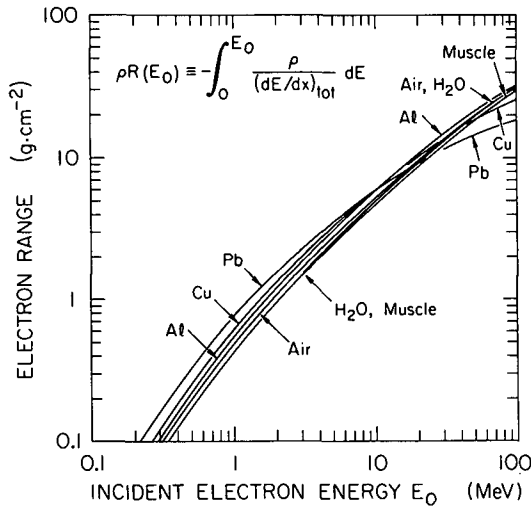


FIG.14. Electron range as given by the continuous-slowing-down approximation (CSDA) in several materials, as a function of incident electron energy. See inset for definition. The data are from Berger and Seltzer [1]. The crossover of the range of heavier elements (Cu, Pb) is due to the relatively greater importance of bremsstrahlung as Z and E_0 increase.

A conservative rule of thumb, useful in the range $E_0 = 1 - 100 \text{ MeV}$, is

$$\dot{H} = 1.6 \times 10^{-4} \varphi \quad (\text{Rule of Thumb: } E_0 = 1 - 100 \text{ MeV}) \quad (11)$$

where \dot{H} is in $\text{rem} \cdot \text{h}^{-1}$ and φ in $\text{electrons} \cdot \text{cm}^{-2} \cdot \text{s}^{-1}$.

Precise dosimetry predictions are somewhat futile because the movements of persons accidentally exposed to narrow beams are not predictable, and the spatial distribution of the beam in transverse planes is usually poorly known and is changing with location. An important point is that these formulae, together with data on average beam currents ($\sim 100 \mu\text{A}$ from Table V) and reasonable beam size of order of magnitude 0.1 cm diameter, clearly show the hazard of direct exposure to electron beams: dose-equivalent rates of $10^{13} \text{ rem} \cdot \text{h}^{-1}$ are easily possible!

If more precise dose determinations are required, such as in a posteriori accidental dose evaluations [6], in-phantom measurements are recommended. The subject of electron-beam dosimetry has been highly developed and more precise data and experimental methods are available. The ICRU Report No.21 is an excellent source of such information [4]. General discussions of radiological safety aspects of electron beams have been published, for example, by Laughlin [7], Patterson and Thomas [8], and by several authors in the Montreux Symposium Proceedings [9].

The range of electrons in materials is difficult to specify in a completely satisfactory way, since there are wide variations in the behaviour of individual particles owing to fluctuations in bremsstrahlung energy loss and direction changes due to Coulomb scattering. The continuous-slowning-down-approximation (CSDA) range is the pathlength which an electron would travel if its rate of energy loss along the entire path were always equal to the mean rate for its energy (Fig.14). Actually, the arithmetic average pathlength will be somewhat greater than this because of the skewness of the energy fluctuations, but the projected range (in the direction of the incident electron) will be shortened because of direction changes induced by scattering. Comprehensive calculations of CSDA ranges have been published by Berger and Seltzer [1, 2] and by Pages et al. [3] for a variety of materials.

A very useful empirical range, called the 'practical range' R_p , can be determined by extrapolation of depth-dose distributions. This is illustrated by the inset of Fig. 15 where R_p , and another empirical quantity, the 'maximum range' R_M , are defined. Where appropriate at higher energies, the extrapolation is made to the bremsstrahlung background, instead of to zero dose.

Both R_p and R_M are almost linear in electron kinetic energy (Fig.15) and are relatively insensitive to beam geometry. Over an energy range extending to about 30 MeV, the Katz-Penfold formula [10] describes the practical-range-energy relationship to an accuracy of about 1.5% for *aluminium*:

$$\rho R_p = 0.530 E_0 - 0.106 \quad (\text{aluminium}) \quad (12)$$

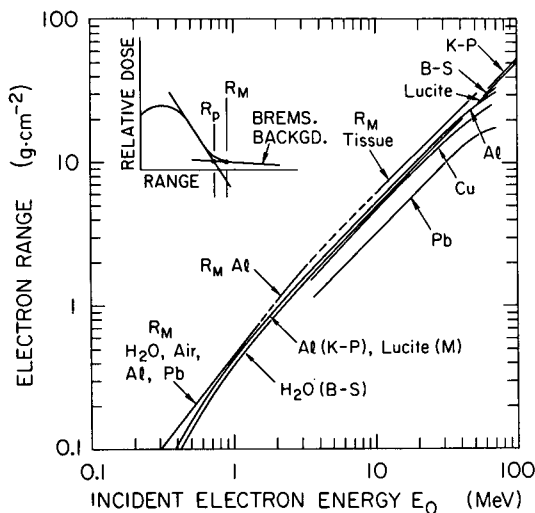


FIG. 15. Electron ranges in several materials, as a function of incident electron energy E_0 . See inset for definitions of maximum range R_M and practical range R_P . The upper curve (broken) shows R_M ; dashed portions separate different sets of measurements (see text). The remaining curves all show R_P . Data for lucite, Al, Cu and Pb are from Harder and Schultz [14]. The other curves shown represent the formula of Katz and Penfold (K-P) [10] for Al which coincides with that of Marcus (M) [12] for low-Z materials, and the formula of Berger and Seltzer (B-S) [11] for H_2O .

where E_0 is in MeV and ρR_P in $g \cdot cm^{-2}$. A relationship in the same units for water has been recommended by Berger and Seltzer [11]:

$$\rho R_P = 0.499 E_0 - 0.111 \quad (\text{water}) \quad (13)$$

This type of relationship has been extended to other materials by the Markus formula [12], which is accurate to about 2% over this energy range for low-Z materials (e.g. water, tissue, plastics) [13]. Using the same units, Markus [12] gives

$$\rho R_P = \left(\frac{A}{Z}\right) (0.285 E_0 - 0.137) \quad (\text{low-Z}) \quad (14)$$

where Z is the atomic number and A the atomic weight of the material in question.⁷

⁷ For mixtures and compounds, Eq.(B.6) (Appendix B) would be used to determine $(Z/A)_{\text{eff}}$ for use in Eq.(14). For Eq.(15), Z_{eff} would be given by $Z_{\text{eff}} = (\sum \rho_i Z_i^2) / (\sum \rho_i Z_i)$, where ρ_i is the fraction (by weight) of the element of atomic number Z_i .

Deviations from these convenient formulae amount to $-(5 \text{ to } 8)\%$ at 50 MeV and become progressively greater at higher energy. Above 30 MeV, the accuracy of Eqs (12) and (14) can be improved by additional factors [14]: $[1 - 0.0018 (E_0 - 30)^{1.27}]$ for aluminium and $[1 - 0.0010 (E_0 - 30)^{1.27}]$ for low-Z materials (E_0 is in MeV).

Curves for R_M (Fig.15) are obtained from measurements of Loevinger et al. [15] and Trump et al. [16, 17]. Loevinger et al. have found that R_M and R_p differ by a constant amount, $\rho(R_M - R_p) = 1.6 \text{ g} \cdot \text{cm}^{-2}$, for electrons in the energy range $E_0 = 10 - 40 \text{ MeV}$ incident on water. A relationship between the R_p and the CSDA range has been derived by Harder and Poschet [18]:

$$R_p = R_{\text{CSDA}} [0.51 (Zm_e/E_0)^{1/2} + 0.69]^{-1} \quad (15)$$

where Z is the atomic number⁷, and m_e is the electron mass, 0.511 MeV.

REFERENCES TO SECTION 2.3

- [1] BERGER, M.J., SELTZER, S.M., Tables of Energy Losses and Ranges of Electrons and Positrons, Paper 10, NAS-NRC Publication 1133, National Academy of Sciences, National Research Council, Washington, DC (1964); and National Aeronautics and Space Administration, Washington, DC, Rep. NASA-SP-3012 (1964).
- [2] BERGER, M.J., SELTZER, S.M., Additional Stopping Power and Range Tables for Protons, Mesons, and Electrons, National Aeronautics and Space Administration, Scientific and Technical Information Division, Washington, DC, Rep. NASA SP-3036 (1966).
- [3] PAGES, L., BERTEL, E., JOFFRE, H., SKLAVENITIS, L., Energy loss, range, and bremsstrahlung yield for 10-keV to 100-MeV electrons in various elements and chemical compounds, *At. Data* 4 1 (1972) 1-127. (This tabulation has particularly extensive tabulations for chemical compounds.)
- [4] INTERNATIONAL COMMISSION ON RADIATION UNITS AND MEASUREMENTS, Radiation Dosimetry: Electrons with Initial Energies Between 1 and 50 MeV, ICRU Report No.21, Washington, DC (1972). (The lower limit of integration in Eq.(2.14) should be zero instead of Δ .)
- [5] INTERNATIONAL COMMISSION ON RADIOLOGICAL PROTECTION, Data for Protection against Ionizing Radiation from External Sources: Supplement to ICRP Publication No. 15, ICRP Publication No.21, Pergamon Press, Oxford (1971).
- [6] LANZL, L.H., TARLOV, A.R., "High-dose human exposure from a 10-MeV linear accelerator", paper presented at the First Symposium on Accelerator Radiation Dosimetry and Experience, held at Brookhaven National Laboratory, 3-5 Nov. 1965, USAEC, Tech. Inf., Washington, DC, Rep. CONF-651109 (1965) 574.
- [7] LAUGHLIN, J.S., "Electron beams", in Radiation Dosimetry, 2nd ed. (ATTIX, F.H., TOCHILIN, E., Eds), Vol. III, Ch.19, Academic Press, New York (1969).
- [8] PATTERSON, H.W., THOMAS, R.H., Accelerator Health Physics, Ch.2, Academic Press, New York (1973).
- [9] ZUPPINGER, A., PORETTI, G., Eds, High-Energy Electrons (Proc. Symp. Montreux, 1964), Springer-Verlag, Berlin (1965).

- [10] KATZ, L., PENFOLD, A.S., Range-energy relations for electrons and the determination of beta-ray endpoint energies by absorption, *Rev. Mod. Phys.* **24** (1952) 28.
- [11] BERGER, M.J., SELTZER, S.M., Penetration of High-Energy Electrons Beams into Water Phantoms, National Bureau of Standards, Washington, DC, unpublished report (1975).
- [12] MARKUS, B., Energiebestimmung schneller Elektronen aus Tiefendosiskurven, *Strahlentherapie* **116** (1961) 280.
- [13] NÜSSE, M., Factors affecting the energy-range relation of fast electrons in aluminium, *Phys. Med. Biol.* **14** 2 (1969) 315.
- [14] HARDER, D., SCHULZ, H.J., "Some new physical data for electron beam dosimetry", *Proc. 2nd Congr. European Association of Radiology, Amsterdam, 14–18 June 1971*, Excerpta Medica, International Congress Series No.249 (ISBN 90 219 0155 2), Amsterdam (1972) 475.
- [15] LOEVINGER, R., KARZMARK, C.J., WEISSBLUTH, M., Radiation therapy with high-energy electrons, Part I: Physical considerations, 10 to 60 MeV, *Radiology* **77** (1961) 906.
- [16] TRUMP, J.G., VAN DE GRAAFF, R.M., CLOUD, R.W., Cathode rays for radiation therapy, *Am. J. Roentgenol., Radium Ther.* **49** (1940) 728.
- [17] TRUMP, J.G., WRIGHT, K.A., CLARKE, A.M., Distribution of ionization in materials irradiated by two- and three-million-volts cathode rays, *J. Appl. Phys.* **21** (1950) 345.
- [18] HARDER, D., POSCHET, G., Transmission und Reichweite schneller Elektronen im Energiebereich 4 bis 30 MeV, *Phys. Lett.* **24B** (1967) 519.

2.4. Photons

2.4.1. External bremsstrahlung

The type of *secondary* radiation of the greatest potential hazard at all energies consists of the photons produced by bremsstrahlung.⁸ Photons are radiated from any object struck by the primary electrons (such as a target designed for that purpose) and form an external secondary beam.

At low energies, the electrons incident on a target lose their energy primarily by ionizing the medium in which they are stopped. Most of this energy reappears in the form of heat and only a small fraction is radiated as external bremsstrahlung.

⁸ The term 'X-ray' is commonly used to denote this kind of radiation in connection with lower-energy equipment. 'Bremsstrahlung' is more descriptive and more often used in relation to higher-energy accelerators to denote both the radiation itself and the underlying physical process by which it occurs. Bremsstrahlung occurs when the path of a moving electron is deflected by an atom. Such a deflection can be regarded as a change in the electric current represented by that moving electron. A changing electric current is always accompanied by the radiation of photons. (For example, in the case of a transmitting antenna, photons are coherently emitted by a regularly changing (RF alternating) current and have a narrow frequency (energy) spectrum. In the case of bremsstrahlung, the photons are randomly emitted and have a very broad energy spectrum.)

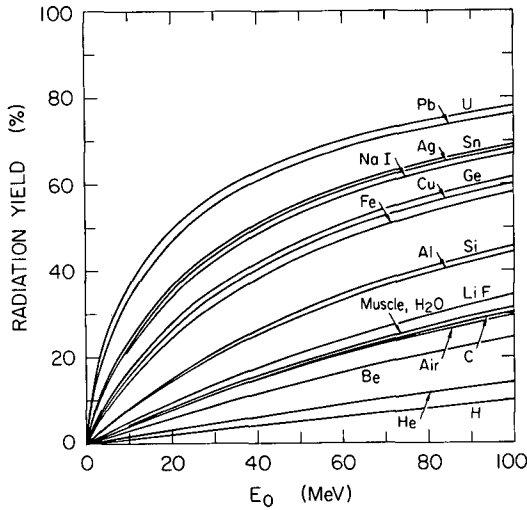


FIG.16. Radiation yield (or bremsstrahlung efficiency) for electrons stopped in various materials. Fraction (in per cent) of kinetic energy of incident electrons converted to radiation, as a function of incident energy E_0 . The remainder is transferred to the medium by ionization and manifests itself as heat. (Data from Berger and Seltzer [2, 3].)

As the electron energy is increased, an increasing fraction is converted to bremsstrahlung [1–4] until at very high energies this mechanism predominates. The ‘critical energy’ E_c for a given material is the electron energy at which the rising dE/dX (radiation) equals the dE/dX (collision). (See Fig.9, Section 2.2, and Table B-I, Appendix B.) Figure 16 shows the percentage average radiation yield of electrons brought to rest in various media.

At high energies (well above E_c), the phenomenon of the electromagnetic cascade or shower plays a dominant role (Section 2.2). Under these conditions it is almost meaningless to specify the depth at which the electron beam is ‘stopped’ because high-energy photons regenerate electrons at all depths of a thick target.

The development of external bremsstrahlung is described by a transition curve: The radiation first increases with increasing target thickness until reabsorption modifies this growth to produce a broad maximum, followed by a decline that becomes approximately exponential at very great thicknesses. A target of thickness corresponding to the maximum radiation is called an ‘optimum’ target and the photon spectrum emanating from such a target is described as ‘thick-target’ bremsstrahlung. The difference between the bremsstrahlung spectra discussed here and the track-length distribution of Section 2.2 is that bremsstrahlung spectra apply to radiation emanating from the target, whereas the track-length distributions are spectra within the target.

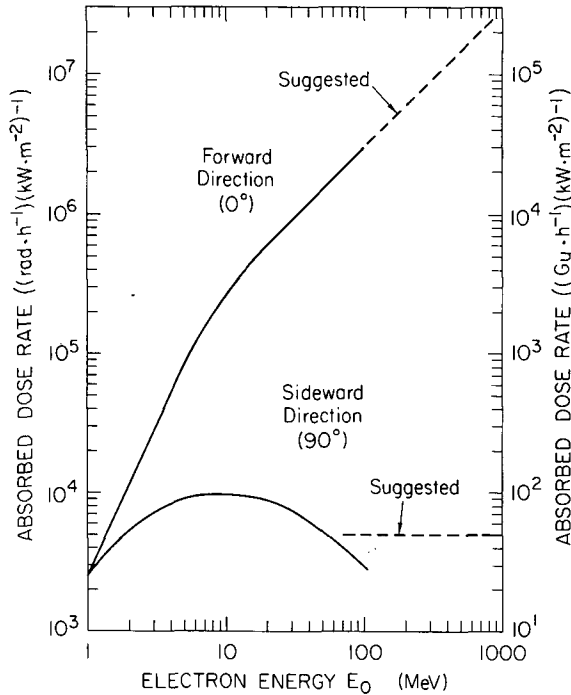


FIG.17. Thick-target bremsstrahlung from a high-Z target. Absorbed dose rate at 1 metre per unit incident electron beam power (kW) as a function of incident electron energy E_0 . The dashed line at 0° represents a reasonable extrapolation of the measured values. The dose rates measured in the sideward direction (smoothed for this figure) depend strongly on target and detector geometry and vary by more than a factor of two. The dashed line at 90° represents the more penetrating radiation component to be considered in room shielding. (See Footnote 9 for references to original sources.)

In radiation protection planning it is conservative practice to assume that all bremsstrahlung sources produce thick-target bremsstrahlung, regardless of the actual thickness of the source.

Some salient properties of thick-target bremsstrahlung are summarized:

- (a) For constant beam current, the intensity in the forward direction (0°) varies rapidly with electron beam energy. Below about 10 MeV the output varies approximately as E_0^3 , and above 10 MeV as E_0^2 , for constant beam current. This

behaviour is illustrated in Fig.17⁹, in which the output is plotted as a function of E_0 , for constant beam *power*. Up to about 20 MeV, the absorbed-dose rate at 0° from an optimum high-Z target is given to within a factor of two by the following Rule of Thumb:

$$\begin{aligned}
 \dot{D} ((\text{Gy} \cdot \text{min}^{-1})(\text{kW} \cdot \text{m}^{-2})^{-1}) &\approx 0.33 E_0^2 \\
 \dot{D} ((\text{rad} \cdot \text{min}^{-1})(\text{kW} \cdot \text{m}^{-2})^{-1}) &\approx 33 E_0^2 \\
 \dot{D} ((\text{Gy} \cdot \text{h}^{-1})(\text{kW} \cdot \text{m}^{-2})^{-1}) &\approx 20 E_0^2 && \text{(Rule of Thumb,} \\
 \dot{D} ((\text{rad} \cdot \text{h}^{-1})(\text{kW} \cdot \text{m}^{-2})^{-1}) &\approx 2000 E_0^2 && 0^\circ, E_0 < 20 \text{ MeV)} \\
 \dot{D} ((\text{Gy} \cdot \text{s}^{-1})(\text{kW} \cdot \text{m}^{-2})^{-1}) &\approx 0.0055 E_0^2 \\
 \dot{D} ((\text{rad} \cdot \text{s}^{-1})(\text{kW} \cdot \text{m}^{-2})^{-1}) &\approx 0.55 E_0^2
 \end{aligned} \tag{16}$$

where E_0 is in MeV. Above 20 MeV, these formulae will begin to overestimate the dose rate substantially. For $E_0 > 20$ MeV, the following Rule of Thumb reflects the change in slope seen in Fig.17 and is more accurate:

$$\begin{aligned}
 \dot{D} ((\text{Gy} \cdot \text{min}^{-1})(\text{kW} \cdot \text{m}^{-2})^{-1}) &\approx 5.0 E_0 \\
 \dot{D} ((\text{rad} \cdot \text{min}^{-1})(\text{kW} \cdot \text{m}^{-2})^{-1}) &\approx 500 E_0 \\
 \dot{D} ((\text{Gy} \cdot \text{h}^{-1})(\text{kW} \cdot \text{m}^{-2})^{-1}) &\approx 300 E_0 && \text{(Rule of Thumb,} \\
 \dot{D} ((\text{rad} \cdot \text{h}^{-1})(\text{kW} \cdot \text{m}^{-2})^{-1}) &\approx 30\,000 E_0 && 0^\circ, E_0 > 20 \text{ MeV)} \\
 \dot{D} ((\text{Gy} \cdot \text{s}^{-1})(\text{kW} \cdot \text{m}^{-2})^{-1}) &\approx 0.083 E_0 \\
 \dot{D} ((\text{rad} \cdot \text{s}^{-1})(\text{kW} \cdot \text{m}^{-2})^{-1}) &\approx 8.3 E_0
 \end{aligned} \tag{17}$$

(b) At 90° (also shown in Fig.17), the absorbed dose rate at high energy is believed to be proportional to power, independent of beam energy. Therefore the suggested behaviour at high energy is constant at

⁹ Figure 17 is adapted in part from Bly and Burrill [5]. Also see Bly [6] and Karzmark and Pering [7] for more recent adaptations of these data. Sources of original data on which this figure is based are Refs [8–14]. Data on which the high-energy behaviour is based may be found in Refs [15, 16]. The behaviour at low energy is consistent with the results of Rassow [17] who found the dose rate for constant current to be proportional to $E_0^{2.87}$ over the energy range $E_0 = 10\text{--}43$ MeV.

$$\dot{D} ((\text{Gy} \cdot \text{min}^{-1})(\text{kW} \cdot \text{m}^{-2})^{-1}) \approx 0.83$$

$$\dot{D} ((\text{rad} \cdot \text{min}^{-1})(\text{kW} \cdot \text{m}^{-2})^{-1}) \approx 83$$

$$\dot{D} ((\text{Gy} \cdot \text{h}^{-1})(\text{kW} \cdot \text{m}^{-2})^{-1}) \approx 50$$

$$\text{(Rule of Thumb, } 90^\circ, E_0 > 100 \text{ MeV)} \quad (18)$$

$$\dot{D} ((\text{rad} \cdot \text{h}^{-1})(\text{kW} \cdot \text{m}^{-2})^{-1}) \approx 5000$$

$$\dot{D} ((\text{Gy} \cdot \text{s}^{-1})(\text{kW} \cdot \text{m}^{-2})^{-1}) \approx 0.014$$

$$\dot{D} ((\text{rad} \cdot \text{s}^{-1})(\text{kW} \cdot \text{m}^{-2})^{-1}) \approx 1.4$$

This amount represents the more penetrating radiation component to be considered in shielding design. Dose rates at 90° from an *unshielded* target may be significantly higher because of the contribution of softer radiation components.

(c) At a given electron energy E_0 the intensity in the forward direction is a slowly varying function of target materials, except at very low Z where it is less. This implies that use of the above dose-rate estimates for radiation protection purposes will not be overly conservative, regardless of the target material used.

(d) At energies above about 1.5 MeV, the intensity peaks in the forward direction. This trend increases markedly with increasing energy, as can be seen in the comparison of 90° and 0° intensities shown in Fig.17. Figure 18 shows a curve of the relative angular distribution, plotted as a function of $E_0\theta$ (the angle at which the bremsstrahlung intensity is measured, relative to the incident beam direction, multiplied by the incident electron energy) [14]. Measurements in the range $E_0 = 2-20$ MeV can be adequately described by a single curve to about $E_0\theta = 400$ MeV·degrees, and a qualitatively similar behaviour is obtained at higher energies. The angular width of the forward lobe at half intensity is given approximately by the relationship

$$E_0\theta_{1/2} \cong 100 \text{ MeV} \cdot \text{degrees} \quad (19)$$

where E_0 is in MeV and $\theta_{1/2}$ is in degrees of angle.

(e) At lower energies, where energy loss by ionization dominates (Fig.16), the width of the forward lobe varies approximately as the square root of the atomic number of the target material. At higher energies ($\gtrsim 20$ MeV in high Z) the width is almost independent of Z .

(f) The hardest radiation (containing the greatest number of the most energetic photons) occurs in the forward direction. The radiation towards the sides becomes progressively softer as the angle is increased. This shift in spectrum may permit economies in shielding at large angles to the incident beam.

(g) The spectra are not as simple as the well-known thin-target spectra which, for $X \ll X_0$, are approximately given by

$$\frac{dN}{dk} \cong X X_0^{-1} k^{-1} \quad (\text{thin: } X \ll X_0) \quad (20)$$

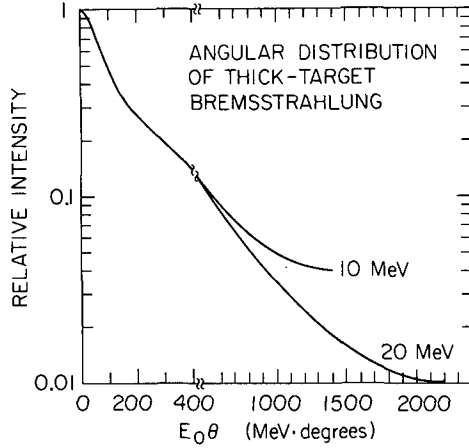


FIG.18. Angular distribution of bremsstrahlung intensity from high-Z targets (relative units), plotted as a function of the variable $E_0\theta$ (the angle at which the bremsstrahlung intensity is observed relative to the incident beam direction, multiplied by the incident electron energy). (Adapted from Ref.[14], with kind permission of A. Brynjolfsson and T.G. Martin, III, and the International Journal of Applied Radiation and Isotopes. See Ref.[14] for references to original work.)

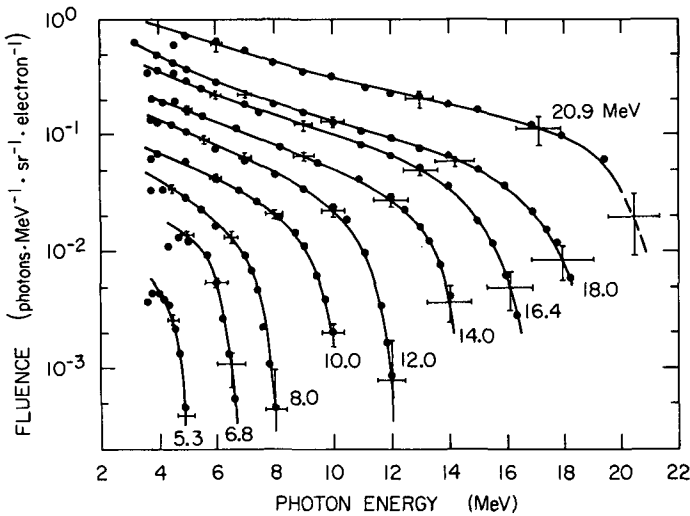


FIG.19. Bremsstrahlung spectra measured at 0° from intermediate-thickness ($0.2 X_0$) targets of high-Z material. The data points are measurements of O'Dell et al. [18]. (Adapted from Ref.[18], with kind permission of the authors and Nuclear Instruments and Methods.)

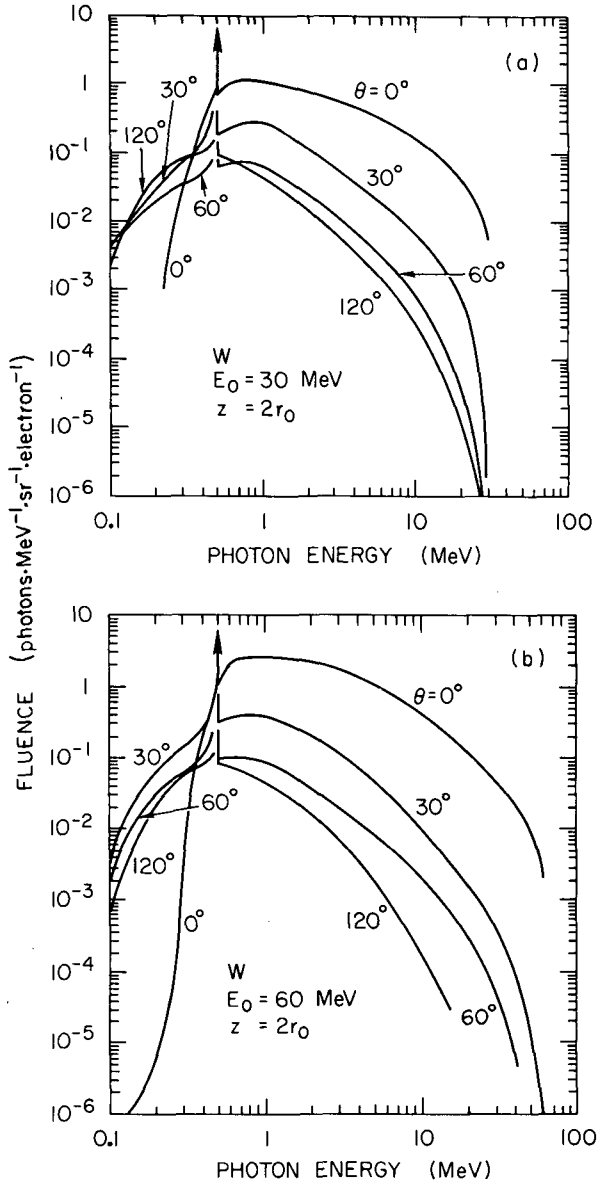


FIG.20. Spectra of bremsstrahlung photons emerging in various directions from thick tungsten targets irradiated by monoenergetic electron beams, normally incident. The target thickness in both cases is $2r_0$, or twice the mean electron range given by the CSD approximation. The arrows indicate positron annihilation radiation at 0.511 MeV. (a) Kinetic energy 30 MeV, thickness $z = 24 \text{ g}\cdot\text{cm}^{-2}$ ($3.6 X_0$); (b) 60 MeV, $z = 33 \text{ g}\cdot\text{cm}^{-2}$ ($4.9 X_0$). (Adapted from Ref.[20], with kind permission of M.J. Berger and S.M. Seltzer.)

where k is the photon energy, X is the target thickness and X_0 the radiation length (Appendix B). The thick-target photon spectrum declines rapidly from low photon energies to the limit E_0 . The fall-off at 0° appears to be more like k^{-2} , and even faster at larger angles. Representative measured spectra are shown in Fig.19 from the work of O'Dell et al. [18]. (Also see Dickinson and Lent [19] for calculations in this energy range.)

Thick-target spectra depend on details such as target materials and shape which may vary. Filtration by the target itself or by separate filters will alter the spectrum. The most satisfactory spectral calculations are by Monte-Carlo methods. Figure 20 shows representative spectra from the work of Berger and Seltzer [20].

References to earlier work on thick-target bremsstrahlung may be found in NBS Handbook No.85 [21]. Other calculations and measurements can be found in Refs [22–37].

2.4.2. Scattered photons

Photons will be scattered from any object placed in the path of a bremsstrahlung beam. This is the normal mode of operation with all radiographic setups and in radiotherapy with photon beams. The main physical process is Compton scattering or elastic collisions of photons with atomic electrons. An important property of Compton scattering is that the energy of scattered photons approaches a limiting value at high initial photon energies (Fig.21). For example, at 90° , the typical angle considered in the design of secondary shielding barriers, the maximum scattered photon energy is $k = m_e c^2 = 0.511$ MeV. At 180° , the maximum energy is half of this, or about 0.255 MeV. It is clear from Fig.21 that any of the bremsstrahlung spectra of Figs 19, 20 will be radically altered by a single scattering. At 90° , for example, the spectrum of scattered photons will be compressed into a secondary spectrum having a maximum energy of 0.511 MeV, with the largest number of photons near this energy. Photons which scatter twice or more at large angles will lose significantly more energy. This energy reduction is entirely a result of two-body kinematics [38], as expressed by the equation

$$k_s = \frac{k m_e}{m_e + k(1 - \cos \theta_s)} \quad (21)$$

in which k is the energy of the incident photon, k_s is the photon energy after scattering, m_e is the electron mass (0.511 MeV) and θ_s is the laboratory angle of scattering. This energy reduction is independent of the nature of the scattering material, but the intensity of scattered radiation does vary with material and

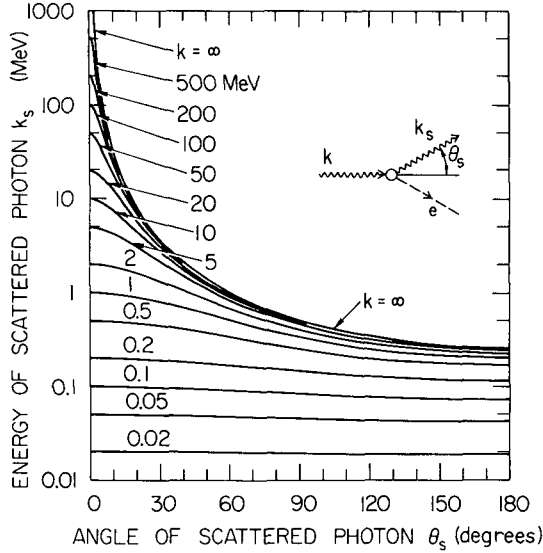


FIG.21. Graph of the energy-angle relationship for Compton scattering. The initial photon has energy k , the scattered photon has energy k_s , and the kinetic energy of the recoiling electron makes up the energy balance. Note that a photon scattered near 0° has the same energy as the initial photon, regardless of energy, but if the photon is scattered at a larger angle, the values of k_s approach a maximum limiting value as k is increased; the upper curve ($k = \infty$) represents the maximum possible energy of a scattered photon.

energy (see Section 3.4) since this also depends on the number of photons scattered and on absorption characteristics of the medium.

In addition to the Compton-scattered photons, a significant number of isotropically distributed 0.511-MeV photons arising from positron annihilations will also be present for $E_0 > 3$ MeV, and will dominate above about 7 MeV.

Because of the lower energy of Compton-scattered and annihilation photons, the shielding for scattered radiation at 90° or larger angles may be designed using beam transmission data appropriate for 1-MeV bremsstrahlung beams, up to about the critical energy E_c for the scattering material. Above this the scattered radiation begins to be dominated by wide-angle bremsstrahlung from the electromagnetic cascade continuing into the scattering medium.

It is important to distinguish between 'leakage' radiation and scattered radiation; leakage radiation is not primarily scattered radiation, but is dominated by thick-target bremsstrahlung at large angles, and its energy spectrum is closer to that of the useful bremsstrahlung beam.

Procedures for shielding against scattered photons are given in Section 3.4.

REFERENCES TO SECTION 2.4

- [1] KOCH, H.W., MOTZ, J.W., Bremsstrahlung cross-section formulas and related data, Rev. Mod. Phys. **31** (1959) 920. (This article reviews the theory of bremsstrahlung, with emphasis on thin-target bremsstrahlung.)
- [2] BERGER, M.J., SELTZER, S.M., Tables of Energy Losses and Ranges of Electrons and Positrons, National Aeronautics and Space Administration, Washington, DC, Rep. NASA SP-3012 (1964).
- [3] BERGER, M.J., SELTZER, S.M., Additional Stopping Power and Range Tables for Protons, Mesons and Electrons, National Aeronautics and Space Administration, Washington, DC, Rep. NASA SP-3036 (1966).
- [4] PAGES, L., BERTEL, E., JOFFRE, H., SKLAVENITIS, L., Energy loss, range, and bremsstrahlung yield for 10-keV to 100-MeV electrons in various elements and chemical compounds, At. Data **4** 1 (1972) 1-127.
- [5] BLY, J.H., BURRILL, E.A., "High-energy radiography in the 6 to 30 MeV range", Symp. Nondestructive Testing in the Missile Industry, American Society for Testing Materials, Special Technical Publication STP278 (1959) 20.
- [6] BLY, J.H., High-energy radiography: 1-30 MeV, Mater. Eval. (Nov. 1964) 1.
- [7] KARZMARK, C.J., PERING, N.C., Electron linear accelerators for radiation therapy: principles and contemporary developments, Phys. Med. Biol. **18** 3 (1973) 338.
- [8] BUECHNER, W.W., VAN DE GRAAFF, R.J., BURRILL, E.A., SPERDUTO, A., Thick-target X-ray production in the range from 1250 to 2350 kilovolts, Phys. Rev. **74** 10 (1948) 1348.
- [9] CLELAND, M.R., "Megaroentgen dose rates", Radiation Review **1** 3, Radiation Dynamics, Inc., Westbury, NY (1961) 1.
- [10] BURRILL, E.A., "Radioisotopes - or particle accelerators?", Radioisotope Engineering (EICHHOLZ, G., Ed.), M. Dekker, New York (1972) 361.
- [11] GOLDIE, C.H., WRIGHT, K.A., ANSON, J.H., CLOUD, R.W., TRUMP, J.G., Radiographic properties of X-rays in the two-to-six million volt range, ASTM Bull. **201** (1954) 49.
- [12] MILLER, C.W., Industrial radiography and the linear accelerator, J. Br. Inst. Radio Eng. **14** 8 (1954) 361.
- [13] WYCKOFF, J.M., PRUITT, J.S., SVENSSON, G., "Dose vs. angle and depth produced by 20 to 100 MeV electrons incident on thick targets", Proc. Int. Congr. Protection Against Accelerator and Space Radiation, held at Geneva, 26-30 April 1971, Rep. CERN 71-16, Vol. 2, European Organization for Nuclear Research, Geneva (1971) 773.
- [14] BRYNJOLFSSON, A., MARTIN, T.G., III, Bremsstrahlung production and shielding of static and linear electron accelerators below 50 MeV. Toxic gas production, required exhaust rates, and radiation instrumentation, Int. J. Appl. Radiat. Isot. **22** (1971) 29.
- [15] DeSTAEBLER, H., JENKINS, T.M., NELSON, W.R., "Shielding and radiation", The Stanford Two-Mile Accelerator, Ch.26 (NEAL, R.B., Ed.), Benjamin, New York (1968).
- [16] DINTER, H., TESCH, K., Measurements of dose and shielding parameters of electron-photon stray radiation from a high-energy electron beam, Deutsches Elektronen-Synchrotron, Hamburg, Rep. DESY-76/19 (1976).
- [17] RASSOW, J., Grundlagen und Planung der Elektronentiefentherapie mittels Pendelbestrahlung, Strahlenklinik des Klinikum Essen der Ruhr-Universität, Habilitationsschrift, Essen (1970) 86.
- [18] O'DELL, A.A., Jr., SANDIFER, C.W., KNOWLEN, R.B., GEORGE, W.D., Measurement of absolute thick-target bremsstrahlung spectra, Nucl. Instrum. Meth. **61** (1968) 340.

- [19] DICKINSON, W.C., LENT, E.M., Calculation of Forward Bremsstrahlung Spectra from Thick Targets, Lawrence Livermore Laboratory, Rep. UCRL-50442 (1968).
- [20] BERGER, M.J., SELTZER, S.M., Bremsstrahlung and photoneutrons from thick tungsten and tantalum targets, *Phys. Rev.* **C2 2** (1970) 621.
- [21] NATIONAL BUREAU OF STANDARDS, Physical Aspects of Irradiation, NBS Handbook No.85, Washington, DC (1964). (References to many earlier papers on bremsstrahlung can be found here.)
- [22] PATTERSON, H.W., THOMAS, R.H., Accelerator Health Physics, Ch.2, Academic Press, New York (1973).
- [23] LANZL, L.H., HANSON, A.O., Z-dependence and angular distribution of bremsstrahlung from 17-MeV electrons, *Phys. Rev.* **83** (1951) 959.
- [24] KOCH, H.W., CARTER, R.E., Determination of the energy distribution of bremsstrahlung from 19.5-MeV electrons, *Phys. Rev.* **77** (1950) 165.
- [25] MOTZ, J.W., MILLER, W., WYCKOFF, H.O., Eleven-MeV thick target bremsstrahlung, *Phys. Rev.* **89** (1953) 968.
- [26] HANSEN, N., BORN, D., DILDINE, R., FULTZ, S., Bremsstrahlung production in thin and thick targets, Lawrence Livermore Laboratory, Document No. Linac-09 (1959).
- [27] HANSEN, N.E., FULTZ, S.C., Cross Sections and Spectra for Negative Electron Bremsstrahlung, Lawrence Livermore Laboratory, Rep. UCRL-6099, Physics and Mathematics, UC-34, TID-4500 (1960).
- [28] JUPITER, C.P., HATCHER, C.R., HANSEN, N.E., Measurements of the Angular Distribution of Bremsstrahlung Intensity for 10-MeV and 20-MeV Electrons on Thick Targets, Lawrence Livermore Laboratory Report (1964).
- [29] SCOTT, W.W., Electron-Bremsstrahlung Differential Cross Sections for Thin and Thick Targets, National Aeronautics and Space Administration, Washington, DC, Rep. NASA TN D-2659 (1965).
- [30] EMIGH, C.R., Thick Target Bremsstrahlung Theory, Los Alamos Scientific Laboratory, Rep. LA-4097 (1969).
- [31] WYCKOFF, J.M., PRUITT, J.S., SVENSSON, G., "Dose vs. angle and depth produced by 20 to 100 MeV electrons incident on thick targets", in *Proc. Int. Congr. Protection Against Accelerator and Space Radiation*, Geneva, 26-30 Apr. 1971, CERN Rep. No. 71-16, Vol.2, Geneva (1971) 773.
- [32] NAKAMURA, T., TAKEMURA, M., HIRAYAMA, H., HYODO, T., Energy spectra transmitted through iron and gold targets by 0.5-1.44 MeV electrons, *J. Appl. Phys.* **43** (1972) 5189.
- [33] HIRAYAMA, H., NAKAMURA, T., Measurement of bremsstrahlung spectra produced in iron and tungsten targets by 15-MeV electrons with activation detectors, *Nucl. Sci. Eng.* **50** (1973) 248.
- [34] NAKAMURA, T., HIRAYAMA, H., Spectra of bremsstrahlung produced in very thick lead targets by 15-, 20-, and 25-MeV electrons measured with activation detectors, *Nucl. Sci. Eng.* **59** (1976) 237.
- [35] LEVY, L.B., WAGGENER, R.G., McDAVID, W.D., PAYNE, W.H., Experimental and calculated bremsstrahlung spectra from a 25-MeV linear accelerator and a 19-MeV beta-tron, *Med. Phys.* **1** (1974) 62.
- [36] NATH, R., SCHULZ, R.J., Determination of high-energy X-ray spectra by photoactivation, *Med. Phys.* **3 3** (1976) 133.
- [37] LEVY, L.B., WAGGENER, R.G., WRIGHT, A.E., Measurement of primary bremsstrahlung spectrum from an 8-MeV linear accelerator, *Med. Phys.* **3 3** (1976) 173.

- [38] NELMS, A.T., Graphs of the Compton Energy-Angle Relationship and the Klein-Nishina Formula from 10 keV to 500 MeV, National Bureau of Standards, Washington DC, Circular No.542 (1953). (The curves for σ_a in Fig.VIIIa and Fig.VIIIb are inaccurate in the low-energy region and should be used with caution.)

2.5. Neutrons

Above a threshold energy which varies from 10 to 19 MeV for light nuclei (but which is 2.23 MeV in deuterium and 1.67 MeV in beryllium) and from 4 to 6 MeV for heavy nuclei, neutron production will take place in any material struck by the electron or bremsstrahlung beam. It should be realized that it is the *photons* interacting with components that release the neutrons, rather than direct interaction of the electrons. The produced neutrons may be a radiation hazard in themselves and are also related to induced activity (this is discussed in Sections 2.6 and 2.7).

In a great many applications, the electron beam is directed onto a special target to produce bremsstrahlung. The bremsstrahlung energy is then absorbed in other media, for example collimators, jaws, object to be radiographed, hydrogen target, beam monitor, concrete floor or ceiling or other shielding. The power remaining in the electron beam may be absorbed entirely in the original target, if it is thick, or be directed towards a separate beam dump, as is often done in high-energy research facilities.

For room shielding, a detailed study of neutron production from all these possible sources is not usually warranted. It is usually adequate to assume that all of the electron beam power is fully absorbed in a single material of the highest Z that an electron or bremsstrahlung beam may strike.

Where neutron production is critical, such as in estimating the integral dose to a patient undergoing radiation therapy, a study of the various neutron sources is essential. The information presented here will be of help in such considerations, as well as in assessing the activity induced in various media (Sections 2.6, 2.7).

Since photoneutron cross-sections have been measured for a wide range of materials, the problem connected with evaluating photoneutron sources is not primarily a lack of data, but rather the formulation of a realistic representation of the photon track-length distribution for the specific materials and geometry at hand, and the estimation of effects of self-shielding and source distribution.

2.5.1. Neutron quality factor and dose equivalent

The interaction of high-energy neutrons in *tissue* is mainly through the release of low-energy protons from elastic collisions with hydrogen nuclei [1, 2].

TABLE XI. CONVERSION FACTORS AND EFFECTIVE QUALITY FACTORS FOR NEUTRONS

Neutron energy (MeV)	Conversion factor ^a (neutrons cm ⁻² s ⁻¹ per mrem h ⁻¹)	Effective quality factor ^b \bar{Q}
2.5×10^{-8} (thermal)	260	2.3
1×10^{-7}	240	2
1×10^{-6}	220	2
1×10^{-5}	230	2
1×10^{-4}	240	2
1×10^{-3}	270	2
1×10^{-2}	280	2
1×10^{-1}	48	7.4
5×10^{-1}	14	11
1	8.5	10.6
2	7.0	9.3
5	6.8	7.8
10	6.8	6.8
20	6.5	6.0
50	6.1	5.0
1×10^2	5.6	4.4
2×10^2	5.1	3.8
5×10^2	3.6	3.2
1×10^3	2.2	2.8
2×10^3	1.6	2.6
3×10^3	1.4	2.5

^a Calculated at maximum of depth-dose equivalent curve.

^b Maximum dose equivalent divided by the absorbed dose at the depth where the maximum dose equivalent occurs.

Reproduced from ICRP-12, Ref.[3], with kind permission of the International Commission on Radiological Protection and Pergamon Press.

Since the recoiling protons are heavily ionizing (high LET), their quality factor is high. At neutron energies less than about 100 eV, (n, γ) and (n, p) reactions predominate. The effective quality factor \bar{Q} of the dose imparted by an external neutron beam of a given energy is derived by an integration over the spectrum of ionizing particles released in tissue by several types of contributing interactions. The resulting \bar{Q} values vary considerably with neutron energy.

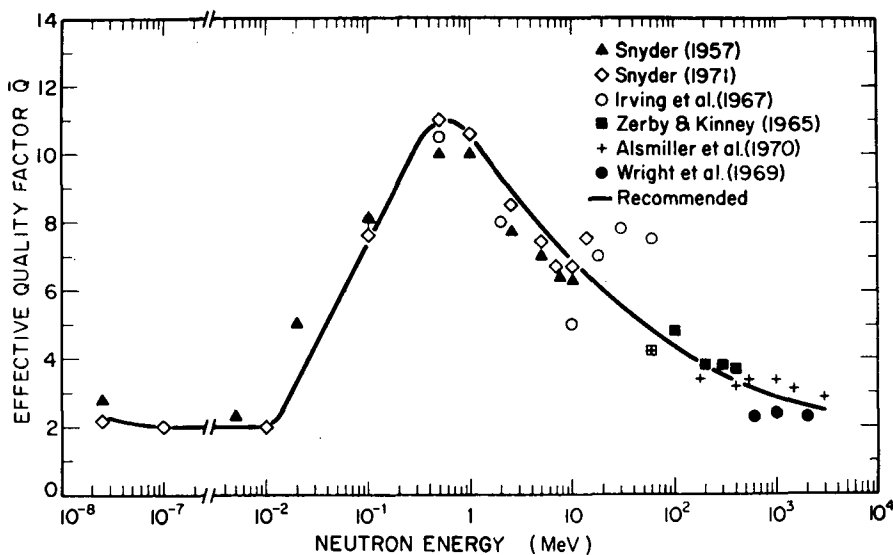


FIG.22. Effective quality factor Q for neutrons as a function of neutron kinetic energy: the maximum dose equivalent divided by the absorbed dose where the maximum dose equivalent occurs. The curve indicates values recommended by ICRP. See ICRP-21 for references to original work. (Reproduced from ICRP-21, Ref.[3], with kind permission of the International Commission on Radiological Protection and Pergamon Press.)

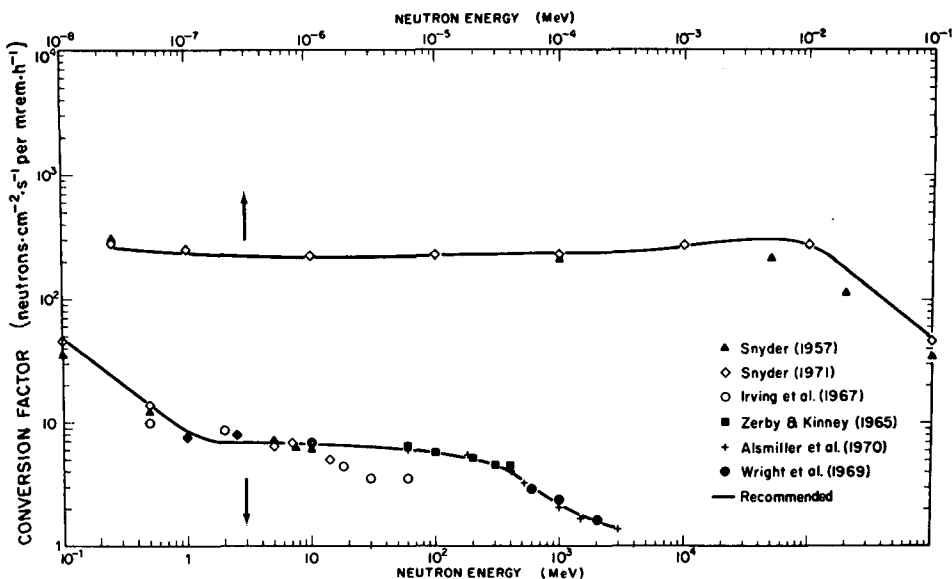


FIG.23. Conversion factors for neutrons as a function of incident neutron kinetic energy. Unidirectional broad beam, normal incidence. The curves indicate the values recommended by ICRP. See ICRP-21 for references to original work. (Reproduced from ICRP-21, Ref.[3], with kind permission of the International Commission on Radiological Protection and Pergamon Press.)

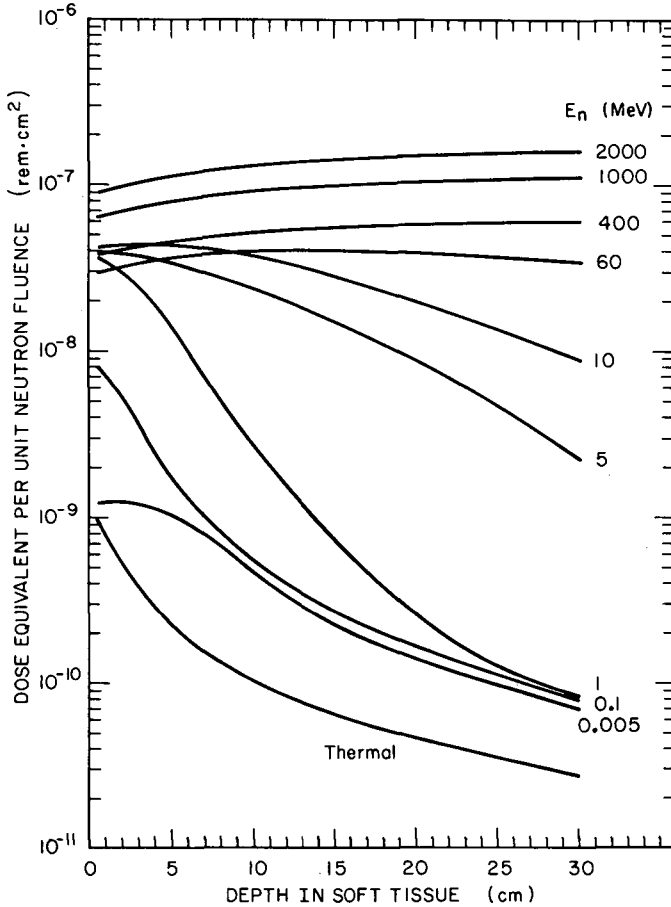


FIG.24. Dose equivalent H per unit neutron fluence, as a function of depth in a 30-cm-thick slab of tissue irradiated normally by a broad beam of monoenergetic neutrons. The labels indicate the energy of the incident neutrons. (Adapted from ICRP-21, Ref.[3], with kind permission of the International Commission on Radiological Protection and Pergamon Press.)

Effective quality factors for neutrons, \bar{Q} , and conversion factors for fluence to dose equivalent, H , recommended by ICRP [3] are shown in Table XI and plotted in Figs 22, 23. They refer to irradiation by a unidirectional broad beam of monoenergetic neutrons at normal incidence and are evaluated at the maxima of the depth-dose equivalent curves (Fig. 24). \bar{Q} is obtained by dividing the maximum dose equivalent by the absorbed dose at the depth where the maximum dose equivalent occurs.

Because neutron spectra found in the radiation environment of electron accelerators peak somewhere near 1 MeV (the *average* energy is somewhat higher; see Section 2.5.2), it is usual to assume that the energy is effectively 1–2 MeV, unless the spectrum at the location in question has been measured and found to be different. A conservative rule of thumb is:

$$\dot{H} \cong 1.4 \times 10^{-4} \varphi \quad (\text{Rule of Thumb}) \quad (22)$$

where \dot{H} is in $\text{rem} \cdot \text{h}^{-1}$, φ is in $\text{n} \cdot \text{cm}^{-2} \cdot \text{s}^{-1}$, and the proportionality constant is derived from Table XI for 2-MeV neutrons.

Because neutrons are attenuated and moderated by transport through tissue, the absorbed-dose and dose-equivalent distributions are non-uniform. The dose equivalent H as a function of depth for broad beams of monoenergetic neutrons is shown as an example in Fig. 24 taken from ICRP-21 [3].

2.5.2. Production mechanisms

(a) The giant resonance

Between threshold and approximately 30 MeV, neutron production results primarily from a process known as the ‘giant photonuclear resonance’ [4–7]. The physical mechanism can be described as one in which the electric field of the photon transfers its energy to the nucleus by inducing an oscillation in which the protons as a group move oppositely to the neutrons as a group.

The cross-section for this process has a large maximum at photon energies of approximately 20–23 MeV for light nuclei (atomic mass number $A \lesssim 40$), and 13–18 MeV for medium and heavy nuclei. For $A \gtrsim 40$, the energy of the peak is approximately given by $k_0 = 80 A^{-1/3}$ MeV. The width of this peaking varies between about 3 MeV (heavy nuclei) and 10 MeV (light nuclei). This phenomenon occurs in all nuclei (except ^1H) and its general features are rather smooth functions of nuclear size. Its relationship to other production mechanisms can be seen in Fig. 25.

It is important to realize that the cross-sections for neutron production depicted as functions of photon energy k are to be folded together with a photon spectrum that declines rapidly with k , in most situations as k^{-2} (Sections 2.2, 2.4). The trend of such a spectrum strongly enhances the importance of the giant-resonance mechanism, relative to mechanisms which dominate at higher energy.

Because of the peaking in the cross-section, we expect a rapid rise in the amount of neutron production as the primary electron energy E_0 is varied through the range 10–20 MeV, followed by a slower rise above 25–30 MeV, for the same electron *current*. When referred to the same beam *power*, giant-resonance neutron production is almost constant with E_0 , for E_0 above about twice k_0 .

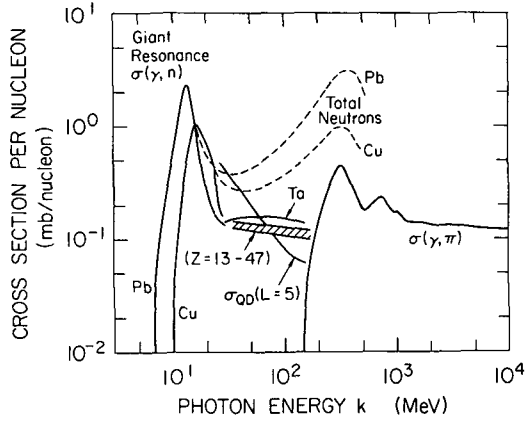


FIG.25. Qualitative picture of neutron-producing mechanisms, expressed as cross-section per target nucleon as a function of photon energy k . To the left are the giant-resonance peaks for Cu and Pb. To the right is the photopion production cross-section (average of proton and neutron). Between these is shown the behaviour found by Jones and Terwilliger [12] for medium- Z targets (hatched), and a calculation for Ta by Alsmiller et al. [44] based on an intra-nuclear cascade model. Also shown for this energy region is the photoneutron cross-section derived from the simple quasi-deuteron model described in the text, assuming $N = Z = A/2$ and $L = 5$. The dashed curves above show the presumed total neutron production per nucleon for Cu and Pb, adapted from Jones and Terwilliger [12], taking neutron multiplicity into account.

The number of neutrons rises systematically with nuclear size, although there are striking variations from the general trend at low Z . The cross-section integrated over photon energies from threshold to 30 MeV has a trend which can be expressed as

$$\sigma_{\text{int}} \sim \int_0^{30 \text{ MeV}} \sigma_n(k) dk \sim \frac{NZ}{A} \quad (23)$$

where $\sigma_n(k)$ is the total photoneutron cross-section as a function of photon energy k , and $N = A - Z$. The upper limit of integration is arbitrary, but 30 MeV is high enough for the region of the peak giant-resonance cross-section for all materials to be integrated over.

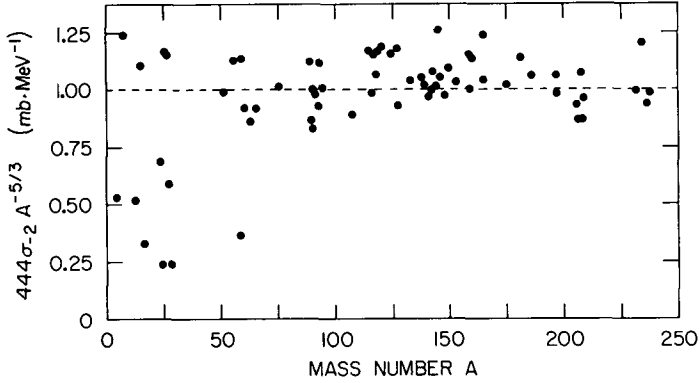


FIG.26. Measured values of the photoneutron integral σ_2 in units of $2.25 \times 10^{-3} A^{5/3} \text{ mb} \cdot \text{MeV}^{-1}$ (or $A^{5/3}/444 \text{ mb} \cdot \text{MeV}^{-1}$). See text for definition. This integral serves as an index of giant-resonance neutron yield from very thick targets. (Adapted from Ref.[8], with kind permission of B.L. Berman and S.C. Fultz, the Lawrence Livermore Laboratory and the Reviews of Modern Physics.)

In radiation protection work, it is usually more appropriate to weight the cross-section by something approximating the actual photon spectrum within a thick target ($\sim k^{-2}$, from Section 2.2). The trend of this integral is given by

$$\sigma_{-2} \sim \int_0^{30 \text{ MeV}} \sigma_n(k) k^{-2} dk \sim A^{5/3} \quad (24)$$

where $\sigma_n(k)$ is the total photoneutron cross-section. Figure 26 shows the actual variation of this integral [8] with atomic mass number A .¹⁰ Above about $A = 60$, the values are well described by this approximation, but there are deviations from Eq. (24) of up to a factor of four for lower A . This integral serves as an index of giant-resonance neutron yield from *very thick* targets ($X \gg X_0$).

¹⁰ It should be noted that the cross-section which correctly gives the neutron yield in the giant-resonance region is the photoneutron *yield* cross-section $\sigma_n = \sigma(\gamma, n) + \sigma(\gamma, np) + 2 \sigma(\gamma, 2n) + \dots$, in which each channel cross-section is multiplied by its neutron multiplicity. The data of Figs 26, 27 and Table XII are mainly integrals of the photoneutron cross-section written as $\sigma_{n, \text{tot}} = \sigma(\gamma, n) + \sigma(\gamma, np) + \sigma(\gamma, 2n) + \dots$, without regard to multiplicity. While this is not strictly correct, the difference is not generally large at giant-resonance energies. The correct integrals have not been conveniently tabulated.

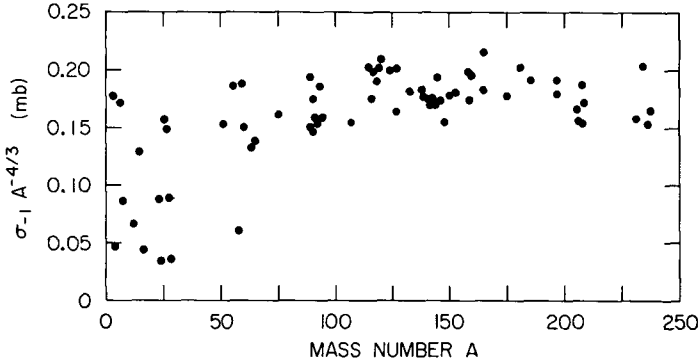


FIG. 27. Measured values of the photoneutron integral σ_{-1} . See text for definition. This integral serves as an index of giant-resonance neutron yield from thin targets. (Adapted from Ref. [8], with kind permission of B.L. Berman and S.C. Fultz, the Lawrence Livermore Laboratory and the Reviews of Modern Physics.)

The bremsstrahlung-weighted integral σ_{-1} is so named because the weighting approximates the photon spectral distribution from thin targets ($\sim k^{-1}$, see Eq. (20)):

$$\sigma_{-1} \sim \int_0^{30 \text{ MeV}} \sigma_n(k) k^{-1} dk \sim A^{-4/3} \quad (25)$$

This integral is useful in estimating yields from *thin* targets and is shown in Fig. 27 as a function of A .

Integrals for photoneutron production, together with values of threshold energy, k_{th} , energy of maximum cross-section, k_0 , maximum cross-section, σ_m , and full width at half maximum, Γ , of the giant resonance peak are given in Table XII for a wide range of nuclei. The upper limit of integration k_{max} is usually of the order of 25–30 MeV, sufficiently high for most of the giant-resonance contribution to be included. This table is adapted from the review article by Berman and Fultz [8] where references to original work may be found. Values of k_0 , σ_m and Γ having decimal points are computer fits to a Lorentz line shape given by these authors for spherical nuclei.¹¹ More than one line for a given nuclide is the result of more than one measurement.

¹¹ A number of peaks are poorly described by this parameterization; low-mass nuclei tend to have broad, skewed peaks, and many of the intermediate and high-mass nuclei have flat tops or are even double-peaked. In these cases, visual estimates of the data in Refs [8, 9] are given in parentheses and are meant to be indicative only.

TABLE XII. PARAMETERS FOR NEUTRON PRODUCTION BY GIANT PHOTONUCLEAR RESONANCE^(a)

Nucleus	k_{th} (MeV)	k_o (MeV)	σ_m (mb)	Γ (MeV)	k_{max} (MeV)	$\sigma_{Int}(\gamma, tot)$ (mb·MeV)	$\sigma_{Int}(\gamma, 1n)$ (mb·MeV)	$\sigma_{Int}(\gamma, 2n)$ (mb·MeV)	$\sigma_{Int}(\gamma, 3n)$ (mb·MeV)	σ_{-1} (mb)	σ_{-2} (mb·MeV ⁻¹)
³ He	7.72	(15)	(0.9)	(14)	30.2	13.0	13.0			0.77	0.050
⁴ He	20.58	(25)	(1.0)	(9)	31.4	7.94	7.94	0		0.30	0.012
⁶ Li	5.67	(12)	(1.7)	(16)	32.0	27.7	27.3	0.4		1.87	0.15
⁷ Li	7.25	(15)	(1.5)	(12)	30.5	20.1	10.1	10.0		1.15	0.071
12C	18.72	(23)	(7)	(5)	26.7	36	36				
					25.5	29.4	29.4				
					37.4	46.8	46.8	0		1.83	0.073
¹⁴ N	10.55	(23)	(15)	(5)	29.5	97.6	97.6			4.36	0.20
¹⁶ O	15.67	(23)	(8)	(4)	26.5	41.5	41.5				
					28.0	41.5	41.5			1.76	0.075
²³ Na	12.44	(26)	(10)	(12)	27.1	119	118	0.6		5.74	0.29
NatMg	7.33	(20)	(11)	(11)	26.0	58 ^b					
					28.0	75.6					
²⁴ Mg	16.55	(19)	(8)	(10)	28.3	51.9	51.9			2.37	0.11
²⁵ Mg	7.33	(24)	(25)	(12)	28.9	247	245	1.5		11.5	0.56
²⁶ Mg	11.15	(22)	(20)	(14)	28.6	236	164	72		11.5	0.59
²⁷ Al	13.03	(22)	(14)	(11)	36.7	167	159	7.6		7.17	0.32
NatSi	17.18	(20)	(11)	(5)	31.0	68.5	68.5	0		3.05	0.14
⁴⁰ Ca	15.63				26.0	73	73				
⁵¹ V	11.04	(18)	(70)	(7)	27.8	552	450	102		28.9	1.56
⁵⁵ Mn	10.22	(18)	(60)	(12)	36.5	798	629	166	3.4	38.8	2.02
⁵⁸ Ni	12.19	(18)	(25)	(10)	33.5	286	278	7.7		13.8	0.70
⁶⁰ Ni	11.38	(17)	(70)	(8)	33.2	704	632	72	0	35.6	1.90
⁵⁹ Co	10.44	(18)	(70)	(12)	36.5	884	741	139	4.2	43.5	2.28
⁶³ Cu	10.84	(16)	(70)	(10)	27.8	604	528	76		33.4	1.92
					25.1	498	43				
⁶⁵ Cu	9.91	16.70	75.2	6.89	27.8	619	421	198		36.0	2.18
NatCu	9.91	(17)	(70)	(7)	27.8	635	525	110			
					19.6	450 ^b					
⁷⁵ As	10.24	(17)	(95)	(8)	29.5	909	688	221	0	51.4	3.05
NatRb	10.53	16.80	190	4.47	24.3	1147	1052	95		67.1	4.04
NatSr	11.12	16.84	206	4.50	27.0	1432	1311	121		80.3	4.68
⁸⁹ Y	11.86	16.79	185	3.95	28.0	1059	960	99		59.8	3.48
		16.74	226	4.25	27.0	1353	1279	74		76.5	4.46
		16.83	205	3.69	18.1	641				40.0	2.52
⁹⁰ Zr	11.94	16.85	185	4.02	27.6	1060	962	98		59.1	3.38
		16.74	211	4.16	25.9	1260	1211	49		70.8	4.08
⁹¹ Zr	7.22	16.58	184	4.20	30.0	1103	903	200	0	65.4	4.07
⁹² Zr	8.67	16.26	166	4.68	27.8	1091	639	452	0	64.2	3.92
⁹⁴ Zr	8.02	16.22	161	5.29	31.1	1121	508	580	33	68.5	4.40
⁹³ Nb	8.81	16.59	200	5.05	24.3	1331	1052	279		78.5	4.80
¹⁰⁷ Ag	9.39	15.90	150	6.71	29.5	1356	1093	263	0	78.7	4.82
¹¹⁵ In	9.03	15.63	266	5.24	31.1	1875	1355	508	13	113	7.13
¹¹⁶ Sn	9.39	15.68	266	4.19	29.6	1669	1255	414	0	99	6.13
¹¹⁷ Sn	7.19	15.66	254	5.02	31.1	1894	1380	476	38	114	7.30

See footnotes at end of table.

TABLE XII. (cont.)

Nucleus	k_{th} (MeV)	k_o (MeV)	σ_m (mb)	Γ (MeV)	k_{max} (MeV)	$\sigma_{int}(\gamma, tot)$ (mb·MeV)	$\sigma_{int}(\gamma, 1n)$ (mb·MeV)	$\sigma_{int}(\gamma, 2n)$ (mb·MeV)	$\sigma_{int}(\gamma, 3n)$ (mb·MeV)	σ_{-1} (mb)	σ_{-2} (mb·MeV ⁻¹)
118Sn	9.25	15.59	256	4.77	30.8	1853	1302	531	20	110	6.83
119Sn	6.58	15.53	253	4.81	31.1	1993	1326	597	69	118	7.55
120Sn	9.24	15.40	280	4.89	29.9	2074	1389	673	12	124	7.79
124Sn	8.56	15.19	283	4.81	31.1	2010	1285	670	55	123	8.02
127I	9.15	(15)	(220)	(5.5)	29.5	1729	1286	443	<20	105	6.70
					24.9	1991	1601	390		128	8.55
133Ca	9.02	15.25	287	5.01	29.5	1986	1475	503	8	124	8.09
138Ba	8.58	15.26	327	4.61	27.1	2040	1550	490	3	130	8.71
NatBa	6.90	15.29	356	4.89	24.3	2248	1877	371		146	9.94
139La	8.78	15.24	336	4.47	21.2	1910 ^b					
					24.3	1978	1687	291		128	8.54
NatCe	9.06	14.95	351	4.64	21.2	1880 ^b					
					25.2	2165	1764	400	1	143	9.83
141Pr	9.37	15.15	324	4.42	29.8	2062	1717	340	5	128	8.37
NatNd	6.07	14.92	315	4.70	18.0	1559	1236	323		112	8.46
NatSm	7.80	(15)	(340)	(6)	25.2	2413	1661	731	21	163	11.5
153Eu	8.65	(14)	(250)	(8)	28.9	2273	1566	670	37	148	10.2
159Tb	8.15	(14)	(250)	(7.5)	28.0	2300	1413	887		151	10.5
					27.4	2557	1936	605	16	170	12.0
160Gd	7.00	(14)	(280)	(7.5)	29.5	2533	1398	1055	80	169	12.1
165Ho	8.12	(14)	(280)	(7.5)	19.6	2540					
					28.9	2523	1735	744	44	166	11.6
					26.8	2871	2090	766	15	194	13.9
NatEr	6.53	(14)	(320)	(7)	21.1	2387	1801	586		172	12.9
175Lu	7.81	(14)	(320)	(7)	23.0	2507	1872	635		173	12.5
181Ta	7.64	(14)	(320)	(7)	22.0	2970 ^b					
					24.6	2181	1300	881		149	10.7
					25.2	2983	2180	790	13	205	14.8
186W	7.27	(14)	(400)	(6)	28.6	3004	1655	1200	149	203	14.5
197Au	8.07				22.0	3000 ^b					
		13.82	560	3.84	24.7	2967	2190	777		205	14.7
		13.72	541	4.61	21.7	3067	2588	479		217	15.9
206Pb	8.12	13.59	514	3.85	26.4	2909	2377	532		203	15.0
207Pb	6.73	13.56	481	3.96	26.4	2718	2169	549		191	14.2
208Pb	7.38	13.46	491	3.90	26.4	2646	1786	860		189	14.3
		13.43	639	4.07	18.9	3059	2731	328		229	17.6
		13.63	645	3.94	14.9	2090 ^b				165	13.3
NatPb	6.73				22.0	4100 ^b					
209Bi	7.43				22.0	3730 ^b					
		13.45	521	3.97	26.4	3058	2344	714		214	15.8
		13.56	648	3.72	14.8	2129 ^b				170	13.8
232Th	6.34	(13)	(440)	(7)	16.3	2694	1728	787	179 ^c	224	19.5
235U	5.24				18.5	3714	1066	1588	1060 ^c	293	24.1
237Np	6.76	(13)	(450)	(7)	16.6	2756	1085	121	1550 ^c	224	19.0
238U	4.76	(13)	(440)	(7)	18.35	3026	1169	899	958 ^c	241	20.2

(a) Table adapted from review article of Berman and Fultz. See Ref.[8] for detailed explanation, additional data and references to original measurements.

(b) Photoneutron yield cross-section $\sigma[(\gamma, n) + (\gamma, pn) + 2(\gamma, 2n)]$.

(c) Photofission cross-section $\sigma_{int}(\gamma, fission)$.

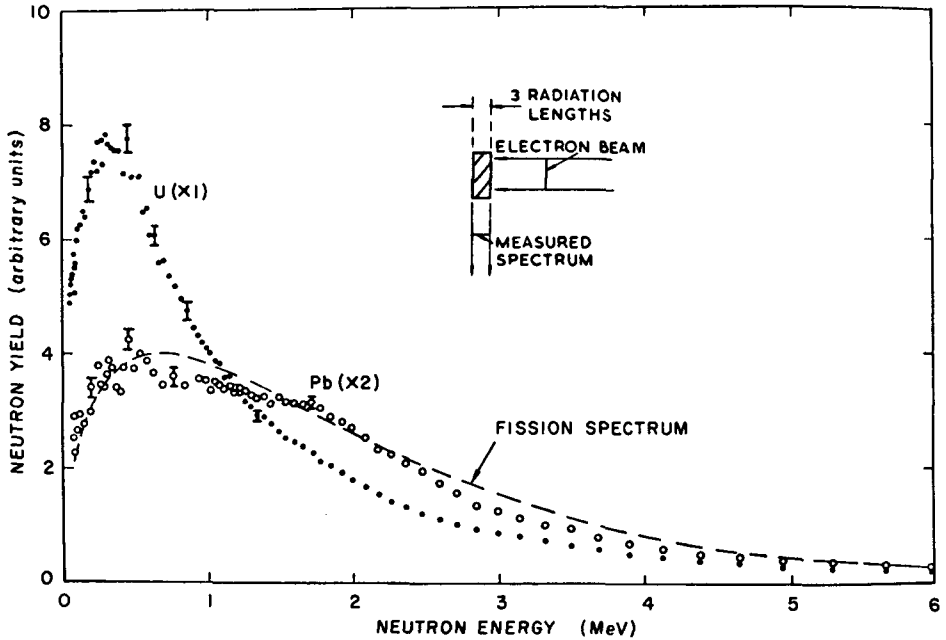


FIG.28. Energy spectra of neutrons released by 45-MeV electrons from three-radiation-length targets of Pb and U. The spectrum from Pb up to 6 MeV is well described by a fission spectrum (dashed curve) or a Maxwellian distribution with $T = 0.98$ MeV. Mean neutron energies are: Pb: 1.92 ± 0.1 MeV; U: 1.37 ± 0.09 MeV. (Adapted from Gayther and Goode [17], with kind permission of the authors and the Journal of Nuclear Energy.)

In addition to the references given, the papers by Price and Kerst [10] and Montalbetti et al. [11], although older, are useful primary sources of photoneutron data for a wide range of substances. The early paper by Jones and Terwilliger [12] covers the energy range to 320 MeV. Data for other nuclei and other types of photonuclear reactions may be found by consulting bibliographies prepared by Fuller et al. [13] (Supplement 1976), Antonescu [14], Ionescu [15], and Bülow and Forkman [16].

Neutron spectra from the giant resonance consist of two distinct components: the 'evaporation spectrum' and the 'direct-emission spectrum'. Evaporation spectra are usually adequately described by a Maxwellian distribution which dominates the low-neutron energy region:

$$\frac{dN}{dE_n} = \frac{E_n}{T^2} \exp(-E_n/T) \quad (\text{Normalized to unit area}) \quad (26)$$

where T is a 'nuclear temperature' (in units of MeV) characteristic of the particular target nucleus and its excitation energy E_{ex} . With this distribution,

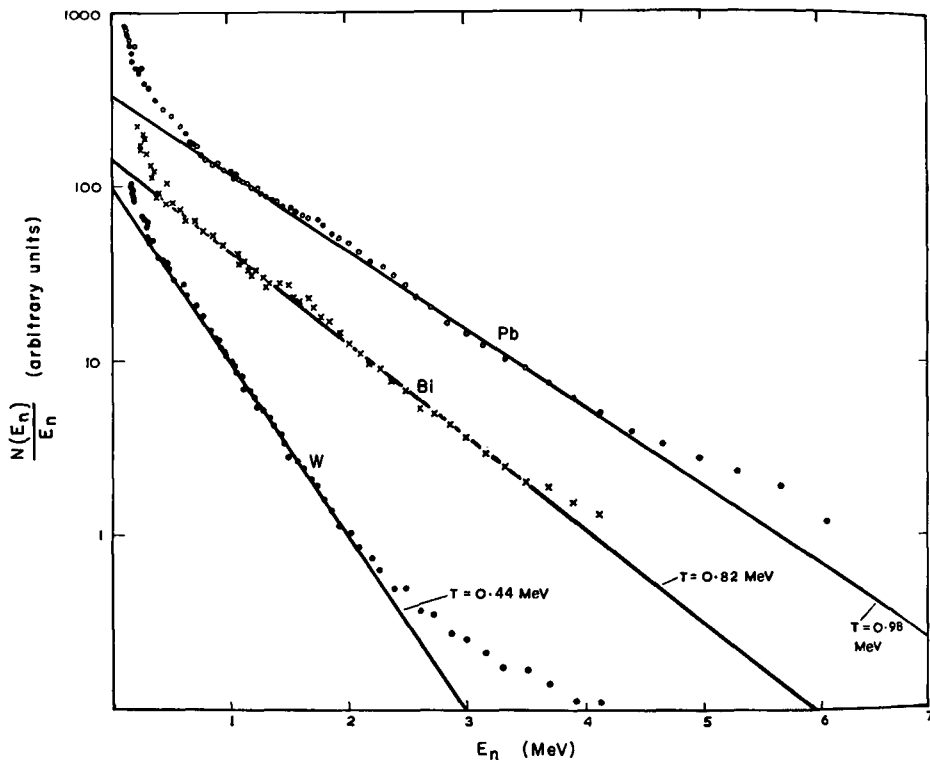


FIG. 29. Spectra of neutrons released by 45-MeV electrons on thick targets of W, Pb and Bi. The data are presented as $E_n^{-1}N(E_n)$ versus E_n , in order to exhibit the characteristic 'temperature' of the three spectra. (Adapted from Gayther and Goode [17], with kind permission of the authors and the *Journal of Nuclear Energy*.)

the most probable neutron energy is $\hat{E}_n = T$ and the average energy is $\bar{E}_n = 2T$. The 'temperature' generally lies in the range $T = 0.5 - 1.0$ MeV for excitations produced in heavy nuclei by the giant-resonance effect. Figure 28 shows experimental spectra of neutrons released by 45-MeV electrons incident on targets of Pb and U [17]. The Pb spectrum is reasonably well described by a Maxwellian with $T = 0.98$ MeV. However, owing to the additional component of photofission neutrons, the uranium spectrum is more strongly enhanced at lower neutron energies than an evaporation spectrum.

When spectra are plotted as $\ln(E_n^{-1} dN/dE_n)$ versus E_n , the Maxwellian distribution appears on semilog paper as a straight line with a slope of $(-1/T)$. Figure 29 shows experimental data for W, Pb and Bi plotted in this manner,

TABLE XIII. NUCLEAR "TEMPERATURES" FOUND IN NEUTRON PHOTOPRODUCTION

Material	Z	Bremsstrahlung End-Point Energy E_0 (MeV)	Nuclear ^(a) "Temperature" (MeV)	Reference
Bi	83	15	0.93	18 Mutchler
		16	0.84	19 Glazunov et al.
		14.1 (monochromatic)	0.72	20 Kuchnir et al.
		18.9	1.1	21 Zatsepina et al.
		45	0.82	17 Gayther and Goode
Pb	82	15	1.31	18 Mutchler
		70	1.0	22 Dixon
		32.5	0.6	23 Breuer
		23	1.35	24 Toms and Stephens
		18.9	1.1	21 Zatsepina et al.
		16	0.98	19 Glazunov et al.
Tl	81	45	0.98	17 Gayther and Goode
		13.5 (b)	1.15	18 Mutchler
Hg	80	14 "	0.93	"
		13 "	0.85	"
Au	79	14 "	0.76	"
		13 "	0.66	"
Pt	78	16	0.48	19 Glazunov et al.
W	74	14 (b)	0.69	18 Mutchler
		45	0.44	17 Gayther and Goode
Ta	73	14 (b)	0.65	18 Mutchler
		13 "	0.64	"
Er	68	14 "	0.71	"
Ho	67	14 "	0.83	"
Sm	62	14 "	0.83	"
Pr	59	14 "	0.77	"
La	57	14 "	0.90	"
I	53	14.4 "	0.82	"
Sn	50	14.4 "	0.79	"
		14.4 (c)	0.69	"
In	49	14.4 (b)	0.69	"

(a) Data uncorrected for direct emission.

(b) Quasi-monochromatic (difference) photons. Neutron energy distribution fit from $E_n = 1$ to 3 MeV.

(c) As (b), but E_n fit from 1 to 2 MeV, instead.

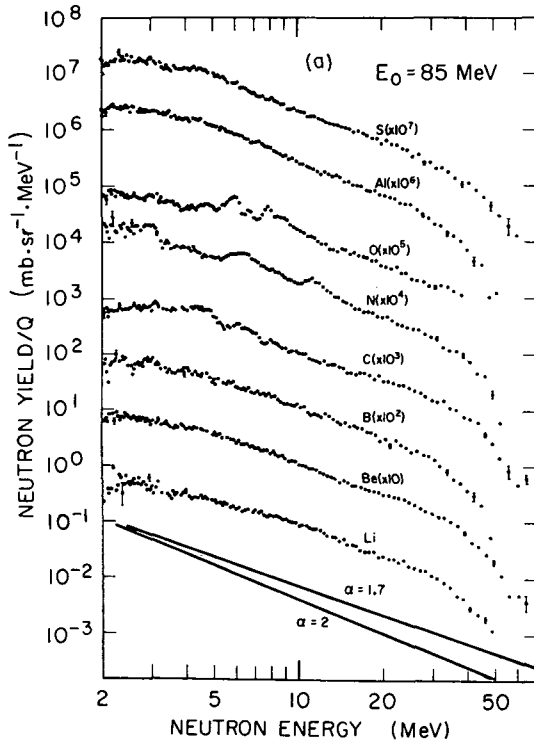


FIG.30a. Energy spectra of neutrons released by bremsstrahlung of end-point energy $E_0 = 85 \text{ MeV}$, incident on various elements. Q , as used in the ordinate title, means 'equivalent quantum'. This is a convenient measure of the amount of bremsstrahlung used to irradiate the material in question and is defined as the total incident bremsstrahlung energy divided by E_0 . Light elements ($Z = 3 - 16$). The lines drawn below show relative spectra of the form $E_n^{-\alpha}$ for comparison. (Adapted from Kaushal et al. [26], with kind permission of the authors and the Journal of Nuclear Energy.)

revealing 'temperatures' of 0.44, 0.98 and 0.82 MeV, respectively [17]. Deviations from this simple model occur for E_n less than 0.5 MeV and also at energies greater than about 3–4 MeV. Above this energy, the spectrum is dominated by direct neutron emission. The relationship between these two processes, as reflected in neutron spectra (and angular distributions), has been extensively investigated by Mutchler [18] for medium- to high- Z materials; for photon energies near the resonance maximum, it was found that direct emission accounts for about 14% of the neutrons emitted, the remainder being evaporation neutrons.

Nuclear temperatures depend somewhat on the average nuclear excitation energy E_{ex} and therefore on the bremsstrahlung spectrum employed. However, average excitation energies tend to be controlled by the peaking in the giant-

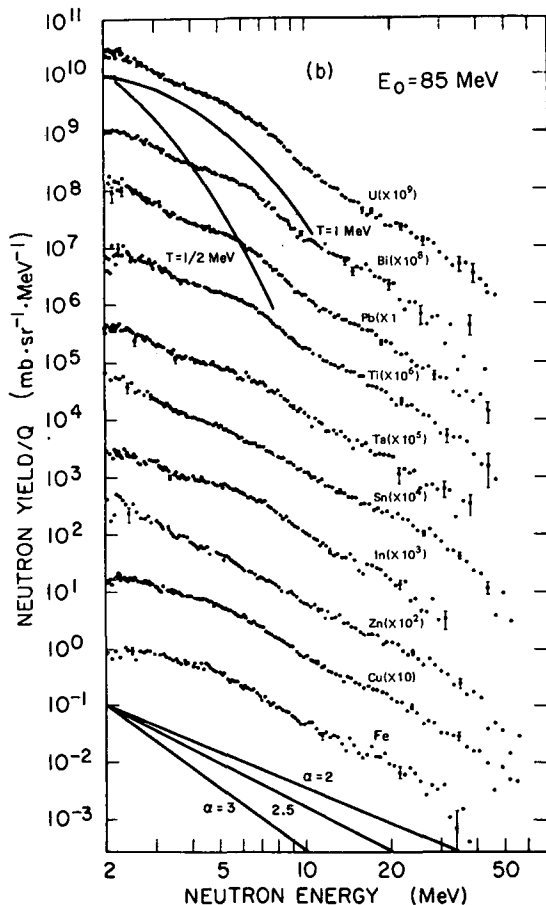


FIG.30b. Energy spectra of neutrons released by bremsstrahlung of end-point energy $E_0 = 85 \text{ MeV}$, incident on various elements. Q , as used in the ordinate title, means 'equivalent quantum'. This is a convenient measure of the amount of bremsstrahlung used to irradiate the material in question and is defined as the total incident bremsstrahlung energy divided by E_0 .

Medium ($Z = 26 - 50$) and heavy ($Z = 73 - 92$) elements. The solid curves above show relative shapes of the Maxwellian distribution for $T = \frac{1}{2}$ and 1 MeV , and the lines below show relative spectra of the form $E_n^{-\alpha}$ for comparison. (Adapted from Kaushal et al. [26], with kind permission of the authors and the Journal of Nuclear Energy.)

resonance cross-section and therefore tend to be near $E_{\text{ex}} \approx k_0 - k_{\text{th}}$, where k_0 is the photon energy of the peak of the (γ, n) giant-resonance cross-section and k_{th} is the threshold energy (see Table XII). Typical values of T , uncorrected for direct emission, are summarized by Mutchler for a variety of materials irradiated at various bremsstrahlung end-point energies, and with quasi-monochromatic photons, as shown in Table XIII.

The relative shapes of the spectra are not strongly dependent on target thickness. The trend, however, will be a small shift of the average energy towards a lower value with thicker targets. Of course, the spectrum emanating from a thick target will be influenced by inelastic collisions and absorption within the target itself, which are not considered here.

The evaporation spectra closely resemble the fission spectrum (Fig. 28 for Pb) [25]. This is convenient because there is a large body of data for shielding against neutrons with this energy distribution (Section 3.5).

Spectra of neutrons released by 55 and 85-MeV bremsstrahlung from a wide range of nuclei have been published by Kaushal et al. [26], as shown in Fig. 30 for $E_0 = 85$ MeV. All spectra seem qualitatively quite similar when plotted in this manner, but closer examination shows a systematic trend towards more rapid fall-off with increasing Z . The curves are reasonably well described by the Maxwellian (Eq. (26)) with $T \approx 1$, only for elements heavier than $Z \approx 30$ (zinc), and then only up to about 4 MeV. For lower Z , direct nucleon emission takes place more frequently, compared with evaporation, and the spectra are shifted towards higher energy.

The data of Fig. 30 were taken with thin-target bremsstrahlung incident on thin samples. For the case of neutrons produced in *thick* materials by incident bremsstrahlung or electrons, we would expect relatively more neutrons at lower energy.

(b) The quasi-deuteron effect

At photon energies above the giant resonance, the dominant neutron production mechanism remaining is one in which the photon interacts initially with a neutron-proton pair within the nucleus, rather than with the nucleus as a whole [4]; hence the name ‘quasi-deuteron’. The cross-section for this mechanism is about an order of magnitude below the giant-resonance peak (Fig. 25). The cross-section is related to the deuteron photodisintegration cross-section $\sigma_D(k)$ qualitatively as [27]:

$$\sigma_{QD}(k) \cong L \frac{NZ}{A} \sigma_D(k) \quad (27)$$

where N , A and Z are for the target nucleus ($N + Z = A$), σ_D is the cross-section for deuteron photodisintegration as a function of photon energy k , and the dimensionless coefficient L is in the range 3–13. L may be regarded as a measure of the probability that a neutron-proton pair is within a suitable interaction distance relative to the deuteron.¹² Direct evidence for this mechanism may be

¹² The value of L depends greatly on the assumptions of the analysis used. Values close to 10 take into account details of quasi-deuteron kinematics and undetected residual states. Discussions of these points are given by Garvey et al. [28] who quote $L = 10.3 \pm 2.6$, and Gabriel and Alsmiller [29, 30] who find that $L = 7.1$ best fits low- Z data, while $L = 12.5$ is required for Au.

found in the observation that the (γ, np) process is dominant in the energy region where the quasi-deuteron effect is expected to be most important.

The photodisintegration cross-section σ_D varies approximately as k^{-1} in the region extending up to the photopion threshold (see curve $\sigma_{QD}(L = 5)$ of Fig. 25):

$$\left. \begin{aligned} \sigma_D &= 7 \times 10^3 k^{-1} && (50 \lesssim k \lesssim 125) \\ &= 57 && (125 \lesssim k \lesssim 300) \\ &= 1.3 \times 10^9 k^{-3} && (300 \lesssim k) \end{aligned} \right\} \quad (28)$$

If k is in MeV, σ_D is in μb . When this trend is combined with the k -dependence of the bremsstrahlung spectrum (k^{-1} for thin targets, k^{-2} for thick targets, Sections 2.2, 2.4), we see that the low-energy region is heavily weighted.

The effect is to add a tail of higher-energy neutrons to the giant-resonance spectrum (Fig. 30). For example, at $E_0 = 100$ MeV, the additional yield released by photons above 30 MeV amounts to $(10 \pm 5)\%$ of the giant-resonance yield. In Fig. 30, most of the neutrons above 5 MeV are produced by this mechanism. Over the range $5 \text{ MeV} < E_n < E_0/2$ the spectrum of quasi-deuteron neutrons varies approximately as

$$\frac{dN}{dE_n} \approx E_n^{-\alpha} \quad (29)$$

where α increases slowly with Z :

Light nuclei	($Z = 3-16$)	$\alpha = 1.7-2.0$
Medium nuclei	($Z = 26-50$)	$\alpha = 2.6-2.8$
Heavy nuclei	($Z = 73-83$)	$\alpha = 3.0-3.3$
Fissionable nuclei	($Z = 92$)	$\alpha \approx 3.6$

These values apply to neutrons released by *thin*-target bremsstrahlung and the rapid fall-off with neutron energy reflects both the decline in the photon spectrum and in σ_D with photon energy k . For *thick*-target situations, the spectral fall-off with E_n would be steeper. For $E_n \geq E_0/2$, there are negligible numbers of neutrons; because it is a quasi-two-body final state, each nucleon takes typically about half of the available energy, and the maximum available energy is always less than E_0 .

The relatively smaller cross-sections and the rapid fall-off in neutron energy make the neutrons released by the quasi-deuteron effect relatively less of a hazard than giant-resonance neutrons, even though they are more penetrating.

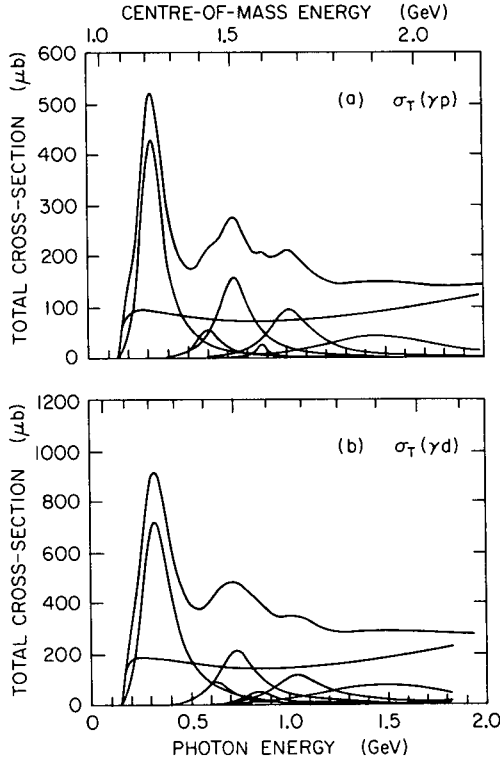


FIG.31. Elementary total cross-sections for photopion production as functions of photon energy. The solid curves drawn below show the contributions of resonances to the total. (a) Proton targets. (b) Deuteron targets. (Adapted from Ref. [35], with kind permission of the Glasgow-Sheffield-Daresbury Collaboration and Nuclear Physics.)

If adequate protection is provided against giant-resonance neutrons and, if needed, high-energy neutrons (discussed below), the quasi-deuteron neutrons are not generally a special problem.

(c) High-energy neutrons

Above 140 MeV, the cross-section for photons on nuclei rises again, owing to the opening of channels for photopion production. The cross-section goes through a number of resonance peaks, which all lie at about 1.1 GeV or below and are caused by nucleon isobar formation [31–33]. The largest peak is the first one, centred at about 300 MeV with a width of about 110 MeV (Figs 25, 31).

Above this, the γp and γn total cross-sections both decline at a very slow rate toward asymptotic values close to $100 \mu\text{b}$.¹³ In the region of a few GeV, $110 \mu\text{b}$ could represent an average cross-section value for purposes of calculation [34–37]. These peaks are only a fraction of the cross-section of the giant resonance, but the neutrons liberated in these reactions are *much more penetrating* than giant-resonance neutrons. In fact, at high-energy accelerators, these neutrons make the dominant contribution to dose rates outside of the massive concrete shields employed, even though the reverse is true on the inside of the shields where bremsstrahlung and giant-resonance neutrons dominate completely (Fig. 6) [38].

At high photon energies, the average momentum squared transferred to a nucleon tends toward a constant value $q^2 = 400 (\text{MeV}/c)^2$, independent of photon energy. This corresponds to an average kinetic energy of the released neutrons of approximately $q^2/2M \approx 200 \text{ MeV}$ at energies far above the pion threshold.

The weighting of the photon spectrum emphasizes the lowest energies, and we may expect the ‘first’ resonance, near 300 MeV, to contribute the most high-energy neutrons.

2.5.3. Neutron yields from electron beams

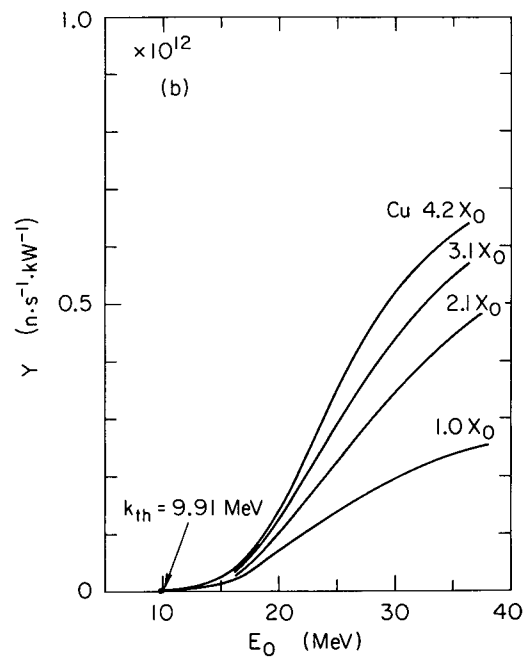
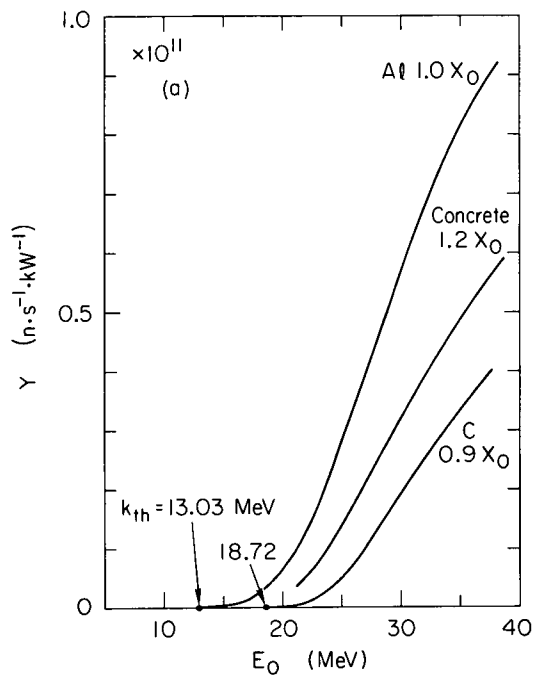
To assess the radiological significance of neutrons released at electron accelerators, it is necessary to combine the cross-sections for photoneutron production (the material of Section 2.5.2) with a realistic energy spectrum of the photons released within materials struck by the electrons (Section 2.2). In the estimation of yields in the following paragraphs, the point of view first taken is that the electron beam power is totally absorbed in a single medium. Such maximum yields set an upper limit from which one may scale to the actual situation. If, at the same time, we assume that the medium provides no self-shielding, we obtain a conservative starting point for the assessment of the neutron hazard. If warranted, self-shielding can be considered in a subsequent step of the assessment.

Where the yield, Y , is expressed in units of $\text{n} \cdot \text{s}^{-1} \cdot \text{kW}^{-1}$, the flux density (in $\text{n} \cdot \text{cm}^{-2} \cdot \text{s}^{-1}$) from a spherically symmetric source is obtained from the relationship:

$$\varphi = Y \cdot P / (4\pi d^2) \quad (30)$$

where P is the electron beam power in kW and d is the distance from the source to the location in question (for these flux-density units, d is in cm). To convert to dose-equivalent rate \dot{H} , a value for the average effective quality factor \bar{Q} is

¹³ Caldwell et al. [34] find a photon energy dependence in the range 4–18 GeV of $\sigma_T(\gamma p) = (98.7 \pm 3.6) + (65.0 \pm 10.1) k^{-\frac{1}{2}}$ and $\sigma_T(\gamma n) = (103.4 \pm 6.7) + (33.1 \pm 19.4) k^{-\frac{1}{2}}$, where k is the photon energy in GeV, and the cross-sections are in μb .



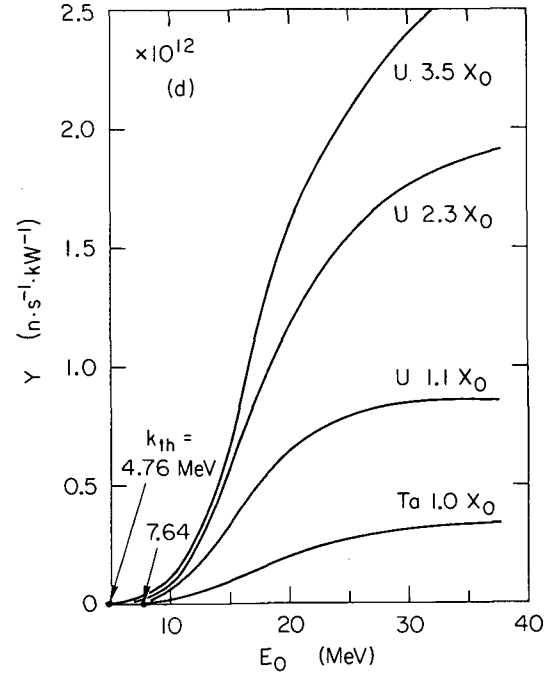
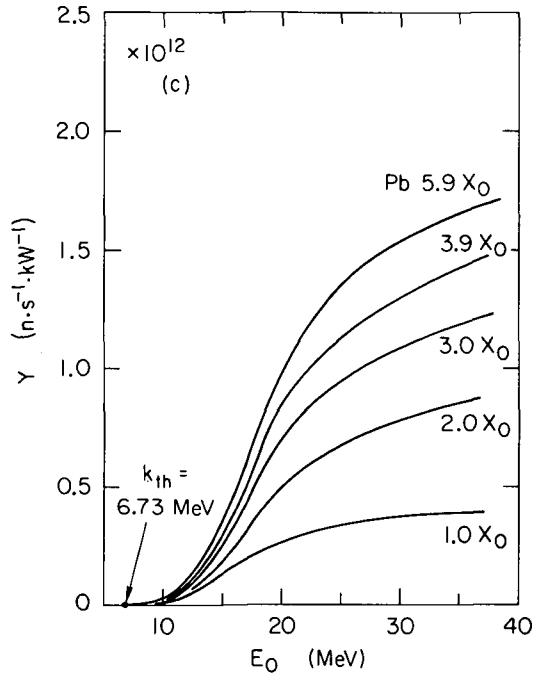


FIG.32. Yield of neutrons from electrons incident on various target materials, adapted from the work of Barber and George [39]. All targets contain isotopes in their naturally occurring abundances. Labels indicate thicknesses in radiation lengths. (Adapted from Ref.[39], with kind permission of W.C. Barber and W.D. George and the Physical Review.)

(a) Carbon, aluminium and concrete. The concrete was a simple 3:1 sand-cement mixture of unspecified elemental composition.

(b) Copper. (c) Lead. (d) Tantalum and uranium.

needed (Section 2.5.1). The Rule-of-Thumb equation (22) for 1-MeV neutrons provides a conservative but reasonable conversion for the dose-equivalent rate in the absence of shielding:

$$\dot{H} \cong 1.2 \times 10^{-8} Y \cdot P / (4\pi d^2) \quad (31)$$

where \dot{H} is in $\text{rem} \cdot \text{h}^{-1}$, and d is in metres for this and subsequent equations. As is shown below, we may take 2×10^{12} neutrons $\cdot \text{s}^{-1} \cdot \text{kW}^{-1}$ as indicative of the maximum neutron yield for *high-Z* materials (if photofissionable materials, $Z > 82$, are excluded). This gives the rule of thumb for the unshielded dose-equivalent rate:

$$\dot{H} \cong 2 \times 10^3 P/d^2 \quad (\text{Rule of Thumb}) \quad (32)$$

for accelerators operating above the giant-resonance energy. (One might use as a mnemonic: “The dose-equivalent rate at 1 m is twice the power in watts”.)

2.5.3.1. The giant-resonance region ($E_0 \gtrsim 35$ MeV)

The electron energy $E_0 = 35$ MeV is a convenient delimiter for the discussion of neutron yields because: (a) the giant resonance is well past its peak for all materials, and yields per unit electron beam power are close to saturation; (b) many of the published photoneutron integral cross-sections useful in estimating yields have their upper limit of integration near 30–35 MeV (Table XII); (c) good experimental and Monte-Carlo calculations on thick-target neutron yields are available near this energy.

(a) Experimental data and Monte-Carlo calculations

Barber and George [39] have measured total neutron yields released by electron beams at $E_0 = 34$ MeV from thick targets of natural materials. Their data are reproduced in Fig. 32 (a–d) and may be used to interpolate to other target thicknesses and materials, as discussed below.

Several Monte-Carlo calculations have also been made based on the elementary photoneutron cross-sections. A list of these calculations and their salient parameters is given in Table XIV.

(b) Yield as a function of target thickness

Figure 33 shows the yield in lead as a function of target thickness in radiation lengths (see Appendix B) for $E_0 = 34$ and 100 MeV, based on Monte-Carlo calculations of Alsmiller and Moran [42] and Hansen et al. [43]. Both curves are normalized to 1.0 at $10 X_0$. At $10 X_0$, the 34-MeV curve appears to

TABLE XIV. MONTE-CARLO CALCULATIONS OF THICK-TARGET
PHOTONEUTRON YIELDS

Authors	Ref.	Target Material	E_0 Range (MeV)	Thicknesses (Radiation Lengths)
Berger and Seltzer	40	Ta	7.8 - 20	0 - 1.87
		W	6.4 - 20	0 - 1.85
		W-Be ^(a)	10	0.44 W + 0 - 0.15 Be
Alsmiller and Moran	41	U	34, 100	1 - 10
Alsmiller and Moran	42	Cu	34	1 - 5
			100	1 - 10, 20
			200	1 - 10, 20
		Ta	30	1 - 10
			100	1 - 10, 20
			150	1 - 10, 20
Hansen, Bartoletti and Daitch	43	Cu	34	0 - 5
			15 - 34	1.04, 2.08, 3.13, 4.17
		Ta	100	0 - 10
			Pb	34
		U	100	0 - 10
			34	0 - 10
Alsmiller, Gabriel and Guthrie	44	Be	150	1, 20
		Ta	150	1, 20
Alsmiller and Barish	45	Cu	400	∞
Gabriel and Alsmiller	46	Cu	50, 400	∞
Gabriel	47	Cu	50 - 400	∞

(a) Composite target: 3 g.cm^{-2} ($0.44 X_0$) W followed by Be.

be fully saturated, but the 100-MeV curve continues to rise slightly to 1.04 at $20 X_0$ [42].

These integral curves indicate that most of the yield comes from the region $1-2 X_0$ where the slopes are greatest. Half of the yield is produced in the first two radiation lengths at 34 MeV, and in 2.7 radiation lengths at 100 MeV.

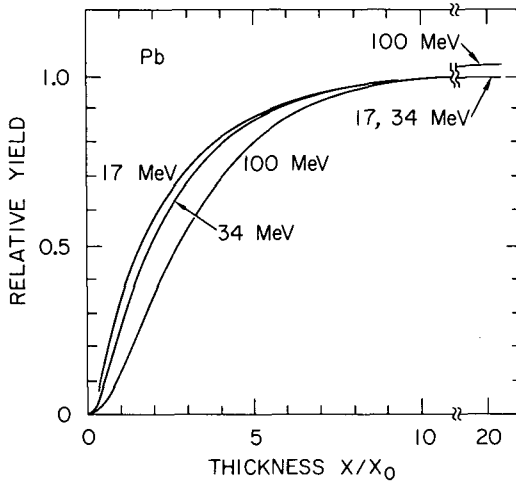


FIG.33. Relative yields of neutrons released by electron beams incident on lead targets at energies $E_0 = 100, 34$ and 17 MeV, as a function of target thickness in radiation lengths X_0 . The curves are qualitatively similar for other materials and energies, but the initial rise will tend to be steeper, and saturation will be more quickly achieved, for lower E_0 or lower Z . The curves for $E_0 = 34$ and 100 MeV are adapted from Alsmiller and Moran [42] and Hansen et al. [43]. The curve for $E_0 = 17$ MeV is an interpolation meant to be indicative of lower-energy behaviour.

At 100 MeV, the electromagnetic cascade continues deeper into the medium, regenerating the photon fluence in the giant-resonance region, thus explaining the small shift in the two curves.

When plotted in terms of radiation lengths, such yield curves should be relatively insensitive to type of material. The yield curves for Cu and Pb have been compared over the range $1-5 X_0$ and found to agree reasonably well [43]; the difference is that there is a steeper initial rise for Cu. Saturation is expected to occur somewhat sooner in lower- Z media because the incident electron loses its energy and ceases to be a source of neutron-producing bremsstrahlung in a shorter distance (measured in radiation lengths). The central portion (as represented, say, by the point at which the relative yield is 0.5) will be displaced from the curve for Pb at 100 MeV by an increment in X/X_0 roughly equal to $\ln(E_0/E_c) - 2.35$, where E_c is the material's critical energy (Section 2.2).

The integral yield curves of Fig. 33 are used to interpolate from a known yield at a given target thickness to obtain the yield at another thickness, or to extrapolate to the maximum possible yield. The curves are qualitatively similar

TABLE XV. APPROXIMATE NEUTRON YIELDS FROM THICK TARGETS

Z Material	Atomic Weight	Yield (10^{12} neutrons \cdot s $^{-1}$ \cdot kW $^{-1}$) ^(a)	
		34 MeV	100 MeV
6 Carbon	12.011	(0.05)	(0.1)
7 Nitrogen	14.007	(0.1)	(0.3)
8 Oxygen	15.999	(0.05)	(0.1)
13 Aluminum	26.982	0.2	0.5
Concrete		(0.09)	(0.2)
26 Iron	55.847	0.5	0.7
28 Nickel	58.710	0.4	0.6
29 Copper	63.546	0.8	1.0
73 Tantalum	180.948	(1.2)	(1.3)
74 Tungsten	183.850	(1.5)	(1.7)
78 Platinum	195.090	(1.6)	(1.8)
79 Gold	196.967	1.6	1.8
81 Thallium	204.370	(1.7)	(1.9)
82 Lead	207.190	1.6	1.8
Lead (b)		1.3 - 2.4	1.6 - 3.2
83 Bismuth	208.981	(1.5)	(1.7)
90 Thorium	232.038	(2.6)	(2.9)
92 Uranium (c)	238.029	3.5	3.9

(a) Unless otherwise indicated, yields obtained by numerical integration. Figures in parentheses represent interpolations based on published cross sections for the naturally-occurring element.

(b) Alsmiller and Moran, Ref. [42].

(c) Alsmiller and Moran, Ref. [41].

for other materials and energies. However, the trend is towards a steeper rise for lower E_0 or Z . Thus if the 34-MeV yield curve for lead is used for E_0 in the giant-resonance region, it will give an overestimate if extrapolated to thicker targets and an underestimate if interpolated to thinner targets.

For very thin targets ($X \ll X_0$), the yield from incident electron beams is approximately quadratic in X , for E_0 well above the giant-resonance energy (Table XII):

$$Y(X) \cong \frac{1 N_A \rho}{2 A} \frac{X^2}{X_0} \sigma_{-1} \quad (33)$$

where σ_{-1} is as defined in the preceding section (Table XII and Fig. 27). In this case, $Y(X)$ is the number of neutrons released *per incident electron*, N_A is Avogadro's number, ρ is the material density ($\text{g} \cdot \text{cm}^{-3}$), A is the gram-atomic weight (g) and X and X_0 (see Appendix B) are both in centimetres.

(c) Yields from semi-infinite targets

It is important to estimate the yield from infinitely thick media because in practice most of the neutrons to be shielded against are released in beam dumps that absorb virtually all of the electron beam energy. Regardless of the actual thickness, the assumption of infinite thickness is a conservative one when considering the object as a neutron source.

Recommended values of neutron yields per unit electron beam power for 34 MeV are shown in Table XV. They are based in part on the experiment of Barber and George [39], corrected for target thickness by means of the curve just described. After correction, the 34-MeV values are probably accurate to about $\pm 20\%$. Values in parentheses are more uncertain than this. Yields for other materials are interpolations made using published cross-sections for the natural materials, where available.

Total yields from infinitely thick targets of selected materials are calculated as a function of E_0 from threshold to 100 MeV, using a corrected version of Approximation B of the analytical shower theory (Section 2.2) and integrating over the elementary cross-sections compiled by Berman [9]. The resulting curves (Fig. 34) show the sigmoid rise of neutron yields (per incident beam power) with E_0 , and the absolute accuracy is about $\pm 20\%$ except for portions very close to the threshold [51].

There is more than an order of magnitude difference between the smallest and largest yields in Table XV and Fig. 34. This spread in values is largely systematic with Z , but there are also considerable deviations due to properties of specific nuclei, viz. nickel, calcium, titanium (anomalously low yield), beryllium (anomalously high), and uranium and thorium (high owing to photofission).

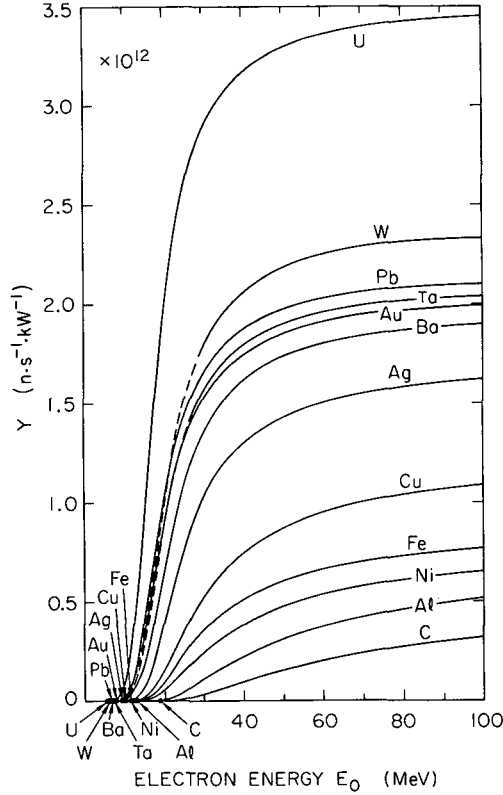


FIG. 34. Neutron yields from infinitely thick targets, per kW of electron beam power, as a function of electron beam energy E_0 , disregarding target self-shielding.

In order to interpolate the neutron yield to another material, Z_2 , it is best to take a value from Table XV at a nearby Z_1 and scale by the ratios of σ_{-2} (from Table XII):

$$Y(Z_2) = \frac{\sigma_{-2}(Z_2)}{\sigma_{-2}(Z_1)} Y(Z_1) \quad (34)$$

It should also be noted that some composite targets may produce more neutrons than can be inferred from these data: A high-Z target followed by a low-Z target will produce more neutrons than the low-Z target alone, even if the high-Z target is thin, because of the enhanced bremsstrahlung yield of high-Z materials (Fig. 16).

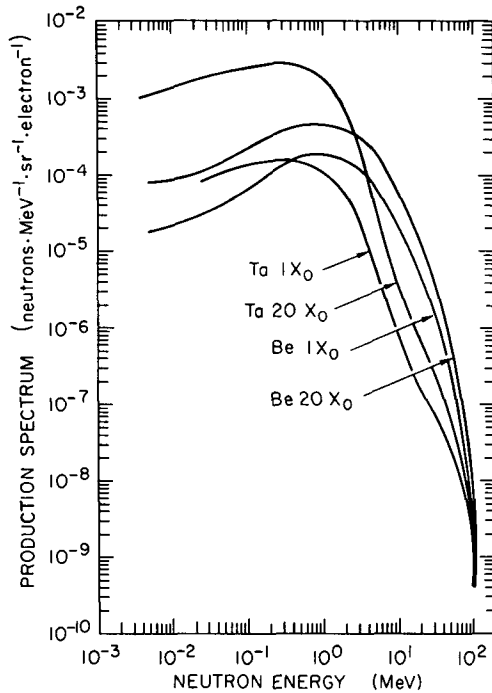


FIG.35. Total photon-neutron-production spectra released by 150-MeV electrons incident on Be and Ta targets $1 X_0$ and $20 X_0$ thick. (Adapted from Ref. [44], with kind permission of R.G. Alsmiller, Jr., T.A. Gabriel and M.P. Guthrie, and Nuclear Science and Engineering.)

The angular distribution of giant-resonance neutrons tends to be enhanced near 90° , typically by about a factor of 1.5 above the fluence averaged over all directions. For radiation protection purposes, it is recommended that the estimated yields be augmented by this amount at 90° , particularly as the shielding is usually thinnest in this direction from the target.

2.5.3.2. Neutron production for $34 < E_0 < 150$ MeV

In this energy region, between the giant-resonance and the onset of photopion production, neutron yields are relatively constant when normalized to unit electron beam power. Table XV shows estimated yields at 34 and 100 MeV. These may be extrapolated without much error to even higher energies.

The qualitative change that takes place as the energy is increased through this region is the increase in a small 'tail' of high-energy quasi-deuteron neutrons added to the much more copious giant-resonance distributions. These additional higher-energy neutrons tend to be more forward-peaked in their angular distribution.

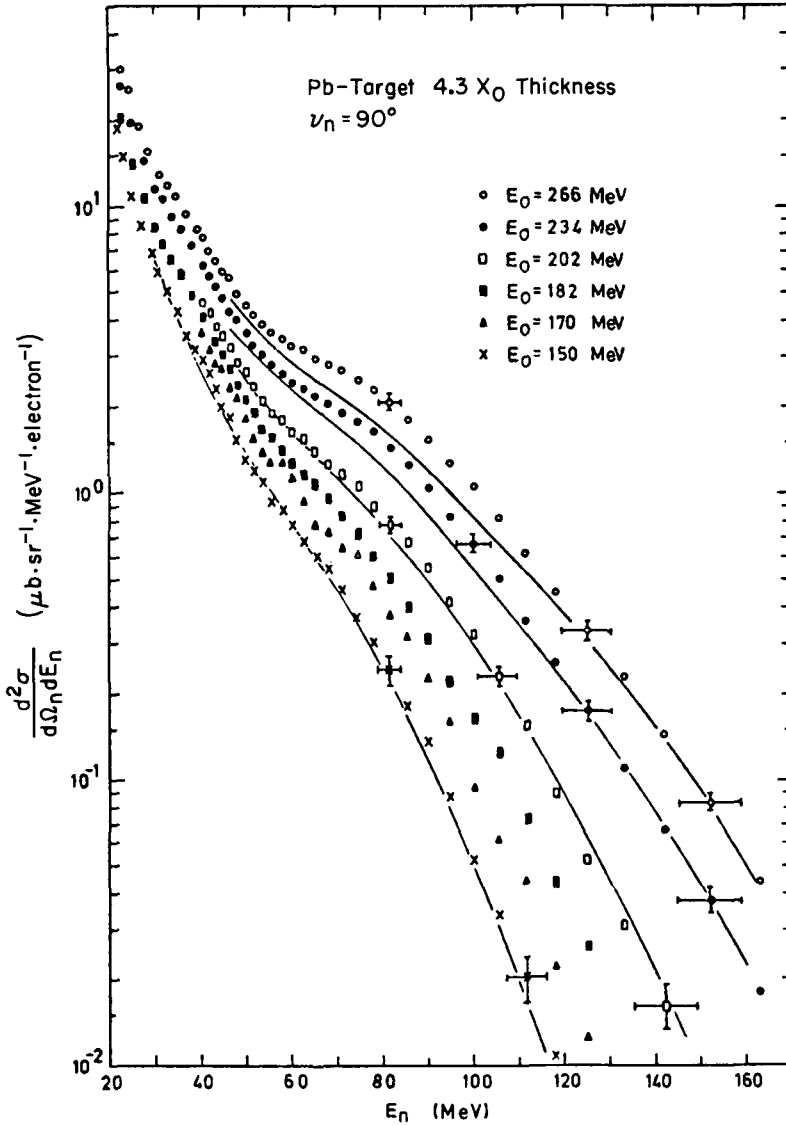


FIG.36. Photoneutron spectra produced at 90° by electrons of energy $E_0 = 150, 170, 182, 202, 234$ and 266 MeV, incident on a thick lead target ($4.3 X_0$). The solid lines are predictions of a quasi-deuteron model. (Adapted from Ref.[48], with kind permission of H.J. von Eyss and G. Lührs, and Zeitschrift für Physik.)

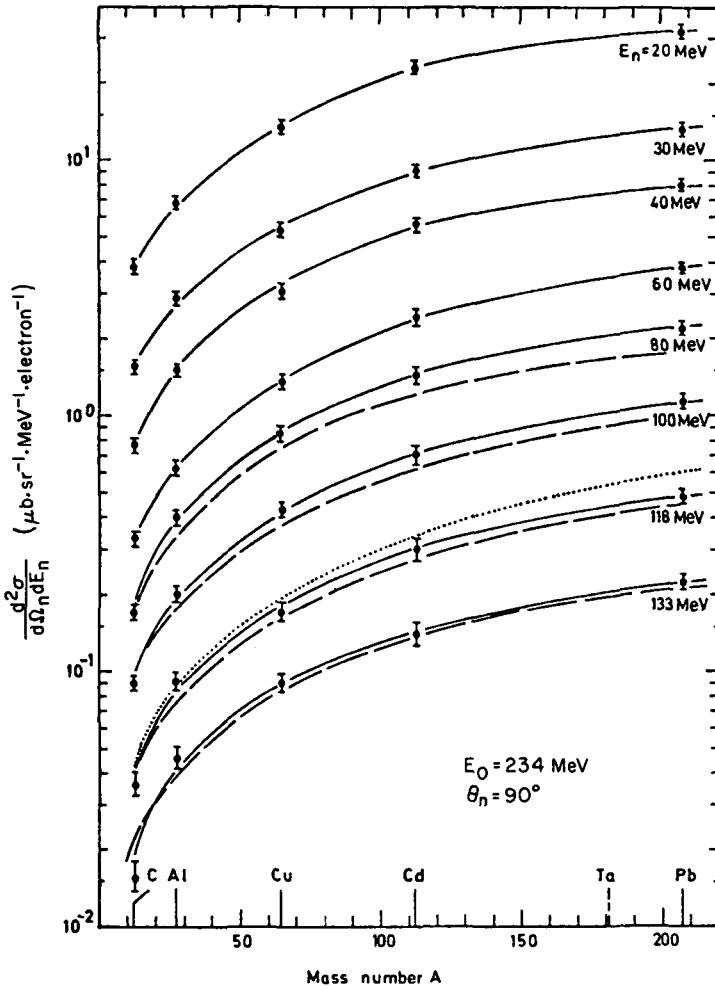


FIG.37. Neutron yields released at 90° by 234-MeV electrons incident on thin ($<1 X_0$) targets. Dependence of the cross-section on the mass number A of the target material, for a range of neutron energies. The solid curves connect the data points. The dashed curves are predictions of a quasi-deuteron model. The dotted curve represents the approximation NZ/A . (Adapted from Ref. [48], with kind permission of H.J. von Eyss and G. Lührs, and Zeitschrift für Physik.)

Monte-Carlo calculations have been done at various energies, particularly by the Alsmiller group, and references are shown in Table XIV. Figure 35, adapted from the Monte-Carlo calculations of Alsmiller et al. [44], shows total photon-neutron production spectra from 150-MeV electrons on Be and Ta, for targets of 1 and 20 radiation lengths. The 20 X_0 Ta spectral shape has been essentially verified in an experiment by von Eyss and Lührs [48].

Monte-Carlo calculations for infinitely thick copper targets have been made by Gabriel and Alsmiller for the energy range above 30 MeV [46, 47]. Neutron spectra are given by these authors for $E_0 = 50 - 400$ MeV. A particularly useful parameterization of the yields, based on the Monte-Carlo work, has been compiled by Gabriel for the same energy range [47]. Analytic forms for $E_0 = 50, 100, 300$ and 400 MeV, in five angular intervals, are given.

2.5.3.3. Neutron production for $E_0 > 150$ MeV

Neutron fluence and spectral measurements over the energy range $E_0 = 150$ to 270 MeV have been made by von Eyss and Lührs [48] for electron beams striking thick lead targets, and at 234 MeV for electrons incident on targets of C, Al, Cu, Cd and Pb. Absolute spectra for Pb are shown in Fig. 36. These data may be used directly as representative spectra from thick high- Z targets.

It was found that the relative shapes of the neutron spectra (Fig. 37) are relatively insensitive to target material (for the *thin* targets used in this portion of the experiment: $0.026-0.3 X_0$). The scale of the cross-section is closely proportional to NZ/A , consistent with the quasi-deuteron model (Section 2.5.2(b)). This behaviour is illustrated in Fig. 37, which shows the systematic rise of cross-section with A .

This spectral information is useful in making detailed shielding calculations. When making such calculations, it should be borne in mind that the effect of a thick target would be to distort the spectra obtained with thin targets, and to relatively enhance the lower-neutron-energy portion.

Qualitatively, the photon track length within thick targets scales as the radiation length X_0 (Eq. (6)). Because the radiation length (in units of $g \cdot cm^{-2}$) shortens with increasing Z approximately as $AZ^{-2} \propto Z^{-1}$ (Eq. (3)), the net result is that the total yield of high-energy neutrons actually decreases with increasing Z , approximately as Z^{-1} . This is illustrated in Fig. 35, which shows that the yield of high-energy neutrons (above 3 MeV neutron energy) from 20 X_0 of Be exceeds that from 20 X_0 of Ta.

For a rough estimate of a source term to estimate shielding needs in the energy region above $E_0 = 150$ MeV, it would be adequate to take the results for a *thick* lead (Fig. 36) or copper (Fig. 38) target and scale to the material in question by Z^{-1} . To scale to a different energy, one may assume that the neutron yield scales as electron beam *power*, over the electron range considered.

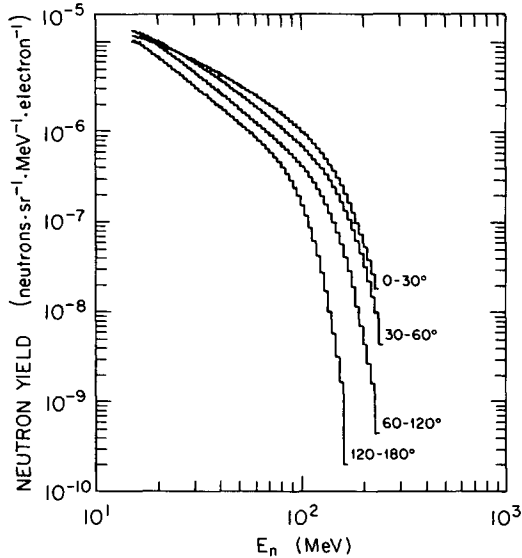


FIG.38. Neutron yield as a function of neutron energy, averaged over the indicated angular intervals, when 400-MeV electrons are incident on a thick copper target. (Adapted from Ref.[45], with kind permission of R.G. Alsmiller, Jr., and J. Barish, and Particle Accelerators.)

Calculations by Gabriel and Alsmiller, cited in the preceding section (Refs [46, 47]), are available in the energy range extending to $E_0 = 400$ MeV for thick copper targets. This energy includes the first pion-nucleon resonance, and the enhanced contribution of high-energy neutrons due to photopion production will be present. Figure 38, adapted from Alsmiller and Barish [45], shows the neutron spectrum in detail.

For very high energies an approach used by DeStaebler et al. [49] for calculating a neutron source term has proved useful. It is based on the following approximations:

(a) The cross-section per nucleus σ_{tot} for photoneutron production is taken to be the average of the γp and γn total cross-sections (Fig. 31), multiplied by the atomic weight A of the target nucleus.

(b) The kinematics of neutron production are considered to be two-body kinematics. That is, the final state is assumed to contain only a pi meson ($M_{\pi^0} = 134.96$ MeV, $M_{\pi^+} = 139.57$ MeV) in addition to the neutron ($M_n = 939.57$ MeV). At a given photon energy k , this determines the kinetic energy of the outgoing neutron at every laboratory angle θ .

(c) The differential cross-section is assumed to be isotropic in the two-body (π , n) centre-of-mass ($d\sigma/d\Omega^* = \sigma_{\text{tot}}/4\pi$). This, together with assumptions (a) and (b), determines completely the magnitude and shape of the laboratory

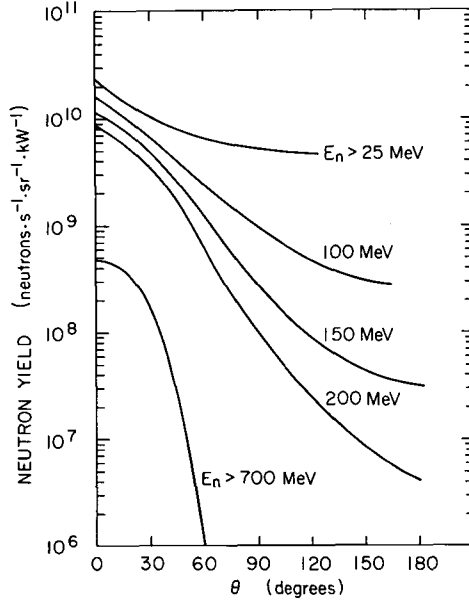


FIG.39. High-energy neutron production by electrons incident on copper, per kilowatt of electron beam power and per unit solid angle, as a function of production angle. The curves indicate the number of neutrons produced with energies greater than E_n (MeV). (Adapted from Ref. [49], with kind permission of H. DeStaebler, the Stanford Linear Accelerator Center, the Energy Research and Development Administration, and Addison-Wesley/Benjamin, New York.)

angular distribution of the outgoing neutrons at each incident photon energy k . When the photon energy spectrum is folded into the calculation, the spectrum of neutron kinetic energies at every laboratory angle can be obtained.

(d) The photon spectrum is expressed in terms of the track-length distribution of Approximation A (Eq. (6)) discussed in Section 2.2.

The integration over photon energy in an infinite copper target from $k = 150$ MeV to 20 GeV yields the laboratory neutron angular distribution of Fig. 39. The neutron energy spectra are shown in integral form, i.e. each curve shows the number of neutrons at each angle having energy *greater* than that indicated by its label. These data are not very sensitive to the primary electron energy E_0 as long as it is well above the first pion-nucleon resonance (Fig. 31).

The distributions of Fig. 39 were calculated for copper ($Z = 29$). For another choice of target material, these distributions would scale approximately as Z^{-1} (or A^{-1}), reflecting the shortening of the radiation length X_0 with increasing Z and thereby of the photon track length in the same proportion, as discussed

TABLE XVI. NEUTRON YIELDS RELEASED BY 6-GeV ELECTRONS INCIDENT ON THICK TARGETS^a

Neutron energy range	Yield ($n \cdot s^{-1} \cdot kW^{-1}$)		
	Al	Cu	Pb
$E_n < 25$ MeV	1.1×10^{12}	2.2×10^{12}	2.6×10^{12}
$E_n > 25$ MeV	1.7×10^{11}	1.2×10^{11}	0.83×10^{11}

^a Adapted from Bathow et al. [50].

above. The yield of neutrons released by 6-GeV electrons incident on thick targets of Al, Cu and Pb has been measured by Bathow et al. [50] (Table XVI). A decreasing trend of high-energy neutrons ($E_n > 25$ MeV) with increasing Z is seen in their data, although not as strong a trend as the simplified theory would predict.

REFERENCES TO SECTION 2.5

- [1] INTERNATIONAL COMMISSION ON RADIATION UNITS AND MEASUREMENTS, Neutron Fluence, Neutron Spectra and Kerma, ICRU Report No.13, Washington, DC (1969).
- [2] NATIONAL COUNCIL ON RADIATION PROTECTION AND MEASUREMENTS, Protection Against Neutron Radiation, NCRP Report No.38, Washington, DC (1971).
- [3] INTERNATIONAL COMMISSION ON RADIOLOGICAL PROTECTION, Data for Protection Against Ionizing Radiation from External Sources: Supplement to ICRP Publication 15, ICRP Publication No.21, Pergamon Press, Oxford (1973).
- [4] LEVINGER, J.S., Nuclear Photodisintegration, Oxford University Press (1960).
- [5] HAYWARD, E., Photonuclear Reactions, National Bureau of Standards, Washington, DC, Monograph 118 (1970).
- [6] FIRK, F.W.K., "Low-energy photonuclear reactions", Annual Reviews of Nuclear Science 20, Annual Reviews, Inc., Palo Alto, CA (1970) 39.
- [7] FULLER, E.G., HAYWARD, E., Photonuclear Reactions, Dowden, Hutchinson and Ross, Stroudsburg, PA (1976).
- [8] BERMAN, B.L., FULTZ, S.C., Giant-Resonance Measurements with Monoenergetic Photons, Lawrence Livermore Laboratory, Rep. UCRL-75383 (1974); Rev. Mod. Phys.47 (1975) 713.
- [9] BERMAN, B.L., Atlas of Photoneutron Cross Sections Obtained with Monoenergetic Photons, Lawrence Livermore Laboratory, Rep. UCRL-74622 (1974); At. Data Nucl. Data Tables 15 (1975) 319.
Supplement: Atlas of Photoneutron Cross Sections Obtained with Monochromatic Photons, Bicentennial Edition, Lawrence Livermore Laboratory, Rep. UCRL-78482 (1976).

- [10] PRICE, G.A., KERST, D.W., Yields and angular distributions of some gamma-neutron processes, *Phys. Rev.* **77** (1950) 806.
- [11] MONTALBETTI, R., KATZ, L., GOLDEMBERG, J., Photoneutron cross sections, *Phys. Rev.* **91** (1953) 659.
- [12] JONES, L.W., TERWILLIGER, K.M., Photoneutron production excitation functions to 320 MeV, *Phys. Rev.* **91** (1953) 699.
- [13] FULLER, E.G., GERSTENBERG, H.M., VANDER MOLEN, H., DUNN, T.C., Photonuclear Reaction Data, 1973, National Bureau of Standards, Washington, DC, NBS Special Publication No. 380 (1973). Supplement (1976).
- [14] ANTONESCU, V.I. (Comp.), Photonuclear Reactions, Bibliographical Series No. 10, IAEA, Vienna (1964).
- [15] IONESCU, V. (Comp.), Photonuclear Reactions, Vol. II, Bibliographical Series No. 27, IAEA, Vienna (1967).
- [16] BÜLOW, B., FORKMAN, B., Photonuclear Cross Sections, University of Lund, Rep. LUNP-7208 (May 1972).
- [17] GAYTHER, D.B., GOODE, P.D., Neutron energy spectra and angular distributions from targets bombarded by 45-MeV electrons, *J. Nucl. Energy* **21** (1967) 733.
- [18] MUTCHLER, G.S., The Angular Distributions and Energy Spectra of Photoneutrons from Heavy Elements, Ph.D. Thesis, Massachusetts Institute of Technology, Rep. MIT-2098-224 (1966) 234–42 (available from ERDA Technical Information Center, Oak Ridge, TN).
- [19] GLAZUNOV, Yu.Ya., SAVIN, M.V., SAFINA, I.N., FOMUSHKIN, E.V., KHOKLOV, Yu.A., Photoneutron spectra of platinum, bismuth, lead and uranium, *Zh. Ehksp. Teor. Fiz.* **46** (1964) 1906; *Sov. Phys. – JETP* **46** (1964) 1284.
- [20] KUCHNIR, F.T., AXEL, P., CRIEGEE, L., DRAKE, D.M., HANSON, A.O., SUTTON, D.C., Univ. of Illinois, Urbana, private communication to G.S. Mutchler (Ref. [18]) (1966).
- [21] ZATSEPINA, G.N., IGONIN, V.V., LAZAREVA, L.E., LEPESTKIN, A.I., Angular and energy distributions of photoneutrons from bismuth, gold and tantalum, *Zh. Ehksp. Teor. Fiz.* **44** (1963) 1787; *Sov. Phys. – JETP* **17** 8 (1963) 1200.
- [22] DIXON, W.R., Energy and angular distributions of photoneutrons produced by 70-MeV X-rays, *Can. J. Phys.* **33** 12 (1955) 785.
- [23] BREUER, H., Die Energieverteilung schneller Photoneutronen aus Blei, *Z. Naturforsch.* **17a** (1962) 584.
- [24] TOMS, M.E., STEPHENS, W.E., Photoneutrons from lead, *Phys. Rev.* **108** 1 (1957) 77.
- [25] NATIONAL BUREAU OF STANDARDS, Shielding for High-Energy Electron Accelerator Installations, NBS Handbook No. 97, Washington, DC (1964).
- [26] KAUSHAL, N.N., WINHOLD, E.J., AUGUSTON, R.H., YERGIN, P.F., MEDICUS, H.A., Absolute neutron yields and energy spectra from 18 targets bombarded by 55 and 85 MeV bremsstrahlung, *J. Nucl. Energy* **25** (1971) 91.
- [27] LEVINGER, J.S., The high energy nuclear photoeffect, *Phys. Rev.* **84** (1951) 43.
- [28] GARVEY, J., PATRICK, B.H., RUTHERGLEN, J.G., SMITH, I.L., Correlated neutron-proton pairs from the photodisintegration of oxygen, *Nucl. Phys.* **70** (1965) 241.
- [29] GABRIEL, T.A., ALSMILLER, R.G., Jr., Photonuclear disintegration at high energies (< 350 MeV), *Phys. Rev.* **182** 4 (1969) 1035.
- [30] GABRIEL, T.A., High-Energy ($40 \text{ MeV} \lesssim E_\gamma \lesssim 400 \text{ MeV}$) Photonuclear Interactions, Oak Ridge National Laboratory, Rep. ORNL-TM-4926 (1975).
- [31] PARTICLE DATA GROUP, Review of Particle Properties, Lawrence Berkeley Laboratory, Rep. LBL-100 (1974); and *Phys. Lett.* **50B** (1974) 1.

- [32] BEALE, J.T., ECKLUND, S.C., WALKER, R.L., Pion Photoproduction Data below 1.5 GeV, Synchrotron Laboratory, California Institute of Technology, Pasadena, CA, Rep. CTSL-42, CALT-68-108 (1966).
- [33] SPILLANTINI, P., VALENTE, V., A Collection of Pion Photoproduction Data: I: From the Threshold to 1.5 GeV, European Organization for Nuclear Research (CERN), Rep. CERN/HERA 70-1 (1970).
- [34] CALDWELL, D.O., ELINGS, V.B., HESSE, W.P., MORRISON, R.J., MURPHY, F.V., Total hadronic photoabsorption cross sections on hydrogen and complex nuclei from 4 to 18 GeV, *Phys. Rev.* **D7** (1973) 1362.
- [35] ARMSTRONG, T.A., HOGG, W.R., LEWIS, G.M., ROBERTSON, A.W., BROOKES, G.R., CLOUGH, A.S., FREELAND, J.H., GALBRAITH, W., KING, A.F., RAWLINSON, W.R., TAIT, N.R.S., THOMPSON, J.C., TOLFREE, D.W.L., The total photon deuteron hadronic cross section in the energy range 0.265–4.215 GeV, *Nucl. Phys.* **B41** (1972) 445.
- [36] JOOS, P., Compilation of Photoproduction Data Above 1.2 GeV, Deutsches Elektronen-Synchrotron, Hamburg, Rep. DESY-HERA 70-1 (1970).
- [37] JOOS, P., Literature on Photoproduction Experiments, Deutsches Elektronen-Synchrotron, Hamburg, Int. Rep. DESY FI-75/04 (1975).
- [38] NELSON, W.R., JENKINS, T.M., Similarities among the radiation fields at different types of high-energy accelerators, *IEEE Trans. Nucl. Sci.* **NS-23** 4 (1976) 1.
- [39] BARBER, W.C., GEORGE, W.D., Neutron yields from targets bombarded by electrons, *Phys. Rev.* **116** (1959) 1551.
- [40] BERGER, M.J., SELTZER, S.M., Bremsstrahlung and photoneutrons from thick tungsten and tantalum targets, *Phys. Rev.* **C2** (1970) 621.
- [41] ALSMILLER, R.G., Jr., MORAN, H.S., Photoneutron production from 34- and 100-MeV Electrons in thick uranium targets, *Nucl. Instrum. Meth.* **51** (1967) 339.
- [42] ALSMILLER, R.G., Jr., MORAN, H.S., Electron-Photon Cascade Calculations and Neutron Yields from Electrons in Thick Targets, Oak Ridge National Laboratory, Rep. ORNL-1502; *Nucl. Instrum. Meth.* **48** (1967) 109.
- [43] HANSEN, E.C., BARTOLETTI, C.S., DAITCH, P.B., Analog Monte Carlo studies of electron-photon cascades and the resultant production and transport of photoneutrons in finite three-dimensional systems, *J. Appl. Phys.* **46** (1975) 1109.
- [44] ALSMILLER, R.G., Jr., GABRIEL, T.A., GUTHRIE, M.P., The energy distribution of photoneutrons produced by 150-MeV electrons in thick beryllium and tantalum targets, *Nucl. Sci. Eng.* **40** (1970) 365.
- [45] ALSMILLER, R.G., Jr., BARISH, J., Shielding against the neutrons produced when 400-MeV electrons are incident on a thick copper target, *Part. Accel.* **5** (1973) 155.
- [46] GABRIEL, T.A., ALSMILLER, R.G., Jr., Photonucleon and Photopion Production from High-Energy (50–400 MeV) Electrons in Thick Copper Targets, Oak Ridge National Laboratory, Rep. ORNL-4443, UC-34-Physics (1969).
- [47] GABRIEL, T.A., Analytic Representation of Photonucleon and Photopion Differential Yields Resulting from High-Energy Electrons ($50 \leq E_0 \leq 400$ MeV) Incident on an Infinite Copper Target, Oak Ridge National Laboratory, Rep. ORNL-4442, UC-34-Physics (1969).
- [48] von EYSS, H.J., LÜHRS, G., Photoproduction of high-energy neutrons in thick targets, *Z. Phys.* **262** (1973) 393.
- [49] DeSTAEBLER, H., JENKINS, T.M., NELSON, W.R., "Shielding and radiation", Ch.26, The Stanford Two-Mile Accelerator (NEAL, R.B., Gen. Ed.), Benjamin, New York (1968).
- [50] BATHOW, G., FREYTAG, E., TESCH, K., Measurements on 6.3 GeV Electromagnetic Cascades and Cascade-Produced Neutrons, *Nucl. Phys.* **B2** (1967) 669.
- [51] SWANSON, W.P., Calculation of neutron yields released by electrons incident on selected materials, *Health Phys.* **35** (1978) 353; also see Stanford Linear Accelerator Center, Rep. SLAC-PUB-2211 (1978).

2.6. Radioactivity induced in components

Radioactivity may be induced in components that are irradiated by an electron or bremsstrahlung beam, to an extent that depends on the energy, beam power, and type of material. Some degree of activity is probable at energies above about 10 MeV. Precise thresholds for various reactions can be found in Ref. [1]. Three types of photon-induced reactions produce most of the activity (see also Section 2.5.2):

- (a) The giant photonuclear resonance
- (b) The quasi-deuteron effect
- (c) High-energy photospallation reactions.

The components to be most suspected for activation are those that absorb most of the bremsstrahlung energy, in particular:

- (a) Beam dumps
- (b) Targets
- (c) Collimators and jaws
- (d) Compensating filters.

To a lesser extent, copper accelerator components, and iron in steel shielding and ferrite materials may also become activated. In addition, significant activity may be induced by secondary neutrons if the beam power is high enough to release large neutron fluences. The photodisintegration of deuterium (threshold = 2.23 MeV), beryllium (threshold = 1.67 MeV), and the photofission of, for example, uranium (threshold = 5.8 MeV) may yield neutron fluences sufficiently large for radioactivity to be induced in nearby components.

The subject of induced activity has been extensively treated by Barbier [2], and a shorter review of the subject has been published by Gollon [3].

Casual observation around high-energy targets and beam dumps suggests a qualitative grouping of common materials as shown in Table XVII. It is evident that lead, concrete and aluminium are preferred, where otherwise suitable, and that fissionable materials such as uranium are undesirable in terms of activation potential.

Operationally, the exposures to accelerator-induced activity are almost entirely direct external exposures. The probability of ingestion of radionuclides from components or even target-room dust is very small. Nevertheless, control over the machining and soldering of radioactive components should be maintained and irradiations of loosely-bound materials should be monitored if the beam energy and power are such that activation may be significant.

Data on induced activity are most conveniently summarized in terms of *saturation* activity, A_s , per unit beam power, following the precedent of NBS Handbook 97, Table VI [4]. This is the amount of activity to be found at the instant of accelerator turnoff if it has been operating steadily for a period of

TABLE XVII. DEGREE OF SUSCEPTIBILITY OF COMMON MATERIALS TO ACTIVATION BY HIGH-ENERGY ELECTRON AND PHOTON BEAMS (QUALITATIVE)

Relatively insensitive to activation	Moderately susceptible to activation	Highly susceptible to activation	Fissionable
Lead (antimony-free)	Iron (steel, ferrites)	Stainless steel	Uranium
Ordinary concrete	Copper	Tungsten	Plutonium
Aluminium		Tantalum	Thorium
Wood		Zinc	
Plastics		Gold	
		Manganese	
		Cobalt	
		Nickel	

time long compared with the half-life of the produced nuclide(s). In practice, two or three times $T_{1/2}$ is a reasonable buildup time for which to assume saturation to be approximately reached. This means that for nuclides with $T_{1/2}$ in the range of seconds or minutes, it may be assumed that saturation is reached each time an irradiation is made. For longer half-lives, the pattern of accelerator use must be considered. For $T_{1/2}$ of the order of several years or more, saturation may never be closely approached. The saturation activities A_s are directly proportional to electron beam power P .

A calculation based on Approximation A (Section 2.2) will yield a value for the saturation activity that is usually accurate enough:

$$A_s \text{ (Ci)} = \left[\frac{P}{eE_0} \right] \cdot \left[\frac{N_0 \rho}{A} \right] \cdot [0.572 E_0 X_0 \sigma_{-2}] \cdot \left[\frac{1}{3.7 \times 10^{10}} \right] \tag{Approx. A} \quad (35)$$

$$A_s \text{ (Bq)} = \left[\frac{P}{eE_0} \right] \cdot \left[\frac{N_0 \rho}{A} \right] \cdot [0.572 E_0 X_0 \sigma_{-2}]$$

in which the first factor converts the average beam power P to electrons per second, using the electronic charge e and energy E_0 . The third factor is an integration of the cross-section $\sigma(k)$ over the Approximation A track-length distribution. After cancelling out E_0 and multiplying by the specific gamma-ray constant Γ [5-7], we may estimate the saturation exposure rate \dot{X}_s for gamma emitters:

$$\dot{X}_s = kP \frac{X_0}{A} \Gamma \sigma_{-2} \quad (36)$$

where P is in kW, X_0 is in $\text{g} \cdot \text{cm}^{-2}$, A is in grams, and σ_{-2} is in $\mu\text{b} \cdot \text{MeV}^{-1}$. If \dot{X}_s is to be in $\text{m}^2 \cdot \text{C} \cdot \text{kg}^{-1} \cdot \text{h}^{-1}$, then Γ will be in $(\text{C} \cdot \text{kg}^{-1} \cdot \text{h}^{-1})(\text{Bq} \cdot \text{m}^{-2})^{-1}$, and the numerical value of k will be 2.15×10^9 ; if \dot{X}_s is to be in $\text{R} \cdot \text{m}^2 \cdot \text{h}^{-1}$, Γ will be in $(\text{R} \cdot \text{h}^{-1})(\text{Ci} \cdot \text{m}^{-2})^{-1}$ and k will be 5.81×10^{-2} .

Parameters that are important in estimating \dot{X} are σ_{-2} , Γ and $T_{1/2}$, the half-life of the produced nuclide. Values of σ_{-2}^{tot} for the giant resonance are shown in Fig.26 and Table XII.

It is useful to remember that the value of σ_{-2} for (γ, n) reactions always dominates, except for $A \lesssim 60$ where $\sigma_{-2}(\gamma, p)$ is comparable. For heavy nuclei ($A \gtrsim 100$), the σ_{-2} values in $\text{mb} \cdot \text{MeV}^{-1}$ for the most common reactions stand in the approximate relation

$$\sigma_{-2}[(\gamma, n):(\gamma, 2n):(\gamma, p):(\gamma, np):(\gamma, \alpha)] \approx [10:3:0.1:0.01:5 \times 10^{-4}] \quad (37)$$

These may be used for order-of-magnitude estimates for $E_0 \gtrsim 20 \text{ MeV}$, if data are not available.

The nuclides listed in Table XVIII will be copiously produced because they are (γ, n) reactions. Whether they pose significant radiation protection problems depends also on their half-lives and the nature of their emissions. Some of them are analysed in greater detail in the following paragraphs.

The exact formula for exposure rate \dot{X} in $\text{m}^2 \cdot \text{C} \cdot \text{kg}^{-1} \cdot \text{h}^{-1}$ ($\text{m}^2 \cdot \text{R} \cdot \text{h}^{-1}$) assuming steady beam power P in kW and saturation activity A_s in $\text{Bq} \cdot \text{kW}^{-1}$ ($\text{Ci} \cdot \text{kW}^{-1}$), is:

$$\dot{X} = A_s \cdot P \cdot \Gamma \cdot [1 - \exp(-0.693 t_b/T_{1/2})] \cdot \exp(-0.693 t_d/T_{1/2}) \quad (38)$$

where t_b is the buildup or irradiation time, t_d is the decay time following turnoff, and $T_{1/2}$ is the half-life of the nuclide. The specific gamma-ray constant Γ in $(\text{C} \cdot \text{kg}^{-1} \cdot \text{h}^{-1})(\text{Bq} \cdot \text{m}^{-2})^{-1}$ ($(\text{R} \cdot \text{h}^{-1})(\text{Ci} \cdot \text{m}^{-2})^{-1}$) relates the exposure rate \dot{X} , produced by gamma rays and internal X-rays from a point source, to the activity of the source and is of primary importance in evaluating the *external* exposure from induced activity. Its value depends on the energy and average number of photons emitted in nuclide decay [8]. Values of Γ are shown for each radio-nuclide in Table XVIII and subsequent tables of this section.¹⁴

¹⁴ The values of Γ given here are based on $W = 33.7 \text{ eV}$ per ion pair for air, the nuclide decay schemes of Lederer et al. [8], and values of (μ_{en}/ρ) of Storm and Israel for air [9]. See Table B-IV, Appendix B. Some Γ -values differ significantly from those found in other tabulations. The main difference is that the present values include the contribution, if any, of K X-rays, whereas other tabulations may not.

TABLE XVIII. RADIONUCLIDES PRODUCED IN (γ, n) REACTIONS

Target nuclide	(γ, n) Threshold energy (MeV)	Product nuclide	Γ , Specific gamma-ray constant ^{a,b}		Product half-life ^a
			$((R \cdot h^{-1})(Ci \cdot m^{-2})^{-1})$	$((C \cdot kg^{-1} \cdot h^{-1})(Bq \cdot m^{-2})^{-1})$	
C-12	18.72	C-11	0.59	4.11×10^{-15}	20.34 min
N-14	10.55	N-13	0.59	4.11×10^{-15}	9.96 min
O-16	15.67	O-15	0.59	4.11×10^{-15}	123. s
Al-27	13.03	Al-26m	0.59	4.11×10^{-15}	6.37 s
Fe-54	13.62	Fe-53	0.65	4.53×10^{-15}	8.51 min
Cu-65	9.91	Cu-64	0.38	2.65×10^{-15}	12.80 h
Zn-70	9.29	Zn-69	0.27	1.88×10^{-15}	13.8 h
			0.00	0	57.0 min
Se-82	9.18	Se-81	0.39	2.72×10^{-15}	56.8 min
			0.003	0.021×10^{-15}	18.6 min
Ag-107	9.39	Ag-106	1.35	9.41×10^{-15}	8.5 d
			0.46	3.21×10^{-15}	23.96 min
In-115	9.03	In-114	0.14	0.976×10^{-15}	50.0 d
			0.004	0.028×10^{-15}	72. s
Sb-121	9.28	Sb-120	0.33	2.30×10^{-15}	15.89 min
			1.43	9.97×10^{-15}	5.8 d
I-127	9.15	I-126	0.25	1.74×10^{-15}	12.8 d
Pr-141	9.37	Pr-140	0.33	2.30×10^{-15}	3.39 min
Ta-181	7.64	Ta-180m	0.04	0.279×10^{-15}	8.15 h
W-182	7.99	W-181	0.07	0.488×10^{-15}	140. d
Au-197	8.07	Au-196	0.14	0.976×10^{-15}	9.7 h
			0.28	1.95×10^{-15}	6.18 d
Pb-204	8.38	Pb-203	0.33	2.30×10^{-15}	6.1 s
			0.18	1.26×10^{-15}	52.1 h

^a Where two values are given, the first refers to the metastable state.

^b See Footnote 14.

The total gamma exposure rate is found by summing the \dot{X} for each radionuclide. Self-shielding, which is not considered in Eqs (36) or (38), will be helpful in reducing exposure rates, particularly for high-Z materials.

For complete information on radiological implications of *all* decay modes (including α and β radiations), nuclide data tabulations should be consulted [8]. This is not normally necessary, but is essential where ingestion is involved.

Fortunately, exposure through ingestion at electron accelerators is insignificant compared with external exposure, except under very special circumstances.

2.6.1. Installations with $E_0 < 35 \text{ MeV}$

Because activation cross-sections are rapidly varying in the energy range 10–20 MeV, a special discussion is devoted to the energy range below 35 MeV in which the majority of electron linacs operate.

The saturation activity A_s in becquerels (1 Bq = 1 disintegration per second) or in curies (1 Ci = 3.7×10^{10} disintegrations per second) per electron beam power (in kW) incident on the 'absorber' is calculated for several materials by numerical integration using published photonuclear cross-sections [10] folded together with the photon track-length distribution used for Section 2.5 from Approximation B (corrected, Section 2.2), consistent with the calculations of neutron production of the previous section. All natural isotopes of the target material are considered as potential sources of radionuclides and the exact thresholds for each reaction are used. At energies below 35 MeV, only reactions of the type (γ, n) , (γ, p) , (γ, np) and $(\gamma, 2n)$ are considered. For more complicated types of photoreactions, thresholds are generally too high and cross-sections too small to be important below 35 MeV. These results are shown in Table XIX. The activities resulting from (γ, n) and $(\gamma, 2n)$ reactions are probably accurate to about $\pm 30\%$. The activities resulting from (γ, p) and (γ, np) reactions are less accurate.

Because cross-sections are rapidly changing in the energy range considered here, the E_0 -dependence of the specific activity, normalized to incident electron beam power, will be sigmoid in nature, resembling the curves of Fig.34, and close to saturation at 35 MeV for high-Z materials.

It is assumed that the material in question absorbs *all* of the beam power. For electrons on thin targets the activity would be proportional to curves similar to those shown in Fig.33.

2.6.2. Activity induced by high-energy beams

At higher energies, reactions involving more emitted nucleons and having correspondingly higher thresholds come into play. Components that are barely activated at therapeutic energies may become quite activated in high-power beams at high energy. At high energy, photospallation plays an important role. This is a process in which any number of nucleons may be ejected by a nucleus, as a result of an intranuclear cascade followed by release of evaporation nucleons.

The activation data in Tables XX–XXVII apply to high-energy electron beams totally absorbed in the materials listed. They are valid (to within a factor of two) for any beam energy E_0 at least somewhat above the nuclide production threshold. The data do not contain corrections for self-shielding of the material

Text continued on p.125

TABLE XIXa. SATURATION ACTIVITY IN VARIOUS TARGET MATERIALS AS A FUNCTION OF ELECTRON BEAM ENERGY E_0 (SI units)

Target material	Radio-nuclide	$T_{1/2}$	Threshold (MeV)	Γ^a ((aC·kg ⁻¹ ·s ⁻¹)(Bq·m ⁻²) ⁻¹)	Saturation activity (GBq·kW ⁻¹) ^b											
					Accelerator energy E_0 (MeV)											
					10	15	20	25	30	35						
Al	Na-24	14.96 h	23.71	3.54	—	—	—	0.02	0.37	1.1						
	Al-26m	6.37 s	13.03	1.14	—	0.74	37.	140.	244.	325.						
Fe	Mn-54	303 d	20.42	2.32	—	—	—	5.9	17.	22.						
	Mn-56	2.576 h	10.57	1.67	—	0.11	0.52	0.89	1.1	1.2						
	Fe-53	8.51 min	13.62	1.30	—	0.37	9.6	19.	25.	27.						
Ni	Ni-56	6.10 d	22.5	3.06	—	—	—	0.11	1.26	2.4						
	Co-56	77.3 d	—	4.40												
	Ni-57	36.0 h	12.19	2.62												
	Co-57	270 d	—	2.50												
Cu	Cu-61	3.32 h	19.73	1.38	—	—	~0.004	8.5	24.	32.						
	Cu-62	9.76 min	10.84	1.16	—	28.	177.	318.	407.	407.						
	Cu-64	12.80 h	9.91	0.74	~0.0004	22.	103.	155.	177.	185.						
W	Ta-182	16.5 min	7.15	0.29	0.629	6.2	11.	13.	13.	13.						
		115.1 d		1.18												
	Ta-183	5.0 d	7.71	0.29							1.0	12.	21.	23.	23.	23.
	W-181	140 d	7.99	0.17							10.	148.	281.	318.	329.	336.
	W-185	1.62 min	7.27	0.35							17.	170.	270.	290.	300.	300.
75 d		no γ														

Target material	Radio-nuclide	$T_{1/2}$	Threshold (MeV)	Γ^a (($\mu\text{C}\cdot\text{kg}^{-1}\cdot\text{s}^{-1}$)($\text{Bq}\cdot\text{m}^{-2}$) $^{-1}$)	Saturation activity ($\text{GBq}\cdot\text{kW}^{-1}$) ^b						
					Accelerator energy E_0 (MeV)						
					10	15	20	25	30	35	
Au	Au-195	30.6	s	14.80	0.29	—	<0.04	74.	159.	196.	203.
		183	d		0.14						
	Au-196	9.7	h	8.07	0.21	55.	740.	1300.	1440.	1480.	1520.
		6.18	d		0.56						
Pb	Pb-203	52.1	h	8.38	0.35	0.48	8.1	15.	17.	17.	17.
	Pb-204m	66.9	min	14.85	2.21	—	<0.004	12.	27.	37.	44.

^a Where two values are given, the first is for the metastable state. See Footnote 14.

^b Activity per incident electron beam power.

^c The first nuclide is parent of the second.

TABLE XIXb. SATURATION ACTIVITY IN VARIOUS TARGET MATERIALS AS A FUNCTION OF ELECTRON BEAM ENERGY E_0 (special units)

Target material	Radionuclide	$T_{1/2}$	Threshold (MeV)	Γ^a ($(R \cdot h^{-1})(Ci \cdot m^{-2})^{-1}$)	Saturation activity ($Ci \cdot kW^{-1}$) ^b					
					Accelerator energy E_0 (MeV)					
					10	15	20	25	30	35
Al	Na-24	14.96 h	23.71	1.83	—	—	—	0.0005	0.010	0.03
	Al-26m	6.37 s	13.03	0.59	—	0.02	1.0	3.8	6.6	8.8
Fe	Mn-54	303 d	20.42	1.20	—	—	—	0.16	0.45	0.59
	Mn-56	2.576 h	10.57	0.86	—	0.003	0.014	0.024	0.030	0.032
	Fe-53	8.51 min	13.62	0.67	—	0.01	0.26	0.52	0.67	0.74
Ni	Ni-56	6.10 d	22.5	1.58	—	—	—	0.003	0.034	0.066
	Co-56	77.3 d	—	2.27						
	Ni-57	36.0 h	12.19	1.35	—	0.10	1.2	2.6	3.6	4.2
	Co-57	270 d	—	1.29						
Cu	Cu-61	3.32 h	19.73	0.71	—	—	$\sim 10^{-4}$	0.23	0.65	0.87
	Cu-62	9.76 min	10.84	0.60	—	0.77	4.8	8.6	11.	11.
	Cu-64	12.80 h	9.91	0.38	$\sim 10^{-5}$	0.62	2.8	4.2	4.8	5.0
W	Ta-182	16.5 min	7.15	0.15	0.017	0.17	0.31	0.35	0.36	0.36
		115.1 d		0.61						
	Ta-183	5.0 d	7.71	0.15	0.027	0.34	0.56	0.61	0.62	0.63
	W-181	140 d	7.99	0.09	0.27	4.0	7.6	8.6	8.9	9.1
	W-185	1.62 min	7.27	0.18	0.47	4.5	7.3	7.9	8.1	8.1
75 d		no γ		} c						

Target material	Radionuclide	$T_{1/2}$	Threshold (MeV)	Γ^a ((R·h ⁻¹)(Ci·m ⁻²) ⁻¹)	Saturation activity (Ci·kW ⁻¹) ^b					
					Accelerator energy E_0 (MeV)					
					10	15	20	25	30	35
Au	Au-195	30.6 s	14.80	0.15	-	<10 ⁻³	2.0	4.3	5.3	5.5
		183 d		0.07						
	Au-196	9.7 h	8.07	0.11						
					1.5	20.	35.	39.	40.	41.
Pb	Pb-203	52.1 h	8.38	0.18	0.013	0.22	0.41	0.45	0.46	0.47
	Pb-204m	66.9 min	14.85	1.14	-	<10 ⁻⁴	0.33	0.74	1.0	1.2

^a Where two values are given, the first is for the metastable state. See Footnote 14.

^b Activity per incident electron beam power.

^c The first nuclide is parent of the second.

TABLE XXa. SATURATION ACTIVITY INDUCED BY HIGH-ENERGY ELECTRONS (SI units)

Material: Concrete^a

Daughter nuclide			Dominant production			Assumed abundance of parent by weight (%)	A _s ^{d,e} Saturation activity (GBq·kW ⁻¹)	Ẋ _s ^f Saturation exposure rate ((μC·kg ⁻¹ ·h ⁻¹)(kW·m ⁻²) ⁻¹)
Nuclide	T _½	Γ ^b ((fC·kg ⁻¹ ·h ⁻¹)(Bq·m ⁻²) ⁻¹)	Parent isotope	Type	Threshold (MeV)			
C-11	20.34 min	4.11	C-12	(γ,n)	18.72	0.10	0.13	0.54
O-15	123 s	4.11	O-16	(γ,n)	15.67	53	96.	400.
Na-22	2.62 a	8.30	Na-23	(γ,n)	12.44	1.6	3.7	31.
Mg-23	12.1 s	4.32	Mg-24	(γ,n)	16.55	0.16	0.27	1.2
Al-26m	6.37 s	4.11	Al-27	(γ,n)	13.03	3.4	0.034	0.14
Si-27	4.14 s	4.11	Si-28	(γ,n)	17.18	31	74.	310.
K-38	7.71 min	10.88	K-39	(γ,n)	13.08	1.2	3.7	40.
Fe-53	8.51 min	4.53	Fe-54	(γ,n)	13.62	0.08	3.7 × 10 ⁻³	0.02

See footnotes on page 122.

TABLE XXb. SATURATION ACTIVITY INDUCED BY HIGH-ENERGY ELECTRONS (special units)

Material: Concrete^a

Daughter nuclide			Dominant production			Assumed abundance of parent by weight (%)	A _s ^{d,e} Saturation activity (Ci·kW ⁻¹)	X _s ^f Saturation exposure rate ((R·h ⁻¹)(kW·m ⁻²) ⁻¹)
Nuclide	T _{1/2}	Γ ^b ((R·h ⁻¹)(Ci·m ⁻²) ⁻¹)	Parent isotope	Type	Threshold (MeV)			
C-11	20.34 min	0.59	C-12	(γ,n)	18.72	0.10	3.5 × 10 ⁻³	2.1 × 10 ⁻³
O-15	123 s	0.59	O-16	(γ,n)	15.67	53	2.6	1.5
Na-22	2.62 a	1.19	Na-23	(γ,n)	12.44	1.6	0.1	0.12
Mg-23	12.1 s	0.62	Mg-24	(γ,n)	16.55	0.16	7.3 × 10 ⁻³	4.5 × 10 ⁻³
Al-26m	6.37 s	0.59	Al-27	(γ,n)	13.03	3.4	9.2 × 10 ⁻⁴	5.4 × 10 ⁻⁴
Si-27	4.14 s	0.59	Si-28	(γ,n)	17.18	31	2.0	1.2
K-38	7.71 min	1.56	K-39	(γ,n)	13.08	1.2	0.1	0.15
Fe-53	8.51 min	0.65	Fe-54	(γ,n)	13.62	0.08	1.0 × 10 ⁻⁴	6.4 × 10 ⁻⁵

See footnotes on page 122.

TABLE XXIa. SATURATION ACTIVITY INDUCED BY HIGH-ENERGY ELECTRONS (SI units)

Material: Natural aluminium ^a										
Daughter nuclide				Dominant production			Cross-section ^c		A _s ^e	Ẋ _s ^f
Nuclide	T _½	Γ ^b	((fC · kg ⁻¹ · h ⁻¹)(Bq · m ⁻²) ⁻¹)	Parent isotope	Type	Threshold (MeV)	Σfσ ₋₂ (μb · MeV ⁻¹)	Note ^d	Saturation activity (GBq · kW ⁻¹)	Saturation exposure rate ((μC · kg ⁻¹ · h ⁻¹)(kW · m ⁻²) ⁻¹)
Be-7	53.6	d	0.20	Al-27	(γ, sp)	32.95	2.3	S	4.8	1.0
C-11	20.34	min	4.11	Al-27	(γ, sp)	33.53	1.0	S	1.9	7.7
N-13	9.96	min	4.11	Al-27	(γ, sp)	25.56	0.3	S	0.5	2.1
O-15	123	s	4.11	Al-27	(γ, sp)	33.43	1.4	S	2.5	10.
F-18	109.7	min	4.04	Al-27	(γ, sp)	34.39	2.8	S	5.2	21.
Ne-24	3.38	min	2.16	Al-27	(γ, 3p)	33.11	0.07	S	0.11	0.26
Na-22	2.62	a	8.30	Al-27	(γ, 3n2p)	22.51	4.7	S	9.3	77.
Na-24	14.96	h	12.62	Al-27	(γ, 1n2p)	23.71	5.4	S	10.	131.
Al-25	7.24	s	4.11	Al-27	(γ, 2n)	24.41	0.75	S	1.4	5.9
Al-26	7.4 × 10 ⁵	a	9.62	Al-27	(γ, n)	13.03	420	B	330.	1550. ^g 670.
Al-26m	6.37	s	4.11							
Mg-27 ⁱ	9.46	min	3.42	Al-27	(γ, π ⁺)	≈140	0.3	S	0.59	2.0

See footnotes on page 122.

TABLE XXIIb. SATURATION ACTIVITY INDUCED BY HIGH-ENERGY ELECTRONS (special units)

Material: Natural aluminium^a

Daughter nuclide				Dominant production			Cross-section ^c		A _s ^e	Ẋ _s ^f
Nuclide	T _{1/2}		Γ ^b ((R·h ⁻¹)(Ci·m ⁻²) ⁻¹)	Parent isotope	Type	Threshold (MeV)	Σfσ ₋₂ (μb·MeV ⁻¹)	Note ^d	Saturation activity (Ci·kW ⁻¹)	Saturation exposure rate ((R·h ⁻¹)(kW·m ⁻²) ⁻¹)
Be-7	53.6	d	0.029	Al-27	(γ,sp)	32.95	2.3	S	0.13	0.004
C-11	20.34	min	0.59	Al-27	(γ,sp)	33.53	1.0	S	0.051	0.03
N-13	9.96	min	0.59	Al-27	(γ,sp)	25.56	0.3	S	0.013	0.008
O-15	123	s	0.59	Al-27	(γ,sp)	33.43	1.4	S	0.067	0.04
F-18	109.7	min	0.58	Al-27	(γ,sp)	34.39	2.8	S	0.14	0.08
Ne-24	3.38	min	0.31	Al-27	(γ,3p)	33.11	0.07	S	0.0031	0.001
Na-22	2.62	a	1.19	Al-27	(γ,3n2p)	22.51	4.7	S	0.25	0.30
Na-24	14.96	h	1.83	Al-27	(γ,1n2p)	23.71	5.4	S	0.28	0.51
Al-25	7.24	s	0.59	Al-27	(γ,2n)	24.41	0.75	S	0.039	0.023
Al-26	7.4 × 10 ⁵	a	1.38	Al-27	(γ,n)	13.03	420	B	8.8	6.0 ^g 2.6 ^g
Al-26m	6.37	s	0.59							
Mg-27 ⁱ	9.46	min	0.49	Al-27	(γ,π ⁺)	≈140	0.3	S	0.016	0.008

See footnotes on page 122.

TABLE XXIIa. SATURATION ACTIVITY INDUCED BY HIGH-ENERGY ELECTRONS (SI units)

Material: Natural iron ^a										
Daughter nuclide				Dominant production			Cross-section ^c		A _s ^e	X _s ^f
Nuclide	T _{1/2}		Γ ^b ((fC·kg ⁻¹ ·h ⁻¹)(Bq·m ⁻²) ⁻¹)	Parent isotope	Type	Threshold (MeV)	Σfσ ₋₂ (μb·MeV ⁻¹)	Note ^d	Saturation activity (GBq·kW ⁻¹)	Saturation exposure rate ((μC·kg ⁻¹ ·h ⁻¹)(kW·m ⁻²) ⁻¹)
Sc-46	83.9 d		7.60	Fe-54	(γ,sp)	37.41	(15)	E	(7.4)	(52.)
V-48	16.0 d		13.60	Fe-54	(γ,sp)	25.86	30	D*	(15.)	(206.)
Cr-51	27.8 d		5.30	Fe-54	(γ,sp)	19.74	(30)	E	(15.)	(77.)
Mn-52	5.60 d		15.20	Fe-54	(γ,np)	20.89		B	1.3	$\left\{ \begin{array}{l} 10. \\ 5.9 \end{array} \right.$ ^g
Mn-52m	21.1 min		9.05							
Mn-54	303 d		8.37	Fe-56	(γ,np)	20.42		B	22.	180.
Mn-56	2.576 h		6.00	Fe-57	(γ,p)	10.57		B	1.2	7.
Fe-52 ^j	8.2 h		5.02	Fe-54	(γ,2n)	24.06		B	2.1	10.
Fe-53	8.51 min		4.67	Fe-54	(γ,n)	13.62		B	27.	126.
Fe-55	2.60 a		4.81	Fe-56	(γ,n)	11.21		B	490.	230.
Fe-59 ^h	45.6 d		4.32	Fe-58	(n,γ)	—		—	—	— ^h

See footnotes on page 122.

TABLE XXIIb. SATURATION ACTIVITY INDUCED BY HIGH-ENERGY ELECTRONS (special units)

Material: Natural iron^a

Daughter nuclide			Dominant production			Cross-section ^c		A _s ^e	Ẋ _s ^f
Nuclide	T _½	Γ ^b ((R·h ⁻¹)(Ci·m ⁻²) ⁻¹)	Parent isotope	Type	Threshold (MeV)	Σfσ ₋₂ (μb·MeV ⁻¹)	Note ^d	Saturation activity (Ci·kW ⁻¹)	Saturation exposure rate ((R·h ⁻¹)(kW·m ⁻²) ⁻¹)
Sc-46	83.9 d	1.09	Fe-54	(γ,sp)	37.41	(15)	E	(0.2)	(0.2)
V-48	16.0 d	1.95	Fe-54	(γ,sp)	25.86	30	D*	(0.4)	(0.8)
Cr-51	27.8 d	0.76	Fe-54	(γ,sp)	19.74	(30)	E	(0.4)	(0.3)
Mn-52	5.60 d	2.18	Fe-54	(γ,np)	20.89		B	0.036	0.039
Mn-52m	21.1 min	1.30							
Mn-54	303 d	1.20	Fe-56	(γ,np)	20.42		B	0.59	0.70
Mn-56	2.576 h	0.86	Fe-57	(γ,p)	10.57		B	0.032	0.027
Fe-52 ^j	8.2 h	0.72	Fe-54	(γ,2n)	24.06		B	0.056	0.040
Fe-53	8.51 min	0.67	Fe-54	(γ,n)	13.62		B	0.74	0.49
Fe-55	2.60 a	0.69	Fe-56	(γ,n)	11.21		B	13.3	9.0
Fe-59 ^h	45.6 d	0.62	Fe-58	(n,γ)	—		—	—	— ^h

See footnotes on page 122.

TABLE XXIIIa. SATURATION ACTIVITY INDUCED BY HIGH-ENERGY ELECTRONS (SI units)

Material: Natural nickel^a

Daughter nuclide			Dominant production			Cross-section ^c		A _s ^e	X _s ^f
Nuclide	T _{1/2}	Γ ^b ((fC·kg ⁻¹ ·h ⁻¹)(Bq·m ⁻²) ⁻¹)	Parent isotope	Type	Threshold (MeV)	Σfσ _s (μb·MeV ⁻¹)	Note ^d	Saturation activity (GBq·kW ⁻¹)	Saturation exposure rate ((μC·kg ⁻¹ ·h ⁻¹)(kW·m ⁻²) ⁻¹)
Ni-56	6.10 d	11.01	Ni-58	(γ, 2n)	22.45		B	3.7	41.
Co-56 ^k	77.3 d	15.83						3.7	57.
Ni-57	36.0 h	9.41	Ni-58	(γ, n)	12.19		B	218.	2040.
Co-57 ^k	270 d	9.00						218.	1940.
Co-60	5.263 a	9.06	Ni-61	(γ, p)	9.86			(3.7)	(26.)

See footnotes on page 122.

TABLE XXIIIb. SATURATION ACTIVITY INDUCED BY HIGH-ENERGY ELECTRONS (special units)

Material: Natural nickel^a

Daughter nuclide			Dominant production			Cross-section ^c		A _s ^e	X _s ^f
Nuclide	T _{1/2}	Γ ^b ((R·h ⁻¹)(Ci·m ⁻²) ⁻¹)	Parent isotope	Type	Threshold (MeV)	Σfσ ₋₂ (μb·MeV ⁻¹)	Note ^d	Saturation activity (Ci·kW ⁻¹)	Saturation exposure rate ((R·h ⁻¹)(kW·m ⁻²) ⁻¹)
Ni-56	6.10 d	1.58	Ni-58	(γ, 2n)	22.45		B	0.1	0.16
Co-56 ^k	77.3 d	2.27						0.1	0.22
Ni-57	36.0 h	1.35	Ni-58	(γ, n)	12.19		B	5.9	7.9
Co-57 ^k	270 d	1.29						5.9	7.5
Co-60	5.263 a	1.30	Ni-61	(γ, p)	9.86			(0.1)	(0.1)

See footnotes on page 122.

TABLE XXIVa. SATURATION ACTIVITY INDUCED BY HIGH-ENERGY ELECTRONS (SI units)

Material: Natural copper^a

Daughter nuclide			Dominant production			Cross-section ^c		A _s ^e	X _s ^f
Nuclide	T _{1/2}	Γ ^b ((fC·kg ⁻¹ ·h ⁻¹)(Bq·m ⁻²) ⁻¹)	Parent isotope	Type	Threshold (MeV)	Σfσ ₋₂ (μb·MeV ⁻¹)	Note ^d	Saturation activity (GBq·kW ⁻¹)	Saturation exposure rate ((μC·kg ⁻¹ ·h ⁻¹)(kW·m ⁻²) ⁻¹)
Co-58	71.3 d	7.87	Cu-63	(γ,sp)	41.75		Sa	~24.	95.
Co-58m	9.2 h	4.53							
Co-60	5.263 a	9.05	Cu-63	(γ,n2p)	18.86		Sa	24.	214.
Ni-63	92 a	no γ	Cu-65	(γ,np)	17.11		B	17.	no γ
Cu-61	3.32 h	4.95	Cu-63	(γ,2n)	19.73		B	32.	157.
Cu-62	9.76 min	4.18	Cu-63	(γ,n)	10.84		B	407.	1680.
Cu-64	12.80 h	2.65	Cu-65	(γ,n)	9.91		B	185.	490.
Cu-66 ^h	5.10 min	0.36	Cu-65	(n,γ)	—		—	—	— ^h

See footnotes on page 122.

TABLE XXIVb. SATURATION ACTIVITY INDUCED BY HIGH-ENERGY ELECTRONS (special units)

Material: Natural copper^a

Daughter nuclide			Dominant production			Cross-section ^c		A _s ^e	Ẋ _s ^f
Nuclide	T _{1/2}	Γ ^b ((R·h ⁻¹)(Ci·m ⁻²) ⁻¹)	Parent isotope	Type	Threshold (MeV)	Σfσ ₋₂ (μb·MeV ⁻¹)	Note ^d	Saturation activity (Ci·kW ⁻¹)	Saturation exposure rate ((R·h ⁻¹)(kW·m ⁻²) ⁻¹)
Co-58	71.3 d	1.13	Cu-63	(γ,sp)	41.75		Sa	~0.66	0.37 ^g
Co-58m	9.2 h	0.65							
Co-60	5.263 a	1.30	Cu-63	(γ,n2p)	18.86		Sa	0.65	0.83
Ni-63	92 a	no γ	Cu-65	(γ,np)	17.11		B	0.45	no γ
Cu-61	3.32 h	0.71	Cu-63	(γ,2n)	19.73		B	0.87	0.61
Cu-62	9.76 min	0.60	Cu-63	(γ,n)	10.84		B	11.	6.5
Cu-64	12.80 h	0.38	Cu-65	(γ,n)	9.91		B	5.0	1.9
Cu-66 ^h	5.10 min	0.052	Cu-65	(n,γ)	—		—	—	— ^h

See footnotes on page 122.

TABLE XXVa. SATURATION ACTIVITY INDUCED BY HIGH-ENERGY ELECTRONS (SI units)

Material: Natural tungsten^a

Daughter nuclide			Dominant production			Cross-section ^c		A _s ^e	X _s ^f
Nuclide	T _{1/2}	Γ ^b ((fC·kg ⁻¹ ·h ⁻¹)(Bq·m ⁻²) ⁻¹)	Parent isotope	Type	Threshold (MeV)	Σfσ ₋₂ (μb·MeV ⁻¹)	Note ^d	Saturation activity (GBq·kW ⁻¹)	Saturation exposure rate ((μC·kg ⁻¹ ·h ⁻¹)(kW·m ⁻²) ⁻¹)
Ta-180m	8.15 h	0.27	W-182	(γ,np)	14.66		B	1.8	0.26 ^g
Ta-182m	16.5 min	1.05	W-183	(γ,p)	7.15		B	13.	{ 7. 28. } ^g
Ta-182	115.1 d	4.25							
Ta-183	5.0 d	1.05	W-184	(γ,p)	7.71		B	23.	23.
Ta-184	8.7 h	5.86	W-186	(γ,np)	14.91		B	1.8	10.
Ta-185	50 min	0.77	W-186	(γ,p)	8.39		B	21.	16.
W-181	140 d	0.63	W-182	(γ,n)	7.99		B	330.	206.
W-183m	5.3 s	0.77	W-184	(γ,n)	7.42		B	320.	110. ^g
W-185	75 d	no γ	W-186	(γ,n)	7.27		B	300.	{ no γ 190. } ^g
W-185m	1.62 min	1.26							
W-187 ^h	23.9 h	1.81	W-186	(n,γ)	—		—	—	— ^h

See footnotes on page 122.

TABLE XXVb. SATURATION ACTIVITY INDUCED BY HIGH-ENERGY ELECTRONS (special units)

Material: Natural tungsten^a

Daughter nuclide			Dominant production			Cross-section ^c		A _s ^e Saturation activity (Ci·kW ⁻¹)	Ẋ _s ^f Saturation exposure rate ((R·h ⁻¹)(kW·m ⁻²) ⁻¹)
Nuclide	T _{1/2}	Γ ^b ((R·h ⁻¹)(Ci·m ⁻²) ⁻¹)	Parent isotope	Type	Threshold (MeV)	Σfσ ₋₂ (μb·MeV ⁻¹)	Note ^d		
Ta-180m	8.15 h	0.038	W-182	(γ,np)	14.66		B	0.049	0.001 ^g
Ta-182m	16.5 min	0.15	W-183	(γ,p)	7.15		B	0.36	0.027 ^g 0.11 ^g
Ta-182	115.1 d	0.61							
Ta-183	5.0 d	0.15	W-184	(γ,p)	7.71		B	0.62	0.09
Ta-184	8.7 h	0.84	W-186	(γ,np)	14.91		B	0.048	0.04
Ta-185	50 min	0.11	W-186	(γ,p)	8.39		B	0.56	0.062
W-181	140 d	0.09	W-182	(γ,n)	7.99		B	8.9	0.80
W-183m	5.3 s	0.11	W-184	(γ,n)	7.42		B	8.6	0.43 ^g
W-185	75 d	no γ	W-186	(γ,n)	7.27		B	8.1	no γ ^g 0.73 ^g
W-185m	1.62 min	0.18							
W-187 ^h	23.9 h	0.26	W-186	(n,γ)	—		—	—	— ^h

See footnotes on page 122.

TABLE XXVIa. SATURATION ACTIVITY INDUCED BY HIGH-ENERGY ELECTRONS (SI units)

Material: Natural gold^a

Daughter nuclide			Dominant production			Cross-section ^c		A _s ^e	X _s ^f
Nuclide	T _{1/2}	Γ ^b ((fC·kg ⁻¹ ·h ⁻¹)(Bq·m ⁻²) ⁻¹)	Parent isotope	Type	Threshold (MeV)	Σfσ ₋₂ (μb·MeV ⁻¹)	Note ^d	Saturation activity (GBq·kW ⁻¹)	Saturation exposure rate ((μC·kg ⁻¹ ·h ⁻¹)(kW·m ⁻²) ⁻¹)
Pt-195m	4.1 d	0.56	Au-197	(γ,np)	13.74		B	3.7	2.1
Au-195	183 d	0.49	Au-197	(γ,2n)	14.80		B	203.5	50. g
Au-195m	30.6 s	1.05							
Au-196	6.18 d	2.02	Au-197	(γ,n)	8.07		B	1517.0	1500. g
Au-196m	9.7 h	0.77							
Au-198 ^h	2.697 d	1.60	Au-197	(n,γ)	—		—	—	h

See footnotes on page 122.

TABLE XXVIb. SATURATION ACTIVITY INDUCED BY HIGH-ENERGY ELECTRONS (special units)

Material: Natural gold^a

Daughter nuclide				Dominant production			Cross-section ^c		A _s ^e	X _s ^f
Nuclide	T _{1/2}		Γ ^b ((R·h ⁻¹)(Ci·m ⁻²) ⁻¹)	Parent isotope	Type	Threshold (MeV)	Σfσ ₋₂ (μb·MeV ⁻¹)	Note ^d	Saturation activity (Ci·kW ⁻¹)	Saturation exposure rate ((R·h ⁻¹)(kW·m ⁻²) ⁻¹)
Pt-195m	4.1	d	0.08	Au-197	(γ,np)	13.74		B	0.10	0.008
Au-195	183	d	0.07	Au-197	(γ,2n)	14.80		B	5.5	0.19 0.41 ^g
Au-195m	30.6	s	0.15							
Au-196	6.18	d	0.29	Au-197	(γ,n)	8.07		B	41	5.9 2.3 ^g
Au-196m	9.7	h	0.11							
Au-198 ^h	2.697	d	0.23	Au-197	(n,γ)	—		—	—	— ^h

See footnotes on page 122.

TABLE XXVIIa. SATURATION ACTIVITY INDUCED BY HIGH-ENERGY ELECTRONS (SI units)

Material: Natural lead ^a									
Daughter nuclide			Dominant production			Cross-section ^c		A _s ^e	X _s ^f
Nuclide	T _{1/2}	Γ ^b ((fC·kg ⁻¹ ·h ⁻¹)(Bq·m ⁻²) ⁻¹)	Parent isotope	Type	Threshold (MeV)	Σfσ ₋₂ (μb·MeV ⁻¹)	Note ^d	Saturation activity (GBq·kW ⁻¹)	Saturation exposure rate ((μC·kg ⁻¹ ·h ⁻¹)(kW·m ⁻²) ⁻¹)
Tl-204	3.81 a	no γ	Pb-206	(γ,np)	14.83		B	0.9	—
Tl-206	4.19 min	no γ	Pb-207	(γ,p)	7.46		B	37.	—
Tl-207m	1.3 s	5.16	Pb-208	(γ,p)	8.04		B	93.	235.
Tl-207	4.79 min	0.01							
Pb-202m	3.62 h	8.09	Pb-204	(γ,2n)	15.32		B	2.2.	7.7 ^g
Pb-202	3.0 × 10 ⁵ a	—							
Pb-203m	6.1 s	2.30	Pb-204	(γ,n)	8.38		B	31.	34. ^g
Pb-203	52.1 h	1.26							
Pb-204m	66.9 min	7.95	Pb-206	(γ,2n)	14.85		B	89.	360. ^g
Pb-204	Stable	—							

See footnotes on page 122.

TABLE XXVIII. SATURATION ACTIVITY INDUCED BY HIGH-ENERGY ELECTRONS (special units)

Material: Natural lead^a

Daughter nuclide			Dominant production			Cross-section ^c		A _s ^e Saturation activity (Ci · kW ⁻¹)	Ẋ _s ^f Saturation exposure rate ((R · h ⁻¹)(kW · m ⁻²) ⁻¹)
Nuclide	T _{1/2}	Γ ^b ((R · h ⁻¹)(Ci · m ⁻²) ⁻¹)	Parent isotope	Type	Threshold (MeV)	Σfσ ₋₂ (μb · MeV ⁻¹)	Note ^d		
Tl-204	3.81 a	no γ	Pb-206	(γ,np)	14.83		B	0.025	—
Tl-206	4.19 min	no γ	Pb-207	(γ,p)	7.46		B	1.0	—
Tl-207m	1.3 s	0.74	Pb-208	(γ,p)	8.04		B	2.5	{ 0.91 0.001 g
Tl-207	4.79 min	8 × 10 ⁻⁴							
Pb-202m	3.62 h	1.16	Pb-204	(γ,2n)	15.32		B	0.06	{ 0.03 — g
Pb-202	3.0 × 10 ⁵ a	—							
Pb-203m	6.1 s	0.33	Pb-204	(γ,n)	8.38		B	0.83	{ 0.13 0.07 g
Pb-203	52.1 h	0.18							
Pb-204m	66.9 min	1.14	Pb-206	(γ,2n)	14.85		B	2.4	{ 1.4 — g
Pb-204	Stable	—							

See footnotes on page 122.

Footnotes to Tables XX–XXVII (a, b)

^a *Composition assumed (%)*:

Concrete (by weight): (C-12, O-16, Na-23, Mg-24, Al-27, Si-28, K-39, Fe-54, others) = (0.10, 53.0, 1.6, 0.16, 3.4, 31.0, 1.2, 0.08, 9.5).

Aluminium: Al-27: 100%.

Iron: Fe-54: 5.84%, Fe-56: 91.68%, Fe-57: 2.17%, Fe-58: 0.31%.

Nickel: Ni-58: 67.76%, Ni-60: 26.16%, Ni-61: 1.25%, Ni-62: 3.66%, Ni-64: 1.16%.

Copper: Cu-63: 69.1%, Cu-65: 30.9%.

Tungsten: W-182: 26.4%, W-183: 14.4%, W-184: 30.6%, W-186: 28.4%.

Gold: Au-197: 100%.

Lead: Pb-204: 1.4%, Pb-206: 25.1%, Pb-207: 21.7%, Pb-208: 52.3%.

^b Specific gamma-ray constant. See Footnote 14 (Section 2.6).

^c Sum of the σ_{-2} for each parent isotope, weighted by the isotope fraction. This is given if Approximation A is used in the estimation of activity.

^d See text for source of data. Activity for concrete from NBS-97 (Ref. [4]).

^e Saturation activity per kW electron beam power.

^f Exposure rate at 1 metre and per kW of electron beam power. The unit m^2 implies an inverse-square dependence on distance. Exposure rates not corrected for self-shielding or distribution of activity.

^g Equal division between metastable and ground state assumed.

^h (n, γ) reaction.

ⁱ Photopion reaction having threshold ~ 140 MeV.

^j Decays to Mn-52m, then to Mn-52.

^k Daughter of Ni isobar.

TABLE XXVIIIa. RADIONUCLIDES DETECTED IN STEEL SHIELDING (SI units)

Nuclide	Half-life	Specific activity ($t = 0$) ^a (kBq·g ⁻¹)	Γ ^b Specific gamma-ray constant ($(\mu\text{C}\cdot\text{kg}^{-1}\cdot\text{h}^{-1})(\text{Bq}\cdot\text{m}^{-2})^{-1}$)	Specific exposure rate ^c ($(\mu\text{C}\cdot\text{kg}^{-1}\cdot\text{h}^{-1})(\text{g}\cdot\text{m}^{-2})^{-1}$)
Mn-56	2.576 h	4800.	6.00	29000
Cr-51	27.8 d	590.	5.30	3100
Mn-52	5.60 d	280.	15.20	4100
Mn-54	303 d	190.	8.37	1600
V-48	16 d	115.	13.60	1500
Fe-59	45.6 d	59.	4.32	260
Sc-44m	2.44 d	37.	10.25 ^d	390 ^d
Sc-46	83.9 d	13.	7.60	95
K-43	22.4 h	7.8	3.97	31
Cr-48	23 h	7.0	6.76	46
Sc-48	1.83 d	6.3	12.41	77
Co-58	71.3 d	4.1	7.88	31
Co-60	5.263 a	2.2	9.06	20
Co-57	270 d	1.9	9.00	17

^a At time of accelerator turnoff, $t = 0$.

^b See Footnote 14 (Section 2.6).

^c Exposure rate at 1 m, per g of activated steel, at time of accelerator turnoff. Uncorrected for self-shielding and distribution of activity.

^d Includes Sc-44 daughter radiations.

TABLE XXVIIIb. RADIONUCLIDES DETECTED IN STEEL SHIELDING (special units)

Nuclide	Half-life	Specific activity ($t = 0$) ^a ($\mu\text{Ci}\cdot\text{g}^{-1}$)	Γ ^b Specific gamma-ray constant ($(\text{R}\cdot\text{h}^{-1})(\text{Ci}\cdot\text{m}^{-2})^{-1}$)	Specific exposure rate ^c ($(\mu\text{R}\cdot\text{h}^{-1})(\text{g}\cdot\text{m}^{-2})^{-1}$)
Mn-56	2.576 h	130.	0.86	111
Cr-51	27.8 d	16.	0.76	12
Mn-52	5.60 d	7.5	2.18	16
Mn-54	303 d	5.2	1.20	6.1
V-48	16 d	3.1	1.95	6.0
Fe-59	45.6 d	1.6	0.62	1.0
Sc-44m	2.44 d	1.0	1.47 ^d	1.5 ^d
Sc-46	83.9 d	0.35	1.09	0.37
K-43	22.4 h	0.21	0.57	0.12
Cr-48	23 h	0.19	0.97	0.18
Sc-48	1.83 d	0.17	1.78	0.30
Co-58	71.3 d	0.11	1.13	0.12
Co-60	5.263 a	0.060	1.30	0.077
Co-57	270 d	0.050	1.29	0.064

^a At time of accelerator turnoff, $t = 0$.

^b See Footnote 14 (Section 2.6).

^c Exposure rate at 1 m, per g of activated steel, at time of accelerator turnoff. Uncorrected for self-shielding and distribution of activity.

^d Includes Sc-44 daughter radiations.

nor for the distributed nature of the activity. Both of these factors will tend to mitigate the associated radiation protection problems. DeStaebler [11] has estimated self-shielding factors in the range of 0.05–0.2 for iron irradiated at high energy, depending on the energy of gamma emissions. Ladu et al. [12] have evaluated self-absorption factors for accelerator components of copper and iron, and find them in the range 0.1–1.0.

Those isotopes of Tables XX–XXVII with note B are from integrations over the photon track length using measured photonuclear cross-sections [10] and Approximation B, corrected as for Section 2.6.1. The data for aluminium in Table XXI are mainly from Ref.[13]. The data marked D are from DeStaebler [11] (D* means rough estimate), and those marked Sa are from Saxon [14]; E indicates a rough estimate.

Nuclides with half-lives less than about one minute or greater than about 100 years do not pose significant radiation protection problems, but some are nevertheless included for comparison.

In a study of radionuclides in shielding steel of unknown composition in the immediate proximity of a 200-kW, 20-GeV electron beam dump the nuclides listed in Table XXVIII were detected. The component studied was not in the direct electron beam but at 90° to the water-cooled aluminium dump. Although not suitable for quantitative use, the list illustrates the variety of possible photon- and photoneutron-produced radionuclides.

REFERENCES TO SECTION 2.6

- [1] HOWERTON, R.J., BRAFF, D., CAHILL, W.J., CHAZAN, N., Thresholds of Photon Induced Reactions, Lawrence Livermore Laboratory, Rep. UCRL-14006 (1964).
- [2] BARBIER, M., Induced Radioactivity, Ch.5, North-Holland, Amsterdam, and John Wiley, New York (1969).
- [3] GOLLON, P.J., Production of radioactivity by particle accelerators, IEEE Trans. Nucl. Sci. NS-23 4 (1976) 1395.
- [4] NATIONAL BUREAU OF STANDARDS, NATIONAL COUNCIL ON RADIATION PROTECTION AND MEASUREMENTS, Shielding for High-Energy Electron Accelerator Installations, NBS Handbook No.97 and NCRP Report No.31, Washington, DC (1964) 31.
- [5] NACHTIGALL, D., Table of Specific Gamma-Ray Constants, Karl Thiernig, Munich (1969).
- [6] See, for example, Radiological Health Handbook, Bureau of Radiological Health, Public Health Service, US Department of Health, Education and Welfare, Rockville, MD (1970) 131–32.
- [7] UNITED KINGDOM DEPARTMENT OF EMPLOYMENT, Handbook of Radiological Protection, Her Majesty's Stationery Office, London (1971), Table 3.1 (1).
- [8] LEDERER, C.M., HOLLANDER, J.M., PERLMAN, I., Table of Isotopes, 6th ed., John Wiley, New York (1967).
- [9] STORM, E., ISRAEL, H.I., Photon Cross Sections from 0.001 to 100 MeV for Elements 1 through 100, Los Alamos Scientific Laboratory, Rep. LA-3753, UC-34, Physics, TID-4500 (1967).

- [10] Cross-sectional data mainly from BERMAN, B.L., Atlas of Photoneutron Cross Sections Obtained with Monoenergetic Photons, Lawrence Livermore Laboratory, Rep. UCRL-74622 (1974); At. Data Nucl. Data Tables 15 (1975) 319.
- [11] DeSTAEBLER, H., Photon-Induced Residual Activity, Stanford Linear Accelerator Center, Rep. SLAC-TN-6392 (1963).
- [12] LADU, M., PELLICIONI, M., ROCCELLA, M., Radioattività residua sulla guida d'onda del linac di Frascati, Minerva Fisiconucl. 11 2 (1967) 103.
- [13] SWANSON, W.P., Activation of aluminum beam dumps by high-energy electrons at SLAC, Health Phys. 28 (1975) 495.
- [14] SAXON, G., "Radioactivity induced by high energy electrons", Radiation Protection in Accelerator Environments (STEVENSON, G.R., Ed.) (Proc. Conf. Rutherford Laboratory, 1969), Rutherford Laboratory, Chilton, Didcot, Oxon. (1969) 8.

2.7. Activity induced in air and water

In considering protection against activated air and water, the possible pathways of exposure should be taken into account. The significant pathways for radiation workers are quite different for air and water. The hazard to the general public from these effluents is negligible, but it may be desirable to assess this risk, at large installations anyway, for reassurance to the general public. The significance of various types of exposure is qualitatively indicated in Table XXIX. Activation is of no concern unless the accelerator energy E_0 exceeds the production threshold (10.55 MeV in air, 15.67 MeV in water).

2.7.1. Airborne radioactivity

There are three forms of airborne activity, listed here in the order of their relative seriousness:

- (a) Direct activation of air by bremsstrahlung
- (b) Radioactive gases formed in water and afterwards released to air (discussed in Section 2.7.2)
- (c) Radioactive dust.

Airborne activity has not been found significant at standard radiotherapeutic and radiographic facilities, and the discussion here is primarily directed towards research facilities.

2.7.1.1. Air activation

Radioactive gases are produced by the interaction of bremsstrahlung with air nuclei if the accelerator is operating above the production threshold (10.55 MeV); air activation is of no concern at energies at or below the threshold (see Table XXX).

TABLE XXIX. PATHWAYS OF EXPOSURE TO ACTIVATED AIR AND WATER

Pathway	Air		Water	
	Radiation Workers	General Public	Radiation Workers	General Public
External	Potential exposure in Containment Area only. Less than from activated components. Region of Containment Area exhaust should be checked.	Concentrations released at site boundary generally negligible, but should be assessed in planning a high-energy, high-power facility.	Potential exposure from water pipes and vessels during operating periods. Exhaust of surge-tank atmosphere should be checked.	Negligible
Internal	Negligible	Negligible	Negligible	Concentrations released at site boundary generally negligible, but should be assessed if direct release is made.

Furthermore, an electron beam without bremsstrahlung will not cause significant air activation¹⁵ because the nuclear cross-sections of *electrons* are smaller by about two orders of magnitude than those of *photons*.

Such airborne activity is in general short-lived, and even if produced in significant amounts, dilution and radioactive decay quickly reduce the concentrations to moderate levels. Only in very unusual circumstances would exposure to radioactive air be the limiting factor for personnel access to a containment area. The limiting factor is almost always external exposure from components.

The total amount of activation is much less in air than in solid materials because the air mass exposed absorbs much less beam energy than the many radiation lengths of solids needed to stop the beam and to shield against prompt radiation. For the same production cross-section, air activation is reduced by a factor of the order of X/X_0 , where X is the bremsstrahlung pathlength in air and

¹⁵ The reverse is true for toxic gas production, which occurs by a chemical, rather than nuclear, transformation and whose reaction rate is closely proportional to the integral dose to air. This is generally higher if the primary electron beam is extracted than if it first strikes a target to make bremsstrahlung.

TABLE XXXa. ACTIVITY INDUCED IN AIR (SI units)

Produced nuclide			Parent nuclide				Cross-section ^b $\Sigma f\sigma_{-2}$ ($\mu\text{b} \cdot \text{MeV}^{-1}$)	A_s^c Saturation activity ($\text{Bq} \cdot \text{m}^{-1} \cdot \text{kW}^{-1}$)
Nuclide	$T_{1/2}$	MPC ($\text{Bq} \cdot \text{cm}^{-3}$)	f Abundance ^a	Nuclide	Reaction type	Threshold (MeV)		
H-3	12.262 a	74 ^d	{ 1.562 0.424	N-14 O-16	($\gamma, \text{H-3}$)	{ 22.73 25.02	(3)	(5×10^6)
Be-7 ^f	53.6 d	37×10^{-3} d	{ 1.562 0.424	N-14 O-16	(γ, sp) ^f	{ 27.81 31.86	(0.6)	(1×10^6) ^f
C-11	20.34 min	111×10^{-3} e	1.5×10^{-4}	C-12	(γ, n)	18.72	0.011	19×10^3
			{ 1.562 0.424	N-14 O-16	(γ, sp) ^f	{ 22.73 25.88	(6)	(10×10^6) ^f
N-13	9.96 min	74×10^{-3} e	1.562	N-14	(γ, n)	10.55	310	520×10^6
O-15	123 s	74×10^{-3} e	0.424	O-16	(γ, n)	15.67	32	56×10^6
N-16	7.14 s	18.5×10^{-3} e	4.0×10^{-4}	O-18	(γ, np)	21.81	(0.01)	(20×10^3)
Cl-38	37.29 min	74×10^{-3} d	4.6×10^{-3}	Ar-40	(γ, np)	20.59	0.13	220×10^3
Cl-39	55.5 min	111×10^{-3} d	4.6×10^{-3}	Ar-40	(γ, p)	12.52	0.86	1.5×10^6
Ar-41 ^g	1.83 h	74×10^{-3} e	4.6×10^{-3}	Ar-40	(n, γ)	—	—	— ^g

^a Fraction of air by volume, multiplied by atoms/molecule.

^b Abundance f times integral cross-section σ_{-2} . Values in parentheses are rough estimates.

^c Per bremsstrahlung pathlength in air (metres) and electron beam power (kW) incident on a thick high-Z target. Values in parentheses are rough estimates.

^d Based on ICRP recommendation for radiation workers, 40-hour week, exposure from inhalation.

^e Based on ICRP recommendation for radiation workers, 40-hour week, semi-infinite cloud (see text).

^f Spallation reaction.

^g Neutron-capture reaction. Occurs where high neutron fluences are moderated by water or concrete shielding.

TABLE XXXb. ACTIVITY INDUCED IN AIR (special units)

Produced nuclide			Parent nuclide			Cross-section ^b $\Sigma f\sigma_{-2}$ ($\mu\text{b}\cdot\text{MeV}^{-1}$)	A_s^c Saturation activity ($\mu\text{Ci}\cdot\text{m}^{-1}\cdot\text{kW}^{-1}$)	
Nuclide	$T_{\frac{1}{2}}$	MPC ($\mu\text{Ci}\cdot\text{cm}^{-3}$)	f Abundance ^a	Nuclide	Reaction type			Threshold (MeV)
H-3	12.262 a	2×10^{-3} d	{ 1.562 0.424	N-14	$(\gamma, \text{H-3})$	22.73	(3)	(140)
				O-16		25.02		
Be-7 ^f	53.6 d	1×10^{-6} d	{ 1.562 0.424	N-14	$(\gamma, \text{sp})^f$	27.81	(0.6)	(30) ^f
				O-16		31.86		
C-11	20.34 min	3×10^{-6} e	1.5×10^{-4}	C-12	(γ, n)	18.72	0.011	0.5
			{ 1.562 0.424	N-14	$(\gamma, \text{sp})^f$	22.73	(6)	(300) ^f
				O-16		25.88		
N-13	9.96 min	2×10^{-6} e	1.562	N-14	(γ, n)	10.55	310	14000
O-15	123 s	2×10^{-6} e	0.424	O-16	(γ, n)	15.67	32	1500
N-16	7.14 s	5×10^{-7} e	4.0×10^{-4}	O-18	(γ, np)	21.81	(0.01)	(0.5)
Cl-38	37.29 min	2×10^{-6} d	4.6×10^{-3}	Ar-40	(γ, np)	20.59	0.13	6
Cl-39	55.5 min	3×10^{-6} d	4.6×10^{-3}	Ar-40	(γ, p)	12.52	0.86	40
Ar-41 ^g	1.83 h	2×10^{-6} e	4.6×10^{-3}	Ar-40	(n, γ)	—	—	— ^g

^a Fraction of air by volume, multiplied by atoms/molecule.

^b Abundance f times integral cross-section σ_{-2} . (See Eq.(8) of Section 2.2). Values in parentheses are rough estimates.

^c Per bremsstrahlung pathlength in air (metres) and electron beam power (kW) incident on a thick high-Z target. Values in parentheses are rough estimates.

^d Based on ICRP recommendation for radiation workers, 40-hour week, exposure from inhalation.

^e Based on ICRP recommendation for radiation workers, 40-hour week, semi-infinite cloud (see text).

^f Spallation reaction.

^g Neutron-capture reaction. Occurs where high neutron fluences are moderated by water or concrete shielding.

X_0 is the radiation length of air (Appendix B). Table XXX lists parameters of reactions leading to air activation [1]. The same formulae for activity buildup and decay apply as for solid materials (Section 2.6).

Even without forced ventilation, a complete air change usually occurs a few times per hour. Therefore it is not possible to accumulate more than a fraction of the saturated activity of ^3H or ^7Be , and the only nuclides that need be considered are ^{13}N and ^{15}O , and possibly ^{11}C , ^{38}Cl , ^{39}Cl and ^{41}A . The *relative* saturation activities of the first two, produced by (γ, n) reactions, can be readily calculated from published cross-sections [2] and are in the ratio 11 : 1 for energies well above the respective thresholds. For energies closer to threshold, the sigmoid rise of activity with E_0 illustrated in the previous section should be considered. Argon-41 is produced in (n, γ) reactions, especially in high fluences of moderated neutrons. Thus it occurs more frequently near water-cooled targets and beam dumps and concrete secondary enclosures, but its production rate is less because of the small concentration of parent ^{40}A and smaller neutron fluences. Argon-41, ^{11}C and ^{39}Cl are considered together with the other nuclides because of their longer half-lives.

Absolute activation predictions are tenuous, but with simple physical assumptions saturation activities, A_s , per bremsstrahlung pathlength in air and unit electron beam power have been calculated [3] and are shown in Table XXX. These predictions correspond approximately to the maximum activation likely to be produced in a situation where the electron beam showers in a high-Z target before entering the air. In many situations, for example at lower energy ($E_0 < 30$ MeV), or for thinner or low-Z targets, air activation may be significantly less. Absolute predictions have also been calculated by Kase [4] and Ladu et al. [5] for specific targeting conditions.

To predict an average room concentration using Table XXX, it is necessary to multiply by the bremsstrahlung pathlength in air and divide by the room volume. For a target room of 10^6 litres containing a 1-metre beam path, 1 kW of electron beam power would produce about $0.5 \text{ Bq} \cdot \text{cm}^{-3}$ ($14 \times 10^{-6} \text{ } \mu\text{Ci} \cdot \text{cm}^{-3}$) or a few times the indicated maximum permissible concentration (MPC). George et al. [6] have found typical concentrations of the order of $0.9 \text{ Bq} \cdot \text{kW}^{-1} \cdot \text{cm}^{-3}$ ($25 \times 10^{-6} \text{ } \mu\text{Ci} \cdot \text{kW}^{-1} \cdot \text{cm}^{-3}$) in areas of a room of about this volume in which normal air mixing could occur ($E_0 = 50$ MeV). Vialettes [7] has reported concentrations above the listed MPCs at Saclay, where the beam power was 100 kW (330 and 530 MeV).

Where air is confined in a small volume, such as a target cave, the concentrations may be 2–3 orders of magnitude above those of a larger room [6].

The MPCs indicated in Table XXX for the most copiously produced nuclides are derived on the basis of external whole-body exposure of radiation workers for a 40-hour week from immersion in an infinite hemispherical cloud [8, 9]; internal doses are smaller by comparison. In smaller gas volumes, of less than

about 12 m radius, the direct beta radiations to the skin become the limiting factor [10]. Because of this and other mitigating factors evaluated by Kase [11], a more appropriate choice of MPC for the smaller 'cloud' of accelerator room air containing ^{13}N is about $0.75 \text{ Bq} \cdot \text{cm}^{-3}$ ($2 \times 10^{-5} \mu\text{Ci} \cdot \text{cm}^{-3}$). Similar arguments have been made by Höfert [12] and Jones et al. [13]. Therefore, the MPCs based on the semi-infinite cloud are to be regarded as very conservative. MPC values calculated by Höfert are shown in Table XXXI for a range of choices of radioactive cloud radius and for four sets of assumptions. The assumptions for columns III and IV give MPCs that more realistically assess the hazard to radiation workers within accelerator target rooms. Small occupancy factors and delays in entry to the containment area mitigate the problem further.

In the unusual circumstance where activated air is a limiting factor, the amount of activated air can be reduced considerably by the following steps:

(a) Shortening of the bremsstrahlung air path by terminating it in shielding, or by the use of evacuated beam pipes or helium bags, will reduce the activity proportionately. Lead shielding, such as beam-pipe 'collars' around every point where the electron beam can strike solid material, will reduce the amount of stray radiation and consequently reduce the amount of air activation, toxic gas production and radiation damage to other objects as well.

(b) Unless continuous ventilation is used, it may be advisable to confine the activated air long enough for most of the ^{13}N to decay (10–20 min) and then to use ventilation before entry.

(c) If continuous forced ventilation is used instead, it can be expected to reduce saturation concentrations by about a factor of two [6].

(d) Local forced ventilation applied directly to the activated air volume may be helpful.

When considering the effect of ventilation on activity removal, the effective half-life is calculated by the equation

$$T_{1/2}(\text{effective}) = \frac{T_{1/2}(\text{physical}) \cdot T_{1/2}(\text{vent})}{T_{1/2}(\text{physical}) + T_{1/2}(\text{vent})} \quad (39)$$

where $T_{1/2}(\text{vent}) = 0.693 \cdot T$ (air change), and T (air change) is the room volume divided by the air volume exhausted per unit time.

2.7.1.2. Dust

All studies indicate that, except under very unusual conditions, external and internal human exposures due to airborne radioactive dust are negligible compared with other potential exposures, including the radioactive gases discussed above [8].

Text continued on p.136

TABLE XXXIa. MAXIMUM PERMISSIBLE CONCENTRATIONS IN AIR FOR RADIOISOTOPES FOUND IN HIGH-ENERGY ACCELERATOR INSTALLATIONS ($\text{Bq} \cdot \text{cm}^{-3}$), FOR DIFFERENT SIZES OF THE RADIOACTIVE CLOUD IN WHICH THE BODY IS SUBMERGED (BASED ON 40-HOUR WEEK)

Radius of radioactive cloud	Ar-41				O-15				C-11				N-13			
	I	II	III	IV												
1 m	0.29	23.38	1.72	2.04	0.24	25.35	1.32	1.50	0.29	25.35	1.85	2.38	0.26	25.35	1.53	1.84
2 m	0.22	11.69	1.51	1.81	0.16	12.69	1.02	1.14	0.24	12.69	1.72	2.20	0.20	12.69	1.32	1.56
4 m	0.20	5.85	1.47	1.75	0.13	6.44	0.92	1.02	0.23	6.44	1.71	2.18	0.17	6.44	1.28	1.52
10 m	0.19	2.41	1.47	1.75	0.12	2.54	0.91	1.00	0.21	2.54	1.71	2.18	0.16	2.54	1.28	1.51
100 m	0.11	0.28	1.47	1.75	0.08	0.30	0.91	1.00	0.11	0.30	1.71	2.18	0.10	0.30	1.28	1.51
∞	0.07 ^a	0.08	1.47	1.75	0.07 ^b	0.10	0.91	1.00	0.10 ^c	0.10	1.71	2.18	0.09 ^b	0.10	1.28	1.51

Assumptions for MPC derivation:

- I. Values calculated according to ICRP Publication II (Ref. [9]) assuming the whole body as the critical organ.
- II. Values calculated critically, taking the gamma component of the nuclide responsible for the whole-body irradiation.
- III. Values calculated critically, based on the beta component of the nuclide responsible for the skin irradiation.
- IV. Same as III, but taking into account the absorption of the beta rays in the outer layer of the skin ($7 \text{ mg} \cdot \text{cm}^{-2}$, according to ICRP).

^a Value from ICRP Publication II [9].

^b Value calculated by George et al. [6] using the ICRP formula (pp. 22, 28 of ICRP Publication II).

^c Value calculated by Höfert using the ICRP formula (pp. 22, 28 of ICRP Publication II).

(Table adapted from Ref. [12], with kind permission of M. Höfert and the European Organisation for Nuclear Research (CERN).)

TABLE XXXIb. MAXIMUM PERMISSIBLE CONCENTRATIONS IN AIR FOR RADIOISOTOPES FOUND IN HIGH-ENERGY ACCELERATOR INSTALLATIONS ($\text{pCi}\cdot\text{cm}^{-3}$), FOR DIFFERENT SIZES OF THE RADIOACTIVE CLOUD IN WHICH THE BODY IS SUBMERGED (BASED ON 40-HOUR WEEK)

Nuclide Radius of radio- active cloud	Ar-41				O-15				C-11				N-13			
	I	II	III	IV												
1 m	7.9	632	46.5	55.0	6.4	685	35.8	40.6	7.8	685	49.9	64.2	6.9	685	41.3	49.8
2 m	6.0	316	40.7	48.8	4.3	343	27.6	30.9	6.6	343	46.5	59.4	5.3	343	35.7	42.2
4 m	5.4	158	39.6	47.4	3.5	174	24.9	27.6	6.2	174	46.2	59.0	4.7	174	34.5	41.0
10 m	5.1	65.0	39.6	47.3	3.2	68.7	24.5	27.1	5.7	68.7	46.2	59.0	4.4	68.7	34.5	40.8
100 m	3.0	7.5	39.6	47.3	2.2	8.2	24.5	27.1	2.9	8.2	46.2	59.0	2.6	8.2	34.5	40.8
∞	2.0 ^a	2.2	39.6	47.3	2.0 ^b	2.6	24.5	27.1	2.6 ^c	2.6	46.2	59.0	2.3 ^b	2.6	34.5	40.8

Assumptions for MPC derivation:

- I. Values calculated according to ICRP Publication II (Ref. [9]) assuming the whole body as the critical organ.
- II. Values calculated critically, taking the gamma component of the nuclide responsible for the whole-body irradiation.
- III. Values calculated critically, based on the beta component of the nuclide responsible for the skin irradiation.
- IV. Same as III, but taking into account the absorption of the beta rays in the outer layer of the skin ($7 \text{ mg}\cdot\text{cm}^{-2}$, according to ICRP).

^a Value from ICRP Publication II [9].

^b Value calculated by George et al. [6] using the ICRP formula (pp. 22, 28 of ICRP Publication II).

^c Value calculated by Höfert using the ICRP formula (pp. 22, 28 of ICRP Publication II).

(Table adapted from Ref. [12], with kind permission of M. Höfert and the European Organisation for Nuclear Research (CERN).)

TABLE XXXIIa. PHOTOACTIVATION PRODUCTS FROM O-16 IN WATER (SI units)

Nuclide	$T_{1/2}$	MPC _w ^a (Bq·cm ⁻³)	Γ ^b Specific gamma-ray constant ((fC·kg ⁻¹ ·h ⁻¹)(Bq·m ⁻²) ⁻¹)	Reaction type	Threshold (MeV)	Cross-section ^c σ_{-2} ($\mu\text{b}\cdot\text{MeV}^{-1}$)	A_s ^{c, d} Saturation activity (GBq·kW ⁻¹)
O-15	123 s	—	4.11 (β^+)	(γ, n)	15.67	75	330
O-14	70.91 s	—	11.16 (β^+)	($\gamma, 2n$)	28.89	(1)	(3.7)
N-13	9.96 min	—	4.11 (β^+)	($\gamma, 2np$)	25.02	0.9	3.7
C-11	20.34 min	—	4.11 (β^+)	($\gamma, 3n2p$)	25.88	3	15.
C-10	19.48 s	—	7.04 (β^+)	($\gamma, 4n2p$)	38.10	(1)	(3.7)
Be-7	53.6 d	740	0.20 —	($\gamma, 5n4p$)	31.86	0.3	1.5
H-3	12.262 a	1110	— (β^-)	($\gamma, \text{H-3}$)	25.02	1.5	7.4

^a ICRP recommendation for the general public, 168-hour week occupancy. See text for discussion.

^b See Footnote 14 (Section 2.6).

^c Values in parentheses are rough estimates.

^d Saturation activity in water per unit electron beam power. Assume 100% direct absorption of electron beam power in water. Activity in water will be less in most situations where the beam absorber is water-cooled metal. Values shown are obtained directly from Approximation A and apply at high energies. For $E_0 \gtrsim 50$ MeV, the value for O-15 may be reduced by a factor of two, and others by an even larger factor.

TABLE XXXIIb. PHOTOACTIVATION PRODUCTS FROM O-16 IN WATER (special units)

Nuclide	$T_{1/2}$	MPC_w^a ($\mu\text{Ci}\cdot\text{cm}^{-3}$)	Γ^b Specific gamma-ray constant ($(\text{R}\cdot\text{h}^{-1})(\text{Ci}\cdot\text{m}^{-2})^{-1}$)	Reaction type	Threshold (MeV)	Cross-section ^c σ_{-2} ($\mu\text{b}\cdot\text{MeV}^{-1}$)	$A_s^{c,d}$ Saturation activity ($\text{Ci}\cdot\text{kW}^{-1}$)
O-15	123 s	—	0.59 (β^+)	(γ,n)	15.67	75	9
O-14	70.91 s	—	1.60 (β^+)	($\gamma,2n$)	28.89	(1)	(0.1)
N-13	9.96 min	—	0.59 (β^+)	($\gamma,2np$)	25.02	0.9	0.1
C-11	20.34 min	—	0.59 (β^+)	($\gamma,3n2p$)	25.88	3	0.4
C-10	19.48 s	—	1.01 (β^+)	($\gamma,4n2p$)	38.10	(1)	(0.1)
Be-7	53.6 d	0.02	0.029 —	($\gamma,5n4p$)	31.86	0.3	0.04
H-3	12.262 a	0.03	— (β^-)	($\gamma,H-3$)	25.02	1.5	0.2

^a ICRP recommendation for the general public, 168-hour week occupancy. See text for discussion.

^b See Footnote 14 (Section 2.6).

^c Values in parentheses are rough estimates.

^d Saturation activity in water per unit electron beam power. Assume 100% direct absorption of electron beam power in water. Activity in water will be less in most situations where the beam absorber is water-cooled metal. Values shown are obtained directly from Approximation A and apply at high energies. For $E_0 \gtrsim 50$ MeV, the value for O-15 may be reduced by a factor of two, and others by an even larger factor.

In assessing potential exposures to radioactive dust, one should begin by considering what materials are exposed to bremsstrahlung at the particular installation. Concrete, steel, lead, aluminium, brass and organic materials are commonly found. Lead and concrete have very little activation potential, but the other materials may be activated.

Violettes [7] has studied dusts at the Saclay Electron Linac (330 and 530 MeV) and found evidence for ${}^7\text{Be}$, ${}^{24}\text{Na}$, ${}^{56}\text{Mn}$, ${}^{57}\text{Ni}$ and ${}^{152}\text{Gd}$. Their concentrations ranged between 3.7×10^{-5} and $3.7 \times 10^{-3} \text{ Bq} \cdot \text{m}^{-3}$ (10^{-15} and $10^{-13} \text{ Ci} \cdot \text{m}^{-3}$), normalized to 1 kW·h beam energy. These are negligible compared with the smallest MPC_a for these particulates, estimated as $(11-22) \times 10^3 \text{ Bq} \cdot \text{m}^{-3}$ ($(3-6) \times 10^{-7} \text{ Ci} \cdot \text{m}^{-3}$).

At the CERN Proton Synchrotron, St. Charalambus and Rindi [14] have detected ${}^{54}\text{Mn}$, ${}^7\text{Be}$, ${}^{51}\text{Cr}$, ${}^{59}\text{Fe}$ and ${}^{48}\text{V}$, ranked in the order listed. Although the CERN PS is a proton accelerator, four of the five nuclides on this list are quite consistent with the dominant longer-lived nuclides of Table XXVIII, found on the surface of steel shielding at SLAC.

Dusts are, of course, raised at the time when personnel first enter the containment area after a period of operation, and their presence should be assessed at such times rather than during the operating cycle. If dust is a problem, recommended steps are to vacuum clean the surfaces in the accelerator room periodically, and to immobilize particulates with paint or varnish.

2.7.2. Activity induced in water

Radioactivity in water is formed by the interaction of bremsstrahlung with the ${}^{16}\text{O}$ component of water-cooled targets and beam dumps. Many of the considerations applying to air activation apply to water as well, including methods of estimating the production, and the time dependence of activity buildup and decay. However, the manner of personnel exposure is different.

Table XXXII lists parameters of reactions leading to water activation. The dominant radionuclides in terms of saturation activity are easily identified as ${}^{15}\text{O}$ and ${}^{11}\text{C}$. The saturation activities shown correspond to 100% energy absorption in water and are normalized to incident electron beam power in kW. If the water is used for cooling, rather than as the primary beam-stopping medium, the fraction of energy directly absorbed in water is much less than 100%. In water-cooled metal-plate beam dumps the fraction of energy absorbed directly by water is of the order of 10%. For most cases the saturation activities of Table XXXII may be reduced by a factor of about this magnitude, depending on the design of the device.¹⁶

¹⁶ To estimate this factor for high-energy operation, it is appropriate to use the ratio of pathlength in water to that in metal, where both pathlengths are expressed in radiation lengths X_0 (Appendix B).

Fortunately, these nuclides are short-lived so that they do not constitute a storage problem, except perhaps for ^3H and to a limited extent for ^7Be . However, they can produce unacceptable radiation levels near accessible water pipes and heat exchangers, and the possibility of spills should be considered. Exhaust atmospheres of cooling water surge tanks and standpipes may be a source of air contamination.

Saturation activities, based on calculations by DeStaeblcr [15] and Coward [16], are shown in Table XXXII. Without question, ^{15}O is produced most abundantly, but it decays quickly. It is generally agreed that ^{11}C is the dominant radio-nuclide 1–5 hours after irradiation. Nitrogen-13 and ^7Be are difficult to detect in water without special effort; ^{13}N is always masked by ^{11}C , and the ^7Be concentration is low.

In considering external exposures of workers, one must consider how the water is circulated. In cases where a low-power facility uses once-through cooling and water is released to a sanitary sewage system or to groundwater, the activities circulated within the facility are a small fraction of those indicated in the table. In these cases, only the environmental impact of released ^3H and ^7Be need be considered further, and dilution by other effluents should be taken into account. Disposal to the groundwater would normally be controlled by the ^3H content, since ^7Be is readily adsorbed on rock surfaces and decays away relatively soon. A comparison with the MPC (Table XXXII) for 168-hour occupancy for the general public should be made [9]. For sewer disposal, one may average the effluent over a period of one year and use MPC_w values for radiation workers (40-hour per week exposure) instead.¹⁷

Yamaguchi [17] has calculated MPC_w values for the other nuclides of Table XXXII, but they are not shown here because these nuclides are not ingested and are not generally of environmental concern.

A significant source of *airborne* activity may be found in the exhaust atmosphere of surge tanks and standpipes of open cooling-water systems [10]. The water of an open system is likely to be chemically saturated with gases of the type bearing the radioactive nuclides, and a significant fraction of the produced radio-nuclides will come out of solution. If vented, the released activity could be a more serious cause of concern than the directly activated air discussed in the previous section.

Average concentrations released from a vented system depend on such factors as:

- (a) Electron beam power (Table XXXII)
- (b) Fraction of beam power directly absorbed in water (typically 10% for water-cooled metal dumps) and operating cycle

¹⁷ Governmental authorities and a qualified expert should be consulted to determine the legal requirements concerning effluents.

- (c) Volume of the system
- (d) Delay in transport of radioactivity to venting point
- (e) Area and other characteristics of the air/water interface which affect the exchange rate (e.g. whether there is splashing or an unperturbed surface within the surge tank)
- (f) Amount of dilution by forced ventilation, if any.

Possible methods of management of this problem are:

- (a) Once-through cooling and release to the sanitary sewer. This is practical only for low-power operation ($\lesssim 10$ kW)
- (b) Venting to a closed containment area
- (c) Direct exhaust to a stack
- (d) Holdup tank followed by exhaust or other release
- (e) Closed system with catalytic recombiners to remove H_2 .

The best management of this problem varies with the nature of the facility and its environment. For electron beam powers below about 10 kW, once-through cooling and release to the sanitary sewer may be satisfactory and is customary for radiotherapeutic and radiographic installations. Water quality or legal requirements may prohibit this in some localities. Where recirculated cooling is used, one of the other solutions must be chosen.

For low-power operation, the primary cooling system can be vented directly to the radiation room. The releases from the water system then mix with the radioactive air and a separate venting system is not needed. This arrangement is permissible only if the amount of radiolytic hydrogen evolved is so small that explosive mixtures cannot be formed at the room ventilation rate used.¹⁸ If problematical, the hydrogen gas can be continuously removed by catalytic recombiners (Pt – Pd, for example) [19] before venting to the atmosphere, or an external vent can be used. Where possible, it is advantageous to vent to the containment area, as this affords additional holdup time to allow ^{15}O and ^{11}C to decay before release to the environment.

¹⁸ Walz [18] has measured the radiolytic yield, $G(H_2)$, under typical conditions of linac irradiation, and found it to be: $G(H_2) = 0.14 \pm 0.02$ molecules/100 eV, which is equivalent to $(3.0 \pm 0.4) \times 10^{-4}$ litre·s⁻¹ at an energy absorption rate in water of 1 kW. From this value, together with the known primary electron beam power and the estimated fraction of that power absorbed directly by the water, the rate of hydrogen evolution can be determined. The room volume together with the ventilation rate then determines the saturation concentration of hydrogen. The lowest hydrogen concentration at which an explosion can occur in air is 4% (by volume). The permitted concentration should be kept below half of that, or below 2%.

The problem has been examined by Warren et al.[10] for the case of high-power beam dumps (100–1000 kW, directly absorbed in water). It was found that the radioactive nuclides ^{15}O and ^{11}C in the surge-tank atmosphere were mainly in the form of O_2 and CO_2 , respectively. Venting to the environment, either directly or via a holdup tank, was unacceptable because of the quantities involved. Venting to the containment area was a possible solution, but it was found more economical to operate with a closed system and to provide catalytic recombiners to prevent the accumulation of explosive concentrations of H_2 . The system is operated at atmospheric pressure and relief valves exhaust to the containment area.

At accelerator facilities of intermediate power (up to ≈ 100 kW), venting of relief valves to the containment area without recombiners has been found acceptable.

In closed-loop cooling systems, one must consider external exposures of personnel due to accessible water pipes and heat exchangers, evaporation from open standpipes and surge tanks, and accumulations such as the concentration of ^7Be in demineralizers [20].¹⁹ By careful layout of pipes and possibly additional shielding, the radiation hazard of cooling-water pipes can be minimized. Where otherwise feasible, it is good practice to install all piping of a primary cooling water circuit, including the heat exchanger and water treatment elements, within the room containing the radiation-absorbing components cooled by that circuit. In this manner, all types of radiation associated with a particular beam are efficiently contained and controlled. Where separate radiation rooms are provided, it may be advantageous to have a separate primary circuit for each. If radioactive water is piped to heat exchangers outside the containment area, a holding tank may be helpful in delaying the transport long enough for the amount of ^{15}O to be significantly reduced. However, it may be more economical to simply shield or fence off the heat exchanger area.

In planning radiation protection for cooling circuits, the following points should be considered:

(a) Only ^{15}O , ^{11}C and ^7Be need be considered unless it is known or suspected that additives or impurities will be present. If demineralizers are used in a cooling circuit, ^7Be will be accumulated there.

(b) Because resin beds are more than 99% efficient in filtering ^7Be , concentrations in water may remain at low levels. On the other hand, one should assume that *all* the ^7Be will be contained in the resin beds and these should be shielded and handled accordingly.

(c) To obtain the applicable concentration, saturation activities (Table XXXII) are divided by system volume. In planning the layout and shielding of the piping and other elements of the water system, transit times from the beam dump to

¹⁹ The concentration of ^7Be in demineralizers actually occurs by filtration rather than by chemical removal. Therefore it would occur with any type of filter element used in the system.

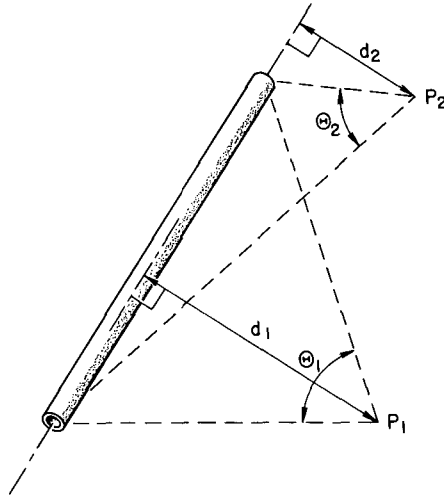


FIG.40. Determination of distance d and angle θ for use in estimating exposure rates at two positions (P_1 and P_2) near a pipe segment carrying radioactive water. The distances are measured perpendicular to the pipe axis and the angles are measured in radians. The total exposure rate at a given position can be estimated by adding together the contributions from all nearby pipes.

the location in question should be estimated and used to determine the concentration of ^{15}O remaining in the water.

(d) Depending on the materials of the system²⁰, oxygen removal elements may be effectively employed to reduce the amount of free oxygen circulated by the water. In this manner the ^{15}O will be concentrated and oxidation with the system will also be reduced.

(e) It may be assumed that the β^+ from all the significant nuclides are absorbed in the pipe wall and only gammas will contribute outside the pipe.

(f) The following formula will provide an estimate of the unshielded exposure rate from a pipe carrying radioactive water at a distance d from the pipe axis (d must be much greater than the pipe radius):

$$\dot{X} = \theta \frac{S}{d} \sum_n \Gamma_n \cdot C_n \quad (40)$$

where \dot{X} is in $\text{C} \cdot \text{kg}^{-1} \cdot \text{h}^{-1}$ ($\text{R} \cdot \text{h}^{-1}$), S (in m^2) is the pipe (inside) cross-sectional area, d (in m) is the distance from the pipe axis to the point in question, Γ_n in

²⁰ For example, the use of these elements in copper systems has been found to be highly beneficial; however they may be detrimental to aluminium or stainless-steel systems.

$(C \cdot \text{kg}^{-1} \cdot \text{h}^{-1})(\text{Bq} \cdot \text{m}^{-2})^{-1} ((\text{R} \cdot \text{h}^{-1})(\text{Ci} \cdot \text{m}^{-2})^{-1})$ is the specific gamma-ray constant (Table XXXII) and C_n in $\text{Bq} \cdot \text{m}^{-3}$ ($\text{Ci} \cdot \text{m}^{-3}$) is the concentration of nuclide within the pipe. The angle θ is the angle (in radians) subtended by the pipe segment at the location in question, as illustrated in Fig.40. For an infinite pipe segment $\theta = \pi$. The index n is for the nuclides (generally only ^{15}O and ^{11}O) to be added to give the total exposure rate. The exposure rate from any number of pipe segments may be added in this manner. More exact methods of dealing with complicated geometries may be found, for example, in the Reactor Shielding Design Manual [21].

(g) Data for calculating the necessary shielding for 0.511-MeV gamma rays may be found in Section 3.4. The data given for 1-MeV bremsstrahlung should be used.

(h) To estimate the buildup of ^3H , the rate at which water is lost from the primary system by evaporation and leakage should be estimated and an approximate effective half-life used, as in Eq.(39).

Warren et al.[10] have reported exposure rates of up to a few hundred $\text{mR} \cdot \text{h}^{-1}$ from cooling water circuits from the SLAC accelerator structures. However, considerably higher levels are found near heat exchangers for high-power beam dumps operating at a few hundred kW electron beam power, totally absorbed in water. There, rates up to $30 \text{ mC} \cdot \text{kg}^{-1} \cdot \text{h}^{-1}$ ($120 \text{ R} \cdot \text{h}^{-1}$) are observed at contact.

REFERENCES TO SECTION 2.7

- [1] LEDERER, C.M., HOLLANDER, J.M., PERLMAN, I., Table of Isotopes, 6th ed., John Wiley, New York (1967).
- [2] BERMAN, B.L., FULTZ, S.C., Giant-Resonance Measurements with Monoenergetic Photons, Lawrence Livermore Laboratory, Rep. UCRL-75383 (1974); Rev. Mod. Phys. 47 (1975) 713.
- [3] SWANSON, W.P., Note on Air Activation by Bremsstrahlung, Stanford Linear Accelerator Center, Internal Note (1976).
- [4] KASE, K.R., Radioactive gas production at a 100-MeV electron linac facility, Health Phys. 13 (1967) 869.
- [5] LADU, M., PELLICIONI, M., ROCCELLA, M., Produzione e Scarico di Gas Tossici e Radioattivi nel Tunnel del Linac di Frascati, Laboratori Nazionali di Frascati del CNEN, Internal Note LNF-65/21, No.282 (1965); Translation: Production and Discharge of Toxic and Radioactive Gases in the 'Linac' Tunnel in Frascati, National Research Council of Canada, Ottawa, Technical Translation No. NRC TT-1332 (1968).
- [6] GEORGE, A.C., BRESLIN, A.J., HOSKINS, J.W., Jr., "Evaluation of the hazard from radioactive gas and ozone at linear electron accelerators", Proc. First Symp. Accelerator Radiation Dosimetry and Experience, Brookhaven National Laboratory, USAEC, Washington DC, Rep. CONF-65119 (1965) 513-55.

- [7] VIALETTES, H., "Gas and dust activation in the target room of the Saclay Electron Linac", Proc. Second Int. Conf. Accelerator Dosimetry and Experience, Stanford Linear Accelerator Center, USAEC, Washington, DC, Rep. CONF-691101 (1969) 121.
- [8] PATTERSON, H.W., THOMAS, R.H., Accelerator Health Physics, Academic Press, New York (1973) 526.
- [9] INTERNATIONAL COMMISSION ON RADIOLOGICAL PROTECTION, Report of Committee II on Permissible Dose for Internal Radiation, ICRP Publication 2, Pergamon Press, Oxford (1960).
- [10] WARREN, G.J., BUSICK, D.D., McCALL, R.C., "Radioactivity produced and released from water at high energies", Proc. Second Int. Conf. Accelerator Dosimetry and Experience, Stanford Linear Accelerator Center, USAEC, Washington, DC, Rep. CONF-691101 (1969) 99.
- [11] KASE, K.R., (MPC)_a for ¹³N, Health Phys. 15 (1968) 283.
- [12] HÖFERT, M., "Radiation hazard of induced activity in air as produced by high energy accelerators", Proc. Second Int. Conf. Accelerator Dosimetry and Experience, Stanford Linear Accelerator Center, USAEC, Washington, DC, Rep. CONF-691101 (1969) 111.
- [13] JONES, T., TURNER, B.A., FOWLER, J.F., "Calculation of the maximum permissible concentration of oxygen 15 in the air", Proc. Conf. Radiation Protection in Accelerator Environments (STEVENSON, G.R., Ed.), Rutherford Laboratory, Chilton, Didcot, Oxon. (1969) 13.
- [14] St. CHARALAMBUS, S., RINDI, A., Aerosol and dust radioactivity in the halls of high-energy accelerators, Nucl. Instrum. Meth. 56 (1967) 125.
- [15] DeSTAEBLER, H., Photon-Induced Residual Activity, Stanford Linear Accelerator Center, Rep. TN-63-92 (1963).
- [16] COWARD, D.H., Radioactive Water, Stanford Linear Accelerator Center, Technical Memorandum (1964); Addendum (1965).
- [17] YAMAGUCHI, C., MPC calculation for the radionuclides produced during accelerator operation, Health Phys. 29 (1975) 393.
- [18] WALZ, D.R., Radiolysis and Hydrogen Evolution in the A-Beam Dump Radioactive Water System, Stanford Linear Accelerator Center, Rep. SLAC-TN-67-29 (1967).
- [19] WALZ, D.R., LUCAS, L.R., The "sphere dump" – a new low-cost, high-power beam dump concept and a catalytic hydrogen-oxygen recombiner for radioactive water systems, IEEE Trans. Nucl. Sci. NS-16 3 (1969) 613; Stanford Linear Accelerator Center, Rep. SLAC-PUB-555 (1969).
- [20] BUSICK, D.D., ⁷Be Build-Up in a Large Water Beam Dump System at the Stanford Linear Accelerator Center, Stanford Linear Accelerator Center, Rep. SLAC-PUB-521 (1966).
- [21] ROCKWELL, T., III (Ed.), Reactor Shielding Design Manual, Ch.9, Van Nostrand, Princeton, NJ (1956).

2.8. Muons

Above an energy of ($2 \times 105.66 \text{ MeV} \approx 211 \text{ MeV}$), muon pair (μ^+ , μ^-) production by photons in the Coulomb field of target nuclei becomes possible. This is a process analogous to ordinary electron-positron pair production, except that the cross-sections are smaller by several orders of magnitude ($\sim 1/40\,000$), owing to the larger muon mass. The dominant process is one in which the target

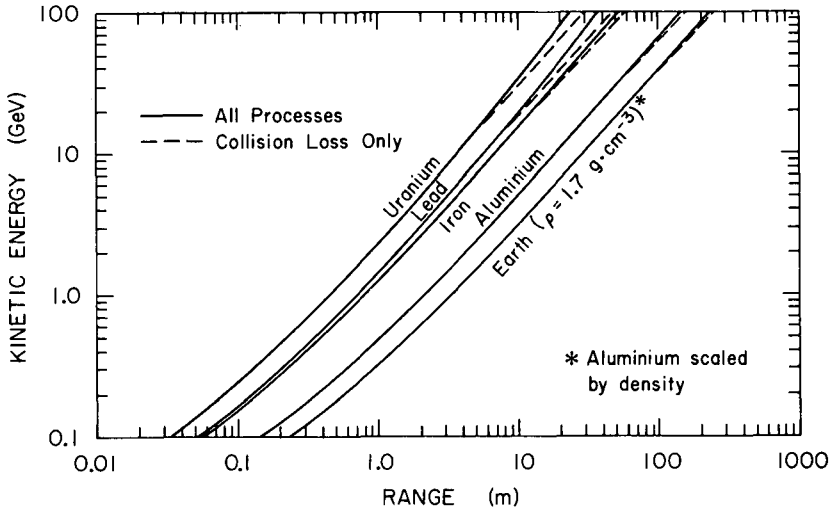


FIG.41. Range-energy curves for muons in various materials. (Adapted from Ref.[10], with kind permission of W.R. Nelson and K.R. Kase, the Stanford Linear Accelerator Center, and Nuclear Instruments and Methods.)

nucleus remains intact as it recoils from the interaction (coherent production), although some reactions involving nuclear breakup (a few per cent) also occur. Muons are also present as decay products of photoproduced π^\pm and K^\pm mesons, but these additional sources are relatively small compared with the direct production of muon pairs, provided that the π^\pm , K^\pm decay path is not too long [1, 2].

Muon production will not present a radiation problem at an installation which is otherwise adequately shielded, unless the beam energy exceeds about 1 GeV. The muon fluence is very highly peaked in the forward direction, with typical beam diameters of 10–20 cm outside of the thick shielding. In cases where additional muon shielding is needed, it usually takes the form of iron blocks, one to several metres in length, positioned only in the forward direction.

Although similar in every respect to electrons, their large mass does not permit muons to radiate energy as readily by bremsstrahlung. Being leptons, they also do not interact with nuclei via the hadronic interaction. The only significant stopping mechanism remaining is energy loss by ionization. Extensive tables of muon stopping power and ranges in various materials are published by Barkas and Berger [3] and Berger and Seltzer [4]. Figure 41 shows a plot of muon ranges in several materials as a function of energy.

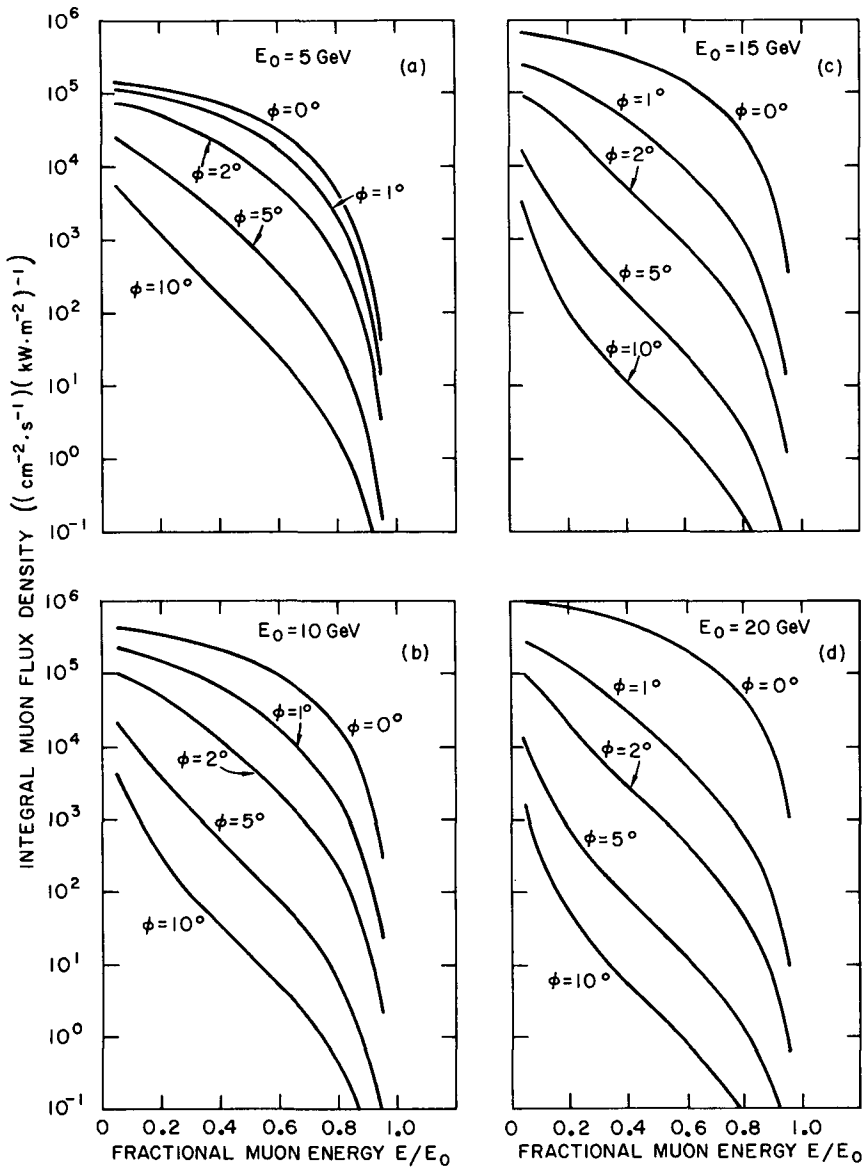


FIG. 42. Integral muon flux density at 1 m, per unit electron beam power, versus fractional muon energy, E/E_0 , for electron energies E_0 incident on a thick iron target. These data are normalized to 1 kW beam power, 1 m from the target. (Adapted from Ref.[9], with kind permission of W.R. Nelson, the Stanford Linear Accelerator Center, and Nuclear Instruments and Methods.)

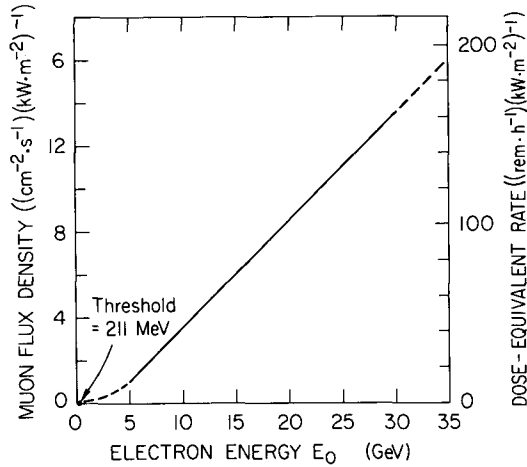


FIG.43. Muon production at 0° from an unshielded thick iron target, as a function of electron energy E_0 . Left-hand scale: muon flux density at 1 m, per unit electron beam power $((\text{cm}^{-2} \cdot \text{s}^{-1})(\text{kW} \cdot \text{m}^{-2})^{-1})$. Right-hand scale: unshielded dose-equivalent rate \dot{H} normalized to 1 m, per unit electron beam power $((\text{rem} \cdot \text{h}^{-1})(\text{kW} \cdot \text{m}^{-2})^{-1})$. (Adapted from W.R. Nelson [9].)

At the higher energies ($E_0 \gtrsim 10 \text{ GeV}$), it is often impractical to attempt to stop a significant fraction of muons, as their range extends to about 10 m in iron. The alternative is to reduce absorbed dose rates in the forward direction by multiple scattering [5–7] in iron blocks and rely on distance, if necessary. A fraction of the muons stops in the material, but scattering is the dominant mechanism for reducing fluences, provided that ample distance from the shield exit is allowed for the beam to diverge. Energy degradation in the material increases the effectiveness of scattering.

Muon photoproduction in thick targets has been discussed by Clément and Kessler [8] and by Nelson et al. [9–11]. Transport and shielding through thick barriers have been discussed by Nelson et al. [10,11], Alsmiller and Barish [12], and Ladu et al. [13].

Figure 42 shows calculated integral energy spectra of muons produced in a thick target of iron at various angles and incident electron energies [9].

Figure 43 plots the μ^\pm fluence at 0° integrated over all muon energies as a function of primary electron energy, E_0 , as derived from Fig.42. The fluence rate per kW beam power is approximately proportional to E_0 , and we may reasonably expect this linear trend to continue to higher values of E_0 . Although the *total* number of muons produced per kW does not rise very rapidly, those produced tend to be more tightly collimated.

To estimate the dose-equivalent rate to tissue due to muons, the integral muon flux density at 0° for the highest average beam power at the highest accelerator energy (Fig.43) should be determined. This flux density should then be corrected by the inverse square law to the closest occupied area at 0° . For purposes of this estimate, the fluence may be considered to be independent of target material because the Z^2 rise in the production cross-section is approximately offset by a shortening of the thick-target track length (Section 2.2). The fluence rate may be converted to dose-equivalent rate in tissue by the relationship

$$\dot{H} (\text{rem} \cdot \text{h}^{-1}) = 1.2 \times 10^{-4} \varphi \quad (41)$$

where φ is in $\mu^\pm \cdot \text{cm}^{-2} \cdot \text{s}^{-1}$, based on an average stopping power for muons in tissue [4] and a quality factor $Q = 1$. This dose-equivalent rate corresponds to an unshielded situation. To approximately account for the scattering effect of an existing or contemplated shield of thickness X , the above unshielded dose-equivalent rate is corrected by means of the formula

$$\dot{H} (\text{scattered}) = \left[\frac{25}{25 + X/X_0} \right] \left[\frac{X(E_0) - X}{X(E_0)} \right] H (\text{unshielded}) \quad (42)$$

in which the radiation length X_0 is used (Appendix B). The first factor in Eq.(42) accounts for multiple Coulomb scattering of muons in the shield, and the second for the fraction which is stopped. In this factor, $X(E_0)$ is the maximum possible muon range at the primary beam energy E_0 (Fig.41). Negative values of this term simply mean that all muons are stopped. The constant 25 is the ratio squared of the muon mass, 105.66 MeV, to the constant, $E_s = 21.2$ MeV, which appears in the theory of multiple Coulomb scattering [5-7]. Thus $(105.66/21.2)^2 = 24.84 \approx 25$. This correction is applied to an arrangement in which the shield begins close to the electron beam dump and the location to be protected is at a considerably greater distance than the shield thickness. It is quite accurate for the first decade of attenuation; thereafter it gives an overestimate of the dose equivalent. A more accurate estimate can be made by numerical integration [10].

A direct measurement of the dose rate in the closest occupied area should be made before routine operation of the accelerator. It should be remembered during the radiation protection survey that the muons will form a narrow beam that may not be evident in a casual area survey.

REFERENCES TO SECTION 2.8

- [1] TSAI, Y.-S., WHITIS, V., Thick-target bremsstrahlung and target considerations for secondary-particle production by electrons, Phys. Rev. **149** (1966) 1248.
- [2] KIM, K.J., TSAI, Y.-S., Improved Weizsäcker-Williams method and its application to lepton and W-boson pair production, Phys. Rev. **D8** (1973) 3109.

- [3] BARKAS, W.H., BERGER, M.J., Tables of Energy Losses and Ranges of Heavy Charged Particles, National Aeronautics and Space Administration, Rep. NASA SP-3013 (1964).
- [4] BERGER, M.J., SELTZER, S.M., Additional Stopping Power and Range Tables for Protons, Mesons, and Electrons, National Aeronautics and Space Administration, Rep. NASA SP-3036 (1966).
- [5] MOLIERE, G., Theorie der Streuung schneller geladener Teilchen II: Mehrfach- und Vielfachstreuung, *Z. Naturf.* 3a (1948) 78.
- [6] ROSSI, B., GREISEN, K., Cosmic ray theory, *Rev. Mod. Phys.* 13 (1941) 240.
- [7] ROSSI, B., High-Energy Particles, Ch.2, Prentice-Hall, Englewood Cliffs, NJ (1952).
- [8] CLEMENT, G., KESSLER, P., Electroproduction de muons de très haute énergie, *Nuovo Cim.* 37 (1965) 876.
- [9] NELSON, W.R., The shielding of muons around high energy electron accelerators: Theory and measurement, *Nucl. Instrum. Meth.* 66 (1968) 293.
- [10] NELSON, W.R., KASE, K.R., Muon shielding around high-energy electron accelerators, Part I, Theory, *Nucl. Instrum. Meth.* 120 (1974) 401.
- [11] NELSON, W.R., KASE, K.R., SVENSSON, G.K., Muon shielding around high-energy electron accelerators, Part II, Experimental investigation, *Nucl. Instrum. Meth.* 120 (1974) 413.
- [12] ALSMILLER, R.G., Jr., BARISH, J., High-energy (>18 GeV) muon transport calculations and comparison with experiment, *Nucl. Instrum. Meth.* 71 (1969) 121.
- [13] LADU, M., PELLICIONI, M., PICCHI, P., ROCCELLA, M., Shielding for ultra-relativistic muons, *Nucl. Instrum. Meth.* 104 (1972) 5.

2.9. Charged-particle secondary beams

At some high-energy research accelerators, secondary beams of mesons and other particles are used. The radiation protection needs for charged-particle beam lines vary considerably, but the following points may serve as guidelines:

(a) The extent of the radiation hazard can only be roughly estimated a priori. An estimate can be based on the following factors:

- (i) The total particle current in the beam line should be estimated from data on target yields and beam-line acceptance, in terms of solid angle and momentum interval ($\Delta\Omega \cdot \Delta p$). Data on yields can be obtained from Refs [1–4]. The beam-line acceptance can be obtained from the beam-line designer.
- (ii) The smallest area that the beam can have in an accessible location should be ascertained. Some high-energy beams have been focussed to spots of the order of 1 mm dia.
- (iii) Data for conversion to dose-equivalent rates for electrons (Section 2.3) may be used to conservatively evaluate the hazard for relativistic particles. For non-relativistic particles, the LET and corresponding quality factor should be used (Section 2.1).

(b) The secondary beam should be contained and considered as part of the containment area, where dose-equivalent rates can rise to unsafe levels.

(c) Fluences should be limited by controlling the primary beam power by redundant electronic devices rather than by reliance on the attentiveness of the operator.

(d) It should be assured that the primary beam cannot inadvertently enter the secondary beam line. This can be done by adequately cooled collimators which spatially restrict both primary and secondary beams, and by designing secondary beams to have initial directions different from those of the primary beam, operating them at different momenta and different polarity, if possible.

(e) The initial magnetic deflection of a secondary beam should be in a plane different from that of the primary beam steering.

(f) Positive secondary beams are inherently safer than negative beams because the (negative) primary beam cannot be transported by the secondary line. Every particle that is transported is the product of a two-step production process which reduces the maximum possible fluence well below that of the primary beam. For this reason, secondary positrons should be used in preference to electrons when feasible.

(g) A procedure should be devised to positively test the containment of the primary beam by steering it while remotely observing its location on a ZnS screen, and simultaneously observing ionization-chamber measurements in the secondary line.

(h) Once the beam is established, the hazard can be better evaluated by direct measurement of particle currents by scintillation counters or ionization chamber readings. The beam area can best be determined by sweeping horizontally and vertically with a smaller detector mounted on a remotely controlled positioning device. At higher fluences, photographic film or plastic colouration dose meters may be useful.

(i) In using ordinary survey instruments, it should be borne in mind that the area of a narrow beam may introduce a geometrical correction factor that can be very large: easily a factor of 1000. One should also be aware that high fluence rates and the duty factor together may cause erroneous readings in a narrow beam because of ion recombination within the chamber (Section 5.2).

(j) Adequate provision should be made to terminate the beam in shielding material.

The accessibility of beam lines is often a point of controversy between beam-line users and persons responsible for radiation safety. In such cases, the following guidelines for the radiation safety committee are suggested for compromise:

(a) Where there is no essential reason to expose a beam line, the definitions and controls for radiation areas and high-radiation areas (Sections 6.3, 6.4) should

be implemented, just as for broad radiation fields, using the best estimates of the maximum dose-equivalent rate at the location in question.

(b) Where the radiation safety committee agrees that the work of the facility really demands that the beam line be exposed, the standards for treating an area as a *high-radiation area* may be relaxed by as much as a factor of ten, based on the highest possible dose equivalent within the beam. The implicit assumption is that the occupancy factor for an eye in an open beam line is less than a tenth of that of the entire body in the beam proximity. It must be made difficult or inconvenient (by height or partial barriers) for personnel to be exposed to the beam and improbable that any individual would have reason to be so exposed. Such an accommodation should be accompanied by intensified educational efforts and alerting of experimenters and other personnel to the hazard of the open beam line. Careful attention should be given to maintenance of radiation signs, ropes and lights.

(c) Where a gap in an otherwise fully enclosed line is sufficiently small so that a head cannot be inserted, the standard for a high-radiation area may be relaxed by a factor of thirty instead of ten.

(d) *Primary* beams and bremsstrahlung beams produced by primary beams constitute another category of danger (Sections 2.3, 2.4) and must always be fully contained and shielded.

REFERENCES TO SECTION 2.9

- [1] STANFORD LINEAR ACCELERATOR CENTER, The SLAC Users Handbook, SLAC Internal Report, Stanford, CA (1971).
- [2] FLATTE, S.M., MURRAY, J.J., KLEIN, P.R., JOHNSTON, L.H., WOJCICKI, S.G., Particle yields at the Stanford Linear Accelerator Center and the photon-nucleus interaction in the 5-18 GeV region, Phys. Rev. **166** (1968) 1482.
- [3] COX, J., MARTIN, F., PERL, M.L., TAN, T.H., TONER, W.T., ZIPF, T.F., A high energy, small phase-space volume muon beam, Nucl. Instrum. Meth. **69** (1969) 77.
- [4] TSAI, Y.-S., Pair production and bremsstrahlung of charged leptons, Rev. Mod. Phys. **46** 4 (1974) 815.

2.10. Production of toxic gases

Toxic gases produced by ionizing radiation are listed in Table XXXIII. Of these, ozone (O₃) is the most toxic and may be produced in such quantities as to constitute a health hazard within the radiation room. Ozone and nitric acid formed by the interaction of nitrogen oxides and water vapour may also gradually damage equipment by corrosion. The highest local concentrations will be in the region where the highest radiation doses (to air) are imparted. In addition to personnel

TABLE XXXIII. TOXIC GASES PRODUCED BY RADIATION AT ELECTRON LINAC INSTALLATIONS

Gas	TLV ^a (ppm)	G (air) ^b (molecules per 100 eV)		Decomposition time assumed ^c (min)	
		Low \dot{D}	High \dot{D}		
Ozone	O ₃	0.1	7.4	10.3	50
Nitric oxide	NO	25			
Nitrogen dioxide	NO ₂	5 ^d	(4.8)	(<0.15)	
Nitrogen trioxide	NO ₃				
Nitrogen tetroxide	N ₂ O ₄	5 ^d			
Nitric anhydride	N ₂ O ₅				
Nitrous oxide	N ₂ O				

^a Threshold limit value. Maximum concentration averaged over any 8-hour work shift, assuming 40-hour work week.

^b Values from Willis et al. [11]. High dose rate means instantaneous dose rate (during beam pulse) greater than about $5 \times 10^8 \text{ Gy} \cdot \text{s}^{-1}$ ($5 \times 10^{10} \text{ rad} \cdot \text{s}^{-1}$) ($\approx 3 \times 10^{24} \text{ eV} \cdot \text{g}^{-1} \cdot \text{s}^{-1}$) to air. Theoretical values are in parentheses.

^c Decomposition time for ozone may depend strongly on size of room and nature of materials present.

^d Value also represents ceiling value: maximum concentration allowed at any time.

safety, the effect of these enhanced concentrations on the irradiated materials must be considered. This is especially true, for example, for food preservation by radiation.

Of the gases listed, ozone production will almost always be the limiting factor, owing to its much lower threshold limit value (0.1 ppm) [1–3], high radiolytic yield and chemical reactivity.

The production rate p of a chemical species is related to the integral dose to the air volume irradiated via the radiolytic yield, G , the number of molecules formed per unit of energy deposited. Recent work has found the radiolytic yield of O₃ in *pure oxygen* to be around $G = 13$ molecules per 100 eV [4–11].

In *air*, an efficient charge-transfer mechanism (positive charge transfer from N₂⁺ ions to O₂) enhances the O₃ yield, and G -values are believed to be in the range 7.4–10.3 molecules per 100 eV, depending on the instantaneous dose rate, even though air is only one-fifth oxygen [11]. Such values imply that more than one ozone molecule is formed for every ion formed (34 eV per ion pair). This yield

represents an efficient conversion mechanism for O₃; the yields for the other toxic gases are smaller. NO is consumed by the more copious O₃ to produce NO₂, and therefore NO₂ is the predominant oxide of nitrogen.

Ozone decomposes spontaneously, reacts chemically with air impurities and other materials, and is decomposed by the radiation itself. The effective decomposition time will therefore depend on room size, wall material, temperature, and impurities in the air and ozone concentration. The decomposition time has been found to be about 50 min in a typical research installation [12].

The provisions for mitigating the effects of toxic gases are the same as those for reducing the concentrations of radioactive gases (Section 2.7.1) and include reduction of the integral dose imparted to the air by limiting the beam pathlength, and increasing the ventilation. The pattern of accelerator usage and radiation room occupancy (no personnel present during irradiation times and no ozone produced during off-times) provides considerable protection in itself and should be considered in assessing these risks. The smell of ozone can be detected at 0.1 ppm or below, so that any room free of the characteristic odour may be regarded as safe from this radiolytic gas. On the other hand, if the odour is strong or frequently detected, an assessment should be made with monitoring equipment.

2.10.1. Concentration buildup and removal

The first step in estimating the concentration of ozone is the determination of its production rate p for the situation in question (see examples below). In this discussion we express p in units of litres per minute, which is convenient when the room volume is also expressed in litres (a large room is of the order of 10⁶ litres), and buildup and decay times are expressed in minutes. Once the production rate p has been determined, factors to account for buildup and removal are applied to determine the concentration at any time, just as for radioactivation. The pattern of accelerator use should be considered here.

The concentration buildup is described by the formula

$$C(t_b) = \frac{p\bar{T}}{V} [1 - \exp(-t_b/\bar{T})] \quad (43)$$

where C is the concentration (dimensionless), t_b is the 'on-time' or buildup time in minutes, V is the room volume in litres, and \bar{T} is determined by the removal processes:

$$\bar{T} = \frac{T(\text{vent}) \cdot T(\text{decomp})}{T(\text{vent}) + T(\text{decomp})} \quad (44)$$

where $T(\text{vent})$ is the room volume divided by the air volume exhausted per unit time. For ozone, we take the decomposition time $T(\text{decomp})$ to be 50 min.

In the usual situation, the ventilation time T (vent) is sufficiently less than the decomposition time so that it essentially controls ozone removal, and $\bar{T} \approx T$ (vent) can often be used without serious error.

Equation (43) shows that the concentration buildup for running times short compared with the effective removal time \bar{T} is proportional to the buildup time:

$$C(t_b) = \frac{pt_b}{V} \quad (\text{short running times; } t_b \ll \bar{T}) \quad (45)$$

The *saturation* concentration C_s derived from Eq.(43) for long buildup times is evidently

$$C_s = \frac{p\bar{T}}{V} \quad (\text{saturation; } t_b \gg \bar{T}) \quad (46)$$

In the case of *no* ventilation, the saturation concentration of ozone is proportional to the effective decomposition time:

$$C_s = \frac{p \cdot (50 \text{ min})}{V} \quad (\text{ozone, no ventilation}) \quad (47)$$

Following turnoff, the concentration will diminish exponentially with decay time t_d :

$$C(t_d) = C_{\text{turnoff}} \exp(-t_d/\bar{T}) \quad (48)$$

The ventilation time T (vent) during periods of ‘accelerator off’ is frequently different from that during ‘on’ periods, and the appropriate value of T (vent) should be used in Eq.(44). For example, if there is no ventilation at all during ‘on’ periods, T (vent) = ∞ , and Eq.(44) gives $\bar{T} = T$ (decomp) = 50 min. The buildup expressed by Eq.(43) will approach the highest possible saturation concentration, as given by Eq.(47). If the ventilation is then switched on, preparatory to personnel entry, \bar{T} will be considerably reduced and the concentration expressed by Eq.(48) will decrease rapidly in comparison with the buildup.

2.10.2. Production rates

Production rates for toxic gases and their radiological safety implications are discussed in Refs [13–18]. We consider here the production rate of ozone for four cases frequently encountered at electron linear accelerators.

(a) External electron beam without showering

The rate of ozone production by an external electron beam is based on an assumed average collision mass stopping power of $2 \text{ MeV} \cdot \text{cm}^2 \cdot \text{g}^{-1}$, and a

G value of 10.3 molecules per 100 eV, corresponding to high instantaneous dose rates to air within a narrow beam path. These assumptions lead directly to

$$p = 350 \text{ IL} \tag{49}$$

where p is in $\text{ltr} \cdot \text{min}^{-1}$, I is the *average* electron current in amperes and L is the pathlength in air (in metres). This situation applies whenever the electron beam does not cause showering in any thick materials before entering the air. This is the case if the beam window is thin ($X < X_0$) or if the energy E_0 is less than about twice the critical energy E_c for the material(s) through which the beam passes. The critical energy is approximately given by Eq.(2) (Section 2.2) (see also Appendix B). Currents accelerated at almost all electron linacs are capable of producing ozone concentrations above the threshold limit value in an average room if an extracted beam is used and the air path is sufficiently long.

(b) External electron beam with showering

Whenever a high-energy electron beam (E_0 greater than about twice E_c) passes through a solid material (such as a beam window, pipe or flange) before entering the air path, buildup of particle fluence can enhance the ozone production considerably, easily by an order of magnitude or more in some cases. The extreme situation is where the thickness of solid material corresponds to the shower maximum. In this case the enhancement factor is approximately proportional to E_0/E_c [19].

$$\left[\begin{array}{l} \text{Maximum} \\ \text{enhancement} \\ \text{of electron} \\ \text{fluence} \end{array} \right] = \frac{0.31 (E_0/E_c)}{[\ln(E_0/E_c) - 0.37]^{1/2}} \quad (\text{Approx. B})^{21} \tag{50}$$

The shower maximum occurs at a thickness X_{max} which increases as the logarithm of the energy. It can be estimated in terms of the radiation length X_0 (Section 2.2 and Appendix B) by:

$$X_{\text{max}}/X_0 = 1.01 [\ln(E_0/E_c) - 1] \quad (\text{Approx. B}) \tag{51}$$

²¹ The use of Approximation B appears to be a conservative choice; for example, the experiment of Jakeways and Calder [20] gives $(E_0/12.7 E_c)^{0.9}$ as the maximum enhancement factor for lead (for $E_0/E_c = 50-400$). The experiment of Müller [21] gives $(E_0/8.33 E_c)^{0.935}$ for lead ($E_0/E_c = 200-1500$). These formulae, generalized to other materials, give enhancement factors lower than Approximation B by about 50% and 25%, respectively, in the range for which they have been determined. (For comparison, Approximation B gives approximately $(E_0/6.6 E_c)$ at $E_0/E_c = 100$.) All of these formulae yield values less than one for small values of E_0/E_c . In such cases the enhancement factor should be taken as one (instead of 'no enhancement').

It should be assumed that the maximum enhancement will occur, unless there is positive assurance that this condition cannot be achieved.

The production rate given by Eq.(49) should be multiplied by the enhancement factor.

- (c) Bremsstrahlung or diffuse electron beams specified in units of exposure rate or dose rate

At radiotherapeutic and radiographic installations, a bremsstrahlung or diffuse electron beam is usually specified in terms of exposure rate or absorbed dose rate in $(\text{C} \cdot \text{kg}^{-1})(\text{m}^2 \cdot \text{s}^{-1})^{-1}$ ($\text{R} \cdot \text{m}^2 \cdot \text{min}^{-1}$) or $(\text{Gy} \cdot \text{m}^2 \cdot \text{s}^{-1})(\text{rad} \cdot \text{m}^2 \cdot \text{min}^{-1})$, in a field area S determined at 1 m from the target. Here we make the simplifying assumption that the absorption dose to the irradiated air at the same distance is equal to the dose to tissue in the case of a therapeutic installation. If the exposure X is specified instead, we can assume that the dose to air (in rad) is equal to the exposure (in R). If the exposure is given in $\text{C} \cdot \text{kg}^{-1}$, we obtain the air dose (in Gy) from $D = 33.7 X$. This leads directly to the production rate for ozone:

$$\begin{aligned} p (\text{ltr} \cdot \text{s}^{-1}) &= 2 \times 10^{-9} \dot{D} (\text{Gy} \cdot \text{m}^2 \cdot \text{s}^{-1}) \text{SL} \\ p (\text{ltr} \cdot \text{min}^{-1}) &= 2 \times 10^{-7} \dot{D} (\text{rad} \cdot \text{m}^2 \cdot \text{min}^{-1}) \text{SL} \end{aligned} \quad (52)$$

assuming $G = 7.4$ molecules per 100 eV, appropriate for 'low' dose rates typically found in situations where the accelerator output is specified in this manner. The field size S is in m^2 and the air pathlength L in metres. The accelerator parameters shown in Tables III and IV (Section 1.3) indicate that the ozone production rate is generally not critical for standard medical and radiographic installations under normal operating conditions.

- (d) Uncollimated bremsstrahlung beam from an optimum high-Z target, where the incident electron beam power is specified in kW

For this case, we make use of the approximation for the absorbed dose rate from bremsstrahlung at 0° from optimum targets (Eq.(16), Section 2.4.1):

$$\begin{aligned} \dot{D} ((\text{Gy} \cdot \text{s}^{-1})(\text{kW} \cdot \text{m}^{-2})^{-1}) &\approx 0.0055 E_0^2 \\ \text{or } \dot{D} ((\text{rad} \cdot \text{min}^{-1})(\text{kW} \cdot \text{m}^{-2})^{-1}) &\approx 33 E_0^2 \end{aligned}$$

where \dot{D} is the bremsstrahlung dose rate and E_0 is in MeV. We further assume that all of the bremsstrahlung dose to air is imparted within a solid angle of

100 E_0^{-2} steradians.²² These approximations, together with a G value of 7.4 molecules per 100 eV, directly yield

$$p (\text{ltr} \cdot \text{s}^{-1}) = 1.2 \times 10^{-5} \text{ LP}$$

$$p (\text{ltr} \cdot \text{min}^{-1}) = 7 \times 10^{-4} \text{ LP} \tag{53}$$

where L is in metres, and the electron energy E_0 cancels and we have a production rate proportional to the incident electron beam power P in kW, independent of energy.

The approximations used are valid (to within a factor of two) for $E_0 \leq 50$ MeV. In this energy range, the lower G value of 7.4 molecules per 100 eV would normally hold. At higher energies, the effect of showering in the target material complicates the situation and case (b) would apply instead. The parameters of typical research accelerators are such that ozone production by bremsstrahlung may be a problem if there is a need for frequent access without adequate ventilation.

REFERENCES TO SECTION 2.10

- [1] AMERICAN CONFERENCE OF GOVERNMENTAL INDUSTRIAL HYGIENISTS, Threshold Limit Values of Airborne Contaminants and Physical Agents with Intended Changes Adopted by ACGIH for 1971, ACGIH, Cincinnati, Ohio (1971).
- [2] AMERICAN CONFERENCE OF GOVERNMENTAL INDUSTRIAL HYGIENISTS, Documentation of the Threshold Limit Values for Substances in Workroom Air, 3rd ed., ACGIH, Cincinnati, Ohio (1971).
- [3] OCCUPATIONAL SAFETY AND HEALTH ADMINISTRATION, Occupational Safety and Health Standards, US Department of Labor, Washington, DC, Federal Register 39 125 (1974) 23541.
- [4] RILEY, J.F., Chemistry Division Annual Report, Oak Ridge National Laboratory, Rep. ORNL-3320 (1962). (This author reports $G = 12.5$.)
- [5] JOHNSON, G.R.A., WARMAN, J.M., Formation of ozone from oxygen by the action of ionizing radiations, Discuss. Faraday Soc. 37 (1964) 87. (The value 12.8 given by these authors has been corrected to 10.2 ± 0.6 by Ghormley et al. (Ref.[9].)
- [6] SHAH, J., MAXIE, E.C., Gamma-ray synthesis of ozone from air, Int. J. Appl. Radiat. Isot. 17 (1966) 155. (These authors find $G = 11$ for flowing air.)
- [7] MEABURN, G.M., PERNER, D., LeCALVE, J., BOURENE, M., A pulsed-radiolysis study of atomic oxygen reactions in the gas phase, J. Phys. Chem. 72 11 (1968) 3922 ($G = 10.5$).

²² The energy dependence of the solid angle, E_0^{-2} , is based on Eq.(19) (Section 2.4.1). The coefficient 100 is chosen to be consistent with the bremsstrahlung yield at 10 MeV from high-Z targets and an average photon mass-energy absorption coefficient for a 10-MeV thick-target bremsstrahlung spectrum in air.

- [8] SEARS, J.T., SUTHERLAND, J.W., Radiolytic formation and decomposition of ozone, *J. Phys. Chem.* **72** 4 (1968) 1166 ($G = 10.5 \pm 0.5$).
- [9] GHORMLEY, J.A., HOCHANADEL, C.J., BOYLE, J.W., Yield of ozone in the pulse radiolysis of gaseous oxygen at very high dose rate. Use of this system as a dosimeter, *J. Chem. Phys.* **50** 1 (1969) 423 ($G = 13.8 \pm 0.7$).
- [10] BOYD, A.W., WILLIS, C., CYR, R., New determination of stoichiometry of the iodometric method for ozone analysis at pH 7.0, *Anal. Chem.* **42** 6 (1970) 670 ($G = 12.8 \pm 0.6$).
- [11] WILLIS, C., BOYD, A.W., YOUNG, M.J., Radiolysis of air and nitrogen-oxygen mixtures with intense pulses: determination of a mechanism by comparison of measured and computed yields, *Can. J. Chem.* **48** (1970) 1515.
- [12] GEORGE, A.C., BRESLIN, A.J., HASKINS, J.W., Jr., RYAN, R.M., "Evaluation of the hazard from radioactive gas and ozone at linear electron accelerators", *Proc. USAEC First Symp. Accelerator Radiation Dosimetry and Experience*, Brookhaven National Laboratory, USAEC, Washington, DC, Rep. CONF-651109 (1965) 539.
- [13] BRYNJOLFSSON, A., MARTIN, T.G., III, Bremsstrahlung production and shielding of static and linear electron accelerators below 50 MeV. Toxic gas production, required exhaust rates and radiation protection instrumentation, *Int. J. Appl. Radiat. Isot.* **22** (1971) 29.
- [14] BROBECK, W.M., *Particle Accelerator Safety Manual*, US Department of Health, Education and Welfare, Rockville, MD (1968).
- [15] NATIONAL BUREAU OF STANDARDS, and NATIONAL COUNCIL ON RADIATION PROTECTION AND MEASUREMENTS, *Shielding for High-Energy Electron Accelerator Installations*, NBS Handbook No.97 and NCRP Report No.31, Washington, DC (1964) 8.
- [16] NATIONAL COUNCIL ON RADIATION PROTECTION AND MEASUREMENTS, *Radiation Protection Design Guidelines for 0.1–100 MeV Particle Accelerator Facilities*, NCRP Rep. No.51, Washington, DC (1977).
- [17] LADU, M., PELLICIONI, M., ROCCELLA, M., *Produzione e scarico di gas tossici e radioattivi nel tunnel del Linac de Frascati*, Laboratori Nazionali di Frascati del CNEN, Internal Rep. No. 282 (1965); Translated as *Production and Discharge of Toxic and Radioactive Gases in the Linac Tunnel in Frascati*, National Research Council of Canada, Ottawa, Technical Translation No. NRC-TT-1332 (1968).
- [18] LESS, L.N., SWALLOW, A.J., Estimating the hazard due to radiolytic products from air, *Nucleonics* **22** 9 (1964) 58.
- [19] ROSSI, B., *High-Energy Particles*, Prentice-Hall, Englewood Cliffs, NJ (1952) 257.
- [20] JAKEWAYS, R., CALDER, I.R., An experimental study of the longitudinal development of electron initiated cascades in lead in the energy range 0.5–4.0 GeV, *Nucl. Instrum. Meth.* **84** (1970) 79.
- [21] MÜLLER, D., Electron showers of high primary energy in lead, *Phys. Rev.* **5** (1970) 2677.

2.11. X-rays generated by microwave systems

2.11.1. Oscillators and amplifiers

Klystrons in accelerator service operate under pulsed conditions with peak beam voltages in the range 200–300 kV and peak currents of 100–300 A, and are therefore efficient generators of low-energy X-rays. The X-ray output may

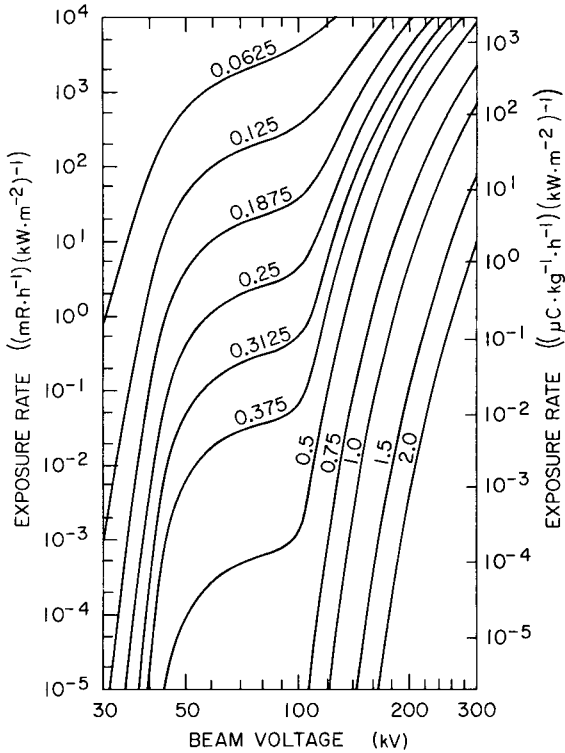


FIG.44. X-ray exposure rate at 1 m, per kW of average beam power from a klystron collector, for various thicknesses of lead shielding (in inches), as a function of supply voltage. (Adapted from Ref.[2], with kind permission of R.B. Nelson and Varian Associates.)

be higher with the RF drive on than with the unit in a quiescent state, and this should be checked. A conservative upper limit to the unshielded output can be calculated from the known operating voltage, current and pulse rate, by using published data for diagnostic X-ray machines [1]. In so doing, one should refer to kVp tables corresponding to *twice* the klystron supply voltage and use half the average current.

A calculation of X-ray exposure rates through various thicknesses of lead shielding, as a function of voltage, has been made by Nelson [2], assuming a current-voltage phase relationship within the operating klystron that would produce the most radiation (see Fig.44).

Experience has shown that a typical thickness of 2–5 cm of lead in areas not shielded by the iron magnet is satisfactory for high-power klystrons (20–40 MW peak power). Because of the irregular geometry of the klystron, particularly in

the region of the RF output waveguide and the collector cooling connections, special care must be taken to avoid radiation leakage due to inadequate overlap or fitting of the shielding material. Normally the shielding provided by the vendor is adequate. However, an evaluation of the shielding should be a phase of the acceptance procedure and should be repeated regularly. A thin-window ionization-chamber survey meter should be used. It is recommended that a wrap-around film technique be adopted as a radiation survey procedure to detect and localize emissions from small shielding gaps.

It has been observed that, as klystrons approach the end of their useful life, the X-ray output sometimes increases sharply. This is due to a distortion of the electron beam path and a consequent change in the effective X-ray source.

Where klystrons are operated only within the containment area (Section 6.4) and are subject to the same interlock protection and other safety provisions as the accelerator itself, the klystron shielding requirements may be relaxed. However, at a clinical facility, possible radiation doses from klystrons to patients undergoing therapy should be assessed and abated, if necessary.

Magnetrons contain cyclical currents operating at much lower voltage (up to 50 kV d.c.) and usually do not produce X-rays of sufficient intensity to be harmful. However, every microwave generator should be checked in this regard.

All microwave generators, including magnetrons, can emit *RF radiation* of harmful intensity and precautions should be taken in *electrical shielding* (Section 6.6).

2.11.2. Microwave cavities

Any vacuum cavity containing high-power microwave fields, such as an RF separator or accelerating cavity, can produce X-ray emissions which may be intense. This radiation is unpredictable and may be erratic, depending on microscopic surface conditions which change with time. The X-ray output is a rapidly increasing function of RF power.²³ All such devices operated outside of the containment area should be carefully shielded and controlled in the same manner as other radiation sources.

An upper limit to the effective X-ray energy can be estimated by obtaining from the designer an indication of the maximum potential difference between surfaces within the cavity. This knowledge is helpful in predicting the efficacy of shielding, after radiation has been measured.

In the case of an RF particle separator, the metal walls provide some degree of shielding, but it is advisable to sheath them entirely with about 2 mm of lead and to provide 5-mm-wall iron 'beam pipes' extending for about one metre along

²³ For example, measurements made on a SPEAR cavity at SLAC indicated an X-ray output dependence on RF power proportional to P^5 (Ref.[3]).

the axis in both directions and then abutting against regular beam pipes of larger diameter. These protection items should be 'permanently' installed and a prominent label affixed warning against their removal.

REFERENCES TO SECTION 2.11

- [1] See, for example, NATIONAL COUNCIL ON RADIATION PROTECTION AND MEASUREMENTS; Structural Shielding Design and Evaluation for Medical Use of X-Rays and Gamma Rays of Energies up to 10 MeV, NCRP Rep. No.49, Washington, DC (1976). (This report supersedes NCRP-34.)
- [2] NELSON, R.B., Theory of X-Ray Shielding for Klystrons, Varian Associates, Palo Alto, CA, Internal Rep. TDM-42 (1965).
- [3] SWANSON, W.P., X-Ray Radiation Observed Around a SPEAR Cavity, Stanford Linear Accelerator Center, Internal Report (1975).

3. RADIATION SHIELDING

3.1. Types of areas and shielding criteria

Because radiation protection standards may vary in different localities and are being revised from time to time, the actual legal requirements for the place in which the facility is to be established should be determined at an early planning stage. A qualified expert and governmental authorities should be consulted. Additional guidance may be found in Refs [1–6], for example.

The controlled area should be a work area where the only regular activity is related to accelerator operation, so that it is occupied for a major portion of each work week only by persons administratively regarded as radiation workers. Occupancy by other persons is only occasional (say, less than 10% of their working time) and only under supervision of the accelerator staff. In clinical situations, those rooms of the radiology department directly connecting to entrances to the treatment rooms are customarily defined as the controlled area, but areas more removed from radiation-producing equipment are not.

For the planning of radiation shielding, it is convenient to express the criteria in terms of a maximum average dose-equivalent rate \dot{H}_M in units of $\text{rem} \cdot \text{week}^{-1}$. Table XXXIV summarizes shielding criteria in these terms for controlled areas and non-controlled areas, suggested for use unless differing legal requirements are applicable.

In assessing shielding requirements, it is appropriate to take into account the accelerator operating schedule or workload, W , together with other factors that would affect the average weekly dose equivalent to individuals in occupiable areas. These factors include the beam orientation (use) factor U and the area occupancy factor T .²⁴

3.1.1. Accelerator scheduling and workload factor W

For radiation therapy, it is customary to express the equipment workload W in Gy(rad) per week produced at 1 metre from the therapy unit target ($\text{Gy}(\text{rad}) \cdot \text{m}^2 \cdot \text{week}^{-1}$). Because the routine for radiation therapy procedures

²⁴ The method of using the factors W , U and T in shielding design is adapted from a system for shielding medical accelerators given in NCRP Reports Nos 34 and 49 [3, 4]. The recommendations given here are broadly consistent with these reports, but also reflect other sources, and differ in details. The use of values of U and T less than one in shielding design is generally considered to be a valid radiation protection concept and, if the choice of values is realistic, serves to avoid unnecessary shielding overdesign. However, in some jurisdictions the use of values of U or T (or both) less than one may not be allowed for some types of installations.

TABLE XXXIV. RADIATION-PROTECTION CRITERIA BY TYPE OF AREA

Type of Area ^(a)	Category of ^(b) Persons	Occupancy Factor T	Dose-Equivalent Rate \dot{H}_M ^(c) (Maximim Average) (rem·week ⁻¹)
Controlled Area	Radiation Workers	1	0.100
Non-Controlled Area	General Public	≤ 1, depending on use of area	0.010
Containment Area	No person (except patient if under treatment)	0	No limit

(a) Terminology and definitions may vary. For example, definitions adopted by the European Community (Ref. [1]), expressed in these terms are: Controlled Area: $0.030 < \dot{H}_M < 0.100$ rem·week⁻¹, Supervised Area: $0.010 < \dot{H}_M < 0.030$ rem·week⁻¹. These standards also provide for two categories of Radiation Workers. DIN-6847 (Ref. [6]) specifies in addition a limit of 0.010 rem·week⁻¹ for persons other than adults in the Supervised Area, and a limit of $\dot{H}_M = 0.003$ rem·week⁻¹ for areas "where there is no possibility of monitoring." Also see NCRP-49 and NCRP-51 (Refs [4, 5]).

(b) Administrative category of persons normally occupying the type of area.

(c) Considering accelerator scheduling (workload W), beam orientation (use) factor U and area occupancy factor T.

TABLE XXXV. SUGGESTED SCHEDULING AND WORKLOAD PARAMETERS W^a

Type of installation	Weekly operating schedule (hours of operation per 40-hour week)	Workload ^b W
Radiation therapy	(Governed by treatment routine; use workload W)	(1000 Gy·m ² ·week ⁻¹) (100 000 rad·m ² ·week ⁻¹)
Industrial radiography	10 hours/week	Multiply accelerator rating (Gy·m ² ·min ⁻¹) or (rad·m ² ·min ⁻¹) by 600 min·week ⁻¹
Other industrial accelerators Research accelerators	40 hours/week	Multiply accelerator DE rate at 1 metre ^c (rem·m ² ·h ⁻¹) by 40 hours·week ⁻¹

^a For use where specific scheduling information is not available.

^b Dose-equivalent rate at 1 m from electron target. Units of rem·m²·week⁻¹ are suggested for shielding calculations. One may assume 0.01 Gy (1 rad) photon dose or 258 μC·kg⁻¹ (1 R) exposure to be equivalent to 1 rem.

^c Estimate dose equivalent of secondary radiations using material of Section 2.

is well established, a workload $W = 1000 \text{ Gy} \cdot \text{m}^2 \cdot \text{week}^{-1}$ ($100\,000 \text{ rad} \cdot \text{m}^2 \cdot \text{week}^{-1}$) is known to be representative of a busy facility and is suggested unless specific scheduling information or equipment specifications indicate a different choice (see Table XXXV). (Such a value corresponds, for example, to 250 treatments per week at 4 Gy (400 rad) per treatment.)

As the output of industrial radiographic units is much more variable, a standard workload figure is not given. Instead, it is suggested that the radiation protection be planned assuming that the unit is operated for 10 hours per 40-hour work week. A workload W for each installation can then be derived from the output specified for the unit to be installed. (Workloads based on 10 hours per week lie in a broad range: 10^2 to $5 \times 10^4 \text{ Gy} \cdot \text{m}^2 \cdot \text{week}^{-1}$ (10^4 to $5 \times 10^6 \text{ rad} \cdot \text{m}^2 \cdot \text{week}^{-1}$)).

A schedule of 40 hours of operation per 40-hour work week is suggested for radiation protection planning for accelerators used for other industrial purposes, such as radiation processing, or in research.

Even if the facility is operated for more than 40 hours per week, these scheduling data may still be applicable, because the dose to individuals is the underlying consideration, and each worker is likely to be present only 40 hours per week.

In estimating the workload, one may assume 0.01 Gy (1 rad) of absorbed dose imparted by photons or electrons, or $258 \mu\text{C} \cdot \text{kg}^{-1}$ (1 röntgen) of exposure to be equivalent to 1 rem.

3.1.2. Primary and secondary barriers and the orientation (use) factor U

A barrier towards which the useful beam can be directed is called a primary barrier; all others are secondary barriers. The orientation factor (use factor) U is used to account for the average fraction of the accelerator 'on-time' for which the radiation is directed towards a given barrier. For facilities where there is no provision for changing the beam direction, there is a single primary barrier; the orientation factor associated with it is $U = 1$. Since secondary barriers *always* protect against stray radiation, regardless of beam direction, they are also ascribed an orientation factor $U = 1$. Where the useful beam orientation is changeable, orientation factors less than 1 may be used for those primary barriers that are less frequently used (see Table XXXVI for suggested orientation factors for radiotherapeutic facilities). Specific factors for therapeutic facilities are also given in NCRP Rep. No. 49 [4] and DIN-6847 [6] (see also Ref. [7]).

For radiographic installations, the nature of the work is so variable that specific orientation factors for the primary barriers are not suggested here. (For secondary barriers $U = 1$, however.) Certain walls are designated as 'target walls', and unless the cost is prohibitive, it is suggested that the entire area of the target

TABLE XXXVI. SUGGESTED ORIENTATION (USE) FACTORS FOR THERAPEUTIC FACILITIES

Type of Barrier	Type of Radiation	U ^(a)
Primary Barrier ^(b)		
Floor	Useful beam	1
Walls toward which useful beam can be directed	Useful beam	1/4
Ceiling	Useful beam	1/4
Areas towards which useful beam is directed only in moving-beam therapy	Useful beam	1/10
Secondary Barrier		
	Leakage radiation	1
	Scattered radiation	1

(a) Note that NCRP-49 (Ref.[4]) recommends: Floor: U = 1, Walls: U = 1/4. DIN-6847 (Ref.[6]) recommends: Floor and one wall: U = 1, directions seldom used (< 10%) or used only for moving beam therapy: U = 0.1. A study of actual treatment practices by Cobb and Björngard gives: Floor: 0.48, Walls (approximately horizontal irradiation): 0.06, Ceiling: 0.29, and all other directions combined: 0.10 (Ref.[7]).

(b) The portion of a floor, wall or ceiling which the useful beam can irradiate with the largest possible radiation field plus a margin of 30 cm (or 10°, whichever is larger) is to be shielded as a Primary Barrier. All other barriers may be considered as Secondary.

walls be ascribed U = 1. Where it is known that an area of a target wall will be infrequently used, it is reasonable to use an orientation factor less than 1 for that area.

Some judgement is always involved in the choice of U for a given facility. Note that the sum of U for all directions in Table XXXVI is greater than 1. This reflects an uncertainty which attends any prediction of clinical procedure usage.

TABLE XXXVII. SUGGESTED OCCUPANCY FACTORS T^(a)

Type of Area	Occupancy Factor T
Full Occupancy	1
Controlled Area	
Offices and Laboratories	
Work areas	
Living quarters	
Nearby buildings	
Partial Occupancy	1/4 ^(b)
Occasional Occupancy	1/16 ^(b)

(a) NCRP-49 (Ref.[4]) recommends **occupancy** factors ranging from T = 1 for full occupancy, T = 1/4 for partial occupancy and T = 1/16 for occasional occupancy, and gives several examples of each category. DIN-6847 (Ref.[6]) recommends T = 1 for workplaces and areas of continuous occupancy outside of the Controlled Area, T = 1/3 for public traffic areas and T = 1/10 for areas outside of the controlled area, where it can be ensured that the occupancy is limited. DIN-6847 furthermore recommends that the product UT not be made less than 1/10, unless either U or T is zero.

(b) Note that the use of occupancy factors less than 1 for shielding design may not be allowed in some jurisdictions.

Different values of U may be chosen if the type of equipment and probable mode of use would so indicate.

3.1.3. Occupancy factor T

The area occupancy factor T (Table XXXVII) is meant to take into account the average time per 40-hour work week spent by any individual in the occupiable areas to be shielded. The value T = 1 is used for the entire controlled area, including adjacent radiation rooms if designed to be occupied while the accelerator

in question is operating. Frequently occupied areas outside of the controlled area, such as offices, laboratories, shops, living quarters and nearby buildings, are also ascribed $T = 1$. Areas expected to be occasionally used by individuals, such as corridors, waiting rooms and elevators, may be ascribed $T = 1/4$. For areas outside of the controlled area but within the institution's grounds, where it can be ensured that no individual does remain more than a small fraction of the time, an occupancy factor $T = 1/16$ is suggested. Public areas where it is clearly unreasonable to expect that any individual would consistently linger more than, say, two hours per week (such as streets, sidewalks, parking lots or lawns) may also be ascribed $T = 1/16$.

It is recommended that values of the product ($U \cdot T$) smaller than $1/16$ should not be used in radiation protection planning, because the occupancy of a given area and the relevant beam orientation may be correlated in some unforeseen way and may lead to undesirably high individual exposures. Judgement is always involved in the choice of these operational parameters. A discussion with the facility management and an inspection of the facility can be very valuable. A scale drawing showing the intended use of surrounding space is essential. Some specialists in radiation protection require values of W , U and T to be specified in writing by the facility management if less conservative values are to be used.

3.2. Shielding materials

It is clear that any material can serve for radiation shielding if the thickness is sufficient to reduce the average dose-equivalent rate to an acceptable level in occupied areas. The main considerations in the choice of materials are cost and availability of space. Of the common shielding materials given in Table XXXVIII, ordinary concrete is usually the most suitable and economical one and should be used where possible. It can be cast in arbitrary shapes, and it has excellent structural properties. It is almost always most economical to order a type of concrete that the contractor customarily installs and to adjust the design thickness to correspond to that density.

In radiotherapy installations, typical concrete barriers may range from 60 cm (secondary barriers) to 2 m (primary barriers) of ordinary concrete (see Section 4.1). Accelerators of higher energy and power may require considerably greater thicknesses, but this is also very dependent on the distances from the radiation source(s) to the occupiable areas and therefore on the size of the radiation rooms.

Where space is at a premium, barite (barytes, or naturally occurring BaSO_4), or iron-bearing aggregates, such as ilmenite or magnetite, are sometimes used in concrete because of their higher densities (Table XXXVIII). Concrete can also be loaded with iron (in the form of shot, punchings, sheared bars, etc.). Densities as high as $6 \text{ g} \cdot \text{cm}^{-3}$ can be achieved by a combination of shot and punchings, but

TABLE XXXVIII. COMMONLY USED SHIELDING MATERIALS

Material	Range of Density ($\text{g}\cdot\text{cm}^{-3}$)	Nominal Density ($\text{g}\cdot\text{cm}^{-3}$)
Earth	1.5 - 1.9	1.7
Sand	1.6 - 1.9	1.6
Concretes:		
ordinary (silicacious)	2.2 - 2.4	2.35
barite (barytes, nat. BaSO_4)	3.0 - 3.8	---
limonite (Goethite, hyd. Fe_2O_3)	2.6 - 3.7	---
ilmenite (nat. FeTiO_3)	2.9 - 3.9	---
magnetite (nat. Fe_3O_4)	2.9 - 4.0	---
iron (shot, punchings, etc.)	4.0 - 6.0	---
Brick (soft)	1.4 - 1.9	1.65
Brick (hard)	1.8 - 2.3	2.05
Granite	2.6 - 2.7	2.65
Limestone	2.1 - 2.8	2.46
Marble	2.6 - 2.86	2.7
Water	1.00	1.0
Wood	0.5 - 0.9	0.7
Lead glass	3.3 - 6.2	3.3
Aluminum	2.70	2.70
Copper	8.96	8.96
Steel	7.8	7.8
Lead	11.35	11.35

at considerable cost. The costs of materials for special concretes are at least several times those of ordinary concrete, for a shield of the same effectiveness, and increase rapidly with the density required. The extra cost must be balanced against the saving in space achieved. Where high-density concrete is needed, a careful investigation of availability and price of heavy aggregates in the locality is definitely worth while. The densities of heavy concrete given in Table XXXVIII are meant to be indicative only, as they depend on the mix, the grade(s) of aggregate and on placement techniques (e.g. puddled, prepacked or conventional pouring, and whether tamping, rodding or mechanical vibration is used); typical densities are not given. If an unusual concrete is to be used, density specifications should be included in the construction contract. Reference [8] contains valuable discussions of concrete types used for radiation shielding and a great deal of data on all types of shielding materials.

Earth is frequently used to cover the accelerator vault and target rooms of large research accelerators (see Section 4.3), but it can also be used to advantage at any type of facility, regardless of size. Facilities located below ground level generally have the benefit of more than adequate shielding on the sides by this inexpensive natural material.

Other construction materials, especially brick or stone, provide a significant degree of radiation attenuation and may be used for new shielding, or regarded as a portion of the shield if already standing in proper relationship to the radiation room. Outside walls of brick or stone are sometimes used to advantage in this manner.

When concrete blocks or bricks are used, the density should be obtained directly from a sample of the material. Hollow or irregular blocks should be used with caution; the effect of inhomogeneities may be difficult to take into account properly.

Where earth, sand, brick, stone or heavy concrete are used, an equivalent thickness X of ordinary concrete ($2.35 \text{ g}\cdot\text{cm}^{-3}$) can be calculated from the ratio of densities:

$$X(\text{concrete}) = \frac{\rho(\text{material})}{\rho(\text{concrete})} X(\text{material}) \quad (54)$$

In situations where space is very restricted, denser materials such as steel or lead²⁵ may be required. This is frequently true where new equipment is to be installed in an existing room; steel plates can often be used to augment the already standing barriers without other expensive modifications. Lead can also

²⁵ Note that lead is easily melted and that a narrow electron beam can 'drill' a clean hole through thick pieces at beam powers as low as about 1 kW! However, there is no such problem in the use of lead for ordinary room shielding as discussed here.

be used in this manner, for a thinner shield, but the total cost is greater. Lead sheets are usually used to line doors because a relatively small thickness is effective in attenuating scattered photons.

Lead and steel find frequent application in local shielding near targets and collimators where the area required is not large. Tungsten is also used for this purpose because of its much higher density, although it has a greater activation potential than either lead or steel. Where lead is used for shielding, consideration should be given to its support, as it tends to creep.

Where ductings or recesses are put into an otherwise integral shielding barrier, a layer of lead or steel should be installed over the area of the opening to compensate for the material removed.

For shielding against neutrons, any material can be used, but hydrogenous materials are most effective (per areal density) because elastic scattering by hydrogen is the most efficient slowing-down mechanism for intermediate-energy neutrons. If the main material is not hydrogenous, at least the portion of the shield away from the radiation source should be of hydrogenous material. About 30 cm of water, or the equivalent amount in hydrogen content of other material, is the right amount to render the non-hydrogenous material most effective.

Because of its water content, ordinary concrete makes an effective neutron shield and is generally the most economical choice. Materials such as wood, paraffins, plastics or water are also effective because of their hydrogen content, but consideration should also be given to the fire hazard represented by some materials, especially organic liquids. Special materials such as boron or cadmium are sometimes used to attenuate thermal neutrons. Boron can be used in the form of borated concrete, boron-loaded plastic, boral²⁶ or borax ($\text{Na}_2\text{B}_4\text{O}_7$). A thin sheet of cadmium is sometimes used to line the door to the radiation room.

3.3. Physical considerations

Whereas the primary electron beam is actually stopped in a modest amount of material (Section 2.3), photons and neutrons are 'attenuated' instead; each thickness of material reduces the photon or neutron fluence by a fractional amount. The shielding is 'adequate' for these radiations if the fluences are reduced by such a large factor that the dose-equivalent rates in accessible areas are acceptably low.

If adequate room shielding is provided for the maximum possible thick-target bremsstrahlung and scattered photons, shielding for the electron beam and scattered electrons is adequate by a very large margin and need not be considered further.

²⁶ A sintered dispersion of boron carbide (35% by weight of B_4C) in aluminium, clad with aluminium sheet.

The attenuation factor B of a barrier of thickness X may be expressed in the following equivalent ways:

$$B(X) = 10^{-X/\text{TVL}} = 2^{-X/\text{HVL}} = \exp(-X/\lambda) \quad (55)$$

This equation expresses the assumption that each additional equal increment in barrier thickness corresponds to a reduction of the radiation by an additional constant multiplicative factor. When expressed in this manner and plotted on a semi-log graph as a function of X , $B(X)$ will appear as a straight line. There are actually deviations from this ideal behaviour for real conditions, especially for small X (i.e. in the shielding layers closest to the radiation source), but for most cases, Eq. (55) provides a description that is accurate enough. This equation defines the frequently used shielding parameters TVL, HVL and the attenuation length λ . The tenth-value layer TVL is the thickness which attenuates the radiation in question by one tenth; the half-value layer HVL is the thickness which attenuates radiation by one half, and the attenuation length is the thickness which attenuates radiation by a factor of $1/e$. The relationships between these parameters are shown in Table XXXIX.

For rapid estimates of shielding needs, the TVLs are convenient and are generally used in this manual. (For rapid estimates, the HVL is about $1/3$ of the TVL for a given material.) The TVL and HVL values given in this manual are usually in units of $\text{g} \cdot \text{cm}^{-2}$ (thickness multiplied by material density) because no particular value of material density is implied, and interpolations to materials of similar atomic number are easily made.

The intensity of unshielded radiation fields decreases approximately inversely as the distance from the source squared (inverse-square law). Exceptions to this general behaviour occur only if the radiation source is spatially extended (by at least a significant fraction of the distance to the occupied area). This situation is not ordinarily found in the types of installations discussed in this manual. If no shielding is provided, the average dose-equivalent rate at a distance d in the direction of the useful beam is given by $\dot{H} = W/d^2$. When the orientation and occupancy factors (U and T) are included, we have:

$$\dot{H} = WUT/d^2 \quad (56)$$

The rapid fall-off in radiation-field intensity with distance, as represented by the inverse-square law, is such that, where space is available, it may occasionally be more economical to use a larger room, with a corresponding saving in wall thickness. In some cases, the distance to occupied areas can be increased by a fence or a lighter wall at some distance from a radiation barrier that would otherwise be inadequate. (See, for example, typical installations for industrial radiography, Section 4.2.)

TABLE XXXIX. MEANING AND RELATIONSHIPS OF SHIELDING PARAMETERS

Symbol	Description	Use (a)	Relationships (b)
TVL	Tenth-Value Layer: Thickness which will attenuate dose-equivalent by 1/10.	$10^{-X/\text{TVL}}$	$\text{TVL} = \text{HVL} / 0.30103 = 2.3026 \lambda$
HVL	Half-Value Layer: Thickness which will attenuate dose-equivalent by 1/2.	$2^{-X/\text{HVL}}$	$\text{HVL} = 0.30103 \text{ TVL} = 0.69315 \lambda$
λ	Attenuation length: Thickness which will attenuate dose-equivalent by 1/e.	$e^{-X/\lambda}$	$\lambda = \text{TVL} / 2.3026 = \text{HVL} / 0.69315$

(a) Expression for calculating approximate attenuation of shielding thickness X . X may be in units of $\text{g}\cdot\text{cm}^{-2}$, cm or equivalent units. Shielding parameter used must be in same units as X .

(b) Conversion factors are based on: $\log_{10} 2 = 0.30103$, $\ln 2 = 0.69315$, $\ln 10 = 2.3026$.

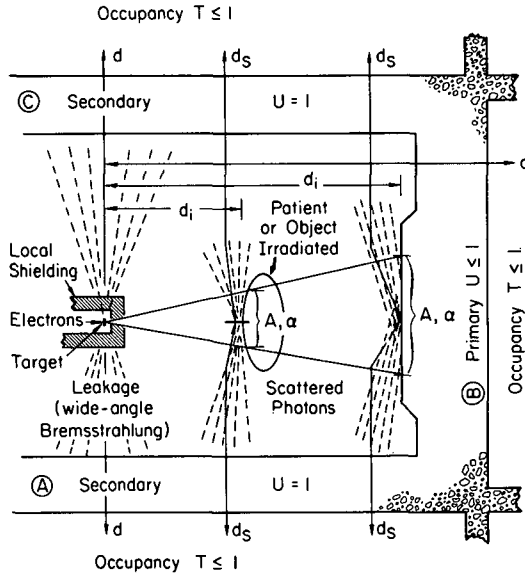


FIG.45. Conceptual plan of a radiation room for one accelerator orientation, showing the relationships of primary ($U \leq 1$) and secondary ($U = 1$) barriers to radiation sources (not to scale). Each barrier is ascribed an orientation (use) factor U , and each occupied area an occupancy factor T . The distances d are measured from the electron target to the nearest point of each occupied area. The distances d_i are measured from the electron target to each scattering surface, and d_s from each such surface to the nearest point of each occupied area. Each source of scattered photons is characterized by its area A (in a plane perpendicular to the beam direction) and differential dose albedo α , depending on the material, its orientation, the scattering angle and primary energy E_0 .

In calculating the shielding, it is important to utilize scale drawings which show the radiation area in relation to other areas and indicate the type of activity in each. Radiation protection needs should be calculated for the nearest point of the area to be protected. (Figure 45 illustrates the determination of the distances d for one accelerator orientation.) However, in determining the distance it is reasonable to assume that individuals will be 30 cm or more from any shielding wall and to augment the value of d used for calculation by such an amount. Similarly it is reasonable to augment d by 50 cm when measuring from the radiation source upwards to the floor of an occupiable area above, and to measure d downwards from the radiation source to the point 2 m above the floor of the room beneath. Margins such as these provide useful flexibility, particularly when radiation protection needs for more powerful equipment to be installed in an existing radiation room are assessed.

For scattered radiation, two distances are involved. First, the distance d_i from the target to the surface irradiated by the direct bremsstrahlung beam, and second, the distance d_s from that surface to the area to be protected. In Fig. 45, a value of d_i is indicated for the distance from the target to the patient or irradiated object and a second value d_i to the nearest wall in the direction of the direct beam. Values of d_s from both of these surfaces to the occupied areas are also indicated.

A 'beam stopper' is sometimes provided with a therapy unit (Figs 57, 60, Section 4) in order to reduce the required thickness of the primary barriers. These are shields mounted directly on the therapy unit that attenuate the forward radiation, usually by a factor of 0.001. In such cases the radiation scattered by the patient at a forward angle of 90° which just misses the beam stopper and strikes the primary barrier may be significant. Data on scattered radiation at 6 MV published by Karzmark and Capone are useful in assessing situations of this type (Ref. [13] and p. 99–100 of Ref. [4]).

For rotational therapy units, the source location and therefore the distances for each barrier are unique for each accelerator orientation. (For example, for units with 100 cm SAD, the source is moved 200 cm by a rotation of 180° , and different values of d , d_i and d_s will generally apply for each barrier for the two orientations. Values of each can be easily read from a simple diagram. See Figs 58, 60, Section 4.) Where accelerator positioning is widely variable, as with crane-mounted radiographic units, the determination of an effective value of d may be unclear for some barriers and a standard way to define an average distance is not practical. One method that might be useful in some cases would be to divide the area of movement into several imaginary 'stations', and to determine an average value of (d^{-2}) , or inverse distance squared, weighted by the estimated fraction of the time each station will be in use. To be on the safe side, the station with the smallest distance to a given barrier can be given extra weight.

The entire area that may be struck by the useful beam at the largest field size should be designed as a primary barrier. An adequate margin about this area should also be provided (a margin of 30 cm or 10° , whichever is larger, is suggested for radiotherapeutic or radiographic facilities).

It is recommended that radiation attenuation by movable objects placed in the beam should *not* be considered in shielding evaluation for primary barriers. On the other hand, for scattered radiation, it should be assumed that a phantom or other object of a type likely to produce the maximum scattered radiation is positioned at the usual distance from the target, using a typical field size.

If a facility is installed in a basement or on the ground floor with no occupancy below, no special shielding is needed beneath the facility.

If no occupancy is planned in nearby spaces on higher levels, the thickness of shielding barriers which shadow areas above about 2.5 m may be reduced (by, say, one TVL). Shielding may even be omitted above this height, if means are

provided to prevent persons from climbing into regions of high radiation above the height shadowed by the barriers; a lower ceiling over the occupied area in question, a high fence at some distance from the shielding wall, or control of roof access by locks or interlocks would be needed in such a case. However, a heavy ceiling must be provided if the space above the facility is accessible. In deciding on barrier height and roof thickness, the possibility of excessive radiation doses to persons in upper stories of nearby existing and future buildings extending above the shadow of radiation barriers should be considered. Both direct radiation and radiation scattered by the air (skyshine) may contribute significantly to the radiation field beyond the facility walls as well as to areas within the facility.

The methods outlined in this section assume only one radiation source for each occupiable area. In case there is more than one radiation source, adequate protection can be obtained by augmenting the shielding for each source (by one HVL, in the case of two sources of approximately equal penetrating power) or by reducing the radiation of all but one of the sources by shielding to levels negligible in comparison with the one remaining.

As a first step, it is recommended that shielding barriers be calculated using the most accurate information available (rather than the most conservative). For the final design, it is good practice to then augment the preliminary design by a safety factor of two, in the form of an additional HVL of shielding material on all sides. This is to allow for small variations in material density and for unanticipated changes in operation that may later make narrowly designed shielding inadequate. The additional expense involved in providing a safety factor of two for new construction is relatively small compared with other installation costs, and much less than later modifications or forced reductions in operation would be. A safety factor of two should be routinely provided where neutrons are expected to be the dominant radiation in occupied areas.

An additional safety factor may be applied to the result of these calculations to reflect the radiation protection philosophy of the facility's management. Where cost is not too high, additional shielding may provide a feeling of security to both management and personnel, justifying the extra expense.

Repeated calculations are generally required to arrive at a final design. One usually begins with requirements for interior room dimensions in addition to the physical data discussed above. At this stage, trial values of d and d_s (including a first guess for the barrier thickness) are chosen. The result of this calculation will provide a better estimate of d and d_s to be used in a repeated calculation. Two such trials are usually enough. If the resulting dimensions are unacceptable because of space limitations, the procedure should be repeated with a denser material or a combination of materials. Consultation with the architect or contractor may show that a different approach is needed. The final drawings should be reviewed for specified materials, thicknesses and intended routing of ductings and conduits. If required, these plans should also be submitted for review by governmental authorities before construction begins.

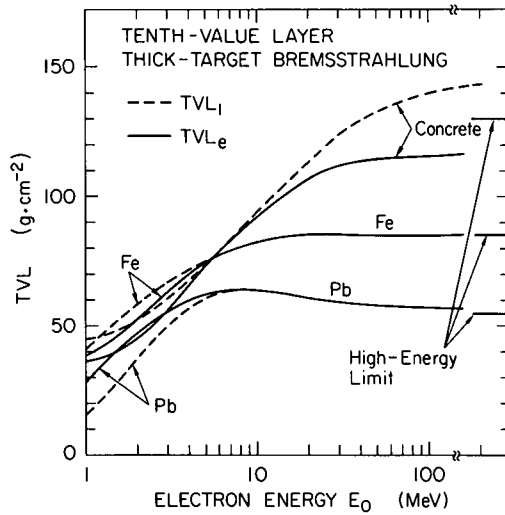


FIG.46. Values of dose-equivalent tenth-value layers (TVLs) in ordinary concrete, iron (steel) and lead, for thick-target bremsstrahlung under broad beam conditions at 0° , as a function of the energy E_0 of electrons incident on a high-Z target. The solid curves show the 'equilibrium' tenth-value layer, TVL_e , the dashed curves the 'first' tenth-value layer, TVL_1 , or the thickness closest to the radiation source needed to reduce the dose equivalent by a factor of ten. The TVLs are plotted in units of $g \cdot cm^{-2}$ to facilitate comparison and interpolation to other materials. Presumed high-energy values are indicated at the right (see Section 3.4.3). The smoothed curves are adapted from several sources, taking into account the behaviour at both lower and higher energies.

The curves shown represent a subjective average of data from several sources and are believed accurate enough for most room shielding calculations. There is a surprising lack of consistency among the reported shielding measurements (for iron and lead, up to 15–20% deviation from the curves shown). These variations may indicate that the effective TVL for these materials is very geometry and/or spectrum dependent. In critical applications, it is suggested that the chosen shielding thickness be based on measurements for the specific radiation source and geometry at hand. Sources of original data are:

DIN-6847 [6]: Concrete, steel, lead: 1–50 MeV

NCRP-34 [3]: Concrete, lead: <1, 1, 2, 3, 4 MeV

Steel: <1, 4, 6 MeV

EMI Therapy Systems [9]: Concrete, steel, copper, tungsten, lead: 4 MeV

Varian Associates [10]: Concrete, steel, lead: 4, 8, 15 MeV

Maruyama et al. [11]: Concrete, heavy concrete, steel, lead: 4, 6, 10, 20, 30, 32 MeV

Coleman [12]: Concrete, steel, lead: 5, 8, 16 MeV

Karzmark and Capone [13]: Concrete, steel, lead: 6 MeV

Kirn and Kennedy [14]: Concrete: 6, 10, 20, 30, 38 MeV

Miller and Kennedy [15]: Concrete, lead: 86, 178 MeV

Buechner et al. [16]: Steel: 1, 2 MeV

Goldie et al. [17]: Steel: 3 MeV

Scag [18]: Steel: 6–90 MeV

O'Connor et al. [19]: Steel: 10 MeV

Westendorp and Charlton [20]: Steel: 4–100 MeV; Pb: 10–100 MeV

Adams and Girard [21]: Steel: 20 MeV

Wideröe [22]: Steel: 31 MeV

The higher-energy behaviour of shielding materials considered is discussed in Section 3.4.3. Similar adaptations, involving mostly the same data sources, are published by Bly and Burrill [23], Bly [24], and Burrill [25], and in Ref. [54], p.37. See also NBS Handbooks 55 and 97 [26, 27], and NCRP-51 [5]. Shielding data specifically for heavy concretes are given by Maruyama et al. [11] and Lokan et al. [28].

3.4. Shielding against photons

3.4.1. Primary barriers ($E_0 < 100$ MeV)

Because bremsstrahlung is the dominant secondary radiation, a photon shield is needed at every installation and is usually the determining consideration for shielding thickness. The equation giving the necessary barrier attenuation factor B is

$$B = \dot{H}_M d^2 / (WUT) \quad (57)$$

which follows directly from Eq. (56). Here, \dot{H}_M is the maximum permitted average dose-equivalent rate ($\text{rem} \cdot \text{week}^{-1}$, Table XXXIV, Section 3.1).

Figure 46 gives values of dose-equivalent TVLs in $\text{g} \cdot \text{cm}^{-2}$ for the most commonly used materials: concrete, iron (steel) and lead. Interpolation to other materials can easily be made from these data. Depending on the material and energy, there may be a transition region (a change in slope in the attenuation curves, see Figs 47a, b, c). This can be taken into account by using a different value (TVL_1) for the first TVL nearest the radiation source. Values of TVL_1 are shown as dashed lines in Fig. 46. Total barrier thickness is determined using

$$n_{\text{TVL}} = -\log_{10}(B) = \log_{10}(1/B) \quad (58)$$

Therefore the total thickness X in centimetres is:

$$X = n_{\text{TVL}} \text{TVL} / \rho \quad (59a)$$

where TVL is in $\text{g} \cdot \text{cm}^{-2}$ and ρ is the material density in $\text{g} \cdot \text{cm}^{-3}$. If TVL_1 is significantly different from the equilibrium value (TVL_e), it is advisable to take this into account, especially if TVL_1 is larger:

$$X = (\text{TVL}_1 + (n_{\text{TVL}} - 1) \text{TVL}_e) / \rho \quad (59b)$$

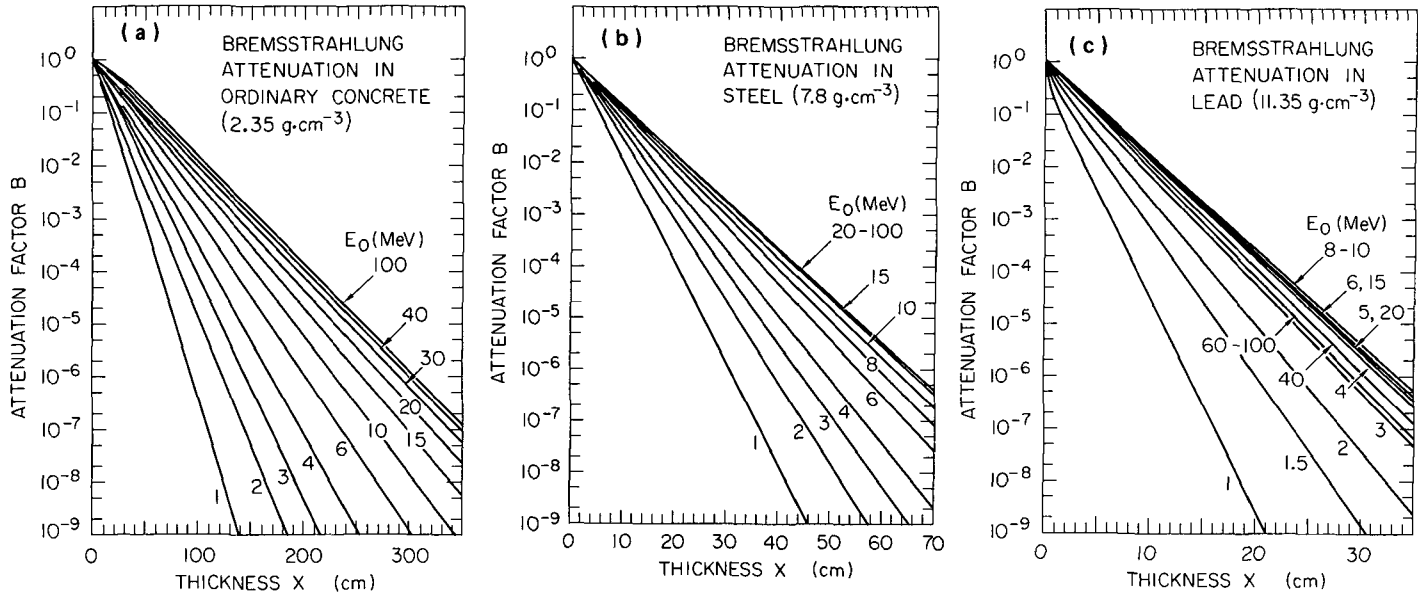


FIG.47. Attenuation factor B of thick-target bremsstrahlung by selected materials under broad-beam conditions at 0° to the incident electron beam, as a function of shielding thickness X . The energy designation for each curve refers to the monoenergetic electron energy E_0 incident on a thick, high- Z target. The curves are derived from Fig.46.
 (a) Ordinary concrete ($2.35 \text{ g}\cdot\text{cm}^{-3}$); (b) Iron (steel, $7.8 \text{ g}\cdot\text{cm}^{-3}$); (c) Lead ($11.35 \text{ g}\cdot\text{cm}^{-3}$).

The use of TVLs is particularly convenient if the total shielding barrier is to be composed of more than one kind of material; it is only necessary to adjust the material thicknesses such that the number of TVLs of all the materials combined is equal to n_{TVL} .

Alternatively, it may be more convenient to read the necessary barrier thickness directly from attenuation curves. These are given in Figs 47a, b, c for ordinary concrete ($2.35 \text{ g} \cdot \text{cm}^{-3}$), iron (steel) and lead.

Figure 48 shows a worksheet for shielding calculation at a therapeutic installation. Most of the symbols for primary barriers are self-explanatory: The left-most portion is meant to describe the barrier and to arrive at a value of WUT ($\text{rem} \cdot \text{m}^2 \cdot \text{week}^{-1}$). The next major portion tabulates the various factors for calculating the unshielded dose rate (space is reserved for calculating scattered radiation, see Section 3.4.2). The factor F_{BS} is for beam-stopper attenuation, if this is used ($F_{\text{BS}} \cong 10^{-3}$). A column is reserved for the sine of the angle of incidence ($\sin = 1$ for perpendicular irradiation), which may be used as a factor in computing the necessary wall thickness. Unless space is very restricted, making this special obliquity correction is not usually worth while. If used for $|\sin| < 0.7$, one or more half-value layers should be added to the recommended thickness (Ref. [4], p. 53).

After the attenuation factor B is calculated, one may use the attenuation curves (Figs 47a, b, c) or continue by taking the logarithm (Eq. (58)) and using TVL values as in Eqs (59a, b). Under the heading 'type' the symbols C, B, S, etc., could indicate ordinary concrete, barytes concrete, steel, etc., and the density would be given in the adjacent column. Space is provided to enter both the 'minimum thickness' and a 'recommended thickness' which may include a safety factor. This worksheet is readily adaptable for industrial radiographic and other types of facilities.

3.4.2. Secondary barriers ($E_0 < 100 \text{ MeV}$)

Secondary barriers are barriers towards which the useful beam cannot be directed. Two sources of photon radiation must be considered in the design of these barriers: bremsstrahlung at wide angles (the 'leakage' radiation of radio-therapeutic or radiographic units is dominated by wide-angle bremsstrahlung) and photons scattered from objects placed in the direct bremsstrahlung beam. The secondary barrier thicknesses calculated for these sources should be compared and the larger thickness used in the final barrier design. If the two thicknesses differ by less than one HVL (for bremsstrahlung), one additional HVL (for bremsstrahlung) should be added to the calculated thickness.

(a) Wide-angle bremsstrahlung (leakage radiation)

In the case of therapeutic and radiographic installations, shielding is provided around the electron target to reduce 'leakage' radiation to a small fraction of

useful-beam radiation, measured at the same distance from the target. The fractional leakage radiation (called F_L in the worksheet, Fig. 48) is obtained from the manufacturer. It is of the order of 0.001 for radiotherapeutic units and generally larger than this for radiographic units (see Tables III and IV in Section 1.3).

For research and industrial installations, levels of unshielded bremsstrahlung at 90° may be obtained from Fig. 17, and for other angles from Fig. 18 (Section 2.4).

If space and/or economic considerations are at a premium economies may be achieved by the fact that the radiation at 90° to the useful beam is somewhat less penetrating. Over an energy range up to $E_0 = 100$ MeV, one may assume the shielding parameters of materials for bremsstrahlung at 90° to be the same as those for bremsstrahlung produced at 0° by electrons of energy $2/3 E_0$ (or E_0 , whichever results in the thinner shield) [5, 12].

(b) Scattered photons

Photons scattered by objects in the direct bremsstrahlung beam must be considered in the calculation of shielding barrier thicknesses, as well as in the design of labyrinths and ducts (Section 3.6). In the case of radiation therapy, scattering from the patient and from walls of the treatment room (or beam stopper, if one is used) must be considered. In the case of radiography, scattering from the object being inspected and from the target walls must be considered. Photons scattered at large angles are relatively low in energy and intensity, but they may dominate shielding considerations in certain instances where local shielding within the radiation head attenuates the large-angle bremsstrahlung, as in radiotherapeutic and radiographic units.

The amount of radiation scattered is proportional to such factors as the radiation intensity incident on the surface and the area of the surface irradiated, and it is inversely proportional to the distance d_s from the irradiated surface to the location in question. These factors are multiplied by a dimensionless coefficient α , called the differential dose albedo, which depends on the photon energy spectrum, the type of material irradiated, the angle of scattering θ_s , and the orientation of the surface. A practical expression for the dose rate of radiation scattered from objects in the direct bremsstrahlung beam is

$$\dot{H} = \left(\frac{WUT}{d_f^2} \right) \cdot \left(\frac{\alpha A}{d_s^2} \right) \quad (60)$$

in which the factor (W/d_f^2) expresses the bremsstrahlung dose rate at the scattering surface. For consistency with the methods outlined for primary barriers, the dimensionless factors U and T are included with W, so that Eq. (60) will reflect the average dose equivalent rate to individuals in the affected

occupied area. Representative values of W , U and T may be found in Tables XXXV–XXXVII. (U would be set equal to 1 for secondary barriers.) It is convenient to express both \dot{H} and W (Table XXXV) in $\text{rem} \cdot \text{m}^2 \cdot \text{week}^{-1}$, d_i and d_s both in metres, and the area A in m^2 .

These relationships are illustrated in Fig. 45, in which d_i represents distances from the target to each of two scattering surfaces — the patient or irradiated object and the wall behind. Each scattering surface is characterized by the incident beam area A and a value of the differential dose albedo α . The distances d_s from these sources to the occupied areas behind barriers A and C are also marked. The distances d_s to occupied areas above and beneath the radiation room are determined in a similar manner. Regardless of the orientation of the irradiated surface, the beam area A is determined in the plane perpendicular to the incident beam direction. In the worksheet of Fig. 48, columns are provided for d_i , α and A , to be used together with WUT and d_s in Eq. (60). For a therapeutic facility, a field size of 0.040 m^2 (corresponding, for example, to a $20 \times 20 \text{ cm}^2$ treatment field) at $d_i = 1 \text{ m}$ is adequately conservative for typical use.²⁷ For a radiographic unit, the largest area obtainable from the equipment at the distance in question should generally be assumed.

The differential dose albedo α may be regarded as a combination of two terms whose relative importance depends on irradiation conditions; one term contains the angular dependence of Compton scattering and the second, which is essentially isotropic, is dominated by positron-annihilation photons (0.511 MeV) for incident photon energy above 7 MeV. Both terms are modified by absorption within the scattering material in a way that depends on the angles of incident and outgoing radiation relative to the surface. For example, for perpendicular incidence, the albedo for θ_s close to 180° is larger than for sideward directions, because the outgoing radiation has less material to penetrate.

Values of the differential dose albedo α are given in Fig. 49 for the scattering of monoenergetic photons of energy k from ordinary concrete, for two orientations of the scattering surface. These data are obtained from an interpolation in photon energy, based mainly on the Chilton-Huddleston [29–31] parameterization for the differential dose albedo, and are useful in labyrinth design. Extensions to energies above 10 MeV are suggested extrapolations.

Values of the differential dose albedo α are given in Figs 50a–d for the scattering of bremsstrahlung beams of endpoint energy E_0 incident on selected materials. These data are based on the same type of parameterization as for Fig. 49 and are obtained by a simple average of the albedo over the photon energy range 0.5 MeV to E_0 . Although parameters are available only for photon

²⁷ A recent study of actual treatment practices at three hospitals by Cobb and Bjärngård [7] reports average treatment fields to be 196, 272 and 296 cm^2 . The overall average is 253 cm^2 (0.0253 m^2).

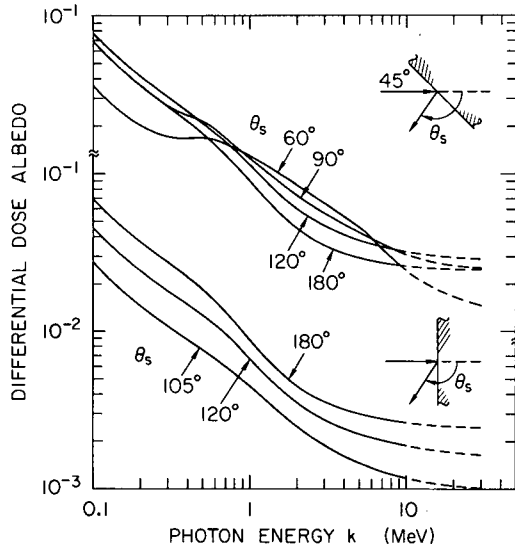
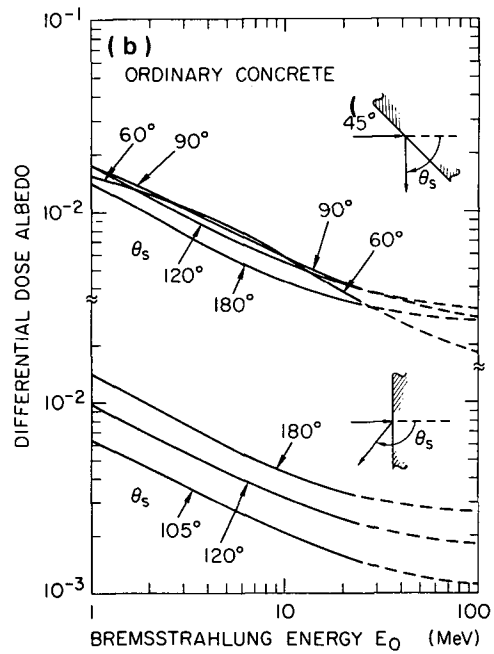
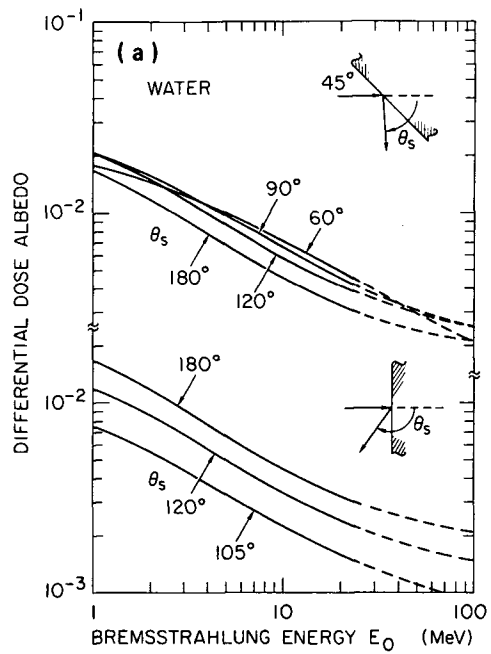


FIG.49. Differential dose albedo α for monoenergetic photons incident on ordinary concrete, for 45° incidence (upper curves) and perpendicular incidence (lower curves), for representative scattering angles θ_s . For 45° incidence, the albedo given is for scattered radiation in the plane containing the normal to the surface and the direction of incident radiation. The formulation used to calculate the albedo for $k = 0.2-10$ MeV is that of Chilton and Huddleston [29], with parameter values based on those given for discrete energies in Ref.[31], but adjusted and interpolated to facilitate computation. The extensions of the curves above 10 MeV are suggested extrapolations, obtained from the parameterization for 10 MeV.

energies up to 10 MeV, this energy range contributes substantially to the effective bremsstrahlung albedo at all energies. The effective bremsstrahlung albedo at higher E_0 is therefore relatively insensitive to the behaviour at high photon energies, and extrapolations to higher bremsstrahlung energies are given. These extrapolations are consistent with measurements of total energy albedo at high energies [32–34].

Albedo values from Figs 50a–d may be used directly in Eq. (60) for a direct bremsstrahlung beam (the useful beam in radiotherapy or radiography) striking a surface. For movable objects, it is advisable to use the albedo values for 45-degree orientation of the scattering surface, as these are generally larger than those for perpendicular incidence. The albedo for water may be used for calculating radiation scattered from a patient. As the behaviour of the differential dose albedo is not strongly dependent on material type, interpolations to other materials can be made easily.



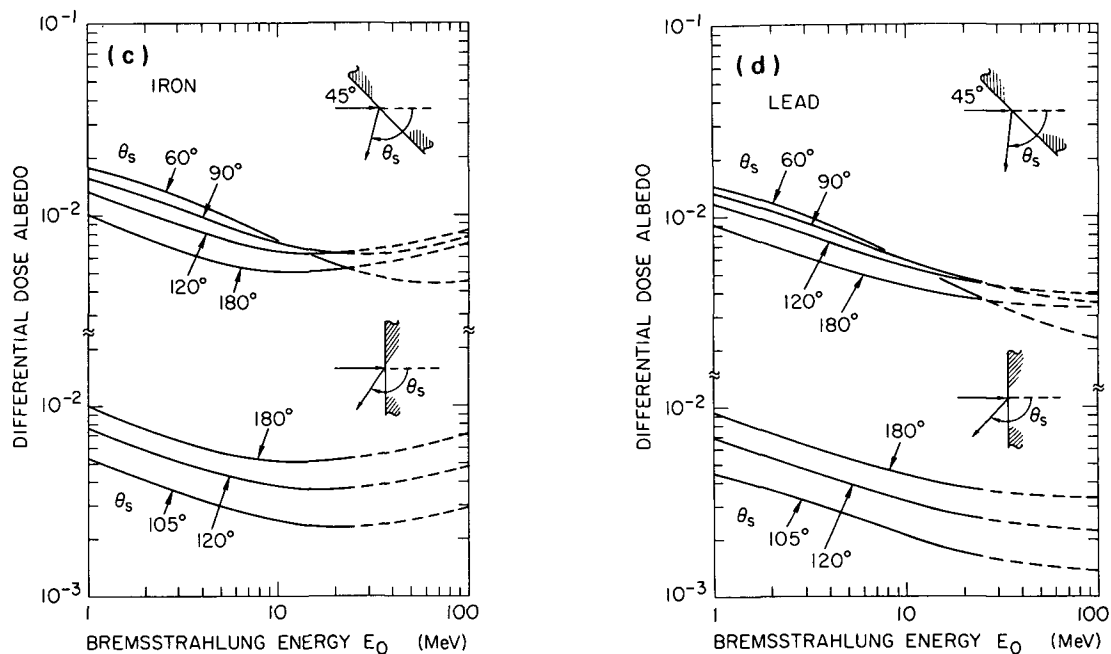


FIG.50. Effective differential dose albedo α for bremsstrahlung beams of endpoint energy E_0 , incident on selected materials, for 45° incidence (upper curves) and perpendicular incidence (lower curves), for representative scattering angles θ_s . For 45° incidence, the albedo given is for scattered radiation in the plane containing the normal to the surface and the direction of incident radiation. The data are interpolated by the type of Chilton-Huddleston parameterization described for Fig.49. Extensions to higher energies are suggested extrapolations. (a) Water (this may also be used for tissue); (b) Ordinary concrete; (c) Iron (steel); (d) Lead.

TABLE XL. TVL SUGGESTED FOR SHIELDING AGAINST SCATTERED PHOTONS^(a)

Shielding Material	TVL ($\text{g}\cdot\text{cm}^{-2}$)	
	After 1 Scattering ^(b)	After 2 or more Scatterings ^(c)
Ordinary concrete ($2.35 \text{ g}\cdot\text{cm}^{-3}$)	37	21
Barytes concrete	29	
Iron (steel)	38	
Lead glass	23	
Lead	17	3.4

(a) Assuming each scattering angle is about 90° or more.

(b) From DIN-6847 (Ref. [6]).

(c) TVL_e estimated from attenuation curves for 250 kVp given in NCRP-49 (Ref. [4]).

The kinematics of Compton scattering are such that the maximum energy of a photon scattered at 90° is 0.511 MeV and the maximum energy of a photon scattered at 180° is $0.511 \text{ MeV}/2 = 0.255 \text{ MeV}$, regardless of the energy of the incident photon (Eq. (21) and Fig. 21, Section 2.4.2). However, above 3 MeV primary electron energy, electron-positron annihilation radiation (0.511-MeV photons) will be present in the radiation scattered once at large angles (and will be dominant above about 7 MeV).²⁸ Therefore the shielding data for 1-MeV bremsstrahlung should be used for estimating shielding needs for photons scattered from one surface at 90° or more. Specific values of the TVL for several materials are given in Table XL, for calculation of shielding against singly scattered photons.

²⁸ There is also a small component of higher-energy photons which undergo two or more scatterings at smaller angles before leaving the scattering material. To illustrate: An incident 5-MeV photon scattered once at 90° has 0.464 MeV. If scattered twice at 45° it has 0.743 MeV, and if scattered thrice at 30° it has 1.01 MeV (Eq. (21)). This component is not significant in scattered radiation except if filtered by thick shielding.

At accelerators operating at very high energies, the electromagnetic cascade will continue into the material first struck by the bremsstrahlung beam. In this case, the radiation at large angles may be dominated by large-angle bremsstrahlung rather than annihilation or Compton-scattered photons. For this reason it is advisable to assume the same shielding characteristics (i.e. the same TVLs) for scattered photons from the first scattering as for large-angle bremsstrahlung if the energy E_0 is above the critical energy E_c of the material first struck (see preceding section). The critical energy is given by Eq. (2) (Section 2.2) (or obtained from Table B-II of Appendix B). For ordinary concrete it is approximately 66 MeV. Albedo α values at high energies will not be significantly different from those indicated by Figs 49 and 50.

To evaluate the case in which photons scatter twice, Eq. (60) may be generalized in the following manner:

$$\dot{H}_2 = \left[\left(\frac{WUT}{d_1^2} \right) \left(\frac{\alpha_1 A_1}{d_{s1}^2} \right) \right] \left(\frac{\alpha_2 A_2}{d_{s2}^2} \right) \quad (61a)$$

where the first factor, from Eq. (60), gives the dose rate incident on the second surface of area A_2 and albedo α_2 , and d_{s2} is the distance from that surface to the point at which the dose rate is to be calculated. Values of α_2 for concrete may be obtained from Fig. 49 for the geometry at hand (assume $k = 0.5$ MeV for the second scattering of about 90° or more).

For subsequent scatterings, additional terms of the form $(\alpha A/d_s^2)$ are factored in the equation:

$$\dot{H}_n = \frac{WUT}{d_1^2} \left(\frac{\alpha_1 A_1}{d_{s1}^2} \right) \left(\frac{\alpha_2 A_2}{d_{s2}^2} \right) \dots \left(\frac{\alpha_n A_n}{d_{sn}^2} \right) \quad (61b)$$

in which the values of each additional α , d_s and A depend on details of the geometry and materials. For concrete, values of α can be obtained from Fig. 49, assuming $k = 0.25$ MeV for the third or subsequent scattering of about 90° or more.

Because the annihilation photons (0.511 MeV) from the first scattering are degraded in energy by each subsequent scattering, the effective radiation energy may be taken as 0.25 MeV for shielding after the second scattering of 90° or more. Since the shielding effectiveness of practical materials is greatly enhanced as the effective photon energy is reduced to such low values²⁹, it is

²⁹ While remaining valid for concrete, the generalization is misleading for very low-Z materials such as water, organics and boron. Because photon absorption by the photoelectric effect (which is important at typical energies of scattered photons) is proportional to Z^4 , it is relatively weak at low Z, but becomes very significant for high-Z materials such as lead. This is easily seen in the shape of the photon attenuation coefficient curves shown in Fig. B1 (Appendix B).

TABLE XL1. EQUILIBRIUM TENTH-VALUE LAYER FOR HIGH-ENERGY BROAD-BEAM BREMSSTRAHLUNG ATTENUATION

Material	TVL Values (g.cm ⁻²)						
	From (a) (μ_{tot}/ρ) _{min}	Highest Values for $E_0 < 100$ MeV (b)	Experiment (E_0)				
			4.8 GeV ^(c)	6.3 GeV ^(d)	6 GeV ^(e)	3-7 GeV ^(f)	1 GeV ^(g)
Sand (SiO ₂)	114	---	---	---	---	119	---
Concrete	114	115	---	---	---	101	---
Heavy concrete	---	---	{100 - 122 100 - 131	122	---	106	---
Aluminium	107	---	---	---	146	---	---
Iron (or steel)	78	85	---	---	---	78	---
Copper	76	---	---	82	89	---	91
Lead	55	55 - 65	---	52	56	55	56

(a) Based on values of the minimum photon attenuation coefficient (Table B.1, Appendix B).

(b) From Fig. 46, for 0° bremsstrahlung.

(c) Bathow et al., Ref. [38], $E_0 = 4.8$ GeV. This paper gives TVL values of 100 to 122 or 100 to 131 g cm⁻² (increasing from 0° to 90°), depending on instrumentation (DESY).

(d) Bathow et al., Ref. [39], $E_0 = 6.3$ GeV (DESY).

(e) Bathow et al., Ref. [40], $E_0 = 6$ GeV (DESY).

(f) Dinter and Tesch, Ref. [41], $E_0 = 3 - 7$ GeV, $\theta = 30 - 90^\circ$ (DESY).

(g) Nelson et al., Ref. [42], $E_0 = 1$ GeV (SLAC).

good practice to design labyrinths in such a manner that each photon arriving at the door is first scattered at least twice (see Table XL).

Because of the approximations made in deriving data for Figs 49 and 50 it is recommended that any shielding design for scattered photons based on these data be provided with a safety factor of two. Useful primary references on the photon differential dose albedo are the articles by Raso [35] and Vogt [36]. Present knowledge concerning albedos is well summarized, for example, by Leimdörfer (Ref. [54], p. 233, photons) and Selph (Ref. [37], photons and neutrons).

3.4.3. Accelerators operating above 100 MeV

The shielding data for electron accelerators operating above 100 MeV have not been so extensively investigated as those for the lower-energy region just discussed. However, at these high energies where the electromagnetic cascade plays an important role, there is evidence that the attenuation parameters for various materials are slowly varying. For many radiation lengths into the cascade, it is believed that the energy is transported mainly by photons with an energy spectrum

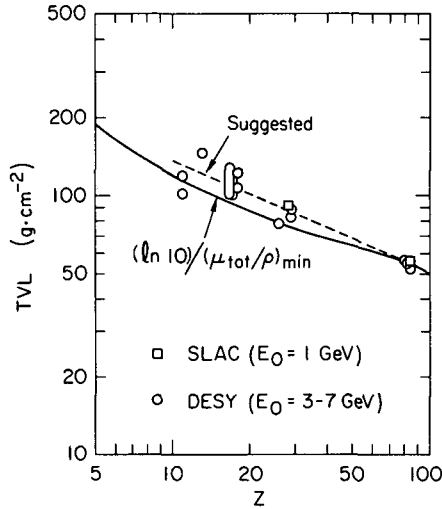


FIG. 51. Trend of equilibrium TVL for photons produced by high-energy electron beams ($E_0 > 100$ MeV), as a function of atomic number Z of the shielding material. The solid curve is for $(\ln 10)/(\mu_{\text{tot}}/\rho)_{\text{min}}$, where $(\mu_{\text{tot}}/\rho)_{\text{min}}$ is the minimum attenuation coefficient for the material. The points are measurements for 1–7 GeV. Sand and ordinary concrete are plotted at $Z = 11$ and heavy concrete at $Z = 18$. The dashed curve is suggested for the design of shielding barriers for all energies above 100 MeV for broad-beam conditions.

that has been modified by the shape of the photon attenuation curve; the absorbed-dose attenuation coefficient is nearly constant with initial electron energy E_0 and is close to its minimum value, $(\mu_{\text{abs. dose}}/\rho) \approx (\mu_{\text{tot}}/\rho)_{\text{min}}$, where $(\mu_{\text{tot}}/\rho)_{\text{min}}$ is the minimum photon attenuation coefficient (see Appendix B). Thus, the TVLs (in $\text{g} \cdot \text{cm}^{-2}$) will be given approximately by:

$$\text{TVL} = (\ln 10)/(\mu_{\text{tot}}/\rho)_{\text{min}} \quad (62)$$

TVL values so derived are shown in Table XLI and may be compared with the maximum TVL values taken from Fig. 46 for the range below 100 MeV. Experimental values for 1–7 GeV, obtained primarily in work at DESY [38–42], are also shown for comparison.

The overall trend of these data is shown in Fig. 51 in which the solid curve is derived from $(\mu_{\text{tot}}/\rho)_{\text{min}}$ (Eq. (62)). Also shown are the data points of Table XLI and a suggested curve (dashed) which should be valid for all initial energies E_0 above 100 MeV and for all bremsstrahlung angles.

The following approximate procedure is suggested for planning the shielding of a target or beam dump for high-energy electrons.

(a) Design the beam dump such that it is adequate to thermally absorb all of the beam power; it should be at least fifteen radiation lengths ($15 X_0$) long and provide an adequate radial margin about the beam area.

(b) For 0° bremsstrahlung, extrapolate the absorbed dose curve of Fig. 17 (Section 2.4.1) to the desired energy E_0 (in MeV), assuming that the absorbed dose (for constant beam power) is proportional to E_0 :

$$\dot{D}((\text{Gy} \cdot \text{h}^{-1})(\text{kW} \cdot \text{m}^{-2})^{-1}) \approx 300 E_0$$

$$(\dot{D}((\text{rad} \cdot \text{h}^{-1})(\text{kW} \cdot \text{m}^{-2})^{-1}) \approx 30\,000 E_0)$$

(Eq. (17), Section 2.4.1).

(c) Determine the total shielding requirements in terms of TVL, using Eqs (57) and (58) and the result of step (b). Call this number n_{TVL} .

(d) Determine the length of the beam dump in terms of TVL, assuming the values shown in Fig. 51 (dashed curve). Call this value n_{BD} .

(e) Determine the necessary amount of additional shielding of the chosen material or combination of materials by the equation $n_{\text{BARRIER}} = n_{\text{TVL}} - n_{\text{BD}}$, again assuming values taken from Fig. 51 (dashed curve).

(f) For shielding at 90° , assume that the radiation is given by

$$\dot{D}((\text{Gy} \cdot \text{h}^{-1})(\text{kW} \cdot \text{m}^{-2})^{-1}) = 50 \quad (\dot{D}((\text{rad} \cdot \text{h}^{-1})(\text{kW} \cdot \text{m}^{-2})^{-1}) = 5000)$$

(Fig. 17), and follow the same procedure. To approximately account for the absorption of the beam dump, use the beam-dump radial margin about the beam as in the previous step.

As the same beam dump may not always be used, it is good practice to assume $n_{\text{BD}} = 0$ for steps (e) and (f), regardless of what is actually installed. Any location where the beam can strike should be shielded in the same manner.

See Refs [38–41] for more complete discussions of shielding against high-energy bremsstrahlung. References [38] and particularly [41] are recommended for their discussions of shielding parameters at large angles to the incident beam direction.

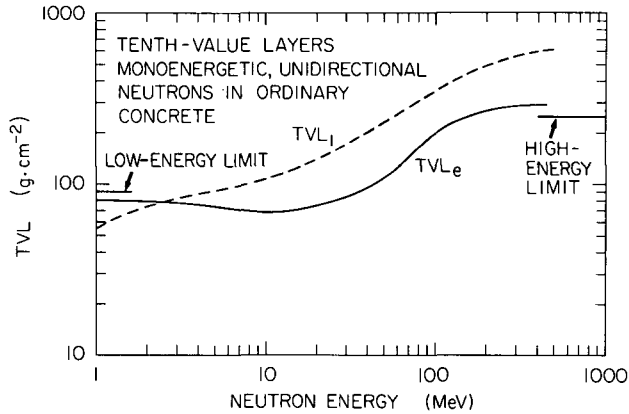


FIG.52. Dose-equivalent tenth-value layer, TVL, for broad beams of monoenergetic, unidirectional neutrons incident on ordinary concrete, as a function of neutron energy E_n . The dashed curve represents TVL_1 (the 'first' TVL) and the solid curve is for TVL_e , corresponding to the nearly exponential attenuation of subsequent layers. The dose equivalent from n-capture gamma rays is implicitly taken into account. The curves are based on discrete-ordinate calculations of Roussin and Schmidt [44], Roussin et al. [45], and Alsmiller et al. [46], using in part the smoothed data of Wyckoff and Chilton [43]. The low-energy limit is to indicate that the TVL_e does not vary greatly below the energy range shown. The high-energy limit is based on semi-empirical considerations (see Section 3.5.2).

3.5. Shielding against neutrons

With currently accepted standards for the evaluation of neutron dose equivalent, the dose-equivalent rates due to photoneutrons from an unshielded target are below those attributable to bremsstrahlung by a comfortable margin for all energies of the incident electron (Fig.6, Section 2.1). Furthermore, the equilibrium TVL in concrete lies in a narrow range, $75\text{--}85\text{ g}\cdot\text{cm}^{-2}$ [43], for neutron energies up to 30 MeV (Fig.52), as compared with the TVL for bremsstrahlung beams, which is in the range of $90\text{--}130\text{ g}\cdot\text{cm}^{-2}$ for accelerator energies above about 10 MeV (Fig.46). These factors indicate that a facility adequately shielded by concrete for bremsstrahlung in all directions is generally also well shielded for neutrons if the number of neutrons having energies above about 50 MeV is negligible. Because of the rapid falloff of the neutron spectrum with energy (Section 2.5.2) the number of such neutrons will not be large until the linac energy exceeds the energy for photopion production. All radiotherapy and industrial radiographic installations, and most research accelerators operate below the pion threshold (Section 1.3).

However, the following reservations must be added:

- (a) In a situation where the electron target is locally well shielded for bremsstrahlung, with correspondingly thinner room shielding, the room shielding should be evaluated for protection against neutrons;
- (b) Neutrons may stream through labyrinths and other openings in otherwise well-designed shielding;
- (c) For facilities with thin roofs, neutron skyshine should be evaluated;
- (d) Radiation doors of materials other than concrete should be evaluated for neutron leakage.

At installations operating above about 10 MeV, the labyrinth and door (Section 3.6) should be designed for protection against neutrons as they have been found to dominate in this area.

As with photons, neutrons are attenuated approximately exponentially through thick shielding barriers. However, the change in effective quality factor \bar{Q} with energy as the neutrons progress through the shielding must also be factored into an evaluation of dose equivalent. Gamma rays released within the shielding material by absorbed neutrons contribute to the dose equivalent at the surface of the shielding barrier, and a complete assessment will take this into account.

Since neutron source data as well as shielding calculations are more tenuous than those for photons, and since shielding effectiveness is more sensitive to material composition (e.g. water content), it is recommended that any shielding design for neutrons be provided with at least a safety factor of two.

3.5.1. Energies below the photopion threshold ($E_0 < 140$ MeV)

Neutron yields may be estimated from data in Section 2.5 for the angle, energy, target material and beam power anticipated. For bremsstrahlung energies above about 15 MeV, a conservative rule of thumb is 2×10^{12} n·s⁻¹ per kW of electron beam power incident on a high-Z target.

In order to treat the neutron component in a manner consistent with the method outlined in the previous paragraphs for photons (Sections 3.1–3.4), it is convenient to begin with an estimate of the neutron flux density φ at 1 m from the electron target in units of (n·cm⁻²·week⁻¹) (m²) (where the units m² imply an inverse-square dependence of the unshielded neutron fluence on distance). This should be estimated for the direction in question and for the average accelerator operating schedule per 40-hour work week (Table XXXV). In the following, the estimate of φ plays a role analogous to that of the workload W .

The required dose-equivalent attenuation factor for neutrons can be derived using:

$$B_n = \dot{H}_M d^2 / (\varphi UT) \quad (63)$$

- where B_n is the factor relating the dose-equivalent at the location in question to the unshielded neutron fluence ($\text{rem} \cdot \text{cm}^2 \cdot \text{n}^{-1}$) at the same location;
- φ is the neutron flux density at the standard distance of one metre from the target in the direction in question ($\text{n} \cdot \text{cm}^{-2} \cdot \text{week}^{-1}$) (m^2);
- d is the distance between the neutron source and the location to be protected (metres);
- \dot{H}_M is the maximum permissible dose-equivalent rate for the type of area ($\text{rem} \cdot \text{week}^{-1}$) (see Table XXXIV);
- U is the orientation (use) factor, taken to be 1 if the calculation is for a secondary barrier;
- T is the occupancy factor of the area to be protected (Table XXXVII).

Equation (63) resembles Eq.(57) except that φ is used in place of the workload W and therefore B_n has a different meaning than B of Eq.(57); B_n contains the fluence-to-dose-equivalent conversion (including the gamma-ray contribution), based on the spectrum at the shielding depth in question.

Curves for B_n for monoenergetic, unidirectional broad neutron beams perpendicularly incident on concrete barriers are shown in Fig.53 as functions of shielding thickness X ($\text{g} \cdot \text{cm}^{-2}$). The intercept at $X = 0$ is equivalent to the fluence-to-dose conversion factor for no shielding (see Table XI and Fig.23, Section 2.5).

Effective dose-equivalent tenth-value layers (TVL) for monoenergetic, unidirectional broad-beam neutrons incident perpendicularly on ordinary concrete are given in Fig.52. The changing slopes of the attenuation curves (for $X < 200 \text{ g} \cdot \text{cm}^{-2}$, Fig.53) are reflected in this figure as a large variation in TVL_1 , whereas TVL_e varies by a smaller amount.

For accelerators operating at energies near the peak of the giant resonance (k_0 in Table XII, Section 2.5) or below, attenuation data for monoenergetic neutrons corresponding to twice the nuclear 'temperature' may be used for neutrons produced in medium- Z or high- Z targets (Table XIII, Section 2.5). (Note that the average neutron energy for neutrons of this energy distribution is twice the nuclear 'temperature' (Eq.(26), Section 2.5).) As the 'temperature' generally lies in the range 0.5–1 MeV, $\bar{E}_n = 2 \text{ MeV}$ is representative of the highest average energy of evaporation neutrons, and the number of direct-emission neutrons emitted from medium- Z or high- Z targets is not large at this operating energy.

For electron energies above the peak of the giant resonance, the data for a monoenergetic energy equal to $E_n = (E_0 - k_0)/2$ would be a conservative choice.

Attenuation curves in concrete for a variety of photoneutron spectra released by bremsstrahlung beams on thin targets are shown in Fig.54. These curves are derived by Wyckoff and Chilton [43] by folding the monoenergetic neutron dose-equivalent attenuation data (from which Figs 52, 53 were adapted)

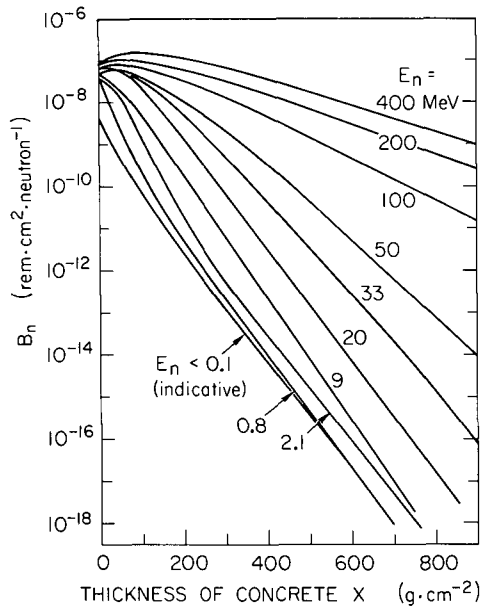


FIG.53. Attenuation of broad beams of monoenergetic, unidirectional neutrons perpendicularly incident on ordinary concrete. The abscissa is the thickness of concrete, X , in $g \cdot cm^{-2}$, and the ordinate is the ratio B_n of dose equivalent in rem at shielding thickness X to unshielded neutron fluence in $n \cdot cm^{-2}$. The dose-equivalent contribution of gamma rays is implicitly included. (References as for Fig.52.)

together with measured photoneutron spectra. Since these curves are based on photoneutron production from thin targets, they assume a spectrum relatively richer in high-energy neutrons than is often the case. They therefore represent a conservative choice of attenuation curve, if used together with a neutron fluence for a thick target (Section 2.5).

The curves shown are mostly for high- Z or medium- Z materials and for 90° neutron emission. The trend will be for a more penetrating neutron spectrum at higher energy E_0 , lower Z , and more forward angles. Thus the three curves at a somewhat more forward angle (67°) lie highest in Fig.54. Curves for light elements ($Z < 10$) will be relatively richer in fast neutrons from direct emission and will therefore show lesser attenuation.

The attenuation curve for neutrons from a PuBe source is shown for comparison with the curves for low-energy photoneutrons. The attenuation curve for neutrons from Cu at $E_0 = 400$ MeV and the presumed behaviour at very high energies ($E_0 \gg 150$ MeV) are also shown.

The data of Figs 52–54 can be adapted to such materials as earth, heavy concrete and stone, assuming that the water content of these materials is not significantly less, by scaling by density, as in Eq.(54) (Section 3.2).

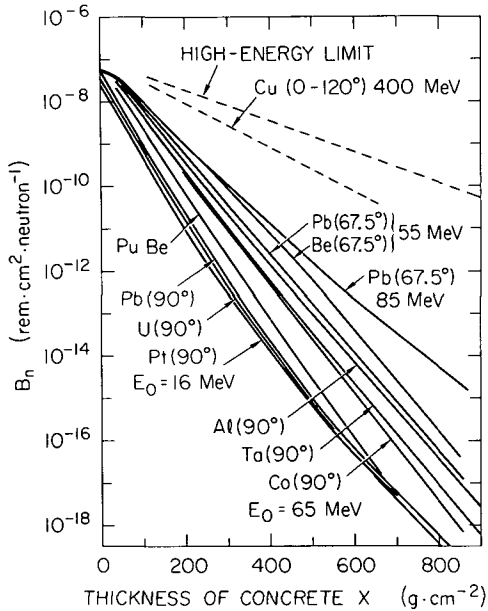


FIG.54. Attenuation of unidirectional broad beams of neutrons, for representative photo-neutron spectra, perpendicularly incident on ordinary concrete. The abscissa is the thickness of concrete, X , in $g \cdot cm^{-2}$, and the ordinate is the ratio B_n of dose equivalent to unshielded neutron fluence. The labels indicate target material, laboratory angle of neutron emission and endpoint energy E_0 of the bremsstrahlung beam. The dose equivalent from gamma rays is implicitly included. The curves are derived by folding the monoenergetic neutron shielding data cited for Fig.52 together with measured photoneutron spectra (adapted from Wyckoff and Chilton [43]). Also shown for comparison are curves for neutrons from a PuBe source (*ibid.*), for photoneutrons produced in Cu at $E_0 = 400$ MeV (unnormalized, from Alsmüller and Barish [47]), as well as the presumed high-energy limit (unnormalized; see Section 3.5.2).

To use materials other than concrete for neutron shielding, the 'removal cross-section' method is convenient and usually accurate enough for low-energy accelerators. Original data on removal cross-sections are given by Chapman and Storrs [48] and the method is neatly summarized in NCRP Report No.38 [49]. More complete discussions can be found in the general references on shielding [50–54]. To use the removal cross-section method, the material of the shield must be hydrogenous, mixed intimately with hydrogenous material, or followed by 20–30 cm of water or the equivalent in hydrogen content. An obviously useful combination for such a shield is steel or lead followed by concrete. The method described may be used to advantage, for example in the case where concrete walls are already standing and the designer wishes to estimate the effect of added iron or lead shielding.

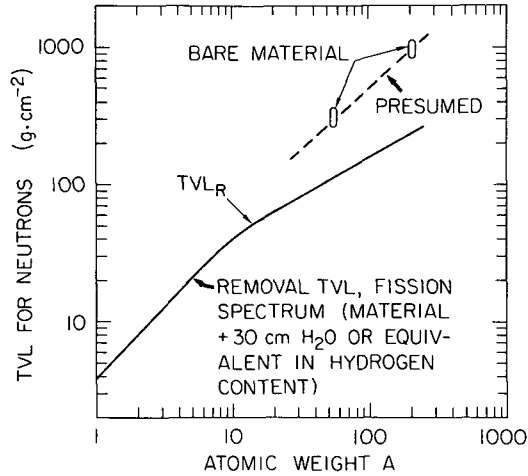


FIG.55. Neutron removal tenth-value layer (TVL_R) as a function of atomic weight A of shielding material. The solid curve is for a fission spectrum, assuming a backing of 30 cm of water or the equivalent in hydrogen content (derived from Chapman and Storrs [48]). The points above show TVL s for the fission spectrum on iron and lead, without hydrogenous backing, for comparison (adapted from Shure et al. [55]). The dashed curve is an interpolation.

The hydrogenous material serves to greatly enhance the effectiveness of the non-hydrogenous portion. Thirty centimetres of water (or the equivalent) is sufficient to bring out the full effectiveness of the non-hydrogenous portion, but any additional hydrogenous material of course provides additional neutron attenuation in itself.

The trend of TVL_R with atomic weight A is shown in Fig.55. For $A > 8$, the TVL_R in $g \cdot cm^{-2}$ is given approximately by

$$TVL_R = 4.76 (\ln 10) A^{0.58} = 11 A^{0.58} \quad (64)$$

These values apply to a fission spectrum and therefore are also suitable for neutrons from thick targets at installations operating at energies E_0 ranging from the photoneutron threshold k_{th} to somewhat above the giant-resonance energy k_0 (Table XII, Section 2.5).

The effectiveness of shields of iron and lead as a function of thickness of the hydrogenous layer have been published by Shure et al. [55], Dudziak [56], and Dudziak and Schmucker [57] (see also, for example, Ref.[58], Ch.4). Their results should be used when it is necessary to evaluate the effect of a hydrogenous layer of less than about 20 cm of water or the equivalent.

TABLE XLII. NEUTRON DOSE-EQUIVALENT TVL VALUES FOR REPRESENTATIVE LOW-ENERGY SPECTRA

Material	Spectrum	TVL ($\text{g}\cdot\text{cm}^{-2}$)	Reference
Paraffin (solid)	AmBe	23	59
Wood	AmBe	28	59
Water	Fission	22	49
Sand (SiO_2)	AmBe	74	59
Ordinary concrete	AmBe	96	59
Heavy concrete	AmBe	110	59
Iron (steel)	Fission	280 - 330	55
Lead	Fission	900 - 1070	55

An indication of the neutron shielding effectiveness of materials other than ordinary concrete can be gained by the fact that the spectrum of giant-resonance neutrons is not very different from that of an Am-Be source. Experimental TVL values for these neutrons for several materials are given in Table XLII [59]. These data, which are useful for shielding accelerators operating at energies near the giant resonance, clearly show the greater effectiveness of low-Z (especially hydrogenous) materials.

The variability of shielding effectiveness of bare non-hydrogenous materials is explained in part by the experimental sensitivity to the detector type. These data are meant to be indicative only and should be used with caution.

The scattering of neutrons, although important for the design of labyrinths and ducts, is too specialized to be treated here. The user of this manual is referred to papers by, for example, French and Wells [60] and Maerker and Muckenthaler [61], as well as general shielding manuals [50-54].

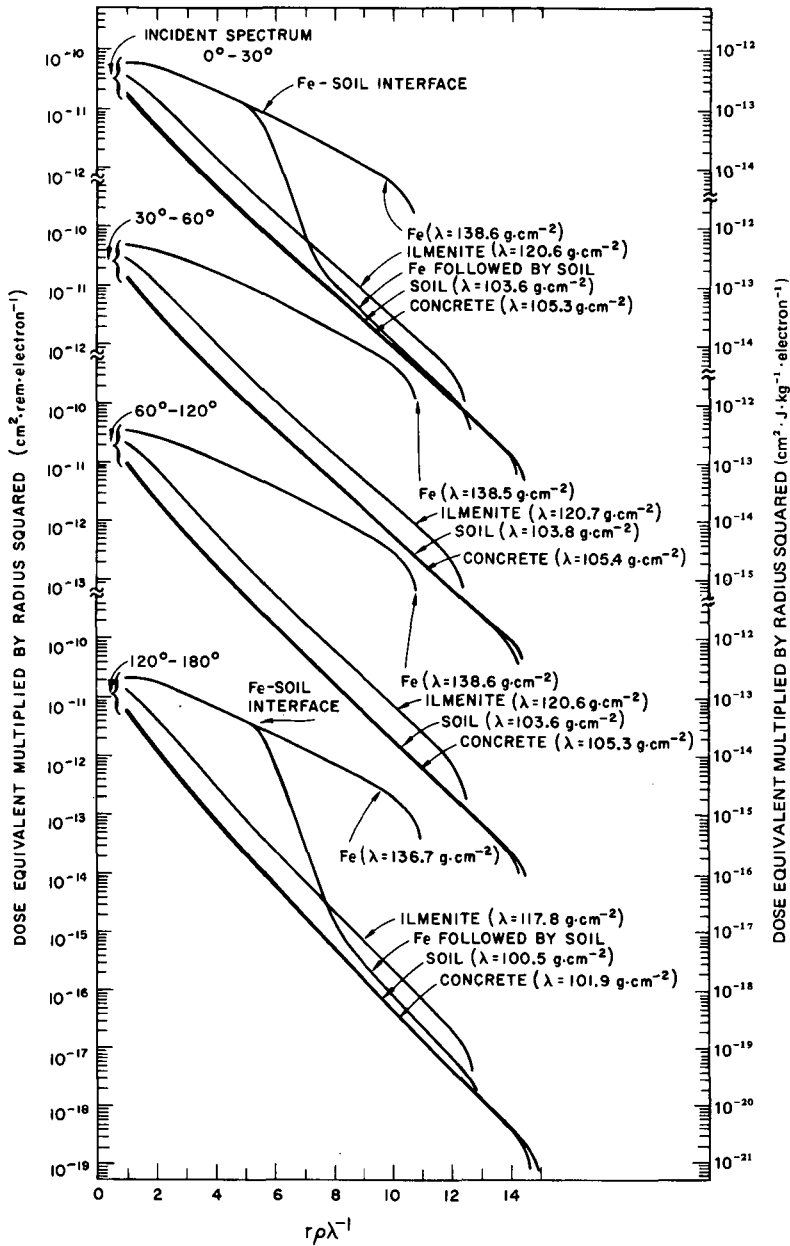


FIG.56. Neutron shielding for 400-MeV electrons incident on a thick copper target. Dose equivalent multiplied by radius squared versus radius for a variety of angles and materials. The ordinate is the dose equivalent multiplied by the distance (radius from target (cm)) squared; the abscissa is in the dimensionless variable $r\rho\lambda^{-1}$, where r is in cm, ρ is in $\text{g}\cdot\text{cm}^{-3}$, and λ is in $\text{g}\cdot\text{cm}^{-2}$. (Adapted from Ref.[47], with kind permission of R.G. Alsmiller, Jr., and J. Barish, and Particle Accelerators.)

3.5.2. High-energy installations ($E_0 > 140 \text{ MeV}$)

Neutron yields have been calculated by Monte-Carlo methods from thick copper targets for incident electron energies up to 400 MeV by Gabriel and Alsmiller [62], and complete calculations of shielding requirements have been published for $E_0 = 400 \text{ MeV}$ by Alsmiller and Barish [47]. This is a particularly useful energy, because it is high enough to include the contribution of the ‘first’ pion resonance (Fig.31, Section 2.5.2) but not high enough that the simplifications used at a much higher energy become valid. The results of this shielding calculation are reproduced in Fig.56.

For materials other than copper, it would be appropriate to scale the yield data by the inverse atomic number Z^{-1} , reflecting the scaling of the photon track-length distribution within the production target by this factor.

At higher energies, the data of Fig.56 would provide only lower limits to the shielding requirements, because the greater penetration of the additional high-energy neutrons added to the spectrum would not be properly accounted for. Nevertheless, when scaled by beam power (rather than energy), they would be useful as a lower limit.

Yields for linacs operating at very high energy ($E_0 \approx 20 \text{ GeV}$) have been estimated by DeStaebler et al. [63], as discussed in Section 2.5.3, also for copper beam dumps ($Z = 29$) (Fig.39). Over a considerable energy range, these yields may be scaled as beam power.

Neutron inelastic cross-sections decrease with increasing energy to essentially a constant value above about 150 MeV, the ‘geometric’ cross-section. Therefore, neutrons with energies above this will ultimately control the neutron radiation protection requirements.

The high-energy neutron fluence is attenuated by an attenuation length³⁰, λ (in cm), given approximately by

$$\lambda = (N \sigma_{\text{in}})^{-1} \quad (65)$$

where N is the number of atoms per cm^3 (given by $N_A \rho / A$) and σ_{in} is the inelastic cross-section in cm^2 [64]. The nucleon-nucleus inelastic cross-section, σ_{in} (in mb), as a function of atomic weight A is well represented by the formula

$$\sigma_{\text{in}} = 43.1 A^{0.70} \quad (66)$$

for $A \gtrsim 3$, $E_n \gtrsim 150 \text{ MeV}$ [65, 66] (see also Appendix B, Table B-I, Footnote F).

³⁰ The attenuation length λ and tenth-value layer are related in the following manner: $\text{TVL} = \lambda \ln 10 = 2.303 \lambda$ (Table XXXIX).

Equations (65) and (66) give the following expression for the high-energy attenuation length (now expressed in $\text{g}\cdot\text{cm}^{-2}$):

$$\lambda = 38.5 A^{0.30} \text{ (derived from } \sigma_{\text{in}}) \quad (67a)$$

Experiments confirm that the attenuation lengths from Eq.(61a) are consistent with this trend. According to a review by McCall and Thomas [64], “. . . while the experimental data show considerable spread, a reasonable choice for λ would be $120 \text{ g}\cdot\text{cm}^{-2}$ for earth or ordinary concrete”. Therefore the coefficient giving a more realistic estimate for shielding purposes is closer to $45 \text{ g}\cdot\text{cm}^{-2}$:

$$\lambda = 45 A^{0.30} \text{ (experimental)} \quad (67b)$$

Surveys of experimental data are given in Ref.[54], p.61–64, and in Ref.[68].

In these considerations, we ignore the much larger yields of lower-energy neutrons from the giant-resonance and quasi-deuteron effects. The lower-energy neutrons have larger cross-sections and correspondingly greater attenuation rates. Studies have shown that the radiation field reaches an equilibrium condition a few attenuation lengths within the shield [67]. Deep within the shield, the ‘original’ lower-energy neutron component has been largely absorbed. A hadronic cascade, fuelled by high-energy neutrons, continually repopulates the lower-energy part of the spectrum, but these low-energy neutrons are also quickly reabsorbed. The shape of the spectrum observed at the shield surface is similar to that which exists within the shield.

Where space is a factor, an efficient shield can be made of iron, followed by about $200 \text{ g}\cdot\text{cm}^{-2}$ (or more) of concrete or the equivalent (in hydrogen content) of other hydrogenous material. For the iron portion of the shield, an attenuation length of $150 \text{ g}\cdot\text{cm}^{-2}$ would be appropriate (Eq.(67b)).³¹ The importance of the hydrogenous backing can be appreciated by examining Fig.56.

A helpful discussion of high-energy neutron shielding can be found in Chapter 6 of Ref.[68]. Of particular usefulness are the review of data on the attenuation lengths and the discussion of the Moyer model for shield calculation.

Table XLIII shows attenuation data for various materials as derived from Eq.(67b)³², and a comparison with the parameters for 400 MeV from Alsmiller and Barish [47].

³¹ A simple average of measurements for steel (Ref.[68], Table 6.IX) gives $\lambda = 152 \pm 6 \text{ g}\cdot\text{cm}^{-2}$.

³² The effective atomic weight A_{eff} for mixtures of elements whose cross-section behaves as Eq.(66) is given by $A_{\text{eff}} = [(\sum \rho_i) / \sum (\rho_i / A_i^{0.3})]^{3.33}$, where ρ_i is the fraction (by weight) of element of atomic weight A_i . See Appendix B for more discussion of this kind of averaging to derive A_{eff} or Z_{eff} .

TABLE XLIII. ATTENUATION PARAMETERS FOR HIGH-ENERGY PHOTONEUTRONS

Material	$A_{\text{eff}}^{(a)}$	$\lambda \text{ (g}\cdot\text{cm}^{-2}\text{)}$		TVL $\text{(g}\cdot\text{cm}^{-2}\text{)}$	
		400 MeV ^(b)	20 GeV	400 MeV ^(b)	20 GeV
Soil ^(c)	20.4	104	120	239	276
SiO ₂	20.6	---	120	---	276
Concrete	21.0	105	120	242	276
Ilmenite	34.4	121	130 ^(d)	279	298 ^(d)
Iron (steel)	55.8	139	150 ^(d)	320	345 ^(d)
Lead	207.2	---	223 ^(d)	---	513 ^(d)

(a) See text for definition of A_{eff} for this context.

(b) After Alsmiller and Barish (Ref. [47]). See Fig. 56.

(c) Assumed composition (by weight): 95% SiO₂, 5% H₂O.

(d) From Eq. (67 b).

A valuable discussion of neutron shielding considerations for 4–6 GeV electron beams at DESY is published by Bathow et al. [69]. Ladu et al. [70] have published detailed considerations for shielding by earth and concrete of neutron fluences released by 400-MeV electrons incident on a Cu-H₂O beam dump at Frascati.

3.6. Labyrinths, doors, voids and penetrations

All types of penetrations should be designed to prevent streaming of scattered photons, and also of neutrons from accelerators operating above 10 MeV. It is important to make these provisions in the initial design, because later modifications may be expensive.

Conduits and pipes entering the radiation room from beneath the floor present no problem if there is no occupancy below the accelerator room. This arrangement is always preferred where possible.

Where penetrations must be made in walls, they should have at least two well-separated bends of about 90° each and be provided with lead baffles. Openings in walls should always be in secondary barriers. The opening into the radiation room should not point towards possible radiation sources, nor should

the outside opening point towards locations likely to be occupied. Preferably they should be close to the floor or above head height. Air-conditioning ducting is best brought in through the labyrinth, and the grille should be provided with a lead baffle. Where voids in the shielding are needed for service boxes (for power, lighting or safety equipment, for example), the shielding should be augmented by an equivalent amount of lead, lining the void. An excellent detailed discussion of these considerations is given in Ch.4 of Ref.[4].

Typical labyrinth designs are illustrated in Section 4. Above 10 MeV, neutrons and scattered photons both must be considered. An important point is that all radiation reaching the door must first be scattered at least twice. In new labyrinth design, the data on scattered radiation of Section 3.4.2 may be of help. It has been found that typical labyrinths used in clinical installations have an effective neutron 'attenuation' of one decade for each 3–4.5 m of labyrinth length. Labyrinths of reasonable dimensions with only one bend do not generally provide sufficient neutron attenuation, and the door must be adequate to shield against the remaining neutrons. There is therefore a trade-off between labyrinth length and door thickness.

At installations of all energies, it is good practice to line the door with 1 cm of lead to shield against scattered photons. An effective combination for installations of energies above 10 MeV is 10 cm of wood, followed by 0.5 mm of cadmium metal, followed by 1 cm of lead. The wood is a neutron shield in itself and serves to thermalize the remaining neutrons to enhance the effectiveness of the cadmium, which has a large cross-section for thermal-neutron capture. The lead then shields against the scattered photons from inside the radiation room and the neutron-capture photons from the labyrinth walls, wood and cadmium. Thus the ordering indicated for the three materials (wood, Cd, then Pb) is the most effective. A layer of boron-loaded material (e.g. polyethylene) can be used in place of Cd. Other materials of equivalent hydrogen content may be substituted for the wood, if desired (see Section 3.5).

Another means of inhibiting neutron streaming is the use of boron-loaded panels for lining the labyrinth walls. These should preferentially be placed along walls nearest the radiation source, or at labyrinth corners to act as neutron 'catchers'. It has been found that up to 20 m² of panels containing 10% borax (Na₂B₄O₇) by weight reduce the amount of neutron streaming by about half [12]. However, because of the greater area involved, this solution may be more expensive than a well-shielded door.

REFERENCES TO SECTION 3

- [1] COUNCIL OF THE EUROPEAN COMMUNITIES, Council directive laying down the revised basic standards for the health protection of the general public and workers against the dangers of ionizing radiation, Official Journal of the European Communities 19 L187 (1976) 1–64.

- [2] NATIONAL COUNCIL ON RADIATION PROTECTION AND MEASUREMENTS, Basic Radiation Protection Criteria, NCRP Rep. No.39, Washington, DC (1971).
- [3] NATIONAL COUNCIL ON RADIATION PROTECTION AND MEASUREMENTS, Medical X-Ray and Gamma-Ray Protection for Energies up to 10 MeV – Structural Shielding Design and Evaluation, NCRP Rep. No.34, Washington, DC (1970). (This report is superseded by NCRP-49 (1976).)
- [4] NATIONAL COUNCIL ON RADIATION PROTECTION AND MEASUREMENTS, Structural Shielding Design and Evaluation for Medical Use of X-Rays and Gamma-Rays of Energies up to 10 MeV (1976), NCRP Rep. No.49, Washington, DC (1976). (This report supersedes NCRP-34. Full-sized reproductions of figures for shielding calculations are available as an adjunct to this report.)
- [5] NATIONAL COUNCIL ON RADIATION PROTECTION AND MEASUREMENTS, Radiation Protection Design Guidelines for 0.1–100 MeV Particle Accelerator Facilities, NCRP Rep. No.51, Washington, DC (1977).
- [6] DEUTSCHER NORMENAUSSCHUSS (DNA), Medizinische Elektronen-Beschleuniger-Anlagen, Draft Rep. No. DIN-6847, Part 2: Radiation Protection Rules for Installation, Beuth-Vertrieb, Berlin (1975).
- [7] COBB, P.D., BJÄRNGARD, B.E., Use factors for medical linear accelerators, Health Phys. **31** (1976) 463.
- [8] HUNGERFORD, H.E., “The nuclear, physical, and mechanical properties of shielding materials”, Reactor Handbook, Ch.51, Vol. I: Materials (TIPTON, C.R., Jr., Ed.), Interscience, New York (1960).
- [9] EMI THERAPY SYSTEMS, private communication, Sunnyvale, California (1977). (TVL_e values of 71, 69, 70, 66 and 56 g·cm⁻² for concrete, steel, copper, tungsten and lead, respectively, at 4 MeV were supplied by C.E. Edgerton.)
- [10] VARIAN, Linatron High-Energy X-Ray Applications, Varian Associates, Radiation Division, Palo Alto, CA (1975). (Lucite, propellant, concrete, aluminium, steel, lead, tungsten: 4, 8, 15 MeV.)
- [11] MARUYAMA, T., KUMAMOTO, Y., KATO, Y., HASHIZUME, T., YAMAMOTO, M., Attenuation of 4–32 MV X-Rays in ordinary concrete, heavy concrete, iron and lead, Health Phys. **20** (1971) 277. (Concrete, heavy concrete, Fe, Pb: 4–32 MeV.)
- [12] COLEMAN, F.J., A Review of Shielding Data for the SL75-20 Linear Accelerator, M.E.L. Equipment Co., Particle Accelerator Division, Publication No. 1013-10-75, Manor Royal, Crawley, Sussex (1975).
- [13] KARZMARK, C.J., CAPONE, T., Measurements of 6 MV X-rays, I. Primary radiation absorption in lead, steel and concrete, Br. J. Radiol. **41** (1968) 33.
- [14] KIRN, F.S., KENNEDY, R.J., How much concrete for shielding?, Nucleonics **12** (1954) 44. (Concrete: 6, 10, 20, 30, 38 MeV.)
- [15] MILLER, W., KENNEDY, R.J., Attenuation of 86 and 176-MeV synchrotron X-rays in concrete and lead, Radiat. Res. **4** (1956) 360. (Concrete: 38, 86, 176 MeV; Pb: 86, 176 MeV.)
- [16] BUECHNER, W.W., VAN DE GRAAFF, R.J., FESHBACH, H., BURRILL, E.A., SPERDUTO, A., McINTOSH, L.R., An investigation of radiography in the range from 0.5 to 2.5 million volts, ASTM Bulletin (Dec. 1948) 54.
- [17] GOLDIE, C.H., WRIGHT, K.A., ANSON, J.H., CLOUD, R.W., TRUMP, J.G., Radiographic properties of X-rays in the two- to six-million volt range, ASTM Bulletin (Oct. 1954) 49.
- [18] SCAG, D.A., Discussion of radiographic characteristics of high-energy X-rays, Nondestr. Test. **12** (1954) 47. (Steel: 6–90 MeV.)

- [19] O'CONNOR, D.T., CRISCUOLO, E.L., PACE, A.L., 10-MeV X-ray technique, Papers on Radiography, Am. Soc. Test. Mater. (1949) 10; and ASTM Spec. Tech. Publ. No.96. (Steel: 10 MeV.)
- [20] WESTENDORP, W.F., CHARLTON, E.E., A 100 million volt induction electron accelerator, J. Appl. Phys. 16 (1945) 581. (Steel: 4, 5, 10, 20, 30, 40, 50, 75, 100 MeV; Pb: 10, 20, 30, 40, 50, 75, 100 MeV.)
- [21] ADAMS, G.D., GIRARD, J.P., Trans. Am. Inst. Electr. Eng. 65 (1946). (Steel: 20 MeV.)
- [22] WIDERÖE, R., The Brown Boveri 31 million volt dual beam betatron, Nondestr. Test. 11 (1953) 23. (Steel: 31 MeV.)
- [23] BLY, J.H., BURRILL, E.A., "High-energy radiography in the 6- to 40-MeV range", Symp. Nondestructive Testing in the Missile Industry, Special Technical Publication No.278, American Society for Testing Materials (1959). (Review: Steel, rocket propellant, concrete, Pb: 0.1–100 MeV.)
- [24] BLY, J.H., High-energy radiography 1–20 MeV, Mater. Eval. (Nov. 1964).
- [25] BURRILL, E.A., The shielding problem with low-energy particle accelerators, Nucl. Saf. 9 6 (1968) 457.
- [26] NATIONAL BUREAU OF STANDARDS, Protection Against Betatron-Synchrotron Radiations up to 100 Million Electron Volts, NBS Handbook No.55, Washington, DC (1954).
- [27] NATIONAL BUREAU OF STANDARDS, Shielding for High-Energy Electron Accelerator Installations, NBS Handbook No.97, Washington, DC (1964).
- [28] LOKAN, K.H., SHERMAN, N.K., GELLIE, R.W., HENRY, W.H., LEVESQUE, R., NOWAK, A., TEATHER, G.G., LUNDQUIST, J.R., Bremsstrahlung attenuation measurements in ilmenite loaded concretes, Health Phys. 23 (1972) 193. (Heavy concrete: 5, 10, 20, 30 and 40 MeV.)
- [29] CHILTON, A.B., HUDDLESTON, C.M., A semiempirical formula for differential dose albedo for gamma rays on concrete, Nucl. Sci. Eng. 17 (1963) 419.
- [30] CHILTON, A.B., DAVISSON, C.M., BEACH, L.A., Parameters for C-H albedo formula for gamma rays reflected from water, concrete, iron and lead, Trans. Am. Nucl. Soc. 8 2 (1965) 656.
- [31] CHILTON, A.B., Backscattering of gamma rays from point sources by an infinite-plane concrete surface, Nucl. Sci. Eng. 21 (1965) 194.
- [32] KRUGLOV, S.P., LOPATIN, I.V., A study of the dispersion of the energy of an impact radiation beam from an absorption calorimeter, Zh. Tekh. Fiz. 30 4 (1960) 424; transl. Sov. Phys. – Tech. Phys. 5 4 (1960) 395.
- [33] PRUITT, J.S., High energy X-ray photon albedo, Nucl. Instrum. Meth. 27 (1964) 23.
- [34] SUGIYAMA, S., TOMIMASU, T., High energy X-ray albedo for Pb, Cu and duralumin, Nucl. Instrum. Meth. 53 (1967) 346.
- [35] RASO, D.J., Monte-Carlo calculations on the reflection and transmission of scattered gamma rays, Nucl. Sci. Eng. 17 (1963) 411.
- [36] VOGT, H.G., Eine Methode zur Bestimmung der differentiellen Albedo für Photonen im Energiebereich von 2 bis 17 MeV, Nucl. Eng. Des. 22 (1972) 138.
- [37] SELPH, W.E., "Albedos, ducts and voids", in Reactor Shielding for Nuclear Engineers (SCHAEFFER, N.M., Ed.), AEC Rep. TID-25921, National Technical Information Service, Springfield, VA (1973).
- [38] BATHOW, G., FREYTAG, E., TESCH, K., Shielding measurements on 4.8-GeV Bremsstrahlung, Nucl. Instrum. Meth. 33 (1965).
- [39] BATHOW, G., FREYTAG, E., TESCH, K., Measurements on 6.3 GeV electromagnetic cascades and cascade-produced neutrons, Nucl. Phys. B2 (1967) 669. (In Table 1, $\lambda(0^\circ)$ for lead should be 0.7, rather than 0.1.)

- [40] BATHOW, G., FREYTAG, E., KOBBERLING, M., TESCH, K., KAJIKAWA, R., Measurements of the longitudinal and lateral development of electromagnetic cascades in lead, copper and aluminum at 6 GeV, Nucl. Phys. **B20** (1970) 592.
- [41] DINTER, H., TESCH, K., Measurements of dose and shielding parameters of electron-photon stray radiation from a high-energy electron beam, Deutsches Elektronen-Synchrotron, Hamburg, Rep. DESY 76/19 (1976).
- [42] NELSON, W.R., JENKINS, T.M., McCALL, R.C., COBB, J.K., Electron-induced cascade showers in copper and lead at 1 GeV, Phys. Rev. **149** 1 (1966) 201.
- [43] WYCKOFF, J.M., CHILTON, A.B., "Dose due to practical neutron energy distributions incident on concrete shielding walls", paper presented at Third Int. Congr. of the International Radiation Protection Association, held at Washington, DC, 9-14 Sep. 1973, IRPA, Washington, DC (1973).
- [44] ROUSSIN, R.W., SCHMIDT, F.A.R., Adjoint Sn calculations of coupled neutron and gamma-ray transport through concrete slabs, Nucl. Eng. Des. **15** 3 (1971) 319.
- [45] ROUSSIN, R.W., ALSMILLER, R.G., Jr., BARISH, J., Calculations of the transport of neutrons and secondary gamma-rays through concrete for incident neutrons in the energy range 15 to 75 MeV, Nucl. Eng. Des. **24** (1973) 2. (Figs 1, 2 of this paper are more accurate than Figs 6, 7 of Ref.[46] and therefore supersede them.)
- [46] ALSMILLER, R.G., Jr., MYNATT, F.R., BARISH, J., ENGLE, W.W., Jr., Shielding against neutrons in the energy range 50 to 400 MeV, Nucl. Instrum. Meth. **72** (1969) 213; also ORNL-TM-2554. (The data of Figs 6, 7 are superseded by Figs 1, 2 of Ref.[45].)
- [47] ALSMILLER, R.G., Jr., BARISH, J., Shielding against the neutrons produced when 400-MeV electrons are incident on a thick copper target, Part. Accel. **5** (1973) 155.
- [48] CHAPMAN, G.T., STORRS, C.L., Effective Neutron Removal Cross Sections for Shielding, Oak Ridge National Laboratory, Rep. AECD-3978 (1955).
- [49] NATIONAL COUNCIL ON RADIATION PROTECTION AND MEASUREMENTS, Protection Against Neutron Radiation, NCRP Rep. No.38, Washington, DC (1971).
- [50] PRICE, B.T., HORTON, C.C., SPINNEY, K.T., Radiation Shielding, Pergamon Press, New York (1957).
- [51] SCHAEFFER, N.M., Ed., Reactor Shielding for Nuclear Engineers, AEC Rep. TID-25921, National Technical Information Service, Springfield, VA (1973).
- [52] BLIZARD, E.P., ABBOTT, L.S., Eds, Reactor Handbook, 2nd ed., Vol. III, Part B, Shielding, Interscience, New York (1962).
- [53] ROCKWELL, T., Reactor Shielding Design Manual, AEC Rep. TID-7004, Technical Information Division, Washington, DC (1956).
- [54] INTERNATIONAL ATOMIC ENERGY AGENCY, Engineering Compendium on Radiation Shielding (JAEGER, R.G., Ed.), Vol.I, Shielding Fundamentals and Methods, Springer-Verlag, New York (1968).
- [55] SHURE, K., O'BRIEN, J.A., ROTHBERG, D.M., Neutron dose rate attenuation by iron and lead, Nucl. Sci. Eng. **35** (1969) 371.
- [56] DUDZIAK, D.J., Attenuation of Fast Neutron Biological Dose in Nonhydrogenous Shields Followed by Thin Hydrogenous Shields, Los Alamos Scientific Laboratory, Rep. LA-DC-9418 (1968).
- [57] DUDZIAK, D.J., SCHMUCKER, J.E., Hydrogenous-Material-Dependent Removal Cross Section of Lead for Fast Neutron Biological Dose, Bettis Atomic Power Laboratory, Pittsburgh, PA, Rep. WAPD-TM-662 (1968).
- [58] STEVENS, P.N., TRUBEY, D.K., GARRETT, C.W., SELPH, W.E., "Radiation transport", in Reactor Shielding for Nuclear Engineers (SCHAEFFER, N.M., Ed.), Ch. 4, AEC Rep. TID-25921, National Technical Information Service, Springfield, VA (1973).

- [59] TESCH, K., Deutsches Elektronen-Synchrotron DESY, Hamburg, private communication (1976).
- [60] FRENCH, R.L., WELLS, M.B., An angle-dependent albedo for fast neutron reflection calculations, *Nucl. Sci. Eng.* **19** (1964) 441.
- [61] MAERKER, R.E., MUCKENTHALER, F.J., Calculation and measurement of the fast-neutron differential dose albedo for concrete, *Nucl. Sci. Eng.* **22** (1965) 455.
- [62] GABRIEL, T.A., ALSMILLER, R.G., Jr., Photonucleon and Photopion Production from High-Energy (50–400 MeV) Electrons in Thick Copper Targets, Oak Ridge National Laboratory, Rep. ORNL-4443 (1969).
- [63] DeSTAEBLER, H., JENKINS, T.M., NELSON, W.R., "Shielding and radiation", The Stanford Two-Mile Accelerator (NEAL, R.B., Ed.), Ch.26, Benjamin, New York (1968).
- [64] McCALL, R.C., THOMAS, R.H., "The radiation environment of high-energy accelerators", Basic Aspects of High-Energy Particle Interactions and Radiation Dosimetry, ICRU, Washington, DC, Rep. ICRU-28 (1978).
- [65] KEEFE, D., SCOLNICK, M., Table of Mean Free Path and Radiation Length for Various Materials, Lawrence Berkeley Laboratory, Internal Rep. AS/EXP 01 (1966).
- [66] SCHIMMERLING, W., DEVLIN, T.J., JOHNSON, W., VOSBURGH, K.G., MISCHKE, R.F., Neutron-nucleus total and inelastic cross sections: 900 to 2600 MeV/c, *Phys. Rev.* **7C** (1973) 248.
- [67] SMITH, A.R., "Some experimental shielding studies at the 6.2 BeV Berkeley Bevatron", Proc. USAEC First Symp. Accelerator Radiation Dosimetry and Experience, held at Brookhaven National Laboratory, 3–5 Nov. 1965, USAEC Rep. CONF-651109, Division of Technical Information, Washington, DC (1965) 365.
- [68] PATTERSON, H.W., THOMAS, R.H., Accelerator Health Physics, Ch.6, Academic Press, New York (1973).
- [69] BATHOW, G., FREYTAG, E., TESCH, K., Shielding of high-energy electrons: the neutron and muon components, *Nucl. Instrum. Meth.* **51** (1967) 56.
- [70] LADU, M., PELLICIONI, M., ROCCELLA, M., Frascati National Laboratory, CNEN Report, Series LNF-66/44, No.332 (1966); Transl.: Shielding for the Frascati Linear Accelerator Quench Tanks, Stanford Linear Accelerator Center, Rep. SLAC-TRANS-60 (1966).

4. TYPICAL INSTALLATIONS

Examples of actual accelerator installations used for medicine, industrial radiography and research are presented in this section, together with a number of general points to be considered in the planning of new facilities. However, a qualified radiation protection expert should be consulted at an early planning stage of a new facility because the management may not be familiar with the detailed requirements for radiation safety or have sufficient time to attend to them. Expert advice should be obtained at the architectural planning stage to ensure that adequate provision is made for radiation shielding. At the same time, provision for interlocks, other safety devices and utilities requirements should be made, and features of the eventual radiation safety programme should be considered in relation to the physical layout.

Because of the weight of shielding barriers, a basement or ground-level location is preferred for radiation facilities. If this is not possible, consideration must be given to the problem of structural support.

From an economic standpoint, ordinary concrete is usually preferred for new construction, but barite (barytes) concrete or other heavy concrete is sometimes used where space is at a premium. Iron or lead plates are frequently used to augment barriers when new equipment is installed in existing rooms.

Except for some research accelerators operating above about 150 MeV, the thicknesses of barriers (if made of concrete) are determined by photon dose rates (see Section 3). For accelerators operating above 10 MeV, neutron streaming is the main consideration for labyrinth and door design, but streaming of soft scattered photons should also be considered. Where possible, a heavy ceiling which serves as a radiation barrier should be provided and is essential where there is occupancy above the height of the wall barriers. Where a heavy ceiling is impractical, extreme care must be taken in controlling access to the roof and other spaces above the facility. The radiological risk to personnel from neutron and photon skyshine should also be assessed under such circumstances.

4.1. Medical installations

Medical linear accelerators are now regarded as standard products and each manufacturer has proven installation drawings which should be followed where possible. If new equipment is to be installed in an existing room, the facility should be evaluated by a qualified expert. It is likely that the new equipment will have a higher energy and output than the equipment being replaced, and some barriers may have to be augmented. If new equipment capable of rotational therapy is being installed, walls or ceiling barriers may have to be augmented or switches may have to be provided to limit the range of rotation.

In evaluating radiation protection requirements, consideration should be given to the workload factor W , the orientation (use) factor U and the area occupancy factor T , and the amount of leakage and scattered radiation. In cases where a beam stopper is provided, the attenuation requirements of primary barriers can be reduced correspondingly. The use of a beam stopper does not affect secondary barriers, however.

The labyrinth and door should be designed together to inhibit radiation streaming (see Section 3.6). Of course the labyrinth should provide adequate passage for hospital gurneys and the equipment to be installed. If possible, the connections for the utilities should be brought into the room through the floor.

The following provisions should be discussed with the manufacturer and architect before installation plans are completed:

- (a) Provision for radiation warning lights and emergency shut-off switches and a 'hazard/safe' switch just inside the door.
- (b) Provision for closed-circuit TV for patient observation.
- (c) Provision for aural communication with patients.
- (d) Provision for lasers or other alignment devices.
- (e) Electrical power, three-phase, of voltage and $kV \cdot A$ rating (10–75 $kV \cdot A$) as specified by the manufacturer. Regulation to $\pm 5\%$ is usually required, and separate power may be needed for vacuum pumps and auxiliary equipment.
- (f) Cooling water (10–70 $\text{ltr} \cdot \text{min}^{-1}$) at adequate pressure (3–5 $\text{kgf} \cdot \text{cm}^{-2}$), depending on the unit. In some units closed-circuit cooling is employed.
- (g) Air conditioning as needed for patient comfort and proper equipment operation, capable of removing a heat load of 2–6 kW, depending on the unit.
- (h) Crane or eyebolt and hoist of 1–2 t capacity.
- (i) Some installations may require a pit for full rotation of the therapy unit or for full treatment table movement.
- (j) Provision for electrical grounding (1 ohm maximum).
- (k) Electrical shielding against RF interference to equipment outside the treatment room.
- (l) Where space limitations prohibit sufficiently thick primary barriers, a beam stopper may be indicated (Fig.57).
- (m) Especially in a clinical setting, attention should be given to the visual impact of the treatment facility as it affects the comfort and morale of patients.

Figures 57–60 illustrate typical clinical installations. The barrier thicknesses shown are indicative only and should be evaluated by a qualified expert for each new installation. Section 3 outlines methods of barrier calculation, including the use of a sample worksheet.

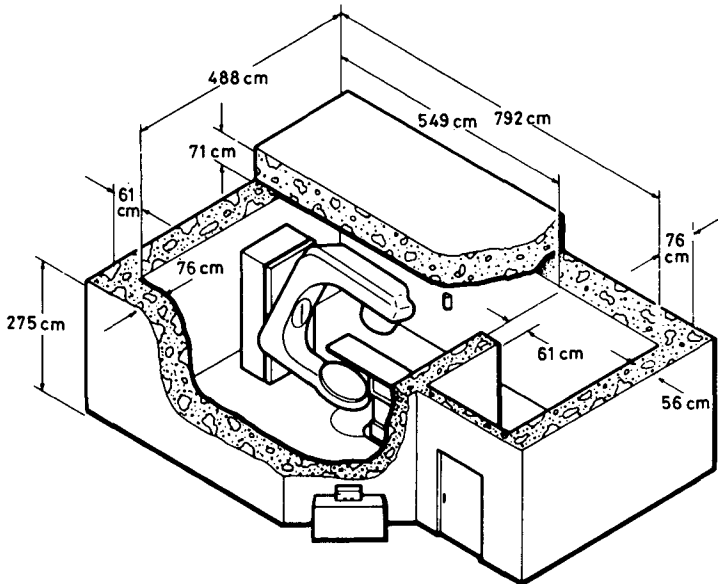
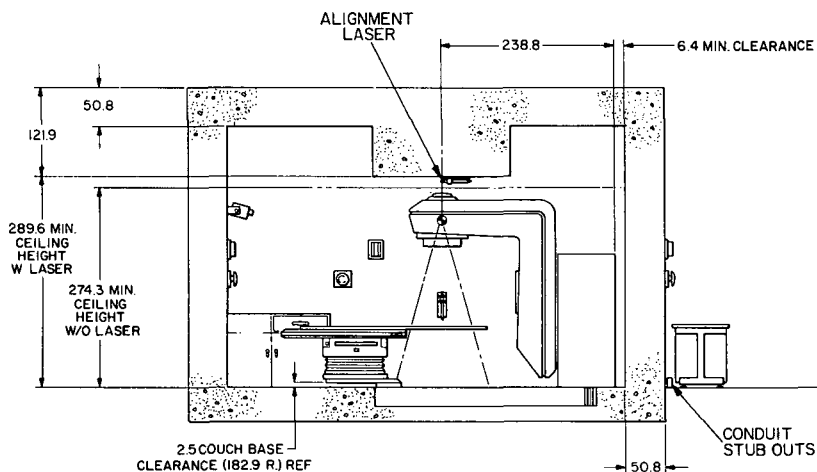
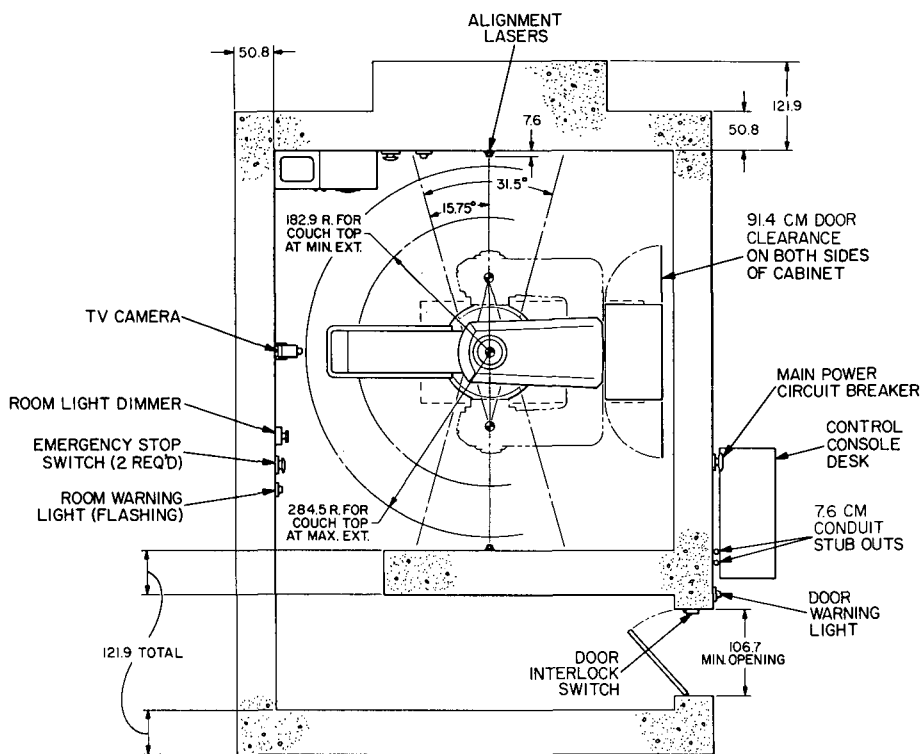


FIG. 57. Cutaway view of a frequently used clinical accelerator arrangement for rotational therapy. The dimensions shown are typical for a 4-MeV, $1000 \text{ Gy} \cdot \text{m}^2 \cdot \text{week}^{-1}$ ($100\,000 \text{ rad} \cdot \text{m}^2 \cdot \text{week}^{-1}$) installation. The lower therapy-unit member is a beam stopper which permits a reduction in primary barrier thickness. Without the beam stopper, the primary barriers (the ceiling and two 76 cm walls) would have to be augmented by about 85 cm of concrete or the equivalent of other materials (original data in inches). (Adapted with kind permission of Varian Associates.)

Reference [1] contains further information on the planning of new radiotherapeutic installations, and Ref.[2] is an international directory of existing facilities.

4.2. Industrial radiographic installations

Although industrial radiographic accelerators are now regarded as standard products (Table IV, Section 1.3), they are employed to inspect all sorts of objects. Therefore finished installations show considerable diversity, reflecting the users' needs and the physical accommodations available. For standard units, the installation plans provided by the manufacturer should be used directly, if possible, or adapted for the facility being planned. Because of their high output and the considerable variation in the nature of their settings, it is especially important that a qualified expert assist in planning such installations.



ALL DIMENSIONS IN CENTIMETRES

FIG. 58. Installation plan for a 4-MeV isocentric therapy unit without beam stopper, showing clearances, auxiliary equipment and typical barrier thicknesses (cm). Compact units of this type are often accommodated in rooms formerly used for ^{60}Co therapy. (Reproduced with kind permission of EMI Therapy Systems Inc.)

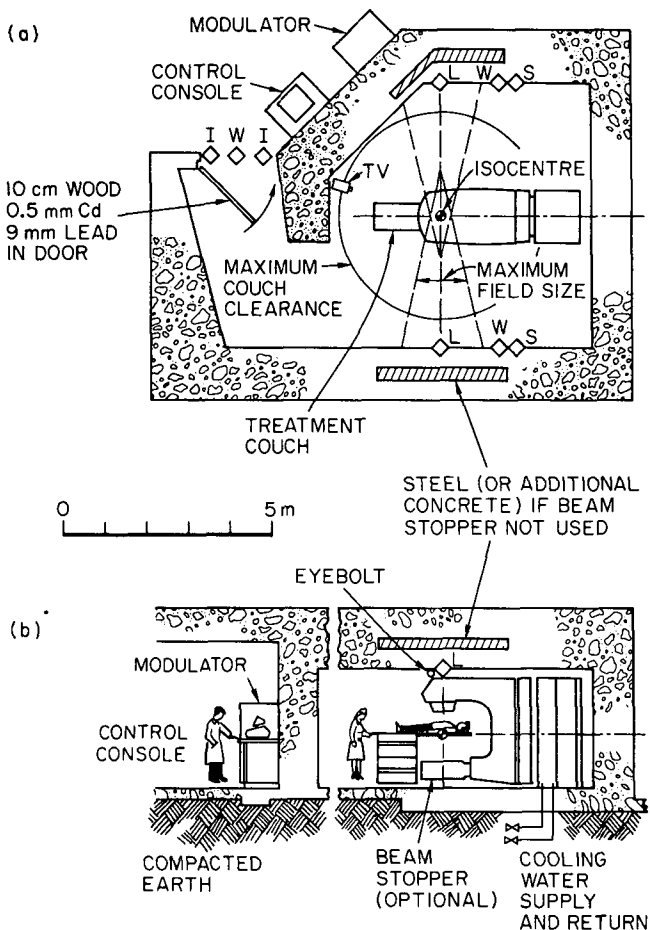


FIG.60. Corner layout of an 18-MeV isocentric therapy unit, designed for efficient space utilization. Note the use of iron plates in the primary barriers to reduce the necessary wall thickness if a beam stopper is not used. Because of the short labyrinth, the door must be made to attenuate neutrons and scattered photons adequately. The symbols L, W, S and I show the locations of alignment lasers, radiation warning lights, emergency cutoff switches and door interlock switches, respectively. The dimensions shown (metres) are only indicative. (Adapted with kind permission of Varian Associates.)

vis-a-vis the workpiece so that irradiation is either directed downward or against one or two 'target walls' only. The accelerator height and the beam direction are then restricted, preferably by limit switches, or by administrative control. In this arrangement, only one or two primary barriers are required; all others are secondary barriers.

In very large radiographic rooms, it is usually impractical to span the entire area with an adequately heavy concrete roof. In such cases it is necessary to control access to the roof and other spaces above the radiation barriers (locked or interlocked access). The possibility of radiological risk to radiation workers and the general public from skyshine should also be evaluated in such circumstances. In some cases an outside fence with interlocked gates is appropriate to delimit the controlled area.

Facilities to be planned in consultation with the manufacturer and architect include:

(a) Support for the accelerator unit (1–4 t, depending on the unit). A bridge crane with trunnion supported from an extensible mast is very well suited for larger accelerator units, and provision for limiting the direction of irradiation is readily made. For smaller units with reduced output, a forklift, pedestal or jib-crane mounting may be suitable. Of course a fixed mounting is most economical, but flexibility is severely limited.

(b) Where a labyrinth is not practical because of workpiece size, a large concrete door on rollers or air bearings is required. When closed, this door is a radiation barrier and must be interlocked. It should be fitted with sufficient overlap so that there are no cracks or openings through which radiation would stream.

(c) Crane, forklift, rails or other means of moving workpieces. Of course, the floor must be designed to bear the heaviest loads contemplated.

(d) Turntable, yokes, or roller supports to facilitate workpiece positioning may be needed.

(e) Public address system and an audible radiation warning device (bell or klaxon).

(f) Emergency shutoff switches and radiation warning lights prominently located in the radiographic room and at each entrance. One or more of the switches can be designed as a 'hazard/safe' switch, to be routinely used to disable the accelerator while personnel occupy the radiographic room.

(g) Electrical power connection (three phases at a rating of 10–50 kV · A, depending on the unit).

(h) Cooling water connection (10–50 ltr · min⁻¹, depending on the unit). Generally, domestic water is used for this, but in some localities a closed-loop system with a heat exchanger may be necessary.

(i) Provision for ventilation, if needed. Heat loads from the accelerator are 2–10 kW, depending on the unit.

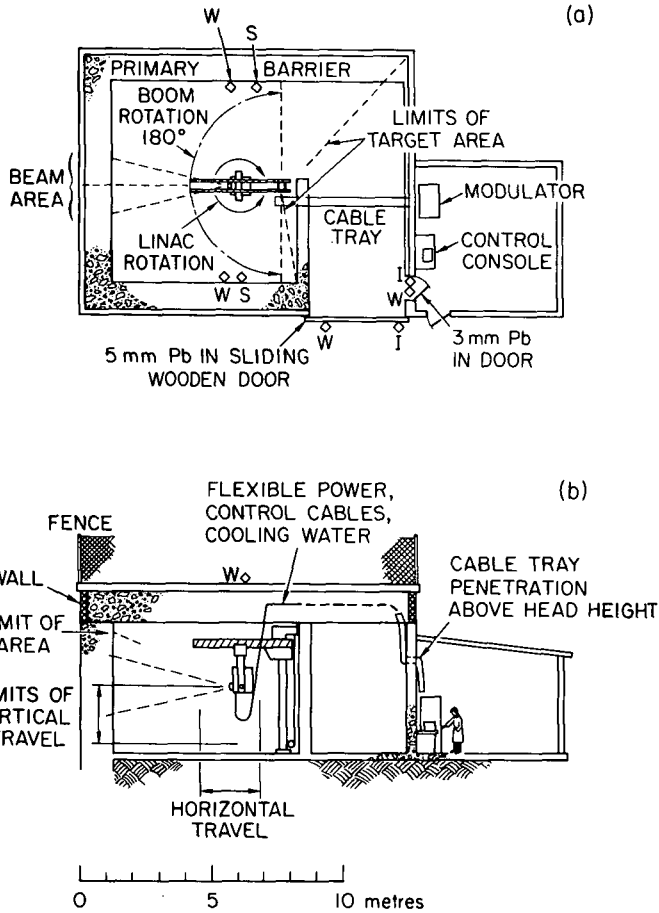


FIG. 61. Layout for a jib-crane-mounted, 2-MeV, $1 \times 10^{-3} \text{ m}^2 \cdot \text{C} \cdot \text{kg}^{-1} \cdot \text{s}^{-1}$ ($\approx 200 \text{ m}^2 \cdot \text{R} \cdot \text{min}^{-1}$) radiographic facility. Limit switches restrict the beam orientation to the area of the three primary barriers. W, S and I indicate the locations of radiation warning lights, emergency cutoff switches and door interlocks, respectively. The roof is designated as a 'high-radiation area' and is fenced and marked by signs and flashing radiation-warning lights. At ground level, the building itself delimits the controlled area. (Adapted with kind permission of Varian Associates.)

(j) In locating the facility, the possibility of RF interference to nearby equipment should be considered.

(k) Vacuum line and/or compressed air may be required.

(l) Support facilities, such as film processing equipment, film densitometer (to density H & D 4.0), film viewers.

(m) Supplies including penetrameters, film holders, lead markers, lead screens, lead sheets and bricks.

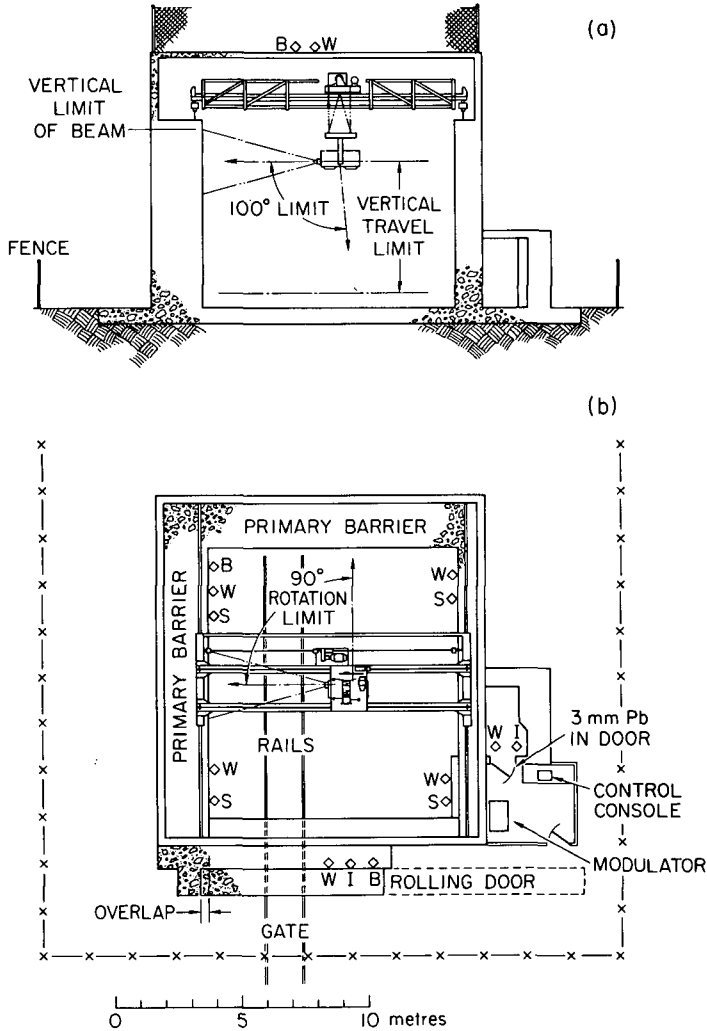


FIG. 62. Large installation for an 8-MeV, $1 \times 10^{-2} \text{ m}^2 \cdot \text{C} \cdot \text{kg}^{-1} \cdot \text{s}^{-1}$ ($\approx 2000 \text{ m}^2 \cdot \text{R} \cdot \text{min}^{-1}$) radiographic facility, illustrating the use of a bridge crane. (a) Elevation. (b) Plan view.

The useful beam can be directed towards either of two primary barriers; limit switches restrict the accelerator height and rotation, about two axes, to the area of these target walls. Note the railroad tracks and overlapping concrete door for workpiece access. The radiation barriers also serve as crane supports. The relatively thin roof is made part of the containment area, and the controlled area is delimited by a surrounding fence at ground level. The safety devices are labelled as follows: I – door interlock, W – warning light, S – emergency shutoff switch, B – audible warning. The scale shown is only indicative. The exact dimensions and the layout of the containment and controlled areas will vary and must be evaluated by a qualified expert for each installation, to ensure compliance with all legal requirements. (Adapted with kind permission of Varian Associates.)

Figures 61 and 62 illustrate typical industrial radiographic installations. The barrier thicknesses shown are only indicative. The exact barrier dimensions as well as the layout of the containment and controlled areas should be evaluated by a qualified radiation protection expert to ensure compliance with all legal requirements. (See Section 3 for methods of barrier calculation).

Reference [3] contains valuable discussions of radiological safety in industrial radiography, in a variety of applications.

4.3. Research and special-purpose installations

The type of facility included in the 'research' category ranges from small installations that resemble the standard clinical installations described in Section 4.1 to facilities capable of acceleration to energies above 20 GeV at hundreds of kilowatts of electron beam power. Special-purpose industrial accelerators, such as for food preservation or industrial radiation processing, are also included in this category. An impression of typical capabilities may be gained from Table V (Section 1.3), which summarizes parameters relevant to radiation protection. The median energy and electron beam power are about 50 MeV and 10 kW, respectively. As a majority of these installations are unique in design, it is essential that a qualified radiation protection expert with accelerator experience be consulted in the planning of the facility and whenever significant changes are contemplated. This consultation is additional to the radiation protection surveys required at certain times (Section 5.4). In addition to the layout of the radiation shielding, it is important to plan the system of safety interlocks, emergency shutoff switches and warning lights at an early stage so that adequate conduits are provided.

Some characteristics that distinguish a research accelerator facility from the installations discussed above are: uniqueness of design, high energy, high power, variability in types of setups and modes of operation, multiple experimental areas and a variety of secondary beam lines.

Because of their size and the problem of leakage of neutron radiation and skyshine, the site for a high-energy accelerator (above about 150 MeV) should be carefully chosen, preferably away from congested urban areas. The layout should be planned with a consideration for annual integrated doses at the site boundary and population doses to present and projected population groups. At larger accelerators, a fence delimiting the controlled area might be appropriate.

The higher energy and higher beam power both aggravate the radiological problems outlined in Section 2. (See Table VI, Section 2.1.1, for a checklist of the types of radiation to be anticipated at various combinations of energy and beam power.)

Because there is almost continual change at an active facility, allowance for flexibility should be made in the initial planning. For example, radiation barriers separating the experimental rooms from each other and from occupied areas can

be modularized so that revisions can be made easily. Adequate crane coverage should be provided for the moving of accelerator sections, shielding blocks, magnets and experimental set-ups. Reinforced floors of experimental halls should be adequate in area to allow flexibility in locating heavy equipment such as magnets and shielding blocks.

Adequate provision should be made for electrical power to equipment in experimental areas, with a view to future needs. An equivalent amount of cooling-water capacity must be provided to these locations. A closed-loop radioactive water system for the accelerator, beam dumps, targets and collimators is needed for high-power installations. This primary system should be separate from cooling-water circuits used for other purposes. The pipes and other components of the radioactive water system should be laid out or shielded to reduce personnel exposure (Section 2.7.2). Where practicable, it is advantageous to provide a separate primary cooling-water circuit for each separate radiation room, and to install the heat exchanger, piping, ballast tanks and other components entirely within that room. In this manner all of the radioactivity associated with a particular radiation facility is efficiently contained and controlled. Whether or not venting of gaseous releases from the water system to the containment area is permitted depends also on the amount of radiolytic hydrogen evolved [4] and on the ventilation rate for the radiation room (see Section 2.7.2). A catalytic gas recombination system [5] may be needed at high-power installations to remove the hydrogen/oxygen mixtures, so that gaseous releases within the containment area can be permitted without the risk of explosive mixtures being formed at any point.

In addition to their function of controlling water quality, demineralizers and oxygen removal elements³³ are useful in concentrating the radionuclides ^7Be and ^{15}O , respectively, and thereby reducing the amount of circulated activity³⁴.

A judicious choice of materials will result in reduced corrosion and therefore in reduced maintenance costs of the cooling-water system. For example, systems containing both aluminium and copper, as well as copper-bearing aluminium alloys, are prone to galvanic corrosion, whereas combinations of copper and stainless steel or aluminium and stainless steel are both satisfactory [6]. Low-carbon stainless alloys are preferred. For the highest reliability, columbium-(niobium-) stabilized alloys are recommended. Careful control of welding procedures is also advised; welding techniques in which an inert gas atmosphere is employed (TIG) will result in relatively corrosion-resistant joints.

³³ Oxygen removal elements are recommended for reducing corrosion in copper systems, for example, but dissolved oxygen actually reduces corrosion in systems of aluminium or stainless steel because it serves to maintain the protective inert oxide film needed by these materials.

³⁴ The concentration of ^7Be in demineralizers actually occurs by filtration, rather than by a chemical process. Therefore the same result could be achieved with ordinary filters. However, demineralizers are invariably needed anyway.

In locating equipment, consideration must be given to possible radiation damage, especially to electrical insulation. Cables should not be routed close to electron targets or beam dumps. Special insulation and connectors may be needed for wiring in regions of intense fields. (For example, ceramic or glass should be used in preference to organics. Special MgO- or Al₂O₃-loaded epoxies are available for magnet coil insulation.) Motors and pumps should be located where radiation is likely to be less intense. Wood should be avoided; it is not only combustible, it loses structural integrity if subjected to high radiation doses. It should be anticipated that glass will be darkened by radiation (e.g. light bulbs, mirrors, TV camera lenses, glass instrument faces).

At multiple-beam facilities where a beam may be transported to one experimental room while other rooms are occupied, careful planning should be made to prevent, by redundant means, an unwanted irradiation of the occupied areas. Examples of such means are interlocked, remotely insertable beam shutters, and power or polarity control of transport magnets by switches that can be locked. Radiation lockout ('hazard/safe') switches, as well as emergency shutoff switches should be provided within the containment area. Radiation area monitors should be installed in such rooms and interlocked so as to turn the accelerator off if the radiation rises to an unacceptable level. It is important that each interlock requires a reset at the location where a trip occurs before the accelerator can be turned on again at the control console.

Because of the size and complexity of the containment area at some installations, procedures for searching and entry control should be carefully developed. A 'captive key' system is a basic provision: The only available key to a portion of the containment area is also required at the control console for a beam to be delivered. In facilities involving more than one room, a 'plug bank' (or 'key bank') is advisable. This can be implemented in various ways, but it is basically a panel mounted near the entrance to the containment area containing a number of connectors wired in series. These are interlocked so that radiation can be delivered only if a complete set of matching devices (plugs) is inserted. Each person entering the containment area is required to remove a plug and keep it until he leaves³⁵.

A key bank is sometimes used in a more elaborate arrangement which combines features of the captive-key and plug-bank systems. It is advantageous only if the containment-area entrance is so far from the control console that the captive-key system is impractical. In this system, a key is electrically released from the key bank by the operator to each person desiring entry, but only after proper identification is made (via closed-circuit TV), and the person is logged in.

³⁵ Entry control may be facilitated if the plug is visibly attached to the bearer's clothing so that it can easily be checked that he is carrying one. It may also be helpful to assign an individual plug to each person frequently requiring entry, so that the operator can easily determine who has taken the missing plugs.

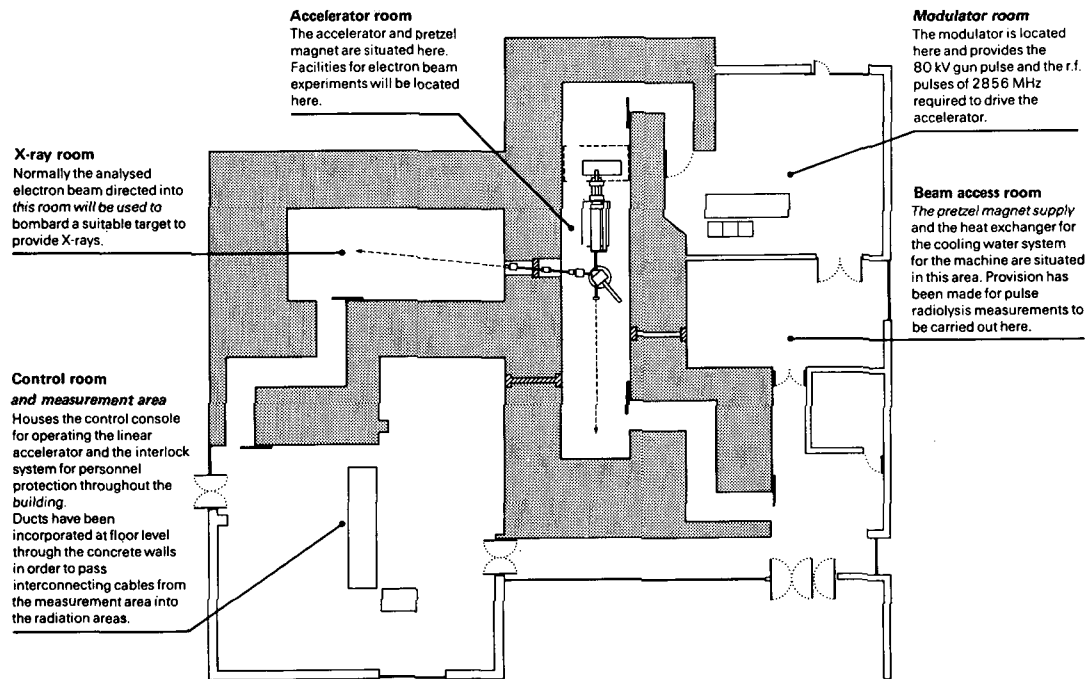
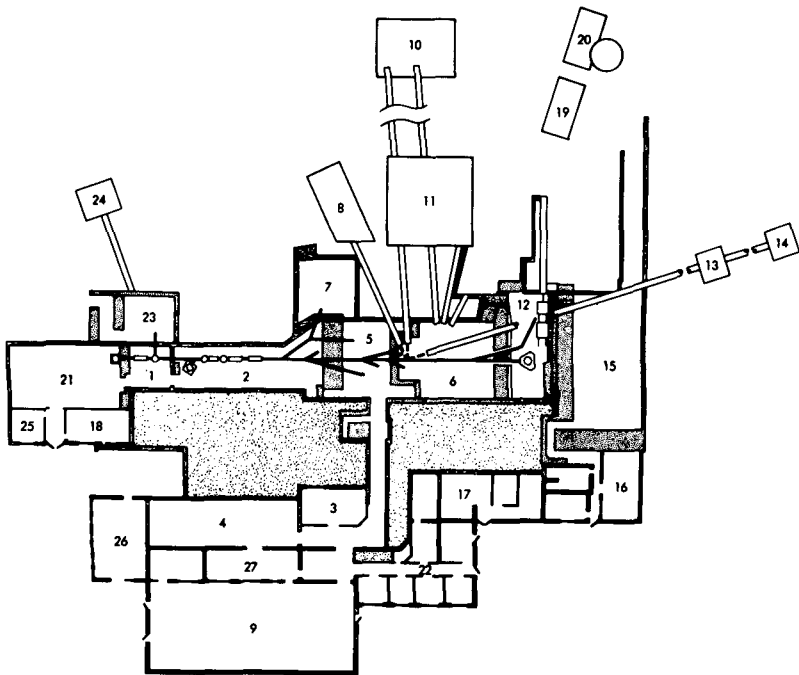


FIG. 63. Building plan for the 22-MeV, 8-kW electron linear accelerator of the National Physical Laboratory, London. The facility is intended mainly for the calibration of secondary-standard dose meters with bremsstrahlung beams between 2 and 12 MeV and electron beams up to 22 MeV. The $1\frac{1}{2}$ -storey building was specifically designed for this work and is entirely above ground. The concrete radiation barriers, shown as shaded areas, are generally 2.5 m thick (3.5 m in primary beam directions). Each radiation area is entered via a labyrinth. Direct access into the exposure rooms is provided for electrical cables through ducts at floor level, and two straight penetrations (normally closed by lead shutters) are provided at beam height for use during low average dose-rate conditions of pulse radiolysis measurements. The pretzel magnet (so called because it is designed to transport the electron beam through an orbit of $\sim 270^\circ$) directs the primary beam to the separate experimental set-ups. Continuous air conditioning provides ten changes per hour in both radiation rooms and exhausts the air at a height just above roof level. (Reproduced with kind permission of the National Physical Laboratory, London.)



- | | |
|--|--|
| <p>1. 25 MeV Accelerator
Pulse Radiolysis Facility
Dosimetry, Detector Calibration, and Radiation Effects Cell</p> <p>2. 75 MeV Accelerator
Accelerator Tuning and Isotope Production Cell</p> <p>3. 75/100 MeV Accelerator Control Room</p> <p>4. Data Acquisition and On-Line Computer Facility</p> <p>5. Radiation Effects Cell</p> <p>6. Neutron Targets Cell</p> <p>7. Electron Penetration Facility
Gamma Ray Penetration Facility
Positron Scattering Facility
Neutron Yield Measurement Cell
Single Electron-per-Pulse Cell
Detector Calibration Cell</p> <p>8. Scintillator Building
Neutron Capture Cross-Section Facility</p> <p>9. Vac Lab, Setup Room, Equipment Storage</p> <p>10. 50-Metre Building
Thermal, Intermediate and Fast Neutron Spectrum Station
Fast Neutron Cross-Section Cell
Neutron Inelastic Scattering Cross-Section Cell</p> | <p>11. 16-Metre Building
Thermal and Intermediate Neutron Spectrum
Thermal Neutron Total Cross-Section Cell
Thermal Neutron Scattering Cross-Section Cell</p> <p>12. Fast Reactor Spectral Test Facility
Split Bed Subcritical Assembly
Lattice Thermal Spectrum Cell</p> <p>13. 100-Metre Building
Fast Neutron Spectrum Station
Neutron Capture Cross-Section Cell</p> <p>14. 200-Metre Building
Fast Neutron Spectrum Station
Neutron Capture Cross-Section Cell</p> <p>15. CF Radiography Cell</p> <p>16. CF Applications Lab</p> <p>17. Chem Lab</p> <p>18. 25-MeV Control and Data Acquisition Room</p> <p>19. CF Control Station</p> <p>20. CF Storage Tower</p> <p>21. Accelerator Modulator Room</p> <p>22. Offices</p> <p>23. Radiation Processing Cell</p> <p>24. Neutron Detector Building</p> <p>25. Data Acquisition Room</p> <p>26. Machine Shop</p> <p>27. Technician Shop</p> |
|--|--|

The released key is used to open the door and is kept by that person until he leaves and is logged out.

In addition to these provisions, a system of 'inspection switches' may be advisable. This is a system of switches that must be manually actuated in a predetermined order, to ensure that all parts of a radiation room are visited during the search. The entrances to the portion of the containment area being searched should be locked so that no one can enter unnoticed after a search has been begun.

Two types of audible warnings are important: A public address system or horn should be used to warn of imminent accelerator turn-on, and a continuously sounding signal should come on at the same time as the accelerator to indicate that radiation is being produced. At single-room facilities, the 'electrical' hum made by the equipment itself may serve this function.

Although the amounts of activated solids, as measured by volume or by total activity, are not large, some provision must be made for their storage and disposal. However, remote-handling equipment is generally not required at electron accelerators. Most maintenance work on activated components can be done with ordinary tools. In some cases the use of such implements as tongs or wrench extenders is indicated to reduce exposures.

Physical planning must provide for such areas as the accelerator vault, pump stations, klystron housing, klystron modulator room, central control room, power supply housing, transformer vault, power distribution centre, heat-exchanger area(s), cooling tower(s), exhaust stack, loading dock with access to radiation room(s) via a large door, crane, utility trenches, and areas for counting equipment and equipment storage. Support facilities might typically include an electronics shop, machine shop, chemistry laboratory, cryogenics laboratory, computation facilities, staging area for future experiments, photographic darkroom, office space and conference area. Auxiliary facilities might include a rotatable carriage

Text continued on p.224

FIG. 64. Plan of the 100-MeV, 35-kW linear accelerator facility of IRT in San Diego. This facility contains two in-line accelerators which can be operated independently (up to 25 and 75 MeV, respectively) or in tandem (up to 100 MeV). Wide variability in energy, pulse width, repetition rate and the arrangement of radiation rooms allow a great deal of experimental flexibility. The principal uses are for nuclear physics research, product sterilization (medical disposables) and radiation processing (e.g. semiconductors). The tubes extending from the main building are for neutron time-of-flight measurements. In addition to the concrete shielding barriers shown (dark shading), the accelerator housing and adjacent radiation rooms are beneath about 15 ft (4.5 m) of earth. The central areas of lighter shading are earth embankments which protect the occupied areas. Separate closed-loop cooling water is provided for each radiation room and the air is exhausted continuously by ventilators just above the earth shielding berm (5–7 air changes per hour). The facility is situated within a fenced enclosure on spacious grounds at the edge of a canyon. (Reproduced with kind permission of IRT Corporation.)



FIG. 65a. The Livermore Electron Linac, a 180-MeV, 45-kW facility situated underground to enhance radiation protection. Above-ground facility. The above-ground buildings include a central office/laboratory, modulator building (right), machine shop, storage building and small detector buildings. The cylindrical building is the neutron 'silo' from which neutron time-of-flight paths (15, 66 and 250 m) radiate. The controlled area is circumscribed by the building complex and a fence (rear). Note earth-mound beam stops at the ends of long flight paths. The stack is 30 m high. Cooling-water pumps and heat exchangers are located in a fenced enclosure near the silo.

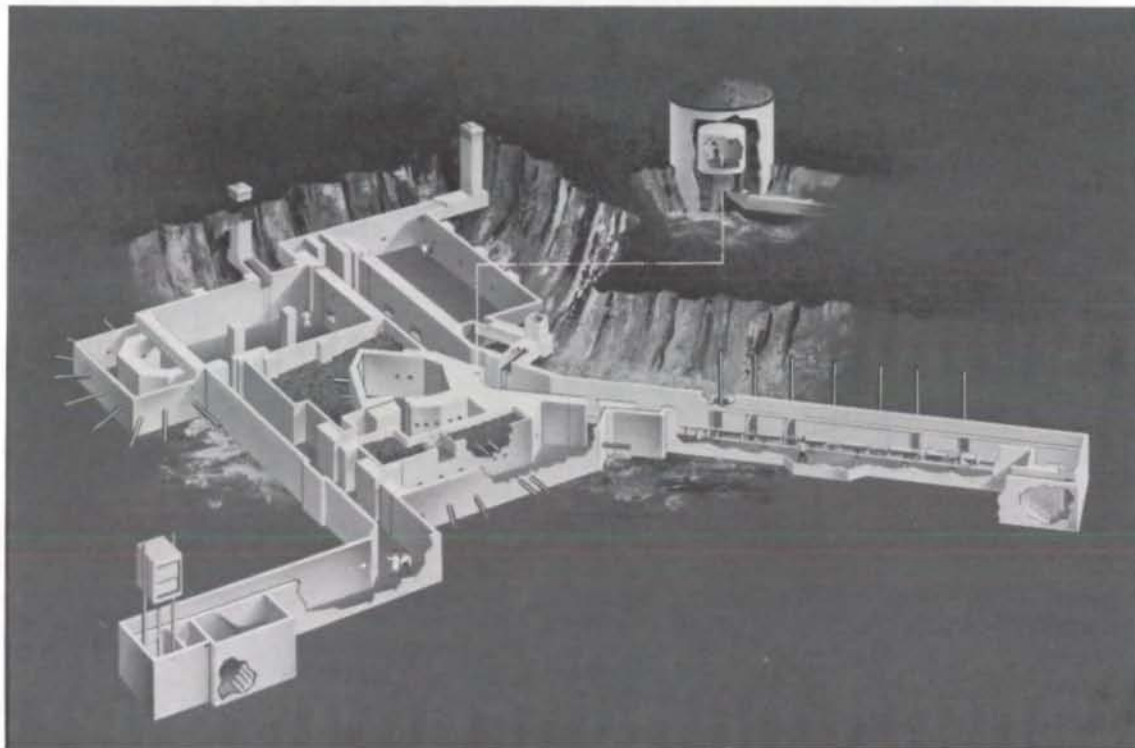


FIG. 65b. The Livermore Electron Linac, a 180-MeV, 45-kW facility situated underground to enhance radiation protection. Underground cave complex. The linac tunnel is at the right, with beams travelling to the left. Electron beams may be transported to three different experimental caves, or upwards to the silo. Secondary beams of neutrons and quasi-monoenergetic photons are available. At the bottom left is an entrance module with a 6000 lb (2700 kg) equipment elevator. A $3 \times 6 \text{ m}^2$ hatch is also provided for large equipment access. The vertical rectangular penetrations are emergency escape hatches. Continuous ventilation exhausts the air from the underground complex via stack (air change time is normally 6 min; for purge before entry, 3 min).

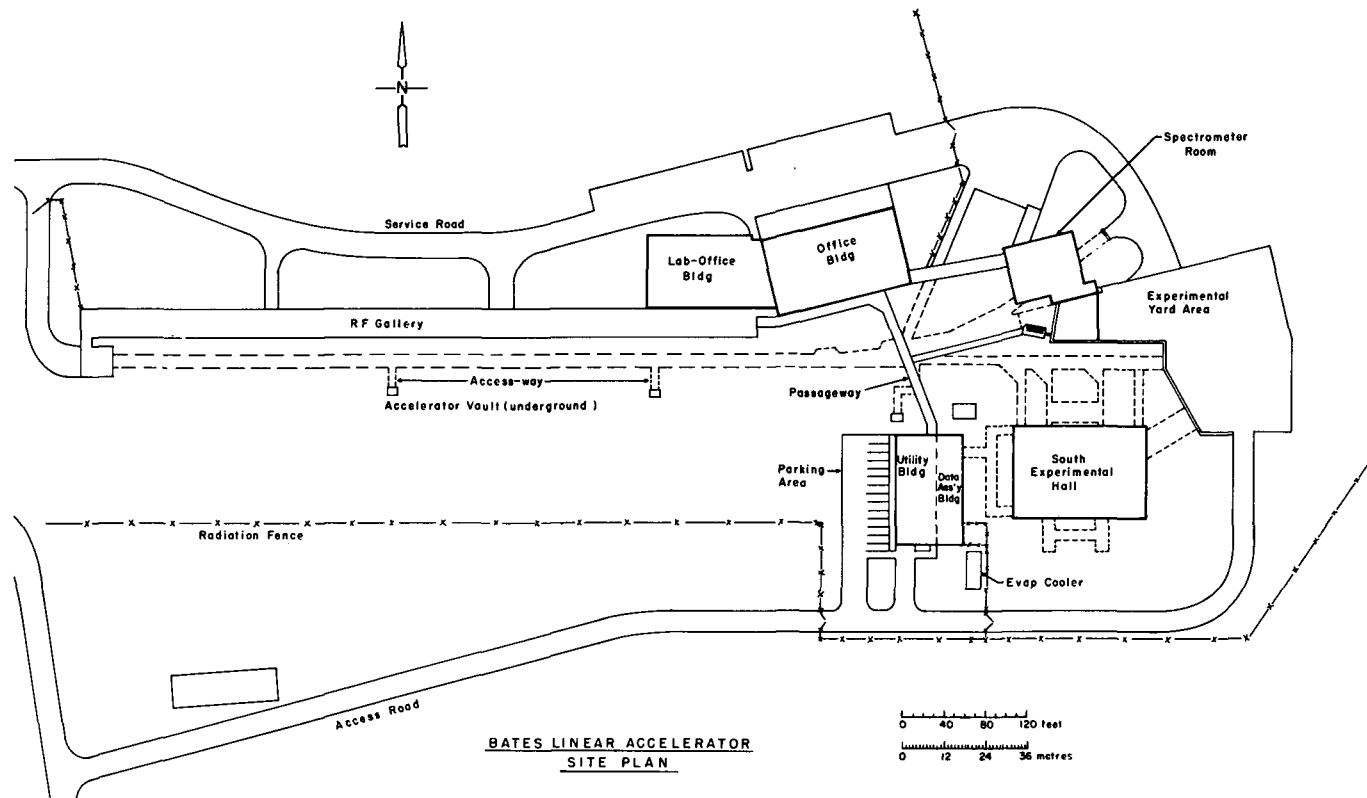


FIG. 66a. Layout of the 400-MeV, 60-kW Bates Linear Accelerator at Massachusetts Institute of Technology. Site plan showing the RF gallery and accelerator vault in relation to the buildings clustered around the experimental area. The vault has 18 in (46 cm) thick concrete walls and ceiling and is 12 ft (3.7 m) underground. The containment area includes the vault, spectrometer room and the south experimental hall. Note the radiation fence delimiting the controlled area to the south and east.

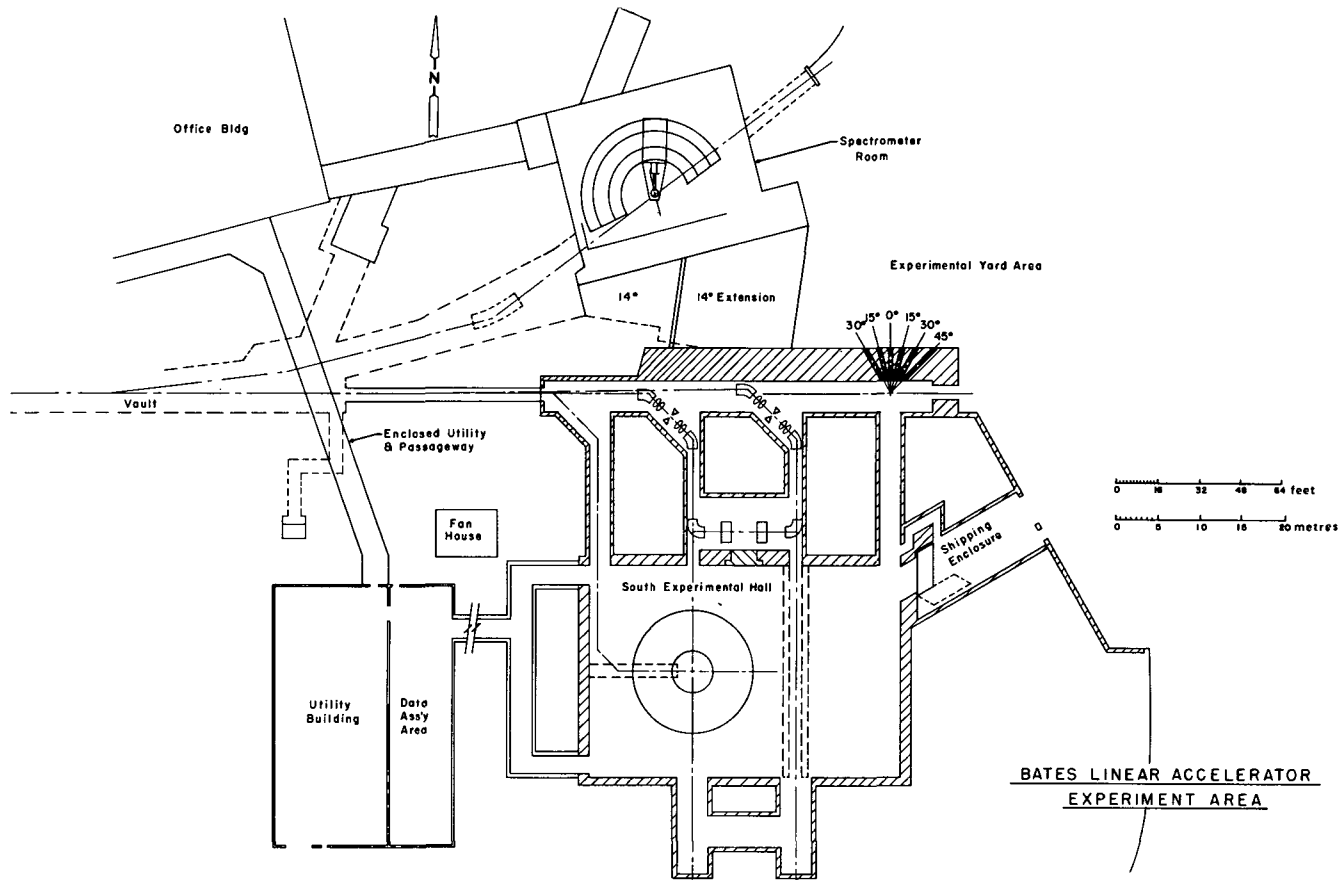


FIG. 66b. Layout of the 400-MeV, 60-kW Bates Linear Accelerator at Massachusetts Institute of Technology. Experimental area. The spectrometer room contains facilities for high-resolution electron scattering experiments on a rotatable carriage. The south experimental hall is designed for maximum flexibility. Note the provisional locations of beam transport magnets and facilities for irradiation and scattering experiments along either of three beam lines. The interior of the hall is 45 ft (13.7 m) high, and the maximum crane hook height is 36 ft (11 m). The ceiling is 5 ft (1.5 m) concrete. The hall is recessed into the hillside so that the walls are backed by earth to the roof on three sides. A utility tunnel extends from the utility building to the west wall of the hall. Water and power connections are provided along north and south walls. A large 6 ft (1.8 m) thick concrete swinging door is provided at the shipping enclosure for equipment access. The adjacent experimental yard area is covered by a 6-in (15-cm) concrete pad to support equipment and is left open for future development. Exhaust air from the accelerator vault, spectrometer room and experimental hall is vented through a 50-ft (15-m) stack located at the fan house.

(gun mount) to support experimental equipment, a pneumatic 'rabbit system', and compressed air and vacuum lines.

Exits from accelerator and radiation rooms should be designed to permit immediate egress at all times, regardless of accelerator status. Larger rooms should have two (or more) well-separated and well-marked exits, in case one is blocked by a fire or other emergency condition. (However, for better access control, only one of these should be routinely used as an entrance, unless operational needs dictate otherwise.) All doors are interlocked, of course.

At high-power installations, continuous ventilation of parts of the containment area may or may not be desired, depending on the amounts of activated air and water, radiolytic hydrogen (Section 2.7) and toxic gases formed (Section 2.10), as well as on heat load and access requirements. In addition to personnel safety, the effect of these reactive gases on equipment and materials irradiated should be considered. Where accelerators are used for food preservation, rapid removal of ozone has been found to be essential, to avoid product damage. The amount of radioactive and toxic gas may be minimized by reducing the amount of stray radiation in the air. Minimizing the air pathlength of straight-ahead beams is an obvious provision. In addition, lead shielding 'collars' around beam pipes at both ends of each deflecting magnet and at collimators and other beam restrictions are helpful in reducing stray radiation.

If ventilation of radioactive or toxic gases in significant amounts is anticipated, provision for an adequate exhaust should be made. This may be in the form of an exhaust stack extending, in some cases, as high as 20–30 m. The required height of the stack will depend on the amount of activity released, the distance to the site boundary, and prevailing meteorological conditions [7]. There is a trade-off between venting speed and stack height; the maximum necessary height at a given activity production rate corresponds to 'immediate' venting of the contaminated air. On the other hand, the stack height may be considerably reduced if most of the activity is contained long enough to decay before venting takes place. Some installations have a two-speed ventilation system: a low ventilation rate to maintain negative pressure and remove the heat load in the radiation rooms, and a high-speed system to purge the area just before personnel entry. Some facilities do not ventilate at all until entry is imminent.

The air conditioning and venting system should be designed to promote good air mixing in the radiation areas. Separate air conditioning should be planned for occupied areas of the facility, where required for personnel comfort or proper equipment operation.

In Figs 63–66, illustrations of selected research accelerator installations are given. Physical considerations in the planning of the Stanford Two-Mile Accelerator are extensively described in Ref.[8]. Examples of radiation safety procedures at research electron linacs can be found in Refs [9–12]. Addresses of over sixty research and special-purpose accelerator installations can be found in Ref.[13].

REFERENCES TO SECTION 4

- [1] WORLD HEALTH ORGANIZATION, Planning of Radiotherapy Facilities, Tech. Rep. Ser. No.328, WHO, Geneva (1966).
- [2] INTERNATIONAL ATOMIC ENERGY AGENCY, Directory of High-Energy Radiotherapy Centres, 1976 ed., IAEA, Vienna (1976).
- [3] UNITED STATES DEPARTMENT OF HEALTH, EDUCATION AND WELFARE, Radiation Safety and Protection in Industrial Applications (Proc. Symp. Washington, DC, 1972), US Dept. of Health, Education and Welfare, Publ. (FDA) 73-8012, BRH/DEP 73-3 (1972).
- [4] WALZ, D.R., Radiolysis and Hydrogen Evolution in the A-Beam Dump Radioactive Water System, Stanford Linear Accelerator Center, Rep. SLAC-TN-67-29 (1967).
- [5] WALZ, D.R., LUCAS, L.R., The "sphere dump" - a new low-cost, high-power beam dump concept and a catalytic hydrogen-oxygen recombiner for radioactive water systems, IEEE Trans. Nucl. Sci. NS-16 3 (1969) 613; Stanford Linear Accelerator Center, Rep. SLAC-PUB-555 (1969).
- [6] WALZ, D.R., Corrosion in an Aluminum-Stainless Steel System, Stanford Linear Accelerator Center, Rep. SLAC-TN-64-17 (1964).
- [7] See, for example, discussions in Meteorology and Atomic Energy 1968 (SLADE, D.H., Ed.), Atomic Energy Commission, Div. Tech. Inf., Rep. TID-24190 (1968). (Available from Clearinghouse for Federal Scientific and Technical Information, Springfield, VA.)
- [8] NEAL, R.B., Gen. Ed., DUPEN, D.W., HOGG, H.A., LOEW, G.A., Eds, The Stanford Two-Mile Accelerator, Benjamin, New York (1968).
- [9] NATIONAL BUREAU OF STANDARDS, NBS Radiation Safety Manual, Internal Report, US Department of Commerce, National Bureau of Standards, Health Physics Section, Washington, DC (1974).
- [10] STANFORD LINEAR ACCELERATOR CENTER, Radiation Rule Book, SLAC Internal Report (updated periodically).
- [11] LAWRENCE LIVERMORE LABORATORY, Operational Safety Procedures, Building 194 General Operations, Lawrence Livermore Laboratory (Sep.1976).
- [12] IRT CORPORATION, IRT Radiological Safety Regulations, Rep. INTEL-RT-4241-004, IRT Corp., San Diego, CA (1975).
- [13] SWANSON, W.P., Addresses of Electron Linear Accelerators Used in Research, Internal Report, Stanford Linear Accelerator Center (in preparation, 1977).

5. RADIATION MONITORING AND INTERPRETATION OF MEASUREMENTS

5.1. Characteristics and choice of monitoring equipment

It is advisable to utilize several different, independent monitoring methods rather than to rely on a single one. This becomes increasingly important as the energy and complexity of operations increase. For example, the portable survey meter will detect radiation areas for which a fixed integrating monitor (film or TLD) may be incorrectly positioned. Area monitors can detect time-varying behaviour missed by a periodic or occasional survey. Redundancy is helpful in detecting inconsistencies in data and malfunctioning equipment.

The measurement of photon radiations (from bremsstrahlung or induced activity) at the levels normally encountered in broad areas is generally straightforward with standard instruments. On the other hand, measurements in beam lines require particular techniques and understanding of beam geometry, buildup, and instrument capabilities.

Radiation due to induced activity can be measured with Geiger-Müller (GM) counters, scintillation counters or ionization chambers, depending on the types of radiation.

Neutron monitoring is much more complicated and has no single complete instrumental solution. Because of its complexities, it should be done with the help of an expert.

Basic information on dosimetry systems may be found in Refs [1–8]. Discussions which illuminate the application of radiation protection instrumentation at particle accelerators are found in Ref. [9]. Articles which review the recent status of accelerator radiation protection instrumentation are found in Refs [10, 11]. Material of an advisory nature which treats instrumentation, calibration and monitoring methods is given in Refs [12–21].

Table XLIV contains recommendations for minimum instrumentation for electron linear accelerators, as a function of accelerator energy and average beam power. It is emphasized that this list reflects the *minimum* needs for safe operation of the facility. Many low-energy installations can safely operate with only a personnel dosimetry system (including pocket ion chambers) which doubles as an integrating area monitoring system, and an ion-chamber survey meter. If the energy exceeds 10 MeV (preferably 6 MeV), a permanently available GM counter should be included. There should always be provision for occasional use of backup instrumentation. Comparative discussions of radiation protection instruments may be found, for example, in Refs [22, 23].

It is interesting to compare this list with the results of a survey by Freytag and Nachtigall [24], in which dosimetry systems used at several types of particle

TABLE XLIV. MINIMUM RECOMMENDED MONITORING EQUIPMENT

Type of Instrument	Always Available or Permanently in Use	For Periodic Surveys or Occasional Use (Loan)
Film or TLD personnel dosimetry system	All installations	—
Film or TLD area monitors	All installations	—
Pocket ion-chamber dose meters	All installations	—
Ion-chamber survey meter (regular window)	All installations	A second instrument should be available for loan.
Ionization-chamber survey meter (thin window)	Wherever low-energy ^a X-ray sources are in use and accessible	If indicated, a second instrument should be available for loan.
Ion-chamber area monitors	Installations with complex or changing operations, especially industrial and research facilities.	—
GM or scintillation counter (portable)	$E_0 > 10 \text{ MeV}$	$E_0 > 10 \text{ MeV}$
GM or scintillation counter for evaluation of smears (laboratory)	$E_0 > 20 \text{ MeV}$, $P > 5 \text{ kW}$	$E_0 > 20 \text{ MeV}$
Moderated BF_3 or equivalent	$E_0 > 10 \text{ MeV}$, $P > 5 \text{ kW}$ $E_0 > 150 \text{ MeV}$: all	$E_0 > 10 \text{ MeV}$
Equipment for neutron spectrum measurements	—	Not normally necessary but may be useful for $E_0 > 150 \text{ MeV}$.
Pulse-height analysis equipment	—	Not normally necessary but may be useful at research installations.

^a Examples are: Exposed klystrons, RF particle separators, RF cavities, and, of course, diagnostic X-ray facilities used in connection with therapy installations.

accelerators are compared. The great variety of dosimetry systems is illustrated by this survey (Table XLV), in which the ranking roughly reflects the 'value' of the method; those at the top of the list are nearly universal and those near the bottom are quite limited in use. This compilation mainly reflects practices found at research laboratories.

TABLE XLV. DOSIMETRY SYSTEMS USED AT PARTICLE-ACCELERATOR INSTALLATIONS^(a)

	Field Dosimetry	Personnel Dosimetry
1	Ionization chamber for photons (not CO ₂ or TE)	
2		Films for photons
3		Gamma pocket ion chambers
4		Films for neutrons
5	Films for photons	
6	Films for neutrons	
7	Moderator techniques: neutrons	
8	GM tubes for photons	
9	BF ₃ tubes for thermal neutrons	
10	TLD for photons	
11	TE ionization chambers	
12		TLD for photons
13	Integration systems for photons	
14	Activation: In foils for neutrons	
15	Integration systems for neutrons	
16	Activation: Al(n,α) ²⁴ Na for neutrons	
17	Activation: All except In, S, P, Hg, Au, Al	
18	BF ₃ long counter plus spectral information or assumptions	
19	Scintillation counters: photons	
20	Activation: S for neutrons	
21	Activation: Al(n,) ²² Na	
22	Fission tracks: neutrons	
23	Scintillation counters: neutrons	
24	Proportional counters: neutrons	
25		Emergency dosimeter
26	Phosphate glass: photons	
27	Activation: Au(n,) ¹⁴⁹ Tb for neutrons	
28	Activation: Hg(n,) ¹⁴⁹ Tb for neutrons	
29	LET spectrometry for neutrons	
30	Moyer counter: neutrons	
31		Activation: Various for neutrons
32	Dennis-Loosemore counter: neutrons	
33	Activation: P for neutrons	

TABLE XLV. (cont.)

	Field Dosimetry	Personnel Dosimetry
34	Thorium fission chamber: neutrons	
35	Proportional chamber: neutrons (except Moyer, Dennis-Loosemore, He)	
36	Ionization chamber: CO ₂	
37	Gas recombination technique for Quality Factor determination	
38	Bismuth fission chamber: neutrons	
39		Phosphate glass: photons
40	Chemical dosimeters: various	
41	Helium counter: neutrons	
42	Liquid dielectricum recombination for Quality Factor determination	

(a) Table adapted from Ref. [23], with kind permission of E. Freytag and D. Nachtigall and the Deutsches Elektronen-Synchrotron.

The application of instruments recommended in Table XLIV at electron accelerators is briefly described.

(a) Personnel dosimetry

In organizations where there are several types of radiation sources, such as a clinic containing nuclear medicine and radiology, or a large research laboratory, a film personnel dosimetry system [12, 13, 21, 22, 25] would be suitable. The strong photon-energy dependence of photographic film, together with the use of a combination of filters incorporated into the holder, affords information for differentiation and analysis of the type and manner of exposure. Some disadvantages of films are their sensitivity to temperature and humidity, and the fading of latent images.

On the other hand, at an installation where there is essentially one kind of source, for instance only radiations produced by high-energy electron beams, thermoluminescent dose meters (TLDs) [26–34] may be more economical. The response of TLDs is nearly independent of photon energy and linear over a wide range of integrated doses. TLDs are capable of greater accuracy than films. Neutron exposures may be estimated by a combination of ⁶LiF and ⁷LiF detectors, if appropriate.

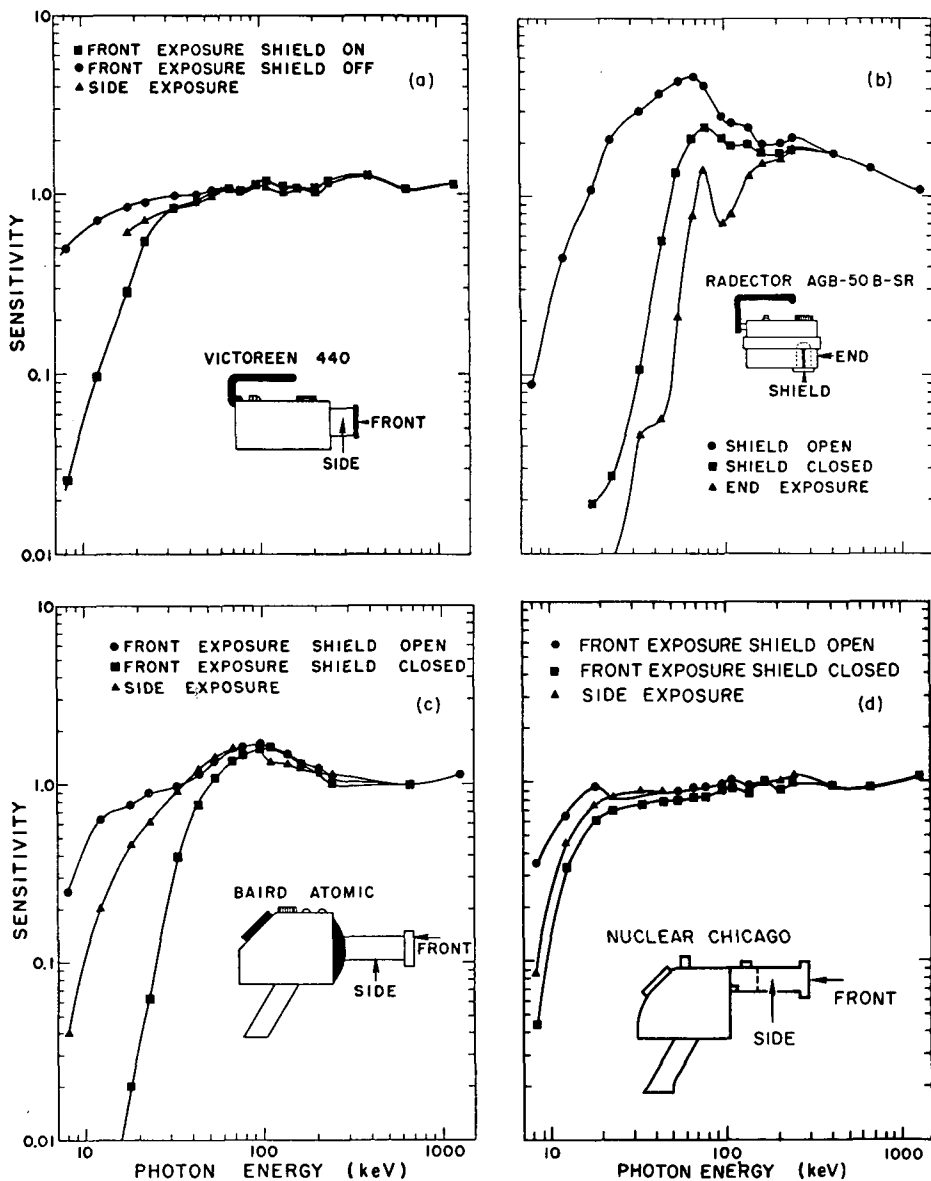


FIG.67. Photon energy response of representative ionization-chamber survey meters. (a) Air-filled chamber with thin window ($3 \text{ mg} \cdot \text{cm}^{-2}$ mylar) having good low-energy sensitivity. (b) Pressurized (10 atm), argon-filled chamber with a logarithmic scale, useful over a wide range of exposure rates. The peaking near 70 keV is characteristic of the argon filling. Models are available having windows of $20 \text{ mg} \cdot \text{cm}^{-2}$ stainless steel and $13.7 \text{ mg} \cdot \text{cm}^{-2}$ aluminium. (c, d) Examples of ambient-pressure air-filled chambers for general use (Cutie Pie). (Adapted from Ref.[41], with kind permission of B.J. Krohn, W.B. Chambers and E. Storm, and the Los Alamos Scientific Laboratory.)

The type of detector used in the personnel dosimetry system is normally also used for integrating area monitors. Personnel dose meters should usually be evaluated at monthly intervals, and a 'background' reading, obtained from a sample of dose meters reserved as a control, subtracted.

Pocket ionization chamber dose meters are recommended for daily assessment of doses to personnel. They are economical, easily checked and reset, and straightforward for untrained personnel to use and interpret [22, 35].

(b) Ionization chamber survey meter

The portable ionization chamber survey meter [8, 22, 23, 35–40] is essential in the radiation survey of all linac installations, regardless of energy. Its sensitivity to photons of a wide energy range makes its interpretation in terms of photon dose equivalent straightforward. It can be considered as a practically complete instrument for this purpose. The energy response of representative instruments is shown in Fig.67 (Ref. [41]).

Survey meters are also useful in assessing induced activity in targets, beam dumps and any object struck by the electron or bremsstrahlung beam. If the radionuclides produced are dominated by γ or β^+ emitters, the instrument will provide a straightforward assessment. In case β^- or α particles predominate, a thin window is required to allow penetration of the particles into the ion chamber. If β^- or α radiations are anticipated or suspected, it is best to have a second instrument with a thin window ($1-2 \text{ mg}\cdot\text{cm}^{-2}$). To assess external exposure from these particles, a correction is generally needed, depending on the energy of the emissions and the geometry of the measurement. Since these activities are generally diffusely embedded solid components and their radiations limited in range (2-8 cm air for α , at most a few $\text{g}\cdot\text{cm}^{-2}$ for β^- , depending on energy), they are usually a minor hazard compared with the γ and β^+ emitters, and generally may be neglected.³⁶

At installations where X-rays from klystrons or vacuum RF cavities may be hazardous, it is recommended that an instrument be available which is sensitive at lower photon energies (down to about 20 keV).

Particularly at high-energy research installations (above 150 MeV), it is advantageous to use a survey instrument sensitive to neutrons, unless other instrumentation for neutron measurements is available. If we consider only absorbed dose (Gy, rad), this requirement is automatically fulfilled if the walls and filling gas are exactly tissue equivalent. Instruments advertised as 'tissue equivalent', employing organic materials, are superior to those filled with air. If it is suspected that the neutron-imparted dose equivalent H dominates the radiation field at a

³⁶ The contribution of β^- to the total dose at the surface of typical activated accelerator components is less than 15% [42]. At greater distances the relative contribution is even less.

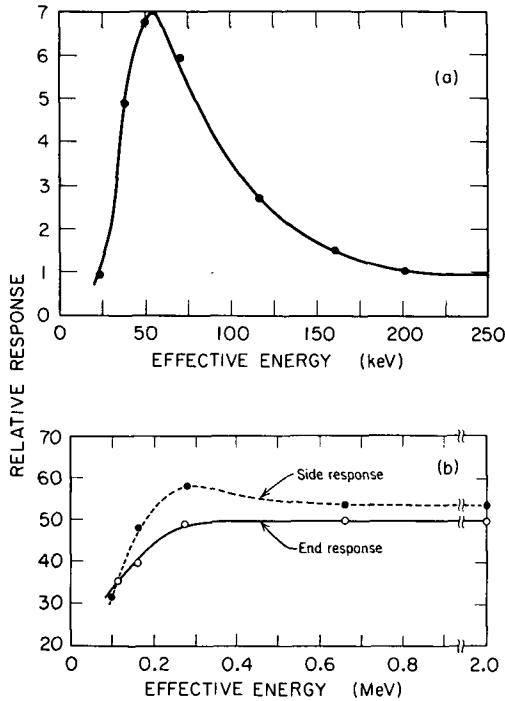


FIG. 68. (a) Energy response of a bare Geiger-Müller counter (typical).

(b) Energy response of a shielded Geiger-Müller counter (typical).

(Adapted from Ref. [4], with kind permission of K.Z. Morgan, J.E. Turner and G.S. Hurst, and John Wiley, New York.)

given location, a conservative estimate of the true H (in rem) can be obtained by multiplying the instrument reading in röntgen or rad by 10, corresponding to the maximum recommended quality factor for neutrons (Table XI, Fig. 22, Section 2.5).

Where a *significant* fraction of the dose equivalent is imparted by neutrons, special survey equipment is essential.

Desirable characteristics of the portable ionization chamber survey meter are:

- (a) Portable, rugged, hand-held and battery operated;
- (b) Range $0.2 \mu\text{C} \cdot \text{kg}^{-1} \cdot \text{h}^{-1}$ to around $1 \text{ mC} \cdot \text{kg}^{-1} \cdot \text{h}^{-1}$ (1 mR/h to several R/h);
- (c) A photon-energy dependence close to that of air or tissue (air or organic gas filling, walls of tissue-equivalent, air-equivalent or other low-Z material);
- (d) Capability of operating in the magnetic fields encountered at the particular facility, if any;

- (e) Capability of operating in microwave RF fields likely to be encountered (klystrons);
- (f) Provision for windows of more than one thickness may be desirable.

Most of the several varieties on the market easily meet these requirements, and a selection can be made on the basis of general quality of manufacture, convenience in operation, and price.

The type of instrument described in this section is *not* designed for calibrating the useful beam of a therapeutic facility, and must not be used for that purpose.

(c) Area monitor

Area monitors are useful where there are time-varying radiation fields, for example, where a change of the accelerator pulse rate, current or beam orientation may produce excessive dose-equivalent rates in accessible areas. An important application is at installations where more than one radiation room is employed; an area monitor in an occupied room will afford additional safety while the beam is delivered elsewhere. These instruments are ionization chamber detectors provided with a connection for remote readout at the main control console, with an audible alarm, and fail-safe relay contacts for an automatic accelerator-shutoff circuit. A self-checking provision is recommended for sensitive applications; a small ionization chamber current produced by an internal radioactive source is required for an accelerator 'permissive'. Where neutrons may be produced, it is desirable that the area monitor be sensitive to neutrons as well as photons.

(d) Geiger-Müller counter

Next to the portable gamma survey meter, the Geiger-Müller (GM) counter is of the greatest all-around utility [22, 23, 37, 43–45]. There are various configurations of this instrument, but the most useful is a portable, battery-operated unit. Its greatest utility is in the *detection* of radiation, rather than its measurement. The audible signal is of great help in searching for radioactivity. At industrial and research installations it is useful for routine surveys of offices and shops, to detect misplaced or unauthorized radioactive materials. It is useful in assessing the degree of radioactivity of targets and beam dumps and all objects struck by the primary electron beam or bremsstrahlung beam. At hospitals with nuclear medicine departments its uses are obvious. A typical GM tube is two orders of magnitude more sensitive than a regular ionization chamber survey meter in this application.

When used to *measure* (rather than detect), the GM counter has limitations which make it incapable of great accuracy, except in restricted applications. First, it has a strong photon energy dependence (Fig.68) compared with an ionization chamber. Second, it must be borne in mind that the duty factor of an operating

linac will usually severely affect the apparent count rate. Some GM counters are known to cease working in high instantaneous fields, giving apparently 'safe' readings. Recalling that the dead time T_D of a GM device³⁷ is of the order of 100–200 μ s, and the radiation pulse length T_p is only of the order of 1 μ s (Table V, Section 1.3), it is clear that not more than one 'event' per pulse can be registered. If the count rate approaches a fraction of the accelerator pulse rate, counts will be lost and must be corrected for (Section 5.2).

REFERENCES TO SECTION 5.1

- [1] ATTIX, F.H., ROESCH, W.C., TOCHILIN, E., Eds, Radiation Dosimetry, 2nd ed. (in three volumes: Vol.I: Fundamentals; Vol.II: Instrumentation; Vol.III: Sources, Fields, Measurements and Applications), Academic Press, New York (1968, 1966, 1969).
- [2] ATTIX, F.H., Ed., Topics in Radiation Dosimetry, Supplement 1 to Radiation Dosimetry, Academic Press, New York (1972).
- [3] FENYVES, E., HAIMAN, O., The Physical Principles of Nuclear Radiation Measurements, Academic Press, New York (1969); Die Physikalischen Grundlagen der Kernstrahlungsmessungen, Akadémiai Kiadó, Budapest (1969).
- [4] MORGAN, K.Z., TURNER, J.E., Eds, Principles of Radiation Protection, Ch. 4–7, John Wiley, New York (1967).
- [5] HINE, G.J., BROWNELL, G.L., Eds, Radiation Dosimetry, Academic Press, New York (1956).
- [6] PRICE, W.J., Nuclear Radiation Detection, McGraw-Hill, New York (1958).
- [7] HANDLOSER, J.S., Health Physics Instrumentation, Pergamon Press, London, New York (1959).
- [8] ROSSI, B.B., STAUB, H.H., Ionization Chambers and Counters: Experimental Techniques, McGraw-Hill, New York (1949).
- [9] PATTERSON, H.W., THOMAS, R.H., Accelerator Health Physics, Ch. 5, Academic Press, New York (1973).
- [10] SULLIVAN, A.H., "The present status of instrumentation for accelerator health physics", in Proc. Second Int. Conf. Accelerator Dosimetry and Experience, held at Stanford Linear Accelerator Center, 5–7 Nov. 1969, USAEC, Washington, DC, Rep. CONF-691101 (1969).
- [11] A number of papers which reflect the status of accelerator dosimetry and monitoring practices may be found in: STEVENSON, G.R., Ed., Proc. Conf. Radiation Protection in Accelerator Environments, held at the Rutherford Laboratory, March 1969, Rutherford Laboratory, Chilton, Didcot, Oxon. (1969).
- [12] INTERNATIONAL ATOMIC ENERGY AGENCY, The Basic Requirements for Personnel Monitoring, Safety Series No.14, IAEA, Vienna (1965).
- [13] INTERNATIONAL ATOMIC ENERGY AGENCY, The Use of Film Badges for Personnel Monitoring, Safety Series No.8, IAEA, Vienna (1962).
- [14] INTERNATIONAL ATOMIC ENERGY AGENCY, Personnel Dosimetry Systems for External Radiation Exposures, Technical Reports Series No. 109, IAEA, Vienna (1970).

³⁷ It is best to determine the dead time by circuitry to a definite value greater than the inherent (and variable) dead time. Methods for experimentally determining the effective T_D for a given instrument are described (Ref. [6], p.126).

- [15] INTERNATIONAL ATOMIC ENERGY AGENCY, Handbook on Calibration of Radiation Protection Monitoring Instruments, Technical Reports Series No.133, IAEA, Vienna (1971).
- [16] INTERNATIONAL COMMISSION ON RADIATION UNITS AND MEASUREMENTS, Radiation Protection Instrumentation and its Application, ICRU Rep. No.20, Washington, DC (1971).
- [17] INTERNATIONAL COMMISSION ON RADIOLOGICAL PROTECTION, General Principles of Monitoring for Radiation Protection of Workers, ICRP Publication No.12, Pergamon Press, London (1969).
- [18] NATIONAL COUNCIL ON RADIATION PROTECTION AND MEASUREMENTS, Instrumentation and Monitoring Methods for Radiation Protection, NCRP Rep. No. 57, Washington, DC (1978).
- [19] NATIONAL COUNCIL ON RADIATION PROTECTION AND MEASUREMENTS, Radiological Monitoring Methods and Instruments, NCRP Rep. No.10 and NBS Handbook No.51, Washington, DC (1952).
- [20] COMMISSION OF THE EUROPEAN COMMUNITIES, Radiation Protection Measurement – Philosophy and Implementation, Rep. No. EUR-5397, Luxembourg (1975).
- [21] COMMISSION OF THE EUROPEAN COMMUNITIES, Technical Recommendations for Monitoring the Exposure of Individuals to External Radiation, Rep. No. EUR-5287, Luxembourg (1975).
- [22] GUPTON, E.D., DAVIS, D.M., “Health physics instruments”, Ch.15, Principles of Radiation Protection (MORGAN, K.Z., TURNER, J.E., Eds), John Wiley, New York (1967).
- [23] SHAPIRO, J., Radiation Protection – A Guide for Scientists and Physicians, Ch.IV, Harvard University Press, Cambridge, MA (1972).
- [24] FREYTAG, E., NACHTIGALL, D., A Comparison of Health Physics Measuring Procedures at Accelerators, Deutsches Elektronen-Synchrotron, Hamburg, Rep. DESY-70/27 (1970).
- [25] DUDLEY, R.A., “Dosimetry with photographic emulsions”, Ch.15, Radiation Dosimetry, Vol.II: Instrumentation, 2nd ed. (ATTIX, F.H., ROESCH, W.C., Eds), Academic Press, New York (1966).
- [26] FOWLER, J.F., ATTIX, F.H., “Solid state integrating dosimeters”, Ch.13, Radiation Dosimetry, Vol.II: Instrumentation, 2nd ed. (ATTIX, F.H., ROESCH, W.C., Eds), Academic Press, New York (1966).
- [27] CAMERON, J.R., SUNTHARALINGAM, N., KENNEY, G.N., Thermoluminescent Dosimetry, Univ. of Wisconsin Press, Madison, WI (1968).
- [28] BECKER, K., Solid State Dosimetry, CRC Press, Cleveland, Ohio (1973).
- [29] BECKER, K., SCHARMANN, A., Einführung in die Festkörperdosimetrie, Karl Thieme, Munich (1975).
- [30] See, for example, papers in: DANISH ATOMIC ENERGY COMMISSION and INTERNATIONAL ATOMIC ENERGY AGENCY, Proc. Third Int. Conf. Luminescence Dosimetry, held at the Danish Atomic Energy Commission Research Establishment, Risø, 11–14 Oct. 1971, Risø Rep. No. 249 (3 Parts) (1971).
- [31] See, for example, papers in: AMELINCKX, S., BATZ, B., STRUMANE, R., Eds, Solid State Dosimetry, Proc. NATO Summer School, held at Brussels, 4–16 Sep. 1967, Gordon and Breach, New York (1969).
- [32] See, for example, papers in: AUXIER, J.A., BECKER, K., ROBINSON, E.M., Eds, Proc. Second Int. Conf. Luminescence Dosimetry, held in Gatlinburg, Tennessee, 23–26 Sep. 1968, USAEC, Washington, DC, Rep. CONF-680920, Health and Safety (TID-4500) (1968).

- [33] See, for example, papers in: ATTIX, F.H., Ed., *Luminescence Dosimetry*, Proc. Int. Conf. Luminescence Dosimetry, held at Stanford University, 21–23 June 1965, USAEC, Washington, DC, Rep. CONF–650637 (1967).
- [34] COMMISSION OF THE EUROPEAN COMMUNITIES, *Technical Recommendations for the Use of Thermoluminescence for Dosimetry in Individual Monitoring for Photons and Electrons from Extended Sources*, Rep. EUR–5358, Luxembourg (1975).
- [35] BEMIS, E.A., Jr., “Survey instruments and pocket dosimeters”, Ch.10, *Radiation Dosimetry* (HINE, G.J., BROWNELL, G.L., Eds), Academic Press, New York (1956).
- [36] BOAG, J.W., “Ionization chambers”, Ch.9, *Radiation Dosimetry*, Vol.II: Instrumentation, 2nd ed. (ATTIX, F.H., ROESCH, W.C., Eds), Academic Press, New York (1966).
- [37] COCHRAN, L.W., “Detection and measurement of ionization”, Ch.5, *Principles of Radiation Protection* (MORGAN, K.Z., TURNER, J.E., Eds), John Wiley, New York (1967).
- [38] BURLIN, T.E., “Cavity-chamber theory”, Ch.8, *Radiation Dosimetry*, Vol.I: Fundamentals, 2nd ed. (ATTIX, F.H., ROESCH, W.C., Eds), Academic Press, New York (1968).
- [39] PRICE, W.J., *Nuclear Radiation Detection*, Ch.4, McGraw-Hill, New York (1958).
- [40] HANDLOSER, J.S., *Health Physics Instrumentation*, Ch.3, Pergamon Press, London, New York (1959).
- [41] KROHN, B.J., CHAMBERS, W.B., STORM, E., *The Photon Energy Response of Several Commercial Ionization Chambers, Geiger Counters and Thermoluminescent Detectors*, Los Alamos Scientific Laboratory, Rep. LA–4052 (1969).
- [42] TESCH, K., *Deutsches Elektronen-Synchrotron DESY, Hamburg*, private communication (1976).
- [43] EMERY, E.W., “Geiger-Mueller and proportional counters”, Ch.10, *Radiation Dosimetry*, Vol.II: Instrumentation, 2nd ed. (ATTIX, F.H., ROESCH, W.C., Eds), Academic Press, New York (1966).
- [44] SINCLAIR, W.K., “Geiger-Mueller counters and proportional counters”, Ch.5, *Radiation Dosimetry*, 2nd ed. (HINE, G.J., BROWNELL, G.L., Eds), Academic Press, New York (1956).
- [45] PRICE, W.J., *Nuclear Radiation Detection*, Ch.5, McGraw-Hill, New York (1958).

5.2. Duty factor effects on radiation measurements

A particular aspect of electron linacs that requires consideration in the choice of instrumentation and evaluation of radiation measurements is the pulsed nature of the prompt radiations. Many common types of monitoring instruments are affected to some extent by a percentage loss in apparent sensitivity which is approximately proportional to the intensity of radiation divided by the accelerator duty factor.

Instruments that are often severely affected include the following:

- (a) GM counters and proportional counters, including bare BF₃ counters
- (b) Scintillation counters

Instruments that may be affected at high dose rates, but not if used in the manner for which they are properly designed:

- (a) Ionization chambers, including survey meters, area monitors and personnel ion-chamber dose meters
- (b) Solid-state detectors such as semiconductor diodes
- (c) *Moderated* BF₃ counters are less prone to this effect, owing to the long moderation time

Instruments that are not affected by the radiation time structure, at least in usual radiation protection applications, include:

- (a) Photographic films
- (b) TLDs
- (c) Neutron threshold detectors and other activation detectors
- (d) Fission-fragment detectors
- (e) Chemical dose meters
- (f) Most dose meters depending on discolouration of glass or other special materials

Because of their frequency of occurrence, two types of instrumental effects are discussed: dead-time effects in pulse counters and ion recombination in ionization chambers.

5.2.1. *Dead-time effects in pulse counters*

In cases where an instrument is used to measure *steady* radiation, as from induced activity, the equation for correction is

$$C_{\text{corr}} = \frac{C}{1 - \frac{CT_D}{T}} \quad (\text{steady radiation}) \quad (68)$$

where C_{corr} is the corrected number of counts, T_D is the dead time or time interval during which the instrument is insensitive following each count, C is the total number of counts *registered* during a total time interval T . T_D and T must be in the same units. The product CT_D can be regarded as the 'total dead time' in the total time interval T .

To see the effect of the accelerator duty factor, first consider the case in which the dead time T_D is *shorter* than the pulse length T_P : ($T_D < T_P$). Then the radiation may be considered 'steady' during the duration of each pulse and Eq.(68) may be modified to apply. For the total time interval, one would substitute PT_P ,

where P is the number of accelerator pulses during the counting time. For the 'total dead time', one would use $CT_D (1 - 1/2 T_D/T_P)$. The second term within the parentheses subtracts the portion of dead time which trails the accelerator pulse while no radiation is being produced. Without this correction the 'total effective dead time' would be overestimated, although the error is small if T_D is very much smaller than T_P .

$$C_{\text{corr}} = \frac{C}{1 - \frac{CT_D}{PT_P} (1 - 1/2 T_D/T_P)} \quad (\text{pulsed, } T_D < T_P) \quad (69)$$

Remembering that the duty factor is proportional to (PT_P) (see Section 1.3), Eq.(69) shows that a small duty factor can have a drastic effect on instrument response.

In order to treat the case in which the dead time is *longer* than the accelerator pulse, we consider that this case results in exactly the same counting losses as does the case $T_D = T_P$. Therefore, we replace (T_D/T_P) by unity in Eq.(69) when $(T_D \geq T_P)$. This will give an expression consistent with the following equation:

$$C_{\text{corr}} = C - P \ln(1 - C/P) \cong C \left[1 + \frac{1}{2} \frac{C}{P} + \frac{1}{3} \left(\frac{C}{P} \right)^2 + \dots \right] \quad (\text{pulsed, } T_D \geq T_P) \quad (70)$$

The first expression in Eq.(70) takes into account fluctuations in the number of counts and is more accurate than the expansion. Whenever the number of counts registered approaches the number of machine pulses ($C \approx P$), the corrected number becomes meaningless for $T_D \gtrsim T_P$.

It may be difficult to accurately determine the pulse length or dead time. The value of either may even vary from pulse to pulse or count to count. Therefore, it is best to avoid situations in which large relative corrections (greater than 10%) are required.

5.2.2. Recombination in ionization chambers

In ionization chambers, there is always some loss in signal current, owing to recombination of the primary ions before they are collected at the electrodes. When a commercially manufactured chamber is used under conditions for which it is designed, there is seldom a significant problem; instruments used as survey meters outside of a reasonable biological shield will not normally be affected. However, because the pulsed conditions of microwave electron linear accelerators

aggravate the recombination, it is an effect of which one should be aware. Significant signal current losses may occur under conditions of very high instantaneous exposure rates:

- (a) Ionization chambers used in a beam or near a target or beam dump will be exposed to intense radiation;
- (b) Where very short intense pulses are used, as at some research facilities, the duty factor may be as small as $10^{-7} - 10^{-6}$, causing large instantaneous bursts of ionization within an instrument.

The *collection efficiency* f is the ratio of the number of ions collected to the number of ions formed by radiation in the gas filling. For *steady* radiation detected by parallel-plate chambers, f is given by [1]:

$$f = (1 + x)^{-1} \approx 1 - x \quad \text{(steady radiation)} \quad (71)$$

where

$$x = \frac{1}{6} \frac{\alpha}{e k_1 k_2} \left(\frac{q d^4}{V^2} \right) = \frac{1}{6} m^2 \left(\frac{q d^4}{V^2} \right)$$

The factors occurring in m^2 depend on the nature of the gas used in the instrument:

- α is the *recombination coefficient* ($\text{cm}^3 \cdot \text{s}^{-1}$). (The rate of charge-carrier recombination ($\text{ion pairs} \cdot \text{s}^{-1} \cdot \text{cm}^{-3}$) is given by $\alpha n_1 n_2$, where n_1, n_2 are the ion densities in $\text{ions} \cdot \text{cm}^{-3}$.) Where the electrons remain free, $\alpha \approx 10^{-10} \text{ cm}^3 \cdot \text{s}^{-1}$; where the electrons attach to molecules, $\alpha \approx 10^{-6} \text{ cm}^3 \cdot \text{s}^{-1}$. For air, $\alpha \approx (1 - 2) \times 10^{-6} \text{ cm}^3 \cdot \text{s}^{-1}$.
- k_1, k_2 are the *mobilities* of positive and negative ions, respectively, in $\text{cm}^2 \cdot \text{s}^{-1} \cdot \text{V}^{-1}$. (For parallel-plate chambers, the ion drift velocity is given by $v = k \cdot V \cdot d^{-1}$.) The mobility is approximately inversely proportional to gas pressure. For air at NTP, $k_1 \approx k_2 \approx (1.3 - 1.4) \text{ cm}^2 \cdot \text{s}^{-1} \cdot \text{V}^{-1}$. For ion diffusion (not electrons), k is of the same order of magnitude for common gases. For electron diffusion, k_2 is not well defined, but is about two orders of magnitude larger.
- q is the ionization rate ($\text{C} \cdot \text{cm}^{-3} \cdot \text{s}^{-1}$); it is equal to the saturation current I_s collected (A), divided by the irradiated gas volume (cm^3).
- e is the electronic charge ($1.602 \times 10^{-19} \text{ C}$).
- d is the electrode spacing (cm).
- V is the chamber bias voltage (V).
- m^2 for air at NTP is $(4.0 \pm 0.5) \times 10^{12} \text{ V}^2 \cdot \text{s} \cdot \text{C}^{-1} \cdot \text{cm}^{-1}$ (Ref. [1], p.16).

In the case of *pulsed* radiation, where the pulse length T_p is much shorter than the ion collection time T_C , the collection efficiency is [1]:

$$f = u^{-1} \ln(1 + u) \approx 1 - 1/2 u \quad (\text{pulsed, } T_p \ll T_C) \quad (72)$$

where

$$u = \frac{\alpha}{(k_1 + k_2) e} \left(\frac{\rho_0 d^2}{V} \right) = \mu \left(\frac{\rho_0 d^2}{V} \right)$$

and ρ_0 is the initial density of positive or negative ionization charge released by one radiation pulse ($C \cdot \text{cm}^{-3}$). For air at NTP, $\mu = 3.3 \times 10^{12} \text{ V} \cdot \text{cm} \cdot \text{C}^{-1}$. The collection time T_C is given by

$$T_C = \frac{2d^2}{(k_1 + k_2) V} \quad (73)$$

For cylindrical or other chamber geometries, closely related formulae apply. Values of the parameters for various gases may be found in Refs [2–5]. In the case of electronegative gases (e.g. air, O_2 , H_2O , NO , NH_3 , SO_2 , Cl , HCl , SiF_4 , etc.) the electrons attach themselves quickly to a molecule. Then k_2 is about equal to k_1 because the negative- and positive-charge carriers have the same mass and therefore diffuse at the same rate. In noble gases and some others (e.g. He , Ne , A , Kr , Xe , H_2 , N_2 , CO_2 , BF_3 , etc.) the negative charge carriers are primarily free electrons with much greater mobility k_2 . In these gases, k_2 is about two orders of magnitude larger, and recombination effects are correspondingly less severe. Special gas mixtures are compounded for use in ionization chambers, notably argon with 10% of CH_4 .

It is always advisable to determine the saturation curve (collected current versus bias voltage at constant exposure rate, or current per unit exposure rate versus exposure rate) for each new chamber design to determine the extremes of operating conditions that will give significant recombination losses. With many chambers, it is not difficult to temporarily modify the bias voltage by substituting a separate battery or power supply. Whenever it is suspected that recombination losses are affecting an instrument, it is a good idea to compare a measurement made at the standard bias voltage with another at about half or less.

The relationship between recombination losses in pulsed and steady radiation fields is quite instructive. Taking the ratios of the quantities of Eqs (72) and (71) which express fractional *loss*, we have

$$\frac{(\text{fractional loss, pulsed})}{(\text{fractional loss, steady})} = \frac{1/2 u}{x} = 3 \left[\frac{k_1 k_2}{k_1 + k_2} \right] \frac{V}{p d^2} \quad (74)$$

where we make use of the relationship $\rho_0 p = q$, which holds for the same average radiation in the pulsed and steady cases (p is the pulse rate in Hz). Because k_1 and k_2 are either about equal, or else k_2 is much larger than k_1 , the quantity in brackets ranges between $1/2 k_1$ and k_1 , and therefore is of the order of unity for common gases. At representative bias voltages (~ 100 V), electrode spacing (~ 1 cm) and accelerator pulse rate (~ 100 Hz), we see that the recombination under pulsed conditions is only a few times larger than the recombination for steady radiation of the same average intensity.

In practice these results indicate that for mean dose rates, even much larger than are allowed in occupiable areas (perhaps up to ~ 0.01 Gy \cdot h $^{-1}$ (~ 1 rad \cdot h $^{-1}$)), and under a wide range of accelerator duty factors, the recombination effects are similar to those found in a constant radiation field of the same average dose rate. Therefore the saturation of instruments for routine survey use may simply be checked with a radioactive source [8].³⁸

More extensive discussions of recombination in ionization chambers can be found in several of the references given [1–7]. Special treatment of ionization-chamber response to pulsed fields can be found in Refs [8, 9].

REFERENCES TO SECTION 5.2

- [1] BOAG, J.W., "Ionization chambers", Ch.9, Radiation Dosimetry, Vol.II: Instrumentation, 2nd ed. (ATTIX, F.H., ROESCH, W.C., Eds), Academic Press, New York (1966).
- [2] FENYVES, E., HAIMAN, O., The Physical Principles of Nuclear Radiation Measurements, Academic Press, New York (1969); Die Physikalischen Grundlagen der Kernstrahlungsmessungen, Akadémiai Kiadó, Budapest (1969).
- [3] PRICE, W.J., Nuclear Radiation Detection, Ch.4, McGraw-Hill, New York (1958).
- [4] ROSSI, B.B., STAUB, H.H., Ionization Chambers and Counters: Experimental Techniques, McGraw-Hill, New York (1949).
- [5] COCHRAN, J.W., "Detection and measurement of ionization", Ch.5, Principles of Radiation Protection (MORGAN, K.Z., TURNER, J.E., Eds), John Wiley, New York (1967).
- [6] BEMIS, E.A., Jr., "Survey instruments and pocket dosimeters", Ch.10, Radiation Dosimetry (HINE, G.J., BROWNELL, G.L., Eds), Academic Press, New York (1956).
- [7] HANDLOSER, J.S., Health Physics Instrumentation, Ch.3, Pergamon Press, New York (1959).
- [8] DINTER, H., TESCH, K., Berechnung des Stromes einer Ionisationskammer im gepulsten elektromagnetischen Feld und Vergleich mit Messungen. Anwendung auf die Strahlungsüberwachung am Elektronenspeicherring, Deutsches Elektronen-Synchrotron, Hamburg, Rep. DESY-73/22 (1973); Calculation of the current of an ionization chamber exposed to a pulsed electromagnetic radiation field and comparison with measurements, Nucl. Instrum. Meth. **120** (1974) 113.
- [9] LEAKE, J.W., WHITE, D.F., "The use of standard radiation survey instruments in pulsed radiation fields", Radiation Protection in Accelerator Environments (Proc. Conf. Rutherford Laboratory, Chilton, 1969) (STEVENSON, R.G., Ed.), Rutherford Laboratory, Chilton, Didcot, Oxon. (1969) 103.

³⁸ It should be noted that these considerations apply only to volume recombination due to minimum-ionizing particles. In neutron fields, columnar recombination occurs which gives much larger effects and is very difficult to handle theoretically.

5.3. Neutron monitoring techniques

Neutron measurements in accessible areas are not normally needed for installations that are adequately shielded on all sides against photons, with a hydrogenous material such as concrete or earth, unless the energy exceeds the pion threshold ($E_0 \gtrsim 140$ MeV). However, new shielding designs for installations operating above 10 MeV should be checked for neutrons, especially at the labyrinth and other openings. At high energies, neutrons will constitute the dominant radiation outside of thick shields and neutron measurements are essential.

There are various levels of complexity that can be employed in neutron monitoring:

(a) The simplest is the use of a tissue-equivalent (TE) ionization chamber to first measure the total absorbed dose. Since dose-equivalent has no SI-derived unit as yet, the dose in rads (if measurements are made in grays convert to rads) is then multiplied by the maximum effective neutron quality factor, $Q = 10$, to obtain a safe overestimate of the dose-equivalent H in rems (Sections 2.1, 2.5). An exposure reading in röntgen (with a TE instrument) can approximately be converted to H by assuming a röntgen-to-rad conversion factor of unity.

(b) The fluence can be determined with an instrument (fluence meter) such as a moderated BF_3 counter or neutron-sensitive TLD system, and the quality factor $Q = 10$ applied to this measurement. This is more satisfactory in that it at least treats the neutron component separately in a mixed radiation field.

(c) The dose equivalent can be determined with a detector moderated to measure dose directly in rem (rem counter). The detector may be a device such as a BF_3 or ^3He tube, LiI scintillator, TLD or activation foil. BF_3 or activation foils provide better discrimination against photons and are recommended. These detectors are placed in moderators whose geometry is designed to give a rem response to the overall system.

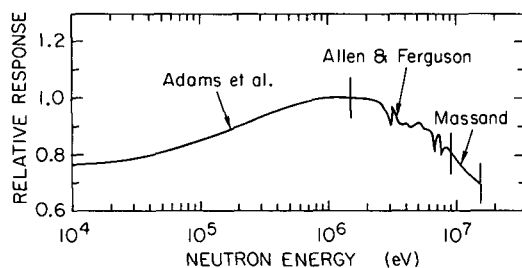


FIG.69. Relative response of the BF_3 long counter to neutron fluence, as a function of neutron energy. See Ref. [5] for references to original work. (Adapted from Ref. [5], with kind permission of D. Nachtigall and G. Burger, and Academic Press, New York.)

(d) Various methods can be used to obtain a relative neutron energy spectrum. Together with a measurement of fluence, this will provide the most accurate dose-equivalent assessment, but it involves a degree of complication which is not warranted at most installations.

An overview of the recent status of neutron monitoring techniques may be gained from Refs [1, 2]. The discussion of Patterson and Thomas [3] is also very useful.

5.3.1. Fluence measurements

(a) Thermoluminescent dose meters

A simple, convenient and sensitive method for *site* monitoring of neutrons is the use of a combination of ^6LiF and ^7LiF thermoluminescent dose meters inside a 15-cm-diameter polyethylene moderator. The response curve of this arrangement makes it suitable as a fluence monitor and its readings can be converted to dose equivalent after calibration against a rem meter exposed to the same neutron spectrum. Although not useful for continuous readings, it is the most economical means of obtaining average readings over an extended period of operation.

(b) BF_3 counter

The portable instrument most generally used for neutron surveys is a version of the BF_3 long counter [4]. This is a proportional counter tube filled with BF_3 gas enriched to about 96% ^{10}B . Its sensitivity to neutrons is based on the reaction



which has a high-cross-section (3000 barns) for thermal neutrons but drops as $(E_n^{-1/2})$ by about four orders of magnitude at fast neutron energies. Several types of information can be obtained with a simple BF_3 counter arrangement.

Thermal fluence. When used with no moderator, the BF_3 counter is practically sensitive to thermal (~ 0.025 eV) neutrons only. The sensitivity of a counter of typical dimensions (about 2 cm diameter \times 15 cm) is of the order of 2–3 counts per unit fluence ($\text{n} \cdot \text{cm}^{-2}$) and is proportional to volume, pressure and degree of enrichment in ^{10}B .

Fluence. With a moderator such as paraffin or polyethylene, some fast neutrons are thermalized and then counted as thermal neutrons. The sensitivity to fast neutrons incident on the moderator surface is of the same order of magnitude as the sensitivity of the bare counter to thermal neutrons. With a

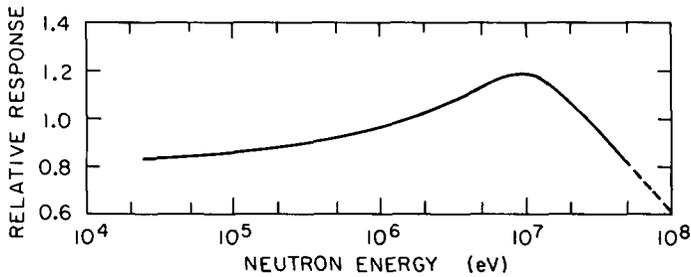


FIG. 70. Relative response of the DePangher (Ref. [6]) cylindrical 'flux meter' to neutron fluence, as a function of neutron energy. (Adapted from Ref. [5], with kind permission of D. Nachtigall and G. Burger, and Academic Press, New York.)

paraffin moderator close to 6.5 cm thick, the sensitivity is almost independent of energy over a large energy range, for example, to within a factor of two over a typical range 10 keV to 3 MeV (see Fig. 69). By means of an 0.5-mm Cd shield outside of the moderator, *incident* thermal neutrons can be eliminated from the measurement.

Rem counter [5]. A similar arrangement, but with a thicker moderator (about 11.5 cm), has the property that the sensitivity to neutron fluence as a function of neutron energy has approximately the same relative shape as the ICRP dose-equivalent curve (Fig. 23, Section 2.5) over a useful energy range extending to about 6 MeV. A rough estimate of the effective energy can be obtained for a given neutron field by the ratio of counts registered with two different moderators.

For more precise work, highly engineered and standardized versions of the BF₃ long counter have been developed. The DePangher Precision Long Counter (PLC) [6] was developed as a fluence meter and can be constructed with a reproducibility from counter to counter of the order of 1%. Figure 70 shows the energy dependence of this instrument.

Andersson and Braun [7] have modified the straightforward BF₃ rem counter by adding intermediate thermal-neutron-absorbing layers of boron plastic within the moderator, to achieve a better approximation to the ICRP response curve.

Counters of cylindrical geometry are directional in response and their orientation with respect to the direction of neutron fluence should be considered when used, in order to obtain the optimum accuracy. Ladu et al. [8, 9] have designed an instrument based on a BF₃ counter with a hollow spherical paraffin moderator (28.4 cm outside diameter, 15 cm inside diameter). This instrument has a uniform angular response and a fluence response uniform over 20 keV – 14 MeV.

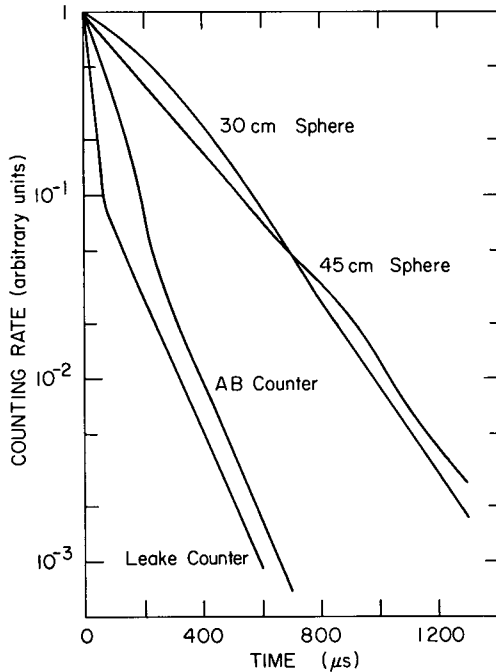


FIG. 71. Distribution of neutron moderation times for four types of rem counter. These distributions effectively make the accelerator duty factor appear much larger than it is. The intrinsic dead times of the bare counters are in the range 2–7 μs , much shorter than the time scale shown. The counters used are: For the 30 cm and 45 cm spheres: ^6LiI scintillator; Andersson-Braun (AB): BF_3 counter; Leake counter: spherical ^3He counter. (Adapted from Ref. [16], with kind permission of H. Dinter and K. Tesch, and the Deutsches Elektronen-Synchrotron, Hamburg.)

Leake [10] has also described a portable spherical apparatus with improved rem response, which utilizes a 20.8-cm-diameter polyethylene moderator and a ^3He counter enclosed in a perforated Cd layer. Spherical units with 9 in (22.5 cm) or 10 in (25 cm) moderators are also commercially available and are discussed in Refs [11–14]. A comparison of the energy dependence of the 9 in (22.5 cm) and 10 in (25 cm) units with the Andersson-Braun instrument is given by Hankins and Cortez [15].

Corrections for instrument dead time may have to be made to the BF_3 counter measurements. In doing so, one must recall that moderation in shielding material and the instrument's special moderator introduces considerable variation in neutron arrival time. Figure 71 illustrates typical distributions of neutron arrival times following the accelerator pulse for four types of moderators [16]. From these data, one would use a value of the order of 200 μs for the 30 cm and 45 cm spheres

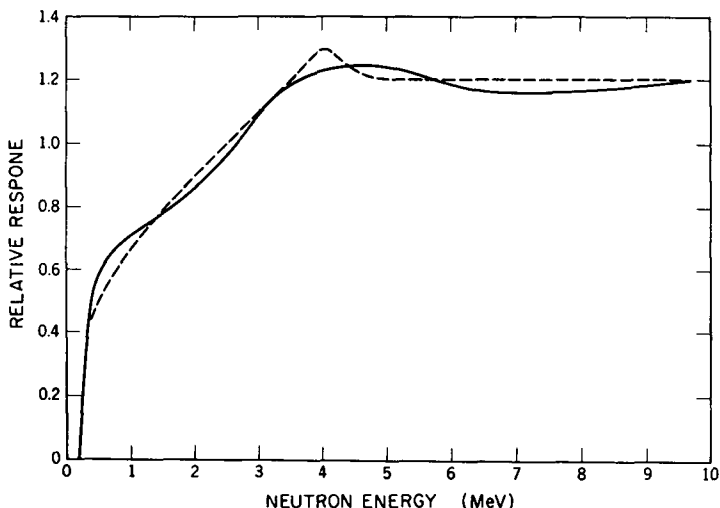


FIG. 72. Relative energy response of the Hurst count-rate dose meter. Its total response is based on the inherent response of a methane-filled proportional counter, combined with the proton recoil distribution from an external paraffin-aluminium sandwich. Dashed curve: calculated response; solid curve: measured response. (After Ref. [17]. Adapted from Ref. [18], with kind permission of G.S. Hurst, K.Z. Morgan and J.E. Turner, and John Wiley, New York.)

in place of the actual T_p value in Eq. (69). At a research installation where facilities are available, this distribution should be measured for each arrangement used. Alternatively, the effective ratio T_D/T_p for use in Eq. (69) can be determined by measurements at various values of C/P . The latter ratio can be varied by changing the accelerator beam current. Trial values of T_D/T_p can be inserted into Eq. (69) until a value is found which best satisfies the data. Moderation times in rem counters and methods of correction have been discussed by Dinter and Tesch [16].

(c) Proton recoil counter

The proton recoil counter is a tube filled with hydrogen gas, or made with hydrogenous walls, or a combination of both, which uses to advantage the properties of n-p scattering. Its sensitivity is quite low compared with the ^{10}B counters. These instruments can be operated either as proportional counters or for large neutron flux densities, as ionization-current-sensitive devices, but this mode would find little application because of sensitivity to photons and other radiations. They are constructed in various configurations, and the moderator thickness may be chosen to obtain arbitrary energy response. Chambers with slowly varying energy dependence from less than 1 MeV to over 10 MeV have been described, for example, in Refs [17–19] (see Fig. 72).

(d) Fission fragment detectors

The use of fission fragment track-etching techniques [3, 20, 21, 22] offers an alternative dosimetry method, especially at higher neutron energies which are found around high-energy accelerators. The method is based on the registration of tracks of fission products induced by the neutrons in the field to be measured. The detection apparatus typically consists of two foils in contact, a fission foil and a detector foil. The fission foil is a high-Z material such as U, Th, Bi, Au or Ta, and the detector foil is a dielectric material such as mica, glass or one of a large variety of plastics (e.g. cellulose nitrates, polycarbonates). If the fission foil is thick compared with the range of the fission fragments, the neutron fluence can be related to the density of the observed fission-fragment tracks approximately by [20]:

$$\rho_t \approx 1.2 \times 10^{19} \varphi \sigma_f \quad (76)$$

where ρ_t is the number of tracks per square centimetre in the detecting foil, φ is the neutron fluence ($\text{n} \cdot \text{cm}^{-2}$), and σ_f is the fission cross-section (cm^2) at the neutron energy in question. The constant of proportionality represents an 'effective thickness' of the thick fission foil, measured in target nuclei per cm^2 , i.e. the thickness of the layer of target foil from which fragments are capable of reaching the detector foil to be registered.³⁹ Because of this relationship, the known fission cross-sections may be used to calculate the neutron energy dependence of various detector combinations. Sets of fissionable materials with different fission thresholds can be used in a manner similar to the way threshold activation detectors are used. The response curve can be altered by moderation techniques, although attempts to achieve a good approximation to the ICRP rem curve have not been as successful as with the rem counters which use detectors that are sensitive only at thermal energies.

³⁹ If we take $\rho_R = 10^{-2} \text{ g} \cdot \text{cm}^{-2}$ as indicative of the fission-fragment range, then the areal density of target nuclei for $A \approx 200$ is:

$$\frac{\rho R N_A}{A} \cong \frac{10^{-2} \text{ g} \cdot \text{cm}^{-2} \times 6.022 \times 10^{23} \text{ mol}^{-1}}{200 \text{ g}} \cong 3 \times 10^{19} \text{ nuclei} \cdot \text{cm}^{-2}$$

Because of the spread in fragment mass and energy, the isotropic distribution of fragments and a registration efficiency less than unity, the resultant effective areal density is less than this, or about $1 \times 10^{19} \text{ nuclei} \cdot \text{cm}^{-2}$.

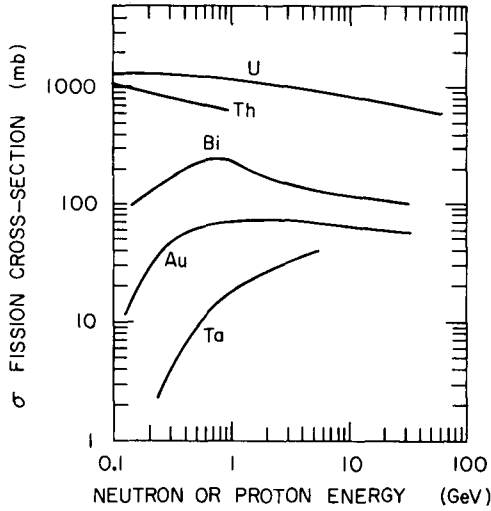


FIG. 73. Fission cross-section of several nuclides suitable for use in high-energy fission fragment detectors, as a function of neutron (or proton) energy. At these high energies, the fission cross-sections of n and p are about equal. (After Wollenberg and Smith [23]. Adapted from Ref.[3], with kind permission of H.W. Patterson and R.H. Thomas, the Lawrence Berkeley Laboratory and Academic Press, New York.)

TABLE XLVI. SENSITIVITIES OF SOME FISSION REACTIONS USED IN NEUTRON DOSIMETRY ^a

Fissionable material	Sensitivity (tracks/neutron)					
	Neutron energy, E_n					
	Thermal	Fission	~ 4 (Pu-Be)	14 MeV	230 MeV	5500 MeV
U (nat)	3.5×10^{-5}	4.2×10^{-6}	4.5×10^{-6}	1.4×10^{-5}		3.6×10^{-6}
U-235	3.5×10^{-3}	1.6×10^{-4}				
Th		4.0×10^{-7}	1.2×10^{-6}	4.5×10^{-6}		
Np-237		1.8×10^{-6}		1.8×10^{-6}		
Ta					5.0×10^{-8}	6.1×10^{-7}
Be					2.0×10^{-6}	
Au					4.5×10^{-7}	9.3×10^{-7}
Bi						1.1×10^{-6}

^a Adapted from Ref.[20], with kind permission of K. Becker and Academic Press.

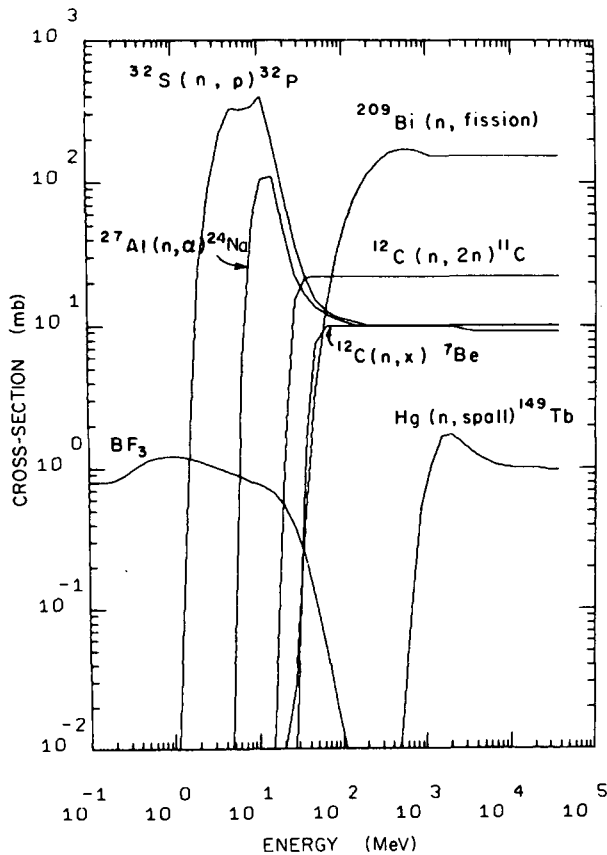


FIG. 74. Energy response functions (activation cross-sections) of selected neutron activation detectors. (Reproduced from Ref.[28], with kind permission of J.T. Routti and the Lawrence Berkeley Laboratory.)

A review of this technique by Becker [20] lists a number of advantages:

“Solid-state track detectors are normally insensitive even to high doses of X, β and γ radiation.”

“There are no deterioration, storage and fading problems involved unless the temperature far exceeds room temperature, and the detectors do not respond to such disturbing environmental influences as light and humidity.”

“The ‘development’ and evaluation are much easier than that of photographic films and can easily be automated. Due to possibility of easily reading larger areas there is also a higher effective sensitivity.”

“A very wide dose range can be covered by simple means such as dilution of the fissile material, or its use in layers of different thickness.”

“The detectors can easily be switched ‘on’ and ‘off’ by coupling or de-coupling during or between irradiations of the fissile foil and the detector foil.”

TABLE XLVII. IMPORTANT CHARACTERISTICS OF VARIOUS NEUTRON DETECTION TECHNIQUES

Detector	Reaction	Energy range (MeV)	Detector size ^a	Response to flux of 1 neutron·cm ⁻² a	Background response ^a
Gold foils moderated	¹⁹⁷ Au(n,γ) ¹⁹⁸ Au	0.02 to 20	2.54 cm dia., 0.5 g foil in paraffin cylinder	2.1 counts/min ^b	10 counts/min
Gold foils bare	¹⁹⁷ Au(n,γ) ¹⁹⁸ Au	thermal	2.54 cm dia., 0.5 g foil	1.8 counts/min ^b	10 counts/min
Sulphur	³² S(n,p) ³² P	> 3	2.54 cm dia., 4 g disk	0.049 counts/min ^c	10 counts/min
Plastic scintillator	¹² C(n,2n) ¹¹ C	> 20	13 to 2700 g	88 counts/min at 85% efficiency ^c 1700 g scintillator	165 counts/min 1700 g scintillator
Mercury	Hg() ¹⁴⁹ Tb	> 600	up to 500 g	0.03 counts/min ^b	0.1 counts/min
Gold foils	¹⁹⁷ Au() ¹⁴⁹ Tb	> 600	2.54 cm dia. 0.5 g	2.7 × 10 ⁻⁶ counts/min ^b	0.1 counts/min
BF ₃ proportional counter moderator	¹⁰ B(n,α) ⁷ Li	0.02 to 20	400 cm ³ at 20 cm Hg, 96% enriched	400 counts/min, 6 cm thick moderator	2 to 3 counts/min
Polyethylene-lined prop. counter	Proton recoil	0.05 to 20	800 cm ² PE radiator, Ar-CO ₂ filled	1 count = 15 MeV/cm ² at zero bias	< 1 count/min
Large bismuth fission counter	²⁰⁹ Bi(n,f)	> 50	30 cm dia. parallel plates 60 g Bi	1.05 counts/min at zero bias, E _n = 220 MeV	< 1 count/h
Small bismuth fission counter	²⁰⁹ Bi(n,f)	> 50	5 cm dia. parallel plates	0.02 counts/min at zero bias	< 1 count/h
Thorium fission counter	²³² Th(n,f)	> 2	5 cm dia. parallel plates	0.017 counts/min at zero bias (PuBe spectrum)	< 1 count/min
Gold foil, moderated	¹⁹⁷ Au(n,γ) ¹⁹⁸ Au	0.02 to 20	5.08 cm dia., 2.0 g foil	10.1 counts/min ^c	48 counts/min NaI(Tl)
Gold foil, bare	¹⁹⁷ Au(n,γ) ¹⁹⁸ Au	thermal	5.08 cm dia., 2.0 g foil	13.4 counts/min ^c	48 counts/min NaI(Tl)
Large indium foil, bare	¹¹⁵ In(n,γ) ¹¹⁶ In ^m	thermal	7.6 cm by 15.2 cm foils (four) 46 g total	300 counts/min (estimated)	75 counts/min NaI(Tl)
Aluminium	²⁷ Al(n,α) ²⁴ Na	> 6	16.9 to 6600 g	101 counts/min, 6600 g ^c , E _n = 14 MeV	111 counts/min, 16.9 g, 118 counts/min, 6600 g NaI(Tl)

Detector	Reaction	Energy range (MeV)	Detector size ^a	Response to flux of 1 neutron · cm ⁻² ^a	Background response ^a
Aluminium	²⁷ Al() ²² Na	> 25	16.9 g	0.21 counts/min ^c	67 counts/min NaI(Tl)
Plastic scintillator	¹² C() ⁷ Be	> 30	2.54 cm dia. by 2.54 cm high	0.0114 counts/min ^c	59 counts/min NaI(Tl)
Emulsion (Ilford)	Proton recoil	2 to 20	600 μm thick		
Emulsion (Ilford)	Star production	> 20	600 μm thick		
Neutron film Kodak Type-B	Proton recoil	0.5 to 25	~ 30 μm thick	0.00083 track per normally incident neutron	
Mica fission-track plates	Fission in Bi, Pb, Au	> 50 in Bi	> 1 cm ²	1.79 × 10 ⁻⁶ tracks per neutron for Bi	

^a Typical values.

^b At saturation, zero decay time and zero bias.

^c Saturation and zero decay time.

(Adapted from the CERN shielding experiment (Gilbert et al., [29]). Reproduced in part with kind permission of the authors and the Lawrence Berkeley Laboratory.)

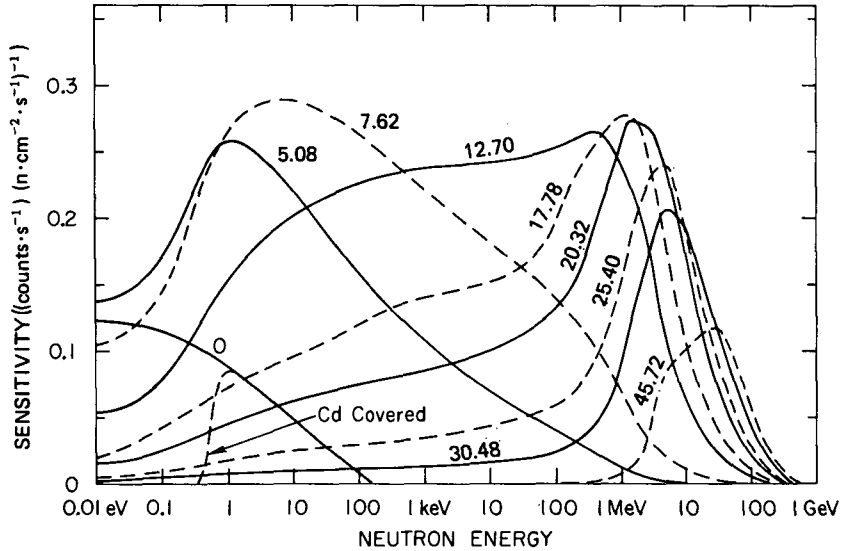


FIG. 75. Detector sensitivities as a function of energy, for a range of moderator thicknesses in centimetres (original data in inches). (Reproduced from Ref.[30], with kind permission of G.R. Stevenson and the Rutherford High-Energy Laboratory.)

However, a correction must be made for a background of photofission tracks if there are significant fluences of high-energy photons ($k \gtrsim 6$ MeV) in the type of mixed radiation field found at electron accelerators.

The fission cross-sections for high-energy neutrons, and sensitivities of fission reactions at representative high neutron energies are shown in Fig. 73 and Table XLVI, respectively. Fission cross-sections in the high-energy range ($E_n > 100$ MeV) are published by Wollenberg and Smith [3, 23]. A compilation of fission cross-sections in the low-energy region is published by Cullen et al. [24]. The application of this technique at a high-energy electron accelerator is described by Gay and Svensson [25].

5.3.2. Spectral measurements

(a) Nuclear emulsions

The nuclear emulsion technique [26] is a primary method of measuring neutron spectra and is useful above about 0.5 MeV. The events actually observed at neutron energies in the range 1–20 MeV are single tracks of recoiling protons arising from n-p elastic scattering in the emulsion. The proton energy, obtainable from its range in emulsion, together with its angle, determines the energy of the incident neutron if its direction is known.

For higher neutron energies the method is more limited, but information can be obtained, with assumptions, from the analysis of neutron-induced stars [27]. This technique does not work in high photon fluences because of emulsion darkening.

(b) Threshold detectors

Threshold detectors, or neutron activation detectors, use to advantage the known rates at which neutrons of different energies can produce radioactivity in particular materials. Although several operations and calculations are always involved, it is a method by which neutron spectra over the full energy range from a few MeV to several hundred MeV may be estimated. Some of its characteristics are:

- Selection of desired energy response by choice of material
- Wide range of sensitivity
- Compactness
- Separation of the activation from the evaluation phases.

However, the method is relatively insensitive compared with other techniques and not useful at low dose rates. Some mathematical manipulation is always involved [3, 28], including corrections for activation and decay time and an integration of the activation cross-section of each material over a presumed neutron spectrum. With a judicious choice of a few materials, a spectrum estimate can be obtained with hand calculations. For more accuracy, several materials can be used, followed by computer analysis including minimization procedures to unfold a smooth spectrum. In all cases, some type of assumptions about the spectrum shape and its parameterization must be given as input.

The energy response of selected threshold detectors is shown in Fig. 74 [28]. A list of convenient threshold detectors, together with other detectors used in a complete neutron study at CERN [29] is contained in Table XLVII.

(c) Bonner spheres

This method uses a detector sensitive to thermal neutrons, usually a LiI counter, together with a series of moderator spheres which impart differing energy response functions to the detector (Fig. 75) [5, 30, 31].

The method involves an unfolding of a smoothed approximation to the true spectrum from the raw measurements. An appropriate form for the spectrum, with variable parameters, must be chosen, and a matrix provided which describes the energy response function for each moderator thickness used. Computer optimization techniques are well suited to the determination of the spectral parameters to be fitted to the data.

REFERENCES TO SECTION 5.3

- [1] Neutron Monitoring for Radiation Protection Purposes (Proc. Symp. Vienna, 1972), IAEA, Vienna (1973).
- [2] Neutron Monitoring (Proc. Symp. Vienna, 1966), IAEA, Vienna (1967).
- [3] PATTERSON, H.W., THOMAS, R.H., Accelerator Health Physics, Ch.5, Academic Press, New York (1973).
- [4] HANSON, A.O., MCKIBBEN, J.L., A neutron detector having uniform sensitivity from 10 keV to 3 MeV, *Phys. Rev.* **72** (1947) 673.
- [5] NACHTIGALL, D., BURGER, G., "Dose equivalent determinations in neutron fields by means of moderator techniques", in Topics in Radiation Dosimetry, Radiation Dosimetry, Suppl. 1, Ch. 7 (ATTIX, F.H., Ed.), Academic Press, New York (1972).
- [6] DePANGHER, J., NICHOLS, L.L., A Precision Long Counter for Measuring Fast Neutron Flux Density, Battelle Memorial Institute, Pacific Northwest Laboratory, Richland, WA, Rep. BNWL-260 (1966).
- [7] ANDERSSON, I.O., BRAUN, J., "A neutron rem counter with uniform sensitivity from 0.025 MeV to 10 MeV", Neutron Dosimetry (Proc. Symp. Neutron Detection and Dosimetry Standards, Harwell, 1963) **2** (1963) 87.
- [8] LADU, M., PELLICIONI, M., ROTONDI, E., On the response to fast neutrons of a BF₃ counter in a paraffin spherical-hollow moderator, *Nucl. Instrum. Meth.* **23** (1963) 173.
- [9] LADU, M., PELLICIONI, M., ROTONDI, E., Flat response to neutrons between 20 keV and 14 MeV of a BF₃ counter in a spherical hollow moderator, *Nucl. Instrum. Meth.* **32** (1965) 173.
- [10] LEAKE, J.W., An improved spherical dose equivalent neutron detector, *Nucl. Instrum. Meth.* **63** (1968) 329.
- [11] HANKINS, D.E., A Modified-Sphere Neutron Detector, Los Alamos Scientific Laboratory, Rep. LA-3595 (1967).
- [12] HANKINS, D.E., The substitution of a BF₃ probe for the LiI crystal in neutron rem-meters, *Health Phys.* **14** (1968) 5; Los Alamos Scientific Laboratory, Rep. LA-DC-9054 (1968).
- [13] HANKINS, D.E., A Neutron Monitoring Instrument Having a Response Approximately Proportional to the Dose Rate from Thermal to 7.0 MeV, Los Alamos Scientific Laboratory, Rep. LA-2717 (1962).
- [14] HANKINS, D.E., "New methods of neutron-dose-rate evaluation", Neutron Dosimetry (Proc. Symp. Harwell, 1962) **2**, IAEA, Vienna (1962) 123.
- [15] HANKINS, D.E., CORTEZ, J.R., Energy dependence of four neutron remmeter instruments, *Health Phys.* **28** (1975) 305.
- [16] DINTER, H., TESCH, K., Moderated Rem Meters in Pulsed Neutron Fields, Deutsches Elektronen-Synchrotron, Hamburg, Rep. DESY-76/08 (1976).
- [17] HURST, G.S., RITCHIE, R.H., WILSON, H.N., *Rev. Sci. Instrum.* **22** (1951) 981.
- [18] MORGAN, K.Z., TURNER, J.E., Eds, Principles of Radiation Protection, John Wiley, New York (1967) 212.
- [19] MOYER, B.J., Survey methods for fast and high-energy neutrons, *Nucleonics* **10** (1952) 14.
- [20] BECKER, K., "Dosimetric applications of track etching", in Topics in Radiation Dosimetry, Suppl. 1, Ch. 2 (ATTIX, F.H., Ed.), Academic Press, New York (1972).
- [21] BECKER, K., Solid State Dosimetry, CRC Press, Cleveland, Ohio (1973).
- [22] BECKER, K., SCHARMANN, A., Einführung in die Festkörperdosimetrie, Karl Thiernig, Munich (1975).

- [23] WOLLENBERG, H.A., SMITH, A.R., "Energy and flux determinations of high-energy nucleons", in Proc. Second Int. Conf. Accelerator Dosimetry and Experience, held at Stanford Linear Accelerator Center, 5–7 Nov. 1969, USAEC, Washington, DC, Rep. CONF-691101 (1969) 586.
- [24] CULLEN, D.E., HAIGHT, R.C., HOWERTON, R.J., MACGREGOR, M.H., PERKINS, S.T., Graphical Experimental Data for Major Neutron-Induced Interactions ($Z > 55$), Lawrence Livermore Laboratory, Rep. UCRL-50400, Vol. 7, Part B (1974).
- [25] GAY, R., SVENSSON, G.K., A Discussion of an Experimental Evaluation of the Use of the Fission Fragment Track Registration Method for Particle Fluence Measurements, Stanford Linear Accelerator Center, Rep. SLAC-TN-70-33 (1970).
- [26] BARKAS, W., Nuclear Research Emulsions, Academic Press, New York (1963).
- [27] PATTERSON, H.W., "New measurements of star production in nuclear emulsions and applications to high-energy neutron spectroscopy", in Proc. Second Int. Conf. Accelerator Dosimetry and Experience, held at Stanford Linear Accelerator Center, 5–7 Nov. 1969, USAEC, Washington, DC, Rep. CONF-691101 (1969).
- [28] ROUTTI, J.T., "Mathematical considerations of determining neutron spectra from activation measurements", Proc. Second Int. Conf. Accelerator Dosimetry and Experience, held at Stanford Linear Accelerator Center, 5–7 Nov. 1969, USAEC, Washington, DC, Rep. CONF-691101 (1969) 494.
- [29] GILBERT, W.S., KEEFE, D., McCASLIN, J.B., PATTERSON, H.W., SMITH, A.R., STEPHENS, L.D., SHAW, K.B., STEVENSON, G.R., THOMAS, R.H., FORTUNE, R.D., GOEBEL, K., 1966 CERN-LRL-RHEL Shielding Experiment at the CERN Proton Synchrotron, Lawrence Berkeley Laboratory, Rep. UCRL-17941 (1968).
- [30] STEVENSON, G.R., Neutron Spectrometry from 0.025 eV to 25 GeV, Rutherford High-Energy Laboratory, Rep. RHEL/R 154 (1967).
- [31] SANNA, R.S., 31-Group Response Matrices for the Multi-Sphere Neutron Spectrometer over the Energy Range Thermal to 400 MeV, ERDA Health and Safety Laboratory, New York, Rep. HASL-276 (1973).

5.4. Radiation surveys

Before *routine* operation, every accelerator should be surveyed by a qualified radiation protection expert. This could be the Radiation Safety Officer (RSO) or an expert designated or hired by him as a consultant. Surveys should be repeated annually or whenever operating conditions are changed in such a way that radiation levels in accessible areas can change significantly. At large research laboratories, for example, this may be a frequent occurrence. If a preliminary survey has shown that shielding is insufficient, the facility should be re-surveyed after the indicated additional shielding has been installed.

During *tune-up* and initial operation of a unique or new type of accelerator, radiation surveys at accessible locations outside the shielding should be performed as soon as doses in excess of 2.5 mrem/h are likely to be delivered. This preliminary survey may be omitted at linac installations of a very standardized type, such as a clinical setting in which previously used installation drawings are followed. However, the tune-up survey is essential in the case of a high-energy

research installation. In this case, continuous readings or frequent sampling with area monitors should be used over the entire time of the initial turn-on.

It is advisable to begin the survey at reduced current. When it appears safe to do so, the survey should be continued at a level sufficiently high that meaningful readings are obtained. In cases where beam power is significantly limited at the highest beam energy, because of accelerator characteristics, it is advisable to repeat part or all of a survey at the energy at which the greatest radiation of the dominant kind can be produced. This will generally occur at an operating energy, E_0 , somewhat above that which permits the greatest beam power to be delivered.

Inspection during construction is advantageous in ensuring compliance with specifications and revealing inadequacies which can be more economically remedied at this stage than later. Where applicable, the following points should be examined:

Thickness of shielding walls

Density of materials used

Possible gaps between shielding elements

Possible inadequate shielding due to penetrations or recesses

Provision for and location of interlock switches, cutoff switches and warning lights

Steps which are recommended for a complete survey following installation are:

(a) Safety devices such as door interlock switches, limit switches for beam orientation, emergency shutoff switches and other necessary devices should be tested. This would include a test of the provision that the interlock or cutoff switch must first be reset at the location at which it was tripped, while the accelerator can only be restarted from the main control console following the reset.

(b) The presence of appropriate warning signs, lights and audible signals should be determined. A red warning light should be located on the control panel, at each entrance to the containment area and at prominent locations within the containment area. Provision for an appropriate audible warning is essential. At the minimum this would be an intercom between the main control console and the containment area used to announce imminent accelerator turn-on. An audible signal continually sounded while radiation is being produced is recommended. In small installations, such as for radiotherapy, this need may be satisfied by the audible 'electrical' hum made by the equipment itself.

(c) The surveyor should check that the controlled and supervised areas are properly demarcated with appropriate signs. However, signs which might alarm patients in a clinical situation may be omitted if personnel occupying the areas

are otherwise informed of the radiation levels to which they could be exposed and the patient entrance to the therapy room is strictly controlled.

(d) Steps which are recommended for assessment of radiation levels are:

Make a continuous survey with a portable gamma survey meter at two heights at least: about eye level and at waist or gonad height. These data should be recorded on a sketch of the installation.

Make a reasonable 'scan' of sample areas from the floor up to about 2 metres, in order to detect areas of general shielding weakness. If higher radiation levels are found, they should be noted on a sketch for future correction. Mark such areas with chalk directly on the wall.

In order to detect narrow regions of higher radiation streaming through hidden gaps or ducts, 'scan' the entire wall with a GM or scintillation counter, while listening to the 'clicks'. Mark any such areas found for future correction, and measure the levels found with an ionization chamber survey meter. It is cautioned that the GM counter may give completely erroneous readings if the count rate observed is comparable with the accelerator pulse rate. The GM counter should not be relied upon for quantitative information when the accelerator is on. The usefulness of the GM counter in the survey is to localize small areas to be later evaluated with an ionization chamber survey meter.

Similar procedures should be followed in accessible areas above and below the accelerator installations.

(e) For the evaluation of a primary barrier (in allowed primary beam directions), removable objects such as phantoms and targets should be removed and the primary beam directed toward the barrier.

(f) For the evaluation of all other (secondary) barriers, the maximum possible scattered radiation should be produced. In a therapy installation, a phantom should be placed at a typical position of a patient and the maximum field size used. In the case of a radiographic installation, a typical object of the largest size to be radiographed should be placed at the normal distance from the target, to produce the maximum scattered radiation. At a research installation, a thick high-Z temporary target should be placed at the normal target position.

(g) Where it is possible to vary the direction of the useful beam by moving the accelerator itself (as with most radiotherapeutic and radiographic units), surveys should be made using representative accelerator orientations. With therapeutic equipment, this generally implies a survey with the useful beam directed at each of two walls, the ceiling and the floor. In radiographic installations a choice of accelerator position as well as beam direction may be permitted by the accelerator mounting. If appropriate, position-limiting switches ('limit switches')

should be tested and their settings noted. Administrative controls on accelerator position and orientation should be reviewed. Where accelerator orientation is limited in part by administrative control, the 'allowable' areas of radiographic target walls should be clearly marked.

(h) Where it is possible to steer an electron beam in different directions with magnets, so that objects such as collimators, beam pipes, or walls can be struck, it is essential to survey accessible areas under a variety of abnormal steering conditions. A recommended procedure is to place an area monitor or survey instrument at an accessible location where stray radiation from a mis-steered beam is likely to be detected. At this location, the reading should be maximized on the instrument by trying various combinations of magnet current settings. When a radiation maximum has been found, an area survey as described above should be repeated to map out the spatial distribution of the stray radiation. Situations such as these can usually be corrected by local shielding at the object struck by the beam.

(i) In evaluating the survey results, consideration should be given to the type of area(s) (whether controlled or non-controlled)⁴⁰, the area occupancy factor T, the orientation (use) factor U for each type of radiation at the barrier in question, and the expected workload W, expressed as $\text{Gy} \cdot \text{m}^2 \cdot \text{week}^{-1}$ ($\text{rad} \cdot \text{m}^2 \cdot \text{week}^{-1}$). At research accelerators, it may be more appropriate to specify the accelerator performance in terms of average beam power transported (kW) at each operating energy E_0 , together with the number of hours per week of operation planned.

At installations operating above about 10 MeV, using previously untested shielding arrangements, a neutron survey should also be included in the initial or periodic survey. It should be done after the photon radiation field has been mapped out with a tissue-equivalent ionization chamber. As the neutron source is more nearly isotropic, greater attention should be paid to the regions of thinner shielding, regardless of their direction from the target or beam dump. Besides these regions, doors, labyrinths and openings of all sizes should be investigated.

A BF_3 counter, moderated for fluence sensitivity uniform with energy (fluence meter) or for direct dose-equivalent response (rem meter), is suitable for this type of survey (Section 5.3).

Unless special measurements have been taken to obtain the neutron spectrum at the location to be evaluated (Section 5.3), use the rule of thumb that a measured fluence rate of $8 \times 10^4 \text{ n} \cdot \text{cm}^{-2} \cdot \text{s}^{-1}$ is equivalent to a dose equivalent of 10 rem/h for all body organs (see Section 2.5).

⁴⁰ The user of this manual is reminded that other terminology and definitions may apply in his locality (see Section 3.1).

TABLE XLVIII. EXAMPLE OF INFORMATION REQUIRED IN ONE JURISDICTION, FOR AN ACCEPTABLE RADIATION-PROTECTION SURVEY REPORT^a

- "1. The name, address and telephone number of the physicist who performed the survey, or under whose direction it was performed.
 2. The name and address of the medical facility, and the telephone number of the person responsible for the therapy installation.
 3. The building and room location of the machine.
 4. Identification of the machine and/or major components thereof, including manufacturer, model designation and serial number.
 5. Scale drawings or carefully dimensioned sketches of the therapy installation and its environs, including both plan and elevation as necessary; direction of North, machine location and orientation, target location and isocenter must be shown.
 6. Identification of the report as one intended to fulfill the requirements of [applicable sections of the radiation control regulations].
 7. A statement of all the working assumptions used in preparing the report, including workload, occupancy factors and use factors.
 8. Measurements of dose rates at the control station and in all other occupiable areas in the vicinity, representative of those beam qualities, beam orientations and field sizes which will be used.
 9. A statement as to whether the machine and door interlocks and limit switches are functioning correctly, and whether warning signals and signs are present as required by the regulations.
 10. A statement as to the integrity of protective barriers, and the manner in which this was determined.
 11. A statement as to the methods of calculation, and a summary of results, including estimates of the maximum expected quarterly exposures to persons under the assumed conditions of use.
 12. The surveyor's conclusions as to whether the therapy installation will meet the requirements of [applicable parts] of the regulations under the assumed conditions of use.
 13. A description of all radiation measuring instruments used, including manufacturer, model designation and serial number.
 14. The calibration record of the instruments, including the method of calibration, name of the reference laboratory, identification of the reference source or instrument, the calibration energies and exposure rates.
 15. The physicist's recommendations to the user for minimization of unnecessary exposure and optimization of radiation safety.
 16. The date of the radiation protection survey and the signature of the surveyor, or of the directing physicist."
-

(a) Quoted from Ref. [1], with kind permission of the Radiologic Health Section, California Department of Health.

Following completion of the radiation survey, a written report should be submitted to the person in charge of the department or facility, and retained for a period of 5 years by the qualified expert who performed or directed the survey. The report should contain at least the following points:

- (a) A statement as to whether the installation is in compliance with applicable recommendations and pertinent government regulations;
- (b) A sketch indicating dose-equivalent rates in nearby occupied areas;
- (c) If the survey indicates that the applicable recommended permissible dose equivalent could be exceeded, taking into account workload W, beam orientation (use) factors U and occupancy factors T, appropriate corrective measures should be recommended;
- (d) Date, time, and a description of conditions such as primary beam energy, output or average beam current, and nature of scattering materials in the beam.

The legal requirements may be quite specific in the information to be supplied. As an example, Table XLVIII contains a detailed description of the contents of an acceptable radiation protection survey report, as set forth by the State of California for radiation-therapy installations [1]. This list may be used for guidance in preparing reports and adapted to other types of installations.

REFERENCE TO SECTION 5.4

- [1] CALIFORNIA DEPARTMENT OF HEALTH, RADIOLOGIC HEALTH SECTION, Contents of an Acceptable Protection Survey Report, Memorandum to radiological and health physicists, Sacramento, CA (June 1975).

5.5. Instrument calibration and maintenance

Each radiation survey instrument should be calibrated at intervals not exceeding three months and after each servicing and repair. Each such quarterly calibration should include a determination or correction of the response of the instrument to the type of radiation which it is designed to detect. An accuracy of $\pm 20\%$ is usually adequate for survey instruments. A record of the results of the most recent calibration should be maintained. The date of the last calibration should be indicated on the instrument.

Calibrations should be performed using radiation fields of known characteristics (energy spectrum, exposure or fluence rate, spatial distribution) of the type for which the instrument is to be used. For photon calibrations, ^{226}Ra , ^{60}Co and

TABLE XLIX. CHARACTERISTICS OF SELECTED RADIOACTIVE NEUTRON SOURCES

Source	Reaction	Half-life	Average neutron energy (MeV)	Yield per Bq (neutrons·s ⁻¹) ^a	Yield per Ci (neutrons·s ⁻¹) ^a
²¹⁰ Po-Be	α, n	138.4 d	4.2	68 × 10 ⁻⁶	2.5 × 10 ⁶
²²⁶ Ra-Be	α, n	1620 a	4.0	351 × 10 ⁻⁶	1.3 × 10 ⁷
²³⁸ Pu-Be	α, n	86.4 a	4.5	62 × 10 ⁻⁶	2.3 × 10 ⁶
²⁴¹ Am-Be	α, n	458 a	4.5	59 × 10 ⁻⁶	2.2 × 10 ⁶
²¹⁰ Po-B	α, n	138.4 d	¹⁰ B: 6.3 ¹¹ B: 4.5	16 × 10 ^{-6b}	6.0 × 10 ^{5b}
¹²⁴ Sb-Be	γ, n	60 d	0.024	35 × 10 ^{-6b,c}	1.3 × 10 ^{6b,c}
²⁵² Cf	spontaneous fission	2.65 a	2.35 (fission spectrum)	62 from 1 g ^d	2.3 × 10 ¹² from 1 g ^d

^a Compacted mixtures.

^b Relatively monoenergetic.

^c Yield can be increased about four times by encasing in beryllium.

^d Specific activity: 19.7 × 10¹² Bq·g⁻¹ (532 Ci·g⁻¹).

(Adapted from ICRP-21, Ref. [1], with kind permission of the International Commission on Radiological Protection and Pergamon Press.)

¹³⁷Cs sources are usually conveniently available, but many others are satisfactory, as long as their photon energy and the instrumental energy response are taken into account.

For neutron calibrations, small sources of the (α, n) type are quite satisfactory. They usually consist of an alpha emitter, such as ²¹⁰Po, ²³⁹Pu, or ²⁴¹Am, in combination with a target material, usually Be, in which the neutron-producing reaction takes place. Such sources are preferred over the (γ, n) type because of their high neutron yields relative to gamma radiations and because of their higher average neutron energies. Their energies, which extend as high as approximately 10 MeV, are more similar to the energies likely to be found in accessible areas around those linac installations where neutron measurements are needed. Table XLIX [1] summarizes characteristics of several types of neutron sources. Californium-252 (half-life 2.65 years) produces a fission spectrum which is also useful.

Care must be taken not to damage the sealed containers of these sources, as the alpha-emitting elements are the most dangerous when ingested or inhaled. Wipe-tests to check for leakage of radioactive materials should be made at the time of periodic instrument calibration.

For accurate neutron calibration, care must be taken to eliminate or reduce the effect of neutrons reflected from the floor or other objects, by keeping the source/detector distance small compared with the distances to reflecting objects.

Manufacturer's performance data should be available for each type of instrument or detector used, including, where appropriate:

- (a) Energy response
- (b) Directional response
- (c) Response as a function of dose rate
- (d) Response to radiations other than the type which the instrument is designed to detect
- (e) Sensitivity to ambient conditions such as temperature and barometric pressure
- (f) Diagrams and maintenance information

Pocket ion-chamber dose meters should be calibrated and checked for leakage at intervals not exceeding one year.

For instruments in regular or continuous use, it is advisable to have a small source located in a convenient place for operational checks.

REFERENCE TO SECTION 5.5

- [1] INTERNATIONAL COMMISSION ON RADIOLOGICAL PROTECTION, Data for Protection Against Ionizing Radiation from External Sources: Supplement to ICRP Publication 15, Report of ICRP Committee 3, ICRP Publication No. 21, Pergamon Press, Oxford (1973).

6. REQUIREMENTS FOR AN EFFECTIVE SAFETY PROGRAMME

6.1. Safety organization

The responsibility, in its broadest sense, for protection of personnel, facilities, the public and the environment from all types of hazards related to linac operations must rest with the management of the organization. Under its direction, a safety organization and programme appropriate to the needs of the project should be developed from the time the facility is first proposed.

The safety organization may include a committee of responsible staff members and individuals, such as the radiation safety officer (RSO), assigned on a continuing basis to specialize in and oversee particular areas. A typical composition of the committee might include the head of the department which operates the linac facility, the RSO, a fire-protection officer and a senior member of the linac operations staff. The committee and the responsible individuals may find it advisable from time to time to consult with qualified experts from outside the organization.

Supervisors of divisions or departments should be made responsible for safety of all kinds within their groups. It is, therefore, essential that they be kept informed of the safety policies and procedures developed for the organization.

During the times the accelerator is operating, the operator in charge should be specifically and directly responsible for its safe operation and be authorized to shut the accelerator off if he feels it is necessary in order to protect personnel or equipment.⁴¹

All employees have the responsibility of complying with safety practices, responding to emergency situations, and reporting unsafe conditions.

6.2. Safety programme

The programme for general facility safety should be developed by the safety committee of the organization, together with individuals responsible for certain aspects and, where appropriate, in consultation with outside experts. Safety practices must conform to government requirements. Although this manual deals primarily with radiological safety, it is to be emphasized that radiation is frequently not the major hazard. At many facilities, electrocution and

⁴¹ Because there is sometimes disagreement on safety matters between accelerator staff members and those who derive direct benefit from the use of the accelerator, it is good practice to provide separate administrative lines of authority for operators and users.

mechanical injury may be potentially more hazardous, and a balanced safety programme will reflect this. All aspects of safety should be considered, but the greatest effort should be directed to the areas of greatest risk.

A comprehensive safety programme for a large organization may typically include the following elements:

(a) The programme should commence when the project is first proposed and attempt to anticipate and avoid future safety problems by proper planning and design.

(b) A body of recent data, recommended practices and other information on relevant safety areas should be accumulated and made available to responsible persons. For radiation safety, a basic library may be chosen from the listing in the General Bibliography (Section 7).

(c) Responsible persons should become familiar with broad aspects of one or more areas of safety, relevant to the accelerator installation.

(d) Written guidelines and procedures for routine operations should be formulated and made widely available to personnel.⁴²

(e) Written procedures for emergency situations, e.g. fire, electrocution, medical emergency or radiation accident, should be formulated, made available to all personnel and posted in conspicuous places.

(f) Appropriate and adequate safety equipment, such as fire extinguishers and first-aid kits, should be provided.

(g) It is advisable to maintain a relationship with the staff of a nearby hospital, so that it can anticipate the facility's needs, and in order that minor injuries as well as emergency situations can be expeditiously treated.

(h) There should be periodic meetings, at least with supervisors, in order that they become familiar with safety guidelines and aware of new potential hazards as they arise.

(i) There should be occasional 'walk-throughs' of the facility by a team made up of members of the management and the safety organization, to gather an impression of the safety practices actually being followed.

(j) The management should enforce the safety programme developed under its direction with appropriate disciplinary measures, if the need arises.

(k) Finally, it is worth noting that a well-conceived safety programme is reasonable in its demands and does not unnecessarily impede normal laboratory activities. An overly rigid programme, zealously imposed, may generate resentment and lack of cooperation, and therefore be self-defeating.

⁴² Some facilities require that personnel sign a statement that they have read and understood the safety procedures.

6.3. Radiation safety

A radiation safety programme should be developed in coordination with the facility's overall safety programme, and in compliance with national, regional and local requirements. Recommendations of international organizations such as the IAEA, ICRP, ICRU, IEC and the Commission of the European Communities, as well as national commissions should be considered in the development of this programme (see General Bibliography, Section 7).

A radiation safety committee should be organized. In a large organization employing several radiation sources, or where the operations are complex or changing, this should be a single-purpose committee. In smaller installations, the functions of the committee may be performed by a general safety committee. Members of the responsible committee should keep informed of the most recent recommendations of advisory organizations, such as those listed above, as well as the legal requirements of their own locality. The functions of the radiation safety committee should include:

- Development of written rules and procedures for radiation safety;
- Review of proposed experiments, facility changes, or deviations from standard operating procedures;
- Advice to management, staff, and user groups on safety matters.

A radiation safety officer (RSO) should be appointed. His qualifications should be determined by the size and complexity of the operations. In a small organization, this may be a part-time responsibility of a technically competent person who is familiar with accelerator operations. In large organizations, the RSO may be the leader of a research-oriented group of radiation protection specialists.

The concepts 'radiation area' and 'high-radiation area' are useful at such installations as research facilities, where much of the work is non-routine. Under unusual beam conditions, radiation fields higher than anticipated in the original planning may temporarily exist in or near beam lines, in portions of an open radiation room adjacent to another room where the beam is being delivered, or near activated materials in an experimental or storage area. Areas so designated may also temporarily exist where radioactive sources are being used.

A *radiation area* is defined for this manual as an accessible area wherein a person could receive a dose equivalent in excess of 5 mrem, but less than 100 mrem, in any one hour if he were continuously present. A *high-radiation area* is an accessible area wherein a person could receive a dose equivalent of 100 mrem or more in any one hour if he were continuously present.⁴³

⁴³ Note that legal terminology and definitions that are different from these may prevail in various localities.

Note that these definitions do not specify the time dependence of the dose-equivalent rate during 'any one hour'. Thus the entire maximum dose equivalent permitted during that hour might be imparted by steady radiation, or it might be imparted by only one or a few accelerator pulses if it could be assured that the accelerator would be promptly turned off before the maximum is reached.

At a facility where operations are highly predictable, such as for radiation therapy, the containment area would include all areas which, under normal operating conditions, would be designated as radiation areas or high-radiation areas if they were accessible.

The radiation safety programme should include the following elements:

(a) A qualified expert should be consulted in the planning or engineering stage of the facility's development, to assist in the shielding design. This individual could be the RSO himself, someone approved by him from within the organization, or an outside consultant.

(b) A radiation survey should be performed by a qualified expert before the accelerator is placed in routine operation. Thereafter surveys should be made at least annually and after every change in equipment or mode of operation that may significantly affect radiation levels in accessible areas.

(c) An area of the facility should be designated as a controlled area.⁴⁴ The precise boundaries may be determined primarily by administrative convenience, but should include all areas within which the radiation level can exceed 0.01 rem/week. Areas designated as radiation areas, high-radiation areas or containment areas should all be within the controlled area.

(d) Criteria for classifying personnel as radiation workers⁴⁴ should be established. An underlying criterion is the likelihood of receiving 10% or more of the recommended annual permissible dose equivalent. Persons whose duties require frequent access to the controlled area are normally classified as radiation workers. Such a classification is needed in the establishment of the personnel dosimetry system.

(e) A personnel dosimetry programme utilizing, for example, film or TLDs should be established for radiation workers. In addition, frequently occupied areas both within and outside of the controlled area should be similarly monitored. A procedure for monitoring of occasional entries to the controlled area by other personnel or visitors from outside should be set up. In a clinical situation, which is normally under strict control during treatment times, no additional monitoring of occasional visits is needed. In an industrial or research setting,

⁴⁴ The user of this manual is reminded that other terminology and definitions may apply in his locality.

it is advisable that all persons entering the controlled area carry a dose meter and that visitors be escorted.

(f) Provision should be made for inventory, control and disposal of radioactive sources, including targets and beam dumps at linacs operating at energies above 6 MeV.

(g) Records of accumulated doses received by personnel should be maintained.

(h) A schedule for instrument calibration should be made and observed.

(i) Where appropriate, an environmental radiation survey programme should be established.

(j) A stock of radiation protection supplies should be maintained. This might include radiation ropes, warning signs, labels for radioactive pieces, instrument batteries, sources for instrument checks, and perhaps padlocks for securing areas and equipment.

(k) Locked cabinets should be reserved for storage of small radioactive sources and radiation safety keys.

(l) Where the possibility of removable radioactivity exists, 'smear tests' should be periodically performed on radioactive sources and other materials. A procedure for smear test evaluation should be designed.

(m) Proper control should be maintained over machining and welding operations on radioactive components. This should include a preliminary assessment of the radiological hazard, including the development of a work 'scenario' in some cases. Other provisions include health physics supervision of transport and setup, use of a lead screen, where possible, to protect the technician, and special personnel dosimetry (finger or hand dose meters in addition to pocket ion chambers). The work should be postponed as long as practicable, to allow the maximum decay time. In many cases it may be more advantageous to fabricate a new component rather than repair one that is radioactive. Face masks are not generally needed unless the work is exceptionally dusty.⁴⁵ Operations that produce coarse chips are preferred (turning, milling); grinding and sanding should be avoided if possible. Provision should be made for collection of chips as they are produced (for example, by a vacuum-cleaner nozzle mounted close to the working surface), and for machine and area decontamination following the work. Hot-cell facilities are not normally needed at electron accelerators.

⁴⁵ Since the electromagnetic cascade induces activity throughout the material, the specific activity of surface material is not likely to be particularly high in comparison with that of the interior. Whole-body exposure from the distributed activity normally dominates over exposure by inhalation or ingestion of surface material and face masks may interfere with efficient completion of the work.

(n) In the case of a high-energy, high-power facility, where an accumulation of tritium (^3H) is possible (Section 2.7.2), provision should be made for periodic tritium assessment, and possibly for storage of water drawn from cooling circuits. Although there is not normally a risk of ingestion, it is good practice to prevent excessive tritium concentrations from accumulating, so that special precautions are not needed in the case of either planned or accidental drainage.

(o) An environmental radiation monitoring programme may be needed for high-energy, high-power facilities. In this case, the monitors used should be capable of distinguishing between neutron and photon radiation. Neutron sensitivity is particularly important where skyshine might be significant. The equipment often can take the form of passive, integrating dose meters (e.g. TLDs), placed at intervals around the site boundary and periodically read. However, such units may not be capable of distinguishing low accelerator-related doses in the presence of a much larger natural background. Where continuous readings are desired or needed, a moderated BF_3 counter for neutrons, together with a scintillation or GM counter to detect photons, would be satisfactory.

6.4. Accelerator safety

The accelerator safety programme should include the following points where appropriate:

(a) An enclosed *containment area* should be constructed which is provided with interlocks to prevent entry while the beam is delivered. This is conceived as a more or less permanent enclosure, integral with the building, which is planned in advance to positively exclude persons from areas that are potentially very hazardous. The containment area will contain at least the accelerator, all primary beam lines, targets, beam dumps, and all other objects that can be struck by the primary beam. All areas that can be anticipated as being potential high-radiation areas should be included in the containment area and, as far as can be foreseen, radiation areas as well. In a clinical situation, the heavily shielded treatment and accelerator rooms comprise the containment area.

(b) Maximum reliance should be placed on passive rather than active elements of a safety system. Where possible, wall barriers and locks should be relied upon, rather than using warning devices or electrical equipment.

(c) The principle of fail-safe design should be utilized wherever possible in the design of safety systems. That is, any type of failure of the safety device or of power to the device will turn the accelerator off.

(d) Redundancy of devices should be employed when it would seem that this can enhance reliability.⁴⁶

⁴⁶ A well-designed interlock will generally have two switches wired in series to provide redundancy.

(e) Primary controls governing the operation of the accelerator should be capable of being locked.

(f) Provision should be made for safety interlocks⁴⁶, particularly door interlocks at entrances to the containment area, but also interlocks on easily removable safety devices such as shielding elements, and interlocks controlling the limits on beam orientation or intensity, where appropriate.

(g) When the accelerator is in operation, the operator in charge should have immediate responsibility for accelerator-related safety. He should be authorized to shut the accelerator off if he feels it is necessary in order to protect personnel or equipment.

(h) Where a radiation area exists outside of the containment area, it should be clearly indicated by a rope enclosing the area and a radiation sign bearing the words RADIATION AREA and indicating the highest approximate dose-equivalent rate within the area. A high-radiation area outside of the containment area should be delimited by a barrier such as a wall or fence. The entrance should be capable of being locked by the RSO or operator in charge. It should be marked by signs bearing the words HIGH-RADIATION AREA. Entrance to the high-radiation area is permitted only under supervision of the RSO. In areas where the only significant radiation is localized within a narrow secondary beam line and the work of the organization requires occasional access to the beam, some accommodation to facilitate such access may be made with the permission of the radiation safety committee (see Section 2.9).

(i) The containment area and all locations designated as high-radiation areas, and entrances to such locations, must be equipped with easily observable flashing or rotating red warning lights that operate automatically when, and only when, radiation is being produced.

(j) Continuously sensitive area radiation monitors should be positioned in high-radiation areas outside of the containment area. A reading of the radiation levels in such areas should be accessible at the main control console together with an audible alarm.

(k) Audible warning must be given prior to start-up of the accelerator. At the minimum, this may be by means of an intercom used to announce imminent accelerator turn-on. An automatically actuated warning used in conjunction with a preset time delay is advised for larger facilities. Because it may alarm patients undergoing radiation therapy, and because room access is under continuous control, the audible warning may be omitted in clinical situations. An audible signal continually sounded while radiation is being produced is recommended. In small installations, such as for radiotherapy, this need may be satisfied by the audible 'electrical' hum made by the equipment.

(l) When an interlock has been tripped, it should be possible to resume operation only by manually resetting controls at the location where the interlock has been tripped, and lastly at the main control console. This is in order

that the cause of the trip be understood and any unsafe condition at the location of the trip is noticed and corrected before resuming operation.

(m) If, for any reason, it is necessary to intentionally bypass a safety interlock, such action should be authorized by the RSO and the operator in charge, recorded in the operations logbook and posted at the control console and location of the interlock. The bypass should be removed as soon as possible.

(n) Emergency shutoff switches should be located within easy reach and be easily identifiable in containment areas and high-radiation areas. Such a switch should have positive indication as to the operative position of the switch and should include a manual reset at the same location so that the accelerator cannot be restarted from the main control console without manually resetting the cutoff switch.

(o) All safety and warning devices, including interlocks and emergency cutoff switches, should be checked for proper operation at intervals not to exceed 6 months.

(p) In large facilities where beams may be transported to more than one containment area, redundant positive means should be provided to prevent beams from being inadvertently directed to an occupied containment area. Examples of such means are the locking off of one or more transport magnets and the insertion of 'beam stoppers' into the beam line well upstream of the containment area to be occupied. In addition, an area monitor interlocked with the accelerator controls will enhance the radiation safety in such areas and is recommended.

(q) If the beam is transported into a vacuum system separate from that of the accelerator and the average beam power can exceed 10 kW, the possibility of collimator, target or beam-dump burnthrough should be considered [1, 2]. Adequate cooling should be provided to such devices, and additional devices to prevent or promptly detect such an occurrence should be provided if warranted.

REFERENCES TO SECTION 6.4

- [1] JENKINS, T.M., BUSICK, D.D., McCALL, R.C., NELSON, W.R., SVENSSON, G.K., WARREN, G.J., BAUMGARTEN, A., HARRIS, J.L., MURRAY, J.J., SEPPI, E.J., VETTERLEIN, R.J., Beam-safety considerations at the Stanford Linear Accelerator Center, Nucl. Saf. 11 6 (1970) 435.
- [2] WALZ, D., BUSICK, D., CONSTANT, T., CROOK, K., FRYBERGER, D., GILBERT, G., JASBERG, J., KELLER, L., MURRAY, J., SEPPI, E., VETTERLEIN, R., Tests and Description of Beam Containment Devices and Instrumentation – a New Dimension in Safety Problems, Stanford Linear Accelerator Center, Rep. SLAC-PUB-1223 (1973).

6.5. Linear accelerators used in radiation therapy

Special consideration must be given to the safe design, installation and utilization of equipment used in radiation therapy, in order to protect patients,

staff and the general public from unnecessary risks. Danger to the patient clearly may arise if the equipment fails to impart the prescribed radiation dose to the defined volume, and could even arise from ordinary mechanical or electrical hazards. Radiation warning devices, radiation interlocks and electrical interlocks are needed to protect the staff and other persons in a clinical environment. The general public is mainly protected by adequate radiation shielding of the radiation facility (Section 3).

References to regulatory and advisory material regarding safety at therapeutic facilities and to discussions of characteristics of electron linear accelerators used in therapy may be found following this section [1–27]. The most recent and detailed of these are the recommendations in preparation by the International Electrotechnical Commission (IEC) [1–3] which set forth safety recommendations as well as much needed standardized nomenclature for operating specifications. Standardized test procedures are also described. The IEC document is designed to become the international standard and should be followed where possible. There may be national and regional legal requirements to be satisfied, and a qualified expert should be consulted when equipment is to be installed. Countries with well-established standards include Canada, the Federal Republic of Germany, France, Japan and the United Kingdom.

The following qualitative discussion is meant as background to complement the detailed recommendations of the IEC. This material may serve as a basis of discussion in facility planning, equipment selection and development of a radiological safety programme. The emphasis is on questions of equipment design and use unique to radiation therapy, but some general points are repeated for completeness.

6.5.1. General radiation safety

Safety provisions such as door interlocks, a key-operated power switch, emergency shutoff switches within the treatment room, and radiation warning lights at each entrance to and within the treatment room are essential (see Sections 6.3, 6.4). Interlocks may also be required for areas such as roofs, basements or other rooms adjacent to the radiation room, if shielding is inadequate. A schedule for the periodic testing of all interlocks should be established.

Provision should be made to lock the equipment into a standby condition to allow safe entry to the radiation room for adjustment and patient set-up, while maintaining the equipment in a state of readiness. A desirable provision is a ‘hazard/safe’ switch⁴⁷ located just inside the door. The staff would be instructed to turn this switch off (‘safe’) upon entry for any reason. Resetting it would be

⁴⁷ The labelling ‘treatment/set-up’ would be more appropriate in a clinical setting, but the function would be identical.

the last operation to be performed when the operator leaves after each treatment set-up. The treatment facility must not be left unattended unless the key-operated power switch is locked off, to prevent unauthorized use.

Because of the very high dose rates delivered, no person is permitted in the treatment room other than the patient during irradiation. An essential step in the start-up procedure is a search of the treatment room by the responsible operator. The 'electrical' hum of the operating accelerator is generally sufficient to satisfy the need for a continuously sounding radiation warning. Since entry to the radiation room is strictly controlled during treatment times, radiation warning signs that may alarm patients may be omitted.

A closed-circuit television viewing system should be provided for continuous observation of the patient to confirm his correct position during treatment. Because of shielding requirements, transparent windows are not usually practical, and they are quite expensive compared with a closed-circuit television system. Means of aural communication should be provided for giving instructions and reassurance to the patient during treatment.

For accelerators operating above about 10 MeV, there may be activation of compensating filters and other components close to the target. These should be assessed and handled with care when removed or during servicing. If residual radiation is present when the accelerator is off, this should be assessed and personnel instructed as to the relative hazard represented by it. The average exposure over an area up to 100 cm² at 1 m from the housing of the treatment unit may be used for the assessment of residual radiation.

Radiation exposure by ingestion or inhalation is insignificant under normal conditions of use. Concentrations of radioactive air (Section 2.7) are never a problem at accelerators used for therapy, even if operating above the threshold energy (10.55 MeV), if ordinary ventilation is provided. Ozone production (Section 2.10) is never significant for accelerators used for therapy, with ordinary ventilation. (However, significant concentrations of ozone can be produced if an unattenuated electron beam is brought into the air, as is sometimes done at dual-purpose installations.) There are no other environmental implications of the operation of such a facility, apart from direct radiation, which is shielded against by methods outlined in Section 3. Radioactivity in cooling water, which is generally released directly to a domestic sewer system, is of no consequence at the accelerator beam power levels used in these units.

6.5.2. Reliability of dosimetry

A precise control of the dose delivered is achieved, on the one hand, by stability of accelerator energy and beam transport and, on the other, by stability in the mechanical and electronic components of the dosimetry.

Beam-monitor ionization chambers should be sealed to eliminate changes in sensitivity due to atmospheric fluctuations. An ion chamber should be designed to operate with nearly 100% ion collection efficiency at the highest ion density that occurs under normal operation. The stability of dosimetry should be periodically checked against a reference dose meter. The checks should consist of assessments of dosimetry precision (reproducibility of consecutive readings), short-term stability (tests at half-hour intervals), daily stability (at 8-hour intervals) and weekly stability (each day just following the start-up period, or at staggered intervals). A long-term stability of $\pm 2\%$ should be achievable. Periodic tests should be made for dosimetry linearity (by a series of irradiations over a wide range of absorbed dose), and for dependence on dose rate and beam orientation. For moving-beam therapy, the calibration should be checked during continuous movement of the equipment, using a reference dose meter fixed to the treatment head at the standard treatment distance. Tests should be periodically performed to ensure that the ratio of absorbed dose increment to increment of rotation (Gy/degree or rad/degree) corresponds to the prescribed ratio.

There should be two substantially independent dosimetry systems integral with the therapy dose control. They may be arranged as equivalent redundant systems, each of which is independently capable of terminating an irradiation, or as a primary/secondary pair. Either system must be capable of turning off the radiation when a preselected number of dosimetry units is reached, and means of verifying this function should be provided. The secondary dose meter (overdose monitor) should be set to terminate irradiation at a dose somewhat above the setting of the primary system. At least one of the monitors should be a transmission device which samples the entire field for all field sizes. Failure of the radiation-detector supply voltage should prevent irradiation. Provision for electronic self-checking of the dosimetry between irradiations is a valuable safety feature.

Calibrations against a dose meter whose own calibration is traceable to a recognized standards laboratory should be performed quarterly or after any change in the equipment that could cause a shift in calibration. Spot checks should be performed daily. Techniques of calibration dosimetry are too specialized to be treated here, and the protocols given in the General Bibliography (Section 7) should be consulted.

6.5.3. Control of dose distribution

Energy stability, focal spot position and beam direction on the target are fundamental requirements for the control of dose distribution. Energy variation affects both the depth-dose distribution and the lateral dose distribution; the relative distribution becomes narrower with increasing energy. If a magnetic transport system is used, adequate regulation of beam direction and focal spot

position must be provided. These properties are inherent in a well-designed magnetic transport system. In a treatment unit employing a scanned beam, adequate provision must be made to ensure proper functioning of the scanning and that no radiation pulses are missed.

One of the dosimetry systems should be sensitive to dose distribution (e.g. by a partitioned ionization chamber whose signals are compared), to detect grossly anomalous dose distributions that would be caused by the absence of a filter or scattering foil or by malfunctioning of a magnetic beam scanning system, if used.

The dose distribution for each beam-shaping device should be known from ionization chamber measurements in a water phantom at least 5 cm larger than the field size at the incident surface. The symmetry and 'flatness' of the beam should be verified by transverse radiation scans or isodose measurements.

The proper choice must be ensured of modality (electron or photon irradiation), compensating filters, scattering foils, collimation, and field shaping blocks, if used. All movable beam-shaping devices should be clearly labelled as to function. Devices attachable to the treatment head should be interlocked in such a manner as to guarantee correct positioning, where appropriate. Beam-shaping devices such as wedge filters should be designed to project an optical indication of field variation onto the patient's skin. The selection of devices should be made in two separate operations: by physically positioning the device, and by confirming its selection by a switch at the control console. The rationale for redundancy in selection is that the same mistake is much less likely to be made in two repeated operations separated by a small time interval than in a single operation.

Possible failures in some of these measures could result in a narrow beam of electrons in the centre of the intended radiation field and care must be taken that such serious accidents are prevented.

6.5.4. Safe delivery of the prescribed treatment

Specific equipment design features to ensure safe and precise dose delivery are briefly outlined:

(a) Because of the high dose rates used, the normal manner of terminating an irradiation must be by automatic shutoff when a number of dosimetry units, preset by the operator for each treatment, is reached.

(b) A timer should be provided which will terminate an irradiation if a time interval preselected by the operator is exceeded.

(c) The control panel should include a device, such as a dose-rate meter, which gives a positive indication of radiation production so that the operational status of the unit is immediately apparent to the operator at all times.

(d) A device to limit the accelerator beam current must be provided if an excessive dose rate is possible for any choice of operating parameters. This is of particular importance for electron therapy, because electron dose rates are very high compared with those imparted by photons produced on a target by the same electron current. Most accelerators are inherently capable of delivering unsafe currents, if not limited in some way.

(e) A dose-rate monitoring system should be provided which will automatically terminate an irradiation if the dose rate is higher than preset. A suggested setting of the dose-rate cut-off is at approximately twice the highest dose rate for normal operation to allow some margin for unimportant momentary variations. This provision is separate from the current-limiting system just described.

(f) The dosimetry systems should have sufficient range so that the actual dose delivered can be determined for any treatment, even if the irradiation is accidentally terminated by the secondary dose meter system (overdose monitor) or the timer at its maximum setting.

(g) Readout scales of the separate dosimetry systems, energy setting and maximum treatment time should be easy to read and interpret. To avoid confusion, only one fixed scale factor should be provided for the dosimetry readouts. The display of irradiation time should be in seconds or minutes, expressed as decimal numbers, but not in minutes and seconds together, in order to avoid misunderstanding.

(h) The unit should be incapable of beginning an irradiation until all relevant treatment parameters have been selected. These may include the prescribed modality (electron or photon irradiation), energy, number of dosimetry units, maximum elapsed time, fixed or moving-beam therapy, and additional filters, if prescribed. A specific provision should be that the number of dosimetry units is set anew for each irradiation, rather than permitting treatment with a setting remaining from the previous irradiation.

(i) Interlocks should prevent irradiation unless the parameters selected at the control console agree with the corresponding physical settings. This is particularly important where a choice of modality (electron or photon irradiation) is possible.

(j) A treatment parameter should not be displayed on the console until all required selection operations are made for that parameter, so that the operator will be made cognizant of any steps in the treatment set-up that have been overlooked. Alternatively, inconsistent selections should be flagged and treatment not allowed until the conflicting settings are resolved or the interlock is overridden in a separate step by an authorized person.

(k) If treatment parameters are digitally read in (via punched or magnetic cards), the operator should also have to manually confirm the treatment parameters, in order to satisfy the need for redundancy in parameter selection.

(l) There should be provision for manual treatment interruption, in case the treatment does not proceed as intended. In case of either automatic or manual

interruption, the dosimetry and elapsed time readings should be retained by the equipment, in order that the treatment can be immediately resumed. If the treatment cannot be completed at that time, this information can be used for later reassessment of the treatment plan.

(m) During stationary-beam treatment, unwanted movement of the therapy unit should not be possible.

(n) In moving-beam therapy, the speed of movement should be servo-controlled to be proportional to the dose rate, so that a constant value of dose per unit of motion results (e.g. constant gray/degree (rad/degree) for rotational therapy). Alternatively, the same end may be achieved by automatically controlling the dose rate to match the speed of movement. As a safeguard against failure of the movement control system, an interlock should terminate the irradiation if the prescribed motion is not actually followed.

(o) To avoid transcription errors, a provision for automatic generation of a record of the actual treatment parameters (independent of those prescribed) following treatment is desirable. Such records are useful in checking on treatment accuracy and may be of legal importance.

(p) If the accelerator stops for any cause other than the operation of the primary dose meter (e.g. equipment malfunction or actuation of an interlock), it should be immediately apparent to the operator. Ideally, the cause of the shutdown is automatically identified.

(q) The functioning of interlocks and trips which are seldom called into play should be regularly (and, if possible, automatically) checked.

6.5.5. Provisions to facilitate accurate patient positioning

(a) Scales for reading translational and rotational settings should be easy to read and interpret. The units used should be centimetres and degrees. To avoid ambiguity, the coordinate system should be so defined that negative coordinates are not used to describe position or orientation.

(b) The treatment unit and treatment table should be mechanically stable so that reliable and reproducible positioning is possible in all coordinates.

(c) A light beam with cross-hairs indicating the central axis, and an optical means of determining the SSD should be provided. The light field must be of adequate illumination and coincide, within limits, with the radiation field for all field geometries obtainable from the treatment head. For this purpose, the dimensions of the radiation field are defined by the 50% isodose, measured at the standard treatment distance.

(d) A system of backpointer, wall-mounted and/or ceiling-mounted alignment lasers or the equivalent should be available to facilitate patient positioning to within ± 2 mm relative to the beam axis and target distance, or to the beam isocentre in the case of isocentric equipment.

(e) The following mechanical adjustments directly affect the precision with which the treatment volume can be defined. Provision should be made to facilitate these adjustments, and the equipment should be sufficiently stable to retain adjustments over extended periods of time.

- Alignment of collimator assembly axis of rotation and beam central axis.
- Coincidence of axis of collimator assembly rotation and central axis of light beam and cross-hairs.
- Coincidence of the light beam with the useful beam and calibration of the collimator beam sizes for the standard treatment distance (SAD or standard SSD).
- Where isocentric therapy is used, the axes of collimator assembly rotation, gantry rotation and treatment table rotation should all intersect, within limits, at the beam isocentre.
- The treatment table vertical motion should be parallel to the downward-directed beam.
- Faces of collimator jaws should accurately describe a rectangle, when projected onto the patient plane.

6.5.6. Control of unwanted dose to patient

It is important to minimize the unwanted dose to healthy tissue, in order to limit the side effects of radiation treatment. The margin of healthy tissue surrounding the target volume which is irradiated by high treatment doses should be as small as possible, consistent with adequate treatment within the target volume. Large-area doses of stray radiation should also be limited by controlling the amount of 'leakage' radiation from the treatment head.

The use of computer-assisted treatment planning to complement the treatment unit is very useful in optimizing the accuracy of the dose delivered to the treatment volume, and in reducing unnecessary dose to healthy tissue, particularly sensitive organs in the proximity of the treatment volume.

The penumbra (defined, for example, as the distance at the field edge over which the field decreases from 80% to 20% of the central axis dose at the same depth) should be as narrow as possible to permit precise definition of the irradiated volume. In this regard, an advantage of the linear accelerator is the small beam diameter (spot or focal size) at the target. This is usually only a few millimetres and therefore small compared with radioactive gamma sources of comparable strength. Because of scattering of radiation within tissue or phantom material, there is a physical limitation on penumbra width, however, and it cannot be reduced to zero even with a point focal spot and perfectly aligned equipment. The penumbra should be measured using a small detector (e.g. an ionization chamber of 0.1 cm³ volume) for each treatment unit. A large penumbra may indicate that adjustment is needed.

With electron therapy, the most important clinical requirement is a rapid fall-off in dose with depth from 80% to 20% of the maximum dose, in order that healthy tissue beyond the treatment volume is protected. (The 80% isodose profile is typically considered the boundary of the treatment volume, and doses of the order of 20% of the treatment dose are tolerated by essentially all organs.) The slope of this portion of the depth-dose curve is very dependent on the amount of energy degradation by bremsstrahlung in any material in the electron beam (Section 2.4). Some means of diffusing the electron beam over the treatment area is necessary, and scattering foils are frequently used. These should be reduced to the minimum thickness that is still consistent with adequate beam diffusion. Magnetic beam scanning systems require no material in the beam path, but they lack the inherent simplicity of scattering foils. Because the practical range of electrons depends on their energy (Section 2.3), the primary electron beam should be almost monoenergetic. This can be achieved by magnetic analysis of the beam by a slit or collimator within the transport magnet, before the beam reaches the diffusing device. Electron energy spectra of a width of $\pm 10\%$ are generally considered sufficiently narrow.

In the case of photon irradiation, the amount of surface (skin) dose due to soft photons and electrons in the useful beam should be as low as possible. In the case of electron therapy, the amount of stray photon radiation in the useful beam, which imparts dose beyond the maximum electron range, should be kept low by minimizing the amount of material in the beam. Magnetic beam scanning systems are superior to scattering foils in this respect, but because they are not passive devices, additional protection must be added to ensure their correct functioning. The degree of beam contamination in either treatment mode can be read directly from a measured depth-dose profile.

A basic means of limiting the integral dose to the patient is by control of 'leakage' radiation by adequate thickness of the collimator and movable jaws. The leakage radiation in the patient plane should be considered separately from the leakage radiation at other angles. The leakage at other angles is primarily an economic problem, to be considered in evaluating room shielding requirements, whereas leakage in the patient plane may impart a significant radiation dose to the patient which is of no benefit to him.

Two regions within the patient plane are also distinguished: the area of the largest treatment field at the standard treatment distance and the area outside of this. The region which coincides with the largest treatment field is protected only by movable jaws when smaller fields are in use. Because of additional fixed collimation, the leakage radiation is smaller outside the area of the largest field size. In assessing leakage radiation it is customary to average the exposure rate over an area up to 100 cm^2 at 1 m from the target, but 'hot spots' should also be noted. These can most easily be detected by a wrap-around film technique using large-sized X-ray film, and later evaluated with survey instruments. The leakage

photon radiation in the patient plane (outside of the largest useful field) is generally specified as 0.1–0.2% of the useful beam at the same distance (Table III, Section 1.3).

Above about 10 MeV accelerator energy, neutrons contribute to the integral dose. They are difficult to assess and awkward to shield against, but their fluences can be reduced somewhat by the choice of materials used in the treatment head. The dose equivalent (rem) imparted by neutrons increases rapidly with energy and at 20–25 MeV is about $(3-5) \times 10^{-1}$ rem/Gy ($(3-5) \times 10^{-3}$ rem/rad) relative to the useful beam at the same distance from the target. The relative neutron dose does not vary as rapidly above this energy range. The manufacturer should state the amount of neutron leakage radiation in the patient plane, both within and outside of the useful beam, for each therapy unit produced by him. Facilities for neutron measurements are not usually available at hospitals and outside help should be obtained to make these measurements, if they are required (see Section 5.3).

6.5.7. Protection against other risks

(a) *Mechanical.* The emergency cut-off switches in the treatment room and at the control console should also be connected to turn off power to positioning motors within the treatment unit and treatment table, as well as the radiation. Power-driven movements that are used to position the accelerator and the patient for treatment should be controlled by switches which are spring-biased to the 'off' position so that continuous actuation is required for movement. Because of the great danger to the patient from failures in such control systems, there should be a backup. This may take the form of a second 'motion-off' switch at the therapy unit or a system of contact-sensing anti-collision guards. Automatic collision protection may also be obtained by computer monitoring of machine motions. Interlocks should prevent simultaneous manual control of machine motions from the control console and the treatment unit, thus ensuring that there is no unexpected movement during patient set-up, in the cases where automatic collision protection is not provided.

Assurance should be obtained that the treatment unit and table are securely anchored to the building.

(b) *Microwave radiation.* Assurance should be obtained that stray microwave radiation from the RF system is at an acceptable level (Sections 2.1.1, 6.6).

(c) *Electrical.* The accelerator should be installed in compliance with local electrical codes. It should be of Class-1 construction, i.e. all circuits and other conductive parts should be connected to ground by a low-resistance path. All equipment of the accelerator installation should be connected to the same grounding point.

All enclosures around live circuits should be secured with locks or special tools. Alternatively, cabinets should be interlocked so that power is disconnected when they are opened. A grounding hook at each high-voltage supply is essential. Pendant-type hand switches are prone to damage from being dropped onto the floor, with the risk of exposure of live parts. They should therefore be operated at low voltage (less than 24 V a.c. or 50 V d.c.). The IEC document "General Requirements for Safety of Electrical Equipment Used in Medical Practice" (Ref.[28]) gives useful guidance on standards of construction and methods of testing for electrical safety.

REFERENCES TO SECTION 6.5

- [1] INTERNATIONAL ELECTROTECHNICAL COMMISSION, Medical Electron Accelerators in the Range 1–50 MeV, Section 1: General, IEC Technical Committee No.62 C, Draft Standard No.62 C (Central Office) 4, Geneva (Nov. 1976, in preparation).
- [2] INTERNATIONAL ELECTROTECHNICAL COMMISSION, Medical Electron Accelerators in the Range 1–50 MeV, Section 2: Safety Requirements for Equipment (Manufacturers), IEC Technical Committee No.62, Draft Standard No.62 C (Central Office) 4, Geneva (Nov. 1976, in preparation).
- [3] INTERNATIONAL ELECTROTECHNICAL COMMISSION, Medical Electron Accelerators in the Range 1–50 MeV, Section 3: Performance Tolerances, IEC Technical Committee No.62, Draft Report No.SC62C-WG1 (Secretary) 24, Geneva (Oct.1978).
- [4] INTERNATIONAL COMMISSION ON RADIOLOGICAL PROTECTION, Protection Against Ionizing Radiation from External Sources, ICRP Publication 15, Pergamon Press, Oxford (1970).
- [5] UNITED KINGDOM DEPARTMENT OF HEALTH AND SOCIAL SECURITY, Code of Practice for the Protection of Persons Against Ionizing Radiations Arising from Medical and Dental Use, Her Majesty's Stationery Office, London (1972).
- [6] UNITED KINGDOM DEPARTMENT OF HEALTH AND SOCIAL SECURITY, Recommendations of the Radiotherapy Apparatus Safety Measures Panel, RASMP/75, London (1975).
- [7] DEUTSCHES INSTITUT FÜR NORMUNG (DIN), Medizinische Elektronenbeschleuniger-Anlagen, Strahlenschutzregeln für die Herstellung und Errichtung, Deutsche Normen DIN 6847, Beuth, Berlin (1965); This report is undergoing revision: Medizinische Elektronenbeschleuniger-Anlagen, Strahlenschutz für die Herstellung, draft version of Deutsche Normen DIN 6847 (Part I), Beuth, Berlin (1975); Medizinische Elektronenbeschleuniger-Anlagen, Strahlenschutz für die Errichtung, draft version of Deutsche Normen DIN 6847 (Part II), Beuth, Berlin (1975).
- [8] BUNDESMINISTERIUM FÜR ARBEIT UND SOZIALORDNUNG, BUNDESMINISTERIUM FÜR JUGEND, FAMILIE UND GESUNDHEIT, Verordnung über den Schutz vor Schäden durch Röntgenstrahlen (Röntgenverordnung), Bundesgesetzblatt I, No.18, Verlag Bundesanzeiger, Bonn (1973) 173.
- [9] BUNDESMINISTERIUM FÜR ARBEIT UND SOZIALORDNUNG, BUNDESMINISTERIUM FÜR JUGEND, FAMILIE UND GESUNDHEIT, Richtlinien für den Betrieb von Beschleunigeranlagen im medizinischen Bereich (Stand 1.3.73), Gemeinsames Ministerialblatt BMBL, No.5, Carl Heymanns, Cologne (1974) 80.

- [10] BUNDESMINISTERIUM FÜR ARBEIT UND SOZIALORDNUNG, BUNDES-MINISTERIUM FÜR JUGEND, FAMILIE UND GESUNDHEIT, Verordnung über den Schutz vor Schäden durch ionisierende Strahlen (Strahlenschutzverordnung), Bundesgesetzblatt, Verlag Bundesanzeiger, Bonn (1976).
- [11] BUREAU OF RADIOLOGICAL HEALTH, Suggested State Regulations for Control of Radiation in Therapy, Draft Revision, Rockville, MD (Dec. 1975).
- [12] NATIONAL COUNCIL ON RADIATION PROTECTION AND MEASUREMENTS, Medical X-Ray and Gamma-Ray Protection for Energies up to 10 MeV – Equipment Design and Use, NCRP Report No.33, Washington, DC (1968).
- [13] NATIONAL COUNCIL ON RADIATION PROTECTION AND MEASUREMENTS, Medical X-Ray and Gamma-Ray Protection for Energies up to 10 MeV, Structural Shielding Design and Evaluation, NCRP Report No.34, Washington, DC (1970). (This report is superseded by NCRP Report No.49, Ref.[14].)
- [14] NATIONAL COUNCIL ON RADIATION PROTECTION AND MEASUREMENTS, Structural Shielding Design and Evaluation for Medical Use of X-Rays and Gamma Rays of Energies up to 10 MeV, NCRP Report No.49, Washington, DC (1976). Full-sized reproductions of figures for shielding calculations are available as NCRP-49 (Adjunct). (This report supersedes NCRP Report No.34.)
- [15] BUREAU OF RADIOLOGICAL HEALTH, The Use of Electron Linear Accelerators in Medical Radiation Therapy, Overview Report No.1, Physical Characteristics, United States National Technical Information Service, No. PB-253 605, NTIS, Springfield, VA (Feb.1976); also published as HEW Publication No. (FDA) 76-8027, United States Department of Health, Education and Welfare, Rockville, MD (Feb. 1976).
- [16] BUREAU OF RADIOLOGICAL HEALTH, The Use of Electron Linear Accelerators in Medical Radiation Therapy, Overview Report No.2, Market and Use Characteristics: Current Status and Future Trends, United States National Technical Information Service, No.PB-246 226, NTIS, Springfield, VA (Jan. 1975).
- [17] BUREAU OF RADIOLOGICAL HEALTH, The Use of Electron Linear Accelerators in Medical Radiation Therapy, Overview Report No.3, Accident History, United States National Technical Information Service, No. PB-246 227, NTIS, Springfield, VA (May 1975).
- [18] BUREAU OF RADIOLOGICAL HEALTH, The Use of Electron Linear Accelerators in Medical Radiation Therapy, Overview Report No.4, Regulations, Standards and Guidelines, United States National Technical Information Service, No. PB-246 228, NTIS, Springfield, VA (June 1975).
- [19] AMERICAN ASSOCIATION OF PHYSICISTS IN MEDICINE, Code of practice for X-ray therapy linear accelerators, Med. Phys. 2 3 (1975) 110.
- [20] HEALTH AND WELFARE CANADA, Proposed Regulations – Therapy X-Ray Equipment, Radiation Protection Bureau of Health Protection Branch, Health and Welfare, Draft of Proposed Standards, Ottawa (April 1975).
- [21] ENVIRO-MED, INC., Specifications for a Microwave Linear Electron Accelerator for Radiotherapy, Rep. MPD-12, La Jolla, CA (Aug. 1969).
- [22] ENVIRO-MED, INC., The Application of Reliability Engineering Concepts to the Design of Radiation Therapy Accelerators, Rep. ESD-203, La Jolla, CA (Apr. 1970).
- [23] ENVIRO-MED, INC., Field Flatness, Symmetry and Penumbra Specifications for the CRTS Prototype Accelerator, Rep. ESD-207, La Jolla, CA (Apr. 1970).
- [24] ENVIRO-MED, INC., Summary of the CRTS Prototype Accelerator Specifications, Rep. ESD-210, La Jolla, CA (Apr. 1970).
- [25] ENVIRO-MED, INC., A Study of the Automation of Radiation Therapy Treatment Machines, Rep. EMI-273, La Jolla, CA (Feb. 1972).

- [26] KARZMARK, C.J., PERING, N.C., Electron linear accelerators for radiation therapy: history, principles and contemporary developments, *Phys. Med. Biol.* **18** 3 (1973) 321.
- [27] SCHITTENHELM, R., Zur Sicherheit von medizinischen Beschleunigeranlagen, *Strahlentherapie* **148** 5 (1974) 520.
- [28] INTERNATIONAL ELECTRO-TECHNICAL COMMISSION, Safety of Medical Electrical Equipment, Part 1, General Requirements, 1st ed., IEC Publication No.601-1, Geneva (1977).

6.6. Safety at industrial and research installations

The following safety areas are particularly relevant to industrial and research facilities. The suggestions given may be developed to meet the particular needs of the installation.

Emergencies. Notices of emergency procedures should be conspicuously posted. Emergency telephone numbers should be posted at every telephone (fire, emergency paramedical services, ambulance). Periodic instruction should be given in emergency procedures, including resuscitation techniques.

Electrical safety. Because of the variety of unusual circuitry found at research facilities, electrical safety should be given very careful attention. A fundamental aspect of electrical safety is the thorough training of personnel in the operation and safety provisions of the equipment used. All pertinent electrical codes should be well understood by responsible personnel and every attempt made to ensure compliance with them. The physical planning should allow convenient access to electrical equipment that is to be installed in dry, well-lighted locations. The provisions for enclosure, interlocking and grounding of circuits should be adequate. A grounding hook or preferably an automatic mechanical discharging device should be provided for high-voltage power supplies and particularly for capacitor banks. Only connectors approved by the safety organization should be installed, and they should be maintained in good repair at all times. Metal ladders should not be used for electrical work. The equipment should be turned off in an obvious and positive manner before working on it. (This is best accomplished by means of multiple padlocks, one for each person who wishes to lock out the circuit.) Work on energized high-voltage circuits should be undertaken only as a last resort and then only by persons having complete understanding of the equipment, and with cognizance of the responsible authorities. In such cases a standby person is essential.

Fire and explosion. Fire protection should be planned in terms of prevention, provision for prompt detection and containment. Unnecessary sources of ignition should be eliminated and unnecessary combustible loading should be removed. Flammable substances such as solvents, oils, acetylene, propane and hydrogen should be carefully stored, handled and properly disposed of. Cabling is susceptible

to fire and is particularly capable of propagating an existing fire. A smoke detector and automatic sprinkler system is advisable for most areas. Adequate fire extinguishers should be maintained and conveniently available. Adequate means of egress should be provided, particularly for the accelerator and target room(s).

Hydrogen. Liquid hydrogen is frequently used in experiments in nuclear and elementary particle physics. The precautions should include a committee review of each new experiment using hydrogen, ventilation to prevent dangerous accumulations, grounding to prevent electrostatic build-up, sealed wiring and switches, enclosure of necessary nearby electrical equipment in inert atmospheres at positive pressure, elimination of other sources of ignition, mechanical protection of thin target windows, and access control. Although emphasis must be placed on prevention, consideration must also be given to provisions for damage limiting, such as walls or partitions that are swung open by excess pressure. Electrical equipment used in the area should be of a type approved by national or regional authorities for the particular class of hazard.

Gas cylinders should be properly labelled, carefully handled, stored upright and secured to prevent overturning. Proper regulators and other fixtures should be used.

Hazardous materials. A variety of unusual materials may be used at large research institutions. They should be properly labelled, using words such as CAUTION, WARNING, DANGER, POISON, together with a brief explanation of the hazard (such as 'vapour harmful', 'harmful if absorbed through the skin', 'do not machine', etc.), as appropriate. An inventory should be kept of dangerous materials and they should be locked up until released to responsible persons for use. Among the materials sometimes found in laboratories are mercury, beryllium metal, lithium hydride, asbestos, polychlorinated biphenyls (PCBs), epoxy resins, acids, caustic liquids, ether and solvents. Where volatile materials are used, adequate ventilation should be available. Where acids, caustics or strong chemicals are used, emergency eye wash facilities and showers are advisable.

Solvents. Protection against harmful solvents should include breathing protection (ventilation, complete enclosure or respirators) and skin protection (avoidance, gloves or creams), in addition to precautions against fire. Extremely toxic solvents (e.g. carbon tetrachloride and carbon disulphide) should not be used.

Microwaves. Where microwave components, including klystrons, magnetrons, RF separators, RF cavities and connecting waveguides, are operating in accessible areas, there is a possibility of exposure to unsafe microwave intensities from openings in the system. Operating systems should remain entirely shielded and flanges and joints examined for integrity. An instrument, preferably one that does not distort the field appreciably, should be available to ensure that microwave intensities at frequencies between 10 MHz and 100 GHz do not exceed

10 mW·cm⁻² when averaged over any possible 0.1-hour period (there may be other limitations imposed by government authorities).

Rigging and handling of heavy objects. The handling of shielding blocks, large objects to be radiographed, and accelerator and beam-transport equipment gives rise to chances of accidents. Crane and forklift operators should be properly trained and provided with adequate equipment.

Magnetic fields. Magnets should bear a warning sign and, when energized, be marked by a flashing light. There should be positive means of ensuring that they are off for personnel working nearby. There is a risk that tools and other ferrous objects may be pulled into magnetic fields, causing injury or damage. Personnel should not be permitted to enter areas where their bodies are immersed in high magnetic fields, such as between the pole faces or in fringing fields of large magnets.

Noxious gases. Ozone and oxides of nitrogen formed in the air by radiation should be assessed. If necessary, steps should be taken to mitigate this health hazard (Section 2.10).

Noise. In rooms containing large motor-generators, compressors or boilers the limits of noise levels allowed by local standards may be exceeded. When engineering or administrative controls cannot bring the exposure of personnel down to the levels allowed, hearing protectors should be worn.

Vacuum safety. A special hazard is presented by large vacuum systems with thin windows such as, for example, the long, large-diameter pipes used in neutron time-of-flight facilities. The rupture of a window can result in a serious, even fatal, accident to a nearby person. There is danger of objects or persons being drawn into a system through a large window, and some possibility of ear damage, even with a small window, if the vacuum system is large enough. When the system is not in use, thin windows to large vacuum systems should be protected by temporary covers capable of withstanding atmospheric pressure. Alternatively, a gate valve near each end of a large vacuum pipe should be provided which can be closed to isolate the largest volume. Warning signs at the window should be used to alert personnel to this peculiar hazard and remind them to implement these protective measures. Unessential occupancy of the vicinity should be discouraged.

Radiation doors. The heavy, motor-operated doors that are used at many research facilities should be designed to permit safe operation. The operating switch should be designed such that continual manual activation is required for motion of the door to continue. A warning bell should sound while the door is in motion. Limit switches should prevent motion beyond the proper range, and the closing edge should be equipped with a pressure-sensitive safety plate which will disconnect power if a person or object is caught. Each door should also be capable of manual operation in case of power failure.

General provisions for safety should also include the provision and maintenance of emergency lighting and power, ventilation systems, respirators, emergency showers and eye wash facilities, self-contained breathing apparatus, air sampling equipment, safety glasses and safety shoes. Proper walking surfaces should be provided and liquid spills should be cleaned up promptly. Care should be exercised when climbing ladders and on equipment. Neatness, cleanliness and order provide an environment conducive to good safety habits.

Selected references on accelerator safety [1–3], electrical safety [4, 5], fire protection [6, 7], occupational safety [8, 9], and hazardous materials [10–12] are given at the end of this section. Appendix D contains addresses of organizations from which additional safety information of several kinds can be obtained.

REFERENCES TO SECTION 6.6

- [1] UNITED STATES ATOMIC ENERGY COMMISSION, Safety Guidelines for High Energy Accelerator Facilities, National Accelerator Committee, USAEC Division of Operational Safety, Washington, DC (1967).
- [2] UNITED STATES ENERGY RESEARCH AND DEVELOPMENT ADMINISTRATION, Operational Safety Standards, AECM Section 0550, USERDA, Washington, DC (periodically revised).
- [3] UNITED STATES ENERGY RESEARCH AND DEVELOPMENT ADMINISTRATION, Operational Safety Program Appraisals, AECM Section 0504, USERDA, Washington, DC (periodically revised).
- [4] UNITED STATES ATOMIC ENERGY COMMISSION, Electrical Safety Guides for Research, Safety and Fire Protection Technical Bulletin No.13, USAEC Division of Operational Safety, Washington, DC (1967).
- [5] TSENG, A., Safety Guidelines for Working on Energized Electrical Equipment, Supplementary Note to USAEC Safety and Fire Protection Technical Bulletin No.13 (Ref.[4]), Stanford Linear Accelerator Center (1977).
- [6] UNITED STATES ENERGY RESEARCH AND DEVELOPMENT ADMINISTRATION, Industrial Fire Protection, AECM Section 0552, USERDA, Washington, DC (periodically revised).
- [7] NATIONAL FIRE PROTECTION ASSOCIATION, Boston, MA, National Fire Codes, Vol.6 (published periodically).
- [8] OCCUPATIONAL SAFETY AND HEALTH ADMINISTRATION, Occupational Safety and Health Standards, Dept. of Labor, Federal Register, Vol. 39, No.125, Washington, DC (1974).
- [9] NATIONAL SAFETY COUNCIL, Accident Prevention Manual for Industrial Operations, 7th ed., Chicago, IL (1974).
- [10] DEPARTMENT OF HEALTH, EDUCATION AND WELFARE, Registry of Toxic Effects of Chemical Substances, National Institute for Occupational Safety and Health, US Dept. of HEW, Supt. of Documents, US Government Printing Office, Washington, DC (periodically updated).
- [11] SAX, N.I., Dangerous Properties of Industrial Materials, 4th ed., Van Nostrand, New York (1975).
- [12] PATTY, F.A., Industrial Hygiene and Toxicology, 2nd ed., Vol.II, Interscience, New York (1963).

7. GENERAL BIBLIOGRAPHY

Advisory material oriented towards concepts and standards

COUNCIL OF THE EUROPEAN COMMUNITIES, Council Directive Laying Down the Revised Basic Safety Standards for the Health Protection of the General Public and Workers against the Dangers of Ionizing Radiation, Official Journal of the European Communities, Vol.19, No.L187, Luxembourg (1976).

INTERNATIONAL ATOMIC ENERGY AGENCY, Basic Safety Standards for Radiation Protection, Safety Series No.9, 1967 Edition, IAEA, Vienna (1967).

INTERNATIONAL COMMISSION ON RADIATION UNITS AND MEASUREMENTS, Radiation Quantities and Units, ICRU Report No.19, Washington, DC (1971).

INTERNATIONAL COMMISSION ON RADIATION UNITS AND MEASUREMENTS, Dose Equivalent, Supplement to ICRU Report No.19, Washington, DC (1973).

INTERNATIONAL COMMISSION ON RADIATION UNITS AND MEASUREMENTS, Conceptual Basis for the Determination of Dose Equivalent (1976), ICRU Report No.25, Washington, DC (1976).

INTERNATIONAL COMMISSION ON RADIOLOGICAL PROTECTION, Recommendations of the International Commission on Radiological Protection, ICRP Publication No.26, Pergamon Press, Oxford (1977).

NATIONAL COUNCIL ON RADIATION PROTECTION AND MEASUREMENTS, Basic Radiation Protection Criteria, NCRP Report No.39, Washington, DC (1971).

NATIONAL COUNCIL ON RADIATION PROTECTION AND MEASUREMENTS, Review of the Current Status of Radiation Protection Philosophy, NCRP Report No.43, Washington, DC (1975).

Advisory material oriented towards accelerator-produced radiations (general)

AMERICAN NATIONAL STANDARDS INSTITUTE and NATIONAL BUREAU OF STANDARDS, Radiological Safety in the Design and Operation of Particle Accelerators, NBS Handbook No.107, Washington, DC (1970).

GUNDAKER, W.E., BOGGS, R.F., Recommendations for the Safe Operation of Particle Accelerators, United States Department of Health, Education and Welfare, National Center for Radiological Health, Report No. MORP 68-2, Rockville, MD (1968).

INTERNATIONAL COMMISSION ON RADIATION UNITS AND MEASUREMENTS, Basic Aspects of High-Energy Particle Interactions and Radiation Dosimetry, ICRU Rep. No. 28, Washington, DC (1978).

INTERNATIONAL COMMISSION ON RADIOLOGICAL PROTECTION, Protection Against Electromagnetic Radiations Above 3 MeV, and Electrons, Neutrons and Protons, ICRP Publication No.4, Macmillan, New York (1964).

INTERNATIONAL COMMISSION ON RADIOLOGICAL PROTECTION, Protection Against Ionizing Radiation from External Sources, Report of Committee 3, ICRP Publication No.15, Pergamon Press, Oxford (1969).

INTERNATIONAL COMMISSION ON RADIOLOGICAL PROTECTION, Data for Protection Against Ionizing Radiation from External Sources: Supplement to ICRP Publication 15, Report of Committee 3, ICRP Publication No.21, Pergamon Press, Oxford (1973).

NATIONAL COUNCIL ON RADIATION PROTECTION AND MEASUREMENTS, Protection Against Betatron-Synchrotron Radiations up to 100 Million Electron Volts, NCRP Report No.14, published as National Bureau of Standards Handbook No.55, US National Bureau of Standards, Washington, DC (1954).

NATIONAL COUNCIL ON RADIATION PROTECTION AND MEASUREMENTS, Radiation Protection Design Guidelines for 0.1 – 100 MeV Particle Accelerator Facilities, NCRP Report No.51, Washington, DC (1977).

UNITED STATES DEPARTMENT OF HEALTH, EDUCATION AND WELFARE, Particle Accelerator Safety Manual, United States Department of Health, Education and Welfare, National Center for Radiological Health, Report No.MORP 68–12, Rockville, MD (1968).

UNITED STATES NATIONAL BUREAU OF STANDARDS, NATIONAL COUNCIL ON RADIATION PROTECTION AND MEASUREMENTS, Shielding for High-Energy Electron Accelerator Installations, NBS Handbook No.97 and NCRP Report No.31, Washington, DC (1964).

Advisory material which discusses accelerator-produced neutrons

INTERNATIONAL COMMISSION ON RADIATION UNITS AND MEASUREMENTS, Neutron Fluence, Neutron Spectra and Kerma, ICRU Report No.13, Washington, DC (1969).

NATIONAL BUREAU OF STANDARDS, Protection Against Neutron Radiation up to 30 Million Electron Volts, NBS Handbook No.63, Washington, DC (1957).

NATIONAL COUNCIL ON RADIATION PROTECTION AND MEASUREMENTS, Protection Against Neutron Radiation, NCRP Report No.38, Washington, DC (1971).

Advisory material oriented towards medical accelerator safety

DEUTSCHER NORMENAUSSCHUSS (DNA), Medizinische Elektronenbeschleuniger-Anlagen, Draft Reports No.DIN-6847, Part 1: Radiation Protection Rules for Manufacture, Part 2: Radiation Protection Rules for Installation, Beuth-Vertrieb, Berlin (1975).

INTERNATIONAL ELECTROTECHNICAL COMMISSION, Medical Electron Accelerators in the Range 1 – 50 MeV, Section 1: General, IEC Technical Committee No.62, Draft Standard No.62C (General Office) 4, Geneva (Nov.1976).

INTERNATIONAL ELECTROTECHNICAL COMMISSION, Medical Electron Accelerators in the Range 1 – 50 MeV, Section 2: Safety Requirements for Equipment (Manufacturer), IEC Technical Committee No.62, Draft Standard No.62C (General Office) 4, Geneva (Nov.1976).

INTERNATIONAL ELECTROTECHNICAL COMMISSION, Medical Electron Accelerators in the Range 1 – 50 MeV, Section 3: Performance Tolerances, IEC Technical Committee No.62, Draft Report No.SC62C-WG1 (Secretary) 24, Geneva (Oct.1978).

NATIONAL COUNCIL ON RADIATION PROTECTION AND MEASUREMENTS, Medical X-Ray and Gamma-Ray Protection for Energies up to 10 MeV – Equipment Design and Use, NCRP Report No.33, Washington, DC (1970).

NATIONAL COUNCIL ON RADIATION PROTECTION AND MEASUREMENTS, Medical X-Ray and Gamma-Ray Protection for Energies up to 10 MeV – Structural Shielding Design and Evaluation, NCRP Report No.34, Washington, DC (1970). (Superseded by NCRP Report No.49.)

NATIONAL COUNCIL ON RADIATION PROTECTION AND MEASUREMENTS, Structural Shielding Design and Evaluation for Medical Use of X-Rays and Gamma-Rays of Energies up to 10 MeV (1976), NCRP Report No.49, Washington, DC (1976). (This report supersedes NCRP Report No.34 of 1970. Full-sized reproductions of figures for shielding calculations are available as an adjunct to this report.)

WORLD HEALTH ORGANIZATION, Planning of Radiotherapy Facilities, Technical Report Series No.328, WHO, Geneva (1966).

Advisory material on radiological protection, useful at accelerator installations, but broader in scope

INTERNATIONAL ATOMIC ENERGY AGENCY, The Provision of Radiological Protection Services, Safety Series No.13, IAEA, Vienna (1965).

INTERNATIONAL ATOMIC ENERGY AGENCY, Radiation Protection Procedures, Safety Series No.38, IAEA, Vienna (1973).

NATIONAL BUREAU OF STANDARDS, A Manual of Radioactivity Procedures, NBS Handbook No.80 and NCRP Report No.28, Washington, DC (1961).

NATIONAL BUREAU OF STANDARDS, Physical Aspects of Irradiation, NBS Handbook No.85 and ICRU Report No.10b, Washington, DC (1964).

NATIONAL COUNCIL ON RADIATION PROTECTION AND MEASUREMENTS, Safe Handling of Radioactive Materials, NCRP Report No.29 and NBS Handbook No.92, Washington, DC (1964).

Advisory material related to radiation monitoring

INTERNATIONAL ATOMIC ENERGY AGENCY, The Use of Film Badges for Personnel Monitoring, Safety Series No.8, IAEA, Vienna (1962).

INTERNATIONAL ATOMIC ENERGY AGENCY, The Basic Requirements for Personnel Monitoring, Safety Series No.14, IAEA, Vienna (1965).

INTERNATIONAL ATOMIC ENERGY AGENCY, Personnel Dosimetry Systems for External Radiation Exposures, Technical Reports Series No.109, IAEA, Vienna (1970).

INTERNATIONAL ATOMIC ENERGY AGENCY, Handbook on Calibration of Radiation Protection Monitoring Instruments, Technical Reports Series No.133, IAEA, Vienna (1971).

INTERNATIONAL COMMISSION ON RADIATION UNITS AND MEASUREMENTS, Radiation Protection Instrumentation and its Application, ICRU Report No.20, Washington, DC (1971).

INTERNATIONAL COMMISSION ON RADIOLOGICAL PROTECTION, General Principles of Monitoring for Radiation Protection of Workers, ICRP Publication No.12, Pergamon Press, London (1969).

NATIONAL COUNCIL ON RADIATION PROTECTION AND MEASUREMENTS, Radiological Monitoring Methods and Instruments, NCRP Report No.10 and NBS Handbook No.51, Washington, DC (1952).

NATIONAL COUNCIL ON RADIATION PROTECTION AND MEASUREMENTS, Instrumentation and Monitoring Methods for Radiation Protection, NCRP Rep. No.57, Washington, DC (1978).

Handbooks and data tabulations

BERGER, M.J., SELTZER, S.M., Tables of Energy Losses and Ranges of Electrons and Positrons, National Aeronautics and Space Administration, Rep. NASA-SP-3012, Washington, DC (1974); Additional Stopping Power and Range Tables for Protons, Mesons, and Electrons, National Aeronautics and Space Administration, Rep. NASA SP-3036, Washington, DC (1966). (These reports are available at the Office of Technical Services, Washington, DC 20230.)

BUREAU OF RADIOLOGICAL HEALTH, Radiological Health Handbook, Bureau of Radiological Health, Public Health Service, United States Department of Health, Education and Welfare, Rockville, MD (1970).

GOLDMAN, D.T., ROESSER, J.R., Chart of the Nuclides, 9th ed., Knolls Atomic Power Laboratory, General Electric Co., Schenectady, NY (1966).

HUBBELL, J.H., Photon Cross Sections, Attenuation Coefficients, and Energy Absorption Coefficients from 10 keV to 100 GeV, United States National Bureau of Standards, Publication No. NSRDS-NBS 29, Washington, DC (1969).

HUBBELL, J.H., Photon mass attenuation and mass energy-absorption coefficients for H, C, N, O, Ar and seven mixtures from 0.1 keV to 20 MeV, Radiat. Res. **70** (1977) 58.

LEDERER, C.M., HOLLANDER, J.M., PERLMAN, I., Table of Isotopes, 6th ed., John Wiley, New York (1967).

NACHTIGALL, D., Table of Specific Gamma Ray Constants, Karl Thiemiig, Munich (1969).

PAGES, L., BERTEL, E., JOFFRE, H., SKLAVENTIS, L., Energy loss, range, and bremsstrahlung yield for 10-keV to 100-MeV electrons in various elements and chemical compounds, At. Data Nucl. Data Tables **4** 1 (1972) 1-127.

PARTICLE DATA GROUP, Review of Particle Properties, Lawrence Berkeley Laboratory, Rep. LBL-100 (1978); Rev. Mod. Phys. **75B** 1 (1978).

PLECHATY, E.F., CULLEN, D.E., HOWERTON, R.J., Tables and Graphs of Photon Interaction Cross Sections from 1.0 keV to 100 MeV Derived from the LLL Evaluated Nuclear Data Library, Lawrence Livermore Laboratory, Rep. UCRL-50400, Vol.6, Rev.1 (1975).

SEELMANN-EGGEBERT, W., PFENNIG, G., MÜNZEL, H., Nuklidkarte, 3rd ed., Institut für Radiochemie, Kernforschungszentrum Karlsruhe, Bundesminister für Wissenschaftliche Forschung, Bonn (1968).

STORM, E., ISRAEL, H.I., Photon Cross Sections from 0.001 to 100 MeV for Elements 1 through 100, Los Alamos Scientific Laboratory, Rep. LA-3753, UC-34, Physics, TID-4500 (1967); "Photon cross sections from 1 keV to 100 MeV for elements $Z = 1$ to $Z = 100$ ", Nuclear Data Tables **A7**, Academic Press, New York (1970) 565-681.

UNITED KINGDOM DEPARTMENT OF EMPLOYMENT, Handbook of Radiological Protection, Her Majesty's Stationery Office, London (1971).

VEIGELE, W.J., Photon cross sections from 0.1 keV to 1 MeV for elements $Z = 1$ to $Z = 94$, *At. Data Tables* 5 1 (1973) 51–111.

WANG, Y., Ed., *Handbook of Radioactive Nuclides*, Chemical Rubber Co., Cleveland, Ohio (1969).

Conference proceedings on accelerator-produced radiations

“ETTORE MAJORANA” CENTER FOR SCIENTIFIC CULTURE, INTERNATIONAL SCHOOL OF RADIATION DAMAGE AND PROTECTION, First Course on High Energy Radiation Dosimetry and Protection, held at Erice, 1–10 Oct. 1975, *IEEE Trans. Nucl. Sci. NS-23* 4 (1976) 1318.

EUROPEAN ORGANIZATION FOR NUCLEAR RESEARCH, Proc. Int. Congr. Protection Against Accelerator and Space Radiation, held at Geneva, 26–30 Apr. 1971, CERN Rep.No.71–16, Geneva (1971).

STEVENSON, G.R., Ed., Proc. Conf. Radiation Protection in Accelerator Environments, held at the Rutherford Laboratory, Mar. 1969, Chilton, Didcot, Oxon. (1969).

UNITED STATES ATOMIC ENERGY COMMISSION, Proc. USAEC First Symp. Accelerator Radiation Dosimetry and Experience, held at Brookhaven National Laboratory, Upton, NY, 3–5 Nov. 1965, USAEC, Div. Technical Information, Rep. CONF-651109, Washington, DC (1965).

UNITED STATES ATOMIC ENERGY COMMISSION, Proc. Second Int. Conf. Accelerator Dosimetry and Experience, held at the Stanford Linear Accelerator Center, Stanford, CA, 5–7 Nov. 1969, USAEC, Div. Technical Information, Rep. CONF-691101, Washington, DC (1969).

UNITED STATES ATOMIC ENERGY COMMISSION, Conf. Particle Accelerators in Radiation Therapy, held at Los Alamos Scientific Laboratory, 2–5 Oct. 1972, USAEC and Los Alamos Scientific Laboratory Rep. LA-5180-C, available from Technical Information Center, Oak Ridge, TN (1972).

Textbooks and review articles on accelerator health physics

BRYNJOLFSSON, A., MARTIN, T.G., III, Bremsstrahlung production and shielding of static and linear electron accelerators below 50 MeV. Toxic gas production, required exhaust rates, and radiation protection instrumentation, *Int. J. Appl. Radiat. Isot.* 22 (1971) 29.

FREYTAG, E., *Strahlenschutz an Hochenergiebeschleunigern*, G. Braun, Karlsruhe (1972).

LADU, M., “Problems of safety and radiation protection around high-energy accelerators”, *Progress in Nuclear Energy, Ser. XII, Health Physics, Vol. II*, Pergamon Press, Oxford (1969).

NEAL, R.B., Gen. Ed., DUPEN, D.W., HOGG, H.A., LOEW, G.A., Eds, *The Stanford Two-Mile Accelerator*, Benjamin, New York (1968). (Particularly Ch.26, DeSTAEBLER, H., JENKINS, T.M., NELSON, W.R., “Radiation and shielding”.)

PATTERSON, H.W., THOMAS, R.H., *Accelerator Health Physics*, Academic Press, New York and London (1973).

Textbooks on basic radiation protection

LAPP, R.E., ANDREWS, H.L., Nuclear Radiation Physics, 4th ed., Prentice-Hall, Englewood Cliffs, NJ (1972).

MORGAN, K.Z., TURNER, J.E., Eds, Principles of Radiation Protection, John Wiley, New York (1967).

SHAPIRO, J., Radiation Protection – A Guide for Scientists and Physicians, Harvard University Press, Cambridge, MA (1972).

References on nuclear and particle physics

EVANS, R.D., The Atomic Nucleus, McGraw Hill, New York (1955).

HALLIDAY, D., Introductory Nuclear Physics, 2nd ed., John Wiley, New York (1955).

ROSSI, B., High-Energy Particles, Prentice-Hall, Englewood Cliffs, NJ (1956).

Basic references on dosimetry and instrumentation

ATTIX, F.H., ROESCH, W.C., TOCHILIN, E., Eds, Radiation Dosimetry, 2nd ed. (in three volumes: Vol.I: Fundamentals; Vol.II: Instrumentation; Vol.III: Sources, Fields, Measurements and Applications), Academic Press, New York (1968, 1966, 1969).

HANDLOSER, J.S., Health Physics Instrumentation, Pergamon Press, London (1959).

HINE, G.J., BROWNELL, G.L., Eds, Radiation Dosimetry, Academic Press, New York (1956).

KASE, K.R., NELSON, W.R., Concepts of Radiation Dosimetry, Pergamon, Press, New York (1978).

PRICE, W.J., Nuclear Radiation Detection, McGraw-Hill, New York (1958).

ROSSI, B.B., STAUB, H.H., Ionization Chambers and Counters: Experimental Techniques, McGraw-Hill, New York (1949).

General references on radiation shielding

JAEGER, R.G., BLIZARD, E.P., CHILTON, A.B., GROTENHUIS, M., HÖNIG, A., JAEGER, T.A., EISENLOHR, H.H., Eds, Engineering Compendium on Radiation Shielding, Vol.1, Shielding Fundamentals and Methods, IAEA, Vienna, Springer-Verlag, New York (1968).

PRICE, B.T., HORTON, C.C., SPINNEY, K.T., Radiation Shielding, Pergamon Press, Oxford (1957).

ROCKWELL, T., III, Ed., Reactor Shielding Design Manual, Van Nostrand, Princeton, NJ (1956).

SCHAEFFER, N.M., Ed., Reactor Shielding for Nuclear Engineers, United States Atomic Energy Commission, Office of Technical Services, Rep. TID-25951, Oak Ridge, TN (1973).

Calibration and dosimetry for radiation therapy

AMERICAN ASSOCIATION OF PHYSICISTS IN MEDICINE, Protocol for the dosimetry of high energy electrons, *Phys. Med. Biol.* **11** (1966) 505.

AMERICAN ASSOCIATION OF PHYSICISTS IN MEDICINE, A code of practice for the dosimetry of 2 to 35 MV X-ray and caesium-137 and cobalt-60 gamma-ray beams, *Phys. Med. Biol.* **14** (1969) 1.

AMERICAN ASSOCIATION OF PHYSICISTS IN MEDICINE, Protocol for the dosimetry of X- and gamma-ray beams with maximum energies between 0.6 and 50 MeV, by Scientific Committee on Radiation Dosimetry SC(RAD) of the American Association of Physicists in Medicine, *Phys. Med. Biol.* **16** (1971) 377.

AMERICAN ASSOCIATION OF PHYSICISTS IN MEDICINE, Code of practice for X-ray therapy linear accelerators, *Med. Phys.* **2** 3 (1975) 110.

HOSPITAL PHYSICISTS ASSOCIATION, A Practical Guide to Electron Dosimetry (5–35 MeV), HPA Report Series No.4, London (1971).

HOSPITAL PHYSICISTS ASSOCIATION, Central axis depth dose data for use in radiotherapy, *Br. J. Radiol., Suppl.* No.11 (1972).

INTERNATIONAL COMMISSION ON RADIATION UNITS AND MEASUREMENTS, Radiation Dosimetry: X-Rays and Gamma Rays with Maximum Photon Energies Between 0.6 and 50 MeV, ICRU Report No.14, Washington, DC (1969).

INTERNATIONAL COMMISSION ON RADIATION UNITS AND MEASUREMENTS, Electrons with Initial Energies between 1 and 50 MeV, ICRU Report No.21, Washington, DC (1972).

INTERNATIONAL COMMISSION ON RADIATION UNITS AND MEASUREMENTS, Measurement of Absorbed Dose in a Phantom Irradiated by a Single Beam of X or Gamma Rays (1972), ICRU Report No.23, Washington, DC (1972).

INTERNATIONAL COMMISSION ON RADIATION UNITS AND MEASUREMENTS, Determination of Absorbed Dose in a Patient Irradiated by Beams of X or Gamma Rays in Radiotherapy Procedures (1976), ICRU Report No.24, Washington, DC (1976).

INTERNATIONAL COMMISSION ON RADIATION UNITS AND MEASUREMENTS, Dose Specification for Reporting External Beam Therapy with Photons and Electrons, ICRU Report No.29, Washington, DC (1978).

MASSEY, J.B., Manual of Dosimetry in Radiotherapy, IAEA, Vienna (1970).

NORDIC ASSOCIATION OF CLINICAL PHYSICS, Procedures in radiation therapy dosimetry with 5 to 50 MeV electrons and roentgen and gamma rays with maximum photon energies between 1 MeV and 50 MeV, *Acta Radiol.* **11** (1972) 603–24.

Environmental radiation

NATIONAL COUNCIL ON RADIATION PROTECTION AND MEASUREMENTS, Environmental Radiation Measurements, NCRP Report No.50, Washington, DC (1977).

SLADE, D.H., Ed., Meteorology and Atomic Energy 1968, United States Atomic Energy Commission, Div. of Tech. Information, Washington, DC, Rep. No. TID-24190 (1968); available from Clearinghouse for Federal Scientific and Technical Information, Springfield, VA.

APPENDIXES

Appendix A

PHYSICAL AND NUMERICAL CONSTANTS

TABLE A-I. PHYSICAL AND NUMERICAL CONSTANTS^a

PHYSICAL CONSTANTS		UNCERTAINTIES (ppm)
N_A	$= 6.0220943(63) \times 10^{23} \text{ mol}^{-1}$	1.05
V_m	$= 22413.83(70) \text{ cm}^3 \cdot \text{mol}^{-1} = \text{molar volume of ideal gas at STP}$	31
c	$= 2.99792458(1.2) \times 10^{10} \text{ cm} \cdot \text{s}^{-1}$	0.004
e	$= 4.803242(14) \times 10^{-10} \text{ esu} = 1.6021892(46) \times 10^{-19} \text{ C}$	2.9; 2.9
1 MeV	$= 1.6021892(46) \times 10^{-6} \text{ erg}$	2.9
$\hbar = \hbar/2\pi$	$= 6.582173(17) \times 10^{-22} \text{ MeV} \cdot \text{s} = 1.0545887(57) \times 10^{-27} \text{ erg} \cdot \text{s}$	2.6; 5.4
$\hbar c$	$= 1.9732858(51) \times 10^{-11} \text{ MeV} \cdot \text{cm} = 197.32858(51) \text{ MeV} \cdot \text{fm}$ $= 0.6240078(16) \text{ GeV} \cdot \text{mb}^{1/2}$	2.6; 2.6 2.6
α	$= e^2/\hbar c = 1/137.035982(30)$	0.22
$k_{\text{Boltzmann}}$	$= 1.380662(44) \times 10^{-16} \text{ erg} \cdot \text{K}^{-1}$ $= 8.61735(28) \times 10^{-11} \text{ MeV} \cdot \text{K}^{-1} = 1 \text{ eV}/11604.50(36) \text{ K}$	32 32; 32
m_e	$= 0.5110034(14) \text{ MeV} = 9.109534(47) \times 10^{-31} \text{ kg}$	2.8; 5.1
m_p	$= 938.2796(27) \text{ MeV} = 1836.15152(70) m_e = 6.72270(31) m_{\pi^\pm}$ $= 1.007276470(11) \text{ u}$	2.8; 0.38; 46 0.011
1 u	$= (1/12) m_{C^{12}} = 931.5016(26) \text{ MeV}$	2.8
m_d	$= 1875.628(5) \text{ MeV}$	3
r_e	$= e^2/m_e c^2 = 2.8179380(70) \text{ fm}$	2.5
λ_e	$= \hbar/m_e c = r_e \alpha^{-1} = 3.8615905(64) \times 10^{-11} \text{ cm}$	1.6
$a_\infty \text{ Bohr}$	$= \hbar^2/m_e e^2 = r_e \alpha^{-2} = 0.52917706(44) \text{ \AA} = 0.052917706(44) \text{ nm}$	0.82

σ_{Thomson}	$= (8/3) \pi r_e^2 = 0.6652448(33) \times 10^{-24} \text{ cm}^2 (10^{-24} \text{ cm}^2 = 1 \text{ b})$	4.9
μ_{Bohr}	$= e\hbar/2m_e c = 0.57883785(95) \times 10^{-14} \text{ MeV} \cdot \text{G}^{-1} = 0.57883785(95) \times 10^{-10} \text{ MeV} \cdot \text{T}^{-1}$	1.6
μ_p	$= e\hbar/2m_p c = 3.1524515(53) \times 10^{-18} \text{ MeV} \cdot \text{G}^{-1} = 3.1524515(53) \times 10^{-14} \text{ MeV} \cdot \text{T}^{-1}$	1.7
μ_p/μ_{Bohr}	$= 1.520993136(21)$	0.014
$1/2\omega_{\text{cyclotron}}^e$	$= e/2m_e c = 8.794023(25) \times 10^6 \text{ rad} \cdot \text{s}^{-1} \cdot \text{G}^{-1} = 8.794023(25) \times 10^{10} \text{ rad} \cdot \text{s}^{-1} \cdot \text{T}^{-1}$	2.8
$1/2\omega_{\text{cyclotron}}^p$	$= e/2m_p c = 4.789378(13) \times 10^3 \text{ rad} \cdot \text{s}^{-1} \cdot \text{G}^{-1} = 4.789378(13) \times 10^7 \text{ rad} \cdot \text{s}^{-1} \cdot \text{T}^{-1}$	2.8

Hydrogen-like atom (non-relativistic, μ = reduced mass):

$$\left(\frac{v}{c}\right)_{\text{rms}} = \frac{Ze^2}{n\hbar c}, \quad E_n = \frac{\mu}{2} v^2 = \frac{\mu Z^2 e^4}{2(n\hbar)^2}, \quad a_n = \frac{n^2 \hbar^2}{\mu Z e^2}$$

$$R_\infty = m_e e^4 / 2\hbar^2 = m_e c^2 \alpha^2 / 2 = 13.605804(36) \text{ eV (Rydberg)} \quad 2.6$$

$$= m_e c \alpha^2 / 2\hbar = 109737.3143(10) \text{ cm}^{-1} \quad 0.009$$

1 year (sidereal)	$= 365.256 \text{ days} = 3.1558 \times 10^7 \text{ s} (\approx \pi \times 10^7 \text{ s})$
density of dry air	$= 1.205 \text{ mg} \cdot \text{cm}^{-3} \text{ (at } 20^\circ\text{C, 760 torr, i.e. 101.3 kPa)}$
acceleration by gravity	$= 980.62 \text{ cm} \cdot \text{s}^{-2} \text{ (sea level, } 45^\circ \text{ latitude)}$
gravitational constant	$= 6.6732(31) \times 10^{-8} \text{ cm}^3 \cdot \text{g}^{-1} \cdot \text{s}^{-2}$
1 calorie (thermochemical)	$= 4.184 \text{ J}$
1 atmosphere	$= 1033.2275 \text{ gf} \cdot \text{cm}^{-2} = 1.01325 \times 10^6 \text{ dyn} \cdot \text{cm}^{-2} = 1.01325 \text{ bar} = 101.325 \text{ kPa}$
1 eV per particle	$= 11604.50(36) \text{ K (from } E = kT)$

^a Prepared by S.J. Brodsky, based mainly on the adjustment of the fundamental physical constants by Cohen and Taylor: COHEN, E.R., TAYLOR, B.N., *J. Phys. Chem. Ref. Data* 2 (1973) 663. TAYLOR, B.N., COHEN, E.R., *Proc. Fifth Int. Conf. Atom Masses and Fundamental Constants (AMCO-5), Paris (1975)*.

The figures in parentheses correspond to the one-standard-deviation uncertainty in the last digits of the main number.

TABLE A-I. (cont.)

NUMERICAL CONSTANTS					
π	= 3.1415927	1 rad	= 57.2957795°	$\sqrt{\pi}$	= 1.7724539
e	= 2.7182818	1/e	= 0.3678794	$\sqrt{2}$	= 1.4142136
ln2	= 0.6931472	ln10	= 2.3025851	$\sqrt{3}$	= 1.7320508
log ₁₀ 2	= 0.3010300	log ₁₀ e	= 0.4342945	$\sqrt{10}$	= 3.1622777

(Updated April 1976. Table reproduced from: PARTICLE DATA GROUP, Review of particle properties, Rev. Mod. Phys. 48 2, Pt.II (1976), with kind permission of the Particle Data Group and Lawrence Berkeley Laboratory.)

For additional conversion factors, the reader is referred to the Conversion Table at the end of the book.

Appendix B

RADIATION PARAMETERS OF MATERIALS

Tables B-I and B-II show properties of elements and of selected composite materials, respectively.

Table B-III shows the collision mass stopping power $(S/\rho)_{\text{col}}$, in $\text{MeV} \cdot \text{cm}^2 \cdot \text{g}^{-1}$, as a function of electron energy, E , in MeV, for various elements and composite materials. The data are from Berger and Seltzer [3, 4].

Photon mass attenuation coefficients and mass energy-absorption coefficients for a selection of materials, including air and water, are shown in Table B-IV. The data are taken from Storm and Israel [5]. The mass energy-absorption coefficient (μ_{en}/ρ) , which represents the rate at which energy is deposited by monoenergetic photons, takes into account all modes of energy transfer to electrons and is useful in calculating the dose under conditions of charged-particle equilibrium.

The mass attenuation coefficient (μ_{tot}/ρ) includes all photon interactions and represents the attenuation of a narrow beam of monoenergetic photons. Useful discussions and extensive tabulations of photon coefficients for a broad range of materials are given by Storm and Israel [5] and by Hubbell [6].

The relationship between these coefficients can be seen in Fig.B-1, in which the solid curves represent μ_{tot}/ρ , based on the total photon cross-section for all processes, and the dashed curves represent μ_{en}/ρ . The curves differ mainly because, in Compton scattering and bremsstrahlung by secondary electrons, photons carry energy away from the point of initial interaction.

Table B-V shows convenient factors for converting photon *energy* flux density to absorbed dose rate for air, carbon and tissue.

Another extensive compilation of data on energy loss, range and bremsstrahlung yield of electrons in various elements and chemical compounds has been published by Pages et al. [12]. Photon cross-sections for elements $Z = 1$ to 94, from 0.1 keV to 1 MeV, have also been published by Veigele [13]. The most recent and extensive critical tabulation of photon cross-sections is by Plechaty et al. [14].

Radiation lengths of composite materials, including compounds and mixtures, are found by combining reciprocal radiation lengths, weighted by the relative composition

$$\frac{\rho_{\text{tot}}}{X_0} = \sum \frac{\rho_i}{X_{0i}} = \frac{\rho_1}{X_{01}} + \frac{\rho_2}{X_{02}} + \frac{\rho_3}{X_{03}} + \dots \quad (\text{B.1a})$$

Text continued on p.313

TABLE B-I. RADIATION PARAMETERS OF ELEMENTS

Z	A	(A)		(B)		(C)		(D)	(E)		(F)		(F)	
		DENSITY ($g \cdot cm^{-3}$)		RADIATION LENGTH ($g \cdot cm^{-2}$)	(cm)	MINIMUM COLLISION STOPPING POWER ($MeV \cdot cm^2 \cdot g^{-1}$)	(MeV)		CRITICAL ENERGY (MeV)	ATTENUATION COEFF AT COMPTON COEFF ($cm^2 \cdot g^{-1}$)	MINIMUM ENERGY (MeV)	GEOMETRICAL CROSS SECTION (barns)	NUCLEAR COLLISION LENGTH ($g \cdot cm^{-2}$)	(cm)
H	1	1.008	0.071	L	63.0470	890.49	3.745	1.95	403.00	0.0111	300.0	0.039	43.	609.8
He	2	4.003	0.125	L	94.3221	754.58	1.777	1.25	280.00	0.0078	160.0	0.13	50.	401.0
Li	3	6.941	0.534		82.7559	154.97	1.469	1.70	169.00	0.0082	115.0	0.21	54.	101.4
Be	4	9.012	1.848		65.1899	35.28	1.700	1.70	132.00	0.0099	90.0	0.27	56.	30.5
B	5	10.811	2.340	V	52.6868	22.52	1.656	1.63	111.74	0.0118	75.0	0.31	58.	24.8
C	6	12.011	2.250	V	42.6983	18.98	1.613	1.55	97.10	0.0141	60.0	0.34	59.	26.3
N	7	14.007	0.808	L	37.9879	47.01	1.659	1.25	107.00	0.0156	50.0	0.38	61.	75.1
O	8	15.999	1.140	L	34.2381	30.03	1.652	1.20	95.20	0.0168	40.0	0.43	62.	54.5
F	9	18.998	1.108	L	32.9303	29.72	1.612	1.20	86.20	0.0171	35.0	0.49	64.	57.9
Ne	10	20.179	1.207	L	28.9367	23.97	1.572	1.20	78.80	0.0190	30.0	0.52	65.	53.8
Na	11	22.990	0.971		27.7362	28.56	1.545	1.27	66.14	0.0195	27.2	0.57	67.	68.6
Mg	12	24.305	1.738		25.0387	14.41	1.518	1.35	55.40	0.0211	24.4	0.60	67.	38.7
Al	13	26.982	2.699		24.0111	8.90	1.463	1.35	51.00	0.0215	21.6	0.65	69.	25.5
Si	14	28.086	2.330		21.8234	9.37	1.442	1.31	49.64	0.0232	18.8	0.67	69.	29.7
P	15	30.974	1.820	V	21.2053	11.65	1.421	1.27	48.44	0.0233	16.0	0.73	71.	38.9
S	16	32.064	2.070	V	19.4953	9.42	1.400	1.23	47.38	0.0250	15.2	0.75	71.	34.4
Cl	17	35.453	1.560	L	19.2783	12.36	1.379	1.19	46.44	0.0246	14.4	0.81	73.	46.6
Ar	18	39.948	1.400	L	19.5489	13.96	1.358	1.15	45.60	0.0258	13.6	0.89	75.	53.3
K	19	39.098	0.862		17.3167	20.09	1.355	1.17	42.54	0.0265	12.8	0.87	74.	86.2
Ca	20	40.080	1.550		16.1442	10.42	1.351	1.19	39.76	0.0283	12.0	0.89	75.	48.2
Sc	21	44.956	2.989		16.5455	5.54	1.348	1.21	37.24	0.0271	11.4	0.97	77.	25.6
Ti	22	47.900	4.540		16.1745	3.56	1.344	1.22	34.93	0.0273	10.9	1.02	78.	17.1
V	23	50.941	6.110		15.8425	2.59	1.341	1.24	32.81	0.0273	10.3	1.07	79.	12.9
Cr	24	51.996	7.190		14.9444	2.08	1.338	1.26	30.87	0.0285	9.8	1.09	79.	11.0
Mn	25	54.938	7.200	V	14.6398	2.03	1.334	1.28	29.07	0.0285	9.2	1.14	80.	11.1
Fe	26	55.847	7.874		13.8389	1.76	1.331	1.30	27.40	0.0296	9.0	1.15	81.	10.2
Co	27	58.933	8.900		13.6174	1.53	1.317	1.28	26.47	0.0295	8.8	1.20	82.	9.2
Ni	28	58.710	8.902		12.6820	1.42	1.302	1.27	25.61	0.0313	8.6	1.20	81.	9.2
Cu	29	63.546	8.960		12.8616	1.44	1.288	1.25	24.80	0.0304	8.4	1.27	83.	9.3
Zn	30	65.380	7.133		12.4269	1.74	1.276	1.22	24.60	0.0310	8.2	1.30	84.	11.7
Ga	31	69.720	5.904		12.4734	2.11	1.265	1.19	24.40	0.0306	8.0	1.36	85.	14.4
Ge	32	72.590	5.323		12.2459	2.30	1.253	1.16	24.22	0.0308	7.8	1.41	86.	16.1
As	33	74.922	5.730	V	11.9401	2.08	1.242	1.14	24.05	0.0311	7.6	1.44	86.	15.1
Se	34	78.960	4.790	V	11.9082	2.49	1.230	1.11	23.89	0.0309	7.4	1.50	88.	18.3
Br	35	79.904	3.120	L	11.4230	3.66	1.219	1.08	23.74	0.0320	7.2	1.51	88.	28.1
Kr	36	83.800	2.600	L	11.3722	4.37	1.207	1.05	23.60	0.0316	7.0	1.57	89.	34.2
Rb	37	85.468	1.532		11.0272	7.20	1.204	1.06	22.75	0.0323	6.8	1.59	89.	58.3
Sr	38	87.620	2.540		10.7623	4.24	1.202	1.07	21.95	0.0327	6.7	1.62	90.	35.4
Y	39	88.906	4.469		10.4101	2.33	1.199	1.08	21.18	0.0335	6.5	1.64	90.	20.2
Zr	40	91.220	6.506		10.1949	1.57	1.196	1.09	20.45	0.0339	6.3	1.67	91.	13.9

Nb	41	92.906	8.570	9.9225	1.16	1.194	1.10	19.76	0.0344	6.1	1.69	91.	10.6
Mo	42	95.940	10.220	9.8029	0.96	1.191	1.10	19.10	0.0343	5.9	1.73	92.	9.0
Tc	43	98.906	11.500	9.6881	0.84	1.189	1.11	18.46	0.0346	5.7	1.77	93.	8.1
Ru	44	101.070	12.410	9.4825	0.76	1.186	1.12	17.86	0.0350	5.5	1.80	93.	7.5
Rh	45	102.906	12.410	9.2654	0.75	1.183	1.13	17.28	0.0355	5.3	1.83	94.	7.5
Pd	46	106.400	12.020	9.2025	0.77	1.181	1.14	16.73	0.0354	5.1	1.87	94.	7.8
Ag	47	107.868	10.500	8.9701	0.85	1.178	1.15	16.20	0.0360	5.0	1.89	95.	9.0
Cd	48	112.400	8.650	8.9945	1.04	1.163	1.13	15.96	0.0356	4.8	1.95	96.	11.1
In	49	114.820	7.310	8.8491	1.21	1.148	1.12	15.72	0.0359	4.7	1.98	96.	13.2
Sn	50	118.690	7.310 V	8.8170	1.21	1.133	1.10	15.50	0.0356	4.5	2.03	97.	13.3
Sb	51	121.750	6.691	8.7244	1.30	1.125	1.07	15.58	0.0358	4.4	2.07	98.	14.6
Te	52	127.600	6.240	8.8267	1.41	1.118	1.05	15.66	0.0350	4.4	2.14	99.	15.8
I	53	126.905	4.930	8.4803	1.72	1.110	1.02	15.73	0.0362	4.3	2.13	99.	20.0
Xe	54	131.300	3.520 L	8.4819	2.41	1.102	1.00	15.80	0.0359	4.3	2.19	100.	28.3
Cs	55	132.905	1.873	8.3052	4.43	1.099	1.00	15.43	0.0363	4.2	2.21	100.	53.4
Ba	56	137.340	3.500	8.3073	2.37	1.095	1.01	15.06	0.0360	4.2	2.26	101.	28.8
La	57	138.906	6.145	8.1381	1.32	1.091	1.01	14.71	0.0365	4.1	2.28	101.	16.5
Ce	58	140.120	6.657	7.9557	1.20	1.088	1.02	14.38	0.0371	4.1	2.30	101.	15.2
Pr	59	140.908	6.773 V	7.7579	1.15	1.084	1.02	14.05	0.0378	4.0	2.30	102.	15.0
Nd	60	144.240	6.950 V	7.7051	1.11	1.081	1.03	13.74	0.0377	4.0	2.34	102.	14.7
Pm	61	145.000	7.220 U	7.5193	1.04	1.077	1.03	13.43	0.0385	4.0	2.35	102.	14.2
Sm	62	150.400	7.520 V	7.5727	1.01	1.074	1.04	13.13	0.0380	3.9	2.42	103.	13.7
Eu	63	151.960	5.243	7.4377	1.42	1.070	1.05	12.85	0.0384	3.9	2.44	104.	19.8
Gd	64	157.250	7.900	7.4830	0.95	1.067	1.05	12.57	0.0380	3.8	2.50	105.	13.2
Tb	65	158.925	8.229	7.3563	0.89	1.063	1.05	12.30	0.0383	3.8	2.52	105.	12.7
Dy	66	162.500	8.550	7.3199	0.86	1.060	1.06	12.04	0.0385	3.8	2.56	105.	12.3
Ho	67	164.930	8.795	7.2332	0.82	1.056	1.06	11.79	0.0387	3.8	2.59	106.	12.0
Er	68	167.260	9.066	7.1448	0.79	1.053	1.07	11.54	0.0389	3.8	2.61	106.	11.7
Tm	69	168.934	9.321	7.0318	0.75	1.049	1.07	11.30	0.0396	3.8	2.63	107.	11.4
Yb	70	173.040	6.965 V	7.0214	1.01	1.046	1.08	11.07	0.0393	3.8	2.68	107.	15.4
Lu	71	174.970	9.840	6.9237	0.70	1.042	1.09	10.84	0.0396	3.8	2.70	108.	10.9
Hf	72	178.490	13.310	6.8907	0.52	1.039	1.09	10.62	0.0398	3.8	2.74	108.	8.1
Ta	73	180.948	16.654	6.8177	0.41	1.035	1.10	10.41	0.0399	3.7	2.77	109.	6.5
W	74	183.850	19.300	6.7630	0.35	1.032	1.10	10.20	0.0403	3.7	2.80	109.	5.7
Re	75	186.200	21.020	6.6897	0.32	1.029	1.08	10.09	0.0404	3.7	2.82	109.	5.2
Os	76	190.200	22.570	6.6763	0.30	1.026	1.06	9.98	0.0405	3.7	2.87	110.	4.9
Ir	77	192.220	22.420	6.5936	0.29	1.024	1.04	9.87	0.0407	3.7	2.89	110.	4.9
Pt	78	195.090	21.450	6.5433	0.31	1.021	1.02	9.76	0.0411	3.6	2.92	111.	5.2
Au	79	196.967	19.320	6.4608	0.33	1.018	1.00	9.66	0.0416	3.6	2.94	111.	5.8
Hg	80	200.590	13.546 L	6.4368	0.48	1.013	0.99	9.61	0.0414	3.6	2.98	112.	8.3

TABLE B-I. (cont.)

Z	A	(A)		(B)		(C)		(D)			(E)		(F)	
		DENSITY ($\text{g}\cdot\text{cm}^{-3}$)		RADIATION LENGTH ($\text{g}\cdot\text{cm}^{-2}$)	(cm)	MINIMUM STOPPING POWER ($\text{MeV}\cdot\text{cm}^2\cdot\text{g}^{-1}$)	COLLISION POWER (MeV)	CRITICAL ENERGY (MeV)	ATTENUATION COEFF ($\text{cm}^2\cdot\text{g}^{-1}$)	AT COMPTON MINIMUM ENERGY (MeV)	GEOMETRICAL CROSS SECTION (barns)		NUCLEAR COLLISION LENGTH ($\text{g}\cdot\text{cm}^{-2}$)	(cm)
Tl	81	204.370	11.850	6.4176	0.54	1.007	0.99	9.56	0.0416	3.6	3.02	112.	9.5	
Pb	82	207.190	11.350	6.3688	0.56	1.002	0.98	9.51	0.0419	3.6	3.05	113.	9.9	
Bi	83	208.981	9.747	6.2899	0.65	0.998	0.98	9.38	0.0424	3.6	3.07	113.	11.6	
Po	84	210.000	9.320	6.1907	0.66	0.994	0.98	9.26	0.0427	3.6	3.08	113.	12.1	
At	85	210.000	--	6.0651	--	0.990	0.99	9.14	0.0436	3.6	3.08	113.	--	
Rn	86	222.000	4.400	6.2833	1.43	0.986	0.99	9.02	0.0421	3.6	3.21	115.	26.1	
Fr	87	223.000	--	6.1868	--	0.982	0.99	8.90	0.0427	3.6	3.22	115.	--	
Ra	88	226.025	5.000	6.1477	1.23	0.978	0.99	8.79	0.0429	3.7	3.25	116.	23.1	
Ac	89	227.000	10.070	6.0560	0.60	0.974	0.99	8.68	0.0435	3.7	3.26	116.	11.5	
Th	90	232.038	11.720	6.0726	0.52	0.970	1.00	8.57	0.0433	3.7	3.31	116.	9.9	
Pa	91	231.036	15.370	5.9319	0.39	0.966	1.00	8.46	0.0443	3.7	3.30	116.	7.6	
U	92	238.029	18.950	5.9990	0.32	0.962	1.00	8.36	0.0438	3.8	3.37	117.	6.2	
Np	93	237.048	20.250	5.8647	0.29	0.959	1.00	8.27	0.0447	3.8	3.36	117.	5.8	
Pu	94	239.130	19.840	5.8090	0.29	0.955	1.00	8.18	0.0446	3.9	3.38	117.	5.9	
Am	95	243.000	13.670	5.7974	0.42	0.951	1.00	8.10	0.0453	3.9	3.42	118.	8.6	
Cm	96	247.000	13.510	5.7886	0.43	0.947	1.00	8.02	0.0453	3.9	3.46	119.	8.8	
Bk	97	247.000	14.000	5.6874	0.41	0.943	1.00	7.93	0.0457	3.9	3.46	119.	8.5	
Cf	98	251.000	--	5.6797	--	0.939	1.00	7.85	0.0461	4.0	3.50	119.	--	
Es	99	254.000	--	5.6495	--	0.935	1.00	7.78	0.0462	4.0	3.53	119.	--	
Fm	100	257.000	--	5.6197	--	0.931	1.00	7.70	0.0474	4.0	3.56	120.	--	

FOOTNOTES TO TABLE B-I

- (A) Except where noted, the density given is for the solid. The letters in this column have the following meanings: L: The density given is for the liquid state at 20°C, or at the boiling point if below 20°C. V: The density of the solid shows considerable variation, or there is more than one allotropic state. Density variation ranges: for amorphous carbon: $1.8 - 2.1 \text{ g}\cdot\text{cm}^{-3}$; for graphite: $1.9 - 2.3 \text{ g}\cdot\text{cm}^{-3}$; for diamond: $3.15 - 3.53 \text{ g}\cdot\text{cm}^{-3}$. Consult standard handbooks for other elements marked by V. U signifies density uncertain and E indicates estimated density.
The densities are mainly from the Handbook of Chemistry and Physics, 56th ed. (1975) (Ref.[1]).
- (B) Radiation lengths from Tsai [2] extrapolated to $Z = 100$ by his Eq.3.65, assuming linear behaviour in the Coulomb correction f over the range $Z = 80 - 100$.
- (C) Minimum collision stopping power for *electrons*. (Values for heavy particles are generally 10–15% greater.) The electron kinetic energy at which the minimum occurs is also indicated. Data are interpolated from Berger and Seltzer [3, 4].
- (D) Critical energy, defined as kinetic energy at which mean values of electron collision and radiative energy losses are equal. Data are interpolated from Table II of Berger and Seltzer [3]. The critical energy (in MeV) may also be approximated by the convenient formula $E_c = 800/(Z + 1.2)$.
- (E) The Compton minimum is defined as the photon energy at which the attenuation coefficient is minimum. Values given for the minimum attenuation coefficient are based on Storm and Israel [5] for $Z > 3$. For $Z \leq 3$, the compilation by Hubbell [6] is used. As the minima are generally broad, the energies shown should be considered uncertain by about $\pm 10\%$ for $1 \leq Z \leq 10$, by $\pm 5\%$ for $10 < Z \leq 20$, and $\pm 2\%$ for higher Z .
- (F) Nuclear total cross-sections, based on the parameterization of Carlson et al. (Ref.[7], p.13), with nuclear radius (in centimetres) $R = 1.23 \times 10^{-13} A^{1/3}$ and nuclear absorption length $X_{\text{on}} = 3.05 \times 10^{-13} \text{ cm}$, corresponding to 21 GeV/c. The corresponding collision lengths are obtained from $L_{\text{coll}} = A/(N_A \sigma)$. The nuclear *absorption* lengths (not shown) correspond to inelastic processes only and are larger, for example, by factors of about 1.5, 1.7 and 1.9 for Al, Fe and Pb, respectively. The data given here are reasonably representative of real n-nucleus (and p-nucleus) cross-sections (to within $\pm 10\%$) as low as 150 MeV kinetic energy, and are considerably more accurate than this at higher energies.

TABLE B-II. RADIATION PARAMETERS OF SELECTED COMPOSITE MATERIALS

MATERIAL	Z	A	(A)		(B)		(C)		(D)		(E)		(F)	
			DENSITY (g·cm ⁻³)	RADIATION LENGTH (g·cm ⁻²)	(cm)	MINIMUM COLLISION STOPPING POWER (MeV·cm ² ·g ⁻¹)	(MeV)	CRITICAL ENERGY (MeV)	ATTENUATION COEFF AT COMPTON COEFF (cm ² ·g ⁻¹)	MINIMUM ENERGY (MeV)	GEOMETRICAL CROSS SECTION (barns)	NUCLEAR COLLISION LENGTH (g·cm ⁻²)	(cm)	
Deuterium (² H ₂)			0.165 L	126.1	764	1.874	1.95	403	0.00555	300	0.074	45.1	273	
Water (H ₂ O)			1.000 L	36.08	36.1	1.852	1.55	92	0.0166	55	0.51	59.2	59	
Air ^(H)			(1.205 G)	36.61	30 380	1.653	1.20	102	0.0160	45	--	61.2	50 800	
CO ₂			(1.79 G)	36.20	20 220	1.658	1.25	100	0.0161	43	1.19	61.3	34 200	
Polyethylene (CH ₂) _n			0.92-0.95	44.78	47.9	1.906	1.65	119	0.0140	70	--	56.1	60	
Plexiglass (Lucite) (C ₅ H ₈ O ₂) _n			1.16-1.20	40.55	34.4	1.774	1.55	100	0.0151	55	--	58.3	49	
Polystyrene (C ₈ H ₈ O ₂) _n			1.03-1.07	41.10	39.1	1.783	1.60	109	0.0142	60	--	58.5	56	
Mylar (C ₅ H ₄ O ₂) _n			1.39	39.95	28.7	1.73	1.6	110	0.0151	60	--	59.1	43	
Nylon (C ₆ H ₁₁ NO) _n			1.09-1.14	41.92	37.6	1.83	1.6	115	0.0146	60	--	57.6	52	
Bakelite (C ₇ H ₅ O) _n			1.3-1.4	41.77	30.9	1.74	1.6	110	0.0147	55	--	58.5	43	
Cellulose (C ₆ H ₁₀ O ₅) _n (amorph wood)			1.3-1.6 0.5-0.9)	38.75	26.7 55.4	1.77	1.6	110	0.0155	55	--	59.2	41 85	
Film emulsion ^(H)			3.815	11.33	2.97	1.296	1.20	22.3	--	--	--	83.5	22	
Muscle ^(H)			1.00	36.66	36.7	1.829	1.55	112	0.0164	50	--	59.2	59	
Bone ^(H)			1.7-2.0	30.49	16.5	1.709	1.50	81.9	0.0189	37	--	61.6	33	
SiO ₂			2.32	27.05	11.7	1.583	1.25	66	0.0202	27	1.53	65.3	28	
CaCO ₃		(marble)	2.5-2.9)	24.03	8.9	--	--	--	0.0219	25	2.51	66.2	25	
BaSO ₄		(barite)	4.5)	11.64	2.59	--	--	--	0.0322	7.3	4.72	82.1	18	
Concrete ^(H)			2.35	25.71	10.9	1.58	1.25	--	0.0209	25	--	65.8	28	
Pyrex glass ^(H)			2.23	28.17	12.6	1.58	1.25	--	0.0195	30	--	64.7	29	
LiF			2.64	39.25	14.9	1.473	1.55	81	0.0149	43	0.70	61.1	23	
NaI			3.67	9.49	2.59	1.179	1.15	17.4	0.0348	5.3	2.71	91.9	25	

FOOTNOTES TO TABLE B-II

- (A) The densities of most solids listed may be quite variable. Where critical, the density of the material used should be measured. L: The density is given for the liquid state (at boiling point for deuterium, and 20°C for water). G: Gas at STP (in units of $\text{g} \cdot \text{litre}^{-1}$).
- (B) Radiation lengths (in $\text{g} \cdot \text{cm}^{-2}$) derived from Table B-I. The *median* density indicated is used to obtain the equivalent in cm.
- (C) Minimum collision stopping power for *electrons* (values for heavy particles are generally 10–15% greater), and kinetic energy at which it occurs. The values of stopping power with four significant figures are from Berger and Seltzer [3,4]; the others are interpolated from Table B-I.
- (D) Critical energy from Berger and Seltzer [3], or interpolated from Table B-I. (See footnote D, Table B-I.)
- (E) Values of attenuation coefficient are interpolated from Storm and Israel [5] or Hubbell [6]. (See footnote E, Table B-I.)
- (F) See footnote F, Table B-I. The geometrical cross-sections indicated are for molecules. Collision lengths ($\text{g} \cdot \text{cm}^{-2}$) are derived from Table B-I. The *median* density indicated is used to obtain the equivalent in cm.
- (H) *First column: Material*
 Composition assumed (by weight), normalized to unit density:
 Air: (N:O:Ar) = (0.755:0.232:0.013)
 Film emulsion: (H:C:N:O:S:Br:Ag:I) = (0.0141:0.0723:0.0193:0.0661:0.0019:0.3491:0.4741:0.0031)
 Muscle: (H:C:N:O:Na:Mg:P:S:K:Ca) = (0.102:0.123:0.0350:0.7289:0.0008:0.0002:0.002:0.002:0.005:0.003:0.0001)
 Bone: (H:C:N:O:Mg:P:S:Ca) = (0.064:0.278:0.027:0.41:0.002:0.07:0.002:0.147)
 Concrete: (H:O:Na:Mg:Al:Si:S:K:Ca:Fe) = (0.0056:0.4983:0.0171:0.0024:0.0456:0.3158:0.0012:0.0192:0.0826:0.0122)
 Pyrex glass: (B:O:Na:Al:Si:K) = (0.0401:0.5396:0.0282:0.0116:0.3772:0.0033)

TABLE B-III. COLLISION MASS STOPPING POWER, $(S/\rho)_{col}$, IN $\text{MeV} \cdot \text{cm}^2 \cdot \text{g}^{-1}$ AS A FUNCTION OF ELECTRON ENERGY, E , IN MeV, FOR VARIOUS ELEMENTS (ATOMIC NUMBER) AND OTHER MATERIALS [3, 4]

E (MeV)	H (1)	C (6)	N (7)	O (8)	Al (13)	Fe (26)	Cu (29)	Pb (82)	Air ^a	Water	Muscle ^a	Bone ^a	Poly- methyl meth- acrylate	Poly- ethylene	Poly- styrene	Silicon	LiF	Film emulsion ^a
0.010	51.47	20.15	19.81	19.64	16.57	14.07	13.28	8.419	19.70	23.20	22.92	21.01	22.51	24.65	22.60	16.92	18.17	13.15
0.015	36.97	14.72	14.49	14.37	12.25	10.53	9.973	6.556	14.41	16.90	16.70	15.36	16.40	17.91	16.46	12.53	13.30	9.884
0.020	29.28	11.78	11.60	11.52	9.885	8.553	8.120	5.450	11.55	13.50	13.34	12.31	13.11	14.29	13.15	10.11	10.66	8.050
0.030	21.18	8.634	8.515	8.454	7.316	6.385	6.078	4.179	8.475	9.879	9.763	9.030	9.588	10.44	9.617	7.491	7.823	6.028
0.04	16.93	6.958	6.866	6.819	5.932	5.204	4.962	3.462	6.835	7.951	7.859	7.281	7.717	8.390	7.739	6.077	6.311	4.922
0.05	14.29	5.909	5.834	5.795	5.059	4.455	4.252	2.997	5.808	6.747	6.669	6.186	6.548	7.113	6.565	5.185	5.363	4.219
0.06	12.49	5.188	5.124	5.091	4.456	3.935	3.759	2.669	5.101	5.919	5.851	5.434	5.746	6.237	5.760	4.568	4.711	3.730
0.08	10.18	4.259	4.208	4.182	3.676	3.259	3.118	2.237	4.190	4.854	4.799	4.463	4.712	6.110	4.723	3.769	3.870	3.094
0.10	8.766	3.685	3.642	3.621	3.191	2.838	2.717	1.964	3.627	4.197	4.149	3.862	4.074	4.415	4.083	3.273	3.350	2.697
0.15	6.840	2.900	2.868	2.852	2.526	2.257	2.164	1.584	2.856	3.299	3.261	3.041	3.202	3.466	3.208	2.592	2.639	2.148
0.20	5.869	2.493	2.475	2.462	2.188	1.961	1.882	1.389	2.466	2.844	2.811	2.625	2.761	2.986	2.766	2.246	2.277	1.869
0.30	4.912	2.097	2.089	2.078	1.848	1.667	1.603	1.196	2.081	2.394	2.366	2.210	2.326	2.513	2.330	1.904	1.916	1.593
0.4	4.458	1.907	1.906	1.897	1.691	1.526	1.473	1.106	1.899	2.181	2.155	2.011	2.106	2.200	2.119	1.739	1.742	1.464
0.5	4.205	1.801	1.806	1.798	1.603	1.449	1.396	1.059	1.800	2.061	2.036	1.901	1.987	2.148	1.999	1.651	1.645	1.394
0.6	4.053	1.735	1.747	1.739	1.551	1.403	1.353	1.033	1.740	1.989	1.964	1.835	1.914	2.067	1.925	1.598	1.585	1.353
0.8	3.893	1.665	1.687	1.680	1.496	1.356	1.310	1.010	1.681	1.911	1.887	1.762	1.835	1.979	1.846	1.544	1.521	1.314
1.0	3.826	1.634	1.665	1.658	1.473	1.337	1.293	1.002	1.659	1.876	1.852	1.728	1.799	1.937	1.809	1.522	1.492	1.299
1.5	3.798	1.613	1.664	1.658	1.464	1.333	1.291	1.015	1.659	1.852	1.829	1.709	1.774	1.906	1.783	1.514	1.473	1.301
2.0	3.833	1.619	1.688	1.682	1.476	1.346	1.305	1.036	1.683	1.858	1.835	1.717	1.779	1.909	1.787	1.528	1.478	1.318
3.0	3.933	1.645	1.744	1.738	1.508	1.378	1.338	1.076	1.738	1.884	1.861	1.747	1.805	1.934	1.813	1.562	1.502	1.355

4	4.029	1.670	1.794	1.788	1.537	1.406	1.367	1.109	1.789	1.909	1.886	1.775	1.832	1.960	1.838	1.593	1.524	1.387
5	4.112	1.692	1.837	1.831	1.561	1.430	1.391	1.135	1.831	1.931	1.908	1.798	1.854	1.982	1.861	1.618	1.544	1.413
6	4.184	1.710	1.874	1.868	1.581	1.450	1.411	1.157	1.868	1.949	1.927	1.818	1.873	2.002	1.879	1.639	1.560	1.435
8	4.304	1.739	1.935	1.929	1.613	1.481	1.442	1.191	1.929	1.978	1.956	1.850	1.903	2.032	1.909	1.673	1.586	1.469
10	4.400	1.761	1.983	1.977	1.637	1.505	1.466	1.217	1.978	2.000	1.978	1.874	1.926	2.056	1.932	1.698	1.606	1.495
15	4.580	1.798	2.075	2.069	1.679	1.545	1.507	1.262	2.068	2.038	2.017	1.915	1.971	2.098	1.972	1.743	1.641	1.541
20	4.707	1.825	2.139	2.133	1.709	1.575	1.535	1.293	2.133	2.064	2.043	1.945	1.994	2.125	1.998	1.773	1.664	1.571
30	4.890	1.859	2.231	2.225	1.747	1.612	1.573	1.334	2.225	2.100	2.079	1.983	2.030	2.163	2.034	1.812	1.695	1.611
40	5.013	1.882	2.288	2.288	1.773	1.637	1.597	1.360	2.283	2.125	2.103	2.010	2.055	2.189	2.059	1.839	1.716	1.638
50	5.089	1.899	2.330	2.324	1.792	1.656	1.616	1.380	2.324	2.144	2.123	2.029	2.074	2.209	2.077	1.859	1.733	1.658
60	5.141	1.914	2.361	2.352	1.808	1.671	1.631	1.396	2.355	2.160	2.138	2.045	2.089	2.225	2.093	1.875	1.746	1.674
80	5.211	1.936	2.408	2.394	1.831	1.694	1.653	1.419	2.400	2.185	2.163	2.070	2.113	2.251	2.117	1.899	1.766	1.698
100	5.258	1.953	2.440	2.425	1.849	1.711	1.670	1.436	2.433	2.204	2.182	2.089	2.132	2.270	2.135	1.917	1.782	1.716

^a Composition (fraction by weight)

Air: 0.755 N; 0.232 O; 0.013 Ar.

Muscle: 0.1020 H; 0.1230 C; 0.0350 N; 0.7290 O; 0.0008 Na; 0.0002 Mg; 0.0020 P; 0.0050 S; 0.0030 K.

Bone: 0.064 H; 0.278 C; 0.027 N; 0.410 O; 0.002 Mg; 0.070 P; 0.002 S; 0.147 Ca.

Film emulsion: 0.0141 H; 0.0723 C; 0.0193 N; 0.0661 O; 0.0019 S; 0.3491 Br; 0.4741 Ag; 0.0031 I.

Adapted from Berger and Seltzer [3, 4].

TABLE B-IVa. COEFFICIENTS FOR PHOTON TRANSPORT (in $\text{cm}^2 \cdot \text{g}^{-1}$)^(a)

Energy (MeV)	1 Hydrogen		6 Carbon		7 Nitrogen		8 Oxygen		Water		13 Aluminum	
	$(\mu/P)_{\text{tot}}$	$(\mu/P)_{\text{en}}$										
0.001	9.86	9.44	2010.	2010.	3140.	3140.	4520.	4520.	4020.	4020.	1230.	1230.
0.0015	3.62	3.23	632.	632.	989.	989.	1430.	1430.	1280.	1280.	395.	393.
.001560											355.	353.
.001560											4890.	4750.
0.002	1.85	1.45	281.	280.	434.	434.	636.	636.	567.	566.	2410.	2370.
0.003	0.842	0.455	88.2	87.7	138.	137.	205.	201.	180.	179.	777.	763.
0.004	0.568	0.181	37.8	37.3	59.8	58.9	87.3	86.6	77.8	77.0	346.	339.
0.005	0.471	0.0866	19.4	18.9	30.5	29.9	45.2	44.4	40.2	39.5	184.	181.
0.006	0.430	0.0472	10.8	10.4	17.5	17.0	26.2	25.6	23.4	22.8	111.	109.
0.008	0.399	0.0202	4.56	4.01	7.27	6.88	11.2	10.7	10.0	9.54	50.0	48.9
0.01	0.388	0.0129	2.21	1.91	3.69	3.35	5.72	5.31	5.12	4.72	26.3	25.7
0.015	0.376	0.0112	0.742	0.493	1.15	0.881	1.74	1.45	1.59	1.29	7.97	7.50
0.02	0.369	0.0131	0.419	0.197	0.585	0.350	0.817	0.565	0.769	0.505	3.41	3.06
0.03	0.357	0.0184	0.250	0.0577	0.296	0.0972	0.363	0.155	0.363	0.140	1.09	0.830
0.04	0.346	0.0229	0.205	0.0296	0.225	0.0447	0.252	0.0670	0.263	0.0620	0.545	0.335
0.05	0.335	0.0269	0.186	0.0220	0.196	0.0292	0.210	0.0395	0.224	0.0383	0.355	0.169
0.06	0.326	0.0305	0.175	0.0198	0.181	0.0237	0.189	0.0295	0.204	0.0296	0.270	0.101
0.08	0.308	0.0361	0.160	0.0197	0.164	0.0213	0.167	0.0234	0.183	0.0249	0.200	0.0516
0.1	0.294	0.0406	0.151	0.0211	0.153	0.0218	0.155	0.0228	0.171	0.0248	0.169	0.0362
0.15	0.265	0.0480	0.135	0.0244	0.135	0.0245	0.136	0.0248	0.151	0.0274	0.138	0.0277
0.2	0.243	0.0525	0.123	0.0264	0.123	0.0265	0.123	0.0266	0.137	0.0295	0.122	0.0272
0.3	0.211	0.0569	0.107	0.0287	0.107	0.0287	0.107	0.0287	0.119	0.0319	0.104	0.0279
0.4	0.189	0.0587	0.0958	0.0295	0.0955	0.0295	0.0956	0.0295	0.106	0.0328	0.0926	0.0286
0.5	0.173	0.0592	0.0867	0.0297	0.0873	0.0298	0.0873	0.0298	0.0969	0.0331	0.0844	0.0290
0.6	0.160	0.0587	0.0802	0.0294	0.0804	0.0295	0.0809	0.0295	0.0896	0.0328	0.0779	0.0283
0.8	0.140	0.0571	0.0707	0.0288	0.0705	0.0287	0.0708	0.0287	0.0787	0.0319	0.0683	0.0277
1.0	0.126	0.0554	0.0637	0.0279	0.0636	0.0279	0.0636	0.0279	0.0707	0.0310	0.0614	0.0268
1.5	0.103	0.0508	0.0516	0.0255	0.0516	0.0254	0.0516	0.0254	0.0574	0.0283	0.0500	0.0243
2.0	0.0872	0.0463	0.0443	0.0234	0.0443	0.0233	0.0444	0.0234	0.0493	0.0260	0.0431	0.0225
3.0	0.0693	0.0399	0.0355	0.0204	0.0357	0.0205	0.0359	0.0206	0.0396	0.0227	0.0355	0.0220
4.0	0.0581	0.0352	0.0305	0.0185	0.0307	0.0186	0.0310	0.0188	0.0341	0.0207	0.0310	0.0188
5.0	0.0505	0.0318	0.0270	0.0171	0.0274	0.0174	0.0278	0.0176	0.0303	0.0192	0.0283	0.0180
6.0	0.0449	0.0290	0.0247	0.0161	0.0251	0.0164	0.0255	0.0167	0.0277	0.0181	0.0266	0.0175
8.0	0.0375	0.0253	0.0215	0.0147	0.0220	0.0152	0.0225	0.0156	0.0242	0.0167	0.0243	0.0169
10.0	0.0325	0.0227	0.0195	0.0139	0.0201	0.0144	0.0207	0.0149	0.0221	0.0158	0.0230	0.0167
15.0	0.0254	0.0186	0.0168	0.0127	0.0177	0.0134	0.0185	0.0141	0.0193	0.0146	0.0218	0.0167
20.0	0.0215	0.0163	0.0156	0.0122	0.0166	0.0130	0.0176	0.0138	0.0181	0.0141	0.0215	0.0167
30.0	0.0174	0.0137	0.0146	0.0117	0.0158	0.0127	0.0169	0.0134	0.0170	0.0135	0.0218	0.0168
40.0	0.0154	0.0124	0.0142	0.0115	0.0156	0.0124	0.0168	0.0133	0.0167	0.0132	0.0223	0.0168
50.0	0.0142	0.0115	0.0142	0.0113	0.0156	0.0123	0.0169	0.0132	0.0166	0.0130	0.0230	0.0166
60.0	0.0133	0.0109	0.0141	0.0111	0.0156	0.0121	0.0171	0.0130	0.0166	0.0128	0.0234	0.0164
80.0	0.0124	0.0103	0.0142	0.0110	0.0159	0.0119	0.0174	0.0128	0.0168	0.0125	0.0243	0.0161
100.0	0.0118	0.00986	0.0145	0.0109	0.0162	0.0118	0.0178	0.0126	0.0171	0.0123	0.0252	0.0159

^a The values are from Storm and Israel [5].

TABLE B-IVb. COEFFICIENTS FOR PHOTON TRANSPORT (in $\text{cm}^2 \cdot \text{g}^{-1}$)^(a)

Energy (MeV)	14 Silicon		18 Argon		20 Calcium		26 Iron		29 Copper		50 Tin	
	(μ/ρ) _{tot}	(μ/ρ) _{en}	(μ/ρ) _{tot}	(μ/ρ) _{en}	(μ/ρ) _{tot}	(μ/ρ) _{en}	(μ/ρ) _{tot}	(μ/ρ) _{en}	(μ/ρ) _{tot}	(μ/ρ) _{en}	(μ/ρ) _{tot}	(μ/ρ) _{en}
0.001	1650.	1650.	3540.	3540.	5640.	5640.	12100.	12100.	13800.	13800.	11400.	11400.
.001096									11300.	11300.		
.001096									12700.	12700.		
0.0015	527.	525.	1120.	1110.	1770.	1770.	3830.	3830.	5250.	5240.	5920.	5910.
.001839	296.	294.										
.001839	3900.	3770.										
0.002	3070.	2950.										
0.003	993.	968.	486.	493.	786.	783.	1710.	1710.	2350.	2350.	1830.	1830.
.003203			157.	155.	249.	246.	550.	547.	763.	759.	629.	624.
.003203			131.	129.								
.003929			1480.	1550.								
.003929												
0.004	442.	433.	799.	742.	111.	109.	245.	241.	343.	339.	312.	306.
.004037					108.	106.					1130.	1010.
.004037					1140.	996.					1070.	954.
.004156												
.004156											934.	837.
.004465											1290.	1160.
.004465											1090.	979.
0.005	236.	232.	433.	407.	636.	570.	132.	129.	183.	180.	140.	130.
0.006	141.	139.	262.	249.	385.	352.	78.7	76.5	111.	108.	908.	827.
.007112							49.	47.2			558.	518.
.007112							442.	529.				
0.008	63.5	62.2	119.	113.	174.	162.	317.	245.			47.9	255.
.008981									49.9	47.9	255.	238.
.008981									36.0	34.2		
									302.	204.		
0.01	34.1	33.0	64.7	62.0	95.0	89.1	170.	139.	224.	157.	139.	131.
0.015	10.4	9.82	20.2	19.3	30.2	28.3	55.3	48.0	73.1	58.2	46.3	43.2
0.02	4.42	4.01	8.61	8.05	13.1	12.3	24.9	22.1	33.1	27.7	21.4	19.6
.029200											7.61	6.70
.029200											44.9	16.2
0.03	1.39	1.10	2.59	2.28	4.03	3.61	8.15	7.28	10.9	9.45	41.9	15.8
0.04	0.673	0.448	1.17	0.938	1.77	1.49	3.63	3.18	4.88	4.22	19.2	10.0
0.05	0.422	0.225	0.673	0.422	0.989	0.751	1.94	1.63	2.60	2.19	10.6	6.39
0.06	0.313	0.133	0.452	0.274	0.642	0.436	1.19	0.944	1.57	1.28	6.55	4.39
0.08	0.219	0.0647	0.273	0.124	0.359	0.188	0.594	0.411	0.761	0.560	3.02	2.14
0.1	0.182	0.0431	0.204	0.0719	0.256	0.107	0.370	0.219	0.459	0.298	1.67	1.21
0.15	0.145	0.0302	0.143	0.0368	0.167	0.0484	0.196	0.0800	0.222	0.104	0.619	0.420
0.2	0.128	0.0287	0.121	0.0299	0.138	0.0362	0.146	0.0483	0.156	0.0589	0.331	0.209
0.3	0.108	0.0294	0.0955	0.0274	0.111	0.0314	0.110	0.0336	0.112	0.0361	0.265	0.0852
0.4	0.0963	0.0296	0.0878	0.0273	0.0978	0.0305	0.0939	0.0304	0.0940	0.0314	0.137	0.0538
0.5	0.0875	0.0298	0.0795	0.0271	0.0884	0.0304	0.0840	0.0293	0.0836	0.0297	0.0939	0.0412
0.6	0.0808	0.0294	0.0733	0.0268	0.0823	0.0299	0.0769	0.0286	0.0762	0.0285	0.0817	0.0353
0.8	0.0705	0.0285	0.0641	0.0259	0.0712	0.0287	0.0669	0.0272	0.0660	0.0269	0.0665	0.0292
1.0	0.0635	0.0277	0.0576	0.0250	0.0639	0.0278	0.0598	0.0260	0.0590	0.0257	0.0578	0.0262
1.5	0.0517	0.0253	0.0469	0.0229	0.0520	0.0254	0.0487	0.0237	0.0480	0.0233	0.0463	0.0227
2.0	0.0448	0.0236	0.0406	0.0213	0.0452	0.0237	0.0425	0.0221	0.0419	0.0217	0.0410	0.0211
3.0	0.0367	0.0209	0.0338	0.0192	0.0376	0.0213	0.0360	0.0204	0.0359	0.0202	0.0367	0.0204
4.0	0.0326	0.0197	0.0302	0.0182	0.0340	0.0206	0.0331	0.0199	0.0333	0.0200	0.0337	0.0213
5.0	0.0296	0.0188	0.0280	0.0178	0.0317	0.0201	0.0315	0.0198	0.0318	0.0201	0.0337	0.0223
6.0	0.0279	0.0184	0.0267	0.0176	0.0304	0.0201	0.0306	0.0201	0.0311	0.0205	0.0359	0.0232
8.0	0.0257	0.0179	0.0250	0.0175	0.0287	0.0201	0.0295	0.0206	0.0304	0.0211	0.0369	0.0249
10.0	0.0244	0.0178	0.0244	0.0178	0.0283	0.0206	0.0298	0.0213	0.0306	0.0218	0.0385	0.0264
15.0	0.0234	0.0178	0.0238	0.0181	0.0283	0.0213	0.0306	0.0225	0.0322	0.0236	0.0427	0.0294
20.0	0.0232	0.0179	0.0243	0.0185	0.0289	0.0218	0.0318	0.0231	0.0336	0.0240	0.0464	0.0305
30.0	0.0238	0.0181	0.0255	0.0190	0.0302	0.0221	0.0342	0.0236	0.0365	0.0248	0.0518	0.0316
40.0	0.0244	0.0181	0.0267	0.0190	0.0317	0.0224	0.0363	0.0237	0.0390	0.0249	0.0558	0.0312
50.0	0.0251	0.0180	0.0275	0.0187	0.0331	0.0221	0.0379	0.0233	0.0409	0.0245	0.0584	0.0303
60.0	0.0257	0.0177	0.0284	0.0187	0.0341	0.0218	0.0392	0.0229	0.0423	0.0240	0.0614	0.0299
80.0	0.0266	0.0174	0.0296	0.0181	0.0356	0.0212	0.0412	0.0223	0.0446	0.0234	0.0649	0.0288
100.0	0.0277	0.0170	0.0308	0.0178	0.0373	0.0207	0.0431	0.0218	0.0466	0.0228	0.0685	0.0278

^a The values are from Storm and Israel [5].

TABLE B-IVc. COEFFICIENTS FOR PHOTON TRANSPORT (in $\text{cm}^2 \cdot \text{g}^{-1}$)^(a)

Energy (MeV)	56 Barium		74 Tungsten		82 Lead		92 Uranium		
	$(\mu/\rho)_{\text{tot}}$	$(\mu/\rho)_{\text{en}}$	$(\mu/\rho)_{\text{tot}}$	$(\mu/\rho)_{\text{en}}$	$(\mu/\rho)_{\text{tot}}$	$(\mu/\rho)_{\text{en}}$	$(\mu/\rho)_{\text{tot}}$	$(\mu/\rho)_{\text{en}}$	
0.001	9730.	9730.	5110.	5110.	6510.	6510.	---	---	
.001061	8460.	8460.	} M-III						
.001061	9730.	9730.							
.001135	7720.	7720.	} M-II						
.001135	9210.	9210.							
.001291	6840.	6840.	} M-I						
.001291	8460.	8460.							
.001441									
.001441							M-I	---	
0.0015	5660.	5660.						---	
.001809			} M-V	2130.	2120.	2690.	2680.	} M-I	3950.
.001809									
.001871			} M-IV	4420.	4420.				3570.
.001871									
.002281	2650.	2640.	} M-III	4650.	4650.	1420.	1400.	1880.	1860.
.002281									
.002484			} M-II	2770.	2760.				
.002484									
.002575			} M-I	2300.	2300.	M-V	881.	869.	
.002575									
.002586			} M-IV	2510.	2500.	M-IV	2510.	2500.	
.002586									
.002820			} M-I	2190.	2180.				
.002820									
0.003	899.	890.		2170.	2160.				
.003066						1900.	1880.	746.	736.
.003066						} M-III	1770.	1760.	
.003552									
.003552									
.003554						} M-II	1420.	1410.	M-V
.003554									
.003728									501.
.003728									1570.
.003851						} M-I	1360.	1350.	M-IV
.003851									
0.004	423.	417.	1030.	1020.	1410.	1400.			1420.
.004304									1610.
.004304									1620.
0.005	235.	230.	573.	567.	788.	779.			
.005181									
.005181									
.005247	208.	203.	} L-III						
.005247	688.	596.							
.005448									
.005448									
.005623	557.	487.	} L-II						
.005623	767.	671.							
.005987	653.	574.	} L-I						
.005987	754.	667.							
0.006	745.	658.	354.	347.	491.	483.	708.	701.	
0.008	346.	313.	167.	162.	231.	225.	331.	324.	

^a The values are from Storm and Israel [5].

TABLE B-IVd. COEFFICIENTS FOR PHOTON TRANSPORT (in $\text{cm}^2 \cdot \text{g}^{-1}$)^(a)

Energy (MeV)	56 Barium		74 Tungsten		82 Lead		92 Uranium	
	$(\mu/\rho)_{\text{tot}}$	$(\mu/\rho)_{\text{en}}$	$(\mu/\rho)_{\text{tot}}$	$(\mu/\rho)_{\text{en}}$	$(\mu/\rho)_{\text{tot}}$	$(\mu/\rho)_{\text{en}}$	$(\mu/\rho)_{\text{tot}}$	$(\mu/\rho)_{\text{en}}$
0.01	189.	173.						
.010204			93.4	88.8	129.	124.	186.	180.
.010204			89.4	84.8				
.011541			L-III { 241.	184.				
.011541			L-II { 175.	137.				
.012098			L-I { 239.	187.				
.012098			L-I { 212.	167.				
.013035			L-I { 245.	193.				
.013035					L-III { 64.8	61.0		
0.015	63.1	58.3	138.	114.	L-III { 162.	113.		
.015200					L-III { 114.	82.8	63.8	60.0
.015200					L-II { 110.	80.8		
.015861					L-II { 151.	109.		
.015861					L-I { 135.	98.8		
.015861					L-I { 157.	114.		
.017170							L-III { 45.0	41.7
.017170							L-III { 103.	70.3
0.02	29.2	26.8	65.2	55.7	85.5	66.3	71.6	51.4
.020948							L-III { 64.3	46.8
.020948							L-II { 87.8	62.7
.021759							L-I { 79.2	57.2
.021759							L-I { 92.1	66.5
0.03	9.82	8.73	22.6	19.6	29.9	24.7	40.5	31.6
.037441	5.44	4.69						
.037441	29.6	9.87						
0.04	24.7	9.25	10.6	9.17	14.2	11.9	19.4	15.7
0.05	13.7	6.71	5.93	5.01	7.94	6.63	11.0	9.01
0.06	8.51	4.78	3.67	3.04	4.94	4.10	6.86	5.64
.069525			K { 2.51	2.03				
.069525			K { 11.2	3.41				
0.08	3.95	2.56	7.80	3.03	2.35	1.88	3.29	2.66
.088004					K { 1.85	1.45		
.088004					K { 7.65	2.31		
0.1	2.19	1.50	4.36	2.16	5.52	2.09	1.88	1.49
.115606							K { 1.29	0.992
.115606							K { 4.86	1.48
0.15	0.789	0.548	1.58	0.973	1.99	1.10	2.58	1.14
0.2	0.410	0.271	0.783	0.511	0.985	0.610	1.28	0.703
0.3	0.190	0.108	0.323	0.207	0.395	0.253	0.501	0.311
0.4	0.127	0.0645	0.191	0.115	0.228	0.142	0.286	0.181
0.5	0.0995	0.0469	0.137	0.0780	0.159	0.0951	0.193	0.120
0.6	0.0842	0.0388	0.108	0.0593	0.123	0.0709	0.145	0.0886
0.8	0.0675	0.0307	0.0799	0.0416	0.0875	0.0483	0.0989	0.0582
1.0	0.0579	0.0268	0.0655	0.0334	0.0701	0.0378	0.0774	0.0440
1.5	0.0456	0.0227	0.0498	0.0259	0.0517	0.0278	0.0552	0.0309
2.0	0.0406	0.0209	0.0439	0.0232	0.0456	0.0247	0.0481	0.0268
3.0	0.0367	0.0204	0.0403	0.0227	0.0419	0.0238	0.0443	0.0253
4.0	0.0360	0.0214	0.0403	0.0240	0.0419	0.0250	0.0438	0.0263
5.0	0.0362	0.0226	0.0409	0.0255	0.0424	0.0265	0.0445	0.0276
6.0	0.0366	0.0236	0.0416	0.0266	0.0436	0.0277	0.0453	0.0288
8.0	0.0380	0.0254	0.0439	0.0288	0.0456	0.0297	0.0478	0.0306
10.0	0.0398	0.0271	0.0465	0.0308	0.0488	0.0320	0.0511	0.0329
15.0	0.0443	0.0302	0.0527	0.0341	0.0552	0.0349	0.0589	0.0359
20.0	0.0487	0.0315	0.0583	0.0354	0.0619	0.0366	0.0650	0.0374
30.0	0.0548	0.0325	0.0658	0.0364	0.0698	0.0375	0.0744	0.0382
40.0	0.0588	0.0319	0.0721	0.0357	0.0765	0.0360	0.0810	0.0364
50.0	0.0623	0.0313	0.0767	0.0351	0.0811	0.0355	0.0858	0.0357
60.0	0.0649	0.0305	0.0799	0.0337	0.0849	0.0346	0.0903	0.0347
80.0	0.0697	0.0296	0.0852	0.0326	0.0904	0.0331	0.0959	0.0331
100.0	0.0728	0.0283	0.0891	0.0309	0.0951	0.0314	0.100	0.0311

^a The values are from Storm and Israel [5].

TABLE B-IVe. COEFFICIENTS FOR PHOTON TRANSPORT (in $\text{cm}^2 \cdot \text{g}^{-1}$)^(a)

Energy (MeV)	Air ^(b)		Plexiglass ^(c)		Muscle ^(c)		Compact Bone ^(c)		Sodium Iodide		Concrete ^(b)	
	(μ/P) _{tot}	(μ/P) _{en}	(μ/P) _{tot}	(μ/P) _{en}	(μ/P) _{tot}	(μ/P) _{en}	(μ/P) _{tot}	(μ/P) _{en}	(μ/P) _{tot}	(μ/P) _{en}	(μ/P) _{tot}	(μ/P) _{en}
0.001	3470.	3460.										
-0.001072									9320.	9310.	3550.	3550.
-0.001072									7930.	7920.		
-0.001073									9900.	9890.		
-0.001073									9900.	9890.	2950.	2950.
-0.001305									11200.	11100.	3090.	3090.
-0.001305											1750.	1740.
0.0015	1100.	1090.									Mg K 2760.	2760.
-0.001560									4540.	4520.	1190.	1190.
-0.001560											Al K 1060.	1060.
-0.001839											1270.	1260.
-0.001839											Si K 798.	793.
0.002	483.	482.									2940.	2890.
-0.002472									2120.	2110.	1570.	1490.
-0.002472											S K 845.	827.
0.003	153.	152.							718.	712.	674.	629.
-0.003203	128.	127.	Argon K								492.	483.
-0.003203	145.	143.										
-0.003607												
-0.003607												
0.004	75.7	74.2									Potassium K 290.	287.
-0.004037									337.	331.	314.	307.
-0.004037											335.	329.
-0.004527											Ca K 226.	222.
-0.004527											311.	296.
-0.004527												
-0.004527												
-0.004527												
0.005	39.1	38.2										
-0.005188												
-0.005188												
0.006	22.7	22.0										
-0.007112												
-0.007112												
0.008	9.64	9.16										
-0.008370									262.	242.	103.	98.9
-0.008370											84.3	81.8
-0.008370											69.1	65.2
-0.008370											49.8	47.0
0.01	4.95	4.57	3.25	2.92	5.27	4.96	20.3	19.0	142.	132.	26.6	25.1
-0.015	1.54	1.25	1.06	0.788	1.63	1.36	6.32	5.89	47.3	44.1	8.26	7.65
0.02	0.744	0.501	0.551	0.311	0.793	0.544	2.79	2.51	21.4	20.0	3.60	3.21
0.03	0.342	0.139	0.298	0.0892	0.373	0.154	0.952	0.743	7.25	6.38	1.18	0.919
-0.03170												
-0.03170												
0.04	0.243	0.0616	0.234	0.0426	0.268	0.0677	0.312	0.205	5.53	4.80		
0.05	0.205	0.0374	0.208	0.0288	0.227	0.0409	0.340	0.158	10.4	8.47	0.593	0.380
0.06	0.186	0.0283	0.193	0.0243	0.205	0.0312	0.274	0.0979	6.1	5.73	0.384	0.195
0.08	0.166	0.0231	0.176	0.0226	0.183	0.0255	0.209	0.0520	2.98	2.01	0.210	0.0591
0.1	0.154	0.0227	0.164	0.0235	0.170	0.0252	0.180	0.0386	1.67	1.17	0.178	0.0407
0.15	0.135	0.0247	0.146	0.0267	0.149	0.0276	0.149	0.0304	0.620	0.422	0.143	0.0298
0.2	0.123	0.0265	0.133	0.0289	0.136	0.0297	0.133	0.0302	0.333	0.208	0.127	0.0286
0.3	0.107	0.0287	0.115	0.0334	0.118	0.0317	0.114	0.0311	0.167	0.0863	0.108	0.0293
0.4	0.0953	0.0294	0.103	0.0319	0.105	0.0325	0.102	0.0316	0.118	0.0547	0.0963	0.0298
0.5	0.0870	0.0298	0.0941	0.0320	0.0960	0.0327	0.0927	0.0316	0.0955	0.0420	0.0876	0.0290
0.6	0.0805	0.0295	0.0871	0.0319	0.0888	0.0326	0.0857	0.0315	0.0826	0.0359	0.0810	0.0296
0.8	0.0706	0.0287	0.0765	0.0311	0.0779	0.0318	0.0752	0.0306	0.0675	0.0298	0.0710	0.0287
1.0	0.0636	0.0278	0.0687	0.0301	0.0700	0.0308	0.0676	0.0287	0.0585	0.0266	0.0637	0.0278
1.5	0.0516	0.0254	0.0559	0.0275	0.0570	0.0281	0.0550	0.0270	0.0469	0.0231	0.0518	0.0254
2.0	0.0442	0.0234	0.0480	0.0252	0.0489	0.0257	0.0475	0.0248	0.0415	0.0213	0.0447	0.0236
3.0	0.0357	0.0205	0.0385	0.0220	0.0393	0.0225	0.0383	0.0210	0.0366	0.0205	0.0364	0.0208
4.0	0.0308	0.0187	0.0329	0.0198	0.0337	0.0203	0.0331	0.0199	0.0353	0.0210	0.0319	0.0194
5.0	0.0275	0.0174	0.0292	0.0183	0.0300	0.0188	0.0297	0.0186	0.0348	0.0218	0.0289	0.0183
6.0	0.0252	0.0165	0.0266	0.0172	0.0274	0.0178	0.0274	0.0178	0.0349	0.0226	0.0269	0.0177
8.0	0.0222	0.0153	0.0232	0.0156	0.0240	0.0163	0.0244	0.0165	0.0355	0.0240	0.0244	0.0170
10.0	0.0203	0.0146	0.0211	0.0147	0.0219	0.0154	0.0226	0.0159	0.0367	0.0252	0.0230	0.0166
15.0	0.0179	0.0136	0.0182		0.0192	0.0140	0.0204		0.0402	0.0278	0.0213	0.0162
20.0	0.0169	0.0133	0.0168		0.0179	0.0138	0.0194		0.0434	0.0287	0.0209	0.0162
30.0	0.0162	0.0129	0.0157		0.0168	0.0130	0.0189		0.0483	0.0296	0.0209	0.0161
40.0	0.0160	0.0127	0.0153		0.0165	0.0128	0.0189		0.0518	0.0292	0.0212	0.0160
50.0	0.0160	0.0126	0.0151		0.0164	0.0126	0.0189		0.0549	0.0287	0.0217	0.0159
60.0	0.0161	0.0124	0.0151		0.0165	0.0125	0.0193		0.0569	0.0279	0.0221	0.0157
80.0	0.0164	0.0122	0.0152		0.0167	0.0124	0.0197		0.0604	0.0271	0.0227	0.0154
100.0	0.0167	0.0121	0.0154		0.0170	0.0123	0.0201		0.0634	0.0261	0.0235	0.0151

(a) Except where noted, values are from Storm and Israel, Ref. [5].
 (b) Assumed composition by weight (per cent): Air: (N : O : A) = (75.5 : 23.2 : 1.3); Concrete: (H : O : Na : Mg : Al : Si : S : K : Ca : Fe) = (0.56 : 49.83 : 1.71 : 0.24 : 4.56 : 31.58 : 0.12 : 1.92 : 8.26 : 1.22).
 (c) Values of (μ/P)_{tot} from Hubbell, HSRDS-NBS-29, Table 3 (Ref. 6). Values of (μ/P)_{en} from NBS Handbook 85, p. 3 (Ref. 11).
 Plexiglass (perspex, lucite) composition: C₅H₈O₂. Assumed composition by weight (per cent):
 Muscle (striated): (H : C : N : O : Na : Mg : P : S : K : Ca) = (10.2 : 12.5 : 3.5 : 72.9 : 0.08 : 0.2 : 0.5 : 0.3 : 0.007);
 Compact bone (femur): (6.4 : 27.8 : 2.7 : 41.0 : 0.0 : 0.2 : 7.0 : 0.2 : 0.0 : 14.7).

TABLE B-Va. FACTOR FOR CONVERTING PHOTON ENERGY FLUX DENSITY TO ABSORBED DOSE RATE (SI units) ^a

E_γ (MeV)	$K_\gamma/E_\gamma((\text{Gy}\cdot\text{h}^{-1})(\text{MeV}\cdot\text{cm}^{-2}\cdot\text{s}^{-1})^{-1})$		
	Air	Carbon	Tissue
0.01	2.67×10^{-6}	1.12×10^{-6}	3.38×10^{-6}
0.015	7.59×10^{-7}	2.97×10^{-7}	9.60×10^{-7}
0.02	3.03×10^{-7}	1.16×10^{-7}	3.88×10^{-7}
0.03	8.58×10^{-8}	3.37×10^{-8}	1.11×10^{-7}
0.04	3.74×10^{-8}	1.76×10^{-8}	4.80×10^{-8}
0.05	2.24×10^{-8}	1.30×10^{-8}	2.81×10^{-8}
0.06	1.70×10^{-8}	1.16×10^{-8}	2.05×10^{-8}
0.08	1.37×10^{-8}	1.17×10^{-8}	1.91×10^{-8}
0.10	1.34×10^{-8}	1.24×10^{-8}	1.50×10^{-8}
0.15	1.45×10^{-8}	1.42×10^{-8}	1.58×10^{-8}
0.2	1.55×10^{-8}	1.53×10^{-8}	1.69×10^{-8}
0.3	1.66×10^{-8}	1.66×10^{-8}	1.80×10^{-8}
0.4	1.70×10^{-8}	1.70×10^{-8}	1.85×10^{-8}
0.5	1.71×10^{-8}	1.71×10^{-8}	1.85×10^{-8}
0.6	1.71×10^{-8}	1.71×10^{-8}	1.85×10^{-8}
0.7	1.70×10^{-8}	1.67×10^{-8}	1.84×10^{-8}
0.8	1.66×10^{-8}	1.66×10^{-8}	1.80×10^{-8}
1.0	1.61×10^{-8}	1.61×10^{-8}	1.74×10^{-8}
1.5	1.48×10^{-8}	1.48×10^{-8}	1.60×10^{-8}
2.0	1.37×10^{-8}	1.37×10^{-8}	1.48×10^{-8}
2.5	1.27×10^{-8}	1.27×10^{-8}	1.40×10^{-8}
3.0	1.22×10^{-8}	1.20×10^{-8}	1.31×10^{-8}
4.0	1.12×10^{-8}	1.10×10^{-8}	1.20×10^{-8}
5.0	1.04×10^{-8}	1.02×10^{-8}	1.11×10^{-8}
6.0	9.92×10^{-9}	9.59×10^{-9}	1.05×10^{-8}
8.0	9.23×10^{-9}	8.80×10^{-9}	9.73×10^{-9}
10.0	8.83×10^{-9}	8.37×10^{-9}	9.76×10^{-9}

^a Adapted from Ref.[10], with kind permission of D.C. Layman, G. Thornton, B.J. Henderson, and the General Electric Company.

TABLE B-Vb. FACTOR FOR CONVERTING PHOTON ENERGY FLUX DENSITY TO ABSORBED DOSE RATE (special units)^a

E_γ (MeV)	K_γ/E_γ ((rad·h ⁻¹)(MeV·cm ⁻² ·s ⁻¹) ⁻¹)		
	Air	Carbon	Tissue
0.01	2.67×10^{-4}	1.12×10^{-4}	3.38×10^{-4}
0.015	7.59×10^{-5}	2.97×10^{-5}	9.60×10^{-5}
0.02	3.03×10^{-5}	1.16×10^{-5}	3.88×10^{-5}
0.03	8.58×10^{-6}	3.37×10^{-6}	1.11×10^{-5}
0.04	3.74×10^{-6}	1.76×10^{-6}	4.80×10^{-6}
0.05	2.24×10^{-6}	1.30×10^{-6}	2.81×10^{-6}
0.06	1.70×10^{-6}	1.16×10^{-6}	2.05×10^{-6}
0.08	1.37×10^{-6}	1.17×10^{-6}	1.91×10^{-6}
0.10	1.34×10^{-6}	1.24×10^{-6}	1.50×10^{-6}
0.15	1.45×10^{-6}	1.42×10^{-6}	1.58×10^{-6}
0.2	1.55×10^{-6}	1.53×10^{-6}	1.69×10^{-6}
0.3	1.66×10^{-6}	1.66×10^{-6}	1.80×10^{-6}
0.4	1.70×10^{-6}	1.70×10^{-6}	1.85×10^{-6}
0.5	1.71×10^{-6}	1.71×10^{-6}	1.85×10^{-6}
0.6	1.71×10^{-6}	1.71×10^{-6}	1.85×10^{-6}
0.7	1.70×10^{-6}	1.67×10^{-6}	1.84×10^{-6}
0.8	1.66×10^{-6}	1.66×10^{-6}	1.80×10^{-6}
1.0	1.61×10^{-6}	1.61×10^{-6}	1.74×10^{-6}
1.5	1.48×10^{-6}	1.48×10^{-6}	1.60×10^{-6}
2.0	1.37×10^{-6}	1.37×10^{-6}	1.48×10^{-6}
2.5	1.27×10^{-6}	1.27×10^{-6}	1.40×10^{-6}
3.0	1.22×10^{-6}	1.20×10^{-6}	1.31×10^{-6}
4.0	1.12×10^{-6}	1.10×10^{-6}	1.20×10^{-6}
5.0	1.04×10^{-6}	1.02×10^{-6}	1.11×10^{-6}
6.0	9.92×10^{-7}	9.59×10^{-7}	1.05×10^{-6}
8.0	9.23×10^{-7}	8.80×10^{-7}	9.73×10^{-7}
10.0	8.83×10^{-7}	8.37×10^{-7}	9.76×10^{-7}

^a Adapted from Ref.[10], with kind permission of D.C. Layman, G. Thornton, B.J. Henderson, and the General Electric Company.

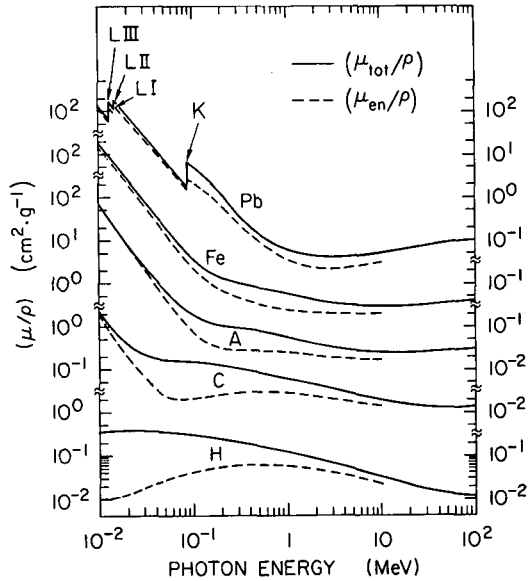


FIG.B-1. Photon transport coefficients for representative elements, as functions of photon energy. The solid curve represents the mass attenuation coefficient (μ_{tot}/ρ). The dashed curve represents the mass energy-absorption coefficient (μ_{en}/ρ), defined as the mass attenuation coefficient multiplied by the fraction of energy deposited locally by photon interactions. (The data are from Hubbell [6]. Adapted from Ref.[9], with kind permission of the Particle Data Group and the Lawrence Berkeley Laboratory.)

where ρ_1, ρ_2, \dots are the relative amounts (by weight) of the components having radiation lengths X_{01}, X_{02}, \dots (in $\text{g} \cdot \text{cm}^{-2}$), and $\rho_{\text{tot}} = \rho_1 + \rho_2 + \dots$.

Nuclear collision lengths and absorption lengths are combined in the same manner.

Attenuation coefficients and mass stopping powers are combined linearly with appropriate weighting:

$$\mu = [\sum \mu_i \rho_i] / \rho_{\text{tot}} = (\mu_1 \rho_1 + \mu_2 \rho_2 + \mu_3 \rho_3 + \dots) / \rho_{\text{tot}} \quad (\text{B.2a})$$

$$S/\rho = [\sum (S/\rho)_i \rho_i] / \rho_{\text{tot}} \quad (\text{B.3a})$$

where all values for μ and S/ρ are in $\text{cm}^2 \cdot \text{g}^{-1}$ and in $\text{MeV} \cdot \text{cm}^2 \cdot \text{g}^{-1}$, respectively, or in equivalent units.

In the case of compounds, one may use the atomic composition directly. For a compound of elements E^1, E^2, E^3, \dots , having atomic weights A_1, A_2, \dots , with chemical formula $E_{n_1}^1 E_{n_2}^2 E_{n_3}^3 \dots$, the equivalent of Eq.(B.1a) is

$$\frac{M}{X_0} = \sum \frac{n_i A_i}{X_{0i}} \quad (\text{B.1b})$$

where M is the molecular weight, $M = \sum n_i A_i = n_1 A_1 + n_2 A_2 + n_3 A_3 + \dots$. Similarly,

$$\mu_{\text{tot}} = [\sum n_i A_i \mu_i] / M \quad (\text{B.2b})$$

$$S/\rho = [\sum n_i A_i (S/\rho)_i] / M \quad (\text{B.3b})$$

For compounds, it is also meaningful to calculate a molecular cross-section, determined in the following manner

$$\sigma_m = \sum n_i \sigma_i = n_1 \sigma_1 + n_2 \sigma_2 + \dots \quad (\text{B.4})$$

In these formulae, the effects of molecular binding are ignored, and this is usually a valid assumption for most purposes.

The effective Z/A and Z of a compound or mixture are useful parameters for interpolation of other physical quantities. Physical quantities that are based on interactions with individual atomic electrons have cross-sections per atom which are proportional to Z . For these quantities, interpolations are best made in terms of the ratio Z/A :

$$(Z/A)_{\text{eff}} = [\sum \rho_i Z_i / A_i] / \rho_{\text{tot}} \quad (\text{B.5})$$

Examples of such physical quantities are the collision stopping power, ranges of particles, and the photon attenuation and energy-absorption coefficients at energies at which the Compton effect would dominate.

For quantities derived from elementary processes whose cross-section per atom is proportional to Z^2 (such as bremsstrahlung and pair production) an effective Z can be approximated by:

$$Z_{\text{eff}} = (Z^2/A)_{\text{eff}} / (Z/A)_{\text{eff}} \quad (\text{B.6})$$

where

$$(Z^2/A)_{\text{eff}} = [\sum \rho_i Z_i^2 / A_i] / \rho_{\text{tot}} \quad (\text{B.7})$$

TABLE B-VI. Z-DEPENDENCE OF CROSS-SECTION PER ATOM ($\sigma \propto Z^m$)

Particle type	Physical effect	Exponent m^a
Photon	Photoelectric effect	4.6
	Coherent scattering	2.6
	Incoherent (Compton) scattering	1
	Pair production	2^b
Electron	Collision (ionization)	1
	Radiation (bremsstrahlung)	2^b
	Angular scattering power	2^b
Hadron (proton, neutron, meson, etc.)	Nuclear scattering	2/3

^a Values of m are both Z - and energy dependent. These should be taken as nominal values.

^b $Z(Z + 1)$ is a better representation of the Z -dependence than is Z^2 .

and $(Z/A)_{\text{eff}}$ is given by Eq.(B.5). Examples of such quantities are the radiation length, the photon attenuation and energy-absorption coefficients at energies above the Compton minimum, and parameters of multiple Coulomb scattering (angular scattering power).

The above examples are specific cases of the general rules

$$(Z^m/A)_{\text{eff}} = [\sum \rho_i Z_i^m / A_i] / \rho_{\text{tot}} = [\sum \alpha_i Z_i^{m-1}] / \rho_{\text{tot}} \quad (\text{B.8})$$

$$Z_{\text{eff}} = \left[\frac{\sum \alpha_i Z_i^{m-1}}{\sum \alpha_i} \right]^{1/(m-1)} \quad (\text{B.9})$$

in which the quantity $\alpha_i = \rho_i Z_i / A_i$ is equal to the density of electrons attributable to element i , and the total density is $\rho_{\text{tot}} = \sum \rho_i$. The parameter m is determined by examining the Z -dependence of the cross-section (per atom) of the underlying physical process: $\sigma \propto Z^m$. Nominal values of the exponent m are shown in Table B-VI. These values vary somewhat with both Z and energy and should be taken as indicative only. A recent discussion of these considerations, together with an analysis of the Z -dependence of photon and electron interactions in light mixtures (including tissue) and compounds is published by White [15].

Where the elementary cross-section per atom is better described as proportional to A^m , we may use

$$A_{\text{eff}} = \left[\sum \rho_i A_i^{m-1} / \sum \rho_i \right]^{1/(m-1)} \quad (\text{B.10})$$

to obtain an effective atomic weight A_{eff} for interpolation.

REFERENCES TO APPENDIX B

- [1] WEAST, R.C., Ed., Handbook of Chemistry and Physics, 56th ed., Chemical Rubber Publishing Company, Cleveland, Ohio (1975) B-1 to B-42.
- [2] TSAI, Y.-S., Pair production and bremsstrahlung of charged leptons, *Rev. Mod. Phys.* **46** 4 (1974) 828.
- [3] BERGER, M.J., SELTZER, S.M., Tables of Energy Losses and Ranges of Electrons and Positrons, National Aeronautics and Space Administration, Washington, DC, Rep. NASA SP-3012 (1964).
- [4] BERGER, M.J., SELTZER, S.M., Additional Stopping Power and Range Tables for Protons, Mesons, and Electrons, National Aeronautics and Space Administration, Washington, DC, Rep. NASA SP-3036 (1966).
- [5] STORM, E., ISRAEL, H.I., Photon Cross Sections from 0.001 to 100 MeV for Elements 1 through 100, Los Alamos Scientific Laboratory, Rep. LA-3753, UC-34, Physics, TID-4500 (1967); *Nucl. Data Tables A7* (1970) 565.
- [6] HUBBELL, J.H., Photon Cross Sections, Attenuation Coefficients, and Energy Absorption Coefficients from 10 keV to 100 GeV, National Bureau of Standards, Washington, DC, Rep. NSRDS-NBS 29 (1969).
- [7] CARLSON, P.J., DIDDENS, A.N., MÖNNIG, F., SCHOPPER, H., "Total np and nN cross sections", in *Numerical Data and Functional Relationships in Science and Technology* (HELLWEGE, K.-H., Ed., Landolt-Börnstein), Group I: Nuclear and Particle Physics, Vol. 7, Elastic and Charge Exchange Scattering of Elementary Particles, Springer-Verlag, Berlin (1973) 14–21.
- [8] INTERNATIONAL COMMISSION ON RADIATION UNITS AND MEASUREMENTS, Radiation Dosimetry: Electrons with Initial Energies Between 1 and 50 MeV, ICRU Report No. 21, Washington, DC (1974).
- [9] PARTICLE DATA GROUP, Review of Particle Properties, *Rev. Mod. Phys.* **48** 2 (1976).
- [10] LAYMAN, D.C., THORNTON, G., Remote Handling of Mobile Nuclear Systems, USAEC, Washington, DC, Rep. TID-21719 (1966).
- [11] NATIONAL BUREAU OF STANDARDS, INTERNATIONAL COMMISSION ON RADIOLOGICAL UNITS AND MEASUREMENTS, Physical Aspects of Irradiation, NBS Handbook No. 85, ICRU Report No. 10b, National Bureau of Standards, Washington, DC (1964) 3.
- [12] PAGES, L., BERTEL, E., JOFFRE, H., SKLAVENITIS, L., Energy loss, range and bremsstrahlung yield for 10-keV to 100-MeV electrons in various elements and chemical compounds, *At. Data Tables* **4** 1 (1972) 1.
- [13] VEIGELE, W.J., Photon cross sections from 0.1 keV to 1 MeV for elements $Z = 1$ to $Z = 94$, *At. Data Tables* **5** 1 (1973) 51.

- [14] PLECHATY, E.F., CULLEN, D.E., HOWERTON, R.J., Tables and Graphs of Photon Interaction Cross Sections from 1.0 keV to 100 MeV Derived from the LLL Evaluated Nuclear Data Library, Lawrence Livermore Laboratory, Rep. UCRL-50400, Vol.6, Rev.1 (1975).
- [15] WHITE, D.R., An analysis of the Z-dependence of photon and electron interactions, Phys. Med. Biol. 22 2 (1977) 219.

Appendix C

RULES OF THUMB

The following formulae, selected for their usefulness at electron linac installations are convenient to remember and use.

1. Dose-equivalent rate imparted by an electron beam of flux density φ (in electrons \cdot cm $^{-2}$ \cdot s $^{-1}$):

$$\dot{H} \text{ (rem} \cdot \text{h}^{-1}) \approx 1.6 \times 10^{-4} \varphi \quad (\text{C.1})$$

(Valid to $\approx \pm 15\%$ for $E = 1 - 200$ MeV.)

2. Dose-equivalent rate imparted by a photon field of *energy* flux density ψ (in MeV \cdot cm $^{-2}$ \cdot s $^{-1}$):

$$\dot{H} \text{ (rem} \cdot \text{h}^{-1}) \approx 1.6 \times 10^{-6} \psi \quad (\text{C.2})$$

(Valid to $\approx \pm 15\%$ for $k = 0.1 - 2.5$ MeV.)

3. Dose-equivalent rate imparted by a neutron field of flux density φ (in neutrons \cdot cm $^{-2}$ \cdot s $^{-1}$):

$$\dot{H} \text{ (rem} \cdot \text{h}^{-1}) \approx 1.4 \times 10^{-4} \varphi \quad (\text{C.3})$$

(This corresponds to an effective energy of about 2 MeV.)

4. The '6CE' rule for a point-source gamma emitter:

$$\dot{H} \text{ (rem} \cdot \text{h}^{-1}) \approx \dot{X} = 5.7 \text{ C E d}^{-2} \approx 6 \text{ C E d}^{-2} \quad (\text{C.4a})$$

(Valid to about $\pm 20\%$ for $0.07 \lesssim k \lesssim 2.0$ MeV)

where X is in R \cdot h $^{-1}$, C is the activity in Ci, E is the total energy released in gammas per disintegration (MeV), and the distance d is in feet.

The metric equivalent is equally convenient:

$$\dot{H} \text{ (rem} \cdot \text{h}^{-1}) \approx \dot{X} = 0.53 \text{ C E d}^{-2} \approx \frac{1}{2} \text{ C E d}^{-2} \quad (\text{C.4b})$$

where C and E have the same meaning but d is in metres.

In SI units the following rules apply:

$$\dot{X} \text{ (C} \cdot \text{kg}^{-1} \cdot \text{s}^{-1}) \approx 1 \times 10^{-18} \text{ B E d}^{-2} \quad (\text{C.4c})$$

$$\dot{D} \text{ (Gy} \cdot \text{s}^{-1}) \approx 35 \times 10^{-18} \text{ B E d}^{-2} \quad (\text{C.4d})$$

where B is the activity in Bq, E is in MeV and the distance d is in metres. (Note that 35 is close to $W = 33.7 \text{ eV}$; see Eqs (C.15a, C.15b).)

5. Dose-equivalent rates of secondary radiations released from targets by electron beams (at 1 m from target, per kW incident beam power)

Type of secondary radiation	\dot{H} (rem · h ⁻¹)(kW · m ⁻²) ⁻¹	Range of validity ^a of E ₀
Bremsstrahlung at 0°	2 000 E ₀ ² (E ₀ in MeV) ^b	1 – 20 MeV
	30 000 E ₀ (E ₀ in MeV) ^c	≳ 20 MeV
at 90°	5 000 ^d	≳ 50 MeV
Giant-resonance neutrons ^e	2 200	≳ 15 MeV
Muons (0° only)	5 E ₀ (E ₀ in GeV)	≳ 2 GeV

^a Range of electron energy for which the rule is valid to within about a factor of two for high-Z targets. Dose-equivalent rates also depend on target material.

^b Equivalent to \dot{H} ((rem · min⁻¹)(kW · m⁻²)⁻¹) ≈ 33 E₀² (E₀ in MeV).

^c Equivalent to \dot{H} ((rem · min⁻¹)(kW · m⁻²)⁻¹) ≈ 500 E₀ (E₀ in MeV).

^d ‘Hard’ bremsstrahlung component, for shielding purposes. Unshielded dose-equivalent rates may be higher by as much as a factor of 10–20, depending on material and angle of incidence.

^e Strongly dependent on material. The value given corresponds approximately to the maximum obtainable from high-Z materials in which fission does not make a significant contribution to the yield. (Mnemonic: “The dose equivalent is twice the power in watts”.)

6. The ‘300A’ rule for dose imparted (at entrance) by β^\pm radiations:

$$\dot{H} \text{ (rem} \cdot \text{h}^{-1}) \approx \dot{D} \approx 300 \text{ A d}^{-2} \quad (\text{C.6a})$$

where \dot{D} is in rad · h⁻¹, A is the activity of a point-source beta emitter in Ci (times the fraction of disintegrations in which a beta ray is emitted), and d is in feet. The equivalent metric rule is

$$\dot{H} \text{ (rem} \cdot \text{h}^{-1}) \approx \dot{D} \approx 30 \text{ A d}^{-2} \quad (\text{C.6b})$$

where d is in metres.

In SI units, the following rules apply:

$$\dot{D} \text{ (Gy} \cdot \text{h}^{-1}) \approx 8 \times 10^{-12} A d^{-2} \quad (\text{C.6c})$$

$$\dot{D} \text{ (Gy} \cdot \text{s}^{-1}) \approx 2 \times 10^{-15} A d^{-2} \quad (\text{C.6d})$$

where A is in Bq and d is in metres. These formulae disregard absorption of beta rays in intervening materials (source material, air, epidermis).

7. Practical range of e^\pm or β^\pm in any material:

$$R \text{ (g} \cdot \text{cm}^{-2}) \approx 1/2 E_0 \quad (\text{C.7})$$

where E_0 is in MeV. (It is almost as easy to remember the formula of Katz and Penfold or that of Markus – see Refs [10, 12] and Eqs (12, 14) in Section 2.3.)

8. Range of energetic muons in any material:

$$R \text{ (g} \cdot \text{cm}^{-2}) \approx 600 E_0 \text{ (GeV)} \approx 1/2 E_0 \text{ (MeV)} \quad (\text{C.8})$$

9. Nucleon-nucleus total cross-section (above 150 MeV):

$$\sigma \text{ (barn)} \approx 0.0496 A^{0.778} \quad (\text{C.9})$$

This is more accurate than $\pi (1.41 \times 10^{-13} A^{1/3})^2 \cdot \text{cm}^2 = 0.0628 A^{2/3}$ barn, which is often used (the ‘natural cross-section’).

10. Critical energy for electrons in material of atomic number Z :

$$E_c \text{ (MeV)} \cong 800/(Z + 1.2) \quad (\text{C.10})$$

11. Ratio of bremsstrahlung to collision (ionization) energy loss per unit track length for electrons of kinetic energy E (MeV) in material of atomic number Z :

$$\frac{(dE/dX)_{\text{rad}}}{(dE/dX)_{\text{col}}} \cong Z E/800 \quad (\text{C.11})$$

12. Fractional radiation yield (bremsstrahlung efficiency) for electrons of initial kinetic energy E_0 (MeV) that are brought to rest in material of atomic number Z :

$$\frac{E_{\text{rad}}}{E_0} \cong \frac{E_0}{1600 + Z E_0} \quad (\text{C.12})$$

13. Thick-target bremsstrahlung: Product of initial electron energy E_0 and $\theta_{1/2}$, the angle at which the bremsstrahlung intensity drops to half:

$$E_0 \text{ (MeV)} \theta_{1/2} \cong 100 \text{ MeV} \cdot \text{degree} \quad (\text{C.13})$$

14. Maximum saturation activity A_s induced by high-energy electron beams, per unit electron beam power:

$$\begin{array}{lll} \text{Light nuclei} & (Z \cong 10 - 40) & A_s \approx 0.75 \text{ TBq} \cdot \text{kW}^{-1} \\ & & A_s \approx 20 \text{ Ci} \cdot \text{kW}^{-1} \end{array} \quad (\text{C.14a})$$

$$\begin{array}{lll} \text{Heavy nuclei} & & \\ \text{(but not photofissionable, } Z \cong 70 - 82) & & A_s \approx 1.5 \text{ TBq} \cdot \text{kW}^{-1} \\ & & A_s \approx 40 \text{ Ci} \cdot \text{kW}^{-1} \end{array} \quad (\text{C.14b})$$

These values apply (to about $\pm 30\%$) where the (γ, n) reaction leads to activity in most or all nuclides of the target. Some notable examples are Cu ($A_s \cong 0.67 \text{ TBq} \cdot \text{kW}^{-1}$ ($18 \text{ Ci} \cdot \text{kW}^{-1}$)) and Au ($A_s \cong 1.7 \text{ TBq} \cdot \text{kW}^{-1}$ ($47 \text{ Ci} \cdot \text{kW}^{-1}$)). However, the induced activity is usually less than these values because the (γ, n) reaction often does not lead to activity of radiological significance.

15. Relationship of exposure to absorbed dose in air and tissue (SI units):
A radiation field which would result in an exposure X (in $\text{C} \cdot \text{kg}^{-1}$) imparts an absorbed dose D (in Gy) to air of:

$$D \text{ (air)} = 33.7 X \quad (\text{C.15a})$$

and, if absorbed in soft tissue:

$$D \text{ (tissue)} = 36.4 X \quad (\text{C.15b})$$

(A useful mnemonic for Eq.(C.15a) derives from its basis in the average energy required to form an ion pair in air: $W = 33.7 \text{ eV}$. Equation (C.15b) is based on ^{60}Co radiation.)

Appendix D

ADDRESSES OF ORGANIZATIONS

The following is a list of addresses of organizations from which additional information on radiological safety and other safety areas may be obtained, and of organizations whose internal reports are cited in the text.

ACGIH	American Conference of Governmental Industrial Hygienists, 1014 Broadway, Cincinnati, OH 45202, United States of America
AIHA	American Industrial Hygiene Association, 14125 Prevost, Detroit, MI 48227, United States of America
ANSI	American National Standards Institute, 1430 Broadway, New York, NY 10018, United States of America
ASTM	American Society for Testing Materials, 1916 Race Street, Philadelphia, PA 19103, United States of America
AEC	Atomic Energy Commission (Superseded in 1975 by the Nuclear Regulatory Commission (NRC) and the Energy Research and Development Administration (ERDA); ERDA was superseded by the Department of Energy (DOE) in 1977.)
BSI	British Standards Institution, 2 Park Street, London W1A 2BS, United Kingdom
BNL	Brookhaven National Laboratory, Upton, Long Island, NY 11973, United States of America

BAM Bundesanstalt für Materialprüfung,
 Unter den Eichen 87,
 1 Berlin 45

Chief Inspector of Factories,
 Ministry of Health and Social Services,
 Fermanagh House,
 Ormean Avenue,
 Belfast, BT2 8GP,
 Northern Ireland

Department of Employment,
 Advisory and Information Unit,
 1 Chepstow Place,
 London W2,
 United Kingdom

DOE Department of Energy,
 Washington, DC 20545,
 United States of America

DHSS Department of Health and Social Security,
 (Scientific and Technical Branch),
 14 Russell Square,
 London WC1B 5EP,
 United Kingdom

Department of National Health and Welfare,
 Radiation Protection Division,
 Brookfield Road,
 Confederation Heights,
 Ottawa, Ontario K1A 1C1,
 Canada

Deutsches Atomforum,
 Allianzplatz,
 53 Bonn,
 Federal Republic of Germany

DESY Deutsches Elektronen-Synchrotron,
 Notkestrasse 85,
 D-2 Hamburg 52,
 Federal Republic of Germany

DIN Deutsches Institut für Normung,
NAR Normenausschuss Radiologie im DIN,
 Alexanderstrasse 1,
 2000 Hamburg,
 Federal Republic of Germany

- ERDA Energy Research and Development Administration,
Washington, DC 20545,
United States of America
(Superseded in 1977 by the Department of Energy (DOE).)
- ERDA Energy Research and Development Administration,
Technical Information Center,
P.O. Box 62,
Oak Ridge, TN 37830,
United States of America
- Environmental Measurements Laboratory,
(formerly Health and Safety Laboratory),
Department of Energy,
New York, NY 10014,
United States of America
- EPA Environmental Protection Agency,
401 M Street S.W.,
Washington, DC 20024,
United States of America
- CERN European Organization for Nuclear Research (CERN),
CH-1211 Geneva 23,
Switzerland
- ESIS European Shielding Information Service,
CCR Euratom,
21020 Ispra, Varese,
Italy
- Geschäftsstelle der Strahlenschutzkommission im
Institut für Reaktorsicherheit,
Glockengasse 2,
5 Cologne 1,
Federal Republic of Germany
- GSU Gesellschaft für Strahlen- und Umweltforschung,
Ingolstädter Landstrasse 1,
8042 Neuherberg/Munich,
Federal Republic of Germany
- Health and Safety Executive,
25 Chapel Street,
London NW1 5DT,
United Kingdom
- HASL Health and Safety Laboratory
(See Environmental Measurements Laboratory)

- HMSO Her Majesty's Stationery Office,
P6A Atlantic House,
Holborn Viaduct,
London EC1,
United Kingdom
- HPA Hospital Physicians' Association,
Tavistock House North,
Tavistock Square,
London WC1,
United Kingdom
- IAEA International Atomic Energy Agency,
Kärntner Ring 11,
P.O. Box 590,
A-1011 Vienna,
Austria
- ICRU International Commission on Radiation Units and Measurements,
7910 Woodmont Avenue, Suite 1016,
Washington, DC 20014,
United States of America
- ICRP International Commission on Radiological Protection,
Clifton Avenue,
Sutton, Surrey SM2 5PU,
United Kingdom
- IEC International Electrotechnical Commission,
1 Rue de Varembe,
CH-1211 Geneva 20,
Switzerland
- ISO International Standards Organization,
23 Rue Notre Dame des Victoires,
Paris,
France
- LNF Laboratori Nazionali di Frascati del CNEN,
Casella Postale No. 70,
00044 Frascati (Rome),
Italy
- LBL Lawrence Berkeley Laboratory,
Berkeley, CA 94720,
United States of America
- LLL Lawrence Livermore Laboratory,
Livermore, CA 94550,
United States of America

LASL Los Alamos Scientific Laboratory,
 Los Alamos, NM 87544,
 United States of America

NASA National Aeronautics and Space Administration,
 Washington, DC 20546,
 United States of America

NBS National Bureau of Standards,
 Radiation Physics Division,
 Washington, DC 20234,
 United States of America

NCRP National Council on Radiation Protection and Measurements,
 7910 Woodmont Avenue, Suite 1016,
 Washington, DC 20014,
 United States of America

NPL National Physical Laboratory,
 Teddington, Middlesex TW11 0LW,
 United Kingdom

NRPB National Radiological Protection Board,
 Harwell, Didcot, Oxon. OX11 0RQ,
 United Kingdom

NRC National Research Council of Canada,
 Ottawa, K1A 0R6,
 Canada

NSC National Safety Council,
 425 North Michigan Avenue,
 Chicago, IL 60611,
 United States of America

NRC Nuclear Regulatory Commission,
 Washington, DC 20545,
 United States of America

ORNL Oak Ridge National Laboratory,
 Oak Ridge, TN 37830,
 United States of America

PTB Physikalisch-Technische Bundesanstalt,
 Bundesallee 100,
 33 Braunschweig,
 Federal Republic of Germany

RSIC Radiation Shielding Information Center,
Oak Ridge National Laboratory,
Oak Ridge, TN 37831,
United States of America

RHEL Rutherford High Energy Laboratory,
Chilton, Didcot, Oxon. OX11 0QX,
United Kingdom

SLAC Stanford Linear Accelerator Center,
P.O. Box 4349,
Stanford, CA 94305,
United States of America

GPO Superintendent of Documents,
United States Government Printing Office,
Washington, DC 20402,
United States of America

NTIS United States Department of Commerce,
National Technical Information Service,
Springfield, VA 22151,
United States of America

USPHS
HEW United States Public Health Service,
Department of Health, Education and Welfare,
Washington, DC 20203,
United States of America

The following conversion table is provided for the convenience of readers and to encourage the use of SI units.

FACTORS FOR CONVERTING SOME OF THE MORE COMMON UNITS TO INTERNATIONAL SYSTEM OF UNITS (SI) EQUIVALENTS

NOTES:

- (1) SI base units are the metre (m), kilogram (kg), second (s), ampere (A), kelvin (K), candela (cd) and mole (mol).
- (2) ► indicates SI derived units and those accepted for use with SI;
 ► indicates additional units accepted for use with SI for a limited time.
 [For further information see *The International System of Units (SI), 1977 ed., published in English by HMSO, London, and National Bureau of Standards, Washington, DC, and International Standards ISO-1000 and the several parts of ISO-31 published by ISO, Geneva.*]
- (3) The correct abbreviation for the unit in column 1 is given in column 2.
- (4) * indicates conversion factors given exactly; other factors are given rounded, mostly to 4 significant figures.
 ≡ indicates a definition of an SI derived unit: [] in column 3+4 enclose factors given for the sake of completeness.

Column 1 Multiply data given in:	Column 2	Column 3 by:	Column 4 to obtain data in:
Radiation units			
► becquerel	1 Bq	(has dimensions of s^{-1})	
disintegrations per second (= dis/s)	1 s^{-1}	≡ 1.00×10^0	Bq *
► curie	1 Ci	= 3.70×10^{10}	Bq *
► roentgen	1 R	[= 2.58×10^{-4}	C/kg] *
► gray	1 Gy	[≡ 1.00×10^0	J/kg] *
► rad	1 rad	= 1.00×10^{-2}	Gy *
sievert (radiation protection only)	1 Sv	[= 1.00×10^0	J/kg] *
rem (radiation protection only)	1 rem	[= 1.00×10^{-2}	J/kg] *
Mass			
► unified atomic mass unit ($\frac{1}{12}$ of the mass of ^{12}C)	1 u	[= 1.66057×10^{-27}	kg, approx.]
► tonne (= metric ton)	1 t	[= 1.00×10^3	kg] *
pound mass (avoirdupois)	1 lbm	= 4.536×10^{-1}	kg
ounce mass (avoirdupois)	1 ozm	= 2.835×10^1	g
ton (long) (= 2240 lbm)	1 ton	= 1.016×10^3	kg
ton (short) (= 2000 lbm)	1 short ton	= 9.072×10^2	kg
Length			
statute mile	1 mile	= 1.609×10^0	km
nautical mile (international)	1 n mile	= 1.852×10^0	km *
yard	1 yd	= 9.144×10^{-1}	m *
foot	1 ft	= 3.048×10^{-1}	m *
inch	1 in	= 2.54×10^1	mm *
mil (= 10^{-3} in)	1 mil	= 2.54×10^{-2}	mm *
Area			
► hectare	1 ha	[= 1.00×10^4	m^2] *
► barn (effective cross-section, nuclear physics)	1 b	[= 1.00×10^{-28}	m^2] *
square mile, (statute mile) ²	1 mile ²	= 2.590×10^0	km ²
acre	1 acre	= 4.047×10^3	m^2
square yard	1 yd ²	= 8.361×10^{-1}	m^2
square foot	1 ft ²	= 9.290×10^{-2}	m^2
square inch	1 in ²	= 6.452×10^2	mm ²
Volume			
► litre	1 l or 1 ltr	[= 1.00×10^{-3}	m^3] *
cubic yard	1 yd ³	= 7.646×10^{-1}	m^3
cubic foot	1 ft ³	= 2.832×10^{-2}	m^3
cubic inch	1 in ³	= 1.639×10^4	mm ³
gallon (imperial)	1 gal (UK)	= 4.546×10^{-3}	m^3
gallon (US liquid)	1 gal (US)	= 3.785×10^{-3}	m^3
Velocity, acceleration			
foot per second (= fps)	1 ft/s	= 3.048×10^{-1}	m/s *
foot per minute	1 ft/min	= 5.08×10^{-3}	m/s *
mile per hour (= mph)	1 mile/h	= 4.470×10^{-1}	m/s
► knot (international)	1 knot	= 1.852×10^0	km/h *
free fall, standard, g		= 9.807×10^0	m/s^2
foot per second squared	1 ft/s ²	= 3.048×10^{-1}	m/s^2 *

This table has been prepared by E. R. A. Beck for use by the Division of Publications of the IAEA. While every effort has been made to ensure accuracy, the Agency cannot be held responsible for errors arising from the use of this table.

Column 1 <i>Multiply data given in:</i>	Column 2	Column 3 <i>by:</i>	Column 4 <i>to obtain data in:</i>
Density, volumetric rate			
pound mass per cubic inch	1 lbm/in ³	= 2.768 × 10 ⁶	kg/m ³
pound mass per cubic foot	1 lbm/ft ³	= 1.602 × 10 ¹	kg/m ³
cubic feet per second	1 ft ³ /s	= 2.832 × 10 ⁻²	m ³ /s
cubic feet per minute	1 ft ³ /min	= 4.719 × 10 ⁻⁴	m ³ /s
Force			
▶ newton	1 N	[≡ 1.00 × 10 ⁰	m · kg · s ⁻²]*
dyne	1 dyn	= 1.00 × 10 ⁻⁵	N *
kilogram force (= kilopond (kp))	1 kgf	= 9.807 × 10 ⁰	N
poundal	1 pdl	= 1.383 × 10 ⁻¹	N
pound force (avoirdupois)	1 lbf	= 4.448 × 10 ⁰	N
ounce force (avoirdupois)	1 ozf	= 2.780 × 10 ⁻¹	N
Pressure, stress			
▶ pascal	1 Pa	[≡ 1.00 × 10 ⁰	N/m ²]*
▶ atmosphere ^a , standard	1 atm	= 1.013 25 × 10 ⁵	Pa *
▶ bar	1 bar	= 1.00 × 10 ⁵	Pa *
centimetres of mercury (0°C)	1 cmHg	= 1.333 × 10 ³	Pa
dyne per square centimetre	1 dyn/cm ²	= 1.00 × 10 ⁻¹	Pa *
feet of water (4°C)	1 ftH ₂ O	= 2.989 × 10 ³	Pa
inches of mercury (0°C)	1 inHg	= 3.386 × 10 ³	Pa
inches of water (4°C)	1 inH ₂ O	= 2.491 × 10 ²	Pa
kilogram force per square centimetre	1 kgf/cm ²	= 9.807 × 10 ⁴	Pa
pound force per square foot	1 lbf/ft ²	= 4.788 × 10 ¹	Pa
pound force per square inch (= psi) ^b	1 lbf/in ²	= 6.895 × 10 ³	Pa
torr (0°C) (= mmHg)	1 torr	= 1.333 × 10 ²	Pa
Energy, work, quantity of heat			
▶ joule (≡ W · s)	1 J	[≡ 1.00 × 10 ⁰	N · m]*
▶ electronvolt	1 eV	[= 1.602 19 × 10 ⁻¹⁹	J, approx.]
British thermal unit (International Table)	1 Btu	= 1.055 × 10 ³	J
calorie (thermochemical)	1 cal	= 4.184 × 10 ⁰	J *
calorie (International Table)	1 cal _{IT}	= 4.187 × 10 ⁰	J
erg	1 erg	= 1.00 × 10 ⁻⁷	J *
foot-pound force	1 ft · lbf	= 1.356 × 10 ⁰	J
kilowatt-hour	1 kW · h	= 3.60 × 10 ⁶	J *
kiloton explosive yield (PNE) (≡ 10 ¹² g-cal)	1 kt yield	≈ 4.2 × 10 ¹²	J
Power, radiant flux			
▶ watt	1 W	[≡ 1.00 × 10 ⁰	J/s]*
British thermal unit (International Table) per second	1 Btu/s	= 1.055 × 10 ³	W
calorie (International Table) per second	1 cal _{IT} /s	= 4.187 × 10 ⁰	W
foot-pound force/second	1 ft · lbf/s	= 1.356 × 10 ⁰	W
horsepower (electric)	1 hp	= 7.46 × 10 ²	W *
horsepower (metric) (= ps)	1 ps	= 7.355 × 10 ²	W
horsepower (550 ft · lbf/s)	1 hp	= 7.457 × 10 ²	W
Temperature			
▶ temperature in degrees Celsius, t	t = T - T ₀		
where T is the thermodynamic temperature in kelvin			
and T ₀ is defined as 273.15 K			
degree Fahrenheit	$\left. \begin{array}{l} t_{\circ F} - 32 \\ T_{\circ R} \\ \Delta T_{\circ R} (= \Delta t_{\circ F}) \end{array} \right\} \times \left(\frac{5}{9} \right) \text{ gives } \left\{ \begin{array}{l} t \text{ (in degrees Celsius) } * \\ T \text{ (in kelvin) } * \\ \Delta T (= \Delta t) * \end{array} \right.$		
degree Rankine			
degrees of temperature difference ^c			
Thermal conductivity^c			
1 Btu · in/(ft ² · s · °F)	(International Table Btu)	= 5.192 × 10 ²	W · m ⁻¹ · K ⁻¹
1 Btu/(ft · s · °F)	(International Table Btu)	= 6.231 × 10 ³	W · m ⁻¹ · K ⁻¹
1 cal _{IT} /(cm · s · °C)		= 4.187 × 10 ²	W · m ⁻¹ · K ⁻¹

^a atm abs, ata: atmospheres absolute;
atm (g), atü: atmospheres gauge.

^b lbf/in² (g) (= psig): gauge pressure;
lbf/in² abs (= psia): absolute pressure.

^c The abbreviation for temperature difference, deg (= degK = degC), is no longer acceptable as an SI unit.

HOW TO ORDER IAEA PUBLICATIONS

An exclusive sales agent for IAEA publications, to whom all orders and inquiries should be addressed, has been appointed for the following countries:

CANADA
UNITED STATES OF AMERICA UNIPUB, 4611-F Assembly Drive, Lanham, MD 20706-4391, USA

In the following countries IAEA publications may be purchased from the sales agents or booksellers listed or through major local booksellers. Payment can be made in local currency or with UNESCO coupons.

ARGENTINA	Comisión Nacional de Energía Atómica, Avenida del Libertador 8250, RA-1429 Buenos Aires
AUSTRALIA	Hunter Publications, 58 A Gipps Street, Collingwood, Victoria 3066
BELGIUM	Service Courrier UNESCO, 202, Avenue du Roi, B-1060 Brussels
CHILE	Comisión Chilena de Energía Nuclear, Venta de Publicaciones, Amunategui 95, Casilla 188-D, Santiago
CHINA	IAEA Publications in Chinese: China Nuclear Energy Industry Corporation, Translation Section, P.O. Box 2103, Beijing IAEA Publications other than in Chinese: China National Publications Import & Export Corporation, Deutsche Abteilung, P.O. Box 88, Beijing
CZECHOSLOVAKIA	S.N.T.L., Mikulandska 4, CS-116 86 Prague 1 Alfa, Publishers, Hurbanovo námestie 3, CS-815 89 Bratislava
FRANCE	Office International de Documentation et Librairie, 48, rue Gay-Lussac, F-75240 Paris Cedex 05
HUNGARY	Kultura, Hungarian Foreign Trading Company, P.O. Box 149, H-1389 Budapest 62
INDIA	Oxford Book and Stationery Co., 17, Park Street, Calcutta-700 016 Oxford Book and Stationery Co., Scindia House, New Delhi-110 001
ISRAEL	Heiliger & Co. Ltd. 23 Keren Hayesod Street, Jerusalem 94188
ITALY	Libreria Scientifica, Dott. Lucio de Biasio "aeiou", Via Meravigli 16, I-20123 Milan
JAPAN	Maruzen Company, Ltd, P.O. Box 5050, 100-31 Tokyo International
PAKISTAN	Mirza Book Agency, 65, Shahrah Quaid-e-Azam, P.O. Box 729, Lahore 3
POLAND	Ars Polona-Ruch, Centrala Handlu Zagranicznego, Krakowskie Przedmiescie 7, PL-00-068 Warsaw
ROMANIA	Ilexim, P.O. Box 136-137, Bucharest
SOUTH AFRICA	Van Schaik Bookstore (Pty) Ltd, P.O. Box 724, Pretoria 0001
SPAIN	Díaz de Santos, Lagasca 95, E-28006 Madrid Díaz de Santos, Balmes 417, E-08022 Barcelona
SWEDEN	AB Fritzes Kungl. Hovbokhandel, Fredsgatan 2, P.O. Box 16356, S-103 27 Stockholm
UNITED KINGDOM	HMSO, Publications Centre, Agency Section, 51 Nine Elms Lane, London SW8 5DR
USSR	Mezhdunarodnaya Kniga, Smolenskaya-Sennaya 32-34, Moscow G-200
YUGOSLAVIA	Jugoslovenska Knjiga, Terazije 27, P.O. Box 36, YU-11001 Belgrade

Orders from countries where sales agents have not yet been appointed and requests for information should be addressed directly to:



**Division of Publications
International Atomic Energy Agency
Wagramerstrasse 5, P.O. Box 100, A-1400 Vienna, Austria**

79-00595

